universität wien

DISSERTATION

Titel der Dissertation

NEW APPROACHES IN THE TARGETING OF CELL CYCLE, CELL DEATH AND CANCER PROGRESSION: MODELS FOR IMPROVED TUMOR THERAPY

Verfasser

Mag.pharm. Benedikt Giessrigl

angestrebter akademischer Grad

Doktor der Naturwissenschaften (Dr.rer.nat.)

Wien, 2011

Studienkennzahl lt. Studienblatt:	A 091 449
Dissertationsgebiet lt. Studienblatt:	Pharmazie
Betreuerin / Betreuer:	Ao. Univ.-Prof. Dr. Walter Jäger

ACKNOWLEDGEMENTS

I would like to express my gratitude to my supervisor, Ao. Univ.-Prof. Dr. Walter Jäger (Department of Clinical Pharmacy and Diagnostics, University of Vienna) for his scientific supervision, his helpful support and his constant encouragement throughout my thesis.

I am extremely grateful to Ao. Univ.-Prof. Dr. Georg Krupitza (Clinical Institute for Pathology, Medical University of Vienna) for providing me with this project, for his cooperativeness and his constant interest and support. His constructive suggestions and critical appreciation throughout my PhD study made the thesis possible.

Finally, I would also like to thank all my other colleagues for their constant interest in my work and their support.

TABLE OF CONTENTS

1 SUMMERY 1

2 ZUSAMMENFASSUNG 3

3 INTRODUCTION 7

3.1 Cancer – a major public health problem 7

3.2 Development and biology of cancer 7

3.2.1 Hallmarks of cancer 8

3.2.1.1 Self-sufficiency in growth signals 8

3.2.1.2 Insensitivity to growth-inhibitory signals 9

3.2.1.3 Evasion of programmed cell death 10

3.2.1.4 Limitless replicative potential 10

3.2.1.5 Sustained angiogenesis 11

3.2.1.6 Metastasis 12

3.2.1.7 Additional hallmarks and enabling characteristics 12

3.2.2 The cell cycle 13

3.2.2.1 Regulation of the cell cycle 14

3.2.2.2 Checkpoints 15

3.2.2.3 Cdc25 phosphatases – important players in cell cycle progression 16

3.2.3 Cell death 19

3.2.3.1 Apoptosis 19

3.2.3.2 Necrotic cell death 20

3.2.4 Metastasis – the leading cause for cancer deaths 21

3.2.4.1 Mechanisms of cell invasion 22

3.2.4.2 Endothelial transmigration 24

3.2.5 The tumor microenvironment 24

3.3 Pancreatic cancer 25

3.3.1 Genetic profiles of pancreatic cancer 25

3.3.2 Treatment options **26**
3.4 Heat shock proteins 27
3.4.1 Hsp90 ..... **27**
4 REFERENCES **29**
5 AIMS OF THE THESIS **47**
6 RESULTS **49**
6.1 Original papers and manuscripts 49
6.1.1 Madlener S., Rosner M., Krieger S., **Giessrigl B.**, Gridling M., Vo T.P., Leisser C., Lackner A., Raab I., Grusch M., Hengstschläger M., Dolznig H. and Krupitza G. Short 42 degrees C heat shock induces phosphorylation and degradation of Cdc25A which depends on p38MAPK, Chk2 and 14.3.3. *Hum Mol Genet.* 18: 1990-2000, **2009.** 53
6.1.2 Ozmen A., Madlener S., Bauer S., Krasteva S., Vonach C., **Giessrigl B.**, Gridling M., Viola K., Stark N., Saiko P., Michel B., Fritzer-Szekeres M., Szekeres T., Askin-Celik T., Krenn L. and Krupitza G. In vitro anti-leukemic activity of the ethno-pharmacological plant Scutellaria orientalis ssp. carica endemic to western Turkey. *Phytomedicine* 17: 55-62, **2010.** 67
6.1.3 Khan M., **Giessrigl B.**, Vonach C., Madlener S., Prinz S., Herbaceck I., Hölzl C., Bauer S., Viola K., Mikulits W., Quereshi R.A., Knasmüller S., Grusch M., Kopp B. and Krupitza G. Berberine and a Berberis lycium extract inactivate Cdc25A and induce alpha-tubulin acetylation that correlate with HL-60 cell cycle inhibition and apoptosis. *Mutat Res.* 683: 123-130, **2010.** 77
6.1.4 Madlener S., Saiko P., Vonach C., Viola K., Huttary N., Stark N., Popescu R., Gridling M., Vo N.T., Herbacek I., Davidovits A., **Giessrigl B.**, Venkateswarlu S., Geleff S., Jäger W., Grusch M., Kerjaschki D., Mikulits W., Golakoti T., Fritzer-Szekeres M., Szekeres T. and Krupitza G. Multifactorial anticancer effects of digalloyl-resveratrol encompass apoptosis, cell-cycle arrest, and

inhibition of lymphendothelial gap formation in vitro. *Br. J. Cancer* 102: 1361-137, **2010.** 87

6.1.5 Saiko P., Graser G., **Giessrigl B.**, Lackner A., Grusch M., Krupitza G., Basu A., Sinha B.N., Jayaprakash V., Jaeger W., Fritzer-Szekeres M. and Szekeres T. A novel N-hydroxy-N'-aminoguanidine derivative inhibits ribonucleotide reductase activity: Effects in human HL-60 promyelocytic leukemia cells and synergism with arabinofuranosylcytosine (Ara-C). *Biochem Pharmacol.* 81: 50-59, **2011.** 99

6.1.6 Jäger W., Gruber A., **Giessrigl B.**, Krupitza G., Szekeres T. and Sonntag D. Metabolomic analysis of resveratrol-induced effects in the human breast cancer cell lines MCF-7 and MDA-MB-231. *OMICS* 15: 9-14, **2011.** 111

6.1.7 Vonach C., Viola K., **Giessrigl B.**, Huttary N., Raab I., Kalt R., Krieger S., Vo T.P., Madlener S., Bauer S., Marian B., Hämmerle M., Kretschy N., Teichmann M., Hantusch B., Stary S., Unger C., Seelinger M., Eger A., Mader R., Jäger W., Schmidt W., Grusch M., Dolznig H., Mikulits W. and Krupitza G. NF-κB mediates the 12(S)-HETE-induced endothelial to mesenchymal transition of lymphendothelial cells during the intravasation of breast carcinoma cells. *Br. J. Cancer* 105: 263-271, **2011.** 119

6.1.8 Bauer S., Singhuber J., Seelinger M., Unger C., Viola K., Vonach C., **Giessrigl B.**, Madlener S., Stark N., Wallnofer B., Wagner K.H., Fritzer-Szekeres M., Szekeres T., Diaz R., Tut F., Frisch R., Feistel B., Kopp B., Krupitza G. and Popescu R. Separation of anti-neoplastic activities by fractionation of a Pluchea odorata extract. *Front Biosci. (Elite Ed)* 1: 1326-36, **2011.** 131

6.1.9 Viola K., Vonach C., Kretschy N., Teichmann M., Rarova L., Strnad M., **Giessrigl B.**, Huttary N., Raab I., Stary S., Krieger S., Keller T, Bauer S, Jarukamjorn K., Hantusch B., Szekeres T., de Martin R., Jäger W., Knasmüller S., Mikulits W., Dolznig H., Krupitza G. and Grusch M. Bay11-7082 and xanthohumol inhibit breast cancer spheroid-triggered disintegration of the lymphendothelial barrier; the role of lymphendothelial NF-κB. *Br. J. Cancer,* ***submitted.*** 145

6.1.10 Seelinger M., Popescu R., Seephonkai P., Singhuber J., **Giessrigl B.**, Unger C., Bauer S., Wagner K.H., Fritzer-Szekeres M., Szekeres T., Diaz R., Tut F.T., Frisch R., Feistel B., Kopp B. and Krupitza G. Fractionation of an anti-neoplastic extract of *Pluchea odorata* eliminates a property typical for a migratory cancer phenotype. *Evidence-based Compl. and Alt. Medicine,* ***submitted.*** 179

6.1.11 **Giessrigl B.,** Yazici G., Teichmann M., Kopf S., Ghassemi S., Atanasov A.G., Dirsch V.M., Grusch M., Jäger W., Özmen A. and Krupitza G. Effects of *Scrophularia* Extracts on Tumor Cell Proliferation, Death and Intravasation through Lymphendothelial Cell Barriers. *Evidence-based Compl. and Alt. Medicine,* ***submitted.*** 205

6.1.12 Saiko P., Graser G., **Giessrigl B.**, Lackner A., Grusch M., Krupitza G., Jaeger W., Golakoti T., Fritzer-Szekeres M. and Szekeres. Digalloylresveratrol, a novel resveratrol analog attenuates the growth of human pancreatic cancer cells by inhibition of ribonucleotide reductase *in situ* activity. *J. of Gastroenterology*, ***submitted.*** 237

6.1.13 **Giessrigl B.,** Krieger S., Huttary N., Saiko P., Alami M., Maciuk A., Gollinger M., Mazal P., Szekeres T., Jäger W. and Krupitza G. Hsp90 stabilises Cdc25A and counteracts heat shock mediated Cdc25A degradation and cell cycle attenuation in pancreas carcinoma cells. *Hum Mol Genet.,* ***submitted.*** 275

7 CURRICULUM VITAE 303

8 LIST OF SCIENTIFIC PUBLICATIONS 305

ABBREVIATIONS

ADP	Adenosine diphosphate
ATM	Ataxia telangiectasia mutated protein
ATP	Adenosine triphosphate
ATR	Ataxia telangiectasia and Rad3-related protein
Bcl-2	B-cell lymphoma 2
BH3	Bcl-2-homology 3
CAK	CDK activation kinase
CAT	Collective to amoeboid transition
Cdc	Cell division cycle
CDK	Cyclin dependant kinase
CDKI	Cyclin dependant kinase inhibitor
Chk	Checkpoint kinase
CSC	Cancer stem cell
DISC	Death-inducing signaling complex
ECM	Extracellular matrix
EMT	Epithelial to mesenchymal transition
FGF	Fibroblast growth factor
HETE	Hydroxyeicosatetraenoic acid
Hsp	Heat shock protein
LEC	Lymphatic endothelial cell
LOX	Lipoxygenase
MAPK	Mitogen activated protein kinase
MAT	Mesenchymal to amoeboid transition
MET	Mesenchymal to epithelial transition
MMP	Matrix-metalloprotease
PARP	Poly-(ADP-ribose) polymerase
PDGF	Platelet derived growth factor
PI3 kinase	Phosphatidylinositol 3-kinase
RB	Retinoblastoma protein
RIP	Ribosome inactivating protein

ROS	Reactive oxygen species
TNF	Tumor necrosis factor
TNFR	Tumor necrosis factor receptor
TSP-1	Thrombospondin 1
VEGF	Vascular endothelial growth factor

1 SUMMERY

Cancer represents a major public health problem in many parts of the world and, besides heart diseases, cancer is the leading cause of death. Although there has been lots of progress in both, the understanding of biological principles leading to tumor development and their treatment, even today therapy concepts are partly limited. Therefore, exploration of new, innovative and target specific therapies represent a major part of cancer research.

The aims of this thesis were investigations about novel therapy concepts for an improved tumor treatment with the main focus to inhibit the increased proliferation of tumor cells, to elicit cell death and to find possibilities to prevent metastasis.

Natural products have played a significant role in human healthcare for thousands of years and even today, more than 60% of all drugs are either natural products or directly derived thereof, and therefore the effects of different natural extracts on various cell lines were investigated. Different medicinal plants, used as folk remedies mainly against acute and chronic inflammations, showed distinct proliferation inhibiting and apoptosis promoting properties and western blot experiments elucidated the underlying mechanisms. Furthermore, a total methanol extract of *Scrophularia lucida*, collected in the south of Turkey, showed anti-metastatic effects in a recently developed in vitro model. In this model, intravasation of tumor cells into the lymphatic vessels is resembled by generating circular defects in the integrity of a lymphatic endothelial cell layer (LEC) by MCF-7 breast cancer spheroids. Formation of these ruptures is known to be mediated by 12(S)-HETE metabolized from arachidonic acid by the hypoxia-inducible enzymes ALOX12 or ALOX15. Inhibition of NF-κB activity with the synthetic inhibitor Bay 11-7082 also repressed the generation of these circular defects and therefore, the NF-κB pathway could be identified as a second mediator leading to the ruptures in the LEC monolayer. As treatment with *Scrophularia lucida* showed a distinct inhibition of NF-κB activity in a luciferase assay, the anti-metastatic properties of this medicinal plant extract could be attributed to NF-κB inhibition.

Inhibition of NF-κB activity represents also one of the anti-neoplastic mechanisms of resveratrol. Its chemo- preventive and growth inhibiting properties are well described. In contrast, there is not much information about metabolic alterations caused by resveratrol and therefore, the influence of this natural compound on the cellular

concentrations of different catabolic metabolites have been investigated in two breast cancer cell lines. It could be demonstrated that treatment with resveratrol leads to increased synthesis of amino acids and biogenic amines. Furthermore, an increased release of arachidonic acid could be observed leading in raised synthesis of 12(S)-HETE. This was most likely the reason that resveratrol, despite inhibiting NF-κB, was only weakly inhibiting the formation of MCF-7 spheroid induced circular defects in LEC monolayers.

Investigations about the influence of short hyperthermia and the inhibition of the heat shock protein 90 (Hsp90) on the proliferation of tumor cells were a second major point of this work. In case of exposure to different stresses such as hypoxia, ischemia, exposure to UV light or chemicals, nutritional deficiencies or increased temperatures, this chaperone protects various client proteins. It could be shown that the dual specific phosphatase Cdc25A, a proto-oncogene over-expressed in various different human cancers, represents a client protein of Hsp90 and that short hyperthermia leads to its degradation in HEK and HELA cells. Furthermore, in combination with the Hsp90 inhibitor geldanamycin the same effect could be observed in different pancreatic and breast cancer cell lines. Regularly, DNA damage leads to activation of ATR and ATM and subsequent phosphorylation and activation of the checkpoint kinases Chk1 and Chk2 resulting in Cdc25A degradation and cell cycle arrest. By western blot analysis and specific knockdown of Hsp90 with lentiviral packaged shRNA we could discover a hitherto unknown cell cycle regulation and demonstrated that the observed Cdc25A degradation by heat shock and Hsp90 inhibition was DNA checkpoint independent. Furthermore, we could show an additive effect on the inhibition of the proliferation in the human pancreatic cancer cell line BxPC3 for the combination of this novel therapy concept together with the checkpoint dependent Cdc25A inhibition by gemcitabine.
In summary, this work demonstrates the huge potential of natural compounds and medicinal plants, that are used since ancient times, regarding their potential as anti cancer remedies. Further investigations and isolation of the active agents could lead to novel lead compounds for potent anti cancer drugs. Furthermore, it could be shown that a comparatively simple and therapy (hyperthermia/fever) can exhibit distinct inhibiting effects on the proliferation of cancer cells and that this innovative therapy concept represents an interesting treatment option against multi resistant pancreatic cancer.

2 ZUSAMMENFASSUNG

In der westlichen Welt stellt Krebs nach Herz Kreislauferkrankungen die zweithäufigste Todesursache dar, und obwohl es in den letzten Jahren zu massiven Fortschritten sowohl in der Aufklärung der biologischen Grundlagen als auch in der Behandlung gekommen ist, sind die Therapiemöglichkeiten auch heute noch teilweise sehr beschränkt, und somit kommt der Erforschung innovativer zielgerichteter Heilverfahren großer Bedeutung zu.

Im Rahmen dieser Arbeit wurden in verschiedenen Projekten neuartige Ansätze für eine verbesserte Tumortherapie untersucht, mit dem Hauptaugenmerk die gesteigerte Proliferationsrate von Tumorzellen zu hemmen, Zelltod auszulösen bzw. Konzepte zum Verhindern von Metastasierung zu erstellen.

Da Naturstoffe selbst oder zumindest als Leitsubstanz mehr als 60% der heute verwendeten Arzneistoffe ausmachen, wurde die Wirkung einiger pflanzlicher Extrakte auf unterschiedliche Zelllinien ausgetestet. Dabei wurden für verschiedene, volksmedizinisch vor allem gegen chronische und akute Entzündungen verwendete Heilpflanzen ausgeprägte wachstumshemmende und Apoptose fördernde Wirkungen nachgewiesen und mittels Western Blot Untersuchungen konnten die zugrunde liegenden Mechanismen erhellt werden. Für die Braunwurz *Scrophularia lucida* konnte neben den schon erwähnten anti-kanzerogenen Eigenschaften auch eine deutliche Metastasierung hemmende Wirkung gezeigt werden. Das hierfür verwendete, erst kürzlich entwickelte in vitro Modell imitiert das Eindringen von Brustkrebszellen in die Lymphgefäße, indem MCF-7 Tumorzellspheroide Spaltformationen in einen Lymphendothelzellen-Monolayer induzieren. Mittels Hemmung der NF-κB Aktivität mit dem synthetischen Inhibitor Bay 11-7082 und damit verbundener stark verminderter Spaltbildung konnte neben der bereits bekannten und beschriebenen Lipoxigenasen abhängigen Sezernierung von 12(S)-HETE auch der NF-κB Pathway als weitere wichtige Signalkaskade für die Lochbildung ausgemacht werden. Behandlung mit *Scrophularia lucida* zeigte in einem NF-κB Luciferase Assay eine ausgeprägte Hemmung dieses Signalweges, wodurch die durch diesen Extrakt hervorgerufene anti-metastatische Wirkung auf NF-κB Inaktivierung zurückzuführen ist.

Hemmung der NF-κB Aktivität ist auch ein Angriffspunkt von Resveratrol, dessen chemopräventive und wachstumshemmende Eigenschaften im Rahmen zahlreicher

Studien belegt sind. Da es jedoch kaum Information über metabolische Veränderungen hervorgerufen durch Resveratrol gibt, wurde der Einfluss dieses Naturstoffes auf die zellulären Konzentrationen verschiedener Stoffwechselprodukte in zwei Brustkrebszelllinien untersucht. Es konnte gezeigt werden, dass Behandlung mit Resveratrol zu gesteigerter Synthese von Aminosäuren und biogenen Aminen führt, sowie die Freisetzung von Arachidonsäure und die damit verbundene erhöhte 12(S)-HETE Konzentration fördert. Dadurch läst sich auch erklären, dass Resveratrol trotz seiner NF-κB hemmenden Wirkung nur einen sehr geringen Einfluss auf das Unterdrücken der MCF-7 Spheroid induzierten Lochbildung in einen LEC Monolayer besitzt.

Untersuchungen über den Einfluss von kurzer Hyperthermie auf die Proliferation von Krebszellen stellten einen weiteren Schwerpunkt dieser Arbeit dar, wobei auf das Heat Shock Protein Hsp90 ein Hauptaugenmerk gelegt wurde. Dieses Chaperon schützt unter verschiedenen Stresssituationen (u. a. unphysiologisch erhöhten Temperaturen) einige Substratproteine. Es konnte gezeigt werden, dass auch Cdc25A, ein Proto-Onkogen, überexprimiert in einer Vielzahl humaner Tumore, ein Targetprotein von Hsp90 ist, und kurze Hyperthermie in HEK- und HELA Zellen zu dessen Degradierung führt. Ferner konnte dieser Effekt in Kombination mit dem Hsp90 Inhibitor Geldanamycin auch für Pankreaskarzinomzellen gezeigt werden. In der Regel führt DNA-Schädigung via ATM/ATR zu Phosphorylierung und damit verbundener Aktivierung der Checkpoint Kinasen Chk 1 und Chk 2 und in weiterer Folge zur Degradierung von Cdc25A und somit zur Arretierung des Zellzyklus. Western Blot Untersuchungen und spezifischer Knockdown von Hsp90 mit lentiviral verpackter shRNA zeigten, dass die Cdc25A Degradierung nach Hsp90 Hemmung und Heatshock jedoch Checkpoint unabhängig ist, und somit konnte im Rahmen dieser Arbeit ein neuer Zellzyklus regulierender Mechanismus ausgemacht werden. Darüber hinaus führte die Kombination dieses neuen Therapieansatzes mit der Checkpoint abhängigen Cdc25A Hemmung durch Gemcitabin, der Standardtherapie für Pankreaskrebs, zu signifikant positivem Effekt auf die Proliferation von Pankreaszellen.

Zusammenfassend veranschaulicht diese Arbeit zum einen das große Potential, das in Naturstoffen steckt, und dass genaue Untersuchungen weiterer verschiedener seit Jahrhunderten volksmedizinisch angewandten Heilpflanzen und Isolierung der wirksamen Bestandteile neuartige Leitsubstanzen für potente Arzneistoffe liefern

können. Zum anderen konnte gezeigt werden, dass sich eine vergleichsweise einfache Therapieform (Hyperthermie/Fieber) deutlich auf das Wachstum von Krebszellen auswirkt, und dass dieser innovative Therapieansatz gerade bei gegenüber fast allen Chemotherapeutika resistentem Pankreaskrebs eine äußerst interessante Option darstellt.

3 INTRODUCTION

3.1 Cancer – a major public health problem

Cancer represents a major public health problem in many parts of the world and currently 1 in 4 deaths in the United States is due to that disease [Jemal et al., 2010]. Besides heart diseases, cancer is the leading cause of death among men and women aged older than 40 years in western countries and the lifetime probability of being diagnosed with an invasive cancer ranges around 40% for men and women. Whereas prostate (28%), lung (15%) colon (9%) and urinary bladder (7%) represent the 4 most common cancers in men, in women cancers of the breast (28%), lung (14%), colon (10%) and uterine corpus (6%) are most frequent cancers [Jemal et al., 2010]. However, in both sexes approx. 30% of cancer deaths is related to lung cancer. Metastasis is the main cancer death reason as 90% of all cancer deaths are not related to the primary tumor but to disseminated tumors that destroy the function of infested organs [Sporn, 1996]. Due to progress in early diagnosis and improved treatment options, there have been notable improvements in the relative 5-year survival rates for many cancer sites with the exception of lung and pancreatic cancer [Jemal et al., 2010]. Although there is huge progress in developing powerful therapies, acquired resistance represents one of the major problems in cancer treatment and therefore, of course besides further improvements in early diagnosis, finding new target specific treatment options must be a focal point of research.

3.2 Development and biology of cancer

Decades of intensive research about development and biology of cancer led to the assumption that different mutations produce oncogenes with increased function and tumor suppressor genes with loss of function [Bishop and Weinberg, 1996]. Generally, transformation of normal cells into malignant derivatives is a multistep process requiring alterations of the genome at multiple sites [Kinzler and Vogelstein, 1996].

3.2.1 Hallmarks of cancer

In their seminal publication [2000] an in an update [2011] D. Hanahan and R. A. Weinberg specified a small number of underlying principles responsible for this transformation:

- Self-sufficiency in growth signals
- Insensitivity to growth-inhibitory signals
- Evasion of programmed cell death (apoptosis)
- Limitless replicative potential
- Sustained angiogenesis
- Tissue invasion and metastasis

These six hallmarks of cancer were proposed to be shared in perhaps all types of cancer leading progressively to a neoplastic state. Furthermore, D. Hanahan and R. A. Weinberg noted that tumors are not just an isolated mass of proliferating cells, but rather a tissue complex of multiple distinct cell types where even normal cells, such as fibroblasts and endothelial cells, are active participants of tumorigenesis and that this "tumor microenvironment" plays a crucial role in understanding the biology of tumors.

3.2.1.1 Self-sufficiency in growth signals

In contrast to normal cells, that require mitogenic growth signals for moving into an active proliferative state, tumor cells show a clearly reduced dependence to exogenous growth stimulation resulting in the disruption of important homeostatic mechanisms. Different reasons for this self-sufficiency have been identified. Besides autocrine stimulation (the ability to produce their growth factors for their own), cancer cells may stimulate normal cells of the tumor-associated stroma to produce various growth factors [Fedi et al., 1997; Cheng et al., 2008]. Over-expression of growth factor receptors accompanying hyper-responsiveness to ambient growth factor levels is another common attitude for increased proliferation in tumor cells [Fedi et al., 1997]. Furthermore, over-expression or structural alteration of growth factor receptors can result in ligand-independent signalling [DiFiore et al., 1987]. Besides these factors related to growth factor receptors, switching the types of extracellular matrix receptors (integrins) to pro-

growth signals transmitting ones [Lukashev and Werb, 1998; Giancotti and Ruoslahti, 1999] and alterations in the downstream cytoplasmic signal cascade (e.g. the SOS-Ras-Raf-MAPK cascade) [Medema and Bos, 1993] are further possibilities for increased proliferation.

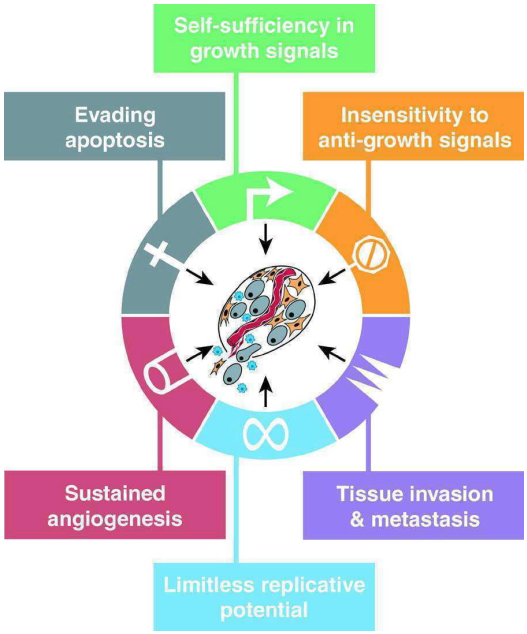

Figure 1 The hallmarks of cancer (Hanahan and Weinberg, 2000)

3.2.1.2 Insensitivity to growth-inhibitory signals

To maintain tissue homeostasis normal cells exhibit multiple anti-proliferative mechanisms including soluble growth inhibitors as well as immobilized inhibitors embedded in the extracellular matrix. These anti-growth signals can force cells into the quiescent (G_0) phase of the cell cycle or, alternatively, may induce cell differentiation associated with attrition of their proliferation potential. Tumor cells have to circumvent these programs. Besides several others, retinoblastoma-associated (RB) and p53 proteins form two prototypical tumor suppressors that are both defective in most, if not all, human cancers [Polager and Ginsberg, 2009]. Besides the prevention of antigrowth signals, tumor cells can avoid cell differentiation by various strategies. Over-expression of the oncogene Myc, as seen in many tumors, for example, has been shown to inhibit cell differentiation [Lüscher, 2001].

3.2.1.3 Evasion of programmed cell death

Beside the cell proliferation rate also the rate of cell death contributes to the population size and acquired resistance toward apoptosis is another hallmark of perhaps all types of cancer. The apoptotic machinery consists of two major circuits – the extrinsic and the intrinsic apoptotic program [Adams and Cory, 2007]. The sensors of the extrinsic program include different cell surface death receptors like the Fas- or the TNF- receptor [Ashkenazi and Dixit, 1999]. In contrast, abnormalities like DNA damage, hypoxia or survival factor insufficiency activate intracellular sentinels [Evan and Littlewood, 1998]. Many of these signals induce release of mitochondrial cytochrome C, the most important pro-apoptotic signalling protein [Green and Reid, 1998]. Cytochrome C release is controlled by bcl-2 family members that have either pro-apoptotic (Bax, Bak, Bim) or anti-apoptotic function (Bcl-2, bcl-x_L) [Adams and Cory, 2007]. However, different intracellular proteases are the ultimate effectors of apoptosis [Thornberry and Lazebnik, 1998]. The two gatekeeper caspases (-8 and -9), triggered by death receptors or cytochrome C, activate different effector caspases, that execute the death program.

Tumor cells can acquire resistance to apoptosis through a variety of strategies and several abnormality sensors have been identified [Lowe et al., 2004], where mutations of the p53 tumor suppressor gene, seen in more than 50% of human cancers, play the most important role [Harris, 1996; Juntilla and Evan, 2009]. Other reasons for resistance to apoptosis include increasing expression of anti-apoptotic regulators (Bcl-2, Bcl-x_L), down-regulation of pro-apoptotic factors (Bax, Bim) or abnormalities in the PI3 kinase-Akt/PKB pathway [Evan and Littlewood, 1998; Juntilla and Evan, 2009].

3.2.1.4 Limitless replicative potential

In contrast to normal cells, cancer cells exhibit unlimited replicative potential in order to generate a macroscopic tumor [Hayflick, 1997]. Normally, cells can pass only through a limited number of cell divisions [Hornsby, 2007]. The two barriers to proliferation are senescence and crisis. Senescence is characterised by irreversible entrance into a non-proliferative but viable state. Cells circumventing this barrier enter a second state (crisis), where most cells of the population die. However, rarely single cells can emerge from a population in crisis and continue proliferating without limit, a trait called immortalization [Wright et al., 1989].

Telomeres, composed of several thousand repeats of a short hexanucleotide element, protect the ends of chromosomes [Blasco, 2005]. Due to the inability of DNA

polymerases to completely replicate 3' ends of chromosomal DNA, each cell cycle leads to loss of small parts of telomeres resulting in the deficit to protect the chromosomal DNA and subsequent crisis [Counter et al., 1992]. In nearly all types of malignant cells telomere maintenance is evident and in about 90% of them telomerase, the specialized DNA polymerase that adds telomere repeat segments, is expressed at functionally significant levels. Hence, the expression of this enzyme correlates with resistance to induction of both senescence and crisis [Zvereva et al., 2010].

Recent research indicates that delayed activation of telomerase may both limit and foster neoplastic progression. Studies demonstrated that some incipient cancer cells undergo telomere loss-induced crisis in a quite early stage of the multistep tumor progression suggesting that these cells have passed through substantial telomere-shortening cell division during their evolution from a normal to a neoplastic cell [Hansel et al., 2006]. In contrast, studies of mutant mice lacking both p53 and telomerase function [Artandi and DePinho, 2010] give indication that the absence of p53 tumor suppressor initiated control permits tumor cells to survive initial telomere loss allowing these cells to become even more malignant because of additional alterations.

3.2.1.5 Sustained angiogenesis

Like normal tissue, tumor cells require blood vessels for the supply of nutrients and oxygen as well as the evacuation of metabolic waste and carbon dioxide. In contrast to normal cells where angiogenesis is only transiently turned on, tumor cells develop an "angiogenic switch", that is almost always activated [Hanahan and Folkman, 1996]. This angiogenic switch is regulated by different factors that either induce (e.g. VEGF, FGF) or inhibit (e. g. TSP-1) angiogenesis [Baeriswyl and Christofori, 2009]. Sustained tumor angiogenesis is generated for example by oncogene mediated up-regulation of pro-angiogenic factors [Ferrara, 2009] or their release and activation out of the extracellular matrix by extracellular matrix-degrading proteases (e.g. MMP-9) [Kessenbrock et al., 2010]. The unbalanced mix of angiogenic signals in tumors lead to blood vessels that are typical aberrant [Nagy et al., 2010]. While historically tumor angiogenesis was thought to occur only in macroscopic tumors, different analyses of premalignant, non-invasive lesions suggest that angiogenesis also occurs quite early in the multistep tumorigenesis, attesting its crucial role [Raica et al., 2009].

3.2.1.6 Metastasis

Like tumorigenesis, invasion and metastasis is a multistep process beginning with local invasion, followed by intravasation into blood and lymphatic vessels, transit through lymphatic and hematogenous systems, extravasation, formation of micrometastases and finally growth of a macroscopic tumor [Fidler, 2003]. Chapter 1.2.4. gives detailed attention to the illustration of this complex process.

3.2.1.7 Additional hallmarks and enabling characteristics

In their updated publication [2011] Hanahan and Weinberg describe two additional hallmarks and two enabling characteristics of tumorigenesis. Although e.g. epigenetic modifications (DNA methylation or histone modifications) can influence gene expression, development of genomic instability represents the basic fundament for the formation and the progression of cancer by generating the mutations that are essential for increased proliferation, prevention of apoptosis and metastasis and cancer cells can increase rates of mutations by increased sensitivity to mutagenic agents and breakdown of different components of the genomic maintenance machinery [Berdasco and Esteller, 2010; Negrini et al. 2010]. Besides that, inflammation by immune cells that are found in virtually every neoplastic lesion supports the multiple hallmark capabilities as a second enabling characteristic. By supplying bioactive molecules to the tumor microenvironment (e.g. growth factors, survival factors, extracellular matrix modifying enzymes etc.) and by the release of different chemicals such as actively mutagenic reactive oxygen species the tumor associated inflammatory response can enhance tumorigenesis and progression [DeNardo et al., 2010; Grivennikov et al., 2010]. Moreover, chronic infections and inflammation frequently lead to cancer development and tumor progression [Mantovani at al., 2010].

Reprogramming of the cancer cells energy metabolism and avoiding of immune destruction are two emerging hallmarks [Hanahan and Weinberg, 2011]. Up-regulation of glucose transporters and a metabolic switch to aerobic glycolysis provide the energy to the cancer cells required for increased proliferation. The fact that cancer cells avoid immunological destruction represents a second emerging hallmark although it is still unresolved how the cancer cells manage to circumvent detection by various arms of the immune system.

3.2.2 The cell cycle

In the development of cancer the disruption of the fine tuned regulation of cell cycle progression and division is an essential step. Lots of different regulatory factors and signals dictate the cell to proliferate or, in case of DNA damage, to die. As mammalian DNA is under constant attack by different agents, cells have developed several defensive mechanisms. Although these repair mechanisms are extremely powerful, they are not perfect, and damage of DNA can result in the development of cancer. DNA breakdown leads to halting of the cell cycle progression via activation of different cell cycle checkpoints until elimination of the damage, or if the cell is not able to repair this defect, to programmed cell death [Hartwell and Weinert, 1989].

The cell cycle is a well regulated series of events in order to duplicate DNA and subsequent cell division and in eukaryotic cell it consists of four distinct phases [Norbury and Nurse, 1992]:

- G1-phase (gap phase 1): cellular growth and preparation for DNA synthesis
- S-phase: duplication of the genome
- G2-phase (gap phase 2): preparation for Mitosis
- M-phase: mitosis (cell division)

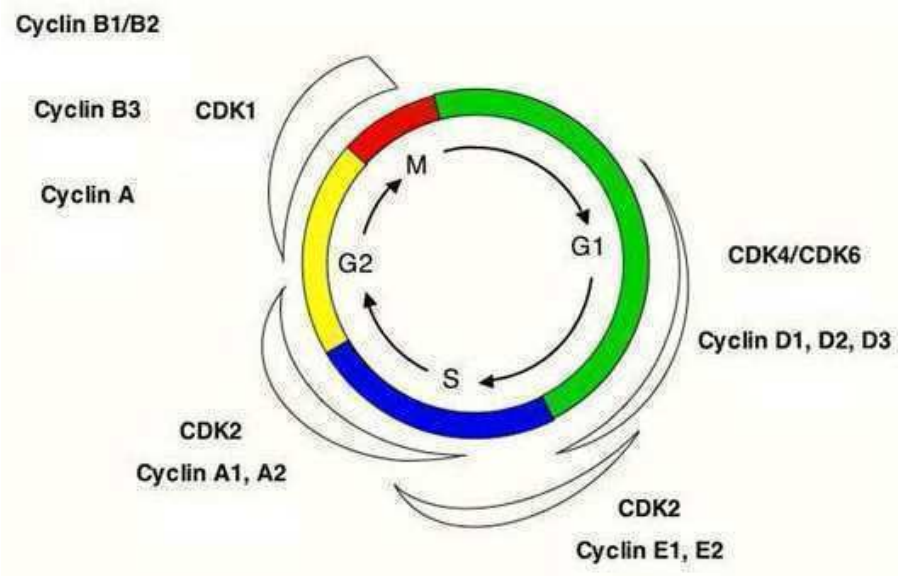

Figure 2 Mammalian cell cycle (simplified) (van den Heuvel 2005)

G1-, S- and G2-phase together form the interphase, while the M-phase could be divided in the metaphase (chromosomal alignment), the anaphase (segregation of sister chromosome) and the telophase (decondensation of chromosomes and formation of nuclear membranes) [McDonald and El-Deiry, 2000]. Besides these four phases, cells in G1-phase may temporarily or permanently leave the cell cycle in dependence on developmental or environmental signals entering a quiescent phase termed G0. Both, cell external and cell intrinsic signals together decide whether cells should enter a division cycle, but after achievement of a restriction point, progression through the cell cycle is controlled only by the intrinsic cell cycle machinery [van den Heuvel at al., 2005].

3.2.2.1 Regulation of the cell cycle

Regulation of the progression from one phase to another is mediated by different cyclin-dependant kinases (CDKs), that are activated after binding to regulatory proteins (cyclins) [Hartwell and Kastan, 1994; Michalides, 1999]. These CDK/Cyclin complexes do not only trigger cell cycle progression, but in case of DNA damage activated checkpoints arrest cells in either G1-, S-, or G2-phase allowing to repair the genetic material [Mailand et al., 2000].

Four CDKs have been identified to be responsible for controlling the different stages of the cell cycle (CDK1, CDK2, CDK4 and CDK6) [Elledge, 1996]. Although CDK protein levels are constant during the cell cycle, they are only functional during distinct intervals [Meeran and Katiyar, 2008]. While CDK4/6 regulate the entry into S-phase, CDK2 remains active through the S-phase and decrease in its activity leads to exit from S-phase. In contrast, CDK1 becomes active in G2-phase and during mitosis [Sherr, 1996].

As mentioned above, association of CDKs with cyclins is essential for their activation. Two types of cyclins have been identified, the cell cycle related cyclins (Cyclins A, B, D and E) and the non cell cycle related cyclins that share structural homology (Cyclins H and C) [Sherr, 1996]. Cyclin D1 and Cyclin E were shown to be frequently deregulated in human cancers [Robles et al., 1998; Porter et al., 2001]. Together with its catalytic subunit, cyclin E has a pivotal role in the regulation of G1-S transition and in the initiation of DNA replication [Krude et al., 1997] and its constitutive over-expression at all phases of the cell cycle was observed in different cancers like breast cancer [Bortner and Rosenberg, 1997] or ovarian cancer [Sui et al., 2001].

Besides the activating cyclins, there are two families of CDK inhibitors (CDKIs) that can repress CDK function, the Cip1/p21 family and the INK4 family. While members of the Cip1/p21 family ($p21^{Cip1}$, $p27^{Kip1}$ and $p57^{Kip2}$) represent universal cyclin/CDK inhibitors, that bind both cyclin and CDK molecules simultaneously, members of the INK4 family ($p15^{INK4}$, $p16^{INK4}$ and $p19^{INK4}$) exhibit specificity for cyclin D/CDK4/6 complexes [Meeran and Katiyar, 2008]. Inhibition of growth stimulatory signaling pathways has been shown to stimulate CDKI expression associated with cell growth arrest [Grana and Reddy, 1995].

3.2.2.2 Checkpoints

Although cells are under constant attack by different agents that may cause mutations of their DNA, manifestation of a mutation and development of a pathological tumor is a rare result. Detection of DNA damage and arresting the cell cycle in order to repair or trigger cell death of the affected cell are the main tasks of different checkpoints and failures of the quality control of these checkpoints or the downstream signal cascades play a major role in the development of cancer [Meeran and Katiyar, 2008]. Besides the ATM/ATR-Chk2/Chk1-mediated response to DNA damage that leads to a delay of cell cycle progression in G1-, S- or G2-phases [Kastan and Bartek, 2004], the tumor suppressor gene p53 is one of the key players in these pathways and mutations or loss of this important tumor suppressor gene are associated with an increased risk of cancer [El-Deiry et al., 1994].

The G1 and G1/S checkpoint

To avoid replication of damaged DNA, the G1/S checkpoint becomes activated and abnormalities at this checkpoint appear to be a crucial step in the development and progression of cancer [Meeran and Katiyar, 2008]. Activation of this checkpoint leads to inhibition of cyclin E/CDK2 complexes via two pathways. Phosphorylation of Chk1 leads to degradation of Cdc25A, with the effect that CDK2 does not get activated. Furthermore, p53 becomes phosphorylated resulting in its stabilization and accumulation and, subsequent, in the activation of Cip1/p21 that silences the G1/S promoting cyclin E/CDK2 complex [Wahl and Carr, 2001]. The Cdc25A degradation cascade is much faster than the slower operating p53 pathway, but delays the G1/S transition only for a few hours in contrast to the p53 dependent mechanism that prolongs the G1 arrest [Kastan and Bartek, 2004].

The S-phase checkpoint

The intra-S-phase checkpoint is regulated by two distinct pathways to avoid duplication of damaged DNA [Falck et al., 2002]. The first one, similar to G1 checkpoint, leads to down-regulation of Cdc25A and subsequent inactivation of cyclin E/CDK2 complexes. Furthermore, inhibition of CDK2 activity blocks the Cdc45 loading onto chromatin, a protein that is required for recruitment of DNA polymerase α. In the second pathway, Nbs1 becomes phosphorylated by ATM on several sites resulting in the activation of the Nbs1-Mre11-Rad50 double strand DNA break repair complex [Lim et al., 2000].

The G2/M checkpoint

The G2/M checkpoint avoids entrance into mitosis when DNA damage occurred during G2-phase or when unrepaired DNA was carried from G1- or S-phase [Nyberg et al., 2002]. The mitosis promoting activity of the cyclin B/CDK1 complex represents the crucial target of this checkpoint. Besides Chk1/2 or p38-kinase mediated degradation of Cdc25 family phosphatases resulting in the prevention of CDK1 activation, p53-dependent mechanisms are also important for the maintenance of G2-phase arrest. P53 activation leads to the up-regulation of cell cycle inhibitors like p21, GADD45a and 14-3-3 proteins [Taylor and Stark, 2001].

3.2.2.3 Cdc25 phosphatases – important players in cell cycle progression

As mentioned before, Cdc25 phosphatases act as key regulators of the cell cycle [Nilsson and Hoffmann, 2000] and especially Cdc25A has been shown to be frequently over-expressed in a wide range of cancers like e.g. breast [Cangi et al., 2000], colorectal [Hernández et al., 2001], head and neck [Gasparotto et al., 1997] or nonsmall cell lung cancers [Wu et al., 1998].

Structure of Cdc25 phosphatases

In mammalian cells, three isoforms of Cdc25 phosphatases have been identified: Cdc25A, Cdc25B and Cdc25C [Boutros et al., 2007]. The human Cdc25 phosphatases are between 300 and 600 amino acids long and can be divided into two regions [Rudolph, 2007]. The N-terminal regulatory domains show low sequence homology and contain several sites for phosphorylation an ubiquitination and modifications at these

sites are involved in cell cycle control and response to checkpoint activation. In contrast, the catalytic C-terminal domains are more homologues.

Function as activators of cell cycle progression

Cyclin dependent kinases and their complexes with cyclins represent the central regulators of the eukaryotic cell cycle and their activation is crucial for cell cycle progression. Different control mechanisms have been elucidated like activating phosphorylations on Thr160/161 by the Cdk-activation kinase (CAK) or inhibitory phosphorylations on Thr14 and Tyr15 by the Wee1 and Myt1 kinases and dephosphorylation of pThr14 and pTyr15 by the dual specific Cdc25 phosphatases represents the essential step of the Cdk/cyclin complexes [Morgan, 1995]. Through their activity on Cdk1/cyclin A and Cdk1/cyclin B complexes, Cdc25B and Cdc25C are regulating the G2/M transition, while Cdc25A also activates the Cdk2/cylin E and Cdk2/Cyclin A complexes and consequently the G1/S transition [Busino et al., 2004; Kristjánsdóttir and Rudolph, 2004].

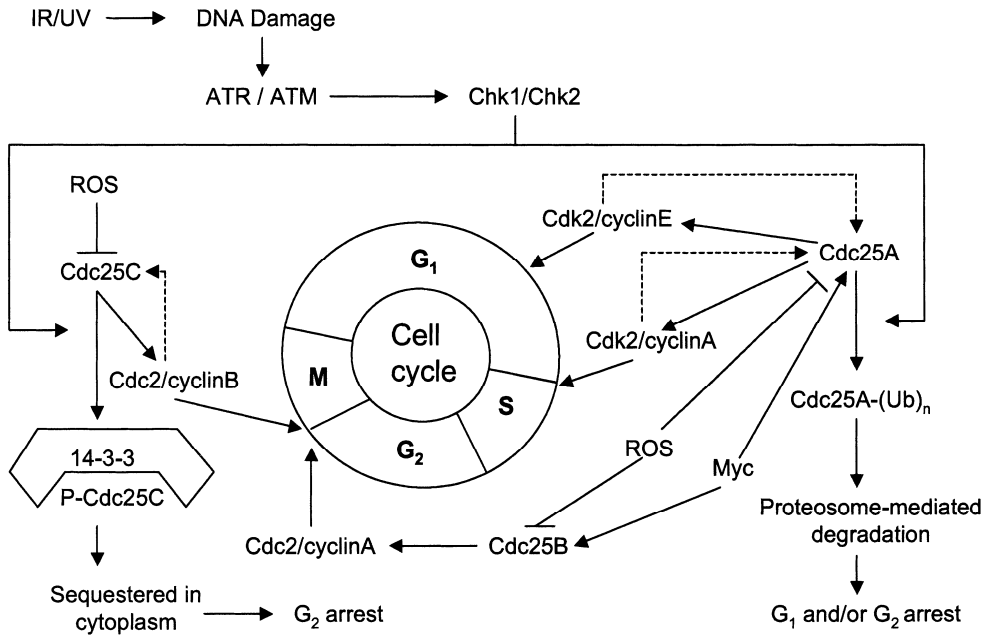

Figure 3 (Kristjánsdóttir and Rudolph, 2004)

Function as regulators after checkpoint activation

Besides the their pivotal role in promoting cell cycle progression, Cdc25 phosphatases are also key components of the checkpoint pathways leading to cell cycle arrest and allowing DNA repair [Bouros et al., 2007]. Mailand et al. [2000] demonstrated that exposure of human cells to ultraviolet light or ionizing radiation resulted in rapid, ubiquitin- and proteasome-dependent protein degradation of Cdc25A and G1/S arrest. Furthermore, it could be shown that this response did not involve the p53 pathway but was a consequence to Chk1 protein kinase activation and that the persisting inhibitory phosphorylation of Tyr15 of Cdk2 blocked the entry into S-phase. Besides ultraviolet light and ionizing radiation also oxidative stress, replication inhibitors and other DNA damaging agents were shown to affect Cdc25 phosphatases expression [Ray and Kiyokawa, 2008; Kristjánsdóttir and Rudolph, 2004] by checkpoint activation via ATM and ATR or activation of the p38 mitogen-activated signalling pathway [Boutros et al., 2007]. While ATM activation occurs primarily in response to double strand DNA breaks, ATR seems to be activated by regions of single stranded DNA [Hurley and Bunz, 2007]. Subsequently, these two kinases phosphorylate and activate the checkpoint kinases Chk1 and Chk2 [Niida and Nakanishi, 2006]. Beside other substrates, Cdc25 phosphatases are important downstream targets of the Chks. Phosphorylation at different inhibitory sites (e.g. Ser75, Ser177 [Goloudina et al. 2003; Karlsson-Rosenthal and Millar, 2006]) creates a docking site for 14.3.3 leading to 14.3.3 mediated sequestration of the phosphatases [Kristjánsdóttir and Rudolph, 2004, Madlener et al., 2009].

Cdc25 phosphatases in cancer

While different studies demonstrate increased expression of Cdc25A, Cdc25B or both in a wide range of human cancers, there is no incidence for Cdc25C over-expression [Rudolph, 2007]. Experimental date gives evidence that over-expression of Cdc25A or Cdc25B to push S-phase or M-phase entry even with incomplete replicated DNA [Karlsson et al., 1999; Sexl et al. 1999], but in different studies there was no correlation between over-expression and an increased rate of proliferation [Kristjánsdóttir and Rudolph, 2004]. As DNA damage results in the degradation of Cdc25 phosphatases it is possible that because of their over-expression these proteins are not completely degraded and inactivated allowing cell cycle expression even in the presence of DNA damages [Kiyokawa and Ray, 2008], thereby accumulating additional mutations.

Mechanisms of over-expression

The mechanisms leading to deregulation and increased Cdc25 phosphatase expression are not fully clarified. Different studies show that there is no evidence that over-expression is a result of gene amplification or other specific genetic mutations [Hernández et al., 2001; Wu et al., 1998; Kudo et al., 1997]. Posttranslational modifications of Cdc25A protein were found to lead to enhanced stability and increased half-life in breast cancer cell lines [Löffler et al., 2003]. Besides alterations concerning Cdc25 phosphatases themselves, changes in regulators of the Cdc25A/B stability could be responsible for increased expression of these oncogenes and in fact mutations of ATR and the Chk kinases have been described [Alderton et al., 2006; Bartek and Lukas, 2003].

3.2.3 Cell death

In multicellular organisms cell death is a crucial process during development, essential for maintaining tissue homeostasis and necessary for immune regulation and its dysregulation is associated with various pathologies [Duprez et al., 2009]. The different types of cell death can be defined by morphological, enzymological (depending on the involved classes of proteases), functional (programmed or accidental) or on immunological aspects (immunogenic or non-immunogenic) [Galluzzi et al., 2007]. Particularly apoptosis represents the major type of programmed cell death.

3.2.3.1 Apoptosis

Apoptosis is a cell-intrinsic programmed suicide and is associated with typical morphological alterations like cell shrinkage, membrane blebbing and chromatin condensation [Duprez et al., 2009]. Apoptotic cell death is immunologically silent without provoking an inflammation because the apoptotic vesicles are recognized and, before losing membrane integrity, taken up by surrounding cells [Krysko and Vandenabeele, 2008].

Cysteinyl aspartate-specific proteases (caspases) have been shown to be crucial for mediating the execution phase of apoptosis [Fuentes-Prior and Salvesen, 2007]. The apoptotic caspases in humans can be divided into initiator (caspase 8, 9, 10) and

executioner (caspase 3, 6, 7) caspases and are expressed as inactive proenzymes. In mammalian cells they can be activated by two different pathways, the intrinsic and the extrinsic pathway.

Different stimuli, like DNA damage or cytotoxic insults, activate the intrinsic pathway that is controlled by the Bcl-2 family of proteins and acts through the mitochondria [Youle and Strasser, 2008]. In case of a DNA damage Bcl-2-homology 3 (BH3)-only proteins are activated and antagonize the anti-apoptotic Bcl-2 family members (Bcl-2, Bcl-x), that prevent the pro-apoptotic family Bcl-2 members Bax and Bak from collapse of the mitochondrial membrane potential Upon activation Bax and Bak, which control mitochondrial membrane pores, allow the release of cytochrome c (Cyt c). This forms a complex with Apaf 1 and recruits procaspase-9 finally resulting in its activation and this furtheron leads to cleavage of the executioner caspases-3, -6 and -7.

The extrinsic pathway is activated upon stimulation of death receptors belonging to the tumor necrosis factor receptor (TNFR) family [Wilson et al., 2009]. Stimulation of these receptors leads to the formation of a death-inducing signaling complex (DISC). Recruitment and activation of the initiator caspases-8 and -10 lead to cleavage of the downstream executioner caspases. Additionally, the BH3-only protein Bid, activated by caspase 8, amplifies the death receptor induced cell death program by activating also the mitochondrial pathway.

3.2.3.2 Necrotic cell death

Necrosis has been considered for a long time as an uncontrolled form of cell death without underlying signaling events and this might be true for severe physical damage such as massive hyperthermia, but there is accumulating evidence for the existence of strictly regulated caspase independent pathways [Chautan et al., 1999]. However, in contrast to apoptosis, necrotic cell death is accompanied with cytoplasmic and organelle swelling and loss of cell membrane integrity resulting in the release of cellular contents into the surrounding extracellular space [Duprez et al., 2009].

Stimulation of death receptors like TNFR1 was shown to activate RIP1 that, after formation of a complex with RIP3, induces a wide range of necrotic mediators [Festjens et al., 2007]. Besides death receptors, pathogen recognition receptors have been shown to mediate necrosis in a RIP1 dependent fashion [Kalai et al., 2002], as well as hyperactivation of poly-(ADP-ribose) polymerase-1 (PARP-1) hyperactivation after extensive DNA damage [Jagtap and Szabo, 2005]. Among others, reactive oxygen

species (ROS), calcium, calpains and phospholipases are important mediators involved in the execution phase of necrotic cell death leading to destabilization of the plasma membrane, mitochondrial permeability and matrix swelling [Vanlangenakker et al., 2008). These phenomena seem to be events resulting from severe cellular disregulations however, which are the result of exploited ATP pools unable to be replenished in time [Nicotera et al. 2001, Tsujimoto 2001, Grusch et al. 2002].

3.2.4 Metastasis – the leading cause for cancer deaths

As about 90% of all cancer deaths are not related to the primary tumor but to metastases that destroy the function of infested organs, prevention of cancer cell dissemination and secondary tumor formation is a major goal of cancer therapy [Sporn, 1996]. Metastasis is a multi-step process existing of a sequence of discrete steps [Eger and Mikulits, 2005]:

- local infiltration of tumor cells into the adjacent tissue
- transendothelial migration of cancer cells into vessels (intravasation)
- transit and survival in the circulatory system
- extravasation
- subsequent proliferation leading to colonization

As less than 0.1% of disseminated cancer cells develop distal metastases, this process is very inefficient [Mack and Marshall, 2010]. There is an ongoing dicussion whether metastatic dissemination is one of the later steps of tumorigenesis or occurs already at the beginning of tumor development and there is evidence for both models [Klein, 2009], but distinct genetic alterations of tumor cells at primary and distal sites argue for an early separation and independent development [van Zijl et al., 2011]. Besides the question about the time point of cancer cell dissemination, it also remains unclear where they develop the ability to colonize foreign tissues and two different models are discussed [Hanahan and Weinberg, 2011]. One the one hand side the capability to colonize may a fortuitous property as a result of a tumor's particular developmental path prior dissemination. In contrast, response to the selective pressure of and adaption to the

foreign microenvironment might induce that ability. However, it was shown that the bone, the lung and the brain represent the major sites of metastasis of breast carcinoma, while colorectal and pancreatic cancer prefers the liver and the lung for distal colonization [Chambers et al., 2002].

Although metastasis is a multistep process, physical dissemination of cancer cells to distant tissues and thereafter the adaption of these cells to foreign microenvironment resulting in successful colonization represent the two major phases [Hanahan and Weinberg, 2011]. The fact, that many patients develop lots of dormant micrometastases, demonstrates that successful colonization is not strictly coupled with physical dissemination [McGowan et al., 2009]. While explosive metastatic growth of dormant micrometastases after resection of the primary tumor substantiate the release of systemic suppressor factors by the primary tumor [Demicheli et al., 2008], other metastases take up to decades to develop macroscopic tumors after surgical removal or destruction of the primary tumor indicating that these micrometastases have solved the complex problem of tissue colonization [Barkan et al., 2010]. Adaption of disseminated cancer cells to the microenvironment, where they have landed, is complex procedure and each disseminated cell has to develop its own solutions to be successful in colonization depending on the cancer cell itself and the new tissue environment. [Gupta et al., 2005]. However, cell invasion and transmigration into blood and lymphatic vessels are the first steps in metastasis and knowledge about the biological mechanisms is essential to find treatment options to inhibit these processes.

3.2.4.1 Mechanisms of cell invasion

Cancer cells can invade other tissues as single cells via mesenchymal or amoeboid cell types or by moving collectively as detached clusters [Friedl and Wolf, 2003]. Tumor cells often experience a change in their plasticity by morphological and phenotypical conversions (epithelial to mesenchymal transition (EMT), collective to amoeboid transition (CAT), mesenchymal to amoeboid transition (MAT)) [van Zilj et al., 2011].

Mesenchymal cell invasion

EMT represents a crucial event in cancer progression and metastasis. This highly conserved process is regulated by different transcriptional factors (e.g. Zeb1/2) and

leads to down-regulation of epithelial and up-regulation of mesenchymal markers [Schmalhofer et al., 2009].

The best characterized alteration of EMT is the change from E- to N-cadherin, termed cadherin switch [Christofori, 2006]. Down-regulation of E-cadherin, an essential component of adherence junctions, and expression of N-cadherin, responsible for rearrangement of the cytoskeleton, leads to enhanced motility of the cancer cells. Furthermore, EMT also exhibits stem cell properties, prevents apoptosis and senescence, suppresses immune reactions and shows resistance against radio- and chemotherapy [Thiery et al., 2009]. Different factors, such as integrins, fibroblast growth factor (FGF), vascular endothelial growth factor (VEGF), platelet derived growth factor (PDGF) or transforming growth factor (TGF)-β have been demonstrated to induce EMT [Thiery et al., 2009]. To form new tumor colonies at a secondary site, cancer cells that have undergone EMT during invasion and dissemination may pass through the reverse process, referred to as mesenchymal to epithelial transition [Hugo et al., 2007].

Amoeboid cell invasion

Cells undergoing CAT show reduced cell-ECM interaction and the ability of chemotaxis and these amoeboid cells are able to squeeze through gaps in the ECM barriers [Condeelis and Segall, 2003]. Motility of these amoeboid cells, in contrast to mesenchymal and collective cell invasion, is not protease dependent without remodeling the ECM and this kind of invasion is described as the fastest migratory phenotype [Friedl and Wolf, 2003]. In melanoma cells integrin blockage was shown to cause CAT resulting in the loss of cell-cell adhesion, cell detachment and transition to an amoeboid single-cell type [Hegerfeldt et al., 2002].

Collective cell invasion

Collective cell invasion can occur either as a two dimensional monolayer or as a three dimensional cell strand or cluster. However, this type of invasion is characterized by three properties: intact cell-cell junctions; remodeling of the ECM and rearrangement of the basement membrane; traction force generation by multi-cellular coordination of polarity and cytoskeletal activity [van Zijl et al., 2011]. While most collectively invading cells maintain their intact epithelial cell to cell contacts, tip cells exhibit a rather mesenchymal phenotype and these leading cells are also mostly responsible for

remodeling the ECM (e.g. by secretion of MMP14) and the generation of traction force by e.g. expression of different substrate binding integrins [Friedl and Gilmour, 2009].

3.2.4.2 Endothelial transmigration

Besides the blood system, the lymphatic system has been shown to be a key player in cancer cell dissemination [Kerjaschki et al., 2004]. There is still discussion whether invasion of cancer cells into the lymphatic system is a passive occurrence or promoted by lymphnodes [Tammela and Alitalo, 2010]. However, recently it could be shown that breast cancer spheroids are able to generate circular defects in the integrity of a lymphatic endothelial cell (LEC) layer resulting in the penetration into lymphatic vessels of cancer cells through these ruptures mediated by 12(S)-hydroxy-eicosatetraenoic acid (12(S)-HETE) metabolized from arachidonic acid by the hypoxia-inducible enzymes ALOX12 or ALOX15 [Madlener et al., 2010; Kerjaschki et al., 2011]. Furthermore, the NF-κB pathway was elucidated as a second signal cascade mediating the intravasation, by inhibiting the NF-κB translocation with Bay11-7082 and subsequent blockage of the MCF-7 spheroid induced gap formation of LECs [Vonach et al., 2011].

3.2.5 The tumor microenvironment

In contrast to the historical reductionist view that a tumor is just a collection of relatively homogeneous cancer cells, there is increasing evidence for heterotypic interactions of cancer cells with cells of the adjacent tumor associated stroma inducing the expression of more malignant phenotypes and that this crosstalk is involved in the acquired capability for invasive growth and metastasis [Karnoub and Weinberg, 2006-2007; Egeblad et al., 2010]. This tumor associated microenvironment is composed of various different cell types including endothelial cells, pericytes, stromal fibroblasts, stem cells and bone marrow derived cells such as macrophages [van Zijl et al., 2011; Hanahan and Weinberg, 2011]. Cancer stem cells (CSC) seem to be a common constituent in many tumors and are defined through their ability to seed new tumors upon inoculation into recipient host mice [Cho and Clark, 2008]. Besides correlation of

the acquisition of CSCs and the EMT transdifferentiation program, CSCs are more resistant to various commonly used chemotherapeutic treatments [Singh and Settleman 2010]. Whereas endothelial cells are necessary to for the tumor associated vasculature, other cell types like cancer associated fibroblasts or tumor associated macrophages promote tumor progression mainly by allocating growth factors, cytokines and matrix degrading enzymes thereby promoting tumor growth, cancer cell invasion and neoangiogenesis [Joyce and Pollard, 2009].

3.3 Pancreatic cancer

Pancreatic cancer is the tenth most common type of cancer in western countries and ranks fourth in cancer mortality statistics and in spite of intensive research there is only little improvement in the survival of pancreatic cancer patients [Mihaljevic et al., 2010, Fahrig et al. 2006, Heinrich et al. 2011]. At the time of diagnosis around 15% of patients have tumors localized in pancreas, 40% have locally advanced cancer with tumors in adjacent organs and nearly 50% already show rapidly progressing aggressive metastatic pancreatic cancer [Borja-Cacho et al., 2008]. Because of the lack of early detection, the absence of symptoms and effective screening tests, high rate of relapse and limited effective therapies, prognosis is very poor with a 5 year survival rate of less than 5% and a 1 year survival rate of less than 20% [Evans et al., 2001]. Age, cigarette smoking, family history and diabetes mellitus have been elucidated as risk factors for pancreatic cancer [Michaud, 2004]. According to the origin of the tumor, there are two types of pancreatic cancer. While endocrine pancreatic cancer, originating from the islet cells, accounts for only 2-4% of the incidence, more than 95% of pancreatic cancer originates in the exocrine pancreas and with more than 80% of this exocrine pancreatic cancer infiltrating ductal adenocarcinoma represents the most common form [Li et al., 2010].

3.3.1 Genetic profiles of pancreatic cancer

Caused by multiple genetic mutations accumulated over years pancreatic cancer is a genetic disease and the earliest recognizable defect is telomeres shortening leading to instability of chromosomes [van Heek et al., 2002]. Alterations of k-Ras, p53 and

SMAD4/DPC4 represent the most common mutations, simultaneously present in more than 75% of all pancreatic cancers [Rozenblum et al., 1997]. Mutations that activate the k-Ras oncogene were seen in more than 90% of pancreatic cancer [Radulovich et al., 2008] resulting in the activation of several downstream effector pathways such as the RAF mitogen activated protein kinase or the phosphoinositide-3-kinase [Maitra and Hruban, 2008]. Activation of these pathways plays a critical role in pancreatic canceroginesis and cell proliferation. Besides k-Ras mutations, inactivation of the p53 tumor suppressor gene, present in up to 75% of all pancreatic cancers, represents another widespread mutation allowing cells to proceed in division in the presence of damaged DNA, thereby leading to accumulation of additional genetic abnormalities [Li et al., 2010]. Amongst other actions, the tumor suppressor gene SMAD4/DPC4 is a mediator of the growth inhibitory effect of TGF-β and its inactivation is found in more than 50% of pancreatic cancers [Koliopanos et al. 2008].

In contrast to normal pancreatic tissues, constitutive NF-κB activity could be found in 70% of pancreatic adenocarcinomas [Chandler et al., 2004]. NF-κB can be activated by the k-Ras pathway leading to activation of multiple genes and pathways including anti apoptotic, cell survival, pro-invasive and angiogenic pathways [Mihaljevic et al., 2010]. Furthermore, pancreatic cancer expresses high levels of chemoresistance factors like mdr1 p-glycoprotein [Miller et al., 1996].

3.3.2 Treatment options

Due to metastasis into adjacent or distant organs more than 80% of these carcinomas are not resectable [Niederhuber et al., 1995] and therefore systemic chemotherapy plays an important role in the treatment of this extremely aggressive cancer with the goal to provide symptomatic relief and prolong survival. Besides 5-fluorouracil, gemcitabine was identified as the two main treatment options [Huguet et al., 2009] but in particular metastatic pancreatic cancer is highly chemoresistant and response rates of single agent therapies are less than 20% [Evans et al., 2001]. Although combinations with other chemotherapeutic agents like topoisomerase I inhibitors (irinotecan), platinums or taxanes improved response rate and progression free survival, there was no longer overall survival [Li et al., 2010]. Because of this lack of effective therapy, research for new capable treatment options represents an important challenge.

3.4 Heat shock proteins

Heat shock proteins (Hsps) represent a highly conserved set of proteins that have a pivotal role in cell cycle progression and cell death (apoptosis) as well as in maintaining cellular homeostasis under stress [Khalil et al., 2011]. Various insults like hypoxia, ischemia, exposure to UV light or chemicals, nutritional deficiencies or other stress rapidly induce their expression [Cotto and Morimoto, 1999; Lindquist and Craig, 1998]. According to their size, mammalian Hsps have been classified into 6 families: Hsp100, Hsp90, Hsp70, Hsp60, Hsp40 and small Hsps (including Hsp27). While high weight Hsps act in an ATP dependent fashion, small Hsps are ATP independent [Khalil et al., 2011]. Due to their function to accompany unfolded proteins during their cellular transport under normal conditions and to help to protect these proteins when subjected to stresses, Hsps are known as molecular chaperones [Kopecek et al., 2001]. These chaperones never work alone but form oligomers and are helped by different co-chaperones such as HSC70 interacting protein (Hip) or Hsp organizing protein (Hop) [Khalil et al., 2011]. Besides their essential functions in the maintenance of normal cellular homeostasis, different Hsps were shown to be over-expressed in a broad range of neoplastic processes and it was shown that the Hsp-induced cytoprotection can be attributed partly to the suppression of apoptosis [Khalil et al., 2011].

3.4.1 Hsp90

Due to the chaotic architecture of the vasculature in solid tumors resulting in hypoxia and acidosis [Issels 2008] and exogenously applied factors, cancer cells have to handle extreme environmental stress and it is not surprising that molecular chaperones in general, and Hsp90 in particular, are highly expressed in most tumor cells [Neckers, 2007]. Hsp90 over-expression was shown among others e.g. for pancreatic, breast and lung cancer and for leukemia [Khalil et al., 2011].

Structure of Hsp90

Hsp90 chaperons contain 3 domains: an N-terminal ATP-binding domain, a middle domain (M-domain) and a C-terminal dimerization domain [Prodromou and Pearl, 2003]. There are two main isoforms of Hsp90, an inducible form (Hsp90α) and a constitutive form (Hsp90β) [Csermely et al., 1998].

Clients, role in cancer and function

The role of Hsp90 includes formation of the correct conformation and activation of a wide range of proteins and more than 200 proteins have been identified as Hsp90 clients [McClellan et al., 2007]. Among these clients, there are several proteins that play pivotal roles in acquisition and maintenance of the six hallmarks of cancer defined by Hanahan and Weinberg [2000] [Neckers 2007]. NF-κB, nuclear receptors (e.g. steroid receptors), protein kinases (e.g. Chk1, Akt, Wee1), Her2 neu, Bcr-Abl or the tumor suppressor protein p53 were for example shown to be Hsp90 clients [Müller et al., 2005; Bottoni et al. 2009; Tse et al., 2008; Fukuyo Y., 2009]. To accomplish its chaperon function, Hsp90 forms a dynamic complex known as the Hsp90 chaperone machinery with Hsp70 and different co-chaperones. [Pratt and Toft, 2003], thereby, besides regulating proteins essential for constitutive cell signaling adaptive stress responses, also protecting mutated and over-expressed oncogenes [Trepel et al., 2010]. Inhibition of Hsp90 by geldanamycin was shown to induce a compensatory induction of other Hsps, in particular Hsp70 and different studies clearly correlate the level of Hsp70 over-expression with therapeutic resistance [Bottoni et al., 2009; Khalil et al., 2011].

Besides geldanamycin, the most prominent inhibitor of Hsp90 binding to the N-terminal ATP-binding pocket [Fukuyu et al., 2010], there are several known Hsp90 inhibitors with potent antitumor-activity in a wide range of malignancies [Taldone et al., 2008] and there are now 14 drug candidates targeting Hsp90 in different clinical trials in multiple indications as single agents or as part of a combination therapy [Khalil et al., 2011].

4 REFERENCES

Adams J.M. and Cory S. The Bcl-2 apoptotic switch in cancer development and therapy. *Oncogene* 26: 1324-1337, **2007.**

Alderton G.K., Galbiati L., Griffith E., Surinya K.H., Neitzel H., Jackson A.P., Jeggo P.A. and O'Driscoll M. Regulation of mitotic entry by microcephalin and its overlap with ATR signaling. *Nature Cell Biol.* 8: 725-733, **2006.**

Artandi S.E. and DePinho R.A. Telomeres and telomerase in cancer. *Carcinogenesis* 31: 9-18, **2010.**

Ashkenazi A. and Dixit V.M. Apoptosis control by death and decoy receptors. *Curr. Opin. Cell Biol.* 11: 255-260, **1999.**

Baeriswyl V. and Christofori G. The angiogenic switch in carcinogenesis. *Semin. Cancer Biol.* 19: 329-337, **2009.**

Barkan D., Green J.E. and Chambers A.F. Extracellular matrix: a gatekeeper in the transition from dormancy to metastatic growth. *Eur. J. Cancer* 46: 1181-1188, **2010.**

Bartek J. and Lukas J. Chk1 and Chk2 kinases in checkpoint control and cancer. *Cancer Cell* 3: 421-429, **2003.**

Berdasco M. and Esteller M. Aberrant epigenetic landscape in cancer: How cellular identity goes awry. *Dev. Cell* 19: 698-711, **2010.**

Bishop J.M. and Weinberg R.A. eds. Molecular Oncology. *New York: Scientific American Inc.*, **1996.**

Blasco M.A. Telomeres and human disease: ageing, cancer and beyond. *Nat. Rev. Genet.* 6: 611-622, **2005.**

Borja-Cacho D., Jensen E.H., Saluja A.K., Buchsbaum D.J. and Vickers S.M. Molecular targeted therapies for pancreatic cancer. *Am J Surg.* 196: 430-441, **2008.**

Bortner D.M. and Rosenberg M.P. Induction of mammary gland hyperplasia and carcinomas in transgenic mice expressing human cyclin E. Mol. *Cell Biol.* 17: 453-459, **1997.**

Bottoni P., Girdina B. and Scatena R. Proteomic profiling of heat shock proteins: an emerging molecular approach with direct pathophysiological and clinical implications. *Proteomics Cli Appl*. 3: 636-653, **2009.**

Boutros R., Lobjois V. and Ducommun B. Cdc25 phosphatases in cancer cells: Key players? Good targets? *Nat Rev Cancer* 7: 495-507, **2007.**

Busino L., Chiesa, M. Draetta G.F. and Donzelli M. Cdc25A phosphatase: combinatorial phosphorylation, ubiquitylation and proteolysis. *Oncogene* 23: 2050-2056, **2004.**

Cangi M.G., Cukor B., Soung P., Signoretti S., Moreira G., Ranashinge M., Cady B., Pagano M. and Loda M. Role of Cdc25A phosphatase in human breast cancer. *J. Clin. Invest.* 106: 753-761, **2000.**

Chambers A.F., Groom A.C. and MacDonald I.C. Dissemination and growth of cancer cells in metastatic sites. *Nat. Rev. Cancer* 2: 563-572, **2002.**

Chandler N.M., Canete J.J. and Callery M.P. Increased expression on NF-kappa B subunits in human pancreatic cancer cells. *J Surg Res.* 118: 9-14, **2004.**

Chautan M., Chazal G., Cecconi F., Gruss P. and Golstein P. Interdigital cell death can occur through a necrotic and caspase independent pathway. *Curr. Biol.* 9: 967-970, **1999.**

Cheng N., Chytil A., Shyr Y., Joly A. and Moses H.L. Transforming growth factor beta signaling-deficient fibroblasts enhance hepatocyte growth factor signaling in mammary

carcinoma cells to promote scattering and invasion. *Mol. Cancer Res.* 6: 1521-1533, **2008.**

Cho R.W. and Clark M.F. Recent advances in cancer stem cells. *Curr. Opin. Genetic. Dev.* 18: 1-6, **2008.**

Christofori G. New signals from the invasive front. *Nature* 441: 444-450, **2006.**

Condeelis J. and Segall J.E. Intravital imaging of cell movement in tumours. *Nat. Rev. Cancer* 3: 921-930, **2003.**

Cotto J.J. and Morimoto R.I. Stress induced activation of the heat shock response: cell and molecular biology of heat shock factors. *Biochem. Soc. Symp.* 64: 105-118, **1999.**

Counter C.M., Avilion A.A., LeFevre C.E., Stewart N.., Greider C.W., Harley C.B. and Becchetti S. Telomere shortening associated with chromosome instability is arrested in immortal cells which express telomerase activity. *EMBO J.* 11: 1921-1929, **1992.**

Csermely P., Schnaider T., Soti C., Prohaszka Z. and Nardai G. The 90-kDa molecular chaperone family: structure, function and clinical applications. A comprehensive review. *Pharmacol. Ther.* 79: 129-168, **1998.**

Demicheli R., Retsky M.W., Hrushesky W.J., Baum M. and Gukas I.D. The effects of surgery on tumor growth: a century of investigations. *Ann. Oncol.* 19: 1821-1828, **2008.**

DeNardo D.G., Andreu P. and Coussens L.M. Interactions between lymphocytes and myeloid cells regulate pro- versus anti-tumor immunity. *Cancer Metastasis Rev.* 29: 309-316, **2010.**

DiFiore P.P., Pierce J.H., Kraus M.H., Segatto O., King C.R. and Aaronson S.A. erbB-2 is a potent oncogene when overexpressed in NIH/3T3 cells. *Science* 237: 178-182, **1987.**

Duprez L., Wirawan E., Berghe T.V. and Vandenabeele P. Major cell death pathways at a glance. *Microbes and Infection* 11: 1050-1062, **2009.**

Egeblad M., Nakasone E.S. and Werb Z. Tumors as organs: complex tissues that interface with entire organism. *Dev. Cell* 18: 884-901, **2010.**

Eger A. and Mikulits W. Models of epithelial-mesenchymal transition. *Drug Disc. Today: Dis. Models* 2: 57-63, **2005.**

El-Deiry W.S., Harper J.W., O'Connor P.M., Velculescu V.E., Canman C.E., Jackman J., Pietenpol J.A., Burrell M., Hill D.E., Wang Y., Wiman K.G., Mercer W.E., Kastan M.B., Kohn K.W., Elledge S.J., Kinzler K.W. and Vogelstein B. WAF1/CIP1 is induced in p53-mediated G1 arrest and apoptosis. *Cancer Res.* 54: 1169-1174, **1994.**

Elledge S.J. Cell cycle checkpoints: preventing an identity crisis. *Science* 274: 1664-1672, **1996.**

Evans D.B., Abbruzzese J.L. and Willett C.G. Cancer of the pancreas. In: DeVita V.T., Hellman S., and Rosenberg S.A., editors. Cancer: principles & practice of oncology. Philadelphia: Lipincott: 1126-1161, **2001.**

Evan G. And Littlewood T. A matter of life and cell death. *Science* 281: 1317-1322, **1998.**

Fahrig R., Quietzsch D., Heinrich J.C., Heinemann V., Boeck S., Schmid R.M., Praha C., Liebert A., Sonntag D., Krupitza G. and Hänel M. RP101 improves the efficacy of chemotherapy in pancreas carcinoma cell lines and pancreatic cancer patients. *Anticancer Drugs* 17: 1045-56, **2006.**

Falck J. Petrini J.H., Williams B.R., Lukas J. and Bartek J. The DNA damage-dependent intra-S phase checkpoint is regulated by parallel pathways. *Nat. Genet.* 30: 290-294, **2002.**

Fedi P., Tronick S.R. and Aaronson S.A. Growth factors. In Cancer Medicine. Holland J.F., Bast R.C., Morton D.L., Frei E., Kufe D.W. and Weichselbaum R.R. eds., *Baltimore, D: Williams ans Wilkins*, 41-64, **1997.**

Ferrara N. Vascular endothelial growth factor. *Arterioscler. Thromb. Vasc. Biol.* 29: 789-791, **2009.**

Festjens N., Vanden Berghe T., Cornelis S. and Vandenabeele P. RIP1, a kinase of the crossroads of a cell's decision to live or die. *Cell Death Differ.* 14: 400-410, **2007.**

Fidler I.J. The pathogenesis of cancer metastasis: the "seed and soil" hypothesis revisited. *Nat. Rev. Cancer* 3: 453-458, **2003.**

Friedl P. and Gilmour D. Collective cell migration in morphogenesis, regeneration and cancer. *Nat. Rev. Mol. Cell Biol.* 10: 445-457, **2009.**

Friedl P. and Wolf K. Tumour cell invasion and migration: diversity and escape mechanisms. *Nat. Rev. Cancer* 3: 362-374, **2003.**

Fuentes-Prior P. and Salvesen G.S. The protein structures that shape caspase activity, specificity, activation and inhibition. *Biochem. J.* 384: 201-232, **2004.**

Fukuyo Y, Clayton R.H. and Horikoshi N. Geldanamycin and its anti-cancer activities *Cancer Letters* 290: 24-35, **2010.**

Galaktionov K., Chen X.C. and Beach D. Cdc25 cell-cycle phosphatase as a target of c-myc. *Nature* 382: 511-517, **1996.**

Galluzzi L., Maiuri M.C., Vitale I., Zischka H., Castedo M., Zitvogel L. and Kroemer G. Cell death modalities: classification and pathophysiological implications. *Cell Death Differ.* 14: 1237-1243, **2007.**

Gasparotto D. Maestro R., Piccinin S., Vukosavljevic T., Barzan L., Sulfaro S. and Boiocchi M. Overexpression of Cdc25A and Cdc25B in head and neck cancers. *Cancer Res.* 57: 2366-2368, **1997.**

Ghebranious N. and Donehower L.A. Mouse models in tumor suppresssion. *Oncogene* 17: 3385-3400, **1998.**

Giancotti F.G. and Ruoslahti E. Integrin signaling. *Science* 285: 1028-1032, **1999.**

Goloudina A., Yamaguchi H., Chervyakova D.B., Appella E., Fornace A.J. Jr. and Bulavin D.V. Regulation of the human Cdc25A stability by serine 75 phosphorylation is not sufficient to activate a A-phase checkpoint. *Cell Cycle* 2: 473-478, **2003.**

Grana X. and Reddy E. P. Cell cyle control in mammalian cells: role of cyclins, cyclin-dependent kinases (CDKs), groth suppressor genes and cyclin-dependent kinase inibitors (CKIs). *Oncogene* 11: 211-219, **1995.**

Green D.R. and Reed J.C. Mitochondria and apoptosis, *Science* 281: 1309-1312, **1998.**

Grivennikov S.I., Greten F.R. and Karin M. Immunity, inflammation and cancer. *Cell* 140: 883-899, **2010.**

Grusch M., Polgar D., Gfatter S., Leuhuber K., Huettenbrenner S., Leisser C., Fuhrmann G., Kassie F., Steinkellner H, Smid K., Peters G.J., Jayaram H., Klepal T., Szekeres T., Knasmüller S. and Krupitza G. Maintainance of ATP favours apoptosis over necrosis triggered by benzamide riboside. *Cell Death Differ.* 9, 169-178. **2002.**

Gupta G.P., Minn A.J., Kang Y., Siegel P.M., Serganova I., Cordón-Cardo C., Olshen A.B., Gerald W.L.. and Massagué J. Identifying site-specific metastasis genes and functions. *Cold Spring Harb Symp. Qunat. Biol.* 70: 149-158, **2005.**

Hanahan D. and Folkman J. Patterns and emerging mechanisms of the angiogenic switch during tumorigenesis. *Cell* 86: 353-364, **1996.**

Hanahan D. and Weinberg R.A. The hallmarks of cancer. *Cell* 100: 57-70, **2000.**

Hanahan D. and Weinberg R.A. Hallmarks of cancer: The next generation. *Cell* 144: 646-674, **2011.**

Hansel D.E., Meeker A.K., Hicks J., De Marzo A.M., Lillemoe K.D., Schulick R., Hruban R.H., Maitra A. and Argani P. Telomere length variation in biliary tract metaplasia, dysplasia and carcinoma. *Mod. Pathol.* 19: 772-779, **2006.**

Harris C.C. p53 tumor suppressor gene: from the basic research laboratory to the clinic – an abridged historical perspective. *Carcinogenesis* 17: 1187-1198, **1996.**

Hartwell L.H. and Kastan M.B. Cell cycle control and cancer. *Science* 266: 1821-1828, **1994.**

Hartwell L.H. and Weinert T.A. Checkpoints: controls that ensure the order of cell cycle events. *Science* 246: 629-634, **1989.**

Hayflick L. Mortality and immortality at the cellular level. A review. *Biochemistry* 62: 1180-1190, **1997.**

Hegerfeldt Y., Tusch M., Brocker E.B. and Friedl P. Collective cell movement in pramry melanoma explants: plasticity of cell-cell interaction, beta1-integrin function and migration strategies. *Cancer Res.* 62: 2125-2130, **2002.**

Heinrich J.C., Tuukkanen A., Schroeder M., Fahrig T. and Fahrig R. RP101 (brivudine) binds to heat shock protein Hsp27 (HspB1) and enhances survival in animals and pancreatic cancer patients. *J Cancer Res Clin Oncol* 1371349-61, **2011.**

Hernández S., Bessa X., Beá S., Hernández L., Nadal A., Mallofré C. Muntane J., Castells A., Fernández P.L., Cardesa A. and Campo E. Differential expression of Cdc25 cell-cycle-activating phosphatases in human colorectal carcinoma. *Lab. Invest.* 81:465-473, **2001.**

Hornsby J. H. “Senescence as an anticancer mechanism”, *Journal of Clinical Oncology*, 25: 1852-1857, **2007.**

Hugo H., Ackland M.L., Blick T. Lawrence M.G., Clements J.A., Williams E.D. and Thompson E.W. Epithelial-mesenchymal and mesenchymal-epithelial transitions in carcinoma progression. *J. Cell. Physiol.* 213: 374-383, **2007.**

Huguet F. Girard N., Guerche C.S., Hennequin C., Mornex F. and Azria D. Chemoradiotherapy in the management of locally advanced pyncreatic carcinoma: a qualitative systematic review. *J Clin Oncol.* 27: 2269-2277, **2009.**

Hurley P.J. and Bunz F. ATM and ATR: components of an integrated circuit. *Cell Cycle* 6: 414-417, **2007.**

Issels R.D. Hyperthermia adds to chemotherapy. *Europ J of Cancer.* 44:2546-2554, **2008.**

Jagtap P. and Szabo C. Poly(ADP-ribose) polymerase and the therapeutic effects of its inhibitors. *Nat. Rev. Drug Disov.* 4: 421-440, **2005.**

Jemal A., Stiegel R., Xu J. and Ward E. Cancer statistics 2010. *Ca Cancer J Clin.* 60: 277-300, **2010.**

Joyce J.A. and Pollard J.W. Microenvironmental regulation of metastasis. *Nat. Rev. Cancer* 9: 239-252, **2009.**

Juntilla M.R. and Evan G.I. p53-a Jack of all trades but master of none. *Nat. Rev. Cancer* 9: 821-829, **2009.**

Kalai M., Van Loo G., Vanden Berghe T., Meeus A., Burm W., Saelens X. and Vandenabeele P. Tipping the balance between necrosis and apoptosis in human and murine cells treated with interferon and dsRNA. *Cell Death Differ.* 9: 981-994, **2002.**

Karlsson C., Katich S., Hagting A., Hoffmann I. and Pines J. Cdc25B and Cdc25C differ markedly in their properties as initiators of mitosis. *J. Cell Biol.* 146: 573-584, **1999.**

Karlsson-Rosenthal C. and Millar J.B.A. Cdc25: mechanisms of checkpoint inhibition and recovery. *Trends Cell. Biol.* 16: 285-292, **2006.**

Karnoub A.E. and Weinberg R.A. Chemokine networks and breast cancer metastasis. *Breast Dis.* 26: 75-85, **2006-2007.**

Kastan M.B. and Bartek J. Cell-cycle checkpoints and cancer. *Nature* 432: 316-323, **2004.**

Kerjaschki D., Regele H.M., Moosberger I., Nagy-Bojarski K., Watschinger B., Soleiman A., Birner P., Krieger S., Hovorka A., Silberhumer G., Laakkonen P., Petrova T., Langer B. and Raab I. Lymphatic neoangiogenesis in human kidney transplants is associated with immunologically active lymphocytic infiltrates. *J. Am. Soc. Nephrol.* 15: 603-612, **2004.**

Kerjaschki D., Bago-Horvath Z., Rudas M., Sexl V., Schneckenleithner C., Wolbank S., Bartel G., Krieger S., Kalt R., Hantusch B., Keller T., Nagy-Bojarsky K., Huttary N., Raab I., Lackner K., Krautgasser K., Schachner H., Kaserer K., Rezar S., Madlener S., Vonach C., Davidivits A., Nosaka H., Hämmerle M., Viola K., Dolznig H., Schreiber M., Nader A., Mikulits W., Gnant M., Hirakawa S., Detmar M., Alitalo K., Nijman S., Offner F., Maier T.J., Steinhilber D. and Krupitza G. Lipoxygenase mediates invasion of intrametastatic lymphatic vessels and propagates lymph node metastais of human mammary carcinoma xenografts in mouse. *J. Clin. Invest.* 121: 2000-2012, **2011.**

Kessenbrock K., Plaks V. and Werb Z. Matrix metalloproteinases: Regulators of the tumor microenvironment. *Cell* 141: 52-67, **2010.**

Khalil A.A., Kabapy N.F., Deraz S.F. and Smith C. Heat shock proteins in oncology: Diagnostic biomarkers or therapeutic targets? *Biochimica and Biophysica*, in press, **2011.**

Kinzler K.W. and Vogelstein B. Lessons from hereditary colorectal cancer. *Cell* 87: 159-170, **1996.**

Kiyokawa H. and Ray D. In vivo roles of Cdc25 phosphatases: Biological insight into the anti-cancer therapeutic targets. *Anticancer Agents Med Chem.* 8: 832-836, **2008.**

Klein C.A. Parallel progression of primary tumours and metastases. *Nat. Rev. Cancer* 9: 302-312, **2009.**

Koliopanos A. Avgerinos C. Paraskeva C. Touloumis Z., Kelgiorgi D. and Dervenis C. Molecular aspects of carcinogenesis in pancreatic cancer. *Hepatobiliary Pancreat Dis Int.* 7: 345-356, **2008.**

Kopecek P., Altmannova K. and Weigl E. Stress proteins: nomenclature, division and functions. *Biomed Papers* 145: 39-47, **2001.**

Kristjánsdóttir K. and Rudolph J. Cdc25 phosphatases and cancer. *Chem Biol* 11: 1043-1051, **2004.**

Krude T. Jackman M., Pines J. and Laskey R. Cyklin/Cdk-dependent initiation of DNA replication in a human cell-free system. *Cell* 88: 109-119, **1997.**

Kryosko D.V. and Vandenabeele P. From regulation og dying cell engulfment to development of anti-cancer therapy. *Cell Death Differ.* 15: 29-38, **2008.**

Kudo Y., Yasui W., Ue T., Yamamoto S., Yokozaki H., Nikai H. and Tahara E. Overexpression of cyclin-dependent kinase-activating Cdc25B phosphatase in human gastric carcinomas. *Jpn. J. Cancer Res.* 88: 947-952, **1997.**

Li J. Wientjes M.G. and Au J.L.S. Pancreatic Cancer: Pathobiology, treatment options and drug delivery. *The AAPS Journal* 12: 223-233, **2010.**

Lim D.S., Kim S.T., Xu B., Maser R.S., Lin J., Petrini J.H. and Kastan M.B. ATM phosphorylates p95/nbs1 in an S-phase checkpoint pathway. *Nature* 404: 613.617, **2000.**

Lindquest S. and Craig E.A. The heat-shock proteins. *Annu Rev Genet.* 22: 631-677, **1998.**

Löffler H., Syljuasen R.G., Bartkova J., Worm J., Lukas J. and Bartek J. Distinct modes of deregulation of the proto-oncogenic Cdc25A phosphatase in human breast cancer cell lines. *Oncogene* 22: 8063-8071, **2003.**

Lowe S.W., Cepero E. and Evan G. Intrinsic tumour suppression. *Nature* 432: 307-315, **2004.**

Lukashev M.E. and Werb Z. ECM signalling: orchestrating cell behaviour an misbehaviour. *Trends Cell Biol.* 8: 4337-441, **1998.**

Lüscher B. "Function and regulation of the transcription factors of the Myc/Max/Mad network", *Gene*, 277: 1-14, **2001.**

Mack G.S. and Marshall A. Lost in migration. *Nat. Biotechnol.* 28: 214-229, **2010.**

Madlener S., Rosner M., Krieger S., Giessrigl B., Gridling M., Vo T.P., Leisser C., Lackner A., Raab I., Grusch M., Hengstschläger M., Dolznig H. and Krupitza G. Short 42 degrees C heat shock induces phosphorylation and degradation of Cdc25A which depends on p38MAPK, Chk2 and 14.3.3. *Hum Mol Genet.* 18:1990-2000, **2009.**

Madlener S., Saiko P., Vonach C., Viola K., Huttary N., Stark N., Popescu R., Gridling M., Vo N.T., Herbacek I., Davidovits A., Giessrigl B., Venkateswarlu S., Geleff S., Jäger W., Grusch M., Kerjaschki D., Mikulits W., Golakoti T., Fritzer-Szekeres M., Szekeres T. and Krupitza G. Multifactorial anticancer effects of digalloyl-resveratrol encompass apoptosis, cell cycle arrest and inhibition of lymphendothelial gap formation in vitro. *Br. J. Cancer* 102: 1361-1370, **2010.**

Mailand N., Falck J., Lukas C., Syljuansen R., Welcker M., Bartek J. and Lukas J. Rapid destruction of human Cdc25A in response to DNA damage. *Science* 288: 1425-1429, **2000.**

Maitra A. and Hruban R.H. Pancreatic cancer. *Annu Rev Pathol.* 3: 157-188, **2008.**

Mantovani A. and Sica A. Macrophages, innate immunity and cancer: balance, tolerance and diversity. *Curr. Opin. Immunol.* 22: 231-237, **2010.**

McClellan A.J., Xia Y., Deutschbauer A.M., Davis R.W., Gerstein M. and Frydman J. Diverse cellular functions of the Hsp90 molecular chaperone uncovered using systems approaches. *Cell* 131: 121-135, **2007.**

McDonald E.R. and El-Deiry W.S. Cell cycle control as a basis for cancer drug development. *Int J. Oncol.* 16: 871-886, **2000.**

McGowan P.M., Kirstein J.M. and Chambers A.F. Micrometastatic disease and metastatic outgrowth: clinical issues and experimental approaches. *Future Oncol.* 5: 1083-1098, **2009.**

Medema R.H. and Bos J.L. The role of p21-ras in receptor tyrosine kinase signaling. *Crit. Rev. Oncog.* 4: 615-661, **1993.**

Meeran S.M. and Katiyar S.K. Cell cycle control as a basis for cancer chemoprevention through dietary agents. *Front. Biosci.* 13: 2191-2202, **2008.**

Michalides R.J. Cell cycle regulators: mechanisms and their role in aetiology, prognosis and treatment of cancer. *J. Clin. Patol.* 52: 555-568, **1999.**

Michaud D.S. Epidemiology of pancreatic cancer. *Minerva Chir.* 59: 99-111, **2004.**

Mihaljevic A.L., Michalski C.W., Firess H. and Kleeff J. Molecular mechanisms of pancreatic cancer – understanding proliferation, invasion and metastasis. *Langenbecks Arch Surg* 395: 295-308, **2010.**

Miller D., Fontain M., Kolar C. and Lawson T. The expression of multidrug resistance associated protein (MRP) in pancreatic adenocarcinoma cell lines. *Cancer Let.* 107: 301-306, **1996.**

Morgan D.O. Principles of CDK regulation. *Nature* 374: 131-134, **1995.**

Müller P., Cekova P. and Vojtesek B. Hsp90 iss essential for restoring cellular functions of temperature sensitive p53 mutant protein but not for stabilization and activation of wild type p53: implications for cancer therapy. *J. Biol. Chem.* 280: 6682-6691, **2005.**

Nagy J.A., Chang S.H., Shih S.C., Dvorak A.M and Dvorak H.F. Heterogeneity of the tumor vasculature. *Semin. Thromb. Hermost.* 36: 321-331, **2010.**

Nardai G., Vegh E.M., Prohaszka Z. and Csermely P. Chaperone related immune dysfunction: an emergent property of distorted chaperone networks. *Trend Immunol.* 27: 74-79, **2006.**

Neckers L. Heat shock protein 90: the cancer chaperone. *J. Biosci.* 32: 517-530, **2007.**

Negrini S., Gorgoulis V.G. and Halazonetis T.D. Genomic instability – an evolving hallmark of cancer. *Nat. Rev. Mol. Cell Biol.* 11: 220-228, **2010.**

Nicotera P. and Leist M. Energy supply and the shape of death in neurons and lymphoid cells. *Cell Death Diff.*4: 435-442, **1997.**

Niederhuber J.E., Brennan M.F. and Menck H.R. The national cancer data base report on pancreatic cancer. *Cancer* 76: 1671-1677, **1995.**

Nilda H. and Nakanishi M. DNA damage checkpoints in mammals. *Mutagenesis* 21: 3-9, **2006.**

Nilsson I. and Hoffmann I. Cell cycle regulation by the Cdc25 phosphatase family. *Prog. Cell Cycle Res.* 4: 107-114, **2000.**

Norbury C. and Nurse P. Animal cell cycles and their control. *Ann. Rev. Biochem.* 61: 441-470, ***1992.***

Nyberg K.A., Michelson R.J., Putnam C.W. and Weinert T.A. Toward maintaining the genome: DNA damage and replication checkpoints. *Annu. Rev. Genet.* 36: 617-656, **2002.**

Polager S. and Ginsberg G. "p53 and E2f: partners in life and death", *Nature Reviews Cancer*, 9: 738-748, **2009.**

Porter D.Z., Zhang N., Danes C., McGahren M.J., Harwell R.M., Faruk S. and Keyomarsi K. Tumor specific proteolytic processing of cyclin E generates hyperactive lower molecule weight forms. *Mol. Cell Biol.* 21: 6254-6269, **2001.**

Pratt W.B. and Toft D.O. Regulation of signalling protein function and trafficking by the hsp90/hsp70 based chaperone machinery. *Exp. Biol. Med. (Maywood)* 228: 111-133, **2003.**

Prodromou C. and Pearl L.H. Structure and functional relationships of Hsp90. *Curr. Cancer Drug Targets* 3: 301-323, **2003.**

Radulovich N., Qian J.Y. and Tsao M.S. Human pancreatic duct epithelial cell model for KRAS transformation. *Methods Enzymol.* 439: 1-13, **2008.**

Raica M., Cimpean A.M. and Ribatti D. Angiogenesis in pre-malignant conditions. *Eur. J. Cancer* 45: 1924-1934, **2009.**

Ray D. and Kiyokawa H. Cdc25A Phosphatase: a rate limiting oncogene that determines genomic stability. *Cancer Res.* 68: 1251-1253, **2008.**

Robles A.I., Rodriguez-Puebla A.L., Glick A.B., Trempus C., Hansen L., Sicinski P., Tennant R.W., Weinberg R.A., Yuspa S.H. and Conti C.J. Reduced skin tumor development in cyclin D1-deficient mice highlights the oncogenic ras pathway in vivo. *Genes Dev.* 12: 2469-2474, **1998.**

Rozenblum E., Schutte M., Goggins M., Hahn S.A., Panzer S., Zahurak M., Goodman S.N., Sohn T.A., Hruban R.H., Yeo C.J. and Kern S.E. Tumor suppressive pathways in pancreatic carcinoma. *Cancer Res.* 57: 1731-1734, **1997.**

Rudolph J. Cdc25 phosphatases: Structure, Specificity and Mechanism. *Biochemistry* 46: 3595-3604, **2007.**

Sexl V., Diehl J.A., Sherr C.J., Ashmun R., Beach D. and Roussel M.F. A rate limiting function of cdc25A for S phase entry inversely correlates with tyrosine dephosphorylation of Cdk2. *Oncogene* 18: 573-82, **1999.**

Schmalhofer O., Brabletz S. and Brabletz T. E-cadherin, beta-catenin and ZEB1 in malignant progression of cancer. *Cancer Metastasis Rev.* 28: 151-166, **2009.**

Singh A. and Settleman J. EMT, cancer stem cells and drug resistance: an emerging axis of evil in the war on cancer. *Oncogene* 29: 4741-4751, **2010.**

Sherr C. Cancer cell cycles. *Science* 274: 1672-1677, **1996.**

Sporn M.B. The war on cancer. *Lancet* 347: 1377-1381, **1996.**

Sui L., Dong Y. Ohno M., Sugimoto K., Tai Y., Hando T. and Tokuda M. Implication of malignancy and prognosis of p27(kip1), cyclin E and Cdk2 expression in epithelial ovarian tumors. *Gynecol. Oncol.* 83: 56-63, **2001.**

Taldone T., Gozman A., Maharaj R. and Chiosis G. Targeting Hsp90: small molecule inhibitors and their clinicall development. *Curr. Opin. Pharmacol.* 8: 370-374, **2008.**

Tammela T. and Alitalo K. Lymphangiogenesis: molecular mechanisms and future promise. *Cell* 140: 460-476, **2010.**

Taylor W.R. and Stark G.R. Regulation of G2/M transition by p53. *Oncogene* 20: 1803-1815, **2001.**

Thiery J.P., Acloque H., Huang R.Y. and Nieto M.A. Epithelial-mesenchmal transitions in development and disease. *Cell* 139: 871-890, **2009.**

Thornberry N.A. and Lazebnik Y. Caspases: enemies within. *Science* 281: 1312-1316, **1998.**

Trepel J., Mollapour M., Giaccone G. and Neckers L. Targeting the dynamic Hsp90 complex in cancer. *Nature Reviews Cancer* 10: 537-549, **2010.**

Tse A.N., Sheikh T.N., Alan H., Chou T.C. and Schwartz G.K. 90-kDa heat shock protein inhibition abrogates the topoisomerase I poison induced G2/M checkpoint in p53-null tumor cells by depleting Chk1 and Wee1. *Mol. Pharmacol.* 75: 124-133, **2009.**

Tsujimoto Y. Apoptosis and necrosis: Intracellular ATP level as a determinant for cell death modes. *Cell Death Diff.* 4: 429-434, **1997.**

van den Heuvel S. Cell-cycle regulation. *Wormbook.* Sep 21, 1-16, **2005.**

van Heek N.T., Meeker A.K., Kern S.E., Yeo C.J., Lillemoe K.D., Cameron J.L., Offerhaus G.J., Hicks J.L., Wilentz R.E., Goggins M.G., De Marzo A.M., Hruban R.H. and Maitra A. Telomere shortening is nearly universal in pancreatic intraepithelial neoplasia. *Am J. Pathol.* 161: 1541-1547, **2002.**

van Zijl F., Krupitza G. and Mikulits W. Initial Stepps of metastasis: Cell invasion and endothelial transmigration. *Mutation Research* 728: 23-34, **2011.**

Vanlangenakker N., Berghe T.V., Krysko D.V., Festjens N. and Vandenabeele P. Molecular mechanisms and pathophysiology of necrotic cell death. *Curr. Mol. Med* 8: 207-220, **2008.**

Wahl G.M. and Carr A.M. The evaluation of diverse biological response to DNA damage: insights from yeast and p53. *Nature Cell Biol.* 3: E277-E286, 2**001.**

Wilson N.S., Dixit V. and Ashkenazi A. Death receptor signal transducers: nodes of coordination in immune signaling networks. *Nat. Immunol.*10: 348-355, **2009.**

Wright W.E., Pereira-Smith O.M. and Shay J.W. Reversible cellular senescence: implications for immortalization of normal human diploid fibroblaasts. *Mol. Cell Biol.* 9: 3088-3092, **1989.**

Wu W., Fan Y.H., Kemo B.L., Walsh G. and Mao.L. Overexpression of Cdc25a and Cdc25B is frequent in primary non-small cell lung cancer but is not associated with overexpression of c-myc. *Cancer Res.* 58, 4082-4085, **1998.**

Youle R.J. and Strasser A. The BCL-2 protein family: opposing activities that mediate cell death. *Nat. Rev. Mol. Cell Biol.* 9: 47-59, **2008.**

Zvereva M. I., Shcherbakova D. M. and Dontsova O. A. Telomerase: structure, functions, and activity regulation", *Biochemistry (Mosc)*, 75: 1563-83, **2010.**

5 AIMS OF THE THESIS

Cancer is a major public health problem in many countries and due to increasing expectancy of life this disease will be even more relevant in future. In the last decades there has been huge progress in early detection and the development of target specific powerful therapies resulting in distinct increased surviving rates for lots of cancers. However, intrinsic and acquired resistance is a major problem in cancer treatment and new therapy concepts are essential to handle this challenge. The major aim of this work was to elucidate innovative strategies in the targeting of cell cycle, cell death and cancer progression.

In former studies we could show that the dual specific phosphatase Cdc25A represents a client of Hsp90 and, because Cdc25 phosphatases act as key regulators of the cell cycle and especially Cdc25A has been shown to be frequently over-expressed in a wide range of cancers, this protein was selected to target via Hsp90 inhibition by geldanamycin. As pancreatic tumors are among the hardest to treat cancers with poor prognosis and high resistance rates, this cancer type was chosen for the investigations. Retardation of cell proliferation by inhibiting ribonucleotide reductase with digalloylresveratrol was another approach to decrease pancreatic cancer cell growth.

Besides elucidating targets for inhibiting the cell cycle in pancreatic cancer cell lines, investigations of different natural compounds and medical plants used in folk medicine as remedies have been the second main objective of this work. Natural products have played a significant role in human healthcare for thousands of years and even today, more than 60% of all drugs are either natural products or directly derived thereof used to treat even diseases such as cancer. Among these are very important agents like vinblastine, vincristine, the camptothecin derivatives, topotecan and irinotecan, etoposide and paclitaxel. The multifactorial anticancer effects of different extracts of medicinal plants collected in Guatemala, Pakistan and Turkey should be tested on HL-60 leukemia cells regarding their ability to inhibit cell growth and elicit cell death.

As about 90% of all cancer deaths are not related to the primary tumor but to metastases that destroy the function of infested organs, prevention of cancer cell dissemination and secondary tumor formation must be a major goal of cancer therapy, investigation of this important step of tumorigenesis has been the third main objective. Breast cancer cells penetrate lymphatic vessels by generating circular defects in the integrity of a lymphatic

endothelial cell layer and that these ruptures are mediated by 12(S)-HETE metabolized from arachidonic acid by the hypoxia-inducible enzymes ALOX12 or ALOX15. Intravasation into blood and lymphatic vessels represents one of the first steps in the multistep process of metastasis and therefore, in this work, different natural compounds, in particular digalloylresveratrol and a methanol extract of *Scrophularia lucida*, should be tested about their ability to inhibit cell intravasation and, besides that, emphasis was placed on investigations about other pathways as the one mediated by 12(S)-HETE.

The results from these studies should allow a better understanding in the role of cell specific targets in frequent human cancers. Knowledge about the underlying mechanisms could also increase the success of different existing and future chemotherapeutic drugs.

6 RESULTS

6.1 Original papers and manuscripts

Madlener S., Rosner M., Krieger S., **Giessrigl B.**, Gridling M., Vo T.P., Leisser C., Lackner A., Raab I., Grusch M., Hengstschläger M., Dolznig H. and Krupitza G. Short 42 degrees C heat shock induces phosphorylation and degradation of Cdc25A which depends on p38MAPK, Chk2 and 14.3.3. *Hum Mol Genet.* 18: 1990-2000, **2009.**

I carried out selected heat shock experiments, proliferation assays and western blots.

Ozmen A., Madlener S., Bauer S., Krasteva S., Vonach C., **Giessrigl B.**, Gridling M., Viola K., Stark N., Saiko P., Michel B., Fritzer-Szekeres M., Szekeres T., Askin-Celik T., Krenn L. and Krupitza G. In vitro anti-leukemic activity of the ethno-pharmacological plant Scutellaria orientalis ssp. carica endemic to western Turkey. *Phytomedicine* 17: 55-62, **2010.**

I carried out different proliferation and cell death experiments.

Khan M., **Giessrigl B.**, Vonach C., Madlener S., Prinz S., Herbaceck I., Hölzl C., Bauer S., Viola K., Mikulits W., Quereshi R.A., Knasmüller S., Grusch M., Kopp B. and Krupitza G. Berberine and a Berberis lycium extract inactivate Cdc25A and induce alpha-tubulin acetylation that correlate with HL-60 cell cycle inhibition and apoptosis. *Mutat Res.* 683: 123-130, **2010.**

I carried out different western blots, the cell cycle distribution and cell death assay.

Madlener S., Saiko P., Vonach C., Viola K., Huttary N., Stark N., Popescu R., Gridling M., Vo N.T., Herbacek I., Davidovits A., **Giessrigl B.**, Venkateswarlu S., Geleff S., Jäger W., Grusch M., Kerjaschki D., Mikulits W., Golakoti T., Fritzer-Szekeres M., Szekeres T. and Krupitza G. Multifactorial anticancer effects of digalloyl-resveratrol encompass apoptosis, cell-cycle arrest, and inhibition of lymphendothelial gap formation in vitro. *Br. J. Cancer* 102: 1361-137, **2010.**

I carried out the cell cycle distribution assay.

Saiko P., Graser G., **Giessrigl B.**, Lackner A., Grusch M., Krupitza G., Basu A., Sinha B.N., Jayaprakash V., Jaeger W., Fritzer-Szekeres M. and Szekeres T. A novel N-hydroxy-N'-aminoguanidine derivative inhibits ribonucleotide reductase activity: Effects in human HL-60 promyelocytic leukemia cells and synergism with arabinofuranosylcytosine (Ara-C). *Biochem Pharmacol.* 81: 50-59, **2011.**

I carried out the western blot experiments.

Jäger W., Gruber A., **Giessrigl B.**, Krupitza G., Szekeres T. and Sonntag D. Metabolomic analysis of resveratrol-induced effects in the human breast cancer cell lines MCF-7 and MDA-MB-231. *OMICS* 15: 9-14, **2011.**

I carried out all cell culture experiments.

Vonach C., Viola K., **Giessrigl B.**, Huttary N., Raab I., Kalt R., Krieger S., Vo T.P., Madlener S., Bauer S., Marian B., Hämmerle M., Kretschy N., Teichmann M., Hantusch B., Stary S., Unger C., Seelinger M., Eger A., Mader R., Jäger W., Schmidt W., Grusch M., Dolznig H., Mikulits W. and Krupitza G. NF-κB mediates the 12(S)-HETE-induced endothelial to mesenchymal transition of lymphendothelial cells during the intravasation of breast carcinoma cells. *Br. J. Cancer* 105: 263-271, **2011.**

I carried out selected western blot experiments.

Bauer S., Singhuber J., Seelinger M., Unger C., Viola K., Vonach C., **Giessrigl B.**, Madlener S., Stark N., Wallnofer B., Wagner K.H., Fritzer-Szekeres M., Szekeres T., Diaz R., Tut F., Frisch R., Feistel B., Kopp B., Krupitza G. and Popescu R. Separation of anti-neoplastic activities by fractionation of a Pluchea odorata extract. *Front Biosci. (Elite Ed)* 1: 1326-36, **2011.**

I carried out different proliferation, cell death and western blot experiments.

Viola K., Vonach C., Kretschy N., Teichmann M., Rarova L., Strnad M., **Giessrigl B.**, Huttary N., Raab I., Stary S., Krieger S., Keller T, Bauer S, Jarukamjorn K., Hantusch B., Szekeres T., de Martin R., Jäger W., Knasmüller S., Mikulits W., Dolznig H., Krupitza G. and Grusch M. Bay11-7082 and xanthohumol inhibit breast cancer spheroid-triggered disintegration of the lymphendothelial barrier; the role of lymphendothelial NF-κB. *Br. J. Cancer,* ***submitted.***

I carried out RNA isolation and different real-time PCR and western blot experiments.

Seelinger M., Popescu R., Seephonkai P., Singhuber J., **Giessrigl B.**, Unger C., Bauer S., Wagner K.H., Fritzer-Szekeres M., Szekeres T., Diaz R., Tut F.T., Frisch R., Feistel B., Kopp B. and Krupitza G. Fractionation of an anti-neoplastic extract of *Pluchea odorata* eliminates a property typical for a migratory cancer phenotype. *Evidence-based Compl. and Alt. Medicine,* ***submitted.***

I carried out selected western blot experiments.

Giessrigl B., Yazici G., Teichmann M., Kopf S., Ghassemi S., Atanasov A.G., Dirsch V.M., Grusch M., Jäger W., Özmen A. and Krupitza G. Effects of *Scrophularia* Extracts on Tumor Cell Proliferation, Death and Intravasation through Lymphendothelial Cell Barriers. *Evidence-based Compl. and Alt. Medicine,* ***submitted.***

Saiko P., Graser G., **Giessrigl B.**, Lackner A., Grusch M., Krupitza G., Jaeger W., Golakoti T., Fritzer-Szekeres M. and Szekeres. Digalloylresveratrol, a novel resveratrol analog attenuates the growth of human pancreatic cancer cells by inhibition of ribonucleotide reductase *in situ* activity. *J. of Gastroenterology*, ***submitted.***

I carried out different proliferation and western blot experiments.

Giessrigl B., Krieger S., Huttary N., Saiko P., Alami M., Maciuk A., Gollinger M., Mazal P., Szekeres T., Jäger W. and Krupitza G. Hsp90 stabilises Cdc25A and counteracts heat shock mediated Cdc25A degradation and cell cycle attenuation in pancreas carcinoma cells. *Hum Mol Genet.,* ***submitted.***

Short 42 degrees C heat shock induces phosphorylation and degradation of Cdc25A which depends on p38MAPK, Chk2 and 14.3.3.

Madlener S., Rosner M., Krieger S., **Giessrigl B.**, Gridling M., Vo T.P., Leisser C., Lackner A., Raab I., Grusch M., Hengstschläger M., Dolznig H. and Krupitza G.

Hum Mol Genet. 18: 1990-2000, **2009.**

Human Molecular Genetics, 2009, Vol. 18, No. 11 **1990–2000**
doi:10.1093/hmg/ddp123
Advance Access published on March 16, 2009

Short 42°C heat shock induces phosphorylation and degradation of Cdc25A which depends on p38MAPK, Chk2 and 14.3.3

Sibylle Madlener[1], Margit Rosner[2], Sigurd Krieger[1], Benedikt Giessrigl[1], Manuela Gridling[1], Thanh Phuong Nha Vo[1], Christina Leisser[1], Andreas Lackner[3], Ingrid Raab[1], Michael Grusch[3], Markus Hengstschläger[2], Helmut Dolznig[1] and Georg Krupitza[1,*]

[1]Institute of Clinical Pathology, Medical University of Vienna, [2]Department of Medical Genetic, Medical University of Vienna and [3]Department of Medicine I, Institute of Cancer Research, Medical University of Vienna, Waehringer Guertel 18-20, A-1090 Vienna, Austria

Received January 14, 2009; Revised and Accepted March 12, 2009

The effects of heat shock (HS; 42°C) on the cell cycle and underlying molecular mechanisms are astonishingly unexplored. Here, we show that HS caused rapid Cdc25A degradation and a reduction of cell cycle progression. Cdc25A degradation depended on Ser75–Cdc25A phosphorylation caused by p38MAPK and Chk2, which phosphorylated Ser177–Cdc25A that is specific for 14.3.3 binding. Upon HS, Cdc25A rapidly co-localized with 14.3.3 in the perinuclear space that was accompanied with a decrease of nuclear Cdc25A protein levels. Consistently, a 14.3.3 binding-deficient Cdc25A double mutant (Ser177/Ala-Tyr507/Ala) was not degraded in response to HS and there was no evidence for an increased co-localization of Cdc25A with 14.3.3 in the cytosol. Therefore, upon HS, p38, Chk2 and 14.3.3 were antagonists of Cdc25A stability. On the other hand, Cdc25A was protected by Hsp90 in HEK293 cells because the specific inhibition of Hsp90 with Geldanamycin caused Cdc25A degradation in HEK293 implicating that Cdc25A is an Hsp90 client. Specific inhibition of Hsp90 together with HS caused and accelerated degradation of Cdc25A and was highly cytotoxic. The results presented here show for the first time that Cdc25A is degraded by moderate heat shock and protected by Hsp90. We describe the mechanisms explaining HS-induced cell cycle retardation and provide a rationale for a targeted hyperthermia cancer therapy.

INTRODUCTION

Severe heat shock (HS; up to 44–45°C) arrests the cell cycle either dependent or independent of p53 through upregulation of p21 and downregulation of cyclin D family members (1–3). Mild to moderate HS (40–43°C) reflects the conditions of very high fever and is reached by hyperthermic cancer therapy (fever range whole body hyperthermia; FR-WBH) but the effects on the cell cycle and its regulators are rather unexplored. Mild HS was shown to upregulate cyclin D1 (4) implicating an induction of the lymphocyte cell cycle although this has so far not been investigated in detail. Furthermore, HS was shown to activate the stress protein p38MAPK (p38) (2,4). Activated p38 can phosphorylate Ser75–Cdc25A (5–7) and phosphorylation of Ser75–Cdc25A destabilizes the protein (5,8). Toxic stress caused by various chemicals and clinical drugs (9,10), UV (11) and ionizing radiation (12,13) leads to degradation of Cdc25A through the activation of checkpoint kinases (Chks) (14), which makes this cell cycle regulator and oncogene a target for anticancer therapy. However, Cdc25A was never studied in response to HS. We found that moderate and short HS (42°C; 20–60 min) destabilized Cdc25A and studied the causal mechanisms. In short, HS caused rapid phosphorylation of Cdc25A by p38 and Chk2, and its nuclear export to the perinuclear space where it accumulated in co-localization with 14.3.3, which was required for its degradation.

There is an ongoing debate on the assumption that the more often high fevers are experienced throughout a lifetime, the

*To whom correspondence should be addressed. Tel: +43 140400 (ext. 3487); Fax: +43 1404003707; Email: georg.krupitza@meduniwien.ac.at

© The Author 2009. Published by Oxford University Press. All rights reserved.
For Permissions, please email: journals.permissions@oxfordjournals.org

lower is the risk to develop certain types of cancer and also hyperthermia treatment of patients suffering from liver, kidney and bone cancer is successful, although locally applied temperatures are much higher than the temperatures described herein. Here, we provide a mechanistic rationale for these observations.

Since Cdc25A is over-expressed in a variety of malignancies such as breast-, pancreatic-, renal-, liver-, lung-, thyroid-, oesophageal-, endometrial-, colorectal cancers, malignant melanoma, glioma, and non-Hodgkin lymphomas (15), the specific response of Cdc25A to HS could be exploited in adjuvant thermo therapy applied either strictly locally at the tumour site or systemically to also reach distant micro-metastases.

RESULTS

Moderate heat shock downregulates Cdc25A and inactivates Cdc2

It was shown that severe HS causes p53−/p21−-dependent as well as p53-independent cell cycle arrest (1,3) suggesting that also different mechanisms are responsible for the inhibition of cell proliferation. Moderate HS was reported to even induce cyclin D1 in lymphocytes implicating a lymphocytic growth response as observed when fevering, i.e. upon infections (2,4). In HEK293 cells, cyclin D1 was also upregulated at 39–40°C (mild HS; Fig. 1A and B). Induction of p21 was not observed at the tested temperatures (37–43°C; data not shown). When analysing the expression of Cdc25A protein in response to moderate HS, we found its rapid downregulation when HEK293 embryonic kidney cells (Fig. 1A–C) or HeLa endometrial carcinoma cells (Fig. 1E) were exposed to 42°C. Thus, HS downregulated the Cdc25A oncogene in different cell types. As a consequence of Cdc25A depletion, the phosphorylation of Tyr15-Cdc2 (Cdk1) peaked (16) (Fig. 1C) because Tyr15-Cdc2 (Cdk1) is a substrate of activated Cdc25A phosphatase (15), and this reduced cell cycle progression. In addition, also Cdc25B and Cdc25C levels dropped in HEK293 cells (Fig. 1D) and HeLa cells (Fig. 1E) upon 42°C HS and this may have contributed to the accumulation of Tyr15-phosphorylation of Cdc2 as well. Conversely, in HEK 293 cells, 40°C HS did not cause Tyr15-phosphorylation of Cdc2 and only in HeLa cells Cdc25B was strongly decreased after 40°C HS. A significant number of HEK293 cells accumulated in the G1 phase upon HS (42°C, 20 min) and subsequent cultivation for 24 and 48 h (Fig. 1F). Heat shocking HEK293 cells for 60 and 90 min (42°C) led to severe apoptosis after 72 h post-incubation time (Fig. 1I), and until the onset of apoptosis cells remained growth retarded. The retardation of cell cycle progression upon 42°C HS was demonstrated by reduced cell proliferation rate (Fig. 1G) and significantly reduced incorporation of BrdU into the nascent DNA (Fig. 1H).

Heat shock activates p38 and induces Ser75–Cdc25A phosphorylation

Searching for Cdc25A degrading signals upon HS, we studied the expression of checkpoint kinase 1 (Chk1), which when phosphorylated destabilizes Cdc25A. However, HS did not activate Chk1 and a specific Chk1 inhibitor (C_1I) did not influence Ser75–Cdc25A phosphorylation or stability (Fig. 2A, left-side panels) and hence, Chk1 did not play a role upon HS-induced destabilization. This was in contrast to UV- or ionizing radiation (IR)-induced Cdc25A degradation, which is triggered by Chk1 (11,12), and for control reasons we show Chk1 activation upon exposure of HEK cells to 50 mJ UV irradiation (Fig. 2A, right-side panels). Also p38 can phosphorylate Ser75–Cdc25A (5–7), and p38 is activated upon severe as well as mild HS (2,4). In the context of HS, this signal cascade (p38 to Ser75–Cdc25A) has not been studied yet. HS induced the phosphorylation of Thr180/182 of p38 (indicative for its activation) and the phosphorylation of Ser75–Cdc25A within 20 min was prevented by the specific p38 inhibitor SB203580 and also the destabilization of the Cdc25A protein level was blocked (Fig. 2B).

Heat shock activates checkpoint kinase 2 and induces Ser177–Cdc25A phosphorylation

In search of downstream degrading mechanisms, the phosphorylation of Ser177–Cdc25A, a site phosphorylated by Chk2 thereby forming a docking site for 14.3.3 (14,16) was analysed. The binding of 14.3.3 to phospho-Ser177 could be demonstrated, and the phosphorylation of Ser177–Cdc25A is known to have a destabilizing effect (9,14,17). HS slightly induced the phosphorylation of Thr68-Chk2 within 20 min. At this time point also a slight electrophoretic upshift became visible (also visible at the 60 min time-point) indicating an increase of additional (likely activating) phosphorylations at different site(s) (Fig. 3). Specific inhibition of Chk2 activity by Chk2 inhibitor (C_2I) caused an electrophoretic downshift equal to the migration of the control band and a reduction of the phospho-specific signal intensity. Upon HS also the phosphorylation of Ser177–Cdc25A became induced within 20 and 60 min, which was reduced (but not reversed to control levels) in the presence of C_2I. This indicated that Chk2 caused Ser177–Cdc25A phosphorylation. The Cdc25A protein level was less reduced after 20 min compared with HS-mediated depletion of Cdc25A protein level shown in Figure 2. There are several reasons for this unsteady response within 20 min of HS. First, the confluence of the cell culture plays a role (the higher the confluence at the time of the experiment, the higher the stability of Cdc25A). Secondly, even slight fluctuations of the incubator temperature (0.5–1.0°C) may cause a remarkable difference in such short time spans of HS (Fig. 1A), and so does the transfer time from the maintenance incubator to the HS incubator. In pilot experiments using water bath-controlled HS, similar fluctuations were observed and therefore, we continued with incubator-controlled HS. However, we want to point out that HS induced the degradation of Cdc25A in every single experiment (at least after 60 min), which is the major finding we want to demonstrate. After 60 min of HS, Cdc25A protein expression was strongly reduced (Fig. 3), whereas the phospho-specific antibody still detected considerable phopho-Ser177 levels. This implicated that low amounts of Cdc25A must have been highly phosphorylated. Specific inhibition of Chk2 by C_2I, which also inhibited phosphorylation of Ser177–

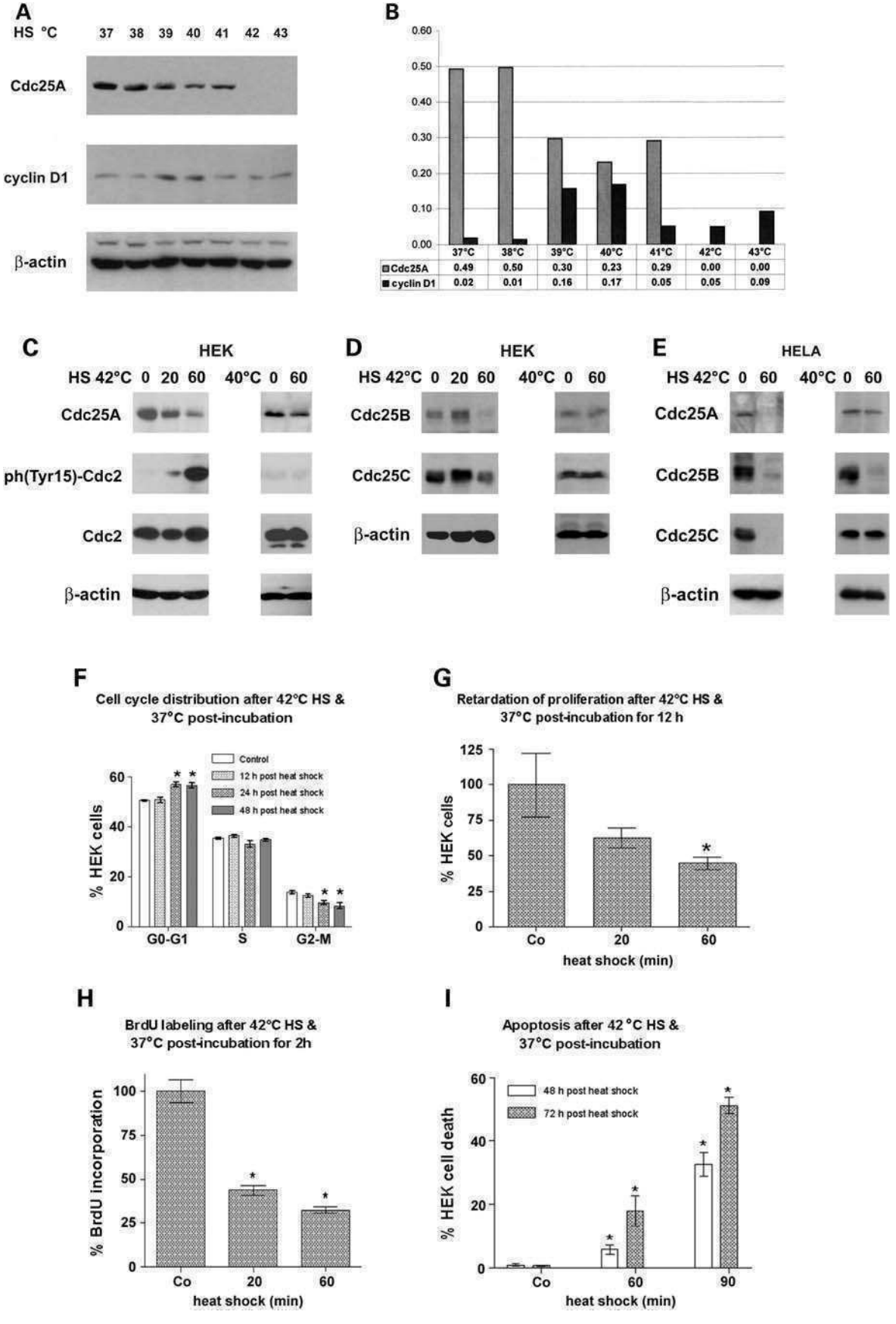
A
HS °C 37 38 39 40 41 42 43
Cdc25A
cyclin D1
β-actin
B
0.60
0.50
0.40
0.30
0.20
0.10
0.00
37°C 38°C 39°C 40°C 41°C 42°C 43°C
Cdc25A 0.49 0.50 0.30 0.23 0.29 0.00 0.00
cyclin D1 0.02 0.01 0.16 0.17 0.05 0.05 0.09
C
HEK
HS 42°C 0 20 60 40°C 0 60
Cdc25A
ph(Tyr15)-Cdc2
Cdc2
β-actin
D
HEK
HS 42°C 0 20 60 40°C 0 60
Cdc25B
Cdc25C
β-actin
E
HELA
HS 42°C 0 60 40°C 0 60
Cdc25A
Cdc25B
Cdc25C
β-actin
F
Cell cycle distribution after 42°C HS & 37°C post-incubation
Control
12 h post heat shock
24 h post heat shock
48 h post heat shock
% HEK cells
G0-G1
S
G2-M
G
Retardation of proliferation after 42°C HS & 37°C post-incubation for 12 h
% HEK cells
Co
20
60
heat shock (min)
H
BrdU labeling after 42°C HS & 37°C post-incubation for 2h
% BrdU incorporation
Co
20
60
heat shock (min)
I
Apoptosis after 42 °C HS & 37°C post-incubation
48 h post heat shock
72 h post heat shock
% HEK cell death
Co
60
90
heat shock (min)

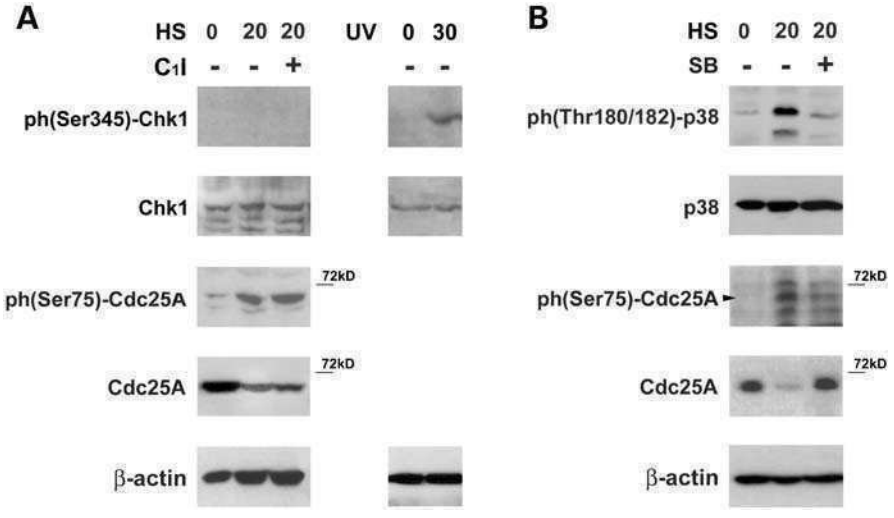

Figure 2. HEK293 cells were exposed to 42°C HS for 20 min and where indicated (**A**) Chk1 inhibitor SB218078 (C_1I, 1 μM; as a phospho-Chk1 antibody control cells were exposed to 50 mJ UV and post-incubated for 30 min, right-side panels), or (**B**) specific p38 inhibitor SB203580 (SB, 1 μM) was included. Then, cells were lysed and subjected to western blot analysis using the indicated antibodies. HS induced Thr180/182-p38 phosphorylation (indicative for its activation) and in consequence phosphorylation of Ser75–Cdc25A within 20 min and the reduction in Cdc25A protein level. The correct position of the phospho Ser75–Cdc25A band was identified by overlaying this luminescence image with that of the Cdc25A blot, which was developed on the same membrane. Chk1, which also phosphorylates Ser75–Cdc25A, did not become activated upon HS. β-Actin was used as loading control.

Cdc25A, somewhat stabilized Cdc25A protein expression (Fig. 3) and this supported the notion that either the inhibition was only partial (the data argue for this interpretation), or once Cdc25A was tagged with destabilizing modifications, the process of degradation was fast, and beyond a certain threshold point, irreversible.

Binding to 14.3.3 destabilizes Cdc25A and heat shock increases 14.3.3–Cdc25A co-localization

To further study the involvement of phosphorylation as trigger mechanism of Cdc25A destabilization, it was tested whether HS-mediated Cdc25A degradation was dependent on 14.3.3. This protein was described as a mediator of nuclear-cytoplasmic transport of Cdc25B and Cdc25C (14,18,19), and as a tag for subsequent proteasomal degradation. A double-mutated (dmt) Cdc25A construct that cannot become phosphorylated at the Ser177Ala and Tyr506Ala mutated residues is 14.3.3 binding-deficient (16). Upon HS, this dmtCdc25A construct exhibited increased stability in transfected HEK293 cells, whereas ectopic wild-type (wt) Cdc25A was degraded, such as endogenous Cdc25A (Fig. 4A, left-side panels show Cdc25A expression of those cells that were transfected with wtCdc25A, right-side panels the expression of dmtCdc25A-transfected cells). Ectopic myc-tagged Cdc25A constructs were detected by an anti-myc antibody and endogenous Cdc25A by a monoclonal antibody against Cdc25A (F6), which does not detect dmtCdc25A. The Cdc25A-specific bands are indicated by arrow heads. The transfection was carefully adjusted not to exceed 2–3-fold overexpression (see Materials and Methods). The experiment analysing the stability of dmtCdc25A supported the hypothesis that Cdc25A stability upon HS was regulated through Chk2 activation and the phosphorylation of Ser177–Cdc25A. Then, it was analysed which of the 14.3.3 isoforms co-precipitated Cdc25A. Co-transfection of wtCdc25A-V5 (fused to a 3′-V5 tag) with each of the 14.3.3 isoforms listed showed that 14.3.3ε and 14.3.3θ (τ) were those isoforms which pulled down high amounts of Cdc25A (Fig. 4B). For unknown reasons HA-antibody precipitated 14.3.3σ inefficiently and therefore we continued the studies with 14.3.3θ and myc-tagged Cdc25A.

Reciprocal pull-down assays confirmed that wtCdc25A co-precipitated HA-14.3.3θ, whereas a binding-deficient HA-mt14.3.3 construct, which cannot associate with natural 14.3.3 binding partners, did not co-precipitate with Cdc25A (20). Also dmtCdc25A was entirely 14.3.3 binding-deficient (Fig. 4C). Next, we investigated where in the cell Cdc25A

Figure 1. (**A**) HEK293 cells were exposed to increasing temperatures (as indicated) for 60 min and the expression of Cdc25A and cyclin D1 was analysed by western blotting and (**B**) measured by densitometry that was calibrated to actin expression (numbers are in proportion to actin expression that was set as 1.0). (**C, D**) HEK293 and (**E**) HeLa cells were exposed to 42°C heat shock (HS; left-side panels) for 20 and 60 min, or 40°C for 60 min (right-side panels), lysed and prepared for western blot analysis using the indicated antibodies. After 60 min HS (42°C), Cdc25A, B and C levels were decreased and phosphoTyr15-Cdc2 levels were increased. β-Actin was used as a loading control. (**F**) HEK293 cells were exposed to HS for 20 min and put back to 37°C for the indicated times. Then cells were prepared for FACS analysis. A significant accumulation of HS-treated cells in G1 was observed after 24 and 48 h. HEK cells were exposed to 42°C HS for 20 and 60 min and set back to 37°C and (**G**) counted after 12 h, or (**H**) pulse-labelled subsequent to HS with BrdU for 2 h. Then, BrdU incorporation was measured using a FACSCalibur flow cytometer, and compared with untreated controls. (**I**) HEK293 cells were exposed to 42°C HS for 60 and 90 min and put back to 37°C for 48 and 72 h. Then, cells were stained with HO/PI, and analysed with fluorescence microscopy using a DAPI filter. Experiments were performed in triplicate, asterisks indicate significance and error bars SEM.

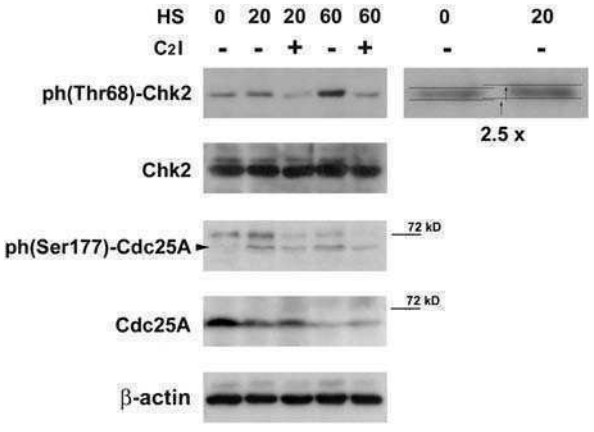

Figure 3. HEK293 cells were exposed to 42°C heat shock (HS) for 20 and 60 min and where indicated a specific Chk2 inhibitor (C_2I, 10 μM) was included. Then cells were lysed and subjected to western blot analysis using the indicated antibodies. After 20 and 60 min HS Chk2 was phosphorylated at the activating Thr68 site. Furthermore, Cdc25A was phosphorylated at the Chk2-specific phospho Ser177 site (arrowhead) after 20 and 60 min and less phosphorylated after treatment with C_2I. Chk2 protein level was unchanged. β-Actin was used as loading control. To better illustrate the HS-mediated phChk2 upshift, the panel at the right side gives a 2.5× magnification of the control- and HS band (20 min). The correct position of the phospho Ser177–Cdc25A bands (or the phospho Thr68-Chk2 bands) was identified by overlaying this luminescence image with that of the Cdc25A blot (or the Chk2 blot, respectively), which was developed on the same membrane.

co-localized with 14.3.3 upon HS and for this, we used confocal microscopy. HEK293 cells were inappropriate for this type of experiment, because they detached from glass slides after HS (even when slides were coated with matrigel or fibronectin), thereby preventing a confocal *in situ* analysis, and therefore, HeLa cells were used for this investigation. Cells were serum-starved overnight to downregulate endogenous *c-Myc* and avoid interference with the myc-tag of the ectopic Cdc25A constructs. In untreated control cells, the majority of wtCdc25A and dmtCdc25A was located in the nucleus. Upon 20 min HS, the levels of nuclear wtCdc25A decreased but the co-localization of wtCdc25A with 14.3.3 increased in the perinuclear space (Fig. 4D and E). dmtCdc25A persisted in the nucleus and HS neither changed the protein level nor the extent of perinuclear co-localization with 14.3.3 (Fig. 4D and E). Zeiss software allowed quantifying the extent of Cdc25A expression as well as 14.3.3 co-localization (Fig. 4D). Since dmtCdc25A was completely 14.3.3 binding-deficient (Fig. 4C), the measured co-localization in untreated and HS-treated dmtCdc25A cells was non-specific (Fig. 4D). Hence, we introduced a threshold (the green dashed line in Fig. 4D) above which the Cdc25A-14.3.3 co-localization was considered specific. This demonstrated that Ser177-phosphorylation-dependent 14.3.3 binding played a role in the subcellular distribution and degradation of Cdc25A upon HS.

Cdc25A is an Hsp90 client in HEK293 cells

Since there exist antagonists of Cdc25A stability, one has to also postulate the existence of protagonists that counteract destabilization. We tested the idea that HS activated chaperones of the heat shock protein family. Hsp90 was shown to interact with its client Chk1 (21), and cytarabine-activated Chk1, which was destabilized by the specific Hsp90 inhibitor 17-AAG, resulted in attenuated degradation of Cdc25A in HL60 cells (22), and this evidenced a connection between Hsp90 and Cdc25A. Garcia-Morales *et al*. (23) demonstrated that Cdc25C and Cdc2 are Hsp90 clients. Further, Akt and Raf1 are Hsp90 clients (24–26) and Galaktionov *et al*. (27) showed that Cdc25A co-immunoprecipitated with Raf and we provided evidence that also Akt was associated with Cdc25A and Raf (28). It therefore seemed likely that also Cdc25A is in complex with Hsp90. Apparently, Hsp90 stabilizes various oncoproteins and/or their oncogenic activity (29) and thus, targeting Hsp90 is evaluated in clinical trials as anticancer therapeutic concept (30–32). Geldanamycin (GD) specifically inhibits Hsp90 by competing with ATP for the ATP/ADP-binding pocket and thereby Hsp90 becomes inactivated in its chaperone function that is required for client stabilization. In case Cdc25A is an Hsp90 client, such as other proto-oncogenes, i.e. Raf1, Akt or c-jun (24,26,33), GD was expected to destabilize Cdc25A. To confirm this, HEK293 and HeLa cells were treated with 1 μM GD for 1 and 24 h and the stability of Cdc25A and Akt (Hsp90 client) was analysed. As expected, Akt was degraded in both cell lines within 24 h, whereas Cdc25A became degraded only in HEK293 cells (Fig. 5A). This implicated that specific co-chaperones required for Cdc25A–Hsp90 binding and activity (34) are limited in HeLa cells but not in HEK293 cells. Therefore, dependent on the cellular context, Cdc25A was an Hsp90 client. Treatment with GD caused an electrophoretic Cdc25A-upshift after 24 h (Fig. 5A) and this phenomenon was accelerated in combination with HS (Fig. 5B). Also Cdc25A depletion was accelerated upon GD and HS co-treatment (after 20), which further confirmed that Cdc25A was an Hsp90 client (Fig. 5B). HS-mediated activation of p38 became additionally induced by GD co-treatment and this correlated with a substantial increase in Ser75–Cdc25A phosphorylation, which faded after 60 min HS.

To formally analyse whether Cdc25A and Hsp90 appear in the same complex, Cdc25A–V5 was transiently overexpressed and immunoprecipitated with anti-Cdc25A antibody

Figure 4. HEK293 cells were transfected with (**A**) wild-type (wt) Cdc25A-myc-tag cDNA (left-side panels) and double-mutated (dmt) Cdc25A-myc-tag cDNA (right-side panels) and then exposed to HS for the indicated times (min). Then cells were lysed and subjected to western blot analysis using the listed antibodies. Endogenous wt- and ectopic wtCdc25A-myc-tag was degraded after 20 min HS, whereas dmtCdc25A protein levels remained unchanged. The bars indicate the 72 kDa weight marker. β-Actin was used as loading control. (**B**) Co-immunoprecipitation of wtCdc25A-V5 with 14.3.3 isoforms: the indicated HA-tagged 14.3.3 cDNA isoforms and V5-tagged wtCdc25AcDNA were co-transfected into HEK293 cells and after 24–36 h cells were lysed and 14.3.3 was immunoprecipitated with HA antibody and co-precipitated Cdc25A was detected with V5 antibody. (**C**) Pull-down assay: HEK293 cells were transfected with the indicated cDNAs (wt14.3.3 θ) and after 24–36 h cells were lysed by repeated freeze-thaw cycles under non-denaturing buffer conditions, and then Cdc25A was immunoprecipitated with monoclonal F6- or polyclonal M191 antibody. F6 was used to check the specificity of the Cdc25A/14.3.3 interaction. mt14.3.3 is a construct

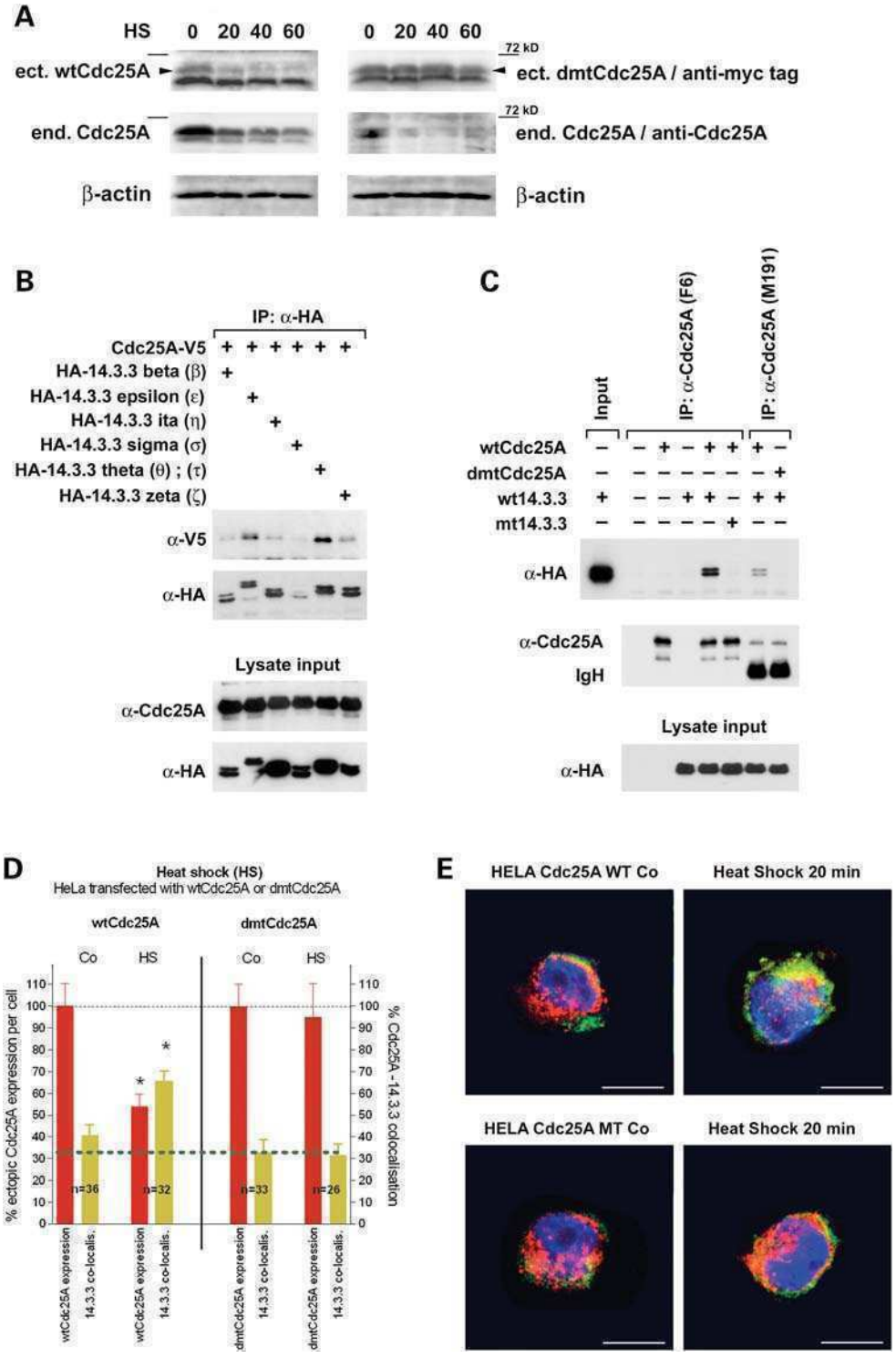

that cannot associate with natural 14.3.3 binding partners. The F6 antibody does not detect dmtCdc25A because it recognizes the C-terminus which is mutated in dmtCdc25A (not shown). Therefore, the analysis was performed with M191 antibody, which also detects dmtCdc25A. 14.3.3 Constructs carried a HA-tag and western blot analyses of co-immunoprecipitated 14.3.3 and lysate input was performed with HA antibody. (**D**) Serum-starved HeLa cells were grown on glass slides, transfected with wtCdc25A-myc-tag cDNA and dmtCdc25A-myc-tag cDNA subjected to HS for 20 min, fixed and prepared for double-immunofluorescence and examined under a confocal microscope. The green dashed line shows the threshold, below which co-localization is arbitrary, whereas above co-localization is specific. After 20 min HS, the co-localization of wtCdc25A/14.3.3 increased approximately 3.5-fold compared with the dmtCdc25A/14.3.3 co-localization, which remained unchanged. (**E**) Representative double immunofluorescence-stained examples of HS-treated HeLa cells expressing wt- or dmtCdc25A. The red colour shows Cdc25A-myc-tag (anti-myc antibody), green 14.3.3, and blue shows the DAPI-stained nuclear chromatin; yellow is the Cdc25A-myc-tag/14.3.3 merge. In controls, most of wtCdc25A and dmtCdc25A was located in the nucleus and the co-localization of wtCdc25A with 14.3.3 was observed predominantly near the nucleus in the cytoplasm. The size bars indicate 10 μm.

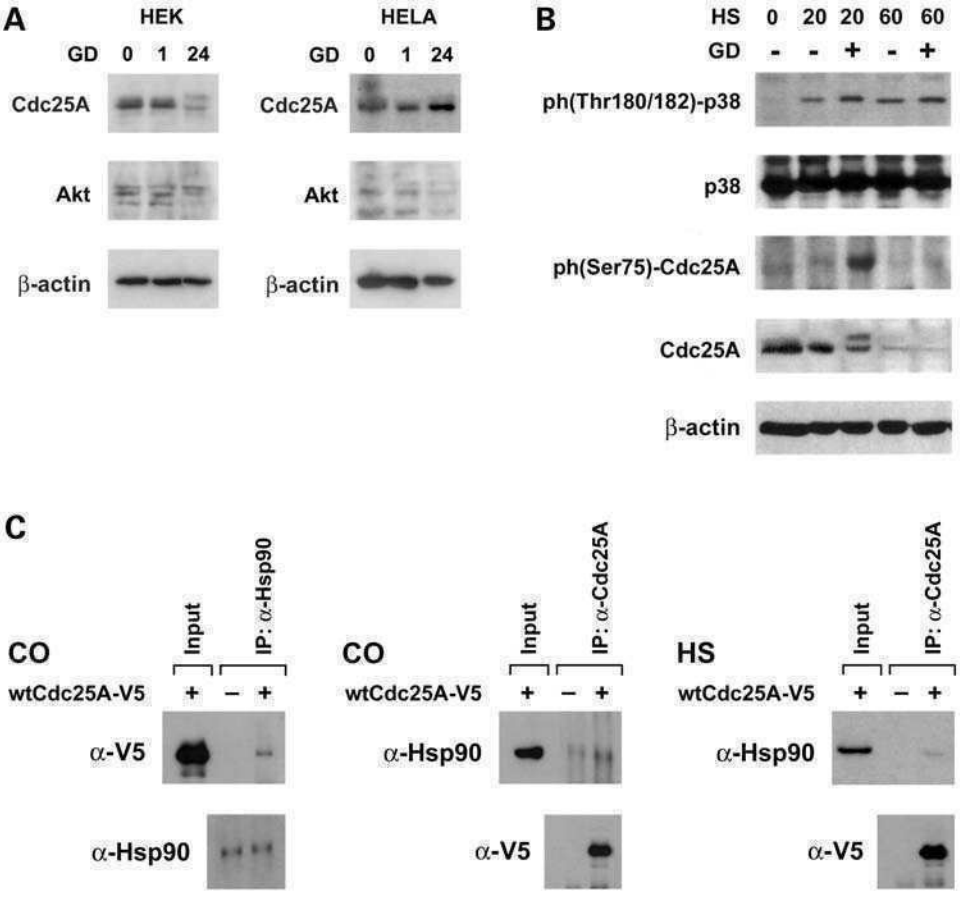

Figure 5. (**A**) HEK293 and HeLa cells were exposed to the specific Hsp90 inhibitor geldanamycin (GD, 1 μM) for 1 and 24 h. After 24 h of treatment, Cdc25A was downregulated in HEK293 cells but not in HeLa cells. GD caused an electrophoretic upshift of Cdc25A in both cell lines after 24 h. (**B**) HEK293 cells were exposed to HS for 20 and 60 min and wherever indicated 1 μM GD was included. Then cells were lysed and subjected to western blot analysis using the indicated antibodies. β-Actin was used as loading control. HS and co-incubation with GD resulted in an increased phosphorylation of Ser75–Cdc25A and electrophoretic retardation and degradation of Cdc25A. Also the phosphorylation of Thr180/182–p38 was increased when cells were treated with HS and GD. β-Actin was used as loading control. (**C**) HEK293 cells were transfected with wtCdc25A-V5 cDNA and after 24–36 h cells were lysed by repeated freeze-thaw cycles under non-denaturing buffer conditions. Then, Hsp90 (left-side panels) was immunoprecipitated with anti-Hsp90 from Abcam and Cdc25A was detected using anti-V5 antibody. Reciprocally, Cdc25A (middle and right-side panels) was immunoprecipitated with M191 antibody and co-precipitated Hsp90 was detected by western blot analysis using anti-Hsp90 antibody from Cell Signaling. In the experiments that are depicted in the left and middle panels, cells were kept under normal culture conditions (CO), and in the experiment that is shown in the right-side panel cells were heat shocked (42°C; HS) for 20 min. Precipitation efficiency was controlled by immunoblotting with anti-Hsp90 antibody from Cell Signaling (left side) or anti-V5 antibody (middle and right side).

under non-denaturing conditions and the presence of Hsp90 in the precipitate was confirmed by western blotting (Fig. 5C, middle panel). The efficiency of the immunoprecipitates (IP) was controlled by anti-V5 immunoblot. Reciprocal IP–western analysis (IP: Hsp90; WB: V5) confirmed the specificity of the Cdc25A–Hsp90 interaction (Fig. 5C, left-side panel). Also, after 42°C HS (20 min) Hsp90 still co-precipitated with Cdc25A (Fig. 5C, right-side panel). Throughout the time span investigated, we did not observe a change in the Hsp90 expression level (data not shown).

DISCUSSION

The dual-specificity phosphatase Cdc25A regulates the cell cycle and was shown to be sensitive to UV, IR, osmotic-, oxidative- and genotoxic stress (9–12). Here, we demonstrate for the first time that Cdc25A was rapidly downregulated upon HS at the high end of the physiological fever range (42°C) (4,35), and reduced cell cycle progression causing an accumulation of cells in G1. Interestingly, also hyperthermic cancer therapy (FR-WBH) is performed around 41.5°C. Upon 40°C, HS Cdc25A expression was only moderately reduced. Unlike UV or IR, which cause Chk1-mediated phosphorylation and degradation of Cdc25A through tagging with the $SCF^{\beta\text{-TrCP}}$ ubiquitin–ligase complex at the phosphodegron around Ser81/87–Cdc25A (13,36,37), HS activated the kinases p38 and Chk2, but not Chk1. p38 phosphorylated Ser75–Cdc25A (such as that described for Chk1) (8) and this may have as well facilitated the subsequent phosphorylation of Ser81/87–Cdc25A and association with the $SCF^{\beta\text{-TrCP}}$ ubiquitin–ligase complex followed by degradation (13,36). Specific inhibition of p38-mediated Ser75–Cdc25A phosphorylation abrogated destabilization of Cdc25A only in a small time-window and this evidenced that an additional degrading mechanism was activated as well. HS-mediated

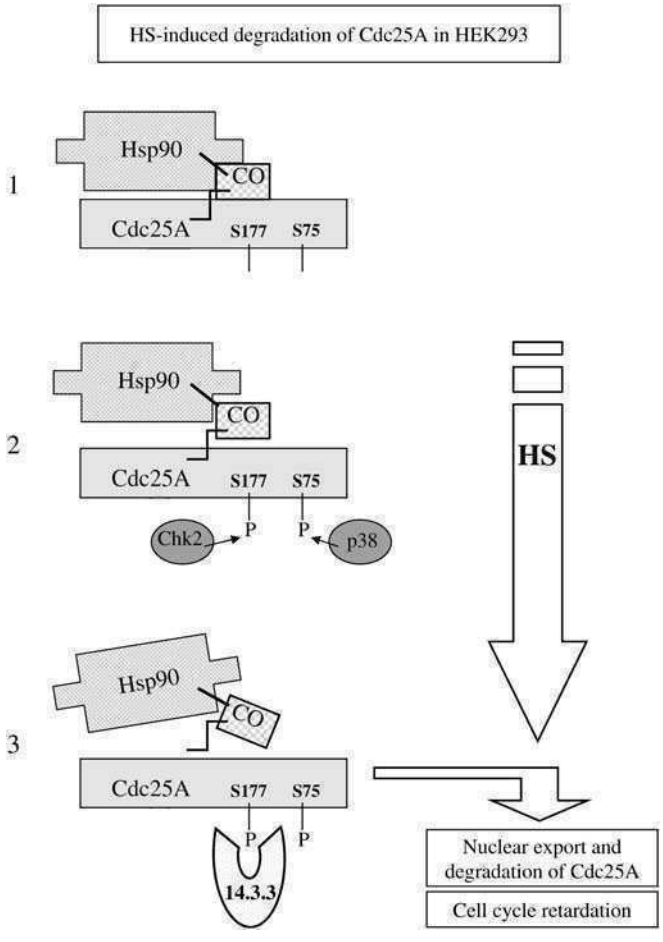

Figure 6. Schematic presentation proposing the mechanism of HS-induced Cdc25A degradation in HEK293 cells. (1) Hsp90 binds through an unidentified co-chaperone (CO) to Cdc25A. (2) 42°C HS activates p38MAPK and Chk2. This causes the phosphorylation of Cdc25A at S75 and S177. Hsp90 is still in complex (perhaps less stable) with Cdc25A. (3) 14.3.3 protein binds to phospho-S177 resulting in nuclear export. Since Cdc25A becomes degraded in the cytoplasm, we postulate that the protection by Hsp90 decreases throughout heat shock response (perhaps through loss of interaction), thereby allowing cell cycle retardation at the extreme end of the fever range.

Chk2 activation led to the phosphorylation of Ser177–Cdc25A (such as formerly described for Chk1) thereby, creating a 14.3.3 docking site (16). It was shown that the binding of 14.3.3 to Cdc25 family proteins is mediated by phosphoserines within 14.3.3-binding consensus sequences of Cdc25 (38). A second 14.3.3 docking site, Tyr506–Cdc25A, was reported to become phosphorylated by Chk1 (14). The prevention of 14.3.3 binding by Ser177Ala-Tyr506Ala mutations (16) inhibited the cytoplasmic sequestration of dmtCdc25A in HeLa cells and its degradation. Since the phosphorylation sites Ser75-, and Ser81/87 of Cdc25A were intact in the dmtCdc25A construct described herein and the degradation of Cdc25A was nevertheless blocked by a 14.3.3-binding mutant, a hypothetic $SCF^{\beta\text{-TrCP}}$ ubiquitin–ligase-dependent scenario was not the only cause for Cdc25A destabilization. Thus, HS-induced Cdc25A destabilization depended on binding to 14.3.3 and the relocation into the perinuclear space (see model suggested in Fig. 6). It has been shown that binding of 14.3.3 to the closely related family members, Cdc25B and Cdc25C, caused their sequestration to the cytoplasm (14,18,19) and finally their degradation. Cdc25A can largely compensate the deficiency in Cdc25B and Cdc25C (demonstrated with respective knockout mice), whereas $Cdc25A^{(-/-)}$ mice are embryonic lethal. Cdc25B and Cdc25C are therefore, not as relevant for survival as Cdc25A (15). Most recently, Cdc25A was identified as a rate-limiting oncogene determining genomic stability and Cdc25A over-expression promotes tumours induced by the ErbB2–Ras pathway. Even a partial repression of Cdc25A is considered beneficial, as it reduces aggressive tumour development and improves prognosis in an MMTV-Ras/Cdc25A mouse model (15). This justifies to search for therapeutic concepts targeting Cdc25A (39).

The results support the interpretation that Hsp90 protected Cdc25A of HEK293 cells through a Hsp90 co-chaperone (Fig. 6), such as the Hsp90 co-chaperone AHA1 maintained the activity of MEK1/2 and Erk1/2 (29). In our case however, the hypothetical co-chaperone was absent in HeLa cells. Currently, also the inhibition of Hsp90 is tested as anti-cancer target and the combination of GD with checkpoint inhibitors is considered as a promising approach. GD and HS (instead of checkpoint inhibitors) seems to be a concept with great potential, since HS treatment can be applied within the physiological range.

Here, a novel regulation of the Cdc25A oncogene was discovered providing a reasonable explanation for HS-induced cell cycle retardation and for the mechanisms destabilizing/stabilizing Cdc25A upon HS and GD treatment and this can form a basis for a tailored Cdc25A-targeting hyperthermia cancer therapy.

MATERIALS AND METHODS

Chemicals

Specific inhibitors against p38 (SB203580; SB), HSP90 (Geldanamycin; GD), Chk1 (SB218078; C_1I) and Chk2 (Chk2 inhibitor; C_2I) were purchased from Calbiochem. Antibodies directed against ph(Tyr15)-Cdc2, ph(Thr180/182)-p38, p38, ph(Ser345)-Chk1, Chk1, ph(Thr68)-Chk2, Chk2 and Hsp90 were from Cell Signaling, against ph(Ser75)-Cdc25A, and Hsp90 from Abcam, against ph(Ser177)-Cdc25A from Abgent, against myc-tag from Invitrogen, against cyclin D1, p21, 14.3.3, Cdc25A (M191) and Cdc25A (F6) from Santa Cruz, against Cdc2 and β-actin from Sigma, V5 from Invitrogen, HA (high affinity, clone 3F10) was purchased from Roche, anti-mouse IgG was from Dako and anti-rabbit IgG from GE-Healthcare. Alexa-Fluor green 488- and Alexa-Fluor red 594-labelled antibodies were purchased from Molecular Probes, and Mowiol from Sigma.

Cell culture

HEK293 and HeLa cells were purchased from ATCC. Cells were grown in logarithmical growth phase at 37°C in a humidified atmosphere containing 5% CO_2 in DMEM high glucose (HEK293) and low glucose (HeLa), both media were supplemented with 10% heat-inactivated fetal

calf serum, 1% L-Glutamine and 1% Penicillin/Streptomycin. All media and supplements were obtained from Life Technologies.

Transfection

HEK293 and HeLa cells were split into a 6-well plate and grown to 70% confluence before transfection in Penicillin/Streptomycin-free medium. 7.5 μl of Lipofectamin 2000 (Invitrogen) and 1 μg of DNA (wtCdc25A-myc, dmtCdc25A-myc, wtCdc25A-V5 or the 14.3.3 isoforms) were mixed into 600 μl of OptiMEM transfection medium and incubated at room temperature for 20 min. In the meantime, cells were washed with phosphate-buffered saline and 1 ml of OptiMEM medium and the DNA and Lipofectamin 2000 mixture was added to the cells and incubated over night.

Cdc25A cDNA (without stop codon) was ligated in frame with a 3-terminal V5 tag into a pcDNA3.1-V5 vector (Invitrogen) and the frame was confirmed by DNA-sequencing.

Double-mutated Cdc25A (dmtCdc25A– Ser177Ala and Tyr506Ala) was a generous gift of Dr Piwnica-Worms—this construct is also referred to as Ser178Ala and Tyr507Ala (when the starting N-terminal methionine is also counted).

Heat shock and inhibitor treatment

HEK293 and HeLa cells were grown to 90% confluence, then cells were pre-incubated with 1 μM of GD for 1 h, or 10 μM of C_2I, 10 μM of SB, 1 μM C_1I for 24 h and exposed to 42°C HS for 20 and 60 min. After HS treatment cells were prepared for analyses as described thereafter.

Western blotting

After incubation with different inhibitors and exposure to 42°C HS HEK293 cells were harvested, washed twice with ice-cold PBS (pH 7.2) and lysed in a buffer containing 150 mM NaCl, 50 mM Tris-buffered saline (Tris pH 8.0), 1% Triton X-100, 1 mM phenylmethylsulfonylfluoride (PMSF) and protease inhibitor cocktail (PIC; from a 100× stock). Then the lysate was centrifuged at 12 000 rpm for 20 min at 4°C, and the supernatant was stored at −20°C until further analysis. Equal amounts of protein samples were separated by polyacrylamide gel electrophoresis (PAGE) and electroblotted onto PVDF membranes (Hybond, Amersham) overnight at 4°C. Equal sample loading was controlled by staining membranes with Poinceau S. After washing with PBS/Tween-20 (PBS/T) pH 7.2 or Tris/Tween-20 (TBS/T) pH 7.6, membranes were blocked for 1 h in blocking solution (5% non-fat dry milk in PBS containing 0.5% Tween-20 or in TBS containing 0.1% Tween-20). Then, membranes were incubated with the first antibody (in blocking solution, dilution 1:500 to 1:1000) by gently rocking at 4°C, overnight. Thereafter, the membranes were washed with PBS or TBS and further incubated with the second antibody (peroxidase-conjugated goat anti-rabbit IgG or anti-mouse IgG, dilution 1:2000 to 1:5000 in PBS/T or TBS/T) at room temperature for 1 h. Chemoluminescence was developed by the ECL detection kit (Amersham, UK) and then membranes were exposed to Amersham Hyperfilms.

Immunoprecipitation

Cells were harvested, washed with PBS and lysed in total lysis buffer (containing 20 mM HEPES, pH 7.9, 0.4 mM NaCl, 2.5% glycerol, 1 mM ethylenediamine tetraaceticacid, 1 mM PMSF, 0.5 mM NaF, 0.5 mM Na_3VO_4 supplemented with 2 μg/ml aprotinin, 2 μg/ml leupeptin, 0.3 μg/ml benzamidin chloride and 10 μg/ml trypsin inhibitor) by repeated freezing and thawing. Supernatants were collected by centrifugation and protein concentrations were determined using the Bio-Rad protein assay. For immunoprecipitation, crude cell extracts (150–300 μg) were precleared with 20 μl Protein G-Sepharose beads at 4°C for 30–60 min. Afterwards, the indicated primary antibodies against Cdc25A (F6), Cdc25A (M191), HA or Hsp90 were added and incubated with constant rotation at 4°C (overnight). After complex formation, immunoprecipitates were washed three times with buffer containing 50 mM Tris–HCl, pH 8.0, 1% NP-40, 150 mM NaCl, 10 mM β-glycerophosphate, 1 mM NaF, 0.1 mM Na_3VO_4, 0.2 mM PMSF supplemented with protease inhibitors. Immunoprecipitated proteins were then denatured and separated from the sepharose beads by adding SDS-sample buffer and boiling for 5 min (40,41).

Cell cycle distribution analysis

HEK293 cells were seeded in 6-wells and incubated at 37°C for 24 h. At a confluence of 70%, cells were exposed to 42°C for 20 min. After 12, 24 and 48 h, cells were harvested, washed with 5 ml cold PBS, centrifuged (600 rpm for 5 min) and re-suspended and fixed in 3 ml cold ethanol (70%) for 30 min at 4°C. After two further washing steps with cold PBS, RNaseA and propidium iodide were added to a final concentration of 50 μg/ml each and incubated at 4°C for 60 min before measurement. Cells were analysed on a FACSCalibur flow cytometer (BD Biosciences, San Jose, CA, USA) and cell cycle distribution was calculated with ModFit LT software (Verity Software House, Topsham, ME, USA).

Immunofluorescence

HeLa cells transiently transfected with wtCdc25A and dmtCdc25A were grown on chamber slides and exposed to 42°C HS for 20 min. Then, cells were washed with PBS and fixed in 4% paraformaldehyde (10 min at room temperature), washed three times with PBS and permeabilized with 0.1% Triton X-100 in PBS at room temperature for 10 min. Then, cells were washed three times with PBS and incubated in 10% goat serum diluted with PBS pH 7.5 for 30 min to block unspecific binding of the antibodies. Thereafter, the cells were incubated with the primary antibody (dilution 1:50 in 2% BSA/PBS) in a humid chamber at room temperature for 45 min and then washed three times with PBS. Afterwards cells were incubated with fluorescence-labelled second antibody (dilution 1:1000 in PBS) in a humid chamber at room temperature for 45 min and then washed three times with PBS. Finally, cells were incubated with DAPI (dilution 1:50 000) at room temperature for 1 min and washed with PBS. The slides were covered with Mowiol and the analysis

was performed using a Zeiss LSM5 Exicter confocal microscope using a 63× objective.

BrdU incorporation

HEK293 cells were seeded in 6-wells, then exposed to 42°C for 20 and 60 min and post-incubated with 10 μM of BrdU for 2 h. Cells were prepared following the instructions of the manufacturer (BrdU Flow Kit, Cat. No.: 552598, BD Pharmingen), except for the incubation with the fluorescent anti-BrdU antibody, which was incubated overnight at 4°C (dilution of 1:50). Afterwards, the BrdU incorporation was measured and analysed by a FACSCalibur flow cytometer.

Determination of cell death—Hoechst 33258/propidium iodide double-staining

To measure apoptosis in MCF-7 clones, cells were seeded in 6-well plates, grown to 30% confluence, treated for increasing times with 42°C HS, and were subsequently post-incubated at 37°C for 48 and 72 h. Then, Hoechst 33258 and propidium iodide (final concentrations 5 μg/ml and 2 μg/ml, respectively) was directly added to the culture medium for 1 h, and stained cells were examined under a fluorescence microscope with a DAPI filter, photographed, analysed and counted. Experiments were performed in triplicate.

Statistics

Experiments were performed in triplicate and analysed using *t*-test (GraphPad Prism 4.0 program).

ACKNOWLEDGEMENTS

We thank Dr Piwnica-Worms for the Ser177Ala-Tyr506Ala-dmtCdc25A construct and Dr Y. Yoneda for the 14.3.3 constructs, Dr David Beach for the cdc25A DNA, Dr Thomas Ströbel for the p38MAPK inhibitor and Toni Jäger for preparing the figures.

Conflict of Interest statement. None declared.

FUNDING

This work was supported by the Herzfeldersche Familienstiftung, the Hochschuljubiläums-stiftung (H-01595/2007) and the Unruhe Privatstiftung to G.K.

REFERENCES

1. Nitta, M., Okamura, H., Aizawa, S. and Yamaizumi, M. (1997) Heat shock induces transient p53-dependent cell cycle arrest at G1/S. *Oncogene*, **15**, 561–568.
2. Park, H.G., Han, S.I., Oh, S.Y. and Kang, H.S. (2005) Cellular responses to mild heat stress. *Cell. Mol. Life Sci.*, **62**, 10–23.
3. Fuse, T., Yamada, K., Asai, K., Kato, T. and Nakanishi, M. (1996) Heat shock-mediated cell cycle arrest is accompanied by induction of p21 CKI. *Biochem. Biophys. Res. Commun.*, **225**, 759–763.
4. Han, S.Y., Oh, S.Y., Jeon, W.J., Kim, J.M., Lee, J.H., Chung, H.Y., Choi, Y.H., Yoo, M.A., Kim, H.D. and Kang, H.S. (2002) Mild heat shock induces cyclin D1 synthesis through multiple Ras signal pathways. *FEBS Lett.*, **515**, 141–145.
5. Goloudina, A., Yamaguchi, H., Chervyakova, D.B., Appella, E., Fornace, A.J. Jr and Bulavin, D.V. (2003) Regulation of human Cdc25A stability by serine 75 phosphorylation is not suficient to activate a S-phase checkpoint. *Cell Cycle*, **2**, 473–478.
6. Khaled, A.R., Bulavin, D.V., Kittipatarin, C., Li, W.Q., Alvarez, M., Kim, K., Young, H.A., Fornace, A.J. and Durum, S.K. (2005) Cytokine-driven cell cycling is mediated through Cdc25A. *J. Cell. Biol.*, **169**, 755–763.
7. Kittipatarin, C., Li, W.Q., Bulavin, D.V., Durum, S.K. and Khaled, A.R. (2006) Cell cycling through Cdc25A: transducer of cytokine proliferative signals. *Cell Cycle*, **5**, 907–912.
8. Hassepass, I., Voit, R. and Hoffmann, I. (2003) Phosphorylation at serine 75 is required for UV-mediated degradation of human Cdc25A phosphatase at the S-phase checkpoint. *J. Biol. Chem.*, **278**, 29824–29829.
9. Xiao, Z., Chen, Z., Gunasekera, A.H., Sowin, T.J., Rosenberg, S.H., Fesik, S. and Zhang, H. (2003) Chk1 mediates S and G2 arrests through Cdc25A degradation in response to DNA-damaging agents. *J. Biol. Chem.*, **278**, 21767–21773.
10. Agner, J., Falck, J., Lukas, J. and Bartek, J. (2005) Differential impact of diverse anticancer chemotherapeutics on the Cdc25A-degradation checkpoint pathway. *Exp. Cell Res.*, **302**, 162–169.
11. Mailand, N., Falck, J., Lukas, C., Syljuâsen, R.G., Welcker, M., Bartek, J. and Lukas, J. (2000) Rapid destruction of human Cdc25A in response to DNA damage. *Science*, **288**, 1425–1429.
12. Falck, J., Mailand, N., Syljuåsen, R.G., Bartek, J. and Lukas, J. (2001) The ATM-Chk2-Cdc25A checkpoint pathway guards against radioresistant DNA synthesis. *Nature*, **410**, 842–847.
13. Busino, L., Donzelli, M., Chiesa, M., Guardavaccaro, D., Ganoth, D., Dorrello, N.V., Hershko, A., Pagano, M. and Draetta, G.F. (2003) Degradation of Cdc25A by beta-TrCP during S phase and in response to DNA damage. *Nature*, **426**, 87–91.
14. Karlsson-Rosenthal, C. and Millar, J.B.A. (2006) Cdc25: mechanisms of checkpoint inhibition and recovery. *Trends Cell. Biol.*, **16**, 285–292.
15. Ray, D. and Kiyokawa, H. (2008) CDC25A phosphatase: a rate-limiting oncogene that determines genomic stability. *Cancer Res.*, **68**, 1251–1253.
16. Chen, M.S., Ryan, C.E. and Piwnica-Worms, H. (2003) Chk1 kinase negatively regulates mitotic function of Cdc25A phosphatase through 14-3-3 binding. *Mol. Cell. Biol.*, **23**, 7488–7497.
17. Busino, L., Chiesa, M., Draetta, G.F. and Donzelli, M. (2004) Cdc25A phosphatase: combinatorial phosphorylation, ubiquitylation and proteolysis. *Oncogene*, **23**, 2050–2056.
18. Davezac, N., Baldin, V., Gabrielli, B., Forrest, A., Theis-Febvre, N., Yashida, M. and Ducommun, B. (2000) Regulation of CDC25B phosphatases subcellular localization. *Oncogene*, **19**, 2179–2185.
19. Esmenjaud-Mailhat, C., Lobjois, V., Froment, C., Golsteyn, R., Monsarrat, B. and Ducommun, B. (2007) Phosphorylation of CDC25C at S263 controls its intracellular localisation. *FEBS Lett.*, **581**, 3979–3985.
20. Sekimoto, T., Fukumoto, M. and Yoneda, Y. (2004) 14-3-3 suppresses the nuclear localization of threonine 157-phosphorylated p27Kip1. *EMBO J.*, **23**, 1934–1942.
21. Arlander, S.J., Felts, S.J., Wagner, J.M., Stensgard, B., Toft, D.O. and Karnitz, L.M. (2006) Chaperoning checkpoint kinase 1 (Chk1), an Hsp90 client, with purified chaperones. *J. Biol. Chem.*, **281**, 2989–2998.
22. Mesa, R.A., Loegering, D., Powell, H.L., Flatten, K., Arlander, S.J., Dai, N.T., Heldebrant, M.P., Vroman, B.T., Smith, B.D., Karp, J.E. *et al.* (2005) Heat shock protein 90 inhibition sensitizes acute myelogenous leukemia cells to cytarabine. *Blood*, **106**, 318–327.
23. García-Morales, P., Carrasco-García, E., Ruiz-Rico, P., Martínez-Mira, R., Menéndez-Gutiérrez, M.P., Ferragut, J.A., Saceda, M. and Martínez-Lacaci, I. (2007) Inhibition of Hsp90 function by ansamycins causes downregulation of cdc2 and cdc25c and G(2)/M arrest in glioblastoma cell lines. *Oncogene*, **26**, 7185–7193.
24. Basso, A.D., Solit, D.B., Chiosis, G., Giri, B., Tsichlis, P. and Rosen, N. (2002) Akt forms an intracellular complex with heat shock protein 90 (Hsp90) and Cdc37 and is destabilized by inhibitors of Hsp90 function. *J. Biol. Chem.*, **277**, 39858–39866.
25. Kamal, A., Boehm, M.F. and Burrows, F.J. (2004) Therapeutic and diagnostic implications of Hsp90 activation. *Trends Mol. Med.*, **10**, 283–290.
26. Schulte, T.W., Blagosklonny, M.V., Ingui, C. and Neckers, L. (1995) Disruption of the Raf-1-Hsp90 molecular complex results in

destabilization of Raf-1 and loss of Raf-1-Ras association. *J. Biol. Chem.*, **270**, 24585–24588.
27. Galaktionov, K., Jessus, C. and Beach, D. (1995) Raf1 interaction with Cdc25 phosphatase ties mitogenic signal transduction to cell cycle activation. *Genes Dev.*, **9**, 1046–1058.
28. Fuhrmann, G., Leisser, C., Rosenberger, G., Grusch, M., Huettenbrenner, S., Halama, T., Mosberger, I., Sasgary, I.S., Cerni, C. and Krupitza, G. (2001) Cdc25A phosphatase suppresses apoptosis induced by serum deprivation. *Oncogene*, **20**, 4542–4553.
29. Holmes, J.L., Sharp, S.Y., Hobbs, S. and Workman, P. (2008) Silencing of HSP90 cochaperone AHA1 expression decreases client protein activation and increases cellular sensitivity to the HSP90 inhibitor 17-allylamino-17-demethoxygeldanamycin. *Cancer Res.*, **68**, 1188–1197.
30. Xiao, L., Lu, X. and Ruden, D.M. (2006) Effectiveness of hsp90 inhibitors as anti-cancer drugs. *Mini Rev. Med. Chem.*, **6**, 1137–1143.
31. Drysdale, M.J., Brough, P.A., Massey, A., Jensen, M.R. and Schoepfer, J. (2006) Targeting Hsp90 for the treatment of cancer. *Curr. Opin. Drug Discov. Devel.*, **9**, 483–495.
32. Sharp, S. and Workman, P. (2006) Inhibitors of the HSP90 molecular chaperone: current status. *Adv. Cancer Res.*, **95**, 323–348.
33. Chen, L., Chen, D., Zhang, Z., Fang, F., Wu, Y., Luo, L. and Yin, Z. (2007) Heat shock protein 90 regulates the stability of c.Jun in HEK293 cells. *Mol. Cells*, **24**, 210–214.
34. Pearl, L.H. and Prodromou, C. (2006) Structure and mechanism of the Hsp90 molecular chaperone machinery. *Annu. Rev. Biochem.*, **75**, 271–294.
35. Murapa, P., Gandhapudi, S., Skaggs, H.S., Sarge, K.D. and Woodward, J.G. (2007) Physiological fever temperature induces a protective stress response in T lymphocytes mediated by heat shock factor-1 (HSF1). *J. Immunol.*, **179**, 8305–8312.
36. Jin, J., Shirogane, T., Xu, L., Nalepa, G., Qin, J., Elledge, S.J. and Harper, J.W. (2003) SCFbeta-TRCP links Chk1 signaling to degradation of the Cdc25A protein phosphatase. *Genes Dev.*, **17**, 3062–3074.
37. Donzelli, M., Busino, L., Chiesa, M., Ganoth, D., Hershko, A. and Draetta, G.F. (2004) Hierarchical order of phosphorylation events commits Cdc25A to betaTrCP-dependent degradation. *Cell Cycle*, **3**, 469–471.
38. Takizawa, C.G. and Morgan, D.O. (2000) Control of mitosis by changes in the subcellular location of cyclin-B1-Cdk1 and Cdc25C. *Curr. Opin. Cell. Biol.*, **12**, 658–665.
39. Boutros, R., Lobjois, V. and Ducommun, B. (2007) CDC25 phosphatases in cancer cells: key players? Good targets? *Nat. Rev. Cancer*, **7**, 495–507.
40. Rosner, M., Freilinger, A., Hanneder, M., Fujita, N., Lubec, G., Tsuruo, T. and Hengstschlaeger, M. (2007) p27Kip1 localization depends on the tumor suppressor protein tuberin. *Hum. Mol. Genet.*, **16**, 1541–1556.
41. Rosner, M. and Hengstschlaeger, M. (2008) Cytoplasmic and nuclear distribution of the protein complexes mTORC1 and mTORC2: rapamycin triggers dephosphorylation and delocalisation of the mTORC2 components rictor and sin1. *Hum. Mol. Genet.*, **17**, 2934–2948.

In vitro anti-leukemic activity of the ethno-pharmacological plant Scutellaria orientalis ssp. carica endemic to western Turkey.

Ozmen A., Madlener S., Bauer S., Krasteva S., Vonach C., **Giessrigl B.**, Gridling M., Viola K., Stark N., Saiko P., Michel B., Fritzer-Szekeres M., Szekeres T., Askin-Celik T., Krenn L. and Krupitza G.

Phytomedicine 17: 55-62, **2010.**

Phytomedicine 17 (2010) 55–62

Contents lists available at ScienceDirect

Phytomedicine

journal homepage: www.elsevier.de/phymed

In vitro anti-leukemic activity of the ethno-pharmacological plant *Scutellaria orientalis* ssp. *carica* endemic to western Turkey

Ali Özmen [a,b], Sibylle Madlener [b], Sabine Bauer [b], Stanimira Krasteva [c], Caroline Vonach [b], Benedikt Giessrigl [b], Manuela Gridling [b], Katharina Viola [b], Nicole Stark [b], Philipp Saiko [d], Barbara Michel [b,d], Monika Fritzer-Szekeres [d], Thomas Szekeres [d], Tülay Askin-Celik [a], Liselotte Krenn [c], Georg Krupitza [b,*]

[a] *Institute of Biology, Fen-Edebiyat Fakültesi, Adnan Menderes Üniversitesi, Aydin, Turkey*
[b] *Institute of Clinical Pathology, Medical University of Vienna, Waehringer Guertel 18-20, A-1090 Vienna, Austria*
[c] *Department of Pharmacognosy, Faculty of Life Sciences, University of Vienna, Austria*
[d] *Clinical Institute of Medical and Chemical Laboratory Diagnostics, Medical University of Vienna, Vienna, Austria*

ARTICLE INFO

Keywords:
Scutellaria orientalis ssp. carica
Leukemia
Apoptosis
Cell cycle inhibition
γ-H2AX

ABSTRACT

Aim of this study: Within the genus *Scutellaria* various species are used in different folk medicines throughout Asia. Traditional Chinese Medicine (TCM) uses *S. baicalensis* (Labiatae) to treat various inflammatory conditions. The root shows strong anticancer properties *in vitro* and was suggested for clinical trials against multiple myeloma. Further, *S. barbata* was successfully tested against metastatic breast cancer in a phase I/II trial. Therefore, we investigated the anti-cancer properties of *S. orientalis* L. ssp. *carica* Edmondson, an endemic subspecies from the traditional medicinal plant *S. orientalis* L. in Turkey, which is used to promote wound healing and to stop haemorrhage.

Materials and methods: Freeze-dried plant material was extracted with petroleum ether, dichloromethane, ethyl acetate, and methanol and the bioactivity of these extracts was analysed by proliferation assay, cell death determination, and by investigating protein expression profiles specific for cell cycle arrest and apoptosis.

Results: The strongest anti-leukemic activity was shown by the methanol extract, which contained apigenin, baicalein, chrysin, luteolin and wogonin, with an IpC50 of 43 μg/ml (corresponding to 1.3 mg/ml of dried plant material) which correlated with cyclin D1- and Cdc25A suppression and p21 induction. At 132 μg/ml (= 4 mg/ml of the drug) this extract caused genotoxic stress indicated by substantial phosphorylation of the core histone H2AX (γ-H2AX) followed by activation of caspase 3 and signature-type cleavage of PARP resulting in a 55% apoptosis rate after 48 hours of treatment.

Conclusions: Here, we report for the first time that *S. orientalis* L. ssp. *carica* Edmondson exhibited potent anti-leukaemic properties likely through the anti-proliferative effect of baicalein and the genotoxic property of wogonin.

© 2009 Elsevier GmbH. All rights reserved.

Introduction

Some 60% of all drugs used in western medicine are derived from natural compounds, which served as leads (Cragg et al. 2006). One approach to discover novel lead compounds against cancer is the consideration of ancient ethno-medicinal knowledge and the investigation of locally available natural resources (Verpoorte 2000, Pieters and Vlietinck 2005).

A very rich plant diversity is found in Western Turkey which includes Scutellaria species such as *S. orientalis* L. traditionally used to promote wound healing or *Scutellaria orientalis* L. ssp. *carica* Edmondson, an endemic subspecies. Recently, the genus *Scutellaria* has gained considerable interest concerning anti-cancer activities. Ethanol extracts of the species *S. barbata* inhibited A549 cell growth with a mechanism that included apoptotic effects (Yin et al. 2004). Three neoclerodane diterpenoids and five new neoclerodane diterpenoid alkoloids isolated from *S. barbata* showed significant cytotoxic activities against three human cancer cell lines; HONE-1, KB and HT29 (Dai et al. 2006, 2007). In HL-60 cells *S. barbata* extract caused apoptosis and decreased the expression of cyclins and cyclin-dependent kinases (Kim et al. 2007), and this plant was tested against metastatic breast cancer in a phase I/II trial (http://tinyurl.com/2oyohu; Rugo et al. 2007). Recent investigations demonstrated the anti-proliferative effects of *S. baicalensis* in acute lymphatic leukaemia (ALL)-, lymphoma- and myeloma cell lines. Growth inhibition

* Corresponding author. Tel.: +43 1 40400 3487; fax: +43 1 40400 3707.
E-mail address: georg.krupitza@meduniwien.ac.at (G. Krupitza).

0944-7113/$ - see front matter © 2009 Elsevier GmbH. All rights reserved.
doi:10.1016/j.phymed.2009.06.001

correlated with increased levels of the Cdk inhibitor p27 and with decreased levels of the *c-myc* proto-oncogene, whereas cytotoxicity was associated with mitochondrial damage and the modulation of the *bcl* gene family (Kumagai et al. 2007). In the two human prostate cancer cell lines LNCaP and PC-3 *S. baicalensis* extract inhibited COX-2 activity and consequently reduced PGE2 synthesis, and this was accompanied by suppression of cyclin D1 and downregulation of Cdk1 activity (Ye et al. 2007). *S. baicalensis*, known as Huang-qin or wogon, is the most commonly prescribed plant in Traditional Chinese Medicine (TCM) and also extensively used in Japanese Kampo medicines. TCM uses the root of *S. baicalensis* (from Huang-Lian-Jie-Du-Tang) to treat various inflammatory conditions and was suggested for clinical trials against multiple myeloma (Ma et al. 2005). *S. baicalensis* and *S. rivularis* have been reported to contain a large number of flavonoids which inhibited the proliferation of HL-60 promyeloic leukaemia cells (Sonoda et al. 2004), and the purified components wogonin and baicalein have been studied in detail (Lee et al. 2008) and showed anticancer effects in human hepatoma cell lines (Himeji et al. 2007). It has not been investigated though, whether wogonin and baicalein are common within the *Scutellaria* genus and causal for the medicinal activity of the other species (Cole et al. 2008). Here we analysed for the first time the anti-leukaemic properties of extracts of *S. orientalis* ssp. *carica* in p53-deficient HL-60 promyeloic leukaemia cells, determined the concentration of wogonin and baicalein and compared the activity profile of the methanolic extract with that of purified wogonin and baicalein to elucidate the respective mechanisms responsible for growth arrest and cell death induction.

Material methods

Plant material

Scutellaria orientalis ssp. *carica* has been collected in April 2007 from South-West of Turkey (Karacasu-AYDIN, 368 m).

The botanical identification was made by Dr. Mesut Kirmaci using the serial "Flora of Turkey and the East Aegean Islands" (Davis et al. 1965–1988). Voucher specimens were deposited in the herbarium of Department of Biology, Adnan Menderes University.

Sample preparation

Plants were freeze dried, then the plant material was milled and extracted in a solvent-series of increasing polarity (petroleum ether, dichloromethane, ethyl acetate and methanol). To 50 g of plant material 500 ml solvent were added. After finishing the first soxhlet extraction (at 40 °C for approximately12 h, until the solvent became colourless) with petroleum ether, subsequent to filtration the plant material was dried and subjected sequentially to the second extraction with dichloromethane, the third extraction with ethyl acetate, and fourth extraction with methanol (Krenn et al. 2003; Marchart et al. 2003; Dolezal et al. 2006). The extracts were evaporated and yielded 8.24 μg, 21.8 μg, 6.48 μg, and 32.98 μg per 1 mg dried plant weight, respectively, and were dissolved in 40 μl ethanol. Baicalein and wogonin were dissolved in DMSO (50 mM stock solutions) and stored under nitrogen gas. For the proliferation- and apoptosis assays following concentrations (as calculated for dried plant material) were used: 500 μg/ml, 1 mg/ml, 4 mg/ml, 20 mg/ml. To exclude the effect of ethanol on cell proliferation and apoptosis, controls were treated with similar concentrations of ethanol as used for sample treatment (in general ~0.4% EtOH). Baicalein (Calbiochem) and wogonin (Biomol) were used in a concentration range which covered the wogonin and baicalein content determined in the methanolic extract (0.1, 1, 5 and 10 μM).

HPLC-analysis

The methanolic extract was analyzed by HPLC under the following conditions: Column: 5 μm ACE 3 C18 (150 × 3 mm, ACE, Aberdeen, Great Britain); mobile phase: acetonitrile (A) and 0.3% acetic acid (B); gradient elution: 0–20 min 12–28% A; 20–50 min 28–32% A; 50–55 min 32–46% A; 55–56 min 46–100% A; 56–66 min 100% A; flow rate 0.4 ml/min; wavelength of detection 270 nm. The content of apigenin, baicalein, chrysin, luteolin and wogonin in the methanolic extract was quantified by external standardisation. Apigenin and luteolin were purchased from Chromadex (USA), wogonin was from Calbiochem (San Diego), baicalein from Biomol (Plymouth Meeting, PA), and chrysin from C. Roth (Germany).

Reagents and antibodies

Hoechst 33258 and propidium iodide were purchased from Sigma. Wogonin was purchased from Calbiochem and baicalein from Biomol. Pierce ECL Western Blotting Substrate Cat# 32106 was from Pierce.

Antibodies: Mouse monoclonal (ascites fluid) anti-acetylated tubulin clone 6-11B1 Cat# T6793, and mouse monoclonal (ascites fluid) anti-β-actin clone AC-15 Cat# A5441, were from Sigma. Rabbit polyclonal anti cdc25A (M191) Cat# sc-7157, anti α-tubulin (TU-02) Cat# sc-8035, PARP-1 (F-2) Cat# sc-8007, anti-cyclin D1 (M-20) Cat# sc-718, and p21 (C-19) Cat# sc-397 were from Santa Cruz Biotec. Inc. Rabbit monoclonal anti-active Caspase-3 (CPP32) clone C92-605 Cat# 58404 was from Research Diagnostics Inc. Polyclonal anti-MEK 1/2 Cat# 9122, polyclonal anti-phospho-MEK 1/2 (Ser 217/221) Cat# 9121 m, monoclonal rabbit anti-p44/42 MAP Kinase (137F5) Cat# 4695, and mouse monoclonal anti-phospho-p44/42 MAPK (Thr202/Tyr204) (E10) Cat# 9106 were from Cell Signaling and rabbit polyclonal phospho detect anti-H2AX (pSER^{139}) Cat# dr-1017 was from Calbiochem. Anti mouse IgG was from Dako and anti rabbit IgG from GE-Healthcare.

Amersham Hyperfilms ECL-High performance chemiluminescence film was from GE-Healthcare.

Cell culture

HL-60 promyeloic leukaemia cells were purchased from ATCC. Cells were grown in RPMI 1640 medium supplemented with 10% heat inactivated fetal calf serum, 1% L-glutamine and 1% penicillin/streptomycin at 37 °C in a humidified atmosphere containing 5% CO_2. All media and supplements were obtained from Life Technologies.

Proliferation inhibition assay

HL 60 cells were seeded in T-25 tissue culture flasks at a concentration of 1×10^5 cells per ml cell culture medium and incubated with increasing concentrations of extracts corresponding to 500 μg/ml, 1 mg/ml, 4 mg/ml, 20 mg/ml of dried plant material and indicated concentrations of baicalein, wogonin, or 2′-deoxy-5-fluorodeoxyuridine (5-FdUrd; Sigma Aldrich), which was used as a positive control. Cell counts and IC_{50} values were determined at 24 and 48 h using the method described earlier (Maier et al. 2006; Strasser et al. 2006).

Hoechst 33258 and propidium iodide double staining

HL-60 cells (1×10^5 per ml) were seeded in T-25 Nunc tissue culture flask and exposed to increasing concentrations of plant extracts corresponding to 500 μg/ml, 1 mg/ml, 4 mg/ml, 20 mg/ml of the drug, or to the indicated concentrations of 5-FdUrd for 24 and 48 hours. Cell death quantification by Hoechst 33258 and propidium iodide staining, which facilitates to distinguish between apoptosis and necrosis, was performed according to the method described by Grusch et al. (2002).

Western blotting

HL-60 cells (1.5×10^7) were seeded into T-75 Nunc tissue culture flasks and incubated with 132 μg/ml methanol extract (corresponding to 4 mg/ml dried plant material, which contains 490 ng/ml and 150 ng/ml baicalein and wogonin, respectively), or with 1, 5 and 10 μM baicalein and wogonin (10 μM baicalein corresponds to 2.7 μg/ml, and 10 μM wogonin corresponds to 2.84 μg/ml) for 0.5, 2, 4, 8 and 24 hours or with 250 nM 5-FdUrd for control reasons. Then 1×10^6 cells were harvested (per experimental point), and prepared for Western blot analyses as described by Gridling et al. (2009).

Statistics

All experiments were done in triplicate and analysed by t-test (GraphPad Prism 4.0 program).

Results

Anti-proliferative activity of the extracts, baicalein, wogonin and 5-FdUrd

Four solvents of increasing polarity were subsequently used to extract bioactive constituents from the freeze-dried material of *S. orientalis* ssp. *carica*. After evaporation the dried extracts were dissolved in ethanol and HL-60 cells were subjected to increasing concentrations of the extracts or baicalein and wogonin. The percentage of HL-60 cell cycle inhibition was calculated. In general, extracts with increasing polarity exhibited increased proliferation-inhibitory activity in HL-60 cells (Fig. 1a-d). The highest activity was determined for the methanol extract with an I_pC_{50} of 43 μg/ml (corresponding to appr. 1.3 mg of dried plant material/ml; Fig. 1d). Hence, further analyses were performed with the methanol extract. As a control the methanol extract of green salad was tested. 4 mg/ml methanol extract of salad did not exhibit cytostatic activity, whereas the 20 mg/ml concentration was slightly anti-proliferative, which suggested that polar plant extracts generally contain weak growth-inhibitory constituents (Fig. 1e). Baicalein inhibited HL-60 growth with a similar efficiency as the methanolic extract, whereas wogonin was almost ineffective (10 μM baicalein = 2.7 μg/ml); 16.5 μg/ml methanolic extract (corresponding to 0.5 mg/ml dried plant material) contain ~61 ng/ml baicalein and ~19 ng/ml wogonin; (Figs. 1f-g). As a positive proliferation-inhibiting control increasing concentrations 5-FdUrd were applied (Fig. 1h).

Downregulation of cyclin D1 and upregulation of p21 by the methanol extract

Due to the strong anti-proliferative activity of the methanol extract the expression profiles of positive and negative cell cycle regulators (cyclin D1 and p21, respectively) were analyzed to investigate by which mechanisms the anti-cancer activity was accomplished. 132 μg/ml extract markedly repressed cyclin D1 expression in HL-60 cells after 2 hours of treatment and Cdc25A levels decreased after 8 hours (Fig. 2a). Furthermore, this extract transiently induced p21 after 30 min, which dropped after 4 hours (Fig. 2b). Since HL-60 cells are p53 deficient (Biroccio et al. 1999), the upregulation of p21, which is a prominent transcriptional target of p53, must have been triggered by another pathway. Besides p53, also the activation of the MEK – Erk pathway was shown to upregulate p21 (Park et al. 2004; Facchinetti et al. 2004). Therefore, MEK – Erk signaling was investigated utilizing phospho-specific antibodies. Erk became phosphorylated at Tyr204 within 30 min of treatment with 132 μg/ml of the extract and this correlated with the timing of p21 upregulation. The phosphorylated form of Erk persisted at least for 8 h and disappeared after 24 h (Fig. 2b). This is an unusually long time period for Erk activity, which is known in other contexts to last only some 10–20 min (Ebner et al. 2007). MEK was constitutively phosphorylated and did not become further induced. Therefore, Erk might have become phosphorylated and induced by a kinase different from MEK. Erk became dose-dependently phosphorylated also upon treatment with Baicalein and wogonin. (Fig. 2c), and baicalein, but not wogonin, inhibited Cdc25A after 8 hours and also p21 was regulated after 24 hours such as by the methanolic plant extract within this time frame. Interestingly, wogonin dose-dependently up-regulated Cdc25A within 8 hours of treatment. Further, we investigated whether the methanol extract contained microtubule-directed activity. Tubulin is the major constituent of microtubules, which facilitate chromosome disjunction during mitosis, and therefore, the affection of tubulin structures is incompatible with functional cell division (Piperno and Fuller 1985). Hence it was investigated whether cell cycle arrest can be attributed to tubulin polymerization/de-polymerization as it is the case e.g. for taxol (Geney et al. 2005). A monoclonal anti-acetylated-α-tubulin antibody was used to analyse acetylated α-tubulin, which is an indirect way of analyzing tubulin status (i.e. polymerization/de-polymerization events). As shown in Fig. 2a, incubation of HL-60 cells with the methanol extract did not change the acetylation pattern of α-tubulin. Therefore, this extract did not contain tubulin-targeting activity. 250 nM 5-FdUrd was used as a control to monitor the effect on relevant cell cycle genes (as indicated in Fig. 2d).

Induction of caspase 3 and apoptosis by the methanol extract

One major property of cytotoxic anticancer drugs is the potential to elicit cancer cell death by apoptosis or by necrosis. Most anti-cancer drugs dose-dependently elicit apoptosis. Beyond a certain threshold level, at which the cellular ATP balance and therefore energy supply becomes corrupted, cells cannot maintain membrane integrity any longer and die by necrosis (Huettenbrenner et al. 2003). The methanol extract elicited predominantly apoptosis at lower concentrations 132 μg/ml), whereas 660 μg/ml resulted in necrosis (Fig. 3a). As a positive apoptosis-inducing control increasing concentrations 5-FdUrd were applied (Fig. 3b).

Western blot analysis showed that the induction of apoptosis with 132 μg/ml methanolic extract (corresponding to 4 mg/ml dried plant material) correlated with the activation of caspase 3 and the cleavage of its target PARP (Fig. 4). Thus, apoptotic cell death triggered by the methanol extract of *S. orientalis* ssp. *carica* was executed by caspase-3. To investigate whether genotoxicity of the methanol extract was responsible for apoptosis induction the phosphorylation status of histone H2AX (γ-H2AX) was analysed, because this core histone variant becomes rapidly phosphorylated

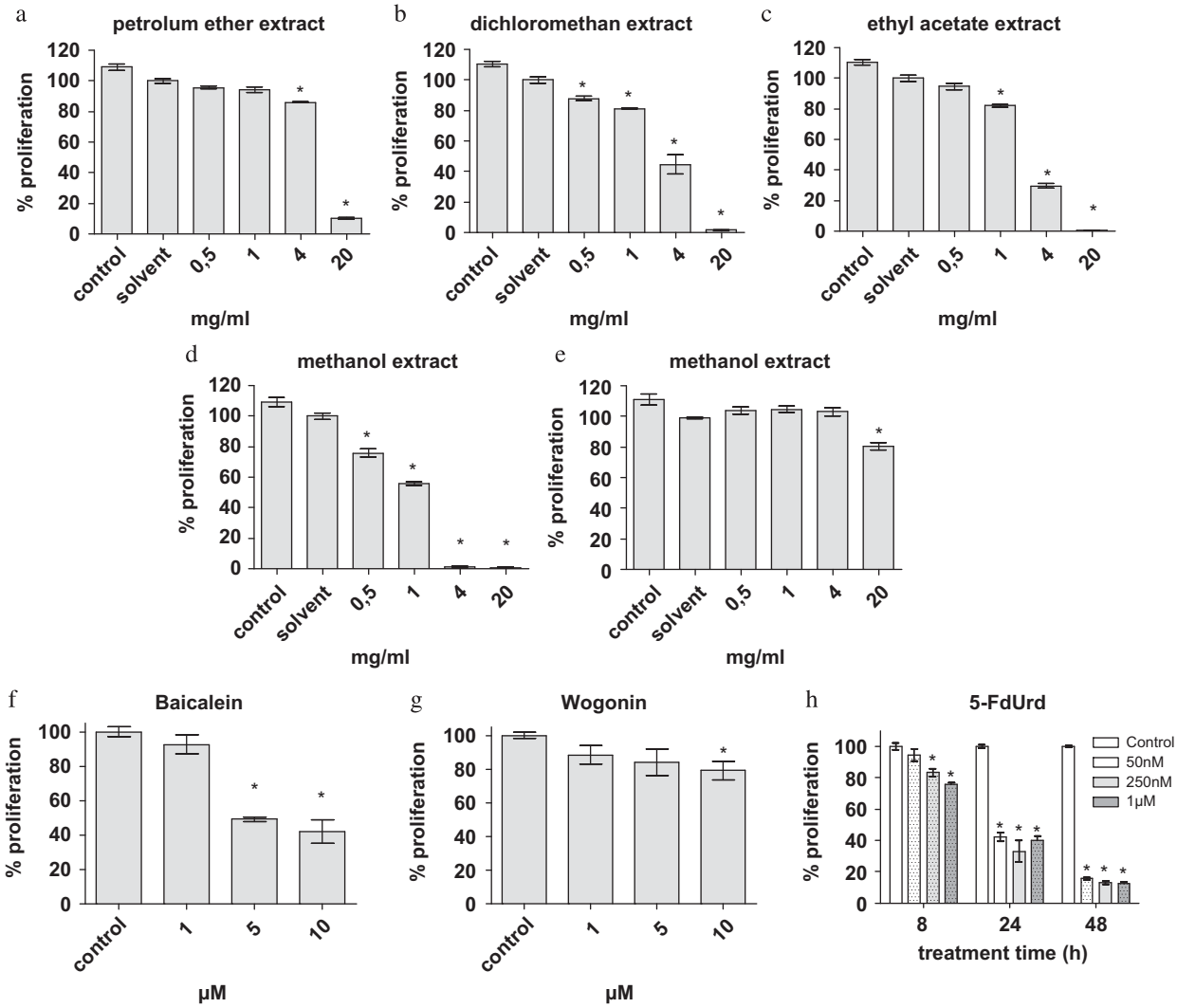

Fig. 1. Anti-proliferative effect of extracts of *Scutellaria orientalis* ssp. *carica* and of methanol extract of green salad (*Lactuca sativa L. var capitata*). HL-60 cells were seeded into T-25 tissue culture flasks (1×10^5 cells/ml), grown for 24 hours to enter logarithmic growth phase, and incubated with amounts of extracts corresponding to 0.5, 1, 4, and 20 mg/ml of dry plant material (a-d), or 1 µM, 5 µM, and 10 µM baicalein and wogonin (f, g) and for control reasons 50 nM, 250 nM and 1 µM 5-FdUrd (h). "Solvent" controls received 0.4% EtOH. The other samples were adjusted to equal ethanol concentrations to achieve similar solvent conditions. "Controls" did not receive any treatment. Cells were counted after 24 and 48 hours of treatment and the percentage of proliferation within this time span was calculated in comparison to controls ("solvent" controls were considered as 100% proliferating cells and all other conditions were set in relation to this). For control reasons, cells were exposed to the methanol extract of green salad (*L. sativa,* e). Error bars indicate SEM, and asterisks significant proliferation inhibition compared to control ($p < 0.05$).

in response to DNA double strand breaks (DSB). Incubation of HL-60 cells with 132 µg/ml methanol extract caused severe phosphorylation of H2AX before a substantial activation of caspase 3 became visible and thereafter γ-H2AX became ubiquitinylated (Fig. 4a). Ubiquitin-conjugated proteins accumulate at sites of DSB and are involved in the reorganization of chromatin in response to DSB (Ikura et al. 2007). It has been recently shown that H2AX also has non-nucleosomal functions, specifically, pro-apoptotic activities in gastrointestinal stroma tumour cells (Liu et al. 2008). Therefore, the methanol extract contained DNA-targeting activities, which triggered cell death. Further, cells were treated with limiting concentrations of baicalein and wogonin to test whether γ-H2AX occurs before caspase 3 cleavage and was therefore the cause for apoptosis and not the consequence of apoptotic DNA fragmentation. Whereas baicalein neither induced Caspase 3 cleavage nor γ-H2AX at the applied concentrations, wogonin induced γ-H2AX but not caspase 3 and this evidenced that γ-H2AX was upstream of caspase 3 cleavage and therefore causal for apoptosis induction and not a consequence of caspase-triggered DNA strand breaks (Fig. 4b). The results support the notion that wogonin was a pro-apoptotic factor and that baicalein caused cell cycle arrest. 250 nM 5-FdUrd was used as a control to monitor the effect on relevant apoptosis-relevant genes (as indicated in Fig. 4c).

Composition of the methanolic extract

HPLC-analyses of the methanolic extract showed flavonoids as major compounds. The genins apigenin, baicalein, chrysin, luteolin, oroxylin A and wogonin were identified by co-chromatography with authentic substances and comparison of PDA spectra (Zhang et al. 2007; Campos and Markham 2007), respectively. Additionally wogonoside, a second, more polar wogoninglycoside, an oroxylinglycoside and a baicaleinglycoside were tentatively identified via the PDA spectra (Fig. 5). The methanolic extract

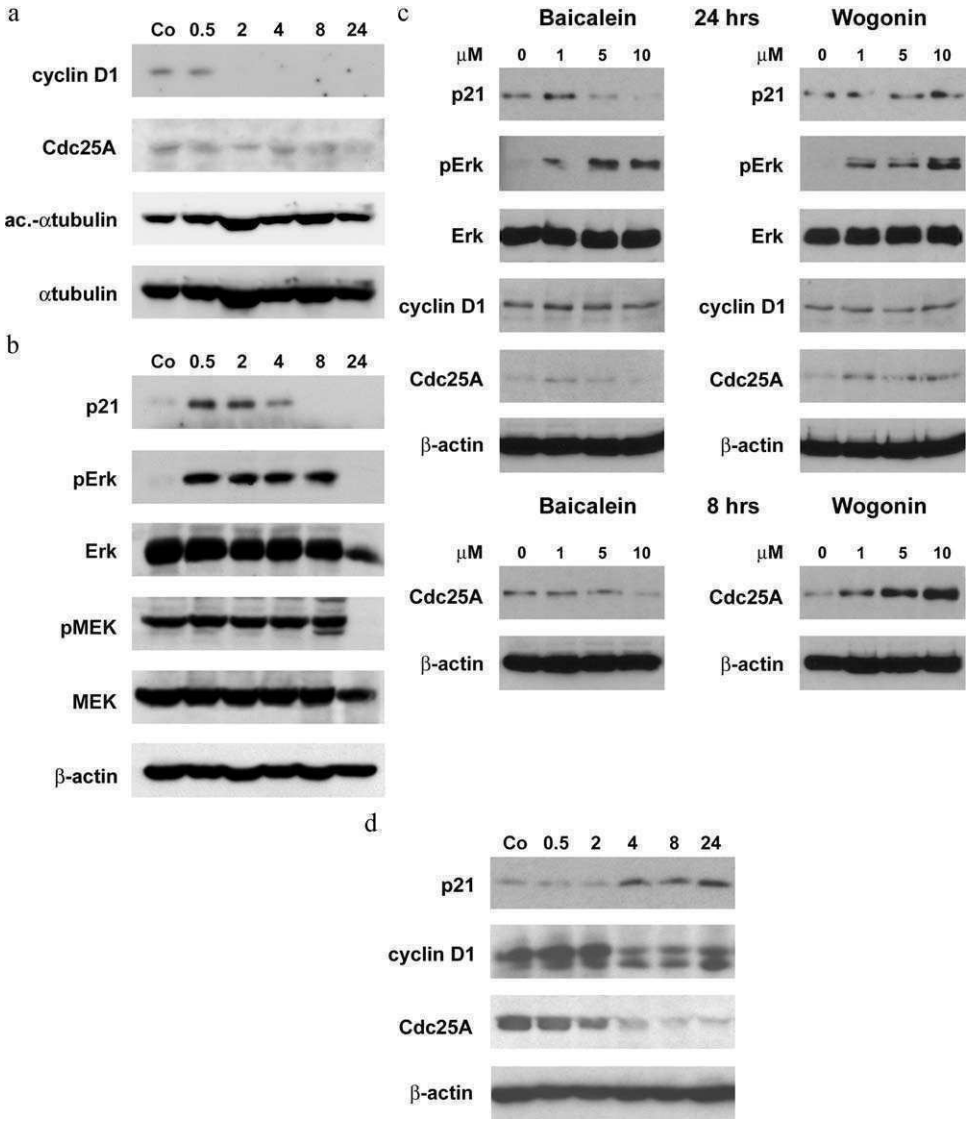

Fig. 2. Analysis of cell cycle-related protein and phospho-protein expression. HL-60 cells (1×10^6 cells) were seeded into T-75 tissue culture flasks and allowed to grow for 24 hours when cells were incubated with 132 μg/ml methanol extract (corresponding to 4mg/ml dried plant material) of *S. orientalis* ssp. *carica* for 0.5, 2, 4, 8, and 24 hours (a, b), with 1 μM, 5 μM and 10 μM concentrations baicalein and wogonin for 8 and 24 hours (c), and for control reasons with 250 nM 5-FdUrd for the indicated times (d). Then, isolated protein samples were subjected to electrophoretic separation and subsequent Western blot analysis using the indicated antibodies (anti phospho-MEK = pMEK, anti phospho Erk = pErk, anti acetylated α-tubulin = ac.α-tubulin). Equal sample loading was controled by Poinceau S staining, β-actin, and α-tubulin analysis.

contained 1.282% apigenin, 1.210% luteolin, 0.374% baicalein, 0.281% chrysin and 0.115% wogonin.

Discussion

Species of the genus *Scutellaria* are used in TCM and particularly the root of *S. baicalensis* (*Scutellariae radix*) is rich in flavonoids and the main constituent from "Huang-Lian-Jie-Du-Tang" (HLJDT) which is used against various inflammations and shows strong anticancer properties *in vitro* (Ma et al. 2005). Flavonoids are of interest for their anti-cancer and antioxidant activity, but previous research has not investigated whether these medicinally active phytochemicals are common to species within the *Scutellaria* genus and may be linked to the medicinal activity of these other species (Cole et al. 2008). Therefore, we studied the anti-leukaemic activity of *S. orientalis* L. ssp. *carica* Edmondson, an endemic medicinal plant used in Turkish folk medicine (called as "Kaside"), which is traditionally used for wound healing and stopping haemorrhage (Baytop 1999).

The major active principles of *Scutellariae radix* are the flavonoids baicalein and wogonin, which exhibited distinct activities on cellular functions (Chang et al. 2002; Nakahata et al. 1998; Yano et al. 1994) and showed anticancer effects on human hepatoma cell lines (Himeji et al. 2007). Other recent reports demonstrated that wogonin significantly inhibited human ovarian cancer cells A2780, human promyeloleukemic cells HL-60, monocytic leukemia THP-1 cells, osteogenic sarcoma HOS cells, bladder cancer KU-1- and EJ-1 cells, prostate cancer LNCaP- and PC-3 cells, hepatocellular carcinoma SK-HEP-1, SMMC-7721 and Bel-7402 cells, and murine sarcoma S180 cells and induced apoptosis in human prostate carcinoma LNCaP and human colon

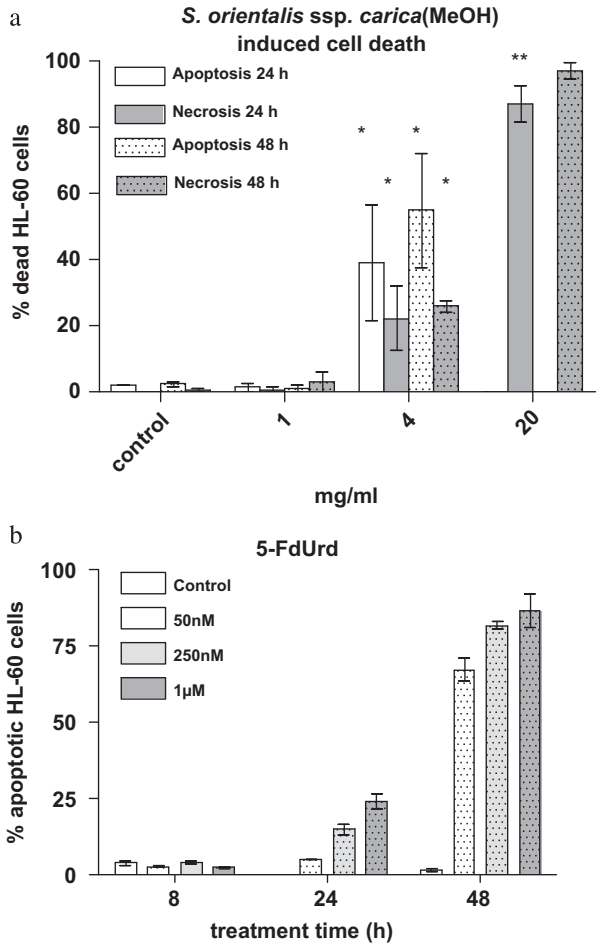

Fig. 3. Induction of apoptosis and necrosis by the methanol extract of *Scutellaria orientalis* ssp. *carica*. Cells were incubated with increasing extract concentrations (a), and for control reasons with 5-FdUrd (b) for 24 and 48 hours and then double stained with Hoechst 33258 and propidium iodide. Afterwards cells were examined under the microscope with UV light connected to a DAPI filter. Nuclei with morphological changes which indicated apoptosis or necrosis (see "Methods") were counted and percentages of vital, apoptotic and necrotic cells were calculated. Error bars indicate SEM, and asterisks significant apoptosis induction compared to control ($p < 0.05$).

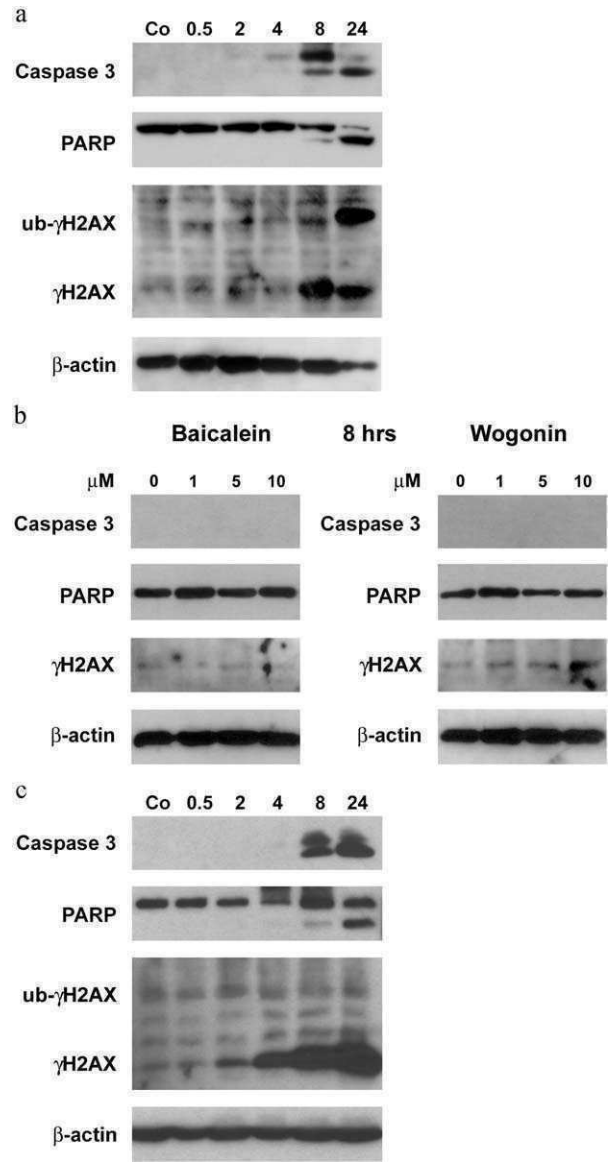

Fig. 4. Western blot analysis of pro-apoptotic Caspase 3, PARP, and phosphorylation of H2AX. HL-60 cells (1×10^6 cells) were seeded into T-75 tissue culture flasks and allowed to grow for 24 hours when cells were incubated with 132 μg/ml methanol extract for 0.5, 2, 4, 8, and 24 hours (a), with 1 μM, 5 μM and 10 μM baicalein and wogonin for 8 hours (b), and for control reasons with 250 nM 5-FdUrd for the indicated times (c). Then, isolated protein samples were subjected to electrophoretic separation and subsequent Western blot analysis with the indicated antibodies (anti phospho H2AX = γ-H2AX) . Equal sample loading was controlled by Poinceau S staining and β-actin analysis. The anti-Caspase 3 antibody recognizes only the cleavage product indicating activation. Anti-PARP antibody recognizes the full length form (116 kDa) and the signature-type cleaved product (85 kDa) which is generated by active Caspase 3.

carcinoma HCT116 cells, whereas normal human prostate epithelial PrEC cells remained unaffected (Chung et al. 2008, Lee et al. 2008). In this study, exposure to wogonin caused an increase in p53, which was in agreement with our results showing an induction of γ-H2AX, because both responses reflect genotoxic stress and DNA damage response (Wasco et al. 2008) which may result in apoptosis. Histone H2AX has also non-nucleosomal functions, specifically, proapoptotic activities in gastrointestinal stromal tumor cells treated with the small molecule protein kinase inhibitor imatinib mesylate (Gleevec) (Liu et al. 2008). The incubation of HL-60 cells with132 μg/ml methanol extract of *S. orientalis* ssp *carica* caused phosphorylation of H2AX within 8–24 hours followed by ubiquitination and activation of caspase 3 and finally cell death. Hence, genotoxic stress was also indicated by ubiquitinated γ-H2AX. Apoptosis induction upon exposure to the methanol extract was independent of p53. Since more than 50% of all cancer types harbour a defective p53 pathway, which is detrimental to successful therapeutic treatment, compounds which exert anticancer activity independent of p53 are of particular interest for clinical applications.

Another major anticancer drug property is to arrest the cell cycle. The methanol extract of *S. orientalis* ssp. *carica* dose-dependently inhibited cell proliferation of HL-60 cells ($I_pC_{50} = 43$ μg methanolic extract/ml culture medium corresponding to 1.3 mg/ml dry plant material). The extract caused cell cycle arrest by two independent mechanisms:

(i) the downregulation of cyclin D1 and presumably inhibition of Cdk4 and/or Cdk6.
(ii) the induction of $p21^{Cip/Waf}$ and therefore most likely the inhibition of Cdk2.

The D-type family of cyclins has been associated with a wide variety of proliferative diseases. Cyclin D1 was identified as the product of the *prad 1* oncogene, which is over-expressed in many

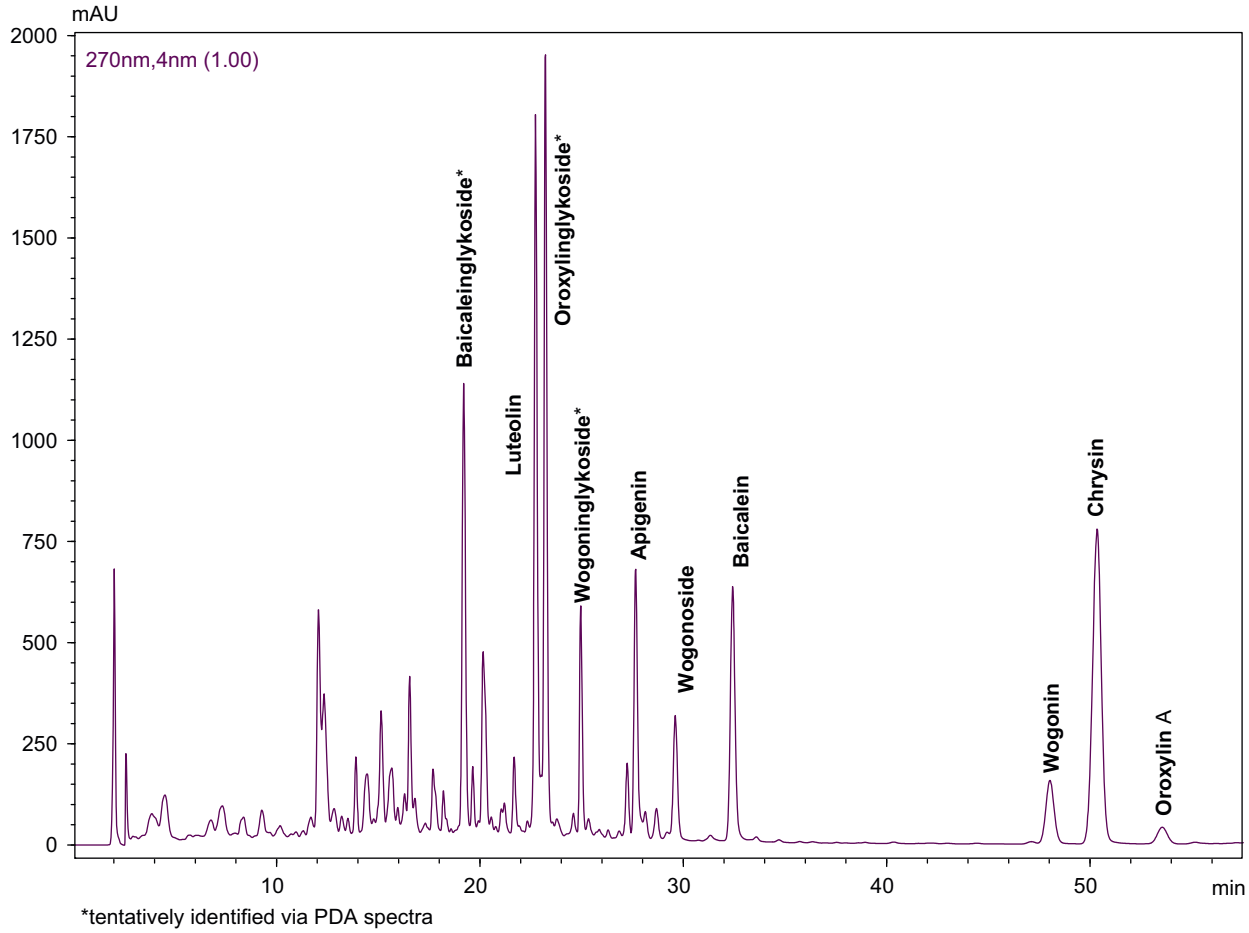

Fig. 5. HPLC of the methanolic extract.

types of cancer (Alao 2007). Therefore, suppression of cyclin D1 is a powerful measure to combat cancer. Since the methanol extract suppressed cyclin D1, a prominent anti-cancer property of this plant was elucidated. Furthermore, p21 as a specific inhibitor of Cdks such as Cdk2, was induced. The p53 tumor suppressor protein is a major regulator of p21. In HL-60 cells the increase in p21 protein levels was independent of p53, because these cells are p53 negative (Biroccio et al. 1999). Also MEK – Erk have been reported to upregulate p21 (Park et al. 2004; Facchinetti et al. 2004). Here we demonstrated that Erk, but not MEK, was activated upon treatment with *S. orientalis* ssp. *carica* extract, which was simultaneous with p21 induction and therefore, this may have caused p21 induction. Since the phosphorylation state of MEK was unchanged upon treatment with the methanolic extract, Erk was either not phosphorylated and activated by MEK, or MEK was activated through phosphorylations at additional amino acid residues, which were not detected by the specific phospho-MEK antibody used in this study.

The flavonoids apigenin and chrysin were reported to exhibit also anti-cancer properties (Hu et al. 2008; Lee et al. 2007). Both phytochemicals were found in the methanolic extract of *S. orientalis* ssp. *carica* and certainly contributed to the bio-activity of the tested constituens (baicalein and wogonin) of the methanolic extract. This warrants further investigations regarding the bio-active properties and constituents of this plant species.

Acknowledgement

We wish to thank Toni Jä]ger for preparing the figures.

The authors are greatly indebted to TUBITAK for providing grant support to A.Ö., the Unruhe Privatstiftung, the Fonds for Innovative and Interdisciplinary Cancer Research, and the Hochschuljubilä]umsstiftung der Stadt Wien to G.K.

References

Alao, J.P., 2007. The regulation of cyclin D1 degradation: roles in cancer development and the potential for therapeutic invention. Mol. Cancer 6, 24.

Baytop, T., 1999. Türkiyede Bitkiler ile Tedavi. Istanbul University Press, Faculty of Pharmacy no: 3255.

Biroccio, A., Del Bufalo, D., Ricca, A., D'Angelo, C., D'Orazi, G., Sacchi, A., Soddu, S., Zupi, G., 1999. Increase of BCNU sensitivy by wt-p53 gene therapy in glioblastoma lines depends on the administration schedule. Gene Therapy 6, 1064–1072.

Campos, M., Markham, K.R., 2007. Structure information from HPLC and on-line measured absorption spectra: flavones, flavonols and phenolic acids. Imprensa da Universidade de Coimbra, Coimbra, ISBN: 978-989-8074-05-8.

Chang, W.H., Chen, C.H., Lu, F.J., 2002. Different effects of baicalein, baicalin and wogonin on mitochondrial function, glutathione content and cell cycle progression in human hepatoma cell lines. Planta Med. 68 (2), 128–132.

Chung, H., Jung, Y.M., Shin, D.H., Lee, J.Y., Oh, M.Y., Kim, H.J., Jang, K.S., Jeosn, S.J., Son, K.H., Kong, G., 2008. Anticancer effects of wogonin in both estrogen receptor-positive and -negative human breast cancer cell lines *in vitro* and in nude mice xenografts. Int. J. Cancer 122, 816–822.

Cole, I.B., Cao, J., Alan, A.R., Saxena, P.K., Murch, S.J., 2008. Comparisons of *Scutellaria baicalensis* and *Scutellaria racemosa* : genome size, antioxidant potential and phytochemsitry. Planta Med. 74, 474–481.

Cragg, G.M., Newman, D.J., Yang, S.S., 2006. Natural product extracts of plant and marine origin having antileukemia potential: the NCI experience. J. Nat. Prod. 69 (3), 488–498.

Dai, S.J., Tao, J.Y., Liu, K., Jiang, Y.T., Shen, L., 2006. *neo*-Clerodane diterpenoids from *Scutellaria barbata* with cytotoxic activities. Phytochemistry 67, 1326–1330.

Dai, S.J., Wang, G.F., Chen, M., Liu, K., Shen, L., 2007. Five new neo-cleodane diterpenoid alkaloids from *Scutellaria barbata* with cytotoxic activities. Chem. Pharm. Bull. 55 (8), 1218–1221.

Davis, P.H., Mill, R.R., Tan, K., 1965–1988. Flora of Turkey and the East Aegean Islands, vols. I–X. Edinburgh University Press, Edinburgh, England.

Dolezal, K., Popa, I., Krystof, V., Spíchal, L., Fojtíková, M., Holub, J., Lenobel, R., Schmülling, T., Strnad, M., 2006. Preparation and biological activity of 6-benzylaminopurine derivatives in plants and human cancer cells. Bioorg. Med. Chem. 14 (3), 875–884.

Ebner, H.L., Blatzer, M., Nawaz, M., Krumschnabel, G., 2007. Activation and nuclear translocation of ERK in response to ligand-dependent and -independent stimuli in liver and gill cells from rainbow trout. J. Exp. Biol. 210 (6), 1036–1045.

Facchinetti, M.M., Siervi, A., Toskos, D., Senderowicz, A.M., 2004. UCN-01-induced cell cycle arrest requires the transcriptional induction of p21(waf1/cip1) by activation of mitogen-activated protein/extracellular signal-regulated kinase kinase/extracellular signal-regulated kinase pathway. Cancer Res. 64 (10), 3629–3637.

Geney, R., Sun, L., Pera, P., Bernacki, R.J., Xia, S., Horwitz, S.B., Simmerling, C.L., Ojima, I., 2005. Use of the tubulin bound paclitaxel conformation for structure-based rational drug design. Chem. Biol. 12 (3), 339–348.

Gridling, M., Stark, N., Madlener, S., Lackner, A., Popescu, R., Benedek, B., Diaz, R., Tut, F.M., Vo, T.P.N., Huber, D., Gollinger, M., Saiko, P., Ozmen, A., Mosgoeller, W., DeMartin, R., Eytner, R., Wagner, K.H., Grusch, M., Fritzer-Szekeres, M., Szekeres, T., Kopp, B., Frisch, R., Krupitza, G., 2009. In vitro anti-cancer activity of two ethno-pharmacological healing plants from Guatemala *Pluchea odorata* and *Phlebodium decumanum*. Int. J. Oncol. 34 (4), 1117–1128.

Grusch, M., Polgar, D., Gfatter, S., Leuhuber, K., Huettenbrenner, S., Leisser, C., Fuhrmann, G., Kassie, F., Steinkellner, H., Smid, K., Peters, G.J., Jayaram, H.N., Klepal, W., Szekeres, T., Knasmuller, S., Krupitza, G., 2002. Maintenance of ATP favours apoptosis over necrosis triggered by benzamide riboside. Cell Death Differ. 9 (2), 169–178.

Himeji, M., Ohtsuki, T., Fukazawa, H., Tanaka, M., Yazaki, S.I., Ui, S., Nishio, K., Yamamoto, H., Tasaka, K., Mimura, A., 2007. Difference of growth-inhibitory effect of *Scutellaria baicalensis*—producing flavonoid wogonin among human cancer cells and normal diploid cell. Cancer Lett. 245, 269–274.

Hu, X.W., Meng, D., Fang, J., 2008. Apigenin inhibited migration and invasion of human ovarian cancer A2780 cells through focal adhesion kinase. Carcinogenesis 29 (12), 2369–2376.

Huettenbrenner, S., Maier, S., Leisser, C., Polgar, D., Strasser, S., Grusch, M., Krupitza, G., 2003. The evolution of cell death programs as prerequisites of multicellularity. Mutat. Res. 543 (3), 235–249.

Ikura, T., Tashiro, S., Kakino, A., Shima, H., Jacob, N., Amunugama, R., Yoder, K., Izumi, S., Kuraoka, I., Tanaka, K., Kimura, H., Ikura, M., Nishikubo, S., Ito, T., Muto, A., Miyagawa, K., Takeda, S., Fishel, R., Igarashi, K., Kamiya, K., 2007. DNA damage-dependent acetylation and ubiquitination of H2AX enhances chromatin dynamics. Mol. Cell. Biol. 27 (20), 7028–7040.

Kim, E.K., Kwon, K.B., Han, M.J., Song, M.Y., Lee, J.H., Ko, Y.S., Shin, B.C., Yu, J., Lee, Y.R., Ryu, D.G., Park, J.W., Park, B.H., 2007. Induction of G1 arrest and apoptosis by *Scutellaria barbata* in the human promyelocytic leukemia HL-60 cell line. Int. J. Mol.Med. 20 (1), 123–128.

Krenn, L., Presser, A., Pradhan, R., Bahr, B., Paper, D.H., Mayer, K.K., Kopp, B., 2003. Sulfemodin 8-O-beta-D-glucoside, a new sulfated anthraquinone glycoside, and antioxidant phenolic compounds from *Rheum emodi*. J. Nat. Prod. 66 (8), 1107–1109.

Kumagai, T., Müller, C.I., Desmond, J.D., Imai, Y., Heber, D., Koeffler, H.P., 2007. *Scutellaria baicalensis*, a herbal medicine: anti-proliferative and apoptotic activity against acute lymphocytic leukemia, lymphoma and myeloma cell lines. Leukemia Res. 31, 523–530.

Lee, S.J., Yoon, J.H., Song, K.S., 2007. Chrysin inhibited stem cell factor (SCF)/c-Kit complex-induced cell proliferation in human myeloid leukemia cells. Biochem. Pharmacol. 74 (2), 215–225.

Lee, D.H., Kim, C., Zhang, L., Lee, Y.J., 2008. Role of p53, PUMA, and Bax in wogonin-induced apoptosis in human cancer cells. Biochem. Pharmacol. 75, 2020–2033.

Liu, Y., Parry, J.A., Chin, A., Duensing, S., Duensing, A., 2008. Soluble histone H2AX is induced by DNA replication stress and sensitizes cells to undergo apoptosis. Mol. Cancer 7, 61.

Ma, Z., Otsuyama, K., Liu, S., Abroun, S., Ishikawa, H., Tsuyama, N., Obata, M., Li, F.J., Zheng, X., Maki, Y., Miyamoto, K., Kawano, M.M., 2005. Baicalein, a component of *Scutellaria radix* from Huang-Lian-Jie-Du-Tang (HLJDT), leads to suppression of proliferation and induction of apoptosis in human myeloma cells. Blood 105 (8), 3312–3318.

Maier, S., Strasser, S., Saiko, P., Leisser, C., Sasgary, S., Grusch, M., Madlener, S., Bader, Y., Hartmann, J., Schott, H., Mader, R.M., Szekeres, T., Fritzer-Szekeres, M., Krupitza, G., 2006. Analysis of mechanisms contributing to AraC-mediated chemoresistance and re-establishment of drug sensitivity by the novel heterodinucleoside phosphate 5-FdUrd-araC. Apoptosis 11 (3), 427–440.

Marchart, E., Krenn, L., Kopp, B., 2003. Quantification of the flavonoid glycosides in *Passiflora incarnata* by capillary electrophoresis. Planta Med. 69 (5), 452–456.

Nakahata, N., Kutsuwa, M., Kyo, R., Kubo, M., Hayashi, K., Ohizumi, Y., 1998. Analysis of inhibitory effects of *Scutellariae radix* and baicalein on prostaglandin E2 production in rat C6 glioma cells. Am. J. Chin. Med. 26 (3–4), 311–323.

Park, K.S., Jeon, S.H., Oh, J.W., Choi, K.Y., 2004. p21Cip/WAF1 activation is an important factor for the ERK pathway dependent anti-proliferation of colorectal cancer cells. Exp. Mol. Med. 36 (6), 557–562.

Pieters, L., Vlietinck, A.J., 2005. Bioguided isolation of pharmacologically active plant components, still a valuable strategy for the finding of new lead compounds?. J. Ethnopharmacol. 100, 57–60.

Piperno, G., Fuller, M., 1985. Monoclonal antibodies specific for an acetylated form of alpha-tubulin recognize the antigen in cilia and flagella from a variety of organisms. J. Cell Biol. 101, 2085–2094.

Rugo, H., Shtivelman, E., Perez, A., Vogel, C., Franco, S., Tan Chiu, E., Melisko, M., Tagliaferri, M., Cohen, I., Shoemaker, M., Tran, Z., Tripathy, D., 2007. Phase I trial and antitumor effects of BZL101 for patients with advanced breast cancer. Breast Cancer Res. Treat. 105 (1), 17–28.

Sonoda, M., Nishiyama, T., Matsukawa, Y., Moriyasu, M., 2004. Cytotoxic activities of flavonoids from two *Scutellaria* plants in Chinese medicine. J. Etnopharmacol. 91, 65–68.

Strasser, S., Maier, S., Leisser, C., Saiko, P., Madlener, S., Bader, Y., Bernhaus, A., Gueorguieva, M., Richter, S., Mader, RM., Wesierska-Gadek, J., Schott, H., Szekeres, T., Fritzer-Szekeres, M., Krupitza, G., 2006. 5-FdUrd-araC heterodinucleoside re-establishes sensitivity in 5-FdUrd- and AraC-resistant MCF-7 breast cancer cells overexpressing ErbB2. Differentiation 74 (9–10), 488–498.

Verpoorte, R., 2000. Pharmacognosy in the new millenium: lead finding and biotechnology. J. Pharm. Pharmacol. 52, 253–262.

Wasco, M.J., Pu, R.T., Yu, L., Su, L., Ma, L., 2008. Expression of γ-H2AX in melanocytic lesions. Hum. Pathol., 23 July, PMID: 18656236 [Epub ahead of print].

Yano, H., Mizoguchi, A., Fukuda, K., Haramaki, M., Ogasawara, S., Momosaki, S., Kojiro, M., 1994. The herbal medicine sho-saiko-to inhibits proliferation of cancer cell lines by inducing apoptosis and arrest at the G0/G1 phase. Cancer Res. 54 (2), 448–454.

Ye, F., Jiang, S., Volshonok, H., Wu, J, Zhang, D.Y., 2007. Molecular mechanism of anti-prostate cancer activity of *Scutellaria baicalensis* extract. Nutr. Cancer 57 (1), 100–110.

Yin, X., Zhou, J., Jie, C., Xing, D., Zhang, Y., 2004. Anticancer activity and mechanism of *Scutellaria barbata* extract on human lung cancer cell line A459. Life Sci. 75, 2233–2244.

Zhang, L., Zhang, R.W., Li, Q., Lian, J.W., Liang, J., Chen, X.H., Bi, K.S., 2007. Development of the fingerprints for the quality evaluation of *Scutellariae radix* by HPLC-DAD and LC–MS–MS. Chromatographia 66, 13–20.

Berberine and a Berberis lycium extract inactivate Cdc25A and induce alpha-tubulin acetylation that correlate with HL-60 cell cycle inhibition and apoptosis.

Khan M., **Giessrigl B.**, Vonach C., Madlener S., Prinz S., Herbaceck I., Hölzl C., Bauer S., Viola K., Mikulits W., Quereshi R.A., Knasmüller S., Grusch M., Kopp B. and Krupitza G.

Mutat. Res. 683: 123-130, **2010.**

Mutation Research 683 (2010) 123–130

Contents lists available at ScienceDirect

Mutation Research/Fundamental and Molecular Mechanisms of Mutagenesis

journal homepage: www.elsevier.com/locate/molmut
Community address: www.elsevier.com/locate/mutres

Berberine and a *Berberis lycium* extract inactivate Cdc25A and induce α-tubulin acetylation that correlate with HL-60 cell cycle inhibition and apoptosis

Musa Khan[a,b,c], Benedikt Giessrigl[b], Caroline Vonach[b], Sibylle Madlener[b], Sonja Prinz[c], Irene Herbaceck[d], Christine Hölzl[d], Sabine Bauer[b], Katharina Viola[b], Wolfgang Mikulits[d], Rizwana Aleem Quereshi[a], Siegfried Knasmüller[d], Michael Grusch[d], Brigitte Kopp[c], Georg Krupitza[b,*]

[a] Department of Plant Sciences, Quaid-i-Azam University Islamabad, Pakistan
[b] Institute of Clinical Pathology, Medical University of Vienna, Waehringer Guertel 18-20, A-1090 Vienna, Austria
[c] Department of Pharmacognosy, Faculty of Life Sciences, University of Vienna, Althanstrasse 14, Austria
[d] Department of Medicine I, Institute of Cancer Research, Medical University of Vienna, Borschkegasse 8a, Austria

ARTICLE INFO

Article history:
Received 22 July 2009
Received in revised form 22 October 2009
Accepted 2 November 2009
Available online 10 November 2009

Keywords:
Berberis lycium
Polar extract
Cancer
Ethnopharmacology

ABSTRACT

Berberis lycium Royle (Berberidacea) from Pakistan and its alkaloids berberine and palmatine have been reported to possess beneficial pharmacological properties. In the present study, the anti-neoplastic activities of different *B. lycium* root extracts and the major constituting alkaloids, berberine and palmatine were investigated in p53-deficient HL-60 cells.

The strongest growth inhibitory and pro-apoptotic effects were found in the n-butanol (BuOH) extract followed by the ethyl acetate (EtOAc)-, and the water (H_2O) extract.

The chemical composition of the BuOH extract was analyzed by TLC and quantified by HPLC. 11.1 μg BuOH extract (that was gained from 1 mg dried root) contained 2.0 μg berberine and 0.3 μg/ml palmatine. 1.2 μg/ml berberine inhibited cell proliferation significantly, while 0.5 μg/ml palmatine had no effect. Berberine and the BuOH extract caused accumulation of HL-60 cells in S-phase. This was preceded by a strong activation of Chk2, phosphorylation and degradation of Cdc25A, and the subsequent inactivation of Cdc2 (CDK1). Furthermore, berberine and the extract inhibited the expression of the proto-oncogene cyclin D1. Berberine and the BuOH extract induced the acetylation of α-tubulin and this correlated with the induction of apoptosis. The data demonstrate that berberine is a potent anti-neoplastic compound that acts via anti-proliferative and pro-apoptotic mechanisms independent of genotoxicity.

© 2009 Elsevier B.V. All rights reserved.

1. Introduction

Berberis taxa are important plants with various healing properties, and *Berberis* species are included in Indian and British pharmacopeias. *Berberis lycium* Royle (Berberidacea) is a widely used medical plant in Pakistan, known by the common name "Zyarh larghai" or "Kashmal", whereas its English name is Barberry [1]. Al-Biruni describes the plant under the name of Ambaribis and mentions its Persian name as Zirkash [2]. The roots of the plant known as "Darhald" are used as astringent, for diaphoretic- and bleeding piles [3]. The roots of *Berberis* species are used for treating a variety of ailments such as eye and ear diseases, rheumatism, jaundice, diabetics, fever, stomach disorder, skin disease, malarial fever and as tonic [4–7]. In particular, the powdered roots of *B. lycium* are used in combination with milk for the treatment of rheumatism and muscular pain in Pakistan folk medicine, probably to protect the gastric mucosa from damage [8]. The potential effectiveness of *Berberis* is also indicated by its use in the Indian Ayurvedic, Unani, and Chinese system of medicine since time immemorial [9]. The active constituents of *B. lycium* are alkaloids and the major compound is berberine [10]. Berberine and several *Berberis* species show a wide range of biochemical and pharmacological activities such as in amoebiasis, cholera and diarrhea [2], possess analgesic and antipyretic effects [11], and were reported to exhibit anti-arrhythmic-, anti-tumor- [12–14], anti-inflammatory- [15], and rheumatic properties [11]. Little is known about the molecular and cellular anti-tumor mechanisms that are triggered by berberine and extracts of *Berberis* species. A recent study addressed the molecular mechanisms of berberine-induced anti-proliferative effects in osteosarcoma cells. The authors showed that berberine inhibited cell proliferation through genotoxicity causing p53-dependent G1 arrest and apoptosis, and p53-independent G2 arrest [16]. We aimed to investigate the effects of berberine and *B. lycium* crude

* Corresponding author. Tel.: +43 1 40400 3487; fax: +43 1 40400 3707.
E-mail address: georg.krupitza@meduniwien.ac.at (G. Krupitza).

0027-5107/$ – see front matter © 2009 Elsevier B.V. All rights reserved.
doi:10.1016/j.mrfmmm.2009.11.001

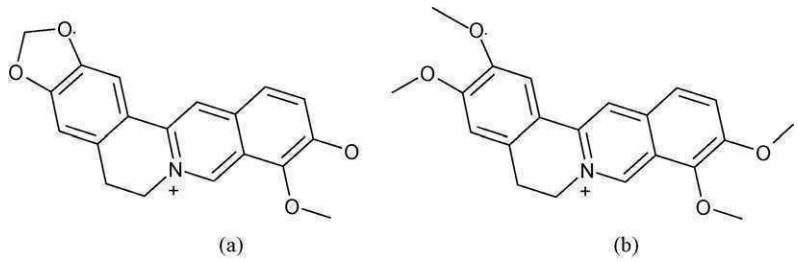

Fig. 1. Chemical structures of (a) berberine and (b) palmatine.

extracts on the expression of cell cycle regulators and to elucidate mechanisms that trigger apoptosis in p53-deficient HL-60 cells.

2. Materials and methods

2.1. Chemicals

Berberine chloride dihydrate (purity 98.92%) and palmatine chloride (purity 96.98%) were purchased from Phytolab (Vestenbergsreuth, Germany). Berbamine dihydrochloride (purity >85%), toluene, ethyl acetate, acetonitrile, sodium 1-heptansulfonate monohydrate, phosphoric acid, isopropanol and HPLC-grade methanol were purchased from Sigma–Aldrich (Schnelldorf, Germany) and were of the highest available purity. Codeine hydrochloride (purity 98.27%) was from Heilmittelwerk Wien (Vienna, Austria). TLC Silica gel 60 F_{254} Aluminum sheets were obtained from Merck (Darmstadt, Germany). All other chemicals and solvents were of analytical grade.

In the experiments berberine chloride dihydrate and palmatine chloride were used because of their improved solubility, and throughout the text and figures the indicated berberine and palmatine concentrations refer to the alkaloid base and not to the salt.

The structural formulas of berberine and palmatine are shown in Fig. 1.

2.2. Cell culture

HL-60 human promyelocytic cells were from the American Type Culture Collection (Manassas, VA, USA). Cells were grown in RPMI 1640 medium supplemented with 10% heat inactivated fetal calf serum, 1% L-glutamine and 1% penicillin/streptomycin (Life Technologies, Paisley, Scotland) at 37 °C in a humidified atmosphere containing 5% CO_2.

2.3. Collection and extraction of root powder

B. lycium was collected from Margalla Hills (Islamabad, Pakistan) and voucher specimens No. 125174 submitted to the herbarium and identified by R.A. Quereshi in the Department of Plant Sciences, Quaid-i-Azam University Islamabad. Roots were washed, air dried and grounded. 20 g of powdered *B. lycium* root were extracted four times with methanol (MeOH). These extracts were collected and concentrated with a Rotavapor at 40 °C. The concentrated MeOH extract was dissolved in distilled water and extracted three times each with ethyl acetate (EtOAc), and n-butanol (BuOH), according to their increasing polarity. Thus, 0.044 g dried EtOAc extract, and 0.222 g dried BuOH extract were obtained. The residue of the aqueous phase – 0.278 g dry weight – was recovered and considered as H_2O extract.

2.4. Thin layer chromatography (TLC) of the different B. lycium extracts

The constituents of the extracts were qualitatively and semi-quantitatively determined by TLC. A solvent system consisting of toluene–ethyl acetate–isopropanol–methanol–water (12:6:3:3:0.6) was used as mobile phase. Two-chambered TLC tanks were used, whereas one chamber was filled with the mobile phase and the other with concentrated ammonia. Prior to chromatographic separation the chamber was saturated for 20 min with the mobile phase. Berberine and related alkaloids were detected under UV_{366}.

2.5. High pressure liquid chromatography (HPLC) analysis of the different B. lycium extracts

HPLC analysis of *B. lycium* extracts was carried out with a Shimadzu™ system consisting of a DGU-14A degasser, a LC-10AD auto sampler, a SPD-M10A VP diode array detector, a LC-10AD liquid chromatograph and a SCL-10A system controller. Data acquisition and processing were performed using Lab-solutions software (Shimadzu). Analysis was carried out on a Hypersil BDS-C18 analytical column (5 μm, 4 mm × 250 mm), protected by a Lichrosphere 100 RP-18 precolumn (5 μm, 4 mm × 4 mm). Baseline separation of the peaks was achieved using gradient elution containing Na^+ heptansulfonate monohydrate (1.0 g in 390 ml H_2O, adjusted to pH 2.8 with phosphoric acid = solvent A) and acetonitrile (solvent B). Gradient was as follows: 0–12 min: 25–70% B, 12–13 min: 90. The flow rate was 1.3 ml/min, injection volume was 10 μl and HPLC chromatogram was monitored at 280 nm. Codeine was used as an internal standard.

2.6. Growth inhibition assay

HL-60 cells were seeded in T-25 tissue culture flasks (Life Technologies, Paisley, Scotland) at a concentration of 1×10^5 per ml and incubated with increasing concentrations of the different extracts of *B. lycium* or with berberine and palmatine. Cell counts and IC_{50} values were determined in the different fractions after 48 and 72 h, using a KX 21 N microcell counter (Sysmex, Kobe, Japan).

2.7. Hoechst dye 33258 and propidium iodide double staining

Hoechst staining was performed according to the method described by Grusch et al. [17]. HL-60 cells (0.1×10^6 per ml) were seeded in T-25 cell culture flasks and exposed to increasing concentrations of *B. lycium* fractions and berberine for 48 h. Hoechst 33258 (HO) and propidium iodide (PI, both Sigma, St. Louis, MO) were added directly to the cells to final concentrations of 5 and 2 mg/ml, respectively. After 60 min of incubation at 37 °C, the cells were examined under a fluorescence microscope (Axiovert, Zeiss) equipped with a DAPI filter and a camera. This method allows to discriminate between early apoptosis, late apoptosis, and necrosis. Cells were judged according to their morphology and the integrity of their cell membranes, which can easily be observed after PI staining.

2.8. Western blotting

HL-60 cells were preincubated for increasing time periods (from 2 to 48 h) with 11.1 μg BuOH extract/ml and 1.2 μg berberine/ml medium. Then, cells were placed on ice, washed with ice-cold PBS (pH 7.2), centrifuged (1000 rpm, 4 °C, 4 min) and the pellets lysed in 150 μl buffer containing 150 mM NaCl, 50 mM Tris pH 8.0, 1% Triton X-100, 2.5% 0.5 mM PMSF and PIC (Sigma, Schnelldorf, Germany). Debris was removed by centrifugation (12,000 rpm, 4 °C, 20 min) and the supernatant collected. Then, equal amounts of protein were loaded onto 10% polyacrylamide gels. Proteins were electrophoresed for 2 h and then electroblotted onto PVDF membranes (Hybond P, Amersham, Buckinghamshire, UK) at 4 °C for 1 h. To confirm equal sample loading, membranes were stained with Poinceau S. After washing with TBS, the membranes were blocked for 1 h in blocking solution containing 5% skimmed milk in TBS and 0.5% Tween 20, washed three times in TBS/T, and incubated by gentle rocking with primary antibodies in blocking solution at 4 °C overnight. Then, the membranes were washed in TBS/T (3× for 5 min) and further incubated with the second antibody (peroxidase-conjugated anti-rabbit IgG, or anti-mouse IgG dilution 1:2000 in Blotto), for 1 h at room temperature. The membranes were washed with TBS/T and the chemoluminescence (ECL detection kit, Amersham, Buckinghamshire, UK) was detected by exposure of the membranes to Amersham Hyperfilm™ ECL. The antibodies against Cdc2-p34 (17), Cdc25A (M-191), phospho-Cdc25A-(phSer17), α-tubulin, PARP and β-tubulin were from Santa Cruz (Santa Cruz, CA, USA), against cleaved caspase-3(Asp17), phospho-p38-MAPK (Thr180/Tyr182), p38-MAPK, cyclin D1, p21, phospho-Cdc2(phTyr15), Chk2, and phospho-Chk2 (Thr68) were from Cell Signaling (Danvers, MA, USA), against γH2AX (phSer139) from Calbiochem (San Diego, CA, USA), and phoshpho-Cdc25A-(phSer177) from Abgent (San Diego, CA, USA), and against acetylated-α-tubulin and β-actin were from Sigma (St. Louis, MO).

2.9. Cell cycle distribution analysis

HL-60 cells (0.5×10^6 per ml) were seeded in T-25 tissue culture flasks and incubated with 5.6 μg/ml BuOH extract, 0.6 μg/ml berberine, or 0.3 μg/ml palmatine, which were equivalent to 0.5 mg/ml dried root powder, respectively. After 24 h, the cells were harvested and suspended in 5 ml cold PBS, centrifuged (600 rpm, 5 min), resuspended and fixed in 3 ml cold ethanol (70%) for 30 min at 4 °C. After two washing steps in cold PBS, RNAse A and PI were added to a final concentration of 50 mg/ml each and incubated at 4 °C for 60 min before analyses. Cells were analyzed with a FACS Calibur flow cytometer (BD Biosciences, San Jose, CA, USA)

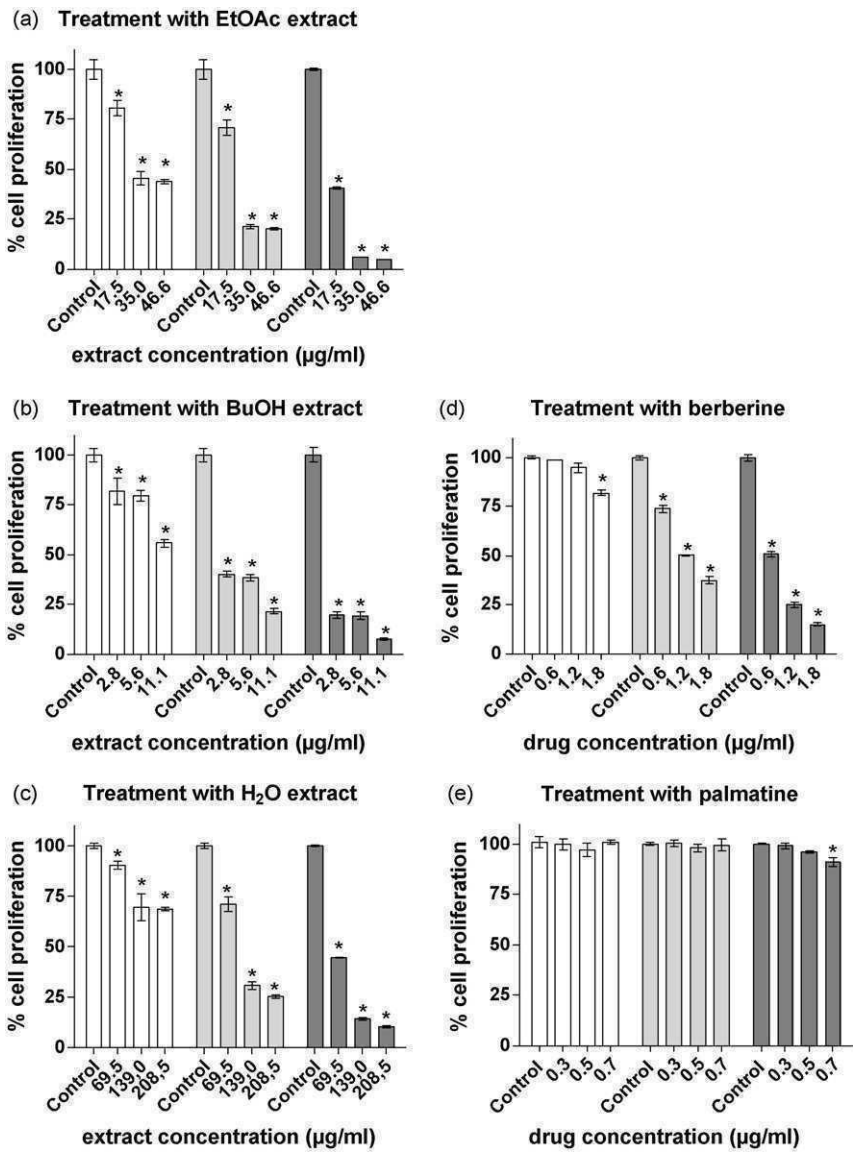

Fig. 2. Anti-proliferative effect of *B. lycium* extracts and its bio-active constituents berberine and palmatine. HL-60 cells were seeded into T-25 tissue culture flasks (1×10^5 cells/ml), grown for 24 h to enter logarithmic growth phase, and incubated with increasing concentrations (a) EtOAc extract (17.5, 35.0 and 46.6 µg/ml medium); (b) BuOH extract (2.8, 5.6 and 11.1 µg/ml); (c) H_2O extract (69.5, 139.0 and 208.5 µg/ml); (d) berberine (0.6, 1.2, and 1.8 µg/ml); and (e) palmatine (0.3, 0.5 and 0.7 µg/ml). Cells were counted after 24, 48 and 72 h of treatment (white, light gray and dark gray columns, respectively) and the percentage of proliferation was calculated and compared to DMSO-controls (Control). Controls were considered as cells with a maximal proliferation rate (100%). Experiments were done in triplicate. Error bars indicate SEM, asterisks significance ($p < 0.05$).

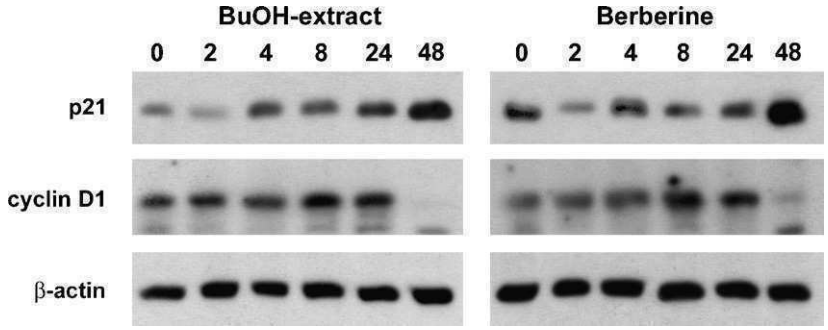

Fig. 3. Analysis of cell cycle proteins. HL-60 cells (1×10^6 cells) were seeded into T-25 tissue culture flasks and allowed to grow for 48 h when cells were incubated with 11.1 µg BuOH extract/ml medium (left side panels) and 1.2 µg berberine/ml medium (right side panels) for 2, 4, 8, 24 and 48 h. Then, isolated protein samples were subjected to 10% SDS-PAGE separation and subsequent Western blot analysis using antibodies against $p21^{waf}$ and cyclin D1. Equal sample loading was controlled by Poinceau S staining and β-actin analysis.

and cell cycle distribution was calculated with ModFit LT software (Verity Software House, Topsham, ME, USA).

2.10. Single cell gel electrophoresis (SCGE)/comet assay

The experiments were conducted according to the guidelines of Tice et al. [18]. After treatment of the cells with BuOH extract or berberine, the cells were centrifuged (400 × *g*, 5 min, 23 °C, Sigma–Aldrich, 4K 15C, Germany) and the pellet resuspended with 200 μl PBS. The cytotoxicity was determined with trypan blue [19], which is a measure for the integrity of the cell membrane. Only cultures with survival rates ≥80% were analyzed for comet formation. To monitor DNA migration 0.05×10^6 cells were mixed with 80 μl low melting agarose (0.5%, Gibco, Paisley, Scotland) and transferred to agarose-coated slides. The slides were immersed in lysis solution (1% Triton X, 10% DMSO, 2.5 M NaCl, 10 mM Tris, 100 mM Na_2EDTA, pH 10.0) at 4 °C for 1 h. After unwinding and electrophoresis (300 mA, 25 V, 20 min) under alkaline conditions (pH > 13), which allows the determination of single and double strand breaks, DNA–protein crosslinks and apurinic sites, the DNA was stained with 40 μl ethidium bromide (20 μg/ml, Sigma–Aldrich, Munich, Germany) and the percentage DNA in tail was analyzed with a computer aided image analysis system (Comet IV, Perceptive Instruments Ltd., Haverhill, UK). From each experimental point, one slide was prepared and 50 cells were scored per slide.

2.11. Statistical analyses

The results of the SCGE (single cell gel electrophoresis) experiments were analyzed with one-way ANOVA followed by Dunnett's multiple comparison test, and the apoptosis and proliferation experiments with *t*-test using GraphPad Prism version 4 (GraphPad Prim Sofware, Inc., San Diego, CA, USA).

3. Results

3.1. Analysis of B. lycium extract constituents by TLC and HPLC

The extraction of 1 g *B. lycium* roots with EtOAc, BuOH, and H_2O yielded 2.2 mg, 11.1 mg, and 13.9 mg extract, respectively. Solutions of the EtOAc, BuOH, and H_2O extracts were applied on TLC plates and chromatographic separation was carried out as previously described (Section 2.4). Berberine, berbamine and palmatine were used as reference compounds since they are known constituents of various *Berberis* taxa with distinct anti-neoplastic properties.

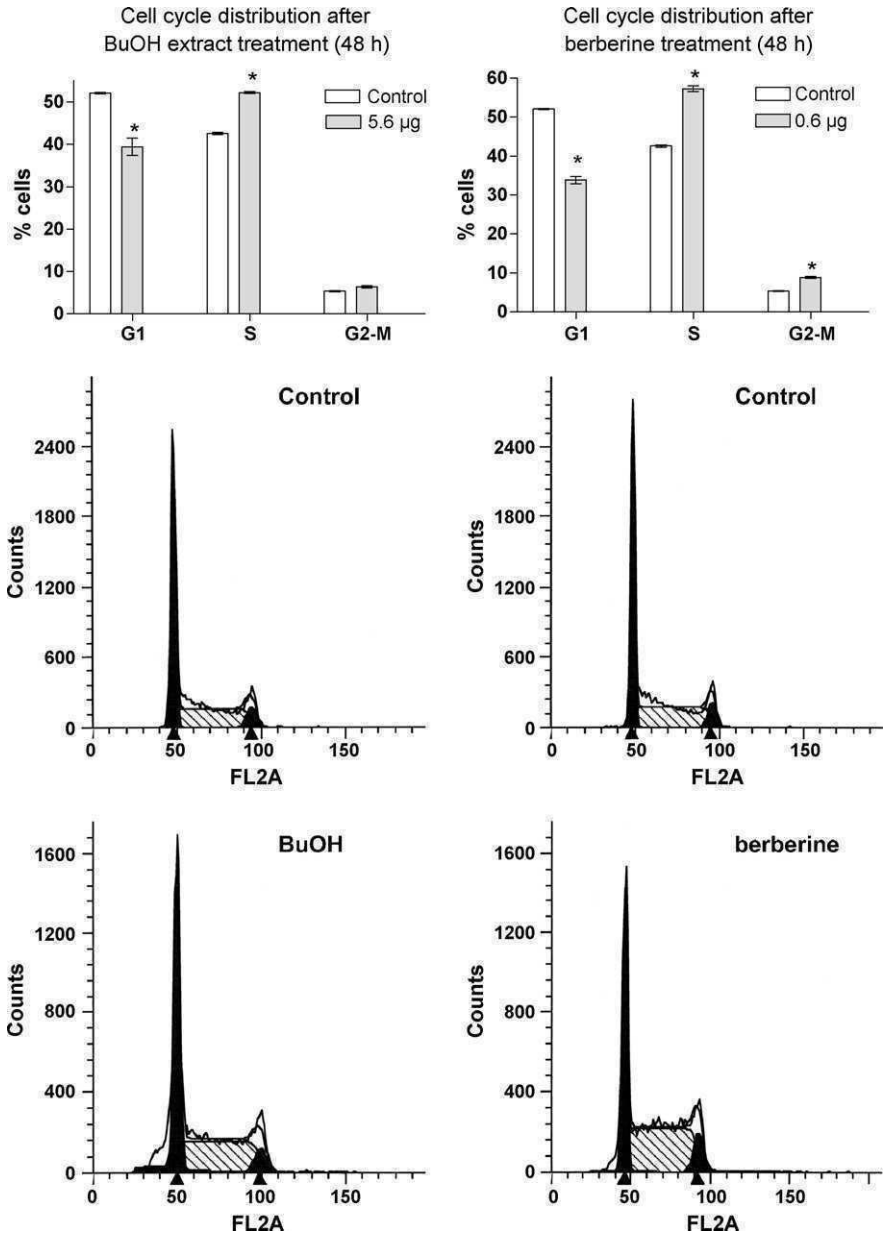

Fig. 4. Cell cycle distribution of HL-60 cells upon treatment with BuOH extract and berberine for 48 h. Logarithmically growing HL-60 cells were incubated with 5.6 μg/ml BuOH extract and 0.6 μg/ml berberine and then subjected to FACS analysis. Experiments were done in triplicate. Representative FACS profiles are shown below the respective diagrams. Error bars indicate SEM, and asterisks significance ($p < 0.05$).

All extracts contained berberine (retention factor, $R_f = 0.151$) and palmatine ($R_f = 0.088$), whereas the highest concentration of both compounds was detected in the BuOH extract. Berbamine ($R_f = 0.405$) was not found in any extract. Besides berberine and palmatine another unknown band was present in all extracts.

For quantification HPLC was used under the above mentioned conditions (Section 2.5). Retention times for codeine (internal standard), berberine, palmatine and berbamine were 4.52, 9.75, 9.19 and 8.06 min, respectively. Berbamine was reported to be a constituent of *B. lycium* [10] while there was no evidence of its presence in the here performed TLC and RP-HPLC analyses. The calculated berberine content was 18.04%, 0.54% and 2.76% and palmatine content was 2.80%, 0.04% and 0.93% in the BuOH, EtOAc and H_2O extracts, respectively (data not shown). Thus, 11.1 μg BuOH extract contained 2.0 μg berberine, and 0.3 μg palmatine.

3.2. Inhibition of HL-60 cell proliferation by extracts of B. lycium, berberine and palmatine

Logarithmically growing cells were incubated with increasing concentrations of EtOAc, BuOH and H_2O extract, or berberine and palmatine for 72 h. Then, cells were counted and the inhibition of proliferation was calculated. The BuOH extract showed the highest toxicity against HL-60 cells (IC_{50} 2.3 μg extract/ml medium after 48 h of treatment), followed by the EtOH extract (23.5 μg/ml) and the H_2O extract (110 μg/ml) (Fig. 2). The data suggest that the measured differences in the extract activities were due to different chemical compositions of the extracts. To evaluate which of the major constituents of the BuOH extract may have caused growth inhibition, HL-60 cells were treated with the measured equivalent concentrations of berberine (0.6–1.8 μg/ml) and palmatine (0.3–0.7 μg/ml). The IC_{50} for berberine was 1.2 μg/ml after 48 h. Palmatine did not inhibit cell growth after 48 h. The inhibition of HL-60 proliferation that was observed upon treatment with BuOH extract or berberine was preceded by the induction of $p21^{waf}$, which has been also observed by Liu et al. [16] and by a dramatic down-regulation of the proto-oncogene cyclin D1 after 48 h (Fig. 3). Both, the up-regulation of $p21^{waf}$ and the suppression of cyclin D1 are potent mechanisms to block cancer cell growth.

3.3. Effect of BuOH extract, berberine and palmatine on cell cycle distribution

HL-60 cells were exposed to 5.5 μg BuOH extract/ml and 0.6 μg berberine/ml for 48 h to investigate the cell cycle distribution. Both, the extract and the pure compound caused a reduction of G1 cells and accumulation of cells in the S-phase (Fig. 4), which was most likely due to activation of intra S-phase checkpoint, because checkpoint kinase 2 (Chk2) became highly activated [20] (Fig. 7). Palmatine had no effect on cell cycle distribution (data not shown) which was consistent with the observation that it did not have an effect on growth inhibition.

3.4. Induction of apoptosis by extracts of B. lycium and berberine

HL-60 cells were treated with the three extracts (EtOAc, BuOH and H_2O) and berberine for 48 h and the induction of cell death was analyzed. The three extract types induced apoptosis and the BuOH extract was the most active followed by the EtOAc- and the H_2O extracts. Berberine was used at a comparable concentration as contained in the BuOH extract and this concentration caused a similar pro-apoptotic effect as the extract (Fig. 5).

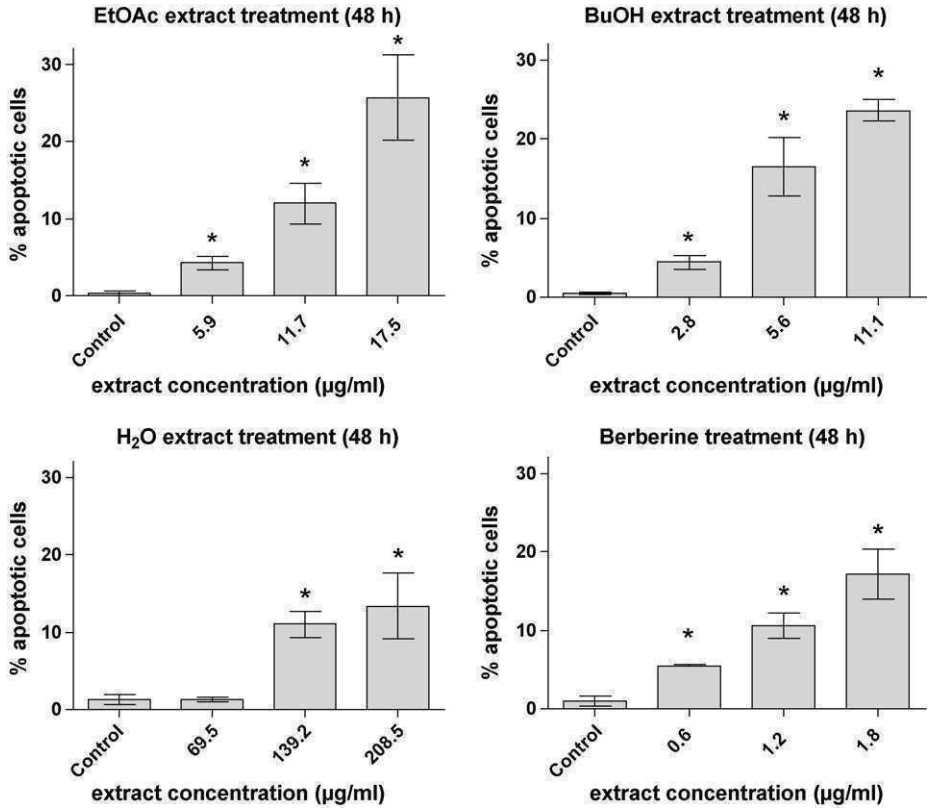

Fig. 5. Induction of apoptosis by the *B. lycium* extracts and berberine. HL-60 cells were incubated with increasing extract and berberine concentrations for 48 h. Then, cells were double stained with Hoechst 33258 and propidium iodide and examined under a fluorescence microscope and a DAPI filter. Nuclei with morphological changes indicating apoptosis (Section 2) were counted and the percentages of vital and apoptotic cells calculated. Experiments were done in triplicate. Error bars indicate SEM, asterisks significance ($p < 0.05$).

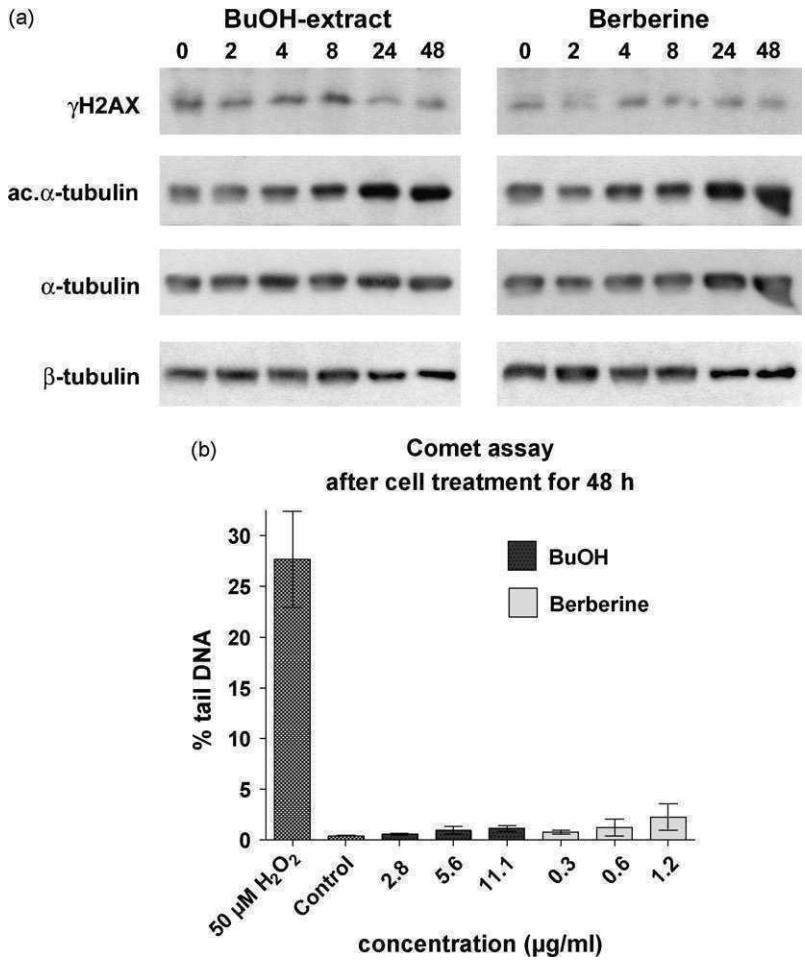

Fig. 6. Analyses of pro-apoptotic mediators and effectors. (a) HL-60 cells (1×10^6 cells) were seeded into T-25 tissue culture flasks and allowed to grow for 48 h when cells were incubated with BuOH extract (11.1 μg/ml medium) and 1.2 μg/ml berberine for 2, 4, 8, 24 and 48 h. Then, isolated protein samples were subjected to 10% SDS-PAGE separation and subsequent Western blot analysis using antibodies against γH2AX, acetylated-α-tubulin and α-tubulin. Equal sample loading was controlled by Poinceau S staining and β-tubulin analysis. (b) Comet assay. The genotoxicity of increasing concentrations of BuOH extract and berberine was investigated in logarithmically growing HL-60 cells. 50 μM H_2O_2 was used as positive control and solvent-treated cells were used as negative control. Bars indicate means ± SD of results obtained with three independent cultures (from each culture 50 cells were evaluated). Statistical analysis: Dunnett's test.

High concentrations of berberine (10–50 μg/ml) were shown to induce H2AX phosphorylation (γH2AX) in osteosarcoma cells indicating genotoxicity [16]. In the present study we demonstrate that 0.6 and 1.2 μg/ml berberine and the corresponding concentration of BuOH extract specifically induced apoptosis in HL-60 cells without concomitant induction of γH2AX (Fig. 6a). This observation indicates that the anti-neoplastic effects have not been triggered by berberine-caused genotoxicity. Comet assay detecting DNA single strand breaks provided no evidence that berberine or the BuOH extract cause DNA damage (Fig. 6b). Thus, other mechanisms must be responsible for cell cycle inhibition and apoptosis. Interestingly, berberine and the BuOH extract caused acetylation of α-tubulin (Fig. 6a), which is indicative for tubulin polymerization reminiscent of the mechanism of taxol. Tilting the fine-tuned equilibrium of polymerized/de-polymerized microtubule is incompatible with normal cell division and this causes not only cell cycle arrest but also apoptosis.

3.5. Induction of stress response by extracts of B. lycium and berberine

Cellular stress is a prominent inducer of apoptosis and cell cycle arrest. Berberine and extract caused the transient phosphorylation of p38-MAPK ~2-fold compared to untreated control after 8 h (Fig. 7). Also Chk2 became activated within 4 h treatment (Fig. 7). This activation pattern correlated with the accumulation of cells in S-phase and this was consistent with intra-S-phase arrest as reported by Luo et al. [20]. Chk1 was not induced (data not shown). Cdc25A became phosphorylated at Ser177 and therefore, Cdc25A became inactivated (within 2 h, Fig. 7) leading finally to its degradation [21]. This resulted in the accumulation of Tyr15 phosphorylation of Cdc2, which is a specific target site of the Cdc25A phosphatase [22]. Tyr15-Cdc2 phosphorylation inactivates this cell cycle specific kinase. The treatment with BuOH extract and berberine changed also the phosphorylation pattern at Ser17 of Cdc25A. The inactivation of the Cdc25A proto-oncogene was the most immediate event elicited by the BuOH extract and berberine (Fig. 7). This was followed by the acetylation of α-tubulin (Fig. 6a), the activation of Chk2 and p38, and the down-regulation of cyclin D1.

4. Discussion

We studied the effects of root extracts of *B. lycium* in HL-60 human leukemia cells and compared them with those of the pure alkaloids, i.e. berberine and palmitine. *B. lycium* is an erect small rigid shrub about 1.0–2.5 m tall, with a thick woody shoot covered with a thin brittle bark [23] and is native to the Himalayan

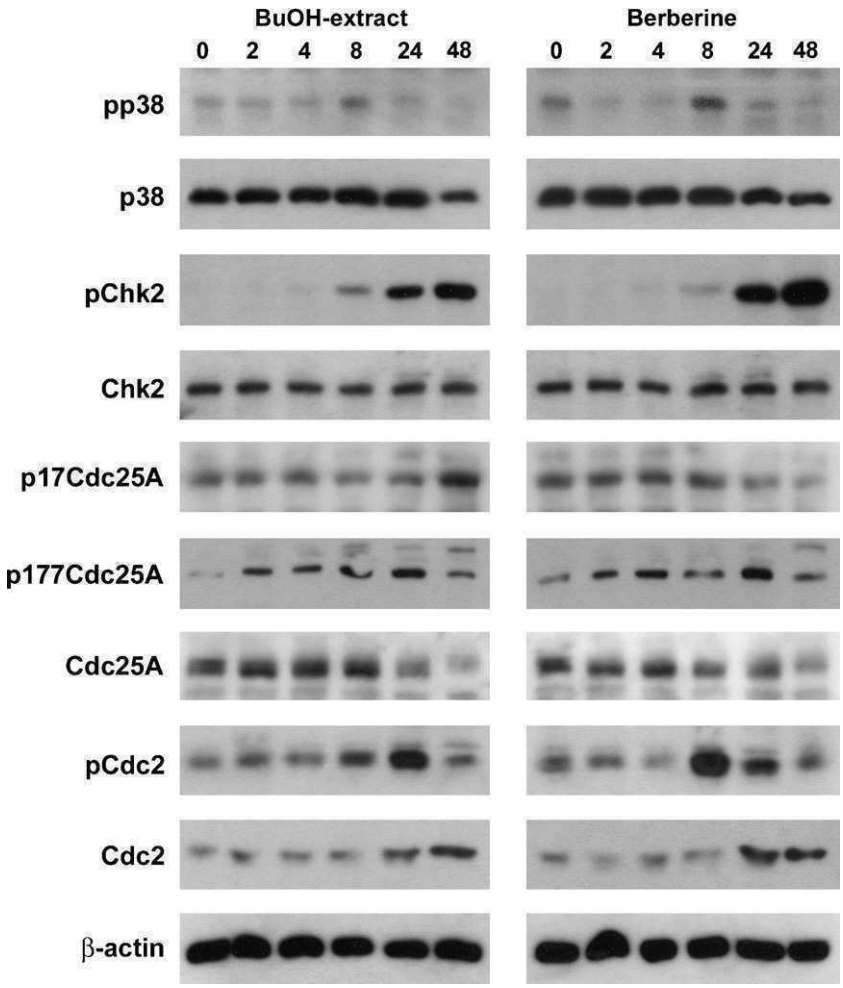

Fig. 7. Induction of stress response by the BuOH extract and berberine. HL-60 cells (1×10^6 cells) were seeded into T-25 tissue culture flasks and allowed to grow for 48 h when cells were incubated with 11.1 μg BuOH extract/ml and 1.2 μg berberine/ml medium for 2, 4, 8, 24 and 48 h. Then, isolated protein samples were subjected to 10% SDS-PAGE separation and subsequent Western blot analysis using antibodies against phospho-p38-MAPK, p38-MAPK, phospho-Chk2, Chk2, phospho-Ser17-Cdc25A, phospho-Ser177-Cdc25A, Cdc25A, phospho-Cdc2, and Cdc2. Equal sample loading was controlled by Poinceau S staining and β-actin analysis.

mountain system and widely distributed in temperate and semi-temperate regions of India, Nepal, Afghanistan, Bangladesh and Pakistan. The active constituents of *B. lycium* are alkaloids. The major alkaloids are umbellatine, berberine [10], and oxyacanthine [24]. Heterocyclic constituents e.g. berberisterol, berberifuranol and berberilycine [25], the alkaloids sindamine, punjabine, gilgitine [26], and berbericine [8] were also found in the roots of *B. lycium*. Besides these, berbamine and tannins are also present in small quantities [10].

In the present investigation berberine and the crude BuOH extract regulated protein expression and protein activation in HL-60 cells similarly. Also the growth inhibiting- and apoptosis-inducing potential was similar and FACS- and Comet data were almost identical. This is a strong indication that BuOH-mediated cell cycle arrest was due to berberine. We show that the growth inhibitory properties of berberine and BuOH extract correlated directly with the inactivation and down-regulation of the proto-oncogene Cdc25A. Also the inhibition of human nasopharyngeal carcinoma CNE-2 cell growth by berberine was associated with suppression of cyclin B1, CDK1 (Cdc2), and Cdc25C proteins [27]. In human glioblastoma T98G cells, berberine induced cell cycle retardation in G1-phase through increased expression of p27 and suppression of CDK2, CDK4, cyclin D, and cyclin E proteins [28]. Also HL-60 cell growth was significantly inhibited by berberine in G1-phase with a decrease in S-phase cells [29]. In another study, FACS analyses indicated that berberine induced G2/M-phase arrest in HL-60 cells and murine myelomonocytic leukemia WEHI-3 cells that was accompanied by increased levels of Wee1 and 14-3-3sigma, and decreased levels of Cdc25C, CDK1 and cyclin B1 [30]. This is in contradiction to the reported G0/G1 arrest [28] and to the intra-S-phase arrest observed in this study, but the differences were most likely due to the different berberine concentrations used in these investigations. Notably, intra-S-phase arrest correlated with the activation of Chk2 and this was also demonstrated in the context of ionizing radiation (20). In addition, the extract and the purified compound caused the down-regulation of the proto-oncogene cyclin D1 after 48 h and this certainly added up to the cell division arrest. Therefore, berberine and the BuOH extract down-regulated two potent oncogenes, Cdc25A and cyclin D1.

Also the proliferation of human umbilical vein endothelial cells (HUVECs) was inhibited upon incubation with 20 μg/ml berberine [31]. This phenomenon was accompanied by a significant decrease of PCNA, and a typical apoptotic appearance correlated with a marked decline in the mitochondrial membrane potential. Berberine-mediated inhibition of vascular endothelial cell proliferation suppressed neo-vascularization, and this might be one of the mechanisms attenuating growth and metastasis of tumors. We tested berberine and the BuOH extract in a 3-D metastasis model. This model utilizes lymphendothelial cells layers onto which MCF-7 cell spheroids are placed that repulse the endothelial cells thereby

generating gaps in the underneath lyphendothelium. Cancer cell bulks penetrate through these gates. 5–50 μM berberine dose-dependently prevented lymphendothelial gap formation induced by MCF-7 spheroids (manuscript submitted).

It was further reported that an ethanol extract of *Coptis teeta*, which contains berberine and other components, as well as purified berberine-induced apoptosis of MCF-7 breast cancer cells [32]. Berberine-triggered cell death was reported also in several other human cancer cell lines [33–35], such as in human glioblastoma T98G cells that was concomitant with an increased Bax/Bcl-2 ratio, disruption of the mitochondrial membrane potential, and the activation of caspase-9 and caspase-3 [28]. Berberine-induced apoptosis of human leukemia HL-60 cells was shown to be associated with down-regulation of nucleophosmin/B23 and telomerase activity [36]. Furthermore, Liu et al. [16] reported a cell cycle inhibitory effect of berberine in a high concentration range (between 10 and 50 μM), which correlated with DNA damage. In this study, the authors show that berberine inhibited osteosarcoma cell proliferation and induced apoptosis through genotoxicity. In contrast, we found that the inhibition of proliferation and the induction of apoptosis occurred at berberine doses and extract concentrations that were devoid of genotoxic activity, although we agree that high berberine concentrations could cause DNA strand breaks. Our data suggest that another molecular/cellular mechanism transduced the pro-apoptotic properties of berberine and BuOH extract and this correlated with α-tubulin acetylation, which is indicative for microfilament polymerization [37]. Therefore, the anticancer properties of berberine and the BuOH extract are reminiscent of that of taxol [38] and independent of genotoxicity. The here used berberine and extract concentrations are equivalent to ~9 g of dried *B. lycium* root per 80 kg body weight.

Conflict of interest

There is no conflict of interests.

Acknowledgements

We wish to thank Toni Jäger for preparing the figures. The authors are indebted the Higher Education Commission of Pakistan for the funding of this project, as well as the Austrian Science Fund, FWF, grant numbers P19598-B13 and SFB F28 (to W.M.), and the Herzfelder Family Foundation (to W.M.), and the Funds for Innovative and Interdisciplinary Cancer Research to G.K. The authors thank the University of Vienna and Medical University of Vienna for technical support.

References

[1] A.K. Anwar, M. Ashfaq, M.A. Nasveen, Pharmacognostic Studies of Selected Indigenous Plants of Pakistan, Pakistan Forest Institute, Peshawar, NWFP, Pakistan, 1979.
[2] H.M. Said, Medicinal Herbal—A Textbook for Medical Students and Doctors, vol. 1, Hamdard Foundation, Nazimabad, Karachi-74600, Sindh, Pakistan, 1996.
[3] K.M. Nadkarni, in: A.K. Nadkarni (Ed.), Indian Material Medica, 3rd ed., Popular Parakashan Depot, Bombay, India, 1980, pp. 180–190.
[4] G. Watt, A dictionary of the economic products of India, Published under the authority of His Majesty's Secretary of State for India in Council, Kolkatta, Yohn Murry, London, 1889, p. 652.
[5] K.R. Kirtikar, B.D. Basu, Indian Medicinal Plants, LM Basu Publication, Allahabad, 1933, p. 2422.
[6] R.N. Chopra, I.C. Chopra, K.L. Handa, L.D. Kapoor, Indigenous Drugs of India, UN Dhur and Sons, Kolkata, 1958, p. 503.
[7] S.P. Ambastha (Ed.), The Wealth of India, vol. 2B, Publication and Information Directorate, CSIR, New Delhi, 1988, p. 118.
[8] M. Ikram, M. Ehsanul, S.A. Warsi, Alkaloids of *Berberis lycium*, Pakistan J. Sci. Indust. Res. 9 (4) (1966) 343–346.
[9] G.V. Sathyavathi, A.K. Guptha, N. Tandon, et al., Medicinal Plants of India, vol. 2, Indian Council Med. Res., New Delhi, India, 1987, pp. 230–239.
[10] M.N. Ali, A.A. Khan, Pharmacognostic studies of *Berberis lycium* Royle and its importance as a source of raw material for the manufacture of berberine in Pakistan, Pak. J. Fore. 28 (1) (1978) 25–27.
[11] E. Yesilada, E. Küpeli, *Berberis crataegina* DC, roots exhibits potent anti-inflammatory, analgesic and febrifuge effects in mice and rats, J. Ethnopharm. 79 (2002) 237–249.
[12] K. Yamamoto, H. Takase, K. Abe, Y. Saito, A. Suzuki, Pharmacological studies on antidiarrheal effects of a preparation containing berberine and geranii herba, Nippon Yakurigaku Zasshi 101 (1993) 169–175.
[13] W.M. Huang, Z.D. Wu, Y.Q. Gan, Effects of berberine on ischemic ventricular arrhythmia, Zhonghua Xin Xue Guan Bing Za Zhi 17 (1989) 300–301, 319.
[14] K. Fukuda, Y. Hibiya, M. Mutoh, M. Koshiji, S. Akao, H. Fujiwara, Inhibition of activator protein 1 activity by berberine in human hepatoma cells, Planta Med. 65 (1999) 381–383.
[15] N. Iizuka, K. Miyamoto, K. Okita, A. Tangoku, H. Hayashi, S. Yosino, T. Abe, T. Morioka, S. Hazama, M. Oka, Inhibitory effect of Coptidis rhizome and berberine on proliferation of human esophagus cancer cell line, Cancer Lett. 148 (2000) 19–25.
[16] Z. Liu, Q. Liu, B. Xu, J. Wu, C. Guo, F. Zhu, Q. Yang, G. Gao, Y. Gong, C. Shao, Berberine induces p53-dependent cell cycle arrest and apoptosis of human osteosarcoma cells by inflicting DNA damage, Mutat. Res. 9 (3) (2009) 75–83.
[17] M. Grusch, D. Polgar, S. Gfatter, K. Leuhuber, S. Huettenbrenner, C. Leisser, et al., Maintenance of ATP favours apoptosis over necrosis triggered by benzamide riboside, Cell Death Differ. 9 (2002) 169–178.
[18] R.R. Tice, E. Agurell, D. Anderson, et al., Single cell gel/comet assay: guidelines for in vitro and in vivo genetic toxicology testing, Environ. Mol. Mutagen. 35 (2000) 206–221.
[19] T. Lindl, J. Bauer, Zell- und Gewebekultur, Stuttgart, Jena, New York, 1994.
[20] H. Luo, Y. Li, J.J. Mu, J. Zhang, T. Tonaka, Y. Hamamori, S.Y. Jung, Y. Wang, J. Qin, Regulation of intra-S phase checkpoint by ionizing radiation (IR)-dependent and IR-independent phosphorylation of SMC3, J. Biol. Chem. 283 (28) (2008) 19176–19183.
[21] S. Madlener, M. Rosner, S. Krieger, B. Giessrigl, M. Gridling, T.P. Vo, C. Leisser, A. Lackner, I. Raab, M. Grusch, M. Hengstschläger, H. Dolznig, G. Krupitza, Short 42 °C heat shock induces phosphorylation and degradation of Cdc25A which depends on p38MAPK, Chk2, and 14.3.3, Hum. Mol. Genet. 18 (11) (2009) 1990–2000.
[22] D. Ray, H. Kiyokawa, CDC25A phosphatase: a rate-limiting oncogene that determines genomic stability, Cancer Res. 68 (2008) 1251–1253.
[23] J.D. Hooker, Flora of British India, vol. 3, Reeve and Co., London, 1882, p. 640.
[24] C.R. Karnick, Pharmacopoeial Standards of Herbal Plants, vol. 1, 1st ed., Satguru Publication, Delhi, India, 1994, p. 51.
[25] Mohd. Ali, S.K. Sharma, Heterocyclic constituents from *Berberis lycium* roots, Indian J. Heterocycl. Chem. 6 (2) (1996) 127–130.
[26] J.E.S. Leet, F. Hussain, R.D. Minard, M. Sharma, Sindamine Punjabine and gilgitine: three new secobisbenzylisoquinoline alkaloids, Heterocycles 19 (12) (1982) 2355–2360.
[27] Y.C. Cai, L.J. Xian, Inhibition of berberine on growth of human nasopharyngeal carcinoma cells CNE-2 in vivo and in vitro, Zhongcaoyao 37 (10) (2006) 1521–1526.
[28] K.S. Eom, J.M. Hong, M.J. Youn, H.S. So, R. Park, J.M. Kim, T.Y. Kim, Berberine induces G1 arrest and apoptosis in human glioblastoma T98G cells through mitochondrial/caspases pathway, Biol. Pharm. Bull. 31 (4) (2008) 558–562.
[29] Z. Wang, J. Lin, Effects of berberine on the proliferation and differentiation of HL-60 cells, Zhongguo Yaolixue Tongbao 20 (11) (2004) 1305–1308.
[30] C.C. Lin, S.Y. Lin, J.G. Chung, J.P. Lin, G.W. Chen, S.T. Kao, Down-regulation of cyclin B1 and up-regulation of Wee1 by berberine promotes entry of leukemia cells into the G2/M-phase of the cell cycle, Anticancer Res. 26 (2A) (2006) 1097–1104.
[31] Y. Hao, B. Xu, H. Zheng, X. Hang, Q. Qiu, Q. Huang, Effects of berberine on proliferation and apoptosis of HUVECs, Zhongguo Bingli Shengli Zazhi 21 (6) (2005) 1124–1127.
[32] J.X. Kang, J. Liu, J. Wang, C. He, F.P. Li, The extract of huanglian, a medicinal herb, induces cell growth arrest and apoptosis by upregulation of interferonbeta and TNF-alpha in human breast cancer cells, Carcinogenesis 26 (2005) 1934–1939.
[33] J.P. Lin, J.S. Yang, J.H. Lee, W.T. Hsieh, J.G. Chung, Berberine induces cell cycle arrest and apoptosis in human gastric carcinoma SNU-5 cell line, World J. Gastroenterol. 12 (2006) 21–28.
[34] S.K. Mantena, S.D. Sharma, S.K. Katiyar, Berberine inhibits growth, induces G1 arrest and apoptosis in human epidermoid carcinoma A431 cells by regulating Cdki-Cdk-cyclin cascade, disruption of mitochondrial membrane potential and cleavage of caspase 3 and PARP, Carcinogenesis 27 (2006) 2018–2027.
[35] J.M. Hwang, H.C. Kuo, T.H. Tseng, J.Y. Liu, C.Y. Chu, Berberine induces apoptosis through a mitochondria/caspases pathway in human hepatoma cells, Arch. Toxicol. 80 (2006) 62–73.
[36] H.L. Wu, C.Y. Hsu, W.H. Liu, B.Y.M. Yung, Berberine-induced apoptosis of human leukemia HL-60 cells is associated with down-regulation of nucleophosmin/B23 and telomerase activity, Int. J. Cancer 81 (6) (1999) 923–929.
[37] A.I. Marcus, J. Zhou, A. O'Brate, E. Hamel, J. Wong, M. Nivens, A. El-Naggar, T.P. Yao, F.R. Khuri, P. Giannakakou, The synergistic combination of the farnesyl transferase inhibitor lonafarnib and paclitaxel enhances tubulin acetylation and requires a functional tubulin deacetylase, Cancer Res. 65 (2005) 3883–3893.
[38] P.J. Wilson, A. Forer, Effects of nanomolar taxol on crane-fly spermatocyte spindles indicate that acetylation of kinetochore microtubules can be used as a marker of poleward tubulin flux, Cell Motil. Cytoskel. 37 (1997) 20–32.

Multifactorial anticancer effects of digalloyl-resveratrol encompass apoptosis, cell-cycle arrest, and inhibition of lymphendothelial gap formation in vitro.

Madlener S., Saiko P., Vonach C., Viola K., Huttary N., Stark N., Popescu R., Gridling M., Vo N.T., Herbacek I., Davidovits A., **Giessrigl B.**, Venkateswarlu S., Geleff S., Jäger W., Grusch M., Kerjaschki D., Mikulits W., Golakoti T., Fritzer-Szekeres M., Szekeres T. and Krupitza G.

Br. J. Cancer 102: 1361-137, **2010.**

British Journal of Cancer (2010) 102, 1361 – 1370
© 2010 Cancer Research UK All rights reserved 0007 – 0920/10 $32.00
www.bjcancer.com

Multifactorial anticancer effects of digalloyl-resveratrol encompass apoptosis, cell-cycle arrest, and inhibition of lymphendothelial gap formation *in vitro*

S Madlener[1], P Saiko[2], C Vonach[1,3], K Viola[1,3], N Huttary[1], N Stark[1], R Popescu[1,4], M Gridling[1], NT-P Vo[1,3], I Herbacek[5], A Davidovits[1], B Giessrigl[1], S Venkateswarlu[6], S Geleff[1], W Jäger[3], M Grusch[6], D Kerjaschki[1], W Mikulits[5], T Golakoti [6], M Fritzer-Szekeres[2], T Szekeres[2] and G Krupitza*[,1]

[1]Institute of Clinical Pathology, Medical University of Vienna, Vienna, Austria; [2]Clinical Institute of Medical and Chemical Laboratory Diagnostics, Medical University of Vienna, Vienna, Austria; [3]Department of Clinical Pharmacy and Diagnostics, University of Vienna, Vienna, Austria; [4]Department of Pharmacognosy, University of Vienna, Vienna, Austria; [5]Department of Medicine I, Institute of Cancer Research, Medical University of Vienna, Vienna, Austria; [6]Laila Impex R&D Center Unit I, Vijayawada, Andhra Pradesh, India

BACKGROUND: Digalloyl-resveratrol (di-GA) is a synthetic compound aimed to combine the biological effects of the plant polyhydroxy phenols gallic acid and resveratrol, which are both radical scavengers and cyclooxygenase inhibitors exhibiting anticancer activity. Their broad spectrum of activities may probably be due to adjacent free hydroxyl groups.

METHODS: Protein activation and expression were analysed by western blotting, deoxyribonucleoside triphosphate levels by HPLC, ribonucleotide reductase activity by ^{14}C-cytidine incorporation into nascent DNA and cell-cycle distribution by FACS. Apoptosis was measured by Hoechst 33258/propidium iodide double staining of nuclear chromatin and the formation of gaps into the lymphendothelial barrier in a three-dimensional co-culture model consisting of MCF-7 tumour cell spheroids and human lymphendothelial monolayers.

RESULTS: In HL-60 leukaemia cells, di-GA activated caspase 3 and dose-dependently induced apoptosis. It further inhibited cell-cycle progression in the G1 phase by four different mechanisms: rapid downregulation of cyclin D1, induction of Chk2 with simultaneous downregulation of Cdc25A, induction of the Cdk-inhibitor p21$^{Cip/Waf}$ and inhibition of ribonucleotide reductase activity resulting in reduced dCTP and dTTP levels. Furthermore, di-GA inhibited the generation of lymphendothelial gaps by cancer cell spheroid-secreted lipoxygenase metabolites. Lymphendothelial gaps, adjacent to tumour bulks, can be considered as gates facilitating metastatic spread.

CONCLUSION: These data show that di-GA exhibits three distinct anticancer activities: induction of apoptosis, cell-cycle arrest and disruption of cancer cell-induced lymphendothelial disintegration.

British Journal of Cancer (2010) **102,** 1361 – 1370. doi:10.1038/sj.bjc.6605656 www.bjcancer.com
© 2010 Cancer Research UK

Keywords: digalloyl-resveratrol; anti-neoplastic; Cdc25A; ribonucleotide reductase; lymphendothelial retraction

Translational Therapeutics

Digalloyl-resveratrol (di-GA) is a synthetic ester of the phytoalexin resveratrol (3,4′,5-trihydroxystilbene; RV) and the polyhydroxy phenolic compound gallic acid (3,4,5-trihydroxybenzoic acid; GA) (Figure 1). Gallic acid can be found in various natural products, such as green tea, pineapples, bananas, apple peels, red and white wine (Sun *et al*, 2002; De Beer *et al*, 2003; Wolfe *et al*, 2003). Resveratrol is a constituent of red wine and grapes. Both compounds are proposed to contribute to the 'French Paradox', a phenomenon of significantly lower (40%) heart infarction incidence in the French population, when compared with other European countries or the United States (Richard, 1987; Renaud and De Lorgeril, 1992; Constant, 1997). Gallic acid and RV were also described as excellent free radical scavengers (Inoue *et al*, 1994; Isuzugawa *et al*, 2001; Kawada *et al*, 2001; Salucci *et al*, 2002; Sohi *et al*, 2003; Horvath *et al*, 2005) and as inducers of differentiation and programmed cell death in a variety of tumour cell lines. Other beneficial properties of GA-containing fruit extracts include anti-diabetic and anti-angiogenic effects (Liu *et al*, 2005; Sridhar *et al*, 2005). Gallic acid is also present at high concentrations in gallnuts (name), which are proliferations of plant leaves that become elicited by gall wasp exudates to build up a hatchery for their larvae. Thus, the secretion of gall wasps stimulates plant cell growth and overrules homeostasis of the affected leaf area – this is similar to tumour outgrowth. In turn, the plant produces GA, which seems to combat the improper growth signals and re-establishes cell-cycle control. This could at least explain why gallnuts are rich in GA and that gallnuts do not grow beyond a certain size. This cytostatic property of GA – which is amplified in

*Correspondence: Dr G Krupitza;
E-mail: georg.krupitza@meduniwien.ac.at
Received 29 September 2009; revised 6 January 2010; accepted 25 January 2010

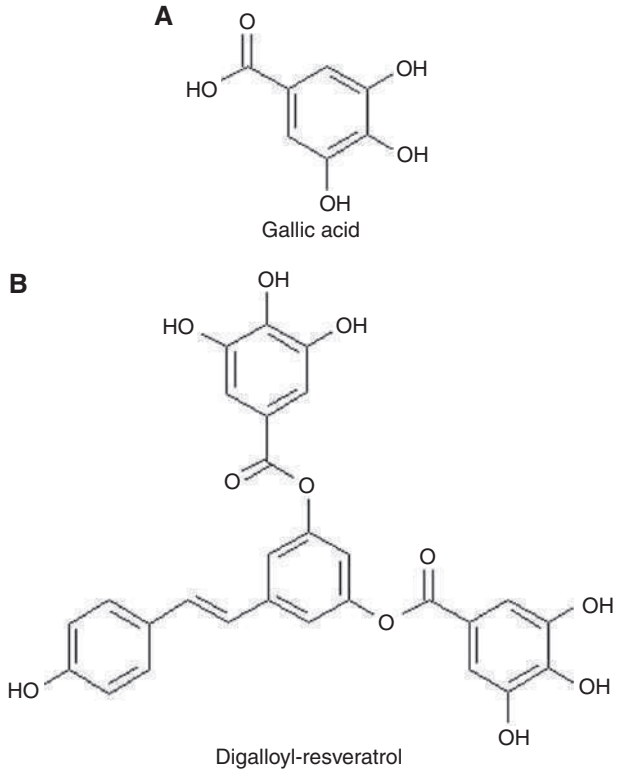

Figure 1 Chemical structures of (**A**) gallic acid (GA) and (**B**) digalloyl-resveratrol (di-GA).

di-GA – seems to be one of the cancer-protective principles of a variety of fruits and this could also be developed for adjuvant therapy.

Gallnuts are not used in modern western medicine, but they were mentioned in the first book of 'De Materia Medica' ascribed to Pedanios Dioscurides (the 'Vienna Dioscurides', Austrian National Library, which was written in the sixth century in Konstantinopolis, East Roman Empire). Interestingly, this manuscript claims that gallnuts 'stop the growth of proliferating tissue'. Other studies showed that RV and GA are effective inhibitors of the enzyme ribonucleotide reductase (RR; EC1.17.4.1) (Fontecave *et al*, 1998; Madlener *et al*, 2007). Ribonucleotide reductase is significantly upregulated in malignant cells compared to non-malignant cells. This enzyme catalyses the rate-limiting step of *de novo* DNA synthesis, which is the reduction of ribonucleotides into the corresponding deoxyribonucleoside triphosphates (dNTPs). This qualifies RR as an excellent target for cancer chemotherapy.

Apart from being a radical scavenger, the multifactorial effects of GA encompass also the inhibition of cyclooxygenases (COXs) and of lipoxygenases (LOXs). Tumours express high levels of COX-2 and 12-LOX (Nie *et al*, 2003; Pidgeon *et al*, 2003; Nassar *et al*, 2007), which metabolise arachidonic acid to prostanoids and to hydroxyeicosatetraenoic acids (12(*S*)-HETE), respectively (Marks *et al*, 2000). Certain HETEs function as inter- and intracellular messengers and cause the repulsion of endothelial cells thereby forming gaps in the endothelial cell layer (Ohigashi *et al*, 1989; Nakamori *et al*, 1997; Uchide *et al*, 2007). Further, these gaps may serve as entry ports for adjacent tumour cells into the lymphatic system. Thus, we hypothesised that GA (and di-GA) may inhibit lymphendothelial gap formation. Here we examine the effects of di-GA on apoptosis, cell-cycle progression and lymphendothelial gap formation.

MATERIALS AND METHODS

Chemicals

Nordihydroguaiaretic acid (NDGA) was from Cayman Chemical (Ann Arbor, MI, USA); and aspirin, mannitol, probucol, GA and RV were from Sigma-Aldrich (Vienna, Austria). Catalase and carboxy-PTIO were from Calbiochem-Merck Biosciences (Nottingham, UK). Berberine chloride dihydrate (purity 98.92%) was from Phytolab (Vestenbergsgreuth, Germany). Experimental stock solutions (in DMSO) were prepared always fresh.

Mouse monoclonal anti-Cdc25A (F-6) Cat. No. 7389; anti-PARP-1 (F-2) Cat. No. sc-8007; anti-cyclin D1 (M-20) Cat. No. sc-718; anti-cyclin E (M20) Cat. No. sc-481 and anti-p21$^{Cip/Waf}$ (C-19) Cat. No. sc-397 antibodies were from Santa Cruz Biotechnology Inc. (Heidelberg, Germany). Polyclonal anti-phospho-Cdc25A (Ser17) Cat. No. ab18321 antibody was from Abcam (Cambridge, UK); and monoclonal anti-p34^{Cdc2} Cat. No. C3085 and anti-β-actin (AC15) Cat. No. A5441 antibodies were from Sigma-Aldrich. Rabbit monoclonal anti-cleaved caspase 3 (CPP32) clone C92-605 Cat. No. 58404 antibody was from Research Diagnostics Inc. (Flanders, NJ, USA). Polyclonal anti-MEK 1/2 Cat. No. 9122; anti-phospho-MEK 1/2 (Ser217/221) Cat. No. 9121 m; anti-phospho-Chk2 (Thr68) Cat. No. 2661; anti-Chk2 Cat. No. 2662 and rabbit monoclonal anti-p44/42 MAP Kinase (137F5) Cat. No. 4695; anti-phospho-Cdc2 (Tyr15) Cat. No. 4539 and mouse monoclonal anti-phospho-p44/42 MAPK (Thr202/Tyr204) (E10) Cat. No. 9106 antibodies were from Cell Signaling Technology Inc. (Danvers, MA, USA). Anti-mouse IgG was from Dako (Vienna, Austria). Anti-rabbit IgG and Amersham ECL – high-performance chemiluminescence film – were from GE Healthcare (Vienna, Austria).

Cell culture

HL-60 human promyelocytic cells were purchased from ATCC (Wesel, Germany). Cells were grown in RPMI-1640 medium supplemented with 10% heat-inactivated fetal calf serum, 1% L-glutamine and 1% penicillin/streptomycin. MCF-7 cells were grown in McCoy 5A medium containing 10% fetal calf serum and 1% penicillin/streptomycin. Human normal lung fibroblasts (HLF) were a generous gift of the Cancer Research Institute of the Medical University of Vienna and were grown in RPMI medium containing 10% fetal calf serum and 1% penicillin/streptomycin. All media, supplements and G418 were obtained from Life Technologies (Lofer, Austria).

Human dermal microvascular endothelial cells (C-12260) were purchased from PromoCell (Heidelberg, Germany). To obtain a population of highly enriched lymphendothelial cells (LECs) dermal microvascular endothelial cells were sorted with polyclonal rabbit anti-human podoplanin antibody and sheep anti-rabbit dynabeads (M-280; Dynal 11203; Invitrogen, Lofer, Austria). Subsequently, residual cells were sorted with anti-CD31 (Dynal 11128). Incubations were performed at 4 °C for 30 min. Such isolated LECs were stable transfected with telomerase cDNA and then maintained in EGM2 Mv medium (EBM2-based medium CC3156 and supplement CC4147; Lonza, Walkersville, MD, USA) and G-418 (Schoppmann *et al*, 2004). All cell types were kept in humidified atmosphere containing 5% CO_2 at 37 °C.

Proliferation inhibition assay

HL-60 cells were seeded in T-25 tissue culture flasks at a concentration of 1×10^5 per ml and incubated with increasing concentrations of di-GA (2.5, 5, 7.5, 10 and 40 μM). Cell numbers and I_pC_{50} values were determined after 24 and 48 h using a CC-108 microcellcounter (Sysmex, Kobe, Japan).

 © 2010 Cancer Research UK

Determination of deoxyribonucleoside triphosphates

The extraction of cellular dNTPs was performed according to a method described previously (Garrett and Santi, 1979). HL-60 cells (7×10^7) were incubated with 5, 10 and 40 μM di-GA for 24 h. Then, 1×10^8 were centrifuged at 1800 r.p.m. and resuspended in 100 μl phosphate-buffered saline (PBS) and extracted with 10 μl trichloroacetic acid. The lysate was rested on ice and neutralised by adding 1.5 vol of freon containing 500 μM tri-n-octylamin. Afterwards the lysate was centrifuged (15 000 r.p.m. for 4 min) and the supernatant was used for periodation (100 μl extract + 30 μl 4 M methylamine (pH 7.5) + 10 μl periodat). Aliquots (120 μl) of each sample were analysed using a Merck 'La Chrom' HPLC-system equipped with D-7000 interface, L-7100 pump, L-7200 autosampler and L-7400 UV-detector. Detection time was set at 80 min, the detector operated on 280 nm for 40 min and then switched to 260 nm for another 40 min. Samples were eluted with a 3.2 M ammonium phosphate buffer, pH 3.6 (pH adjusted by addition of 3.2 M H_3PO_4), containing 20 mol l^{-1} acetonitrile using a 4.6 × 250 mm Partisil 10 SAX column (Whatman Ltd., Kent, UK). Separation was performed at constant ambient temperature and at a flow rate of 2 ml min^{-1}. The concentrations of each dNTP of the experimental samples were then calculated as percent of total area under the control curves. Chemicals were from Sigma-Aldrich and of highest available quality.

Hoechst 33258 and propidium iodide double staining

The vitality staining was performed according to a protocol described before (Grusch *et al*, 2002). HL-60 cells (0.4×10^6 per ml) were seeded in T-25 tissue culture flasks and exposed to increasing concentrations of di-GA (2.5, 5, 7.5, 10 and 40 μM) for 24 h. Hoechst 33258 and propidium iodide were purchased from Sigma-Aldrich and added directly to the cells at final concentrations of 5 and 2 μg/ml, respectively. After 60 min of incubation at 37 °C, we examined cells with a Zeiss Axiovert fluorescence microscope and a DAPI filter (Carl Zeiss, Jena, Germany). Cells were photographed and analysed by visual examination (not by FACS). This method allows to distinguish between early apoptosis, late apoptosis and necrosis. Cells were judged according to their nuclear morphology and the disintegration of their cell membranes, which is indicated by propidium iodide uptake.

Cell-cycle distribution analysis

HL-60 cells (0.4×10^6 per ml) were seeded in T-25 tissue culture flasks and incubated with 2.5, 5, 10 and 40 μM di-GA. After 24 h, cells were harvested, washed with 5 ml cold PBS, centrifuged (600 r.p.m. for 5 min) and resuspended and fixed in 3 ml ethanol (70%) at 4 °C for 30 min. After two further washing steps with cold PBS, RNAse A and propidium iodide were added to a final concentration of 50 μg ml^{-1} each and incubated at 4 °C for 60 min before analysis on a FACSCalibur flow cytometer (BD Biosciences, San Jose, CA, USA). The cell-cycle distribution was calculated with ModFit LT software (Verity Software House, Topsham, ME, USA).

Determination of RR *in situ* activity

Exponentially growing HL-60 cells (5×10^5) were incubated with 1, 2.5 and 5 μM di-GA for 24 h at 37 °C in a humidified atmosphere containing 5% CO_2 to assess changes in RR *in situ* activity. Then, cells were pulsed with ^{14}C-cytidine (Sigma-Aldrich; 3 μl in a 5 ml cell suspension) at 37 °C for 30 min, collected by centrifugation (1200 r.p.m. for 5 min), washed twice with PBS and processed to extract total genomic DNA. Thereafter, the radioactivity, which became incorporated into genomic DNA, was measured.

Western blotting

HL-60 cells (1.5×10^7 cells) were seeded into T-75 tissue culture flasks and incubated with 10 μM di-GA for 0.5, 2, 4, 8 and 24 h. Then, 1×10^6 cells were harvested (per experimental point), washed twice with cold PBS, centrifuged at 1000 r.p.m. for 5 min and lysed in a buffer containing 150 mM NaCl, 50 mM Tris (pH 8.0), 1% Triton X-100, 1 mM phenylmethylsulfonyl fluoride and protease inhibitor cocktail (from a × 100 stock; Sigma-Aldrich). The lysates were centrifuged at 4 °C for 20 min (12 000 r.p.m.) and supernatants stored at −20 °C until further analysis. Equal amounts of protein samples were separated by polyacrylamide gel electrophoresis and electroblotted onto PVDF membranes (Hybond, GE Healthcare) at 4 °C overnight. Equal sample loading was controlled by staining membranes with Poinceau S (Sigma-Aldrich). After washing with PBS/0.5% Tween 20 (PBS/T) (pH 7.2) or TBS/0.1% Tween 20 (TBS/T) (pH 7.6), membranes were blocked for 1 h in blocking solution (5% non-fat dry milk in PBS/T or in TBS/T). The membranes were incubated with the first antibody (in blocking solution, dilution 1 : 500 – 1 : 1000) by gently rocking at 4 °C overnight. Thereafter, the membranes were washed with PBS or TBS and further incubated with the second antibody (peroxidase-conjugated goat anti-rabbit IgG or anti-mouse IgG, dilution 1 : 2000 – 1 : 5000 in PBS/T or TBS/T) for 12 h. Chemoluminescence was developed by the ECL detection kit and the exposure of membranes to Amersham Hyperfilms (GE Healthcare).

MCF-7 spheroid generation

1.2 g of autoclaved methyl cellulose (M-0512; Sigma-Aldrich) was resuspended in 100 ml prewarmed McCoy 5A medium (Life Technologies; 1.2% stock concentration), stirred until the solution turned clear and centrifuged at 4000 r.p.m. (swing out rotor) for 2 h to pellet undesired debris. Then, 1×10^5 MCF-7 cells were transferred to 15 ml McCoy 5A medium containing 0.24% methyl cellulose (final concentration). 150 μl (containing $\sim 1 \times 10^3$ cells) was transferred to each well of a round bottom microtitre plate (96-well) to allow spheroid formation. Cells were allowed to aggregate and grow for 2 days, and then spheroids were sufficiently dense for further manipulations. MCF-7 spheroids had an average diameter of ~ 300 μm.

MCF-7 spheroid/LEC monolayer co-cultivation

LECs were seeded in EGM2 MV medium on 24-well plates and allowed to grow for 2 – 3 days until confluence. Then, LECs were stained with cytotracker green (concentration 2 μg ml^{-1} final concentration, Molecular Probes-C2925, Invitrogen) at 37 °C for 90 min and subsequently rinsed thoroughly. Thereafter, MCF-7 spheroids were washed in EGM2 MV medium to rid off methyl cellulose, and 12 spheroids were carefully transferred using wide bore yellow tips to each well containing LECs.

For those experiments in which inhibitors were used, the indicated inhibitor concentrations (final concentrations) were applied to the spheroids 30 min prior addition of the spheroids to the LEC layers.

Analysis of gap formation

LEC areas with spheroids on top were photographed using an FITC filter, which was used to visualise cytotracker (green)-stained LECs underneath the spheroids. Axiovert software (Carl Zeiss) facilitated to measure the gap areas within the LEC layers.

Statistical calculations

Dose – response curves were calculated using the Prism 4.03 software package (GraphPad, San Diego, CA, USA) and statistical

© 2010 Cancer Research UK

significance was determined by two-tailed paired t-test (significance $P<0.05$).

RESULTS

Quite a few studies on GA and its derivatives, RV and RV analogues were performed in human leukaemia cells (Saiko *et al*, 2008), because these cells are very sensitive to drugs and therefore advantageous to test the efficacy of novel anticancer compounds. HL-60 cells are particularly useful to discriminate the nuclear morphology of necrotic and apoptotic cells (Grusch *et al*, 2002) and hence, we used HL-60 cells to study di-GA facilitating the comparability of our results with published data of other GA and RV analogues.

Di-GA induces caspase 3 and apoptosis

The pro-apoptotic potential of naturally occurring GA was compared to that of synthetic di-GA by incubating HL-60 promyelocytic leukaemia cells to both agents (Figure 2A and B). Increasing concentrations of GA (10, 20, 40 and 80 μM) elicited 4, 10, 34 and 60% apoptosis, respectively. Because the di-GA molecule contains two galloyl residues (as compared to just one gallic acid molecule of GA) we expected that half of the di-GA concentrations would induce similar apoptosis rates as the tested GA concentrations. However, 5, 10 and 40 μM di-GA (to compare it to 10, 20 and 80 μM GA, see above) triggered 12, 39 and 84% apoptosis, respectively. In an earlier study, we showed that 25 and 50 μM RV induced $\sim$18 and 45% apoptosis in HL-60 cells, respectively (Horvath *et al*, 2006). Therefore, the apoptotic efficiency of di-GA is the sum of the apoptotic properties of 2$\times$ GA plus RV. Apoptosis correlated with the activation of caspase 3 and with the signature type cleavage of PARP into an 85 kDa fragment (Figure 2C). Digalloyl-resveratrol did not induce significant numbers of necrotic cells even at high concentrations (data not shown). The data suggest that di-GA is a potent inducer of apoptosis and significantly more effective than GA alone.

Di-GA inhibits G1-S transition

HL-60 cells were exposed to increasing concentrations of GA and di-GA and the cell numbers were measured after 24 and 48 h. The percentages of proliferation inhibition were calculated at both time points. Those concentrations that inhibited 50% proliferation (I_pC_{50}) are shown in Table 1. Digalloyl-resveratrol inhibited proliferation 7–10 times more efficiently than GA during the tested time period. Inhibition of cell proliferation was due to a dose-dependent cell-cycle block in G1 (Figure 3A).

Di-GA modulates mitogenic signalling and the expression of cell-cycle regulators

We next examined the levels of the cell-cycle inhibitor $p21^{Cip/Waf}$, which is known to inhibit Cdk2 by blocking its interaction with cyclin E (Jeon *et al*, 2007). $p21^{Cip/Waf}$ was induced within 4 h (Figure 3B), which was independent of p53, because HL-60 cells are p53 negative (Biroccio *et al*, 1999). Phosphorylation of Erk1 and MEK, which is indicative for their activation, preceded the increase in $p21^{Cip/Waf}$ levels. This is consistent with previous reports that MEK-Erk signalling upregulates $p21^{Cip/Waf}$ (Facchinetti *et al*, 2004; Park *et al*, 2004; Perez-Pinera *et al*, 2006). Phosphorylation of Erk2 (the lower band occurring after 4 and 8 h) was simultaneous to $p21^{Cip/Waf}$ upregulation. Next, we investigated whether the expression of the G1-specific cell-cycle regulators Cdc25A, cyclin D1 and cyclin E was altered by di-GA treatment (10 μM). Western blot analyses showed that cyclin D1 expression decreased after 2 h and remained suppressed, whereas cyclin E expression persisted (Figure 3C). Cyclin D1 is required for the activation of Cdk4 and Cdk6 (Lingfei *et al*, 1998; Alao, 2007),

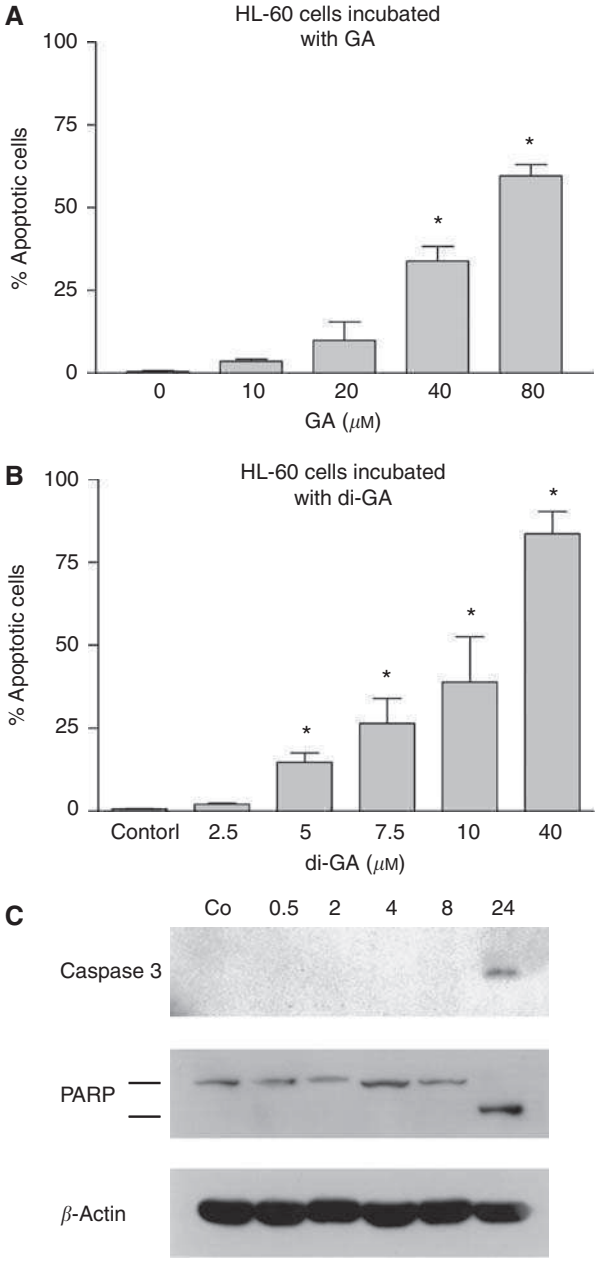

Figure 2 Induction of apoptosis by (**A**) GA and (**B**) di-GA in HL-60 cells. Cells were incubated with increasing concentrations of drugs for 24 h, and then double stained with Hoechst 33258 and propidium iodide. Afterwards cells were examined under the microscope with UV light connected to a DAPI filter. Nuclei with a morphological phenotype indicating apoptosis were counted and percentages of apoptotic cells were calculated. Experiments were conducted in triplicate. Error bars indicate s.e.m., asterisks significance ($P<0.05$). (**C**) Activation of caspase 3 and cleavage of PARP on treatment with di-GA. Logarithmically growing HL-60 cells were incubated with 10 μM di-GA for 0.5, 2, 4, 8 and 24 h. Afterwards cells were lysed and protein expression was analysed by western blotting. The anti-caspase 3 antibody recognises only the cleaved peptide indicating its activation. Anti-PARP antibody recognises the full-length form (116 kDa) and the signature-type cleaved product (85 kDa) that is generated by active caspase 3. The antibody against β-actin was used to monitor equal sample loading.

© 2010 Cancer Research UK

which altogether is controlled by Cdc25A (Iavarone and Massague, 1997). Digalloyl-resveratrol strongly induced serine 17 (Ser17) phosphorylation of Cdc25A after 4 h. Phosphorylation of Ser17-Cdc25A was shown to stabilise this phosphatase at a high activity status specifically in the M phase (Mailand *et al*, 2002), thereby de-phosphorylating and activating its target Cdk1 (Cdc2). This is mandatory for the transit through the G2-M phase (Karlsson-Rosenthal and Millar, 2006). Hence, Cdc25A controls not only the G1-S, but also the G2-M phase. Indeed, di-GA caused the de-phosphorylation of Tyr15-Cdc2 indicating that cells entered the mitotic phase. FACS analysis confirmed that 40 μM di-GA allowed ~90% of the cells to pass through S and M phase (likely due to Cdc25A activity) but accumulated in the subsequent G1 phase because cyclin D1 was repressed. Finally, Cdc25A protein level decreased after 24 h. This was paralleled by Chk2 activation (indicated by its phosphorylation at Thr68), presumably due to replicatory stress. Chk2 targets Cdc25A for proteolytic degradation (Karlsson-Rosenthal and Millar, 2006). In summary, the data suggest that di-GA inhibits cell proliferation by disturbing orchestrated mitogenic signalling.

Table 1 Concentrations of GA and di-GA that inhibit proliferation of HL-60 cells by 50%

	$I_pC_{50\ (24\,h)}$ (μM)	$I_pC_{50\ (48\,h)}$ (μM)
GA	21	24
Di-GA	4	2

Di-GA inhibits RR

Gallic acid is a radical scavenger (Whang *et al*, 2005) and inhibits RR through chelating the tyrosyl radical required for RR activity (Madlener *et al*, 2007). Ribonucleotide reductase is the rate-limiting enzyme for nucleotide metabolism necessary for DNA synthesis during cell division.

Hence, RR activity was investigated by an assay that measures the incorporation of ^{14}C-cytidin into genomic DNA. Figure 4A shows that ^{14}C-cytidin incorporation into genomic DNA decreased with increasing di-GA concentration. Further, RR activity was fully blocked on treatment with 5 μM di-GA. At this concentration the dCTP level (but not dTTP and dATP) dropped significantly (Figure 4B). In HT29 colon carcinoma cells, a similar effect of di-GA on RR activity, dCTP, dTTP and dATP levels was observed (Bernhaus *et al*, 2009).

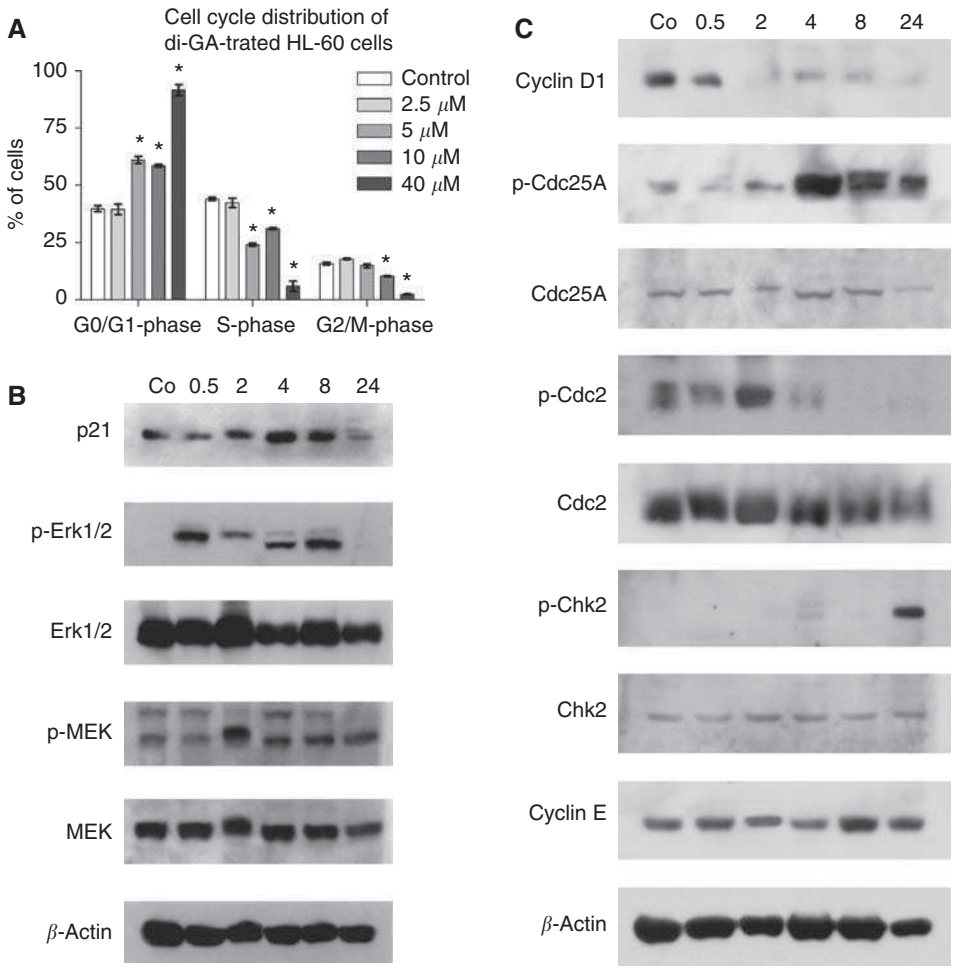

Figure 3 Effect of di-GA on the cell cycle of HL-60 cells. (**A**) Logarithmically growing HL-60 cells were incubated with increasing concentrations of di-GA for 24 h and then subjected to FACS analysis. Experiments were conducted in triplicate. Error bars indicate s.e.m., asterisks significance ($P<0.05$). HL-60 cells were incubated with 10 μM di-GA for 0.5, 2, 4, 8 and 24 h, lysed, and the (**B**) expression of p21$^{Cip/Waf}$, the phosphorylation of threonine202/tyrosine204-Erk1/2 (p-Erk1/2) and serine217/221-MEK1/2 (p-MEK), and (**C**) phosphorylation of threonine68-Chk2 (p-Chk2), serine17-Cdc25A (p-Cdc25A), tyrosine15-Cdc2 (p-Cdc2), and the protein levels of cyclin D1, E were analysed by western blotting. β-Actin served as loading control.

© 2010 Cancer Research UK

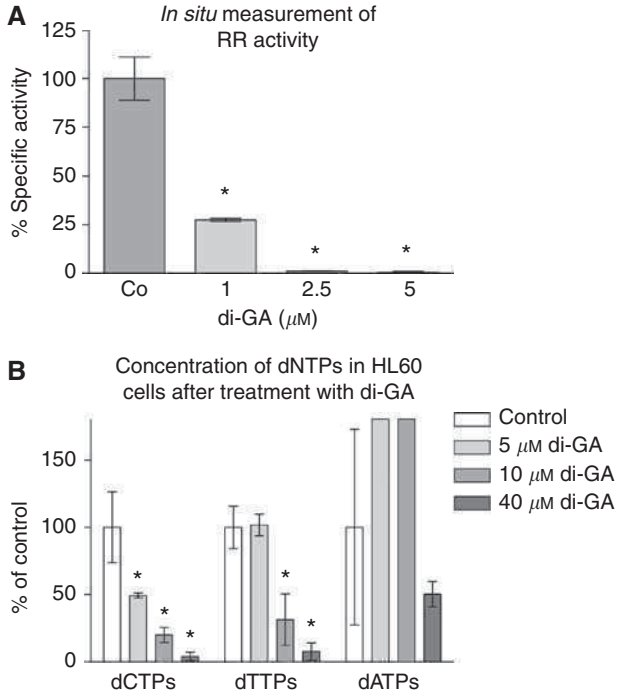

Figure 4 (**A**) Measurement of the *in situ* effect of di-GA on ribonucleotide reductase (RR) activity. HL-60 cells were incubated with 1, 2.5 and 5 μM di-GA for 24 h at 37 °C in a humidified atmosphere containing 5% CO_2 to assess changes in RR *in situ* activity. Then, cells were pulsed with ^{14}C-cytidine (Sigma-Aldrich; 3 μl in a 5 ml cell suspension) for 30 min at 37 °C. Afterwards the cells were collected and the radioactivity that became incorporated into genomic DNA was measured. (**B**) Effect of di-GA on intracellular dNTP pools in HL-60 cells. HL-60 cells were incubated with 5, 10 and 40 μM di-GA for 24 h. Then the cells were prepared for HPLC analysis and the dNTP levels were determined according to the protocol described in the 'Materials and methods' section. Experiments were conducted in triplicate. Error bars indicate s.e.m., asterisks significance ($P<0.05$).

Di-GA inhibits lymphendothelial gap formation induced by co-cultivated tumour cell spheroids

Leukocytes trespass basal membranes and trans-migrate tissues and endothelia as part of their normal physiological function and are therefore, *a priori* 'invasive'. Hence, HL-60 leukaemia cells are inappropriate to study the pathological invasiveness of cancer cells and the anti-invasive/anti-metastatic potential of di-GA. In contrast, solid tumours acquire an invasive potential in course of cancer progression and this particular cancer cell property has to be studied and combated. We developed a novel bulk invasion assay to establish an *in vitro* model resembling the pathologic situation of ductal breast cancer cells invading the lymphatic vasculature and to recapitulate the mechanism of metastasis (Ohigashi *et al*, 1989; Nakamori *et al*, 1997; Uchide *et al*, 2007). For this, telomerase immortalised human LECs were grown to confluent monolayers and MCF-7 tumour spheroids (average diameter $\sim$300 μm, containing $\sim$4000 cells) were placed on top to mimic tumour intrusion into lymphatics. Lymphendothelial cells were pre-labelled with cyto-tracker (green) immediately before co-cultivation, to monitor presence or absence of LECs underneath tumour spheroids (Figure 5A). Normal HLF spheroids served as negative controls, because these primary cells with limited lifespan (Hayflick limit) are non-malignant and do not invade blood or lymphatic vasculature. After 4 h of co-cultivation, gaps formed underneath >99% of the MCF-7 tumour spheroids (gap area was on average $\sim 1.15\times10^5\,\mu m^2$) whereas no or only small gaps were formed underneath normal lung fibroblasts. The gap size area was measured underneath at least 12 spheroids and in triplicate experiments. These gaps resemble entry ports for cancer cell bulks invading the lymphatic system, which is now widely accepted to be a route for the spreading of certain cancers (Alitalo *et al*, 2005; Oliver and Alitalo, 2005; Sipos *et al*, 2005).

Di-GA inhibited gap formation dose-dependently and maximally by >60% (Figure 5B). We have evidence (time-laps movies; data not shown) that gap formation is caused by LEC migration. Berberine was reported to inhibit cell migration and invasion of SCC-4 tongue squamous cancer cells (Ho *et al*, 2009) and HONE1 nasopharyngeal cancer cells (Tsang *et al*, 2009). The chemical structure of berberine is reminiscent to parts of di-GA and for control reasons we tested whether berberine had an effect on MCF-7-induced LEC behaviour. Berberine dose-dependently inhibited gap formation and this confirmed that the assay was functional and responded according to prediction.

Primary cancers and also MCF-7 breast cancer cells express elevated levels of LOXs, which metabolise arachidonic acid to HETEs (Marks *et al*, 2000; Nie *et al*, 2003; Kudryavtsev *et al*, 2005). The migration of endothelial cells was shown to be mediated by LOXs generating 12(*S*)-HETE (Ohigashi *et al*, 1989; Nakamori *et al*, 1997; Uchide *et al*, 2007). 12(*S*)-HETE functions as inter- and intracellular messenger and causes the retraction of endothelial cells, thereby forming gaps into the confluent cell layer. The 12/15-LOX inhibitors baicalein (100 μM) and NDGA (50 μM) reduced the area of MCF-7 spheroid-induced gaps in the LEC monolayers by $\sim$50 and 60%, respectively. Derivatives of GA are also known to inhibit HETE generating LOXs, and prostanoids generating COXs (Christow *et al*, 1991; Ha *et al*, 2004; Kim *et al*, 2006). However, because aspirin had no effect on gap formation (Figure 5B) the contribution of COXs can be excluded. We also took into account that NDGA, baicalein, GA and di-GA are powerful radical scavengers and antioxidants (Sohi *et al*, 2003; Floriano-Sanchez *et al*, 2006). In case LEC gaps were induced by radicals, gap formation should be inhibited by radical scavengers. To test this possibility, we analysed the efficacy of four *bona fide* ROS scavengers. In particular, we used mannitol, which scavenges the OH$^\bullet$ radical; probucol, which is an effective inhibitor of lipid peroxidation; catalase, which is an H_2O_2 catabolising enzyme; and carboxy-PTIO, which scavenges the NO$^\bullet$ radical. These scavengers did not prevent LEC gap formation. Therefore, MCF-7-induced gap formation was independent of a potential radical involvement.

Finally, we tested whether isolated GA and RV inhibited LEC gap formation. Whereas 50 μM RV inhibited gap size by $\sim$25%, 80 μM GA was ineffective. Therefore, GA did not affect cell migration, which was in contrast to a galloyl glucose derivate that inhibited tube formation of human microvessel endothelial cells (Lee *et al*, 2004). Methyl gallate influences 5-LOX (Kim *et al*, 2006) and GA may also inhibit this enzyme. However, 5-LOX did not contribute to LEC gap formation, because 100 μM caffeic acid did not reduce gap size (data not shown). This indicated that RV, but not GA, was the inhibitory principle being improved by the higher complex structure of di-GA.

In summary, di-GA dose-dependently inhibited LEC gap formation with an efficiency similar to that of NDGA. The strong anti-invasive property of di-GA is apparently due to the novel chemical structure of the compound, but not due to the GA residues, and only in part due to RV.

DISCUSSION

Gallic acid is a polyhydroxylated phenol previously known to scavenge radicals, inhibit RR, COXs, LOXs, arrest cell cycle and induce apoptosis (Ha *et al*, 2004; Faried *et al*, 2007; Hsu *et al*, 2007; Madlener *et al*, 2007).

Here we tested a novel synthetic GA derivate, di-GA, assuming that this compound may exhibit superior activity than GA itself.

 © 2010 Cancer Research UK

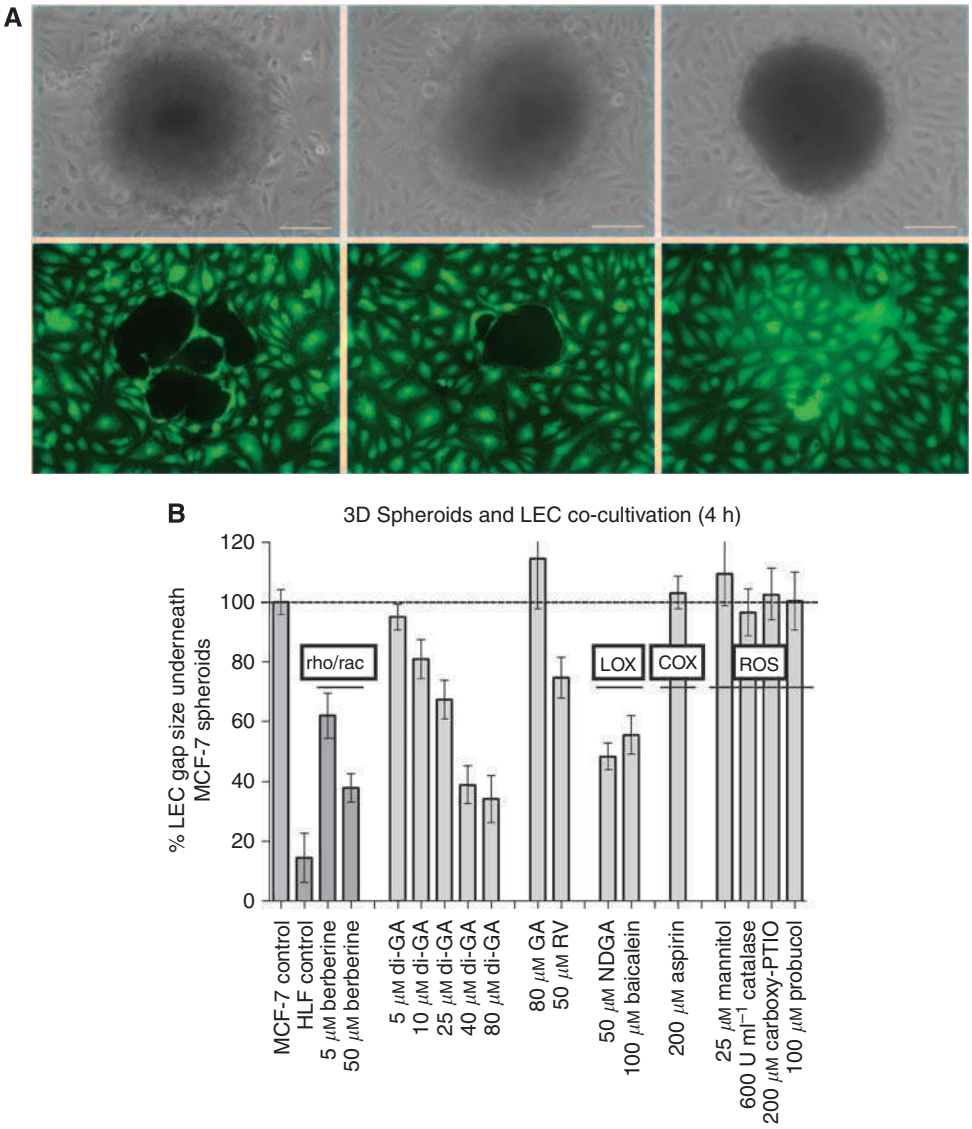

Figure 5 Effect of di-GA on MCF-7 spheroid-induced gap formation in lymphendothelial cell monolayers. (**A**) LEC monolayers that were exposed to MCF-7 spheroid (left side panels), MCF-7 spheroid treated with 40 μM di-GA (middle panels) and HLF spheroid (right side panels). Upper panels are phase-contrast micrographs showing the respective spheroids, the panels below show the identical power fields using FITC filter and exhibit green stained LECs underneath the respective spheroids. Bars in the lower right corners of upper panels indicate 100 μM. (**B**) MCF-7 tumor spheroids were preincubated with solvent (control), or 5 and 50 μM berberine; 5, 10, 25, 40 and 80 μM di-GA; 80 μM GA; 50 μM RV; 50 μM NDGA; 100 μM baicalein; 200 μM aspirin; 25 μM mannitol; 600 U ml^{-1} catalase; 200 μM carboxy-PTIO and 100 μM probucol, and then placed on top of cytotracker stained LEC monolayers that were also treated with respective agents for 4 h. Then, the size of the gaps that were formed in the LEC monolayers by MCF-7 spheroids (through repulsion of LECs) was measured using an inverted microscope connected to an FITC filter and equipped with Axiovision 4.5 software (Carl Zeiss). As negative controls normal human lung fibroblast (HLF) spheroids were used. Rho/rac (small GTPases regulating cell migration), LOX (lipoxygenase), COX (cyclooxygenases) and ROS (reactive oxygen species) indicate which mechanisms and phenomena are inhibited by the respective agents. Experiments were conducted in triplicate, and the underneath areas of at least 12 spheroids were analysed. Error bars indicate s.e.m., asterisks significance ($P<0.05$).

In fact, the pro-apoptotic property of 10 μM di-GA exceeded that of 20 μM GA by four-fold. Thus, an additional pro-apoptotic mechanism, apart from two galloyl residues, contributed to cell death especially at low concentrations. This is of particular interest because such concentrations can be achieved in humans. The RV backbone, to which the galloyl residues are connected, may be responsible for the additive effect, because RV was previously reported to induce apoptosis in HL-60 cells (Horvath *et al*, 2006). The apoptotic activity of di-GA was much higher than the reported RV activity (50 μM RV induced 50% apoptosis in HL-60), but the apoptotic activity of the RV derivative, 3,3′,4,4′,5,5′-hexahydroxystilbene (M8) was even higher than that of di-GA (Horvath *et al*, 2006). In contrast, another RV derivative with anti-neoplastic properties, *N*-hydroxy-*N*′-(3,4,5-trimethoxyphenyl)-3,4,5-trimethoxy-benzamidine (KITC), induced HL-60 apoptosis less efficiently (Saiko *et al*, 2007). Digalloyl-resveratrol triggered apoptosis through the caspase 3 pathway yet independent of p53, because HL-60 cells are p53 deficient (Biroccio *et al*, 1999). Because more than 50% of all cancer types harbour a defective p53 pathway, which is detrimental to successful therapeutic treatment, compounds that exert anticancer activity independent of p53 are of particular interest for clinical applications.

Another prominent anticancer property of therapeutic drugs is to arrest the cell cycle. This can be achieved by blocking distinct mechanisms such as cell-cycle regulators or enzymes involved in DNA-replicative processes etc. Here we show that di-GA inhibited

© 2010 Cancer Research UK

cell proliferation 10-fold more efficiently than GA (Madlener *et al*, 2007). This again suggests that the RV backbone synergised with the two galloyl residues. Similar to GA, di-GA also inhibited HL-60 cell cycle in G1 (Madlener *et al*, 2007). Resveratrol and its analogue M8 were shown to inhibit the cell cycle in S phase (Ragione *et al*, 1998; Horvath *et al*, 2006) and, therefore, the G1-inhibitory effect of the GA moieties was dominant over that of the RV backbone in the di-GA molecule. Interestingly, also KITC inhibited the HL-60 cell cycle in G1 phase (Saiko *et al*, 2007). Digalloyl-resveratrol caused cell-cycle arrest by four independent mechanisms:

(i) Di-GA downregulated cyclin D1 and thus presumably inhibited Cdk4 and/or Cdk6. Cyclin D1 was identified as the Prad 1 oncogene, which is overexpressed in many types of cancer (Lingfei *et al*, 1998; Alao, 2007). Therefore, suppression of cyclin D1 is a relevant target to combat cancer.
(ii) Di-GA induced $p21^{Cip/Waf}$ and, therefore, affected Cdk2. Both Cdk2- and Cdk4-activity are mandatory for G1-S transit. Hence, blocking Cdk4 and Cdk2 inhibits cell division. $p21^{Cip/Waf}$ upregulation was independent of p53, because HL-60 cells are p53 deficient. Consistent with reports that $p21^{Cip/Waf}$ is also induced by the MEK–Erk pathway (Facchinetti *et al*, 2004; Park *et al*, 2004), we found that di-GA triggered Erk1(p44Thr202)-phosphorylation within 30 min and MEK1(Ser217)-phosphorylation within 2 h. Further, Erk2(p42Tyr204)-phosphorylation occurred at 4 h, which was simultaneous with $p21^{Cip/Waf}$-induction.
(iii) Di-GA stabilised Cdc25A by Ser17 phosphorylation and forced cells through S and M phase. In consequence, ~90% of the cells accumulated in the following G1 phase due to cyclin D1 suppression and $p21^{Cip/Waf}$ induction. This may have resulted in replicative stress because after 24 h of di-GA treatment Chk2 became activated, which was paralleled by Cdc25A protein degradation. A similar effect was observed on heat shock treatment, which also induces the ATM–Chk2 pathway resulting in the degradation of Cdc25A (Madlener *et al*, 2009). In contrast, Agarwal *et al* (2006) observed an almost immediate Cdc25ASer17 phosphorylation and Chk2 activation on treatment of DU145 cells with GA that was not accompanied by degradation of Cdc25A.
(iv) Similar to GA, di-GA inhibited RR most probably by chelating the tyrosyl radical that is required for RR activity (Madlener *et al*, 2007). Resveratrol inhibits RR through a similar mechanism (Fontecave *et al*, 1998). At 5 μM di-GA inhibited 50% of dCTP synthesis, whereas it was reported that 50 μM GA did not inhibit dCTP synthesis whatsoever (Madlener *et al*, 2007). Digalloyl-resveratrol inhibited dCTP synthesis also several-fold more efficiently than RV (Horvath *et al*, 2005). This indicated that the galloyl residues synergised with the RV backbone to inhibit DNA replication.

It has been shown that MCF-7 cells induce gap formation into arterial endothelial cell layers by virtue of 12(*S*)-HETE secretion, which is generated by LOXs metabolising arachidonic acid (Kudryavtsev *et al*, 2005; Uchide *et al*, 2007). Gap formation was due to LEC migration (retraction) but not due to apoptosis of LECs, which was evidenced by microscopic time-laps movies (not shown) and by berberine-mediated inhibition of migration (Ho *et al*, 2009; Tsang *et al*, 2009). We extended this cell system using a three-dimensional co-culture model consisting of MCF-7 spheroids and telomerase-immortalised primary human LECs (Schoppmann *et al*, 2004), because this closely resembles ductal breast cancer bulks intruding the lymphatic vasculature. We showed that MCF-7-triggered lymphendothelial gap formation could be reduced to 40% by NDGA, which is a potent inhibitor of 12/15-LOXs but also a radical scavenger. Several gallate derivates are known to inhibit LOXs (Christow *et al*, 1991; Ha *et al*, 2004; Kim *et al*, 2006), to scavenge radicals (Whang *et al*, 2005) and to inhibit COX (Madlener *et al*, 2007; Kim *et al*, 2006). However, neither radicals nor COXs contributed to gap formation. Hence, baicalein- and NDGA-mediated inhibition supports the notion that at least 50–60% of gap formation was due to 12(*S*)-HETE generating LOX activity. The property of di-GA that reduced LEC migration was similar to that of NDGA. Also the tube formation of human microvessel endothelial cells, which was inhibited by a galloyl glucose derivate, was most likely due to the inhibition of cell migration (Lee *et al*, 2004). Because 12/15-LOX contributes to angiogenesis (Nie *et al*, 2000, 2006; Rose and Connolly, 2000) and tumour metastasis (Liu *et al*, 1996; Jankun *et al*, 2006), di-GA may prevent neo-vascularisation of tumours as well as infiltration of cancer cells into the lymphatic vasculature. Another derivate, galloyl glucose, blocked HT-1080 tumour invasion through gelatin by inhibiting matrix metalloprotease-2 (MMP-2) and MMP-9 (Ata *et al*, 1996). In our system, specific inhibition of MMP-2 and MMP-9 with cell permeable small molecules exhibited only a weak effect on MCF-7-mediated gap formation into LEC layers (data not shown). Interestingly, 80 μM GA did not decrease lymphendothelial gap formation whereas 50 μM RV inhibited gap formation by 25% evidencing that the principal inhibitory activity was contributed by RV and that the superior activity of di-GA was not the sum of RV plus GA, but a new property of its own.

This is analogous to the observation that the RV derivate M8 exhibits not only improved but even new anti-neoplastic properties. In particular, M8 inhibits ROCK1 expression in contrast to RV, which even induces ROCK1 protein levels (Paulitschke *et al*, 2009). ROCK1 supports migration, invasivity and lymph node metastasis of melanoma cells. M8 inhibits melanoma lymph node metastasis in an scid mouse model by ~50% at a concentration that is comparable to 50 μM used *in vitro* (Paulitschke *et al*, 2009). Interestingly, LEC gaps induced by melanoma spheroids could not be inhibited by NDGA or baicalein suggesting that different cancer types invade the lymphatic vasculature by a mechanism different of LOX. In addition to the effects described above, RV and M8 are shown to inhibit NF-κB (Holmes-McNary and Baldwin, 2000; Horvath *et al*, 2006). In preliminary investigations we found that specific inhibition of NF-κB by small molecules significantly attenuated LEC gap formation (data not shown). Whether di-GA affects ROCK1 expression and/or NF-κB translocation remains to be established. DMU-212 (3,4,5,4′-tetramethoxystilbene) is another RV derivate that exerts strong anti-neoplastic effects in breast carcinoma cells by tubulin polymerisation, which is a mechanism not induced by RV (Ma *et al*, 2008). Other approaches focus on RV analogues with improved cellular uptake properties such as a triacetate form of RV or vineatrol that both retain the anti-neoplastic properties of RV (Colin *et al*, 2009).

In conclusion, we describe three distinct anticancer effects of di-GA: the induction of apoptosis, the inhibition of cell division and the inhibition of gap formation into lymphendothelial layers. Further, we provide mechanistic explanations for the effect of di-GA on apoptosis and cell cycle. For gap formation, we show the affection of cell motility; however, an exact mechanism awaits elucidation.

ACKNOWLEDGEMENTS

We thank Toni Jäger for preparing the figures, and Professor Max J Scott, Massey University, Palmerston North, NZ, for carefully reading and styling the article. The work was supported by the Unruhe Privatstiftung, the Funds for Innovative and Interdisciplinary Cancer Research, and the Hochschuljubiläumsstiftung der Stadt Wien to GK; the Funds for Innovative and Interdisciplinary Cancer Research, and the Fonds zur Förderung der Wissenschaftlichen Forschung des Bürgermeisters der Bundeshauptstadt Wien, grant number 09059 to MF-S; the Hochschuljubiläumsstiftung der Stadt Wien to TS, and the Austrian Science Fund, FWF, Grant Numbers P19598-B13 and SFB F28, and the Herzfelder Family Foundation (to WM).

 © 2010 Cancer Research UK

REFERENCES

Agarwal C, Tyagi A, Agarwal R (2006) Gallic acid causes inactivating phosphorylation of cdc25A/cdc25C-cdc2 via ATM-Chk2 activation, leading to cell cycle arrest, and induces apoptosis in human prostate carcinoma DU145 cells. *Mol Cancer Ther* **5**(12)**:** 3294 – 3302

Alao JP (2007) The regulation of cyclin D1 degradation: roles in cancer development and the potential for therapeutic invention. *Mol Cancer* **6:** 24

Alitalo K, Tammela T, Petrova TV (2005) Lymphangiogenesis in development and human disease. *Nature* **438:** 946 – 953

Ata N, Oku T, Hattori M, Fujii H, Nakajima M, Saiki I (1996) Inhibition by galloylglucose (GG6-10) of tumor invasion through extracellular matrix and gelatinase-mediated degradation of type IV collagens by metastatic tumor cells. *Oncol Res* **8**(12)**:** 503 – 511

Bernhaus A, Fritzer-Szekeres M, Grusch M, Saiko P, Krupitza G, Venkateswarlu S, Trimurtulu G, Jaeger W, Szekeres T (2009) Digalloyl-resveratrol, a new phenolic acid derivative induces apoptosis and cell cycle arrest in human HT-29 colon cancer cells. *Cancer Lett* **274**(2)**:** 299 – 304

Biroccio A, Del Bufalo D, Ricca A, D'Angelo C, D'Orazi G, Sacchi A, Soddu S, Zupi G (1999) Increase of BCNU sensitivity by wt-p53 gene therapy in glioblastoma lines depends on the administration schedule. *Gene Therapy* **6:** 1064 – 1072

Christow S, Luther H, Ludwig P, Gruner S, Schewe T (1991) Actions of gallic esters on the arachidonic acid metabolism of human polymorphonuclear leukocytes. *Pharmazie* **46**(4)**:** 282 – 283

Colin D, Gimazane A, Lizard G, Izard JC, Solary E, Latruffe N, Delmas D (2009) Effects of resveratrol analogs on cell cycle progression, cell cycle associated proteins and 5fluoro-uracil sensitivity in human derived colon cancer cells. *Int J Cancer* **124**(12)**:** 2780 – 2788

Constant J (1997) Alcohol, ischemic heart disease, and the French paradox, Coro. *Artery Dis* **8:** 645 – 649

De Beer D, Joubert E, Gelderblom WC, Manley M (2003) Antioxidant activity of South African red and white cultivar wines: free radical scavenging. *J Agric Food Chem* **51:** 902 – 909

Facchinetti MM, De Siervi A, Toskos D, Senderowicz AM (2004) UCN-01-induced cell cycle arrest requires the transcriptional induction of p21(waf1/cip1) by activation of mitogen-activated protein/extracellular signal-regulated kinase kinase/extracellular signal-regulated kinase pathway. *Cancer Res* **64**(10)**:** 3629 – 3637

Faried A, Kurnia D, Faried LS, Usman N, Miyazaki T, Kato H, Kuwano H (2007) Anticancer effects of gallic acid isolated from Indonesian herbal medicine, *Phaleria macrocarpa* (Scheff.) Boerl, on human cancer cell lines. *Int J Oncol* **30**(3)**:** 605 – 613

Floriano-Sanchez E, Villanueva C, Medina-Campos ON, Rocha D, Sanchez-Gonzalez DJ, Cardenas-Rodriguez N, Pedraza-Chaverri J (2006) Nordihydroguaiaretic acid is a potent *in vitro* scavenger of peroxynitrite, singlet oxygen, hydroxyl radical, superoxide anion and hypochlorous acid and prevents *in vivo* ozone-induced tyrosine nitration in lungs. *Free Radical Res* **40**(5)**:** 523 – 533

Fontecave M, Lepoivre M, Elleingand E, Gerez C, Guittet O (1998) Resveratrol, a remarkable inhibitor of ribonucleotide reductase. *FEBS Lett* **421**(3)**:** 277 – 279

Garrett C, Santi DV (1979) A rapid and sensitive high pressure liquid chromatography assay for deoxyribonukleoside trisphosphate in cell extracts. *Anal Biochem* **99:** 268 – 273

Grusch M, Polgar D, Gfatter S, Leuhuber K, Huettenbrenner S, Leisser C, Fuhrmann G, Kassie F, Steinkellner H, Smid K, Peters GJ, Jayaram HN, Klepal W, Szekeres T, Knasmüller S, Krupitza G (2002) Maintainance of ATP favours apoptosis over necrosis triggered by benzamide riboside. *Cell Death Differ* **9:** 169 – 178

Ha TJ, Nihei K, Kubo I (2004) Lipoxygenase inhibitory activity of octyl gallate. *J Agric Food Chem* **52**(10)**:** 3177 – 3181

Ho YT, Yang JS, Li TC, Lin JJ, Lin JG, Lai KC, Ma CY, Wood WG, Chung JG (2009) Berberine suppresses *in vitro* migration and invasion of human SCC-4 tongue squamous cancer cells through the inhibitions of FAK, IKK, NF-kappaB, u-PA and MMP-2 and -9. *Cancer Lett* **279**(2)**:** 155 – 162

Holmes-McNary M, Baldwin Jr AS (2000) Chemopreventive properties of trans-resveratrol are associated with inhibition of activation of the IkappaB kinase. *Cancer Res* **60**(13)**:** 3477 – 3483

Horvath Z, Saiko P, Illmer C, Madlener S, Hoechtl T, Bauer W, Erker T, Jaeger W, Fritzer-Szekeres M, Szekeres T (2005) Synergistic action of resveratrol, an ingredient of wine, with Ara-C and tiazofurin in HL-60 human promyelocytic leukemia cells. *Exp Hematol* **33**(3)**:** 329 – 335

Horvath Z, Murias M, Saiko P, Erker T, Handler N, Madlener S, Jaeger W, Grusch M, Fritzer-Szekeres M, Krupitza G, Szekeres T (2006) Cytotoxic and biochemical effects of 3,3′,4,4′,5,5′-hexahydroxystilbene, a novel resveratrol analog in HL-60 human promyelocytic leukemia cells. *Exp Hematol* **34**(10)**:** 1377 – 1384

Hsu CL, Lo WH, Yen GC (2007) Gallic acid induces apoptosis in 3T3-L1 pre-adipocytes via a Fas- and mitochondrial-mediated pathway. *J Agric Food Chem* **55:** 7359 – 7365

Inoue M, Suzuki R, Koide T, Sakaguchi N, Ogihara Y, Yabu Y (1994) Antioxidant gallic acid, induces apoptosis in HL-60 RG cells. *Biochem Biophys Res Commun* **204:** 898 – 904

Isuzugawa K, Inoue M, Ogihara Y (2001) Catalase contents in cells determine sensitivity to the apoptosis inducer gallic acid, Biol. *Pharm Bull* **24:** 1022 – 1026

Iavarone A, Massague J (1997) Repression of the CDK activator Cdc25A and cell-cycle arrest by cytokine TGF-beta in cells lacking the CDK inhibitor p15. *Nature* **387:** 417 – 422

Jankun J, Aleem AM, Malgorzewicz S, Szkudlarek M, Zavodszky MI, Dewitt DL, Feig M, Selman SH, Skrzypczak-Jankun E (2006) Synthetic curcuminoids modulate the arachidonic acid metabolism of human platelet 12-lipoxygenase and reduce sprout formation of human endothelial cells. *Mol Cancer Ther* **5**(5)**:** 1371 – 1382

Jeon Y, Yong Lee K, Ji Ko M, Sun Lee Y, Kang S, Su Hwang D (2007) Human TopBP1 participates in cyclin E/CDK2 activation and preinitiation complex assembly during G_1/S transition. *J Biol Chem* **282**(20)**:** 14882 – 14890

Karlsson-Rosenthal C, Millar JB (2006) Cdc25: mechanisms of checkpoint inhibition and recovery. *Trends Cell Biol* **16**(6)**:** 285 – 292

Kawada M, Ohno Y, Ri Y, Ikoma T, Yuugetu H, Asai T, Watanabe M, Yasuda N, Akao S, Takemura G, Minatoguchi S, Gotoh K, Fujiwara H, Fukuda K (2001) Anti-tumor effects of gallic acid on LL-2 lung cancer cells transplanted in mice. *Anticancer Drugs* **12:** 847 – 852

Kim SJ, Jin M, Lee E, Moon TC, Quan Z, Yang JH, Son KH, Kim KU, Son JK, Chang HW (2006) Effects of methyl gallate on arachidonic acid metabolizing enzymes: cyclooxygenase-2 and 5-lipoxygenase in mouse bone marrow-derived mast cells. *Arch Pharm Res* **29**(10)**:** 874 – 878

Kudryavtsev IA, Gudkova MV, Pavlova OM, Oreshkin AE, Myasishcheva NV (2005) Lipoxygenase pathway of arachidonic acid metabolism in growth control of tumor cells of different type. *Biochemistry (Mosc)* **70**(12)**:** 1396 – 1403

Lee SJ, Lee HM, Ji ST, Lee SR, Mar W, Gho YS (2004) 1,2,3,4,6-Penta-*O*-galloyl-beta-D-glucose blocks endothelial cell growth and tube formation through inhibition of VEGF binding to VEGF receptor. *Cancer Lett* **208**(1)**:** 89 – 94

Lingfei K, Pingzhang Y, Zhengguo L, Jianhua G, Yaowu Z (1998) A study on p16, pRb, cdk4 and cyclinD1 expression in non-small cell lung cancers. *Cancer Lett* **130**(1 – 2)**:** 93 – 101

Liu XH, Connolly JM, Rose DP (1996) Eicosanoids as mediators of linoleic acid-stimulated invasion and type IV collagenase production by a metastatic human breast cancer cell line. *Clin Exp Metastasis* **14**(2)**:** 145 – 152

Liu Z, Schwimer J, Liu D, Greenway FL, Anthony CT, Woltering EA (2005) Black raspberry extract and fractions contain angiogenesis inhibitors. *J Agric Food Chem* **53:** 3909 – 3915

Ma Z, Molavi O, Haddadi A, Lai R, Gossage RA, Lavasanifar A (2008) Resveratrol analog *trans*-3,4,5,4′-tetramethoxystilbene (DMU-212) mediates anti-tumor effects via mechanism different from that of resveratrol. *Cancer Chemother Pharmacol* **63**(1)**:** 27 – 35

Madlener S, Illmer C, Horvath Z, Saiko P, Losert A, Herbacek I, Grusch M, Elford HL, Krupitza G, Bernhaus A, Fritzer-Szekeres M, Szekeres T (2007) Gallic acid inhibits ribonucleotide reductase and cyclooxygenases in human HL-60 promyelocytic leukemia cells. *Cancer Lett* **245**(1 – 2)**:** 156 – 162

Madlener S, Rosner M, Krieger S, Giessrigl B, Gridling M, Vo TP, Leisser C, Lackner A, Raab I, Grusch M, Hengstschläger M, Dolznig H, Krupitza G (2009) Short 42 degrees C heat shock induces phosphorylation and degradation of Cdc25A which depends on p38MAPK, Chk2 and 14.3.3. *Hum Mol Genet* **18**(11)**:** 1990 – 2000

Mailand N, Podtelejnikov AV, Groth A, Mann M, Bartek J, Lukas J (2002) Regulation of G(2)/M events by Cdc25A through phosphorylation-dependent modulation of its stability. *EMBO J* **21**(21)**:** 5911 – 5920

Marks F, Muller-Decker K, Furstenberger G (2000) A causal relationship between unscheduled eicosanoid signaling and tumor development:

cancer chemoprevention by inhibitors of arachidonic acid metabolism. *Toxicology* **153**(1–3): 11–26

Nakamori S, Okamoto H, Kusama T, Shinkai K, Mukai M, Ohigashi H, Ishikawa O, Furukawa H, Imaoka S, Akedo H (1997) Increased endothelial cell retraction and tumor cell invasion by soluble factors derived from pancreatic cancer cells. *Ann Surg Oncol* **4**(4): 361–368

Nassar A, Radhakrishnan A, Cabrero IA, Cotsonis G, Cohen C (2007) COX-2 expression in invasive breast cancer: correlation with prognostic parameters and outcome. *Appl Immunohistochem Mol Morphol* **15**(3): 255–259

Nie D, Krishnamoorthy S, Jin R, Tang K, Chen Y, Qiao Y, Zacharek A, Guo Y, Milanini J, Pages G, Honn KV (2006) Mechanisms regulating tumor angiogenesis by 12-lipoxygenase in prostate cancer cells. *J Biol Chem* **281**(27): 18601–18609

Nie D, Nemeth J, Qiao Y, Zacharek A, Li L, Hanna K, Tang K, Hillman GG, Cher ML, Grignon DJ, Honn KV (2003) Increased metastatic potential in human prostate carcinoma cells by overexpression of arachidonate 12-lipoxygenase. *Clin Exp Metastasis* **20**(7): 657–663

Nie D, Tang K, Diglio C, Honn KV (2000) Eicosanoid regulation of angiogenesis: role of endothelial arachidonate 12-lipoxygenase. *Blood* **95**(7): 2304–2311

Ohigashi H, Shinkai K, Mukai M, Ishikawa O, Imaoka S, Iwanaga T, Akedo H (1989) *In vitro* invasion of endothelial cell monolayer by rat ascites hepatoma cells. *Jpn J Cancer Res* **80**(9): 818–821

Oliver G, Alitalo K (2005) The lymphatic vasculature: recent progress and paradigms. *Annu Rev Cell Dev Biol* **21**: 457–483

Paulitschke V, Schicher N, Szekeres T, Jäger W, Elbling L, Riemer AB, Scheiner O, Trimurtulu G, Venkateswarlu S, Mikula M, Swoboda A, Fiebiger E, Gerner C, Pehamberger H, Kunstfeld R (2009) 3,3′,4,4′,5,5′-Hexahydroxystilbene impairs melanoma progression in a metastatic mouse model. *J Invest Dermatol*; e-pub ahead of print 3 December 2009. doi: 10.1038/jid.2009.376 PMID: 19956188

Park KS, Jeon SH, Oh JW, Choi KY (2004) p21Cip/WAF1 activation is an important factor for the ERK pathway dependent anti-proliferation of colorectal cancer cells. *Exp Mol Med* **36**(6): 557–562

Perez-Pinera P, Menendez-Gonzalez M, del Valle M, Vega JA (2006) Sodium chloride regulates extracellular regulated kinase 1/2 in different tumor cell lines. *Mol Cell Biochem* **293**(1–2): 93–101

Pidgeon GP, Tang K, Rice RL, Zacharek A, Li L, Taylor JD, Honn KV (2003) Overexpression of leukocyte-type 12-lipoxygenase promotes W256 tumor cell survival by enhancing alphavbeta5 expression. *Int J Cancer* **105**(4): 459–471

Ragione FD, Cucciolla V, Borriello A, Pietra VD, Racioppi L, Soldati G, Manna C, Galletti P, Zappia V (1998) Resveratrol arrests the cell division cycle at S/G2 phase transition. *Biochem Biophys Res Commun* **250**: 53–58

Renaud S, De Lorgeril M (1992) Wine, alcohol platelets, and the French paradox for coronary heart disease. *Lancet* **339**: 1523–1526

Richard JL (1987) Coronary risk factors. The French paradox. *Arch Mal Coeur Vaiss* **80**: 17–21

Rose DP, Connolly JM (2000) Regulation of tumor angiogenesis by dietary fatty acids and eicosanoids. *Nutr Cancer* **37**(2): 119–127

Saiko P, Szakmary A, Jaeger W, Szekeres T (2008) Resveratrol and its analogs: defense against cancer, coronary disease and neurodegenerative maladies or just a fad? *Mutat Res* **658**(1–2): 68–94

Saiko P, Ozsvar-Kozma M, Bernhaus A, Jaschke M, Graser G, Lackner A, Grusch M, Horvath Z, Madlener S, Krupitza G, Handler N, Erker T, Jaeger W, Fritzer-Szekeres M, Szekeres T (2007) *N*-hydroxy-*N*′-(3,4,5-trimethoxyphenyl)-3,4,5-trimethoxy-benzamidine, a novel resveratrol analog, inhibits ribonucleotide reductase in HL-60 human promyelocytic leukemia cells: synergistic antitumor activity with arabinofuranosylcytosine. *Int J Oncol* **31**(5): 1261–1266

Salucci M, Stivala LA, Maiani G, Bugianesi R, Vannini V (2002) Flavonoids uptake and their effects on cell cycle of human colon adenocarcinoma cells (Caco2). *Br J Cancer* **86**: 1645–1651

Schoppmann SF, Soleiman A, Kalt R, Okubo Y, Benisch C, Nagavarapu U, Herron GS, Geleff S (2004) Telomerase-immortalized lymphatic and blood vessel endothelial cells are functionally stable and retain their lineage specificity. *Microcirculation* **11**(3): 261–269

Sipos B, Kojima M, Tiemann K, Klapper W, Kruse ML, Kalthoff H, Schniewind B, Tepel J, Weich H, Kerjaschki D, Kloppel G (2005) Lymphatic spread of ductal pancreatic adenocarcinoma is independent of lymphangiogenesis. *J Pathol* **207**(3): 301–312

Sohi KK, Mittal N, Hundal MK, Khanduja KL (2003) Gallic acid, an antioxidant, exhibits antiapoptotic potential in normal human lymphocytes: a Bcl-2 independent mechanism. *J Nutr Sci Vitaminol (Tokyo)* **49**: 221–227

Sridhar SB, Sheetal UD, Pai MR, Shastri MS (2005) Preclinical evaluation of the antidiabetic effect of *Eugenia jambolana* seed powder in streptozotocin-diabetic rats, Braz. *J Med Biol Res* **38**: 463–468

Sun J, Chu YF, Wu X, Liu RH (2002) Antioxidant and antiproliferative activities of common fruits. *J Agric Food Chem* **50**: 7449–7454

Tsang CM, Lau EP, Di K, Cheung PY, Hau PM, Ching YP, Wong YC, Cheung AL, Wan TS, Tong Y, Tsao SW, Feng Y (2009) Berberine inhibits Rho GTPases and cell migration at low doses but induces G2 arrest and apoptosis at high doses in human cancer cells. *Int J Mol Med* **24**(1): 131–138

Uchide K, Sakon M, Ariyoshi H, Nakamori S, Tokunaga M, Monden M (2007) Cancer cells cause vascular endothelial cell (vEC) retraction via 12(S)HETE secretion; the possible role of cancer cell derived microparticle. *Ann Surg Oncol* **14**(2): 862–868

Whang WK, Park HS, Ham IH, Oh M, Namkoong H, Kim HK, Hwang DW, Hur SY, Kim TE, Park YG, Kim JR, Kim JW (2005) Methyl gallate and chemicals structurally related to methyl gallate protect human umbilical vein endothelial cells from oxidative stress. *Exp Mol Med* **37**(4): 343–352

Wolfe K, Wu X, Liu RH (2003) Antioxidant activity of apple peels. *J Agric Food Chem* **51**: 609–614

 © 2010 Cancer Research UK

A novel N-hydroxy-N'-aminoguanidine derivative inhibits ribonucleotide reductase activity: Effects in human HL-60 promyelocytic leukemia cells and synergism with arabinofuranosylcytosine (Ara-C).

Saiko P., Graser G., **Giessrigl B.**, Lackner A., Grusch M., Krupitza G., Basu A., Sinha B.N., Jayaprakash V., Jaeger W., Fritzer-Szekeres M. and Szekeres T.

Biochem Pharmacol. 81: 50-59, **2011.**

Biochemical Pharmacology 81 (2011) 50–59

Contents lists available at ScienceDirect

Biochemical Pharmacology

journal homepage: www.elsevier.com/locate/biochempharm

A novel N-hydroxy-N′-aminoguanidine derivative inhibits ribonucleotide reductase activity: Effects in human HL-60 promyelocytic leukemia cells and synergism with arabinofuranosylcytosine (Ara-C)

Philipp Saiko [a], Geraldine Graser [a], Benedikt Giessrigl [b], Andreas Lackner [c], Michael Grusch [c], Georg Krupitza [b], Arijit Basu [d], Barij Nayan Sinha [d], Venkatesan Jayaprakash [d], Walter Jaeger [e], Monika Fritzer-Szekeres [a], Thomas Szekeres [a,*]

[a] Department of Medical and Chemical Laboratory Diagnostics, Medical University of Vienna, General Hospital of Vienna, Waehringer Guertel 18-20, A-1090 Vienna, Austria
[b] Institute of Clinical Pathology, Medical University of Vienna, Waehringer Guertel 18-20, A-1090 Vienna, Austria
[c] Department of Medicine I, Division of Cancer Research, Medical University of Vienna, Borschkegasse 8a, A-1090 Vienna, Austria
[d] Department of Pharmaceutical Sciences, Birla Institute of Technology, Mesra 835 215, India
[e] Department of Clinical Pharmacy and Diagnostics, Faculty of Life Sciences, University of Vienna, Althanstrasse 14, A-1090 Vienna, Austria

ARTICLE INFO

Article history:
Received 13 July 2010
Accepted 7 September 2010

Keywords:
N-hydroxy-N′-aminoguanidines
Ribonucleotide reductase
Cell cycle arrest
Arabinofuranosylcytosine
Synergistic combination effects

ABSTRACT

Ribonucleotide reductase (RR; EC 1.17.4.1) is responsible for the *de novo* conversion of ribonucleoside diphosphates into deoxyribonucleoside diphosphates, which are essential for DNA replication. RR is upregulated in tumor cells and therefore considered to be an excellent target for cancer chemotherapy.

ABNM-13 (N-hydroxy-2-(anthracene-2-yl-methylene)-hydrazinecarboximidamide), a novel N-hydroxy-N′-aminoguanidine has been designed to inhibit RR activity using 3D molecular space modeling techniques. In this study, we evaluated its effect on human HL-60 promyelocytic leukemia cells. ABNM-13 proved to be a potent inhibitor of RR which was displayed by significant alterations of deoxyribonucleoside triphosphate (dNTP) pool balance and a highly significant decrease of incorporation of radiolabeled cytidine into DNA of HL-60 cells. Diminished RR activity caused replication stress which was consistent with activation of Chk1 and Chk2, resulting in downregulation/degradation of Cdc25A. In contrast, Cdc25B was upregulated, leading to dephosphorylation and activation of Cdk1. The combined disregulation of Cdc25A and Cdc25B was the most likely cause for ABNM-13 induced S-phase arrest. Finally, we combined ABNM-13 with the first-line antileukemic agent arabinofuranosylcytosine (Ara-C) and found that ABNM-13 synergistically potentiated the antineoplastic effects of Ara-C.

Due to these promising results, ABNM-13 deserves further preclinical and *in vivo* testing.

© 2010 Elsevier Inc. All rights reserved.

1. Introduction

Various compounds with hydroxyguanidine, thiosemicarbazide, and substituted benzohydroxamic acid functional groups have shown promising antitumor activity [1–5]. Hydroxyguanidines and hydroxysemicarbazides were especially active against human CCRF-CEM/0 and murine L1210 leukemia cells as well as against human HT-29 colon cancer cells [1–4,6]. These agents inhibited DNA synthesis as a consequence of inhibiting ribonucleotide reductase (RR; EC 1.17.4.1) activity.

RR is significantly upregulated in tumor cells in order to meet the increased need for deoxyribonucleoside triphosphates (dNTPs) of these rapidly proliferating cells for DNA synthesis [7]. The enzyme is an $\alpha2\beta2$ complex consisting of two subunits [8]. The effector binding R1 subunit possesses an $\alpha2$ homodimeric structure with substrate and allosteric effective sites that control enzyme activity and substrate specificity. The nonheme iron R2 subunit, a $\beta2$ homodimer, forms two dinuclear iron centers each stabilizing a tyrosyl radical. The inhibition of the nonheme iron subunit can be caused, for instance, by iron chelation or radical scavenging of the tyrosyl radical [9]. Additionally, a p53-inducible R2-homologue (p53R2) has been described recently [9]. Expression of the R2 and p53R2 subunits is induced by DNA damage and it has been reported that p53R2 supplies dNTPs for DNA repair in G_0/G_1 cells in a p53-dependent manner [10]. Hydroxyurea (HU) is the first RR inhibitor that has been used in clinical practice and is given to treat chronic myeloid leukemia and many other neoplastic diseases [11,12]. Difluorodeoxycytidine (Gemcitabine; dFdC) is applied in chemotherapy regimens against non-small cell lung cancer and pancreatic cancer [13,14].

* Corresponding author. Tel.: +43 1 40400 5365; fax: +43 1 320 33 17.
E-mail address: thomas.szekeres@meduniwien.ac.at (T. Szekeres).

0006-2952/$ – see front matter © 2010 Elsevier Inc. All rights reserved.
doi:10.1016/j.bcp.2010.09.006

HU is believed to destabilize R2 iron centers by scavenging the tyrosyl radical which is essential for enzyme activity [9,15]. Several newer iron chelating agents including tachypyridine [16–20] and a number of thiosemicarbazones such as triapine [9,21] were shown to interact with the iron-containing R2 subunit. These compounds are currently under (pre)clinical development.

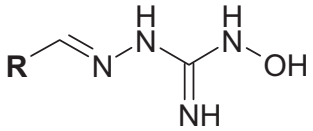

ABNM	R	IC_{50} (μM)
1	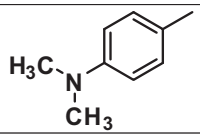	> 100
2	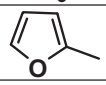	> 100
3	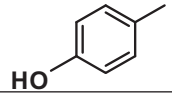	> 100
4	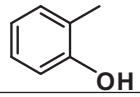	95
5	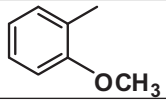	> 100
6	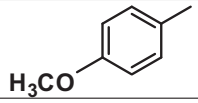	> 100
7	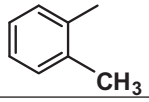	> 100
8	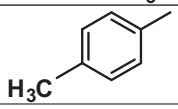	67
9	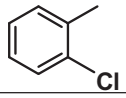	60
10	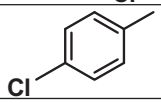	> 100
11	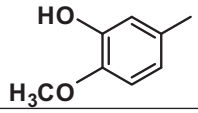	> 100
12	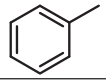	62
13	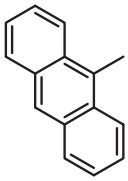	11

Fig. 1. Structural formula and biological activity of ABNM 1-13 in HL-60 cells. HL-60 cells (0.1×10^6 per ml) were incubated with increasing concentrations of drugs for 72 h. Cell counts and IC_{50} values (IC_{50} = 50% growth inhibition of tumor cells) were determined using a microcellcounter CC-110. Viability of cells was determined by trypan blue staining. Results were calculated as number of viable cells. Data are means ± standard errors of three determinations.

Modern drug design uses qualitative and quantitative structure–activity relationship (QSAR) studies as an approach to find relationships between chemical structures or structure-related properties and biological activities of distinct compounds. Based on the prediction of the best QSAR model, we synthesized 13 novel compounds (ABNM-1 to ABNM-13) with potential RR inhibitory capacities. Five of these agents were active in human HL-60 promyelocytic leukemia cells and ABNM-13 was chosen as lead substance because of its pronounced growth inhibitory effects which were up to 10-fold stronger than those of HU. The HL-60 cell line is an excellent *in vitro* model and has been extensively used by our group and others, especially with regard to investigate RR activity after treatment with various drugs. Additionally, growth inhibition and cytotoxicity caused by ABNM-13 were also investigated in human AsPC-1 pancreatic cancer cells. To study the mechanisms by which ABNM-13 influences cell cycle transit in HL-60 cells, we examined the effects on RR and the cell cycle regulators downstream of checkpoint kinase activation.

In general, anticancer drugs are more effective when used in combination. The major advantage of drug combinations is the achievement of additive or synergistic effects through intimidation of distinct molecular pathways and, accordingly, a decrease of drug resistance. For example, administration of leucovorin increases the binding of an active 5-fluorouracil metabolite to its target, thymidylate synthase, thus increasing the antineoplastic effects [22]. In addition, various RR inhibitors caused synergism together with arabinofuranosylctosine (Ara-C), a first line antileukemia drug affecting intracellular dCTP pools [23–27]. Following this strategy, we combined ABNM-13 with Ara-C in order to test potential additive or synergistic properties.

2. Materials and methods

2.1. Chemicals and supplies

ABNM 1-13 were synthesized and provided by the Department of Pharmaceutical Sciences, Birla Institute of Technology, Mesra, India. Structural formulas are shown in Fig. 1. Ara-C, HU and all other chemicals and reagents were commercially available (Sigma–Aldrich, Vienna, Austria) and of highest purity.

2.2. Cell culture

The human HL-60 promyelocytic leukemia and human AsPC-1 pancreatic adenocarcinoma cell lines were purchased from ATCC (American Type Culture Collection, Manassas, VA, USA). Both lines were grown in RPMI 1640 medium supplemented with 10% heat inactivated fetal calf serum (FCS), 1% L-glutamine, and 1% penicillin–streptomycin at 37 °C in a humidified atmosphere containing 5% CO_2 using a Heraeus cytoperm 2 incubator (Heraeus, Vienna, Austria). AsPC-1 cells were grown in a monolayer culture using 25 cm^2 tissue culture flasks and were periodically detached from the flask surface by 0.25% trypsin–ethylenediaminetetraacetic acid (trypsin–EDTA) solution. All media and supplements were obtained from Life Technologies (Paisley, Scotland, UK). Cell counts were determined using a microcellcounter CC-110 (SYSMEX, Kobe, Japan). Cells growing in the logarithmic phase of growth were used for all experiments described below.

2.3. Growth inhibition assay

HL-60 cells (0.1×10^6 per ml) were seeded in 25 cm^2 Nunc tissue culture flasks and incubated with increasing concentrations

of ABNM 1–13 or HU at 37 °C under cell culture conditions. Cell counts and IC_{50} values (IC_{50} = 50% growth inhibition of tumor cells) were determined after 24, 48, and 72 h using a microcellcounter CC-110.

In another set of experiments, AsPC-1 cells were seeded in 25 cm^2 Nunc tissue culture flasks and allowed to attach overnight. Cells were then incubated with increasing concentrations of ABNM-13 for 72 h. After that period, cells were detached from the flask surface by 0.25% trypsin–ethylenediaminetetraacetic acid (trypsin–EDTA) solution. After removal of trypsin–EDTA by centrifugation and suspension of the pellet in RPMI 1640 medium, cells were counted using a microcellcounter CC-110. Viability of cells was determined by staining with trypan blue. Results were calculated as number of viable cells.

2.4. Clonogenic assay

AsPC-1 cells (2×10^3 per well) were plated in 24-well plates and allowed to attach overnight at 37 °C in a humidified atmosphere containing 5% CO_2. Then cells were incubated with increasing concentrations of ABNM-13 for 6 days. Subsequently, the medium was carefully removed from the wells and the plates were stained with 0.5% crystal violet solution for 5 min. Colonies of more than 50 cells were counted using an inverted microscope at 40-fold magnification.

2.5. MTT chemosensitivity assay

AsPC-1 or HL-60 cells (5×10^3 per well) were seeded in 96-well microtiter plates in supplemented RPMI 1640 medium. AsPC-1 cells were allowed to attach overnight. Cells were then incubated with various concentrations of ABNM-13 for 96 h at 37 °C under cell culture conditions. After that period, the reduction of the yellow tetrazolium compound 3-(4,5-dimethylthiazo-2-yl)-2,5-diphenyl tetrazoliumbromide (MTT) by the mitochondrial dehydrogenases of viable cells to a purple formazan product was determined using an assay kit from Promega® according to the supplier's manual. The change in absorbance at 550 nm was tracked on a Wallac 1420 Victor 2 multilabel plate reader (PerkinElmer Life and Analytical Sciences). Drug effect was quantified as the percentage of control absorbance of reduced dye at this wavelength.

2.6. Simultaneous growth inhibition assay using ABNM-13 and Ara-C

HL-60 cells (0.1×10^6 per ml) were simultaneously incubated with various concentrations of ABNM-13 (12.5, 15, 17.5, and 20 μM) and Ara-C (10, 15, and 20 nM) for 72 h. After that period, cells were counted using a microcellcounter CC-110.

2.7. Sequential growth inhibition assay using ABNM-13 and Ara-C

HL-60 cells (0.1×10^6 per ml) were first incubated with different concentrations of ABNM-13 (2.5, 5, 7.5, and 10 μM) for 24 h. Then ABNM-13 was washed out and cells were further exposed to various concentrations of Ara-C (10, 15, and 20 nM) for another 48 h. After that period, cells were counted using a microcellcounter CC-110.

2.8. Cell cycle distribution analysis

Cells (0.4×10^6 per ml) were seeded in 25 cm^2 Nunc tissue culture flasks and incubated with increasing concentrations of drugs at 37 °C under cell culture conditions. After 24 h, cells were harvested and suspended in 5 ml cold PBS, centrifuged, resuspended and fixed in 3 ml cold ethanol (70%) for 30 min at 4 °C. After two washing steps in cold PBS RNAse A and propidium iodide were added to a final concentration of 50 μg/ml each and incubated at 4 °C for 60 min before measurement. Cells were analyzed on a FACSCalibur flow cytometer (BD Biosciences, San Jose, CA, USA) and cell cycle distribution was calculated with ModFit LT software (Verity Software House, Topsham, ME, USA).

2.9. Western blotting

After incubation with 15 μM ABNM-13 and/or 15 nM Ara-C, HL-60 cells (2×10^6 per ml) were harvested, washed twice with ice-cold PBS (pH 7.2) and lysed in a buffer containing 150 mM NaCl, 50 mM Tris-buffered saline (Tris pH 8.0), 1% Triton X-100, 2.5% 100 mM phenylmethylsulfonylfluoride (PMSF) and 2.5% protease inhibitor cocktail (PIC; from a 100× stock). The lysate was centrifuged at 12,000 rpm for 20 min at 4 °C, and the supernatant was stored at −20 °C until further analysis. Equal amounts of protein samples were separated by polyacrylamide gel electrophoresis (PAGE) and electroblotted onto PVDF membranes (Hybond, Amersham) overnight at 4 °C. Equal sample loading was controlled by staining membranes with Ponceau S. After washing with PBS/Tween-20 (PBS/T) pH 7.2 or Tris/Tween-20 (TBS/T) pH 7.6, membranes were blocked for 60 min in blocking solution (5% non-fat dry milk in PBS containing 0.5% Tween-20 or in TBS containing 0.1% Tween-20). Then membranes were incubated with the first antibody (in blocking solution, dilution 1:500 to 1:1000) by gently rocking at 4 °C, overnight. Subsequently, the membranes were washed with PBS or TBS and further incubated with the second antibody (peroxidase-conjugated goat anti-rabbit IgG, anti-mouse IgG, or donkey anti-goat IgG – dilution 1:2000 to 1:5000 in PBS/T or TBS/T) at room temperature for 60 min. Chemiluminescence was developed by the ECL detection kit (Amersham, Buckinghamshire, UK) and then membranes were exposed to Amersham Hyperfilms.

Equal numbers of cells were lysed for each sample, protein content was measured by the Bradford method, and PVDF membranes were checked by Ponceau S staining. Equal sample loading was controlled by β-actin expression which appeared to be stable when inspected in short term exposures to X-ray films. Each Western blot experiment was performed at least twice, and specific experimental points were done more often as they served as internal controls.

Antibodies directed against p(Ser1981)-ATM, p(Ser317)-Chk1, Chk1, p(Thr68)-Chk2, Chk2, p(Tyr15)-Cdc2, cleaved Caspase-3 (Asp175) and anti-rabbit IgG were from Cell Signaling (Danvers, MA, USA), against p(Ser75)-Cdc25A from Abcam (Cambridge, MA, USA), against p(Ser177)-Cdc25A from Abgent (San Diego, CA, USA), against R1 (T-16), R2 (I-15), p53R2 (N-16), Cdc25A (F-6), Cdc25B (C-20), Cdc25C (C-20), Cdc2 p34 (17), and donkey anti-goat IgG from Santa Cruz (Santa Cruz, CA, USA), against ph(Ser139)-γH2AX from Merck (Darmstadt, Germany), against β-actin from Sigma (St. Louis, MO, USA), and anti-mouse IgG was from Dako (Glostrup, Denmark).

2.10. Incorporation of ^{14}C-labeled cytidine into DNA (DNA synthesis assay)

To analyze the effect of ABNM-13 treatment on the activity of DNA synthesis, an assay was performed as described previously [28]. Radiolabeled ^{14}C-cytidine has to be reduced by RR in order to be incorporated into the DNA of HL-60 cells following incubation with ABNM-13 and/or Ara-C. HL-60 cells (0.4×10^6 cells per ml) were incubated with various concentrations of ABNM-13 for 24 h. After that, cells were counted and pulsed with ^{14}C-cytidine (0.3125 μCi, 5 nM) for 30 min at 37 °C. In another set of experiments, cells were treated with ABNM-13 and/or Ara-C for 30 min and simultaneously pulsed with ^{14}C-cytidine (0.3125 μCi,

5 nM). Afterwards, cells were collected by centrifugation and washed with PBS. Total DNA from 5×10^6 cells was purified by phenol–chloroform–isoamyl alcohol extraction and specific radioactivity of the samples was determined using a Wallac 1414 liquid scintillation counter (PerkinElmer, Boston, MA) whose read out was normalized by a Hitachi U-2000 Double Beam Spectrophotometer to ensure equal amounts and purity of DNA.

2.11. Determination of deoxyribonucleoside triphosphates (dNTPs)

Cells were seeded in 175 cm^2 tissue culture flasks (5×10^7 per flask) and incubated with increasing concentrations of ABNM-13 for 24 h. The cells were then centrifuged at $1800 \times g$ for 5 min, resuspended in 100 μl of PBS, and extracted with 10 μl of trichloracetic acid (90%). The lysate was allowed to rest on ice for 30 min and neutralized by the addition of 1.5 volumes of freon containing 0.5 mol/l tri-n-octylamine. Concentrations of dNTPs were then determined using the method described by Garrett and Santi [29]. Aliquots (100 μl) of the samples were analyzed using a Merck "La Chrom" high-performance liquid chromatography (HPLC) system (Merck, Darmstadt, Germany) equipped with D-7000 interface, L-7100 pump, L-7200 autosampler, and L-7400 UV detector. Detection time was set at 80 min, with the detector operating on 280 nm for 40 min and then switched to 260 nm for another 40 min. Samples were eluted with a 3.2 M ammonium phosphate buffer (pH 3.6, adjusted by the addition of 3.2 mM H_3PO_4) containing 20 M acetonitrile using a 4.6×250 mm PARTISIL 10 SAX column (Whatman Ltd., Kent, UK). Separation was performed at constant ambient temperature and a flow rate of 2 ml per min. The concentration of each dNTP was calculated as percentage of the total area under the curve for each sample.

2.12. Hoechst dye 33258 and propidium iodide double staining

The Hoechst staining was performed according to the method described by our group [30]. HL-60 cells (0.2×10^6 per ml) were seeded in 25 cm^2 Nunc tissue culture flasks and exposed to increasing concentrations of ABNM-13 for 24 and 48 h. Hoechst 33258 (HO, Sigma, St. Louis, MO, USA) and propidium iodide (PI, Sigma, St. Louis, MO, USA) were added directly to the cells to final concentrations of 5 μg/ml and 2 μg/ml, respectively, followed by 60 min of incubation at 37 °C. Cells were examined on a Nikon Eclipse TE-300 Inverted Epi-Fluorescence Microscope (Nikon, Tokyo, Japan) equipped with a Nikon DS-5M-L1 Digital Sight Camera System including appropriate filters for Hoechst 33258 and PI. This method allows distinguishing between early apoptosis, late apoptosis, and necrosis and is therefore superior to TUNEL assay which fails to discriminate among apoptosis and necrosis [31,32] and does not provide any morphological information. In addition, the HO/PI staining is more sensitive than a customary FACS based Annexin V binding assay [32–34]. The Hoechst dye stains the nuclei of all cells and thus allows monitoring cellular changes associated with apoptosis, such as chromatin condensation and nuclear fragmentation. In contrast, PI is excluded from viable and early apoptotic cells; consequently, PI uptake indicates loss of membrane integrity being characteristic of late apoptotic and necrotic cells. In combination with fluorescence microscopy to evaluate the morphologies of nuclei, the selective uptake of the two dyes enables studying the induction of apoptosis in intact cultures and to distinguish it from non-apoptotic cell death by means of necrosis. The latter is characterized by nuclear PI uptake without chromatin condensation or nuclear fragmentation [35].

Cells were judged according to their morphology and the integrity of their cell membranes, counted under the microscope and the number of apoptotic cells was given as percentage value.

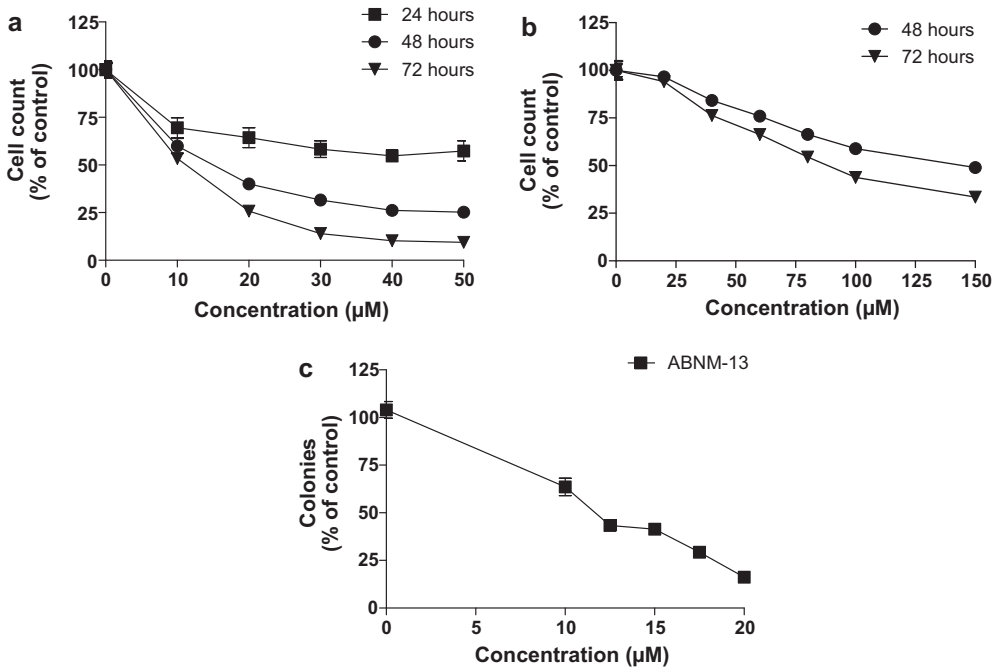

Fig. 2. (a and b) Growth inhibition of HL-60 cells after incubation with ABNM-13 or HU. HL-60 cells (0.1×10^6 per ml) were incubated with increasing concentrations of ABNM-13 or HU. Cell counts and IC_{50} values (IC_{50} = 50% growth inhibition of tumor cells) were determined using a microcellcounter CC-110. Viability of cells was determined by trypan blue staining. Results were calculated as number of viable cells. Data are means ± standard errors of three determinations. (c) Inhibition of colony formation of AsPC-1 cells after incubation with ABNM-13. AsPC-1 cells (2×10^3 per well) were plated in 24-well plates and allowed to attach overnight at 37 °C in a humidified atmosphere containing 5% CO_2. After 24 h, the cells were incubated with increasing concentrations of ABNM-13 for 6 days. Subsequently, the medium was carefully removed from the wells and the plates were stained with 0.5% crystal violet solution for 5 min. Colonies of more than 50 cells were counted using an inverted microscope at 40-fold magnification. Data are means ± standard errors of three determinations.

2.13. Statistical calculations

Dose–response curves were calculated using the Prism 5.01 software package (GraphPad, San Diego, CA, USA) and significant differences between controls and each drug concentration applied were determined by unpaired *t*-test. The calculations of dose–response curves and combination effects were performed using the "Calcusyn" software designed by Chou and Talalay (Biosoft, Ferguson, MO) [36]. The analytical method of Chou and Talalay [36,37] describes the interaction among drugs in a given combination. A combination index (CI) of <0.9 indicates synergism, a CI of 0.9–1.1 indicates additive effects, and a CI of >1.1 indicates antagonism.

3. Results

3.1. Effect of ABNM 1-13 on the growth of HL-60 and AsPC-1 cells

HL-60 cells (0.1×10^6 per ml) were seeded in 25 cm^2 Nunc tissue culture flasks and incubated with increasing concentrations of ABNM 1-13. After 72 h, the cell number of viable leukemia cells was determined. ABNM-4, ABNM-8, ABNM-9, ABNM-12, and ABNM-13 inhibited the growth of HL-60 cells with IC_{50} values (IC_{50} = 50% growth inhibition of tumor cells) of 95 ± 2.2, 67 ± 1.3, 60 ± 1.0, 62 ± 2.0, and 11 ± 1.1 μM, respectively. The IC_{50} values of all other compounds remained beyond 100 μM (Fig. 1). In another set of experiments, AsPC-1 cells (0.2×10^6 per ml) were seeded in 25 cm^2 Nunc tissue culture flasks and allowed to attach overnight. After 72 h, cells were detached and counted using a microcellcounter CC-110. ABNM-13 inhibited the growth of AsPC-1 cells with an IC_{50} of 76 ± 4 μM.

3.2. Effect of ABNM-13 on the growth of HL-60 cells – alone and in combination with Ara-C

HL-60 cells were seeded at a concentration of 0.1×10^6 per ml and incubated with increasing concentrations of ABNM-13. After 24, 48, and 72 h, the cell number of viable leukemia cells was determined. ABNM-13 inhibited the growth of HL-60 cells with IC_{50} values (IC_{50} = 50% growth inhibition of tumor cells) of 15 ± 0.3 and 11 ± 1.1 μM, respectively (Fig. 2a). Exposure to ABNM-13 for 24 h resulted in a cell count of 67 ± 0.6% (33% growth inhibition). Treatment with HU, a RR inhibitor currently used in the clinic for 48 and 72 h resulted in IC_{50} values of 143 ± 0.2 and 88 ± 0.2 μM, respectively (Fig. 2b). These findings are consistent with those obtained by Szekeres et al. who determined an IC_{50} of 73 μM after 96 h of incubation [38].

To investigate the effect of ABNM-13 in combination with Ara-C, HL-60 cells were seeded at a concentration of 0.1×10^6 per ml and simultaneously or sequentially incubated with increasing

Table 1
Synergistic combination effects of ABNM-13 and Ara-C in HL-60 cells employing a sequential growth inhibition assay.

Compound	Concentration (μM/nM)	Cell number ± SD (% of control)	Predicted value[a]	Combination index[b]
ABNM-13 (A)	2.5	88.7 ± 0.78		
(μM)	5.0	61.8 ± 0.16		
	7.5	50.9 ± 0.78		
	10.0	32.6 ± 0.31		
Ara-C (B)	10	72.4 ± 0.94		
(nM)	15	71.8 ± 3.61		
	20	59.3 ± 3.45		
ABNM-13	2.5			
+ Ara-C	10	49.2 ± 4.55	64.2	0.607[c]
ABNM-13	2.5			
+Ara-C	15	25.2 ± 4.87	63.7	0.305[c]
ABNM-13	2.5			
+Ara-C	20	39.8 ± 2.35	52.6	0.607[c]
ABNM-13	5			
+Ara-C	10	15.5 ± 7.85	44.7	0.329[c]
ABNM-13	5			
+Ara-C	15	20.0 ± 5.65	44.4	0.418[c]
ABNM-13	5			
+Ara-C	20	32.1 ± 1.10	36.6	0.692[c]
ABNM-13	7.5			
+Ara-C	10	17.3 ± 5.02	36.9	0.514[c]
ABNM-13	7.5			
+Ara-C	15	26.4 ± 0.00	36.6	0.740[c]
ABNM-13	7.5			
+Ara-C	20	23.2 ± 1.41	30.2	0.695[c]
ABNM-13	10			
+Ara-C	10	17.2 ± 2.04	23.6	0.670[c]
ABNM-13	10			
+Ara-C	15	16.8 ± 1.73	23.4	0.676[c]
ABNM-13	10			
+Ara-C	20	17.9 ± 2.67	19.3	0.727[c]

Cells were sequentially incubated with (1) ABNM-13 for 24 h and (2) Ara-C for 48 h, and then the cell number was determined. Data are means of two determinations ± standard deviations (SD).
[a] Predicted value: $(\%A \times \%B)/100$.
[b] Combination indices according to the equation of Chou and Talalay [36].
[c] Synergistic combination effect.

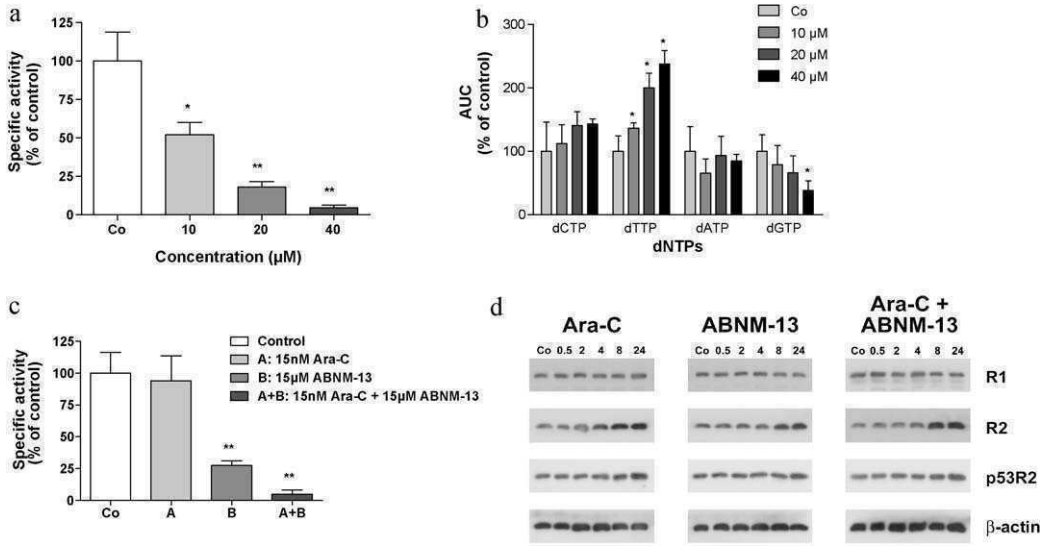

Fig. 3. (a) Inhibition of incorporation of ^{14}C-cytidine into DNA of HL-60 cells after treatment with ABNM-13 for 24 h (DNA synthesis assay). HL-60 cells (0.4×10^6 cells per ml) were incubated with increasing concentrations of ABNM-13 for 24 h. After the incubation period, cells were counted and pulsed with ^{14}C-cytidine (0.3125 μCi, 5 nM) for 30 min at 37 °C. Then cells were collected by centrifugation and washed with PBS. Total DNA was extracted from 5×10^6 cells and specific radioactivity of the samples was determined using a Wallac 1414 liquid scintillation counter (PerkinElmer, Boston, MA). Data are means ± standard errors of three determinations. Values significantly ($p < 0.05$) different from control are marked with an asterisk (*). Highly significant ($p < 0.01$) differences are marked with two asterisks (**). (b) Concentration of dNTP pools in HL-60 cells upon treatment with ABNM-13. HL-60 cells (0.4×10^6 cells per ml) were incubated with 10, 20, and 40 μM ABNM-13 for 24 h. Afterwards, 5×10^7 cells were separated for the extraction of dNTPs. The concentration of dNTPs was calculated as percent of total area under the curve for each sample. Data are means ± standard errors of three determinations. Values significantly ($p < 0.05$) different from control are marked with an asterisk (*). (c) Inhibition of incorporation of ^{14}C-cytidine into DNA of HL-60 cells after treatment with ABNM-13 and/or Ara-C for 30 min (DNA synthesis assay). HL-60 cells (0.4×10^6 cells per ml) were incubated with 15 μM ABNM-13 and/or 15 nM Ara-C and simultaneously pulsed with ^{14}C-cytidine (0.3125 μCi, 5 nM) for 30 min at 37 °C. Then cells were collected by centrifugation and washed with PBS. Total DNA was extracted from 5×10^6 cells and specific radioactivity of the samples was determined using a Wallac 1414 liquid scintillation counter (PerkinElmer, Boston, MA). Data are means ± standard errors of three determinations. Highly significant ($p < 0.01$) differences are marked with two asterisks (**). (d) Expression levels of RR subunits R1, R2 and p53R2 in HL-60 cells upon treatment with ABNM-13 and/or Ara-C. After incubation with 15 μM ABNM-13 and/or 15 nM Ara-C for 0.5, 2, 4, 8, and 24 h, HL-60 cells (2×10^6 per ml) were harvested, washed twice with ice-cold PBS (pH 7.2) and lysed in a buffer containing 150 mM NaCl, 50 mM Tris-buffered saline (Tris pH 8.0), 1% Triton X-100, 1 mM phenylmethylsulfonylfluoride (PMSF) and protease inhibitor cocktail (PIC; from a 100× stock). The lysate was centrifuged at 12,000 rpm for 20 min at 4 °C, and the supernatant was subjected to Western blot analysis.

concentrations of drugs (ABNM-13 first for 24 h and then Ara-C for 48 h as described in the Section 2). All 12 drug combinations yielded additive effects when ABNM-13 and Ara-C were applied simultaneously (data not shown). Moreover, all 12 combinations led to highly synergistic effects when applied sequentially (cells were first incubated with 2.5, 5, 7.5, and 10 μM ABNM-13 followed by the addition of 5, 10, and 20 nM Ara-C, respectively) (Table 1).

3.3. Effect of ABNM-13 on the growth of AsPC-1 cell colonies

AsPC-1 cells were seeded at a concentration of 2×10^3 per well and incubated with increasing concentrations of ABNM-13. Colonies were counted after 6 days of treatment. ABNM-13 inhibited the growth of AsPC-1 cell colonies with an IC_{50} value of 11.5 ± 1.4 μM (Fig. 2c) being almost identical to the IC_{50} seen in HL-60 cells (11 ± 1.1 μM).

3.4. MTT chemosensitivity assay

AsPC-1 or HL-60 cells (5×10^3 per well) were seeded in 96-well microtiter plates and exposed to increasing concentrations of ABNM-13 as described in Section 2. After 96 h of incubation, ABNM-13 reduced the absorbance (viability) of AsPC-1 and HL-60 cells with IC_{50} values of 40 ± 3.4 and 9 ± 1.7 μM, respectively.

3.5. Inhibition of incorporation of ^{14}C-cytidine into DNA of HL-60 cells (DNA synthesis assay) and dNTP alterations after treatment with ABNM-13 and/or Ara-C

Incorporation of ^{14}C-cytidine into nascent DNA was measured in HL-60 cells after incubation with increasing concentrations of ABNM-13. Exposure to 10, 20, and 40 μM ABNM-13 for 24 h significantly decreased ^{14}C-cytidine incorporation to 52 ± 13.9%, 17 ± 6.1%, and 4 ± 2.8%, respectively (Fig. 3a). Constitutive RR activity maintains balanced dNTP pools, whereas RR inhibition tilts this balance. In line with this, ABNM-13 treatment caused also an imbalance of dNTPs in HL-60 cells after 24 h, which was determined by HPLC analysis. Incubation of cells with 40 μM ABNM-13 resulted in a significant depletion of intracellular dGTP pools to 36 ± 15.7%. Treatment with 10, 20, and 40 μM ABNM-13 significantly increased dTTP pools to 134 ± 8.0%, 200 ± 22.7%, and 237 ± 21.3% of control values, respectively. Regarding dCTP and dATP pools, treatment with ABNM-13 led to insignificant changes (Fig. 3b).

To analyze the immediacy of DNA synthesis inhibition, HL-60 cells were exposed to 15 nM Ara-C, 15 μM ABNM-13, and the simultaneous combination of both compounds for only 30 min. Even this short incubation period reduced the incorporation of ^{14}C-cytidine to 93 ± 33.8%, 27 ± 6.3%, and 4 ± 5.7% of controls, respectively (Fig. 3c).

3.6. Expression of RR subunits R1, R2, and p53R2 after treatment with ABNM-13 and/or Ara-C

To monitor the effect of RR inhibitors on the expression of RR subunits, HL-60 cells were incubated with 15 nM Ara-C and/or 15 μM ABNM-13 for 0.5, 2, 4, 8, and 24 h and subjected to Western blot analysis. The protein level of the constitutively expressed R1 subunit remained unchanged during the whole time course. R2 levels showed an increase after 8 and 24 h, and p53R2 levels were elevated after 24 h of incubation (Fig. 3d). Both R2 and p53R2 are S-phase specific.

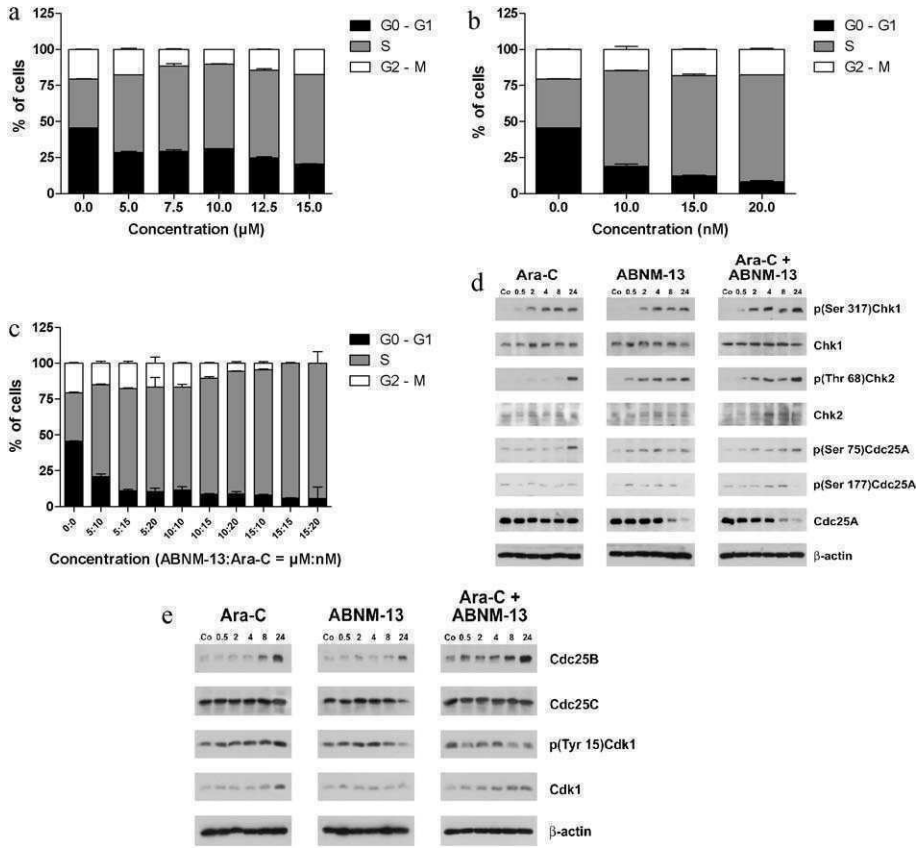

Fig. 4. (a–c) Cell cycle distribution in HL-60 cells after incubation with ABNM-13 and/or Ara-C. HL-60 cells (0.4×10^6 per ml) were seeded in 25 cm^2 Nunc tissue culture flasks and simultaneously incubated with 15 μM ABNM-13 and/or 15 nM Ara-C at 37 °C for 24 h under cell culture conditions. Cells were analyzed on a FACSCalibur flow cytometer (BD Biosciences, San Jose, CA, USA) and cell cycle distribution was calculated with ModFit LT software (Verity Software House, Topsham, ME, USA). Data are means ± standard errors of three determinations. (d) Expression levels of p(Ser 317)Chk1, Chk1, p(Thr 68)Chk2, Chk2, p(Ser 75)Cdc25A, p(Ser 177)Cdc25A, and Cdc25A after incubation with ABNM-13 and/or Ara-C. After incubation with 15 μM ABNM-13 and/or 15 nM Ara-C for 0.5, 2, 4, 8, and 24 h, HL-60 cells (2×10^6 per ml) were harvested, washed twice with ice-cold PBS (pH 7.2) and lysed in a buffer containing 150 mM NaCl, 50 mM Tris-buffered saline (Tris pH 8.0), 1% Triton X-100, 1 mM phenylmethylsulfonylfluoride (PMSF) and protease inhibitor cocktail (PIC; from a 100× stock). The lysate was centrifuged at 12,000 rpm for 20 min at 4 °C, and the supernatant was subjected to Western blot analysis. (e) Expression levels of Cdc25B, Cdc25C, p(Tyr 15)Cdk1, and Cdk1 after incubation with ABNM-13 and/or Ara-C. After incubation with 15 μM ABNM-13 and/or 15 nM Ara-C for 0.5, 2, 4, 8, and 24 h, HL-60 cells (2×10^6 per ml) were harvested, washed twice with ice-cold PBS (pH 7.2) and lysed in a buffer containing 150 mM NaCl, 50 mM Tris-buffered saline (Tris pH 8.0), 1% Triton X-100, 1 mM phenylmethylsulfonylfluoride (PMSF) and protease inhibitor cocktail (PIC; from a 100× stock). The lysate was centrifuged at 12,000 × rpm for 20 min at 4 °C, and the supernatant was subjected to Western blot analysis.

3.7. Cell cycle distribution in HL-60 cells after treatment with ABNM-13 and/or Ara-C

HL-60 cells were simultaneously incubated with 15 μM ABNM-13 and/or 15 nM Ara-C for 24 h. Treatment of HL-60 cells with 15 μM ABNM-13 caused cell cycle arrest in S-phase, increasing this cell population from 34 ± 0.4% to 62 ± 0.0%, whereas G0–G1 phase cells decreased from 46 ± 0.1% to 21 ± 0.1%. 15 nM Ara-C likewise caused an accumulation of 69 ± 1.6% HL-60 cells in S-phase and a concomitant decrease of G0–G1 cells to 12 ± 0.8%. Simultaneous incubation of HL-60 cells with 15 μM ABNM-13 and 15 nM Ara-C led to an even more pronounced growth arrest in the S-phase, increasing this cell population from 34 ± 0.4% to 94 ± 0.5% while decreasing cells in the G0–G1 phase from 46 ± 0.5% to 6 ± 0.5% (Fig. 4a–c). No subG1 peaks could be observed by FACS at the time points measured.

3.8. Expression of checkpoint and cell cycle regulating proteins after treatment with ABNM-13 and/or Ara-C

To investigate whether S-phase inhibition caused activation of cell cycle checkpoint kinases, HL-60 cells were simultaneously treated with 15 nM Ara-C and/or 15 μM ABNM-13 for 0.5, 2, 4, 8, and 24 h and subjected to Western blot analysis (Fig. 4d and e). Chk1 was phosphorylated at the activating Ser317 site within 30 min (Ara-C), 2 h (ABNM-13), and 30 min (Ara-C/ABNM-13). Chk2 was phosphorylated at the activating Thr68 site within 24 h (Ara-C), 30 min (ABNM-13), and 30 min (ABNM-13/Ara-C). Chk1 protein levels remained unchanged, whereas Chk2 protein levels increased transiently, in particular when using the combination of ABNM-13 and Ara-C (Fig. 4d). In addition, ABNM-13 caused phosphorylation at Ser75 and Ser177 of the dual-specificity phosphatase Cdc25A, which are target sites of Chk1 and Chk2, respectively, resulting in its downregulation after 8 and 24 h. On the other hand, ABNM-13 upregulated Cdc25B protein levels after 24 h (Ara-C after 8 and 24 h), resulting in the dephosphorylation of Tyr15 of Cdk1 after 24 h, which is indicative for its activation (Fig. 4e). Ara-C treatment did not cause dephosphorylation of Cdk1. Cdc25C levels remained unchanged throughout the time course.

3.9. Induction of apoptosis in HL-60 cells by ABNM-13 and/or Ara-C

HL-60 cells were exposed to 12.5, 15, 17.5, and 20 μM ABNM-13 and/or 15 nM Ara-C for 24 and 48 h and double stained with Hoechst 33258 and propidium iodide to analyze whether apoptotic cell death was induced. The nuclear morphology of 16 ± 0.9% and 22 ± 2.4% HL-60 cells showed early or late apoptosis stages upon treatment with 15 μM ABNM-13 for 24 and 48 h, respectively (Fig. 5a). Incubation with 15 nM Ara-C or the combination of 15 μM

ABNM-13 and 15 nM Ara-C for 24 h resulted in only 8.2 ± 0.5% and 13 ± 2.7% apoptotic cells, respectively. Even the exposure of cells to 15 nM Ara-C or the combination of 15 μM ABNM-13 and 15 nM Ara-C for 48 h led to no more than 10 ± 0.6% and 28 ± 4.8% apoptotic cells, respectively, suggesting that cell death is at best additive but not synergistic after simultaneous application of both compounds (Fig. 5b). The induction of apoptosis was further substantiated by the cleavage and therefore activation of caspase-3 after 8 and 24 h of treatment with 15 μM ABNM-13 or the combination of 15 μM ABNM-13 and 15 nM Ara-C which in turn led to increased protein levels of γH2AX after 24 h (Fig. 5c). In contrast, 15 nM Ara-C induced activated caspase-3 and γH2AX levels only marginally. Constitutive phospho-ATM levels were not enhanced upon treatment with ABNM-13 and/or Ara-C. Examples of the cellular morphology are provided in Fig. 5d.

4. Discussion

3D molecular space modeling techniques were used to design in silico structures specifically to inhibit the activity of ribonucleotide reductase (RR), which is the rate-limiting enzyme of *de novo* DNA synthesis. From a panel of 13 compounds, we found that ABNM-13 is the most active agent with regard to growth inhibition of HL-60 cells.

The analysis of the *in situ* RR activity evidenced that ABNM-13 is a powerful RR inhibitor even after a short incubation time and at low concentrations. In addition, ABNM-13 caused alterations of deoxyribonucleoside triphosphate (dNTP) pool balance: dGTP pools were significantly depleted while dTTP pools were elevated. By misbalancing the concentration of precursors for *de novo* DNA synthesis, the latter is blocked in proliferating cells. Cell cycle

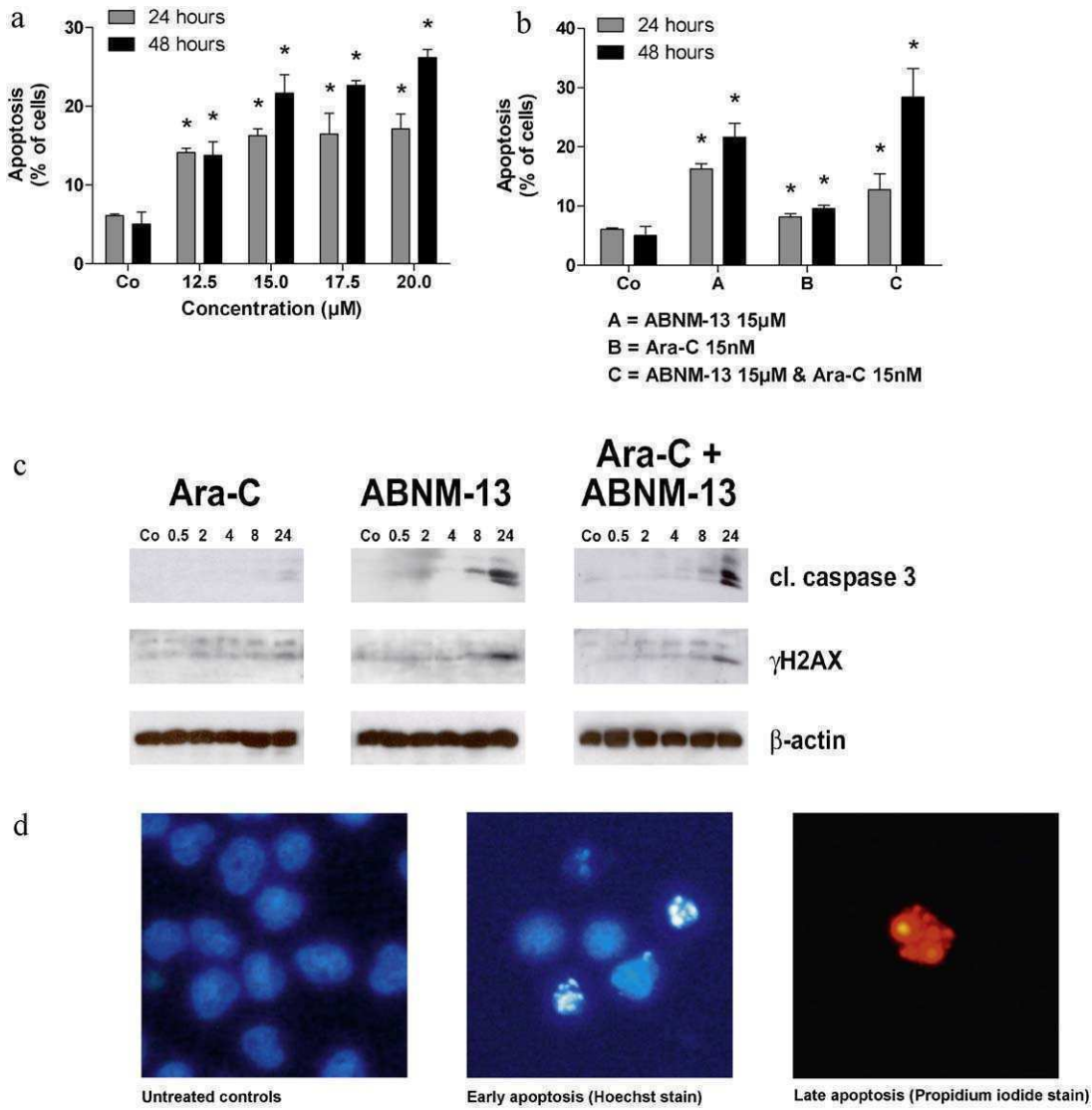

Fig. 5. (a and b) Induction of apoptosis in HL-60 cells after incubation with ABNM-13 and/or Ara-C. HL-60 cells (0.2×10^6 per ml) were exposed to increasing concentrations of ABNM-13 for 24 and 48 h (a) or treated with 15 μM ABNM-13 and/or 15 nM Ara-C for 24 and 48 h (b). Hoechst 33258 (HO, Sigma, St. Louis, MO, USA) and propidium iodide (PI, Sigma, St. Louis, MO, USA) were added directly to the cells to final concentrations of 5 μg/ml and 2 μg/ml, respectively. After 60 min of incubation at 37 °C, cells were counted under a fluorescence microscope and the number of apoptotic cells was given as percentage value. Data are means ± standard errors of three determinations. (c) Expression levels of cleaved caspase-3 and γH2AX after incubation with ABNM-13 and/or Ara-C. After incubation with 15 μM ABNM-13 and/or 15 nM Ara-C for 0.5, 2, 4, 8, and 24 h, HL-60 cells (2×10^6 per ml) were harvested, washed twice with ice-cold PBS (pH 7.2) and lysed in a buffer containing 150 mM NaCl, 50 mM Tris-buffered saline (Tris pH 8.0), 1% Triton X-100, 1 mM phenylmethylsulfonylfluoride (PMSF) and protease inhibitor cocktail (PIC; from a 100× stock). The lysate was centrifuged at 12,000 rpm for 20 min at 4 °C, and the supernatant was subjected to Western blot analysis. (d) Examples of the cellular morphology. After incubation with increasing concentrations of ABNM-13 for 48 h, HL-60 cells were double stained with Hoechst dye 33258 plus propidium iodide. In comparison to untreated controls, the cell morphology of HL-60 cells after treatment showed nuclear condensation and apoptotic bodies (early apoptosis) or loss of membrane integrity (late apoptosis).

perturbations, growth arrest and induction of apoptosis are the consequences, as it was observed in the course of ABNM-13 treatment.

The prime effect of ABNM-13 was a strong S-phase arrest which is consistent with the role of RR as the rate limiting enzyme for S-phase transit and the fact that inhibition of RR leads to inhibition of cells in S-phase [39]. It has been suggested that cells in which RR was inhibited by HU may enter the early S-phase at a normal rate and accumulate there until they undergo apoptosis [40,41]. The protein level of the constitutively expressed R1 subunit of RR remained unchanged. In contrast, the S-phase specific R2 subunit and also the p53R2 subunit of the enzyme were elevated although HL-60 cells are p53 deficient, indicating a compensatory up-regulation through which the cells try to rebalance their dNTP production. However, these findings are in line with the observations made by Yanomoto et al. [42] who demonstrated that basal levels of p53R2 are expressed regardless of the cellular p53 status and of Zhang et al. [43] who showed that up-regulation of the R2 protein levels occurs in response to DNA damage and involves up-regulation and activation of Chk1.

DNA damage or disrupted dNTP balance and incomplete DNA synthesis activate cell cycle checkpoints to prevent DNA synthesis and cell cycle progression [44–46] and to provide time for repair before the damage gets passed on to daughter cells or to allow for the reconstitution of the dNTP pools. These regulatory pathways govern the order and timing of cell cycle transitions to ensure completion of one cellular event prior to commencement of another. Before mitosis, cells have to pass G1–S, intra-S, and G2–M cell cycle checkpoints, which are controlled by their key regulators, ATR and ATM protein kinases, through activation of their downstream effector kinases Chk1 and Chk2, respectively [46,47]. Activated Chk1 and Chk2 phosphorylate the Cdc25A phosphatase at Ser75 and Ser177, respectively, and target it for proteasomal degradation. Cdc25A is an oncogene and required for cell cycle transit. Treatment with ABNM-13 activated both Chk1 and Chk2, the latter being phosphorylated within as little as 30 min.

Both Cdc25B and Cdc25C induce mitosis by activating Cdk1/cyclin B [48], and Cdc25B has been implicated as the initial phosphatase to activate Cdk1/cyclin B [49]. Activated Cdk1/cyclin B then phosphorylates and activates Cdc25C, which in turn keeps Cdk1/cyclin B active, creating a positive feedback loop that drives the cell through mitosis [50]. Cdc25B protein levels were upregulated by ABNM-13, leading to dephosphorylation and activation of Cdk1. Cdc25C levels remained unchanged. In contrast, Ara-C induced Cdk1 protein expression, and co-treatment with Ara-C and ABNM-13 resulted in both an increase of Cdk1 levels and subsequent increase of its activity. Undue overexpression of Cdc25B, i.e. when Cdc25A is unavailable, and consequent dephosphorylation of Cdk1/cyclin B, as observed in this study, was shown to induce cell cycle arrest by abrogating entry into mitosis [51]. Furthermore, Cdk2, as being regulated by Cdc25A, is required for S-phase progression [52]. Therefore, the combined effect of Cdc25A degradation and Cdc25B overexpression most likely caused the almost complete S-phase arrest induced by ABNM-13 alone and together with Ara-C (Fig. 6). Apoptosis upon treatment with ABNM-13 occurred in only 22% of cells (after 48 h), indicating that cell cycle inhibition rather than induction of programmed cell death seems to be the primary antineoplastic effect of ABNM-13. We therefore believe that a portion of treated cells was growing much slower than untreated controls, but did not undergo necrosis or apoptosis. The latter was further determined by the expression of cleaved caspase-3 (after 8 h) which in turn led to elevation of γH2AX protein levels (after 24 h), suggesting that treatment with ABNM-13 was not the primary cause for DNA double strand breaks but the consequence of caspase-3 induced DNAse activation. This was supported by the fact that constitutive phospho-ATM levels were not elevated, either. Cell death via mitotic catastrophe (i.e. the formation of giant cells with two or more nuclei) being promoted by Chk2 inhibition [53,54] could not be observed at any time point.

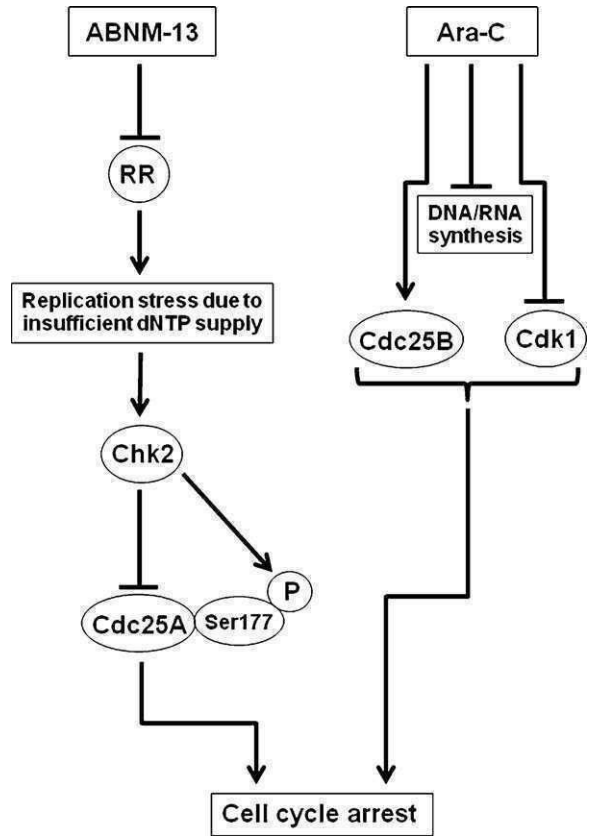

Fig. 6. Proposed mechanism of action of ABNM-13 and Ara-C.

Combination treatment is expected to produce fortified antitumor effects, if the pharmacokinetic and pharmacological properties are different from each other. Accordingly ABNM-13, which disregulated dTTP and dGTP pools and Ara-C, which is known to affect dCTP pools [55–57] inhibited cell proliferation synergistically. Using a sequential combination of ABNM-13 and Ara-C, all 12 concentrations applied yielded highly synergistic antineoplastic effects.

Taken together, we demonstrate that the novel RR inhibitor ABNM-13 exerts pronounced anticancer activity both as single agent and as enhancer of another antitumor drug such as Ara-C. Due to these promising results, ABNM-13 may support conventional chemotherapy of human malignancies and therefore deserves further preclinical and *in vivo* testing.

Acknowledgements

This investigation was supported by the "Fonds zur Foerderung der Wissenschaftlichen Forschung des Buergermeisters der Bundeshauptstadt Wien", grant #09059 to M.F.-S., and the "Hochschuljubilaeumsstiftung der Stadt Wien", grant #H-756/2005 to T.S. The authors wish to thank Toni Jaeger for preparing the Western blotting figures.

References

[1] Koneru PB, Lien EJ. Avramis VI. Synthesis and testing of new antileukemic Schiff bases of N-hydroxy-N′-aminoguanidine against CCRF-CEM/0 human leukemia cells in vitro and synergism studies with cytarabine (Ara-C). Pharmaceutical Research 1993;10:515–20.

[2] Ren S, Wang R, Komatsu K, Bonaz-Krause P, Zyrianov Y, McKenna CE, et al. Synthesis, biological evaluation, and quantitative structure–activity relationship analysis of new Schiff bases of hydroxysemicarbazide as potential antitumor agents. Journal of Medicinal Chemistry 2002;45:410–9.
[3] Tai AW, Lien EJ, Lai MM, Khwaja TA. Novel N-hydroxyguanidine derivatives as anticancer and antiviral agents. Journal of Medicinal Chemistry 1984;27:236–8.
[4] T'Ang A, Lien EJ, Lai MM. Optimization of the Schiff bases of N-hydroxy-N′-aminoguanidine as anticancer and antiviral agents. Journal of Medicinal Chemistry 1985;28:1103–6.
[5] van't Riet B, Wampler GL, Elford HL. Synthesis of hydroxy- and amino-substituted benzohydroxamic acids: inhibition of ribonucleotide reductase and antitumor activity. Journal of Medicinal Chemistry 1979;22:589–92.
[6] Matsumoto M, Fox JG, Wang PH, Koneru PB, Lien EJ, Cory JG. Inhibition of ribonucleotide reductase and growth of human colon carcinoma HT-29 cells and mouse leukemia L1210 cells by N-hydroxy-N′-aminoguanidine derivatives. Biochemical Pharmacology 1990;40:1779–83.
[7] Takeda E, Weber G. Role of ribonucleotide reductase in expression in the neoplastic program. Life Sciences 1981;28:1007–14.
[8] Kolberg M, Strand KR, Graff P, Andersson KK. Structure, function, and mechanism of ribonucleotide reductases. Biochimica et Biophysica Acta 2004;1699: 1–34.
[9] Shao J, Zhou B, Chu B, Yen Y. Ribonucleotide reductase inhibitors and future drug design. Current Cancer Drug Targets 2006;6:409–31.
[10] Bourdon A, Minai L, Serre V, Jais JP, Sarzi E, Aubert S, et al. Mutation of RRM2B, encoding p53-controlled ribonucleotide reductase (p53R2), causes severe mitochondrial DNA depletion. Nature Genetics 2007;39:776–80.
[11] Saban N, Bujak M. Hydroxyurea and hydroxamic acid derivatives as antitumor drugs. Cancer Chemotherapy and Pharmacology 2009;64:213–21.
[12] Tennant L. Chronic myelogenous leukemia: an overview. Clinical Journal of Oncology Nursing 2001;5:218–9.
[13] Noble S, Goa KL, Gemcitabine. A review of its pharmacology and clinical potential in non-small cell lung cancer and pancreatic cancer. Drugs 1997; 54:447–72.
[14] Toschi L, Finocchiaro G, Bartolini S, Gioia V, Cappuzzo F. Role of gemcitabine in cancer therapy. Future Oncology 2005;1:7–17.
[15] Hatse S, De Clercq E, Balzarini J. Role of antimetabolites of purine and pyrimidine nucleotide metabolism in tumor cell differentiation. Biochemical Pharmacology 1999;58:539–55.
[16] Abeysinghe RD, Greene BT, Haynes R, Willingham MC, Turner J, Planalp RP, et al. p53-independent apoptosis mediated by tachpyridine, an anti-cancer iron chelator. Carcinogenesis 2001;22:1607–14.
[17] Samuni AM, Krishna MC, DeGraff W, Russo A, Planalp RP, Brechbiel MW, et al. Mechanisms underlying the cytotoxic effects of Tachpyr—a novel metal chelator. Biochimica et Biophysica Acta 2002;1571:211–8.
[18] Turner J, Koumenis C, Kute TE, Planalp RP, Brechbiel MW, Beardsley D, et al. Tachpyridine, a metal chelator, induces G2 cell-cycle arrest, activates checkpoint kinases, and sensitizes cells to ionizing radiation. Blood 2005;106:3191–9.
[19] Torti SV, Torti FM, Whitman SP, Brechbiel MW, Park G, Planalp RP. Tumor cell cytotoxicity of a novel metal chelator. Blood 1998;92:1384–9.
[20] Greene BT, Thorburn J, Willingham MC, Thorburn A, Planalp RP, Brechbiel MW, et al. Activation of caspase pathways during iron chelator-mediated apoptosis. Journal Biological Chemistry 2002;277:25568–75.
[21] Tsimberidou AM, Alvarado Y, Giles FJ. Evolving role of ribonucleoside reductase inhibitors in hematologic malignancies. Expert Review of Anticancer Theraphy 2002;2:437–48.
[22] Erlichman C, Fine S, Wong A, Elhakim T. A randomized trial of fluorouracil and folinic acid in patients with metastatic colorectal carcinoma. Journal of Clinical Oncology 1988;6:469–75.
[23] Saiko P, Ozsvar-Kozma M, Bernhaus A, Jaschke M, Graser G, Lackner A, et al. N-hydroxy-N′-(3,4,5-trimethoxyphenyl)-3,4,5-trimethoxy-benzamidine, a novel resveratrol analog, inhibits ribonucleotide reductase in HL-60 human promyelocytic leukemia cells: synergistic antitumor activity with arabinofuranosylcytosine. International Journal of Oncology 2007;31:1261–6.
[24] Horvath Z, Saiko P, Illmer C, Madlener S, Hoechtl T, Bauer W, et al. Synergistic action of resveratrol, an ingredient of wine, with Ara-C and tiazofurin in HL-60 human promyelocytic leukemia cells. Experimental Hematology 2005;33:329–35.
[25] Horvath Z, Murias M, Saiko P, Erker T, Handler N, Madlener S, et al. Cytotoxic and biochemical effects of 3,3′,4,4′,5,5′-hexahydroxystilbene, a novel resveratrol analog in HL-60 human promyelocytic leukemia cells. Experimental Hematology 2006;34:1377–84.
[26] Fritzer-Szekeres M, Salamon A, Grusch M, Horvath Z, Hochtl T, Steinbrugger R, et al. Trimidox, an inhibitor of ribonucleotide reductase, synergistically enhances the inhibition of colony formation by Ara-C in HL-60 human promyelocytic leukemia cells. Biochemical Pharmacology 2002;64:481–5.
[27] Fritzer-Szekeres M, Savinc I, Horvath Z, Saiko P, Pemberger M, Graser G, et al. Biochemical effects of piceatannol in human HL-60 promyelocytic leukemia cells—synergism with Ara-C. International Journal of Oncology 2008;33:887–92.
[28] Szekeres T, Gharehbaghi K, Fritzer M, Woody M, Srivastava A, van't Riet B, et al. Biochemical and antitumor activity of trimidox, a new inhibitor of ribonucleotide reductase. Cancer Chemotherapy and Pharmacology 1994;34:63–6.
[29] Garrett C, Santi DV. A rapid and sensitive high pressure liquid chromatography assay for deoxyribonucleoside triphosphates in cell extracts. Analytical Biochemistry 1979;99:268–73.
[30] Grusch M, Polgar D, Gfatter S, Leuhuber K, Huettenbrenner S, Leisser C, et al. Maintenance of ATP favours apoptosis over necrosis triggered by benzamide riboside. Cell Death and Differentiation 2002;9:169–78.
[31] Grasl-Kraupp B, Ruttkay-Nedecky B, Koudelka H, Bukowska K, Bursch W, Schulte-Hermann R. In situ detection of fragmented DNA (TUNEL assay) fails to discriminate among apoptosis, necrosis, and autolytic cell death: a cautionary note. Hepatology 1995;21:1465–8.
[32] Rosenberger G, Fuhrmann G, Grusch M, Fassl S, Elford HL, Smid K, et al. The ribonucleotide reductase inhibitor trimidox induces c-myc and apoptosis of human ovarian carcinoma cells. Life Sciences 2000;67:3131–42.
[33] Grusch M, Fritzer-Szekeres M, Fuhrmann G, Rosenberger G, Luxbacher C, Elford HL, et al. Activation of caspases and induction of apoptosis by novel ribonucleotide reductase inhibitors amidox and didox. Experimental Hematology 2001;29:623–32.
[34] Fritzer-Szekeres M, Grusch M, Luxbacher C, Horvath S, Krupitza G, Elford HL, et al. Trimidox, an inhibitor of ribonucleotide reductase, induces apoptosis and activates caspases in HL-60 promyelocytic leukemia cells. Experimental Hematology 2000;28:924–30.
[35] Huettenbrenner S, Maier S, Leisser C, Polgar D, Strasser S, Grusch M, et al. The evolution of cell death programs as prerequisites of multicellularity. Mutation Research 2003;543:235–49.
[36] Chou TC, Talalay P. Quantitative analysis of dose–effect relationships: the combined effects of multiple drugs or enzyme inhibitors. Advances in Enzyme Regulation 1984;22:27–55.
[37] Chou TC, Talalay P. Generalized equations for the analysis of inhibitions of Michaelis–Menten and higher-order kinetic systems with two or more mutually exclusive and nonexclusive inhibitors. European Journal of Biochemistry (FEBS) 1981;115:207–16.
[38] Szekeres T, Fritzer M, Strobl H, Gharehbaghi K, Findenig G, Elford HL, et al. Synergistic growth inhibitory and differentiating effects of trimidox and tiazofurin in human promyelocytic leukemia HL-60 cells. Blood 1994;84: 4316–4321.
[39] Chimploy K, Diaz GD, Li Q, Carter O, Dashwood WM, Mathews CK, et al. E2F4 and ribonucleotide reductase mediate S-phase arrest in colon cancer cells treated with chlorophyllin. International Journal of Cancer 2009;125:2086–94.
[40] Yarbro JW. Mechanism of action of hydroxyurea. Seminars in Oncology 1992;19:1–10.
[41] Maurer-Schultze B, Siebert M, Bassukas ID. An in vivo study on the synchronizing effect of hydroxyurea. Experimental Cell Research 1988;174:230–43.
[42] Yanamoto S, Iwamoto T, Kawasaki G, Yoshitomi I, Baba N, Mizuno A. Silencing of the p53R2 gene by RNA interference inhibits growth and enhances 5-fluorouracil sensitivity of oral cancer cells. Cancer Letters 2005;223:67–76.
[43] Zhang YW, Jones TL, Martin SE, Caplen NJ, Pommier Y. Implication of checkpoint kinase-dependent up-regulation of ribonucleotide reductase R2 in DNA damage response. Journal of Biological Chemistry 2009;284:18085–9.
[44] Kastan MB, Bartek J. Cell-cycle checkpoints and cancer. Nature 2004;432: 316–23.
[45] Shiloh Y. ATM and related protein kinases: safeguarding genome integrity. Nature Reviews Cancer 2003;3:155–68.
[46] Bartek J, Lukas J. Chk1 and Chk2 kinases in checkpoint control and cancer. Cancer Cell 2003;3:421–9.
[47] Abraham RT. Cell cycle checkpoint signaling through the ATM and ATR kinases. Genes Development 2001;15:2177–96.
[48] Donzelli M, Draetta GF. Regulating mammalian checkpoints through Cdc25 inactivation. EMBO Reports 2003;4:671–7.
[49] Nishijima H, Nishitani H, Seki T, Nishimoto T. A dual-specificity phosphatase Cdc25B is an unstable protein and triggers p34(cdc2)/cyclin B activation in hamster BHK21 cells arrested with hydroxyurea. Journal of Cell Biology 1997;138:1105–16.
[50] Hoffmann I, Clarke PR, Marcote MJ, Karsenti E, Draetta G. Phosphorylation and activation of human cdc25-C by cdc2—cyclin B and its involvement in the self-amplification of MPF at mitosis. EMBO Journal 1993;12:53–63.
[51] Varmeh-Ziaie S, Manfredi JJ. The dual specificity phosphatase Cdc25B, but not the closely related Cdc25C, is capable of inhibiting cellular proliferation in a manner dependent upon its catalytic activity. Journal of Biological Chemistry 2007;282:24633–41.
[52] Donzelli M, Squatrito M, Ganoth D, Hershko A, Pagano M, Draetta GF. Dual mode of degradation of Cdc25 A phosphatase. EMBO Journal 2002;21:4875–84.
[53] Castedo M, Perfettini JL, Roumier T, Andreau K, Medema R, Kroemer G. Cell death by mitotic catastrophe: a molecular definition. Oncogene 2004;23: 2825–2837.
[54] Portugal J, Mansilla S, Bataller M. Mechanisms of drug-induced mitotic catastrophe in cancer cells. Current Pharmaceutical Design 2010;16:69–78.
[55] Gandhi V, Huang P, Chapman AJ, Chen F, Plunkett W. Incorporation of fludarabine and 1-beta-D-arabinofuranosylcytosine 5′-triphosphates by DNA polymerase alpha: affinity, interaction, and consequences. Clinical Cancer Research 1997;3:1347–55.
[56] Wills PW, Hickey R, Malkas L. Ara-C differentially affects multiprotein forms of human cell DNA polymerase. Cancer Chemotherapy and Pharmacology 2000;46:193–203.
[57] Seymour JF, Huang P, Plunkett W, Gandhi V. Influence of fludarabine on pharmacokinetics and pharmacodynamics of cytarabine: implications for a continuous infusion schedule. Clinical Cancer Research 1996;2:653–8.

Metabolomic analysis of resveratrol-induced effects in the human breast cancer cell lines MCF-7 and MDA-MB-231.

Jäger W., Gruber A., **Giessrigl B.**, Krupitza G., Szekeres T. and Sonntag D.

OMICS 15: 9-14, **2011.**

OMICS A Journal of Integrative Biology
Volume 15, Numbers 1 and 2, 2011
© Mary Ann Liebert, Inc.
DOI: 10.1089/omi.2010.0114

Metabolomic Analysis of Resveratrol-Induced Effects in the Human Breast Cancer Cell Lines MCF-7 and MDA-MB-231

Walter Jäger,[1] Alexandra Gruber,[2] Benedikt Giessrigl,[3] Georg Krupitza,[3] Thomas Szekeres,[4] and Denise Sonntag[2]

Abstract

Resveratrol is a naturally occurring anticancer compound present in grapes and wine with antiproliferative properties against breast cancer cells and xenografts. Our objective was to investigate the metabolic alterations that characterize the effects of resveratrol in the human breast cancer cell lines MCF-7 and MDA-MB-231 using high-throughput liquid chromatography-based mass spectrometry. In both cell lines, growth inhibition was dose dependent and accompanied by substantial metabolic changes. For all 21 amino acids analyzed levels increased more than 100-fold at a resveratrol dose of 100 μM with far lower concentrations in MDA-MB-231 compared to MCF-7 cells. Among the biogenic amines and modified amino acids ($n = 16$) resveratrol increased the synthesis of serotonin, kynurenine, and spermindine in both cell lines up to 61-fold indicating that resveratrol strongly interacts with cellular biogenic amine metabolism. Among the eicosanoids and oxidized polyunsaturated fatty acids ($n = 17$) a pronounced increase in arachidonic acid and its metabolite 12S-HETE was observed in MDA-MB-231 and to a lesser extent in MCF-7 cells, indicating release from cell membrane phospholipids upon activation of phospholipase A_2 and subsequent metabolism by 12-lipoxygenase. In conclusion, metabolomic analysis elucidated several small molecules as markers for the response of breast cancer cells to resveratrol.

Introduction

Breast cancer is a major cause of cancer death in women worldwide. Evidence from epidemiological and experimental studies indicates that certain natural constituents of diet may act as chemopreventive agents and inhibit mammary carcinogenesis. One such compound is resveratrol (3,4′,5-trihydroxy-*trans*-stilbene), which is produced by several plants, berries, and fruits, and is mainly found in the skin of grapes and red wine. The antiproliferative property of resveratrol has been demonstrated *in vitro* against hormone-dependent and hormone-independent breast cancer cells and is due to the induction of apoptosis via downregulation of NF-kappa B and Bcl-2 (Bove et al., 2002; Garvin et al., 2006; Nakagawa et al., 2001; Pozo-Guisado et al., 2002). Also, resveratrol significantly decreases extracellular vascular endothelial growth factor (VEGF) and effectively inhibits ribonucleotide reductase, which catalyzes the rate-limiting step of the *de novo* DNA synthesis and is highly upregulated in rapidly proliferating tumor cells (Fontecave et al., 2002; Horvath et al., 2005). Resveratrol has also been shown to arrest cells in the S and G2 phases of the cell cycle (Ragione et al., 1998). Moreover, resveratrol is active in the inhibition of cyclooxygenases (COX-1, COX-2) (Murias et al., 2004), which partly explains why this compound also reduces the occurrence of colon and breast cancer (Anderson et al., 2003). In addition to these *in vitro* data, experiments have shown significantly less tumor growth in human breast cancer xenografts *in vivo*, supporting the use of this polyphenol as a potential chemotherapeutic agent (Nakagawa et al., 2001).

Although gene and protein expression in breast cancer cells after resveratrol treatment have been extensively profiled, there are no data about the metabolic alterations caused by this compound. In contrast to genetics and proteomics, the identification and quantification of specific metabolites in tumor cells provide high-resolution biochemical snapshots depicting the functional endpoints of the physiologic state of an organism, including the effects of drug disposure (Deberardinis et al., 2008; Weinberger and Graber 2005).

Studies conducted on laboratory animals and humans have reported a very low oral bioavailability of resveratrol based

[1]Department of Clinical Pharmacy and Diagnostics, University of Vienna, Vienna, Austria.
[2]Biocrates Life Sciences AG, Innsbruck, Austria.
[3]Institute of Clinical Pathology, Medical University of Vienna, Vienna, Austria.
[4]Department of Medical and Chemical Laboratory Diagnostics, Medical University of Vienna, Vienna, Austria.

on extensive metabolism in gut and liver to several glucuronides and sulfates. In human breast cancer cell lines, however, resveratrol is exclusively metabolized to trans-resveratrol-3-O-sulfate. Surprisingly, in this setting the concentrations of resveratrol glucuronides were below the detection limits (Murias et al., 2008). Furthermore, recent data from our lab also demonstrate that trans-resveratrol-3-O-sulfate was about threefold less cytotoxic against the hormone-dependent MCF-7 and the hormone-independent MDA-MB-231 human breast cancer cell lines with IC_{50} values of about 200 μM, indicating that sulfation of resveratrol has only a minor effect on cell growth inhibition (Miksits et al. 2010). Therefore, we used these cell lines to investigate possible alterations in the cellular concentrations of amino acids, biogenic amines, eicosanoids, and polyunsaturated fatty acids after resveratrol application using a targeted metabolomic approach. This information is important as some small molecules analyzed in this study may act as markers for the anticancer activity of resveratrol.

Materials and Methods

Materials

Resveratrol (3,4′,5-trihydroxy-*trans*-stilbene, 99% GC) and dimethyl sulfoxide (DMSO) were obtained from Sigma-Aldrich (Munich, Germany). All other chemicals and solvents were commercially available, of analytical grade, and used without further purification.

Cell culture

MCF-7 and MDA-MB-231 breast cancer cells were purchased from the American Type Culture Collection (ATCC, Rockville, MD, USA). Both cell lines were grown in phenolred-free RPMI 1640 tissue culture medium including L-glutamine (PAN Biotech, Aldenbach, Germany), supplemented with 10% heat-inactivated fetal bovine serum (FBS) and 1% penicillin-streptomycin (Gibco Invitrogen Corp., Grand Island, NY, USA) under standard conditions at 37°C in a humidified atmosphere containing 5% CO_2 and 95% air. Twenty-four hours before treatment, cells were transferred to a RPMI 1640 medium supplemented with 2.5% charcoal-stripped FBS (PAN Biotech, Aidenbach, Germany) and 1% penicillin–streptomycin. Cells were placed into 15-cm plates and allowed to attach overnight. Resveratrol was dissolved in DMSO and diluted with medium (final DMSO concentration <0.1%) to 5–100 μM. Experiments under each set of conditions were carried out in triplicate. Blank experiments contained DMSO in the medium in place of resveratrol. After 72 h, media were aspirated by suction and aliquots (100 μL) were analyzed by LC-MS/MS. In parallel, cells were scraped off, washed three times with phosphate-buffered saline, and lysed in ethanol/phosphate buffer (85/15 v/v) by repeating (three times) shock freezing in liquid nitrogen, and thawing. After centrifugation at 10,000×*g* for 5 min, 10 or 20 μL of the supernatant (cytoplasm) was subjected to the LC-MS/MS quantification assays.

Cell growth inhibition

The effect of resveratrol (0–100 μM) on the *in vitro* growth of MCF-7 and MDA-MB-231 cells was evaluated after 72 h of resveratrol application under identical conditions (see above) using the CellTiter-Glo® Luminescent Cell Viability Assay (Promega, Madison, WI, USA) and a Victor™ microplate reader (Perkin-Elmer, Waltham, MA, USA) according to the manufacturer's instructions.

Targeted metabolomics

Using a high-throughput liquid chromatography-based mass spectrometry platform for targeted metabolomics, 54 analytes were quantified in cell pellets and in medium at Biocrates Life Sciences AG, Austria. Multiple reaction monitoring detection was performed using a 4000 Q TRAP tandem mass spectrometry instrument (Applied Biosystems, Bedford, MA, USA) to obtain concentration data, which were finally exported for statistical analysis. Metabolomics data were used as received from Biocrates. No data correction or removal of data points was applied. The experimental metabolomics measurement technique was carried out as previously described (Gieger et al., 2008).

Statistical analysis

Unless otherwise indicated, values are expressed as mean ± SD of three individual experiments. Statistical differences from control values were evaluated using the Students' paired *t*-test at a significance level of $p < 0.05$ using the Prism program (version 5.0, GraphPad Software Inc., San Diego, CA, USA).

Results

Amino Acids

Resveratrol significantly reduced cell viability in the cancer cell lines MCF-7 and MDA-MB-231, yielding IC_{50} values of 68.3 ± 2.6 and 67.6 ± 4.1 μM, respectively (data not shown). Cell growth inhibition was accompanied by substantial metabolic changes, which were dose dependent but different between both cell lines. After 72 h of cell growth in the presence of resveratrol, the concentrations in the medium of all 21 analyzed amino acids (19 proteinogenic, 2 nonproteinogenic) were substantially increased compared to resveratrol-free controls. For MDA-MB-231 cells, this effect was less pronounced than for the MCF-7 cell line (data not shown). In the presence of resveratrol, the maximum changes seen between resveratrol-treated cells and controls were 21-fold for serine in MCF-7 cell culture and 63-fold for methionine in MDA-MB-231 cells (Table 1). Significant increases in the synthesis of all amino acids under resveratrol treatment was also observed in the cytoplasm of MDA-MB-231 cells (up to 18-fold), whereas the concentrations of many amino acids, most notably aspartic acid, glutamine, glycine, and ornithine in MCF-7 cells were decreased (0.42 to 0.56-fold) (Table 1).

Biogenic Amines and Modified Amino Acids

Metabolic changes in response to resveratrol were also seen for biogenic amines and modified amino acids (n = 16). As already observed for amino acids, much higher concentrations were seen in the medium of MCF-7 cells than in the MDA-MB-231 cell line. In cytoplasm, however, concentrations in both cell lines were very low or below the detection limit (Table 1). Most important, resveratrol significantly increased the synthesis of serotonin, kynurenine, spermidine, and spermine by up to fivefold in MCF-7 and up to 61-fold in MDA-MB 231 compared with controls (Fig. 1), indicating that resveratrol strongly interacts with cellular biogenic amine metabolism. Furthermore, resveratrol induced the oxidation

Table 1. Influence of Resveratrol (100 μM) on the Metabolite Concentrations in Cells and Medium of MCF-7 and MDA-MB-231 Cells Given as n-Fold Changes to the Control

	MCF-7		*MDA-MB-231*	
Metabolite	*Cells*	*Medium*	*Cells*	*Medium*
Amino acids				
Alanine	0.81	**2.16**	**7.51**	**18.51**
Arginine	0.82	**2.53**	**5.55**	**6.25**
Asparagine	0.75	**5.34**	**9.50**	**15.08**
Aspartic acid	**0.42**	**5.35**	**4.33**	**5.56**
Citrulline	1.33	**3.08**	n.d.	**4.51**
Glutamine	**0.49**	**1.85**	**7.01**	**5.28**
Glutamic acid	1.02	**3.71**	**5.25**	**11.47**
Glycine	0.56	**3.58**	**9.71**	**14.61**
Histidine	0.99	**1.87**	**13.50**	**6.22**
Isoleucine	1.66	**4.03**	**18.02**	**37.7**
Leucine	1.31	**4.01**	**16.32**	**55.25**
Lysine	1.06	**2.59**	**6.33**	**5.53**
Methionine	1.51	**3.20**	**14.99**	**63.44**
Ornithine	0.51	**2.21**	**5.03**	**6.40**
Phenylalanine	1.12	**1.87**	**9.47**	**9.89**
Proline	0.90	**1.55**	**5.69**	**4.46**
Serine	0.83	**21.08**	**5.37**	**18.78**
Threonine	0.86	**2.15**	**8.34**	**5.51**
Tryptophan	1.57	**2.09**	**7.04**	**41.26**
Tyrosine	0.99	**2.01**	**12.87**	**9.21**
Valine	1.34	**2.81**	**18.08**	**29.70**
Biogene amines and modified amino acids				
ADMA (Asymmetric dimethylarginine)	n.d.	1.09	n.d.	**3.52**
SDMA (Symmetric dimethylarginine)	1.0	1.0	n.d.	**3.14**
Creatinine	n.d.	**1.51**	n.d.	**3.53**
Histamine	n.d.	1.08	n.d.	**4.33**
Kynurenine	n.d.	**1.54**	n.d.	**4.01**
Methionine-sulfoxide	n.d.	**1.71**	n.d.	**5.24**
Nitrotyrosine	n.d.	n.d.	n.d.	**4.98**
Hydroxykynurenine	n.d.	**1.62**	n.d.	**7.45**
Hydroxyproline	n.d.	n.d.	n.d.	n.d.
PEA (Phenylethylamine)	n.d.	n.d.	n.d.	n.d.
Putrescine	**0.27**	1.20	n.d.	**4.60**
Sarcosine	0.67	**3.21**	n.d.	**2.91**
Serotonin	n.d.	**5.20**	n.d.	**3.66**
Spermidine	1.78	**5.25**	n.d.	**39.90**
Spermine	1.46	**2.46**	3.12	**61.31**
Taurine	0.61	**11.28**	5.75	**14.38**
Eicosanoids and oxidized polyunsaturated fatty acids				
12S-HETE (12(S)-Hydroxy-5Z,8Z,10E,14Z-eicosatetraenoic acid)	n.d.	**5.98**	n.d.	**5.14**
15S-HETE (15(S)-Hydroxy-5Z,8Z,11Z,13E-eicosatetraenoic acid)	n.d.	n.d.	n.d.	n.d.
5S-HpETE (5(S)-Hydroperoxy-6E,(Z,11Z,14Z-eicosatetraenoic acid)	n.d.	n.d.	n.d.	n.d.
14(15)-EpETE ((±)14,15-Epoxy-5Z,8Z,11Z,17Z-eicosatetraenoic acid)	n.d.	n.d.	n.d	n.d.
15S-EpETE (15(S)-Hydroperoxy-5Z,8Z,11Z,13E-eicosatetraenoic acid)	n.d.	n.d.	n.d.	n.d.
9-HODE ((±)9-Hydroxy-10E,12Z-octadecadienoic acid)	2.86	1.84	0.83	2.33
13S-HODE (13-Hydroxy-9Z,11E-octadecadienoic acid)	2.64	2.11	**2.11**	1.35
Arachidonic acid	1.03	2.90	1.18	**84.03**
Docosahexaenoic acid	**1.88**	2.22	3.16	**9.51**
Leukotriene B4	n.d.	**10.82**	n.d.	n.d.
Leukotriene D4	n.d.	n.d.	n.d.	n.d.
Prostaglandin D2	n.d.	n.d.	n.d.	n.d.
Prostaglandin E2	n.d.	0.35	n.d.	**0.07**
Prostaglandin F2a	n.d.	0.67	n.d.	1.08
6-keto-Prostaglandin F1a	n.d.	n.d.	n.d.	n.d.
8-iso-Prostaglandin F2a	n.d.	n.d.	n.d.	n.d.
Thromboxane B2	n.d.	n.d.	n.d.	n.d.

Values in bold indicate significant changes ($p < 0.05$).
n.d., not detectable.

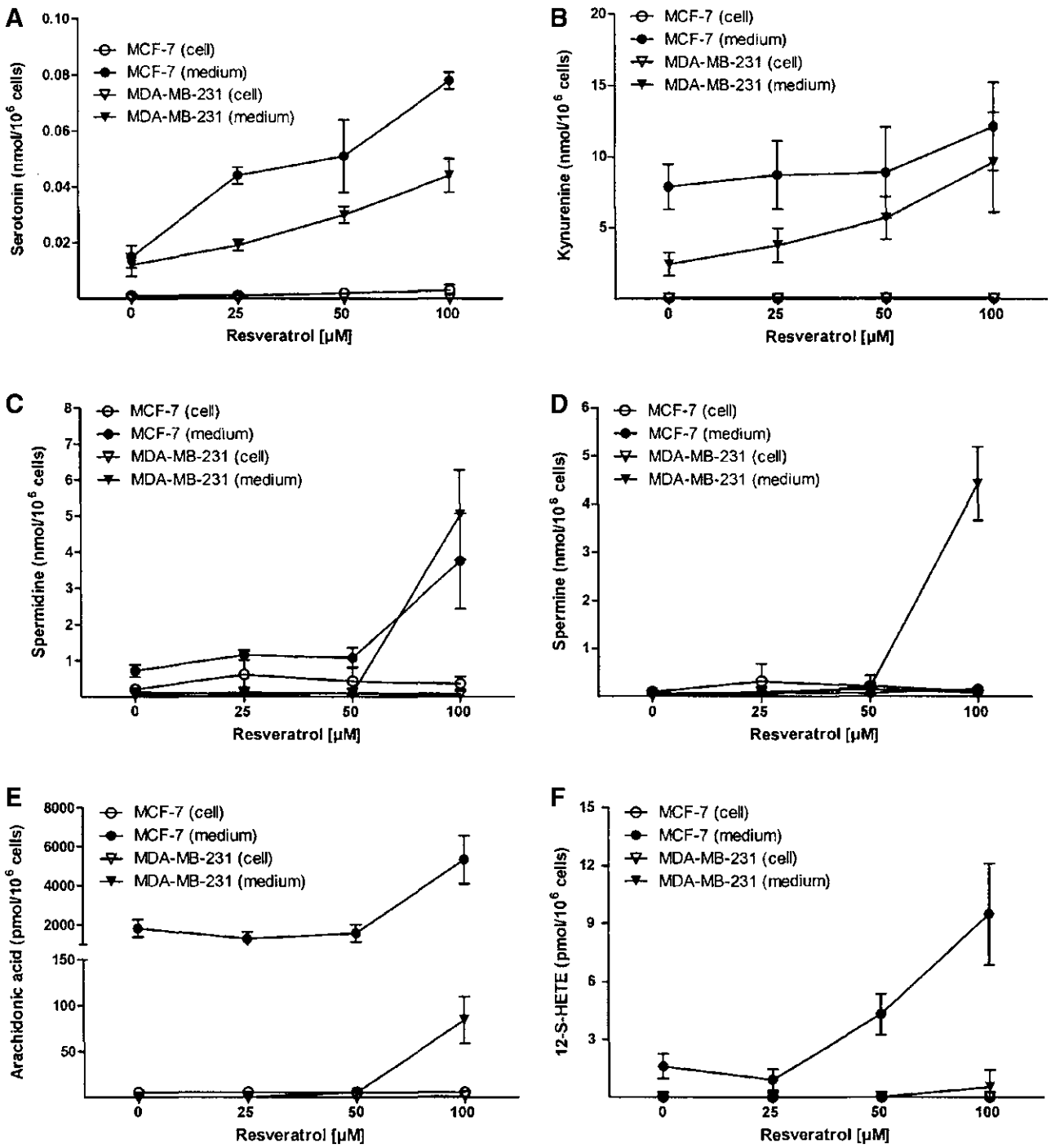

FIG. 1. Induction of serotonin (**A**), kynurenine (**B**), spermidine (**C**), spermine (**D**), arachidonic acid (**E**), and 12S-HETE (**F**) in the human breast cancer cell lines MCF-7 and MDA-MB-231 after incubation with resveratrol (0–100 μM) for 72 h. Data represent the mean ± SD of triplicate determinations.

of methionine to methionine sulfoxide by 1.7- and 5.24-fold in MCF-7 and MDA-MB-231 cells, respectively (Table 1). Phenylalanine and phenylethylamine (PEA) concentrations were below the detection limits in both cell lines.

Eicosanoids and Oxidized Polyunsaturated Fatty Acids

Among the 17 analytes quantified, a marked increase in extracellular arachidonic acid and its metabolite 12S-HETE (12(S)-hydroxy-5Z,8Z,10,E14Z-eicosatetraenoic acid) was observed (Fig. 1). Concentrations of the linoleic acids metabolites 13S-HODE [13(S)-hydroxy- 9Z, 11E-octadecadienoic acid] and 9-HODE [(±)9-hydroxy-10E,12Z-octadecadienoic acid] were also increased by resveratrol. Remarkably, extracellular arachidonic acid concentrations rose 84-fold in MDA-MB-231 cells cultures, but only 2.9-fold in MCF-7 cells compared to control (Fig. 1). Also, resveratrol significantly reduced prostaglandin E2 (PGE2) levels in the medium of MDA-MB-231

cells (>99%), whereas the reduction in MCF-7 cells was less pronounced (65%) (Table 1). Several other oxidized polyunsaturated fatty acids and prostaglandins as well as leucotriene D4 and thromboxane B2 were below the detection limit.

Discussion

In the present study, we investigated the metabolic changes in two human breast cancer cell lines after resveratrol application (5–100 μM). These concentrations were chosen based on daily intake of resveratrol as beverage (red wine) or as dietary supplement (5–100 mg/day). By quantifying 54 analytes, we found that resveratrol significantly induced the synthesis of 21 amino acids with far higher concentrations in MCF-7 than in MDA-MB-231 cells. In both cell lines, all amino acids were substantially released from the cytoplasm into the medium, which is often caused by cell swelling and the occurrence of reactive oxygen species (Lambert, 2007). Resveratrol also profoundly modulated the polyamine biosynthesis in both cell lines. Tryptophan, serotonin, and kynurenine increased significantly in the presence of resveratrol, indicating that enzymatic conversion of tryptophan to the bioactive metabolite serotonin through tryptophanhydroxylase and to kynurenine through tryptophan-2,3-dioxygenase and monooxygenase was stimulated. Kynurenine was further metabolized to hydroxykynurenine3-hydroxy-kynurenine with much higher concentrations in the medium of MDA-MB-231 cells than in the MCF-7 cell line (Fig. 1).

Treatment of both breast cancer cell lines with resveratrol also stimulated the synthesis of putrescine and spermidine indicating activation of ornithine decarboxylase and spermidine synthase, respectively. Interestingly, synthesis of spermine from spermidine was stimulated in MDA-MB-231 cells but inhibited in MCF-7 cells. Because putrescine, spermidine and spermine are essential for a variety of cellular processes related to signal transduction, resveratrol-induced growth and differentiation changes in polyamine metabolism may be directly linked to cell vitality (Takao et al., 2006). Conversion of putrescine to the metabolically active polyamines spermidine and spermine occurs early during cell proliferation. It is mediated by S-adenosylmethionine decarboxylase (SADMC), the rate-limiting enzymes of polyamine biosynthesis. Similar to ornithine decarboxylase (ODC), SADMC activity is increased in proliferating cells (Milovic et al, 2000). In human colon adenocarcinoma CaCo-2 cells, resveratrol, and the analog (Z)-3,5,4′-trimethoxystilbene have been shown to reduce ODC and SADMC activities by depletion of the polyamines putrescine and spermidine, exerting their cytotoxic effects by depleting the intracellular pool of polyamines (Schneider et al., 2003; Wolter et al., 2003). In contrast to colon cancer cells, resveratrol stimulated putrescine and spermidine synthesis in MCF-7 and MDA-MB-231 cells, indicating that cell growth inhibition may rather be caused by high polyamine concentrations, which have also been to induce cell death (Takao et al., 2006).

Our study also showed a pronounced increase in extracellular arachidonic acid and its metabolite 12S-HETE at high resveratrol concentrations, indicating the release of arachidonic acid from cell membrane phospholipids upon activation of phospholipase A_2. Arachidonic acid is subsequently converted to 12S-HETE through the action of 12-lipoxygenase. Increased levels of 12S-HETE may therefore indicate oxidative stress in tumor cells under resveratrol treatment (Nazarewicz et al, 2007). Furthermore, resveratrol also reduced prostaglandin E2 (PGE2) levels, thus confirming that this polyphenol is an inhibitor of cyclooxygenase 2 (Murias et al. 2004). In conclusion, we revealed several small molecules as novel markers for the anticancer activity of resveratrol. Further investigations are required to better understand the resveratrol-induced metabolic differences between hormone-sensitive and hormone-insensitive cell lines.

Acknowledgments

This study was supported by grants of the Jubiläumsfonds der Österreichischen Nationalbank (12600 to W.J.) and FWF (P21083-B11 to W.J.).

Author Disclosure Statement

No competing financial interests exist.

References

Anderson, W.F., Umar, A., and Hawk, E.T. (2003). Cyclooxgenase inhibition in cancer prevention and treatment. Expert Opin Pharmacother 4, 2193–2204.

Bove, K., Lincoln, D.W., and Tsan, M.F. (2002). Effect of resveratrol on growth of 4T1 breast cancer cells in vitro and in vivo. Biochem Biophys Res Commun 291, 1001–1005.

Deberardinis, R.J., Sayed, N., Ditsworth, D., and Thompson, C.B. (2008). Brick by brick: metabolism and tumor cell growth. Curr Opin Genet Dev 18, 54–61.

Fontecave, M., Lepoivre, M., Elleingand, E., Gerez, C., and Guittet, O. (1998). Resveratrol, a remarkable inhibitor of ribonucleotide reductase. FEBS Lett 421, 277–279.

Garvin, S., Ollinger, K., and Dabrosin, C. (2006). Resveratrol induces apoptosis and inhibits angiogenesis in human breast cancer xenografts in vivo. Cancer Lett 231, 113–122.

Gieger, C., Geistlinger, L., Altmaier, E., Hrabe de Angelis, M., Kronenberg, F., Meitinger, T., et al. (2008). Genetics meets metabolomics: a genome-wide association study of metabolite profiles in human serum. PLoS Genet 4, e1000282.

Horvath, Z., Saiko, P., Madlener, S., Hoechtl, T., Bauer, W., Erker, T., et al. (2005). Synergistic action of resveratrol, an ingredient of wine, with Ara-C and tiazofurin in HL-60 human promyelocytic leukemia cells. Exp Hematol 33, 329–335.

Lambert, I.H. (2007). Activation and inactivation of the volume-sensitive taurine leak pathway in NIH3T3 fibroblasts and Ehrlich Lettre ascites cells. Am J Physiol Cell Physiol 293, 390–400.

Milovic, V., Stein, J.E.,Odera, G., Gilani, S., and Murphy, G.M. (2000). Low-dose deoxycholic acid stimulates putresine uptake in colon cancer cells (Caco-2). Cancer Lett 154, 195–200.

Miksits, M., Wlcek, K., Svoboda, M., Kunert, O., Haslinger, E., Thalhammer, T., et al. (2010). Antitumor activity of resveratrol and its sulfated metabolites against human breast cacner cells. Planta Medica 75, 1–4.

Murias, M., Handler, N., Erker, T., Pleban, K., Ecker, G., Saiko, P., et al. (2004). Resveratrol analogues as selective cyclooxygenase-2 inhibitors: synthesis and structure–activity relationship. Bioorg Med Chem 12, 5571–5578.

Murias, M., Miksits, M., Aust, S., Spatzenegger, M., Thalhammer, T., et al. (2008). Metabolism of resveratrol in breast cacner cell lines: impact of sulfotransferase 1A1 expression on cell growth inhibition. Cancer Lett 261, 172–182.

Nakagawa, H., Kiyozuka, Y., Uemura, Y., Senzaki, H., Shikata, N, Hioki, K., et al. (2001). Resveratrol inhibits human breast

cancer cell growth and may mitigate the effect of linoleic acid, a potent breast cancer cell stimulator. J Cancer Res Clin Oncol 127, 258–264.

Nazarewicz, R., Zenebe, W.J., Parihar, A., Parihar, M.S., Vaccaro, M., Rink, C., et al. (2007). 12(S)-hydroperoxyeicosatetraenoic acid (12-HETE) increases mitochondrial nitric oxide by increasing intramitochondrial calcium. Arch Biochem Biophys 468, 114–120.

Pozo-Guisado, E., Alvarez-Barrientos, A., Mulero-Navarro, S., Santiago-Josefat, B., and Fernandez-Salguero, P.M. (2002). The antiproliferative activity of resveratrol results in apoptosis in MCF-7 but not in MDA-MB-231 human breast cancer cells: cell-specific alteration of the cell cycle. Biochem Pharmacol 64, 1375–1386.

Ragione, F.D., Cucciolla, V., Boriello, A., Pietra, V.D., Racioppi, L., Soldati, G., et al. (1998). Resveratrol arrests the cell division cycle at S/G2 phase transition. Biochem Biophys Res Commun 250, 53–58.

Schneider, Y., Chabert, P., Stutzmann, J., Coelho, D., Fougerousse, A., Gosse, F., et al. (2003). Resveratrol analog (Z)-3,5,4′-trimethoxystilbene is a potent anti-mitotic drug inhibiting tubulin polymerization. Int J Cancer 107, 189–196.

Takao, K., Rickhag, M., Hegardt, C., Oredsson, S., and Persson, L. (2006). Induction of apoptotic cell death by putrescine. Int J Biochem Cell Biol 38, 621–628.

Weinberger, K.M., and Graber, A. (2005). Using comprehensive metabolomics to identify novel biomarkers. Screen Trends Drug Discov 6, 42–45.

Wolter, F., Turchanova, L., and Stein, J. (2003). Resveratrol-induced modification of polyamine metabolism is accompanied by induction of c-Fos. Carcinogenesis 24, 469–474.

Address correspondence to:
Prof. Walter Jäger
Department of Clinical Pharmacy and Diagnostics
University of Vienna
A-1090 Vienna, Austria

E-mail: walter.jaeger@univie.ac.at

NF-κB mediates the 12(S)-HETE-induced endothelial to mesenchymal transition of lymphendothelial cells during the intravasation of breast carcinoma cells.

Vonach C., Viola K., **Giessrigl B.**, Huttary N., Raab I., Kalt R., Krieger S., Vo T.P., Madlener S., Bauer S., Marian B., Hämmerle M., Kretschy N., Teichmann M., Hantusch B., Stary S., Unger C., Seelinger M., Eger A., Mader R., Jäger W., Schmidt W., Grusch M., Dolznig H., Mikulits W. and Krupitza G.

Br. J. Cancer 105: 263-271, **2011.**

British Journal of Cancer (2011) 105, 263 – 271
© 2011 Cancer Research UK All rights reserved 0007 – 0920/11
www.bjcancer.com

NF-κB mediates the 12(S)-HETE-induced endothelial to mesenchymal transition of lymphendothelial cells during the intravasation of breast carcinoma cells

C Vonach[1,2], K Viola[1,2], B Giessrigl[1], N Huttary[1], I Raab[1], R Kalt[1], S Krieger[1], TPN Vo[1], S Madlener[1], S Bauer[1], B Marian[2], M Hämmerle[1], N Kretschy[1], M Teichmann[1], B Hantusch[1], S Stary[1], C Unger[1], M Seelinger[1], A Eger[3], R Mader[2], W Jäger[4], W Schmidt[5], M Grusch[2], H Dolznig[1,6], W Mikulits[2] and G Krupitza*[,1]

[1]Institute of Clinical Pathology, Medical University of Vienna, Waehringer Guertel 18-20, A-1090 Vienna, Austria; [2]Department of Medicine I, Institute of Cancer Research, Medical University of Vienna, Vienna, Austria; [3]University of Applied Science, Krems, Austria; [4]Department of Clinical Pharmacy and Diagnostics, University of Vienna, Vienna, Austria; [5]Neuromuscular Research Department, Center for Anatomy and Cell Biology, Medical University of Vienna, Vienna, Austria; [6]Institute of Medical Genetics, Medical University of Vienna, Vienna, Austria

BACKGROUND: The intravasation of breast cancer into the lymphendothelium is an early step of metastasis. Little is known about the mechanisms of bulky cancer invasion into lymph ducts.

METHODS: To particularly address this issue, we developed a 3-dimensional co-culture model involving MCF-7 breast cancer cell spheroids and telomerase-immortalised human lymphendothelial cell (LEC) monolayers, which resembles intravasation *in vivo* and correlated the malignant phenotype with specific protein expression of LECs.

RESULTS: We show that tumour spheroids generate 'circular chemorepellent-induced defects' (CCID) in LEC monolayers through retraction of LECs, which was induced by 12(S)-hydroxyeicosatetraenoic acid (HETE) secreted by MCF-7 spheroids. This 12(S)-HETE-regulated retraction of LECs during intravasation particularly allowed us to investigate the key regulators involved in the motility and plasticity of LECs. In all, 12(S)-HETE induced pro-metastatic protein expression patterns and showed NF-κB-dependent up-regulation of the mesenchymal marker protein S100A4 and of transcriptional repressor ZEB1 concomittant with down-regulation of the endothelial adherence junction component VE-cadherin. This was in accordance with ~50% attenuation of CCID formation by treatment of cells with 10 μM Bay11-7082. Notably, 12(S)-HETE-induced VE-cadherin repression was regulated by either NF-κB or by ZEB1 since ZEB1 siRNA knockdown abrogated not only 12(S)-HETE-mediated VE-cadherin repression but inhibited VE-cadherin expression in general.

INTERPRETATION: These data suggest an endothelial to mesenchymal transition-like process of LECs, which induces single cell motility during endothelial transmigration of breast carcinoma cells. In conclusion, this study demonstrates that the 12(S)-HETE-induced intravasation of MCF-7 spheroids through LECs require an NF-κB-dependent process of LECs triggering the disintegration of cell–cell contacts, migration, and the generation of CCID.

British Journal of Cancer (2011) **105,** 263–271. doi:10.1038/bjc.2011.194 www.bjcancer.com
Published online 31 May 2011
© 2011 Cancer Research UK

Keywords: LEC motility; VE-cadherin; ZEB1; S100A; NF-κB

Molecular Diagnostics

Breast cancer is the most common malignancy causing the highest death rate among women. Noteworthy, patients are not threatened by the primary tumour, but by metastases that destroy the function of infested organs. Breast cancer is believed to spread mainly through the lymphatic vasculature and as soon as carcinoma cell emboli are detectable in intrametastatic lymphatic vessels of sentinel lymph nodes (intrametastatic carcinosis), the postsentinel lymph nodes also fill up with cancer cells (Kerjaschki *et al*, 2011). The number of metastasised lymph nodes is a clinical predictor for the development of distant organ metastases and patient outcome (Carlson *et al*, 2009). Hence, understanding early steps of tumour cell intravasation into the lymphatic vasculature is important for the development of tailored anti-metastatic treatment concepts. Ductal breast cancer accesses the lymphatics in bulks generating gaps in the lymphendothelial cell (LEC) wall that serve as entry gates for the tumour. Therefore, we aimed to investigate the mechanisms of breast cancer cells that generate gaps – and as we now call them – 'circular chemorepellent-induced defects' (CCID) into LEC monolayers to identify potential target molecules for therapy. In a 3-dimensional (3D) co-culture model *in vitro*, we recently demonstrated that human MCF-7 breast cancer spheroids induced the formation of CCID into LEC monolayers right underneath the spheroids through centrifugal LEC migration (Madlener *et al*, 2010), a process closely resembling the situation in

*Correspondence: Dr G Krupitza;
E-mail: georg.krupitza@meduniwien.ac.at
Received 13 December 2010; revised 18 April 2011; accepted 9 May 2011; published online 31 May 2011

human patients. Tumour cells (MCF-7) secrete 12(S)-hydroxy-eicosatetraenoic acid (HETE) (Uchide *et al*, 2007), which is produced by lipoxygenase-15 (ALOX15) in MCF-7 cells. Our recent study identified this arachidonic acid metabolite as one of the major factors in the process of CCID formation (Kerjaschki *et al*, 2011). Notably, 12(S)-HETE was described as the 'endothelial retraction factor' (Honn *et al*, 1994). The NF-κB promotes endothelial cell migration (Flister *et al*, 2010) and in preliminary experiments, we found that NF-κB inhibition reduced CCID formation. As the migration of LECs is an early and relevant event in mammary tumour cell intravasation and metastasis, we investigated the mechanism of 12(S)-HETE and the role of NF-κB on LEC motility.

MATERIALS AND METHODS

Chemicals

The I-κBα phosphorylation inhibitor (E)-3-[(4-methylphenylsulfonyl]-2-propenenitrile (Bay11-7082) was from Biomol (Hamburg, Germany) and 12(S)-HETE was purchased from Cayman Chemical (Ann Arbor, MI, USA).

Monoclonal antibody against CD144 (VE-cadherin) (PN IM1597) was from Beckman Coulter (Fullerton, CA, USA). The polyclonal rabbit anti-paxillin antibody (H-114) (SC-5574), the monoclonal mouse α-tubulin (DM1A) antibody, and rabbit polyclonal anti-ZEB1 (H-102) were purchased from Santa Cruz Biotechnology (Santa Cruz, CA, USA).

Monoclonal mouse antibody phospho-p44/42 MAPK (Erk1/2) (Thr202/Tyr204) (E10), monoclonal rabbit p44/42 MAPK (Erk1/2) (137F5) antibody, polyclonal rabbit antibody phospho-myosin light chain 2 (MLC2) (Ser19), polyclonal rabbit MLC2 antibody, monoclonal mouse antibody phospho-Akt (Ser473) (587F11), polyclonal rabbit Akt antibody, monoclonal rabbit antibody ROCK-1 (C8F7), polyclonal rabbit ILK1 antibody, and polyclonal rabbit MYPT1 antibody were from Cell Signaling (Danvers, MA, USA). Monoclonal mouse anti-β-actin (clone AC-15) and monoclonal mouse anti-acetylated-tubulin (clone 6-11B-1) were from Sigma-Aldrich (Munich, Germany). The polyclonal rabbit IgG anti-phospho-MYPT1 (Thr696) was purchased from Upstate (Lake Placid, NY, USA). The polyclonal rabbit phospho-specific actin (Tyr-53) antibody was from extracellular matrix (ECM) Biosciences (Versailles, KY, USA). Rabbit anti-S100A4 was purchased from Sigma (St Louis, MO, USA). Polyclonal goat ARP2/3 subunit 1B antibody was purchased from Abcam (Cambridge, MA, USA). Polyclonal rabbit anti-mouse and anti-rabbit IgGs were from Dako (Glostrup, Denmark). Alexa-Fluor 488 (green) goat-anti-rabbit and Alexa-Fluor 594 (red) goat-anti-mouse labelled antibodies were purchased from Molecular Probes, Invitrogen (Karlsruhe, Germany).

Cell culture

Human MCF-7 breast cancer cells were grown in MEM medium supplemented with 10% fetal calf serum (FCS), 1% penicillin/streptomycin, 1% NEAA (Invitrogen) at 37°C in a humidified atmosphere containing 5% CO_2. Telomerase-immortalised human LECs were grown in EGM2 MV (Clonetics, Allendale, NJ, USA) at 37°C in a humidified atmosphere containing 5% CO_2.

For gap formation assays, LECs were stained with cytotracker green purchased from Invitrogen.

3D co-cultivation of MCF-7 cancer cells with LECs

Mock cells (MCF-7) were transferred to 30 ml MEM medium containing 6 ml of a 1.6% methylcellulose solution (0.3% final concentration; Cat. No.: M-512, 4000 centipoises; Sigma, Karlsruhe, Germany). A total of 150 μl of this cell suspension were transferred to each well of a 96-well plate (Greiner Bio-one, Cellstar 650185, Kremsmünster, Austria) to allow spheroid formation within the following 2 days. Then, MCF-7 spheroids were washed in phosphate-buffered saline (PBS) and transferred to cytotracker-stained LEC monolayers that were seeded into 24-well plates (Costar 3524, Sigma-Aldrich) in 2 ml EGM2 MV medium.

CCID assay

The MCF-7 cell spheroids (3000 cells/spheroid) were transferred to the 24-well plate containing LEC monolayers. After 4 h of incubating the MCF-7 spheroids-LEC monolayer co-cultures, the gap sizes in the LEC monolayer underneath the MCF-7 spheroids were photographed using an Axiovert (Zeiss, Jena, Germany) fluorescence microscope to visualise cytotracker(green)-stained LECs underneath the spheroids. Gap areas were calculated with the Axiovision Re. 4.5 software (Carl Zeiss, Jena, Germany). The MCF-7 spheroids were treated with solvent (DMSO) as negative control. Each experiment was performed in triplicate and for each condition, the gap size of 12 and more spheroids was measured.

Confocal microscopy and immunofluoresce analysis

Lab-Tek II chambered coverglasses (Nalgen Nunc International, Wiesbaden, Germany) were coated with 10 μg ml^{-1} fibronectin for 1 h at room temperature. Lymphendothelial cells were seeded in 1 ml EGM 2 MV onto chambered coverslips and allowed to grow for 2 days followed by co-cultivation with MCF-7 spheroids on LEC monolayers. After 4 h of incubation, cells were washed with ice-cold PBS and fixed in 4% paraformaldehyde for 15 min at room temperature. Cells were immunostained with various antibodies and analysed by confocal microscopy. For this, cells were washed with PBS and permeabilised with 0.1% Triton X-100 in PBS for 30 min at room temperature, followed by washing with PBS and blocking for 1 h with 10% goat serum diluted in BSA. Thereafter, the cells were incubated with the primary antibody against VE-cadherin diluted 1 : 50 for 1 h at room temperature and washed with PBS. Cells were further incubated with a fluorescence labelled second antibody diluted 1 : 1000 for 1 h at room temperature in the dark and washed with PBS. Cells were counterstained with DAPI (dilution 1 : 50 0000) at room temperature.

Western blotting

Lymphendothelial cells were seeded in 6 cm dishes and treated with the indicated compounds (10 μM Bay11-7082 and or 1 μM 12(S)-HETE). Cells were washed twice with ice-cold PBS and lysed in buffer containing 150 mM NaCl, 50 mM Tris pH 8.0, 0,1% Triton X-100, 1 mM phenylmethylsulfonylfluorid and protease inhibitor cocktail. Afterwards, the lysate was centrifuged at 12 000 r.p.m. for 20 min at 4°C and the supernatant was stored at −20°C until further analysis. Equal amounts of protein samples were separated by SDS polyacrylamide gel electrophoresis and electro-transferred onto Hybond PVDF membranes at 100 V for 1 h at 4°C. To control equal sample loading, membranes were stained with Ponceau S. After washing with PBS/T (PBS/Tween 20; pH: 7.2) or TBS/T (Tris-buffered saline/Tween 20; pH: 7.6), membranes were immersed in blocking solution (5% non-fat dry milk in TBS containing 0.1% Tween or in PBS containing 0.5% Tween 20) at room temperature for 1 h. Membranes were washed and incubated with the first antibody (in blocking solution; dilution 1 : 500 – 1 : 1000) by gently rocking at 4°C overnight or at room temperature for 1 h. Thereafter, the membranes were washed with PBS/T or TBS/T and incubated with the second antibody (peroxidase-conjugated goat-anti-rabbit IgG or anti-mouse IgG; dilution 1 : 2000) at room temperature for 1 h. Chemiluminescence was detected by ECL detection kit (Thermo Scientific, Portsmouth, NH, USA) and the membranes were exposed to Amersham Hyperfilms (GE-Healthcare, Amersham, Buckinghamshire, UK).

© 2011 Cancer Research UK

Transient siRNA transfection

Lymphendothelial cells were grown in 6-well plates to 70% confluence in EGM 2 MV medium. Cells were subsequently transfected using RNAiFect (Qiagen, Hamburg, Germany). siRNA (ZEB1 silencer select pre-designed siRNA ID: s13883, and ID: s13885, and scrambled RNA Ambion; Applied Biosystems, Austin, TX, USA) was diluted in culture medium containing FCS and antibiotics (final volume 100 μl) to a final concentration of 100 nM. A total of 15 μl of RNAiFect transfection reagent was added to the diluted siRNA and incubated for 15 min at room temperature. Then the mixture was added to cells and incubated for 8 h at 37°C. Thereafter, the medium was changed and the cells were incubated further 48 h. ZEB1 expression was analysed by western blotting.

Statistical analysis

Dose–response curves were analysed using Prism 4 software (San Diego, CA, USA) and significance was determined by paired Student's *t*-test. Significant differences between experimental groups were $^*P<0.05$.

RESULTS

12(S)-HETE induces protein expression in LECs associated with motility

Breast cancer cells (MCF-7) secrete 12(S)-HETE (Uchide *et al*, 2007), which has been shown to induce the motility of endothelial cells (Honn *et al*, 1994). The time-dependent formation of CCIDs was caused by MCF-7 spheroids in the underneath growing LEC monolayer (Figures 1A and B). We could demonstrate by time lap microscopy that MCF-7 spheroid-induced CCID formation was the result of rapid cell retraction rather than a cell clearence through apoptosis (Kerjaschki *et al*, 2011). Confocal laser scanning microscopy revealed that cell retraction correlated with the increased phosphorylation of myosin light chain phosphotransferase (MYPT1, synonym: PPP1R12A) threonine-696 and of MLC2 serine-19 in underneath growing LECs at the rim of CCIDs (Figure 1C; upper right corner each, which was covered by the MCF-7 spheroid), indicating a mobile LEC phenotype. To simplify the 3D co-culture model consisting of MCF-7 spheroids and LEC monolayer, in which the role of ALOX15, ALOX12, and 12(S)-HETE was investigated in detail (Madlener *et al*, 2010; Kerjaschki *et al*, 2011) and to analyse protein expression/activation, LECs were treated with 1 μM synthetic 12(S)-HETE. Indeed, purified 12(S)-HETE increased the phosphorylation of MYPT1 in LECs within 1 h (Figure 2A), confirming our recent data (Kerjaschki *et al*, 2011). Furthermore, MLC2 showed increased phosphorylation, which substantiated the fact that 12(S)-HETE induced the motility of LECs.

Akt is an important component in pro-survival pathways but also significantly involved in pro-migratory signalling (Burgering and Coffer, 1995; Franke *et al*, 1997). Treatment with 12(S)-HETE transiently increased the level of phosphorylated Akt within 30 min (Figure 2A).

Arp2/3 activity correlates with mesenchymal-type migration, whereas ROCK-1 is associated with amoeboid migration (Paulitschke *et al*, 2010) and both co-regulate the actin cytoskeleton (Xu *et al*, 2009; To *et al*, 2010). 12(S)-HETE stimulated a marginal increase of ROCK-1 and Arp2/3 expression; however, the constitutive phosphorylation of actin at the Tyr53 activation site remained unchanged (Figure 2B).

Paxillin is a focal adhesion phosphoprotein contributing to the contact between the endothelial cell and the ECM, and its up-regulation associates with a mobile cell phenotype (Huang *et al*, 2003; Webb *et al*, 2004). Treatment of LECs with 12(S)-HETE caused an increase of paxillin after 2 h (Figure 2C) and a transient up-regulation of the pro-metastatic Ca^{2+} signal transducer S100A4, both suggesting a mesenchymal and mobile phenotype (Zeisberg and Neilson, 2009). S100A4 expression was reported to correlate with tubulin polymerisation (Lakshmi *et al*, 1993), which is indicated by increased acetylation of α-tubulin (Piperno and Fuller, 1985). In all, 12(S)-HETE slightly increased tubulin acetylation (Figure 2C) concomittant with S100A4 up-regulation and this was accompanied by dephosphorylation (inactivation) of Erk1/2 (Figure 2D). Active Erk and paxillin mediate disadhesion, a process required for a directionally migrating cell phenotype (Webb *et al*, 2004). The reason for 12(S)-HETE-mediated Erk inactivation upon treatment remains obscure. It might indicate that the migratory stimulus was not an attracting one, but a repelling one, or that 12(S)-HETE-induced LEC adhesion disassemby is independent of Erk. Yet, from the total of the data we conclude that 12(S)-HETE induced a mesenchymal and mobile LEC phenotype mandatory for metastatic intravasation.

12(S)-HETE transiently inhibits VE-cadherin expression and induces endothelial disassembly

For cell–cell cohesion, VE-cadherin is necessary and hence, for vascular integrity. Therefore, VE-cadherin is a marker for an endothelial, immobile phenotype that withstands metastatic cell intravasation. Conversely, metastatic cells have to interefere with VE-cadherin function to facilitate the migration of LECs. In fact, treatment of LECs with 12(S)-HETE transiently down-regulated VE-cadherin expression (Figure 3A).

To investigate the effect of MCF-7 spheroids on VE-cadherin expression of underneath LECs, we analysed VE-cadherin distribution by confocal immunofluorescence microscopy. Lymphendothelial cells at distance of MCF-7 spheroids showed intact VE-cadherin structures (Figure 3B). At the margin of CCID, LECs showed disintegrated and reduced VE-cadherin at cell boundaries, suggesting disassembly of endothelial organisation (Figure 3C). The MCF-7 cells constantly produce 12(S)-HETE and, therefore, the down-regulation of VE-cadherin of underneath growing LECs was observed even after 4 h of co-culture and was not only transiently suppressed as seen upon synthetic 12(S)-HETE treatment.

These data implicate that LEC motility might be caused by the loss of cell–cell contacts through down-regulation of VE-cadherin and suggest an endothelial to mesenchymal transition (EMT)-like process, both by the spheroid as well as by 12(S)-HETE.

ZEB1 contributes to 12(S)-HETE-induced VE-cadherin repression

E-cadherin is negatively regulated by the transcription factor and proto-oncogene ZEB1 (Eger *et al*, 2005; Chua *et al*, 2007; Peinado *et al*, 2007). Therefore, we examined whether VE-cadherin was also regulated by ZEB1. In fact, 12(S)-HETE rapidly induced ZEB1 that was accompanied by VE-cadherin repression (Figure 4). Since it was so far unknown whether ZEB1 also (co)regulates VE-cadherin, we investigated by siRNA approach whether knockdown of ZEB1 causes loss of VE-cadherin regulation by 12(S)-HETE. Two different and validated siRNAs were transiently transfected into LECs to specifically knockdown the expression of ZEB1. This resulted in the loss of VE-cadherin regulation upon 12(S)-HETE stimulation (Figure 4). Unexpectedly, blocking ZEB1 expression down-regulated constitutive VE-cadherin expression, which implicated that VE-cadherin was not directly regulated by ZEB1.

Inhibition of NF-κB blocks MCF-7-induced gap formation of LEC

The inhibition of NF-κB translocation with Bay11-7082 blocked MCF-7 spheroid-induced gap formation of LECs in a

© 2011 Cancer Research UK

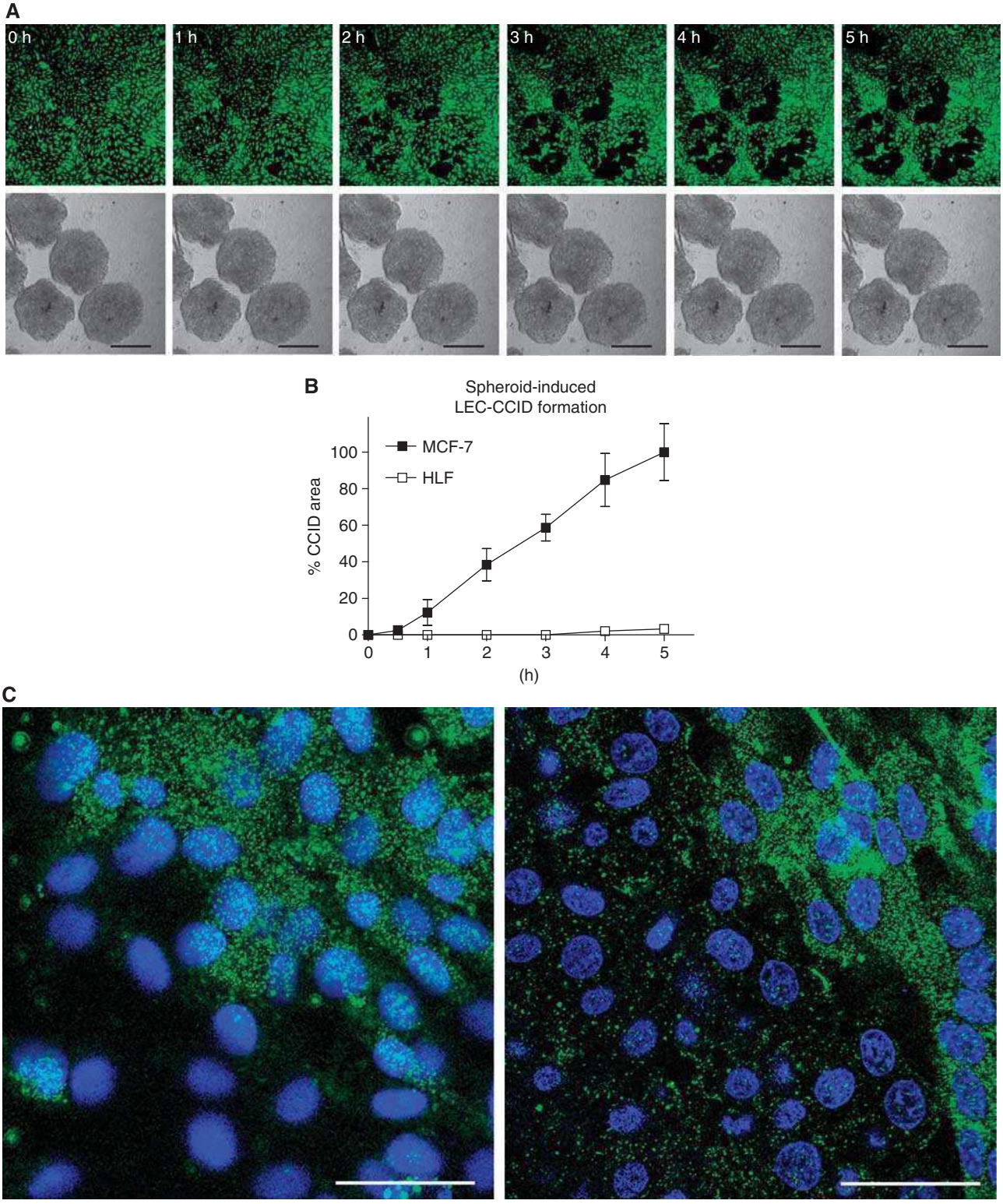

Figure 1 CCID formation by cell migration. (**A**) Time lap experiment show the same microscopic power field after 0–5 h co-culture of LECs (upper panel; cytotracker green, FITC filter) and MCF-7 spheroids (lower panel; phase contrast); The images show the progression of CCID formation over time. No apoptotic features were observed. Scale bars: 200 μm. (**B**) The gradual increase of CCID areas over time was measured underneath five MCF-7 spheroids or human normal lung fibroblast spheroids (HLF) after the indicated time points using Axiovision software (Zeiss). Error bars indicate s.e.m. (**C**) LECs were grown on coverslips until confluence when MCF-7 spheroids were transferred on top of LECs and co-incubated for 4 h at 37°C to allow CCID formation. LECs were stained with respective antibodies. Confocal laser scanning microscopy of immunocytochemically stained LECs at the rim of CCID (upper right diagon each, which was the part covered by the MCF-7 spheroid) show elevated levels of phosphorylation (green; FITC filter) of MYPT threonine-696 (left panel) and MLC2 serine-19 (right panel), indicating increased cell mobility. Nuclei are stained with DAPI (blue). Scale bars: 45 μm.

 © 2011 Cancer Research UK

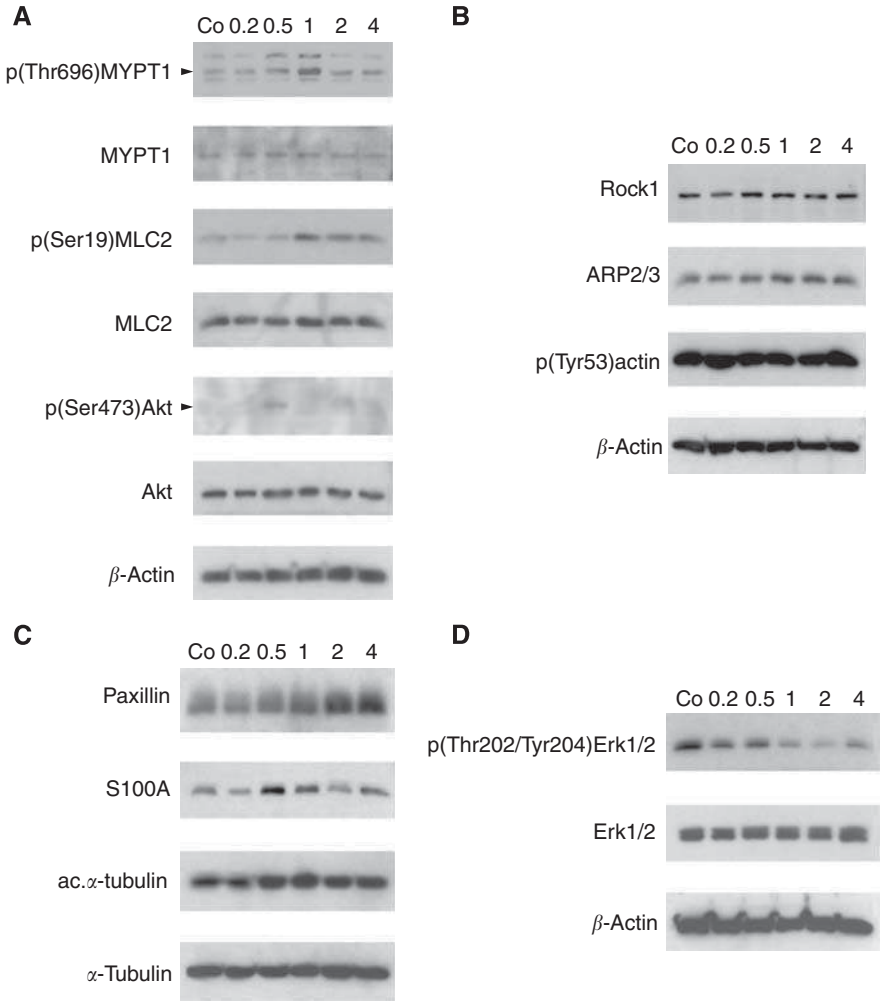

Figure 2 Modulation of protein expression and posttranslational modifications in LECs. LEC monolayers were incubated with 1 μM synthetic 12(S)-HETE and analysed by western blotting after 0.2, 0.5, 1.0, 2.0, and 4.0 h. Equal sample loading was controlled by Ponceau S staining, β-actin (**A**, **B**, **D**), or α-tubulin (**C**) expression. Co, untreated LECs.

dose-dependent fashion. A total of 10 μM Bay11-7082 reduced CCID areas by 50–60% and 15 μM prevented CCID formation almost completely (Figure 5A). Bay11-7082 is an irreversible inhibitor of I-κBα phosphorylation and this allowed a specific experimental design that facilitated to discriminate whether NF-κB activity of MCF-7 cells or of LECs contributed to CCID formation of LECs. Therefore, LEC monolayers or MCF-7 spheroids were each pretreated with Bay11-7082 for 30 min followed by a thorough washing procedure to prevent contaminating spill overs to the respective other cell type. Subsequently, MCF-7 spheroids were placed on the LEC monolayer (Figure 5B). Similar levels of inhibition were achieved when the drug was applied either on MCF-7 spheroids or on LECs, indicating that NF-κB contributed to gap formation by at least two mechanisms. Here, we focussed only on the role of NF-κB in LECs, regulating the change of endothelial plasticity associated with motility, and studied the expression of VE-cadherin and S100A4 by Western blot analysis. For this, LECs were pretreated with Bay11-7082 and then exposed to 12(S)-HETE. Bay11-7082 caused the up-regulation of VE-cadherin and the down-regulation of ZEB1 as well as of the mesenchymal marker protein S100A4 (Figures 6A and B). Immunocytochemistry confirmed that LECs expressed high levels of the mobility marker S100A4 (green) underneath MCF-7 spheroids (Figure 6C), which were down-regulated in the presence of Bay11-7082 (Figure 6D). Bay11-7082 prevented the suppression of VE-cadherin (red) underneath spheroids, although the VE-cadherin patterns appeared disintegrated and unconnected to adjacent cell borders (nuclei are in blue). These data suggest the involvement of NF-κB in the acquisition of a mesenchymal-like phenotype of LECs, which induces single cell motility necessary for intravasation of breast carcinoma cells into the endothelium.

DISCUSSION

The progression of tumours to metastatic outgrowth is the fatal process of most cancer entities. Metastasis includes multiple steps such as intravasation of bulky tumours or dissociated single cells into the vasculature, transport through vessels, extravasation, invasion of tumour cells in target tissues, and manifestation of secondary tumours (Geiger and Peeper, 2009). Therefore, the direct interaction of tumour cells with vascular endothelial cells (Kramer and Nicolson, 1979) is one of the earliest events that facilitates intra- and extravasation into and from the blood or lymphatic vasculature (Honn *et al*, 1987). The break through of tumour emboli into intrametastatic lymphatic vessels of sentinel lymph nodes (Hirakawa *et al*, 2009) is the preceding step for the subsequent colonisation of lymph nodes along efferent axes with

© 2011 Cancer Research UK

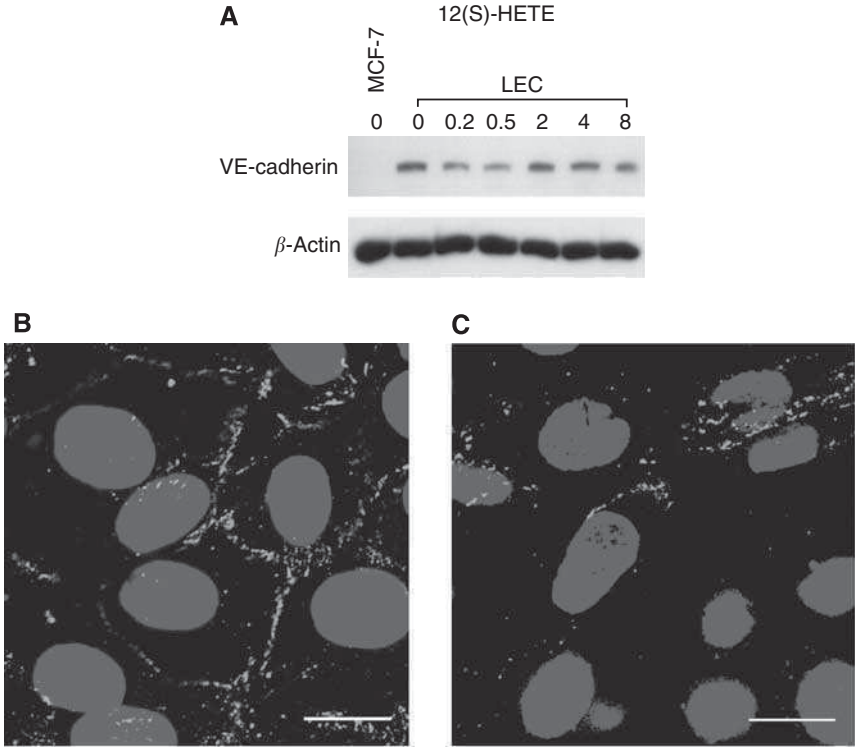

Figure 3 Analysis of VE-cadherin expression in LECs. (**A**) LECs were treated with 1 μM 12(S)-HETE for 0.2, 0.5, 2, 4, and 8 h. Then, cells were harvested and protein lysates were analysed by western blotting. MCF-7 cells were used as negative control. Equal sample loading was controlled by Ponceau S staining and β-actin analysis. Confocal immunofluorescence images of LECs next to a spheroid (**B**) and underneath an MCF-7 spheroid (**C**). LECs were grown on coverslips until confluence when MCF-7 spheroids were transferred on top of LECs and co-incubated for 4 h at 37°C to allow CCID formation. LECs were stained with anti-VE-cadherin antibody (red) and DAPI (blue). (**B**) Distant to a spheroid, VE-cadherin structures appear well developed, whereas (**C**) VE-cadherin interactions are disrupted underneath an MCF-7 spheroid. Scale bar: 15 μM. The colour reproduction of this figure is available at the *British Journal of Cancer* journal online.

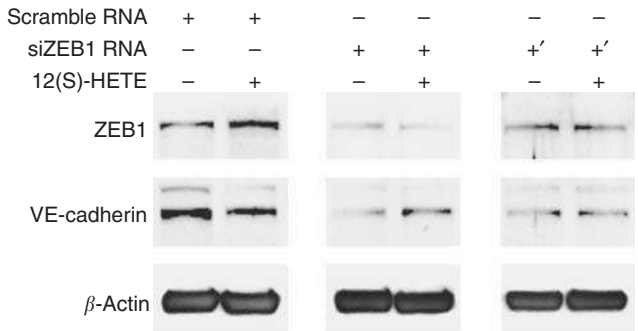

Figure 4 Effect of ZEB1 suppression on VE-cadherin regulation by 12(S)-HETE. LECs were transiently transfected with two different siRNAs against ZEB1 (+: siRNA1; +′: siRNA2), or with scrambled siRNA. LECs were subsequently treated with 1 μM 12(S)-HETE and analysed by western blotting using antibodies against ZEB1 and VE-cadherin. Equal sample loading was controlled by β-actin expression.

carcinoma cells. Notably, this event is indicative for a bad prognosis of ductal breast cancer (Kerjaschki *et al*, 2011). Hence, it is important to understand the mechanisms of tumour/lymph-endothelial interactions. Here, we used a 3D-co-culture system to mimic an early step of trespassing breast cancer cells through the lymphatic vasculature. The generation of CCID into LEC monolayers recapitulated the situation in the sentinel and postsentinel lymph nodes in ductal breast cancer lymph metastasis in humans. Metastasis was shown to depend on the expression and activity of ALOXs that produce 12(S)-HETE as in case of MCF-7 spheroids (Uchide *et al*, 2007; Kerjaschki *et al*, 2011). In all, 12(S)-HETE induces endothelial cell retraction (Honn *et al*, 1994) and stimulates tumour cell spreading on the ECM (Timar *et al*, 1992). Several studies have shown the involvement of ALOXs in tumour differentiation and progression (Chen *et al*, 1994; Jiang *et al*, 2006; Nithipatikom *et al*, 2006) and increased levels of ALOX12 were observed in breast cancer (Jiang *et al*, 2006). We identified that LEC migration was the crucial step for CCID (Kerjaschki *et al*, 2011) and, therefore, LECs were treated with the pro-migratory factor 12(S)-HETE to analyse protein expression that causes or correlates with a mobile cell phenotype. Since 12(S)-HETE is a labile compound that is rapidly metabolised/degraded, the effects observed on protein expression were immediate (0.2–0.5 h) and transient. This was in contrast to the effects on LECs underneath spheroids, which were long lasting (4 h) due to the permanent supply of 12(S)-HETE by MCF-7 cells as *de novo* generated molecules.

Here, we demonstrated that MYPT1 and MLC2 became phosphorylated at the rim of MCF-7 spheroid-induced CCID in LECs. MYPT1 is the regulatory/targeting subunit of the myosin phosphatase, which regulates the interaction of actin and myosin in response to signalling through the GTPase Rho (Feng *et al*, 1999). Phosphorylation leads to the inhibition of MYPT1, cytoskeletal reorganisation and is associated with motility (Birukova *et al*, 2004a, b). In addition, the phosphorylation of MLC2 at Thr18 and Ser19 (Ikebe and Hartshorne, 1985), which is correlated with myosin ATPase activity and contraction of myosine microfilament bundles (Tan *et al*, 1992), became induced in LECs upon 12(S)-HETE treatment, and also ROCK-1 became slightly up-regulated. ROCK is known to phosphorylate MLC2 at

 © 2011 Cancer Research UK

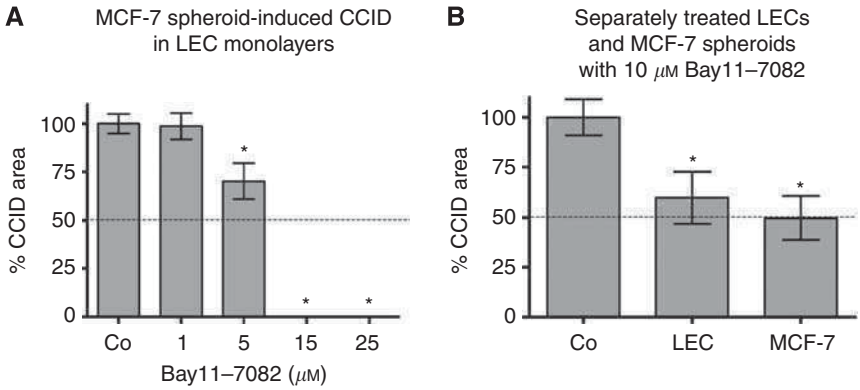

Figure 5 Quantitative analysis of formation and inhibition of CCID in LEC monolayers by MCF-7 spheroids formation. LECs were seeded into 24-well plates and allowed to grow for 2 days until confluence when LECs were stained with cytotracker green. (**A**) MCF-7spheroids, which were treated with different concentrations (solvent, 1, 5, 10, 15, and 25 μM) of Bay11-7082 for 0.5 h at 37°C, were transferred on top of LECs. (**B**) Either LECs or MCF-7 spheroids were treated with the Bay11-7082 for 0.5 h, which was entirely washed off before both cell types were co-cultivated. The 3D-MCF-7 spheroids/LEC monolayer co-cultures were incubated for 4 h at 37°C. The size of CCIDs, which were formed by MCF-7 spheroids in the LEC monolayer in this time period, was measured using a Zeiss Axiovert microscope and Axiovision software. In the solvent treated controls, the CCID sizes in LEC monolayers were set 100%. For each condition, the gap area of at least 12 spheroids was measured. Error bars indicate standard error of the mean. Asterisks show significant differences in the inhibition of CCID formation compared with control (*$P<0.05$).

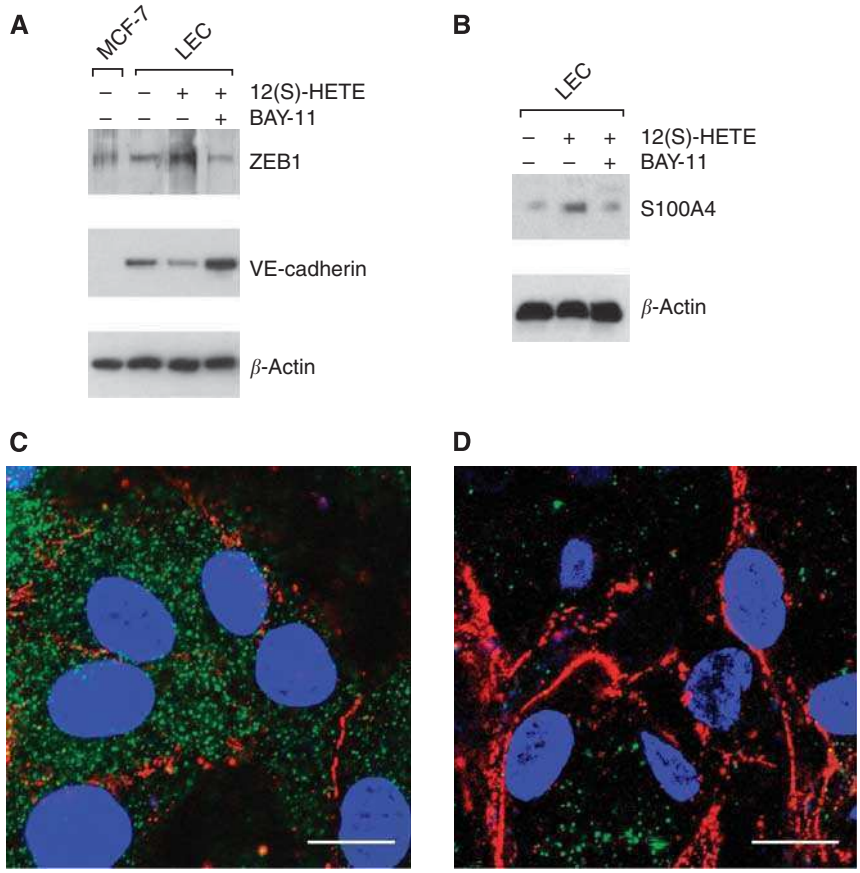

Figure 6 Analysis of mesenchymal marker expression in LECs after intervention with NF-κB signalling. LECs were pretreated with 10 μM of the I-κBα phosphorylation inhibitor Bay11-7082 for 0.5 h and then stimulated with 1 μM 12(S)-HETE for 0.2 h. Cells were harvested and analysed by western blotting using (**A**) anti-ZEB1 and anti-VE-cadherin antibodies. MCF-7 cells were used as negative control. (**B**) Blots were analysed with anti-S100A4 antibody. Equal sample loading was controlled by Ponceau S staining and β-actin analysis. Confocal immunofluorescence images of LECs at the rim of CCID (**C**) induced by an MCF-7 spheroid; (**D**) and from a similar position after treatment with 10 μM Bay11-7082. LECs were grown on coverslips until confluence when MCF-7 spheroids were transferred on top of LECs and co-incubated for 4 h at 37°C to allow CCID formation. LECs were stained with anti-S400A4 antibody (green), anti-VE-cadherin antibody (red), and DAPI (blue). (**C**) S100A4 is well expressed and VE-cadherin interactions are disrupted. (**D**) Upon Bay11-7082 treatment, VE-cadherin structures again appear well developed (although unconnected to VE-cadherin structures of neighbouring cells), whereas S100A4 expression is decreased. Scale bar: 15 μM.

© 2011 Cancer Research UK

Ser19 regulating the assembly of stress fibres (Totsukawa *et al*, 2000) and causes focal adhesions generating an amoeboid movement (Sahai and Marshall, 2003). Moreover, Arp2/3, which levels were also marginally elevated by 12(S)-HETE, regulates mesenchymal invasion (Paulitschke *et al*, 2010).

The mobile state of induced LECs was furthermore confirmed by the increased expression of paxillin and protein S100A4. Paxillin (focal adhesion phosphoprotein) is necessary for cell–ECM contact, and its increased expression could already be associated *in vivo* and *in vitro* with enhanced endothelial cell motility (Lu *et al*, 2006; Deakin and Turner, 2008). S100A4 is a calcium-binding protein that interacts with intracellular target proteins (Mandinova *et al*, 1998) and is a marker for a mesenchymal phenotype and mesenchymal transition of epithelial cells, which encompasses cell mobility (Zeisberg and Neilson, 2009). In epithelial tumours, activation of the embryonic epithelial–mesenchymal transition programme is important for the dissemination and invasion of cancer cells (Yilmaz *et al*, 2007). S100A4 has been associated with migratory and invasive properties and is able to induce metastasis in rodent models of breast cancer (Rudland *et al*, 2000). Noteworthy, the levels of S100A4 mRNA are higher in breast carcinomas than in benign breast tumour specimens (Wang *et al*, 2000). S100A4 acts as an angiogenic factor by stimulating the motility and invasiveness of endothelial cells (Takenaga *et al*, 1994; Ambartsumian *et al*, 2001; Jenkinson *et al*, 2004; Schmidt-Hansen *et al*, 2004). Therefore, S100A4 has a role in both – cancer cells and endothelial cells – to increase malignancy.

Single cell motility can only be realised when cell–cell contacts of the continuous monolayer are disrupted and this was in fact accomplished through both MCF-7 spheroid- and 12(S)-HETE-mediated down-regulation of VE-cadherin. This was consistent with the fact that loss of VE-cadherin is associated with a mobile phenotype. VE-cadherin is expressed specifically in endothelial cells and is important for the maintenance and control of endothelial cell contacts. Hence, VE-cadherin is a marker for a differentiated endothelium and an immobile cellular phenotype. Cadherins (E-, P-, N-, M-, and VE-cadherin) are cell adhesion molecules, which organise contacts via Ca^{2+}-dependent interactions and bind directly to β-catenin, which is required for cohesive function (Vestweber, 2008). Loss of E-cadherin is a key initiating event in EMT (Thiery, 2002). It enables the first step of metastasis – local invasion and dissemination of cancer cells from the primary tumour. ZEB1 is a transcriptional repressor of E-cadherin (Schmalhofer *et al*, 2009) and, therefore, high ZEB1 expression correlates with loss of E-cadherin and an increased migratory and invasive potential and induces EMT (Arumugam *et al*, 2009). Here, we could demonstrate that ZEB1 also regulated 12(S)-HETE-mediated VE-cadherin repression. However, the relation of ZEB1 with VE-cadherin regulation remained unclear. Our results propose that 12(S)-HETE induces an EMT-like phenotype of LECs. This interpretation is problematic, because LECs are of mesenchymal origin yet with an epitheloid phenotype and function.

NF-κB activation was reported to be associated with tumour cell proliferation, survival, angiogenesis, and invasion (Brown *et al*, 2008). Irreversible inhibition of I-κBα with Bay11-7082 (Pierce *et al*, 1997) inhibited MCF-7 spheroid-induced CCID formation of LECs in a dose-dependent manner and at low concentration. Since Bay11-7082 caused a decrease of ZEB1 expression and induction of VE-cadherin expression, NF-κB activation is associated with induction of ZEB1 expression (Chua *et al*, 2007). The mode of 12(S)-HETE-induced activation of NF-κB in LECs remains to be established, as we did not observe an increase in E-selectin mRNA levels upon 12(S)-HETE treatment (data not shown). Interestingly, the extracellular addition of S100A4 activates NF-κB through induction of phosphorylation and subsequent degradation of I-κBα (Boye *et al*, 2008). We found that 12(S)-HETE-induced S100A4 and Bay11-7082 inhibited S100A4 expression. However, since S100A4 up-regulation occurred after NF-κB-dependent ZEB1 induction, an autocrine activation loop can be excluded. Our study provides biochemical data suggesting that 12(S)-HETE induced a migratory phenotype in LECs (Paulitschke *et al*, 2010) that was already microscopically observed during the formation of large CCIDs in the LEC monolayer underneath MCF-7 spheroids (Madlener *et al*, 2010; Kerjaschki *et al*, 2011). The mechanisms of breast cancer cell intravasation require NF-κB activity that is necessary for LEC motility and the here discovered alterations of LEC structural dynamics allow insights into metastatic mechanisms and the search for anti-metastatic compounds.

ACKNOWLEDGEMENTS

We thank Toni Jäger for preparing the figures. This work was supported by the Hochschuljubiläumsstiftung der Stadt Wien (GK), the Fellinger Krebsforschungsverein (GK), the Austrian Science Fund, FWF, Grant numbers P19598-B13 and P20905-B13 (WM), the European Union, FP7 Health Research, project number HEALTH-F4-2008-202047 (WM), and by grants of the Herzfelder Family Foundation AP00420OFF (HD) and AP00392OFF (MG).

Molecular Diagnostics

REFERENCES

Ambartsumian N, Klingelhofer J, Grigorian M, Christensen C, Kriajevska M, Tulchinsky E, Georgiev G, Berezin V, Bock E, Rygaard J, Cao R, Cao Y, Lukanidin E (2001) The metastasis-associated Mts1(S100A4) protein could act as an angiogenic factor. *Oncogene* **20:** 4685–4695

Arumugam T, Ramachandran V, Fournier KF, Wang H, Marquis L, Abbruzzese JL, Gallick GE, Logsdon CD, McConkey DJ, Choi W (2009) Epithelial to mesenchymal transition contributes to drug resistance in pancreatic cancer. *Cancer Res* **69**(5)**:** 5820–5829

Birukova AA, Smurova K, Birukov KG, Kaibuchi K, Garcia JG, Verin AD (2004a) Role of Rho GTPases in thrombin-induced lung vascular endothelial cells barrier dysfunction. *Microvasc Res* **67:** 64–77

Birukova AA, Smurova K, Birukov KG, Usatyuk P, Liu F, Kaibuchi K, Ricks-Cord A, Natarajan V, Alieva I, Garcia JG, Verin AD (2004b) Microtubule disassembly induces cytoskeletal remodeling and lung vascular barrier dysfunction: role of Rho-dependent mechanisms. *J Cell Physiol* **201:** 55–70

Boye K, Grotterod I, Aasheim HC, Hovig E, Maelandsmo GM (2008) Activation of NF-kappaB by extracellular S100A4: analysis of signal transduction mechansims and identification of target genes. *Int J Cancer* **123/6**(p4)**:** 1301–1310

Brown M, Cohen J, Arun P, Chen Z, Van Waes C (2008) NF-B in carcinoma therapy and prevention. *Expert Opin Ther Targets* **12**(9)**:** 1109–1122

Burgering BM, Coffer PJ (1995) Protein kinase B (c-Akt) in phosphatidylinositol-3-OH kinase signal transduction. *Nature* **376:** 599–602

Carlson RW, Allred DC, Anderson BO, Burstein HJ, Carter WB, Edge SB, Erban JK, Farrar WB, Goldstein LJ, Gradishar WJ, Hayes DF, Hudis CA, Jahanzeb M, Kiel K, Ljung BM, Marcom PK, Mayer IA, McCormick B, Nabell LM, Pierce LJ, Reed EC, Smith ML, Somlo G, Theriault RL, Topham NS, Ward JH, Winer EP, Wolff AC (2009) Breast cancer: Clinical Practice Guidelines in Breast Cancer, NCCN Cancer Clinical Practice Panel. *J Natl Compr Canc Netw* **7:** 122–192

Chen YQ, Duniec ZM, Liu B, Hagmann W, Gao X, Shimoji K, Marnett LJ, Johnson CR, Honn KV (1994) Endogenous 12(S)-HETE production by tumor cells and its role in metastasis. *Cancer Res* **54:** 1574–1579

Chua HL, Bhat-Nakshatri P, Clare SE, Moimiya A, Badve S, Nakshatri H (2007) NF-B represses E-cadherin expression and enhances epithelial to mesenchymal transition of mammary epithelial cells: potential involvement of ZEB-1 and ZEB-2. *Oncogene* **26**(p4)**:** 711–724

Deakin NO, Turner CE (2008) Paxillin comes of age. *J Cell Sci* **121:** 2435–2444

 © 2011 Cancer Research UK

Eger A, Aigner K, Sonderegger S, Dampier B, Oehler S, Schreiber M, Berx G, Cano A, Beug H, Foisner R (2005) DeltaEF1 is a transcriptional repressor of E-cadherin and regulates epithelial plasticity in breast cancer cells. *Oncogene* **24**(14): 2375 – 2385

Feng J, Masaaki I, Ichikawa K, Isaka N, Nishikawa M, Hartshorne DJ, Nakano T (1999) Inhibitory phosphorylation Site for Rho-associated kinase on smooth muscle myosin phosphatase. *J Cell Biol* **274:** 37385 – 37390

Flister MJ, Wilber A, Hall KL, Iwata C, Miyazono K, Nisato RE, Pepper MS, Zawieja DC, Ran S (2010) Inflammation induces lymphangiogenesis through up-regulation of VEGFR-3 mediated by NF-kappaB and Prox1. *Blood* **115**(2): 418 – 429

Franke TF, Kaplan DR, Cantley LC (1997) PI3K: downstream AKTion blocks apoptosis. *Cell* **88:** 435 – 437

Geiger TR, Peeper DS (2009) Metastasis mechanisms. *Biochim Biophys Acta* **1796:** 293 – 308

Hirakawa S, Detmar M, Kerjaschki D, Nagamatsu S, Matsuo K, Tanemura A, Kamata N, Higashikawa K, Okazaki H, Kameda K, Nishida-Fukuda H, Mori H, Hanakawa Y, Sayama K, Shirakata Y, Tohyama M, Tokumaru S, Katayama I, Hashimoto K (2009) Nodal lymphangiogenesis and metastasis: role of tumor-induced lymphatic vessel activation in extramammary Paget's disease. *Am J Pathol* **175:** 2235 – 2248

Honn KV, Steinert BW, Moin K, Onoda JM, Taylor JD, Sloane BF (1987) The role of platelet cyclooxygenases and lipoxygenase pathways in tumor cell induced platelet aggregation. *Biochem Biophys Res Commun* **29:** 384 – 389

Honn KV, Tang DG, Grossi I, Duniec ZM, Timar J, Renaud C, Leithauser M, Blair I, Johnson CR, Diglio CA, Kimler VA, Taylor JD, Marnett LJ (1994) Tumour cell-derived 12(S)-hydroxyeicosatetraenoic acid induces microvascular endothelial cell retraction. *Cancer Res* **54:** 565 – 574

Huang C, Rajfur Z, Borchers C, Schaller MD, Jacobson K (2003) JNK phosphorylates paxillin and regulates cell migration. *Nature* **424**(6945): 219 – 223

Ikebe M, Hartshorne DJ (1985) Phosphorylation of smooth muscle myosin at two distinct sites by myosin light chain kinase. *J Biol Chem* **260**(18): 10027 – 10031

Jenkinson SR, Barraclough R, West CR, Rudland PS (2004) S100A4 regulates cell motility and invasion in an *in vitro* model for breast cancer metastasis. *Br J Cancer* **90:** 253 – 262

Jiang WG, Douglas-Jones AG, Mansel RE (2006) Aberrant expression of 5-lipoxygenase-activating protein (5-LOXAP) has prognostic and survival significance in patients with breast cancer. *Prostaglandins Leukot Essent Fatty Acids* **74**(2): 125 – 134

Kerjaschki D, Rudas M, Bartel G, Bago-Horvath Z, Sexl V, Wolbank S, Schneckenleithner C, Dolznig H, Krieger S, Hantusch B, Nagy-Bojarszky K, Huttary N, Raab I, Kalt R, Lackner K, Hämmerle M, Keller T, Viola K, Schreiber M, Nader A, Mikulits W, Gnant M, Krautgasser K, Schachner H, Kaserer K, Rezar S, Madlener S, Vonach C, Davidovits A, Nosaka H, Hirakawa S, Detmar M, Alitalo K, Nijman S, Offner F, Maier TJ, Steinhilber D, Krupitza G (2011) Tumour invasion into intrametastatic lymphatics causes lymph node metastasis. *J Clin Invest* **21**(5): 2000–2012

Kramer RH, Nicolson K (1979) Interactions of tumor cells with vascular endothelial cell monolayers: a model for metastatic invasion. *Proc Natl Acad Sci USA* **76**(11): 5704 – 5708

Madlener S, Saiko P, Vonach C, Viola K, Huttary N, Stark N, Popescu R, Gridling M, Vo NT, Herbacek I, Davidovits A, Giessrigl B, Venkateswarlu S, Geleff S, Jäger W, Grusch M, Kerjaschki D, Mikulits W, Golakoti T, Fritzer-Szekeres M, Szekeres T, Krupitza G (2010) Multifactorial anticancer effects of digalloyl-resveratrol encompass apoptosis, cell-cycle arrest, and inhibition of lymphendothelial gap formation *in vitro*. *Br J Cancer* **102**(9): 1361 – 1370

Lakshmi MS, Parker C, Sherbet GV (1993) Metastasis associated MTS1 and NM23 genes affect tubulin polymerisation in B16 melanomas: a possible mechanism of their regulation of metastatic behaviour of tumours. *Anticancer Res* **13**(2): 299 – 303

Mandinova A, Atar D, Schafer BW, Spies M, Aebi U, Heizmann CW (1998) Distinct subcellular localization of calium binding S100 proteins in human smooth muscle cells and their relocation in response to rises in intracellular calcium. *J Cell Sci* **111:** 2043 – 2054

Nithipatikom K, Isbell MA, See WA, Campbell WB (2006) Elevated 12- and 20-hydroxyeicosatetraenoic acid in urine of patients with prostatic diseases. *Cancer Lett* **233**(2): 219 – 225

Paulitschke V, Schicher N, Szekeres T, Jäger W, Elbling L, Riemer AB, Scheiner O, Trimurtulu G, Venkateswarlu S, Mikula M, Swoboda A, Fiebiger E, Gerner C, Pehamberger H, Kunstfeld R (2010) 3,3′,4,4′,5,5′-Hexahydroxystilbene impairs melanoma progression in a metastatic mouse model. *J Invest Derm* **130**(6): 1668 – 1679

Peinado H, Olmeda D, Cano A (2007) Snail, Zeb and bHLH factors in tumour progression: an alliance against the epithelial phenotype? *Nat Rev Cancer* **7**(6): 415 – 428

Pierce JW, Schoenleber R, Jesmok G, Best J, Moore SA, Collins T, Gerritsen ME (1997) Novel inhibitors of cytokine-induced I-Bα phosphorylation and endothelial cell adhesion molecule expression show anti-inflammatory effects *in vivo*. *J Biol Chem* **272**(34): 21096 – 21103

Piperno G, Fuller MT (1985) Monoclonal antibodies specific for an acetylated form of alpha-tubulin recognize the antigen in cilia and flagella from a variety of organisms. *J Cell Biol* **101:** 2085 – 2094

Lu H, Murtagh J, Schwartz EL (2006) The microtubule binding drug laulimalide inhibits vascular endothelial growth factor-induced human endothelial cell migration and is synergistic when combined with docetaxel (taxotere). *Mol Pharmacol* **69**(4): 1207 – 1215

Rudland PS, Platt-Higgins A, Renshaw C, West CR, Winstanley JHR, Robertson L, Barraclough R (2000) Prognostic significance of the metastasis-inducing protein S100A4 (p9Ka) in human breast cancer. *Cancer Res* **60:** 1595 – 1603

Sahai E, Marshall CJ (2003) Differing models of tumour cell invasion have distinct requirements for Rho/ROCK signalling and extracellular proteolysis. *Nat Cell Biol* **5:** 711 – 719

Schmalhofer O, Brabletz S, Brabletz T (2009) E-cadherin, β-catenin, and ZEB1 in malignant progressio of cancer. *Cancer Metastasis Rev* **28**(p5-6): 151 – 166

Schmidt-Hansen B, Ornas D, Grigorian M, Klingelhöfer J, Tulchinsky E, Lukanidin E, Ambartsumian N (2004) Extracellular S100A4(mts1) stimulates invasive growth of mouse endothelial cells and modulates MMP-13 matrix metalloproteinase activity. *Oncogene* **23:** 5487 – 5495

Takenaga K, Nakamura Y, Endo H, Sakiyama S (1994) Involvement of S100-related calcium-binding protein pEL98 (or mts1) in cell motility and tumor cell invasion. *Jpn J Cancer Res* **85:** 831 – 839

Tan JL, Ravid S, Spudich JA (1992) Control of nonmuscle myosins by phosphorylation. *Annu Rev Biochem* **61:** 721 – 759

Thiery JP (2002) Epithelial-mesenchymal transitions in tumour progression. *Nat Rev Cancer* **2:** 442 – 454

Timar J, Chen YQ, Liu B, Bazaz R, Taylor JD, Honn KV (1992) The lipoxyenase metabolite 12(S)-HETE promotes αIIbβ3 integrin mediated tumor cell spreading on fibronectin. *Int J Cancer* **52:** 594 – 603

To C, Shilton BH, Di Guglielmo GM (2010) Synthetic triterpenoids target the Arp2/3 complex and inhibit branched actin polymerization. *J Biol Chem* **285**(36): 27944 – 27957

Totsukawa G, Yamakita Y, Yamashiro S, Hartshorne DJ, Sasaki Y, Matsumura F (2000) Distinct roles of ROCK (Rho-kinase) and MLCK in spatial regulation of MLC phosphorylation for assembly of stress fibers and focal adhesions in 3T3 fibroblasts. *J Cell Biol* **150:** 797 – 806

Vestweber D (2008) VE-cadherin: the major endothelial adhesion molecule controlling cellular junctions and blood vessel formation. *Arterioscler Thromb Vasc Biol* **28**(p1-2): 223 – 232

Uchide K, Sakon M, Ariyoshi H, Nakamori S, Tokunaga M, Monden M (2007) Cancer cells cause vascular endothelial cell retraction via 12(S)-HETE secretion; the possible role of cancer cell derived microparticle. *Ann Surg Oncol* **14:** 862 – 868

Wang G, Rudland PS, White MR, Barraclough R (2000) Interaction *in vivo* and *in vitro* of the metastasis-inducing S100 protein, S100A4 (p9Ka) with S100A1. *J Biol Chem* **275**(15): 11141 – 11146

Webb DJ, Donais K, Whitmore LA, Thomas SM, Turner CE, Parsons JT, Horwitz AF (2004) FAK-Src signalling through paxillin, ERK and MLCK regulates adhesion disassembly. *Nat Cell Biol* **6**(2): 154 – 161

Xu Y, Li J, Ferguson GD, Mercurio F, Khambatta G, Morrison L, Lopez-Girona A, Corral LG, Webb DR, Bennett BL, Xie W (2009) Immunomodulatory drugs reorganize cytoskeleton by modulating Rho GTPases. *Blood* **114**(2): 338 – 345

Yilmaz M, Christofori G, Lehembre F (2007) Distinct mechanisms of tumor invasion and metastasis. *Trends Mol Med* **13:** 535 – 541

Zeisberg M, Neilson EG (2009) Biomarkers for epithelial-mesenchymal transitions. *J Clin Invest* **119**(6): 1429 – 1437

© 2011 Cancer Research UK

Separation of anti-neoplastic activities by fractionation of a Pluchea odorata extract.

Bauer S., Singhuber J., Seelinger M., Unger C., Viola K., Vonach C., **Giessrigl B.**, Madlener S., Stark N., Wallnofer B., Wagner K.H., Fritzer-Szekeres M., Szekeres T., Diaz R., Tut F., Frisch R., Feistel B., Kopp B., Krupitza G. and Popescu R.

Front Biosci. (Elite Ed) 1: 1326-36, **2011.**

Separation of anti-neoplastic activities by fractionation of a *Pluchea odorata* extract

Sabine Bauer[1], Judith Singhuber[2], Mareike Seelinger[1], Christine Unger[1], Katharina Viola[1], Caroline Vonach[1], Benedikt Giessrigl[1], Sibylle Madlener[1], Nicole Stark[1], Bruno Wallnofer[3], Karl-Heinz Wagner[4], Monika Fritzer-Szekeres[5], Thomas Szekeres[5], Rene Diaz[6], Foster Tut[6], Richard Frisch[6], Bjorn Feistel[7], Brigitte Kopp[2], Georg Krupitza[1], Ruxandra Popescu[2]

[1]Institute of Clinical Pathology, Medical University of Vienna, Waehringer Guertel 18-20, Austria, [2]Department of Pharmacognosy, Faculty of Life Sciences, University of Vienna, Althanstrasse 14, Austria, [3]Department of Botany, Museum of Natural History, Burgring 7, A-1010 Vienna, Austria, [4]Department of Nutritional Sciences, University of Vienna, Althanstrasse 14, Austria, [5]Clinical Institute of Medical and Chemical Laboratory Diagnostics, Medical University of Vienna, Waehringer Guertel 18-20, Austria, [6]Institute for Ethnobiology, Playa Diana, San Jose/Peten, Guatemala, [7]Finzelberg GmbH & Co. KG, Koblenzer Strasse 48-54, D-56626 Andernach, Germany

TABLE OF CONTENTS

1. Abstract
2. Introduction
3. Materials and Methods
- *3.1. Plant material*
- *3.2. Extraction and fractionation*
- *3.3. Cell culture*
- *3.4. Proliferation inhibition analysis*
- *3.5. Cell death analysis*
- *3.6. Western blot analysis*
- *3.7. Statistical analysis*

4. Results and Discussion
- *4.1. Anti-proliferative activity of Pluchea odorata CH2Cl2 crude extract and F1 (VLC) fractions*
- *4.2. Anti-proliferative activity of F2 (CC-I) fractions derived from F1/3*
- *4.3. Anti-proliferative activity of F3 (CC-II) fractions derived from F2/13*
- *4.4. Western blot analysis of cell cycle and checkpoint regulators*
- *4.5. Fractions F2/11, F2/13 and F3/4 induce apoptosis*
- *4.6. Western blot analysis of apoptosis related proteins*

5. Acknowledgements
6. References

1. ABSTRACT

Natural products continue to represent the main source for therapeutics, and ethnopharmacological remedies from high biodiversity regions are a rich source for the development of novel drugs. Hence, in our attempt to find new anti-neoplastic activities we focused on ethno-medicinal plants of the Maya, who live in the world's third richest area in vascular plant species. *Pluchea odorata* (Asteraceae) is traditionally used for the treatment of various inflammatory disorders and recently, the *in vitro* anti-cancer activities of different extracts of this plant were described. Here, we present the results of bioassay-guided fractionations of the dichloromethane extract of *P. odorata* that aimed to enrich the active principles. The separation resulted in fractions which showed the dissociation of two distinct anti-neoplastic mechanisms; firstly, a genotoxic effect that was accompanied by tubulin polymerization, cell cycle arrest, and apoptosis (fraction F2/11), and secondly, an effect that interfered with the orchestrated expression of Cyclin D1, Cdc25A, and Cdc2 and that also led to cell cycle arrest and apoptosis (fraction F3/4). Thus, the elimination of generally toxic properties and beyond that the development of active principles of *P. odorata*, which disturb cancer cell cycle progression, are of interest for potential future therapeutic concepts against proliferative diseases.

2. INTRODUCTION

The majority of medicinal drugs used in western medicine are derived from natural products (1, 2). A success story in natural product drug discovery is paclitaxel (Taxol), which is derived from the bark of the Pacific Yew, *Taxus brevifolia* Nutt. (Taxaceae). The antitumor activity of Taxol is based on its ability to stabilize microtubules in tumor cells, triggering mitotic arrest and cell death (3-5). Several Native American tribes have used *Taxus* species for the treatment of non-cancerous diseases (6). Ethno-pharmacological remedies, particularly from high biodiversity regions such as rainforests, can be a rich source for the development of novel drugs (7) and therefore, we investigate traditional healing plants of the Maya who live in a region which is the world's third richest in vascular plant species (8). Over the centuries and millennia, the Maya developed an advanced pharmaceutical knowledge that is still practiced today. In the attempt to find plants with anti-neoplastic activities we select those traditionally used against severe inflammations, because there are several similar signaling pathways, which are commonly up-regulated in both, in inflammatory conditions and in cancer (9). Maya healers prepare decoctions of the Asteraceae *Pluchea odorata* (L.) Cass. (Itza-Maya vernacular name: "Chal Che"), to treat coughs, cold, neuritis, and arthritis and also swelling, bruises,

Table 1. Fractionation of the *Pluchea odorata* CH_2Cl_2 crude extract by VLC

F1-Fractions	Mobile phase (1000 ml)	Yield (g)
F1/1	PE	0.21
F1/2	$CHCl_3$	1.36
F1/3	$CHCl_3$: MeOH (9:1)	**1.46**
F1/4	$CHCl_3$: MeOH (7:3)	0.45
F1/5	$CHCl_3$: MeOH (5:5)	0.09
F1/6	$CHCl_3$: MeOH (3:7)	0.14
F1/7	$CHCl_3$: MeOH (1:9)	0.09
F1/8	MeOH : H_2O (7:3)	0.08
F1/9	MeOH : H_2O (1:1)	0.05
F1/10	H_2O	0.02

Fractionation of the *Pluchea odorata* CH_2Cl_2 crude extract by VLC. The CH_2Cl_2 extract was chromatographed on a silica gel column using the indicated solvents as mobile phase, which resulted in 10 fractions (F1/1 – F1/10).

Table 2. Fractionation of the *Pluchea odorata* F1/3 extract by column chromatography (CC-I)

F2-Fractions	Mobile phase	Yield (mg)	Yield w/o chlorophyll	
			(mg)	(%)
F2/1	$CHCl_3$ (500 ml)	32.5		
F2/2		30.5		
F2/3		12.2		
F2/4		54.2		
F2/5		17.8		
F2/6	$CHCl_3$:MeOH:H_2O (95:1.5:0.1) (600 ml)	26.4		
F2/7		67.2		
F2/8		24.8		
F2/9		48.5		
F2/10		32.9		
F2/11		113.2	25.7	22.7
F2/12	$CHCl_3$:MeOH:H_2O (90:3.5:0.2) (562 ml)	90.7	16.3	17.9
F2/13		170.6	**41.2**	24.2
F2/14		88.6	27.9	31.5
F2/15		26.3	2.4	9.1
F2/16		148.5	21.6	14.5
F2/17		44.1		
F2/18	$CHCl_3$:MeOH:H_2O (85:8.0:0.5) (2000 ml)	64.9		
F2/19		184.6		
F2/20		268.0		
F2/21	MeOH:H_2O (95:5.0) (500 ml)	213.0		

Fractionation of the *Pluchea odorata* F1/3 extract by column chromatography (CC-I). The extract was applied on a silica gel column and eluted with the indicated solvents and 21 main fractions (F2/1 – F2/21) were obtained. Chlorophyll was removed from fractions F2/11-16 and the fraction-yield (mg, %) before and after chlorophyll separation was calculated.

inflammations, and tumors (10). Recently, the anti-cancer activity of extracts of this medicinal herb was described (11). Here, we focused on the dichloromethane extract of *P. odorata* and performed bioassay-guided fractionations to separate and enrich different bioactive principles.

3. MATERIALS AND METHODS

3.1. Plant material

Pluchea odorata (L.) Cass. was collected in Guatemala, Departamento Peten, near the north-western shore of Lago Peten Itza, San Jose, within an area of four year old secondary vegetation ~1 km north of the road from San Jose to La Nueva San Jose (16°59'30" N, 89°54'00" W). Voucher specimens (leg. G. Krupitza & R. O. Frisch, Nr. 1-2009, 08. 04. 2009, Herbarium W) were archived at the Museum of Natural History, Vienna, Austria. The fresh plant material (the aerial plant parts, leaves, caulis and florescence) of *P. odorata* was stored deep-frozen until lyophilization and subsequent extraction.

3.2. Extraction and fractionation

Aerial plant parts of *P. odorata* were lyophilised, ground and 192 g were taken for extraction using an accelerated solvent extractor (ASE) (ASE® 200, Dionex, California, USA). The first cycle was performed with PE in order to partly eliminate chlorophyll and lipids. Then, the same plant material was extracted x 3 with CH_2Cl_2. The extraction was performed with a pressure of 150 bar and at 40°C. The CH_2Cl_2 extract was evaporated under reduced pressure to yield 4.0 g dried extract. The crude CH_2Cl_2 extract was subjected to vacuum liquid chromatography (VLC) on a silica gel column, eluting with a stepwise gradient from PE to H_2O (Table 1) to provide ten main fractions (F1/1 – F1/10) which were collected based on similar TLC profiles. Fraction F1/3 (1.46 g) was further chromatographed on a silica gel column (CC-I) using a stepwise gradient from $CHCl_3$ to MeOH : H_2O for elution (Table 2) and led to the collection of 21 main fractions (F2/1 – F2/21). Chlorophyll was separated from fractions F2/11 – F2/16 by redissolving the dried fractions in CH_2Cl_2 (1 g fraction / 150 ml CH_2Cl_2) and adding an equal volume of MeOH : H_2O (1 : 1). Then CH_2Cl_2 was evaporated under reduced pressure to precipitate chlorophyll in the MeOH : H_2O phase. Chlorophyll was removed by filtration and the chlorophyll-free MeOH : H_2O layer was dried under reduced pressure. After the removal of chlorophyll, fraction F2/13 (30 mg) was purified on a silica gel column (CC-II) eluting with $CHCl_3$: MeOH in different ratios (Table 3). Fractions with similar TLC profiles were pooled to give five main fractions (F3/1 – F3/5).

Table 3. Fractionation of the *Pluchea odorata* F2/13 extract by column chromatography (CC-II)

F3-Fractions	Mobile phase	Yield (mg)
F3/1	$CHCl_3$: MeOH (95:0.5) (700 ml)	3.41
F3/2		13.03
F3/3		7.87
F3/4	$CHCl_3$: MeOH (95:0.5) (300 ml)	**3.58**
F3/5	$CHCl_3$: MeOH (90:0.5) (300 ml)	21.32

Fractionation of the *Pluchea odorata* F2/13 extract by column chromatography (CC-II). The extract was chromatographed on a silica gel column using the indicated solvents as mobile phase; the separation resulted in 5 main fractions (F3/1 – F3/5).

3.3. Cell Culture

HL-60 promyelocytic leukaemia cells were purchased from ATCC and grown in RPMI 1640 medium and humidified atmosphere containing 5% CO_2 at 37°C. The medium was supplemented with 10 % heat-inactivated fetal calf serum (FCS), 1 % Glutamax and 1 % Penicillin-Streptomycin. The medium and supplements were obtained from Life Technologies (Carlsbad, CA, USA).

3.4. Proliferation inhibition analysis

HL-60 cells were seeded in T-25 tissue culture flasks or in 24-well plates at a concentration of 1 x 10^5 cells/ml and incubated with increasing concentrations of plant extracts or fractions. Cell counts and IC_{50} values were determined within 24 h using a KX-21 N microcell counter (Sysmex Corporation, Kobe, Japan). All experiments were performed in triplicate. Cell proliferation rates were calculated as described (11-13).

3.5. Cell death analysis

In order to determine the type of cell death, HL-60 cells were seeded in 24-well plates at a concentration of 1 x 10^5 cells/ml and grown for 24 h. Then cells were treated with the indicated concentrations of the extract and fractions for 8 h and 24 h. Hoechst 33258 and propidium iodide were added to the cells at final concentrations of 5 and 2 µg/ml, respectively. After 1 h of incubation at 37°C, cells were examined on a Zeiss Axiovert fluorescence microscope equipped with a DAPI filter. Cells were photographed and analyzed by visual examination to distinguish between apoptosis and necrosis (14-16). For this, cells were judged according to their morphology and the integrity of the plasma membrane on the basis of propidium iodide exclusion. Experiments were performed in triplicate.

3.6. Western blot analysis

HL-60 cells were seeded in T-75 tissue culture flasks at a concentration of 1 x 10^6 cells/ml and incubated with 3 µg/ml fractions (F2/11, F2/13, F3/4, respectively) for 0.5 h, 2 h, 4 h, 8 h and 24 h. At each time point, 2 x 10^6 cells were harvested, placed on ice, centrifuged (1000 rpm, 4 ºC, 4 min), washed twice with cold PBS (pH 7.2), and lysed in 150 µl buffer containing 150 mM NaCl, 50 mM Tris pH 8.0, 1 % Triton X-100, 1mM phenylmethylsulfonylfluorid (PMSF) and Protease Inhibitor Cocktail (Sigma, Schnelldorf, Germany). Debris was removed by centrifugation (12,000 rpm, 4 ºC, 20 min) and equal amounts of total protein were electrophoretically separated by SDS polyacrylamide gels (10 %) and then transferred to PVDF membranes (Hybond P, Amersham, Buckinghamshire, UK) at 100 V and 4ºC for 1 h. To confirm equal sample loading, membranes were stained with Ponceau S (17-19). Customary blotting protocol was employed; primary antibodies were diluted 1:500 in blocking solution and incubated with the membrane at 4 ºC, overnight and the secondary antibodies were diluted 1:2000. Blots were analyzed using an enhanced chemoluminescence technique (ECL detection kit) and detected by exposure of the membranes to Amersham Hyperfilm™ (both Amersham, Buckinghamshire, UK). The antibody against Phospho-Cdc25A (S75) was from Abcam (Cambridge, MA, USA) and against phospho-Cdc25A (S177) from Abgent (San Diego, CA, USA). Anti-gamma-H2AX (pSer139) was purchased from Calbiochem (San Diego, CA, USA) and the antibodies against cleaved caspase-3 (Asp175), Chk2, phospho-Chk2 and phospho-Cdc2 (Tyr15) from Cell Signaling (Danvers, MA, USA). The antibodies against Cdc2 p34 (17), Cdc25A (F-6), Cyclin D1 (M-20), PARP-1 (F-2) and alpha-tubulin (DM1A) were from Santa Cruz Biotechnology Inc. (Santa Cruz, CA, USA) and the antibodies against beta-actin (clone 6-11B-1) and acetylated alpha-tubulin (clone 6-11B-1) were from Sigma (St. Louis, MO, USA). The secondary antibodies peroxidase-conjugated anti-rabbit IgG and anti-mouse IgG were purchased from Dako (Glostrup, Denmark).

3.7. Statistical analysis

The apoptosis and proliferation experiments were analyzed by t-test using GraphPad Prism version 4 (GraphPad Prim Sofware, Inc., San Diego, CA, USA).

4. RESULTS AND DISCUSSION

4.1. Anti-proliferative activity of *Pluchea odorata* CH_2Cl_2 crude extract and F1 (VLC) fractions

The activity of the obtained CH_2Cl_2 crude extract, which was 2.1 % of the dried plant material input (196 g), was tested in HL-60 leukemia cells. Cells were incubated with increasing concentrations of crude extract (1-15 µg/ml) and the number of cells was counted twice within a time span of 24 h in order to calculate the proliferation rates. The CH_2Cl_2 crude extract significantly decreased the proliferation rate of HL-60 cells; the concentration which inhibited cell proliferation by 50 % (IC_{50}) was ~10 µg/ml (Figure 1). Subsequently, the crude extract was fractionated by VLC resulting in fraction F1/1 – F1/10 (Table 1). All fractions were tested at concentrations of 10µg/ml. The results showed that fraction F1/3, which represented 36.5 % of the CH_2Cl_2 extract input (4.0 g), inhibited proliferation by ~ 60 %, whereas the other fractions had no effect on cell growth (data not shown). Therefore, the gain of activity was not significant and VLC was an insufficient procedure to enrich the active principles. Based on these results, subsequent fractionation of F1/3 by CC-I followed.

4.2. Anti-proliferative activity of F2 (CC-I) fractions derived from F1/3

Fraction F1/3 was further subjected to CC-I to provide 21 main fractions (Table 2). The anti-proliferative

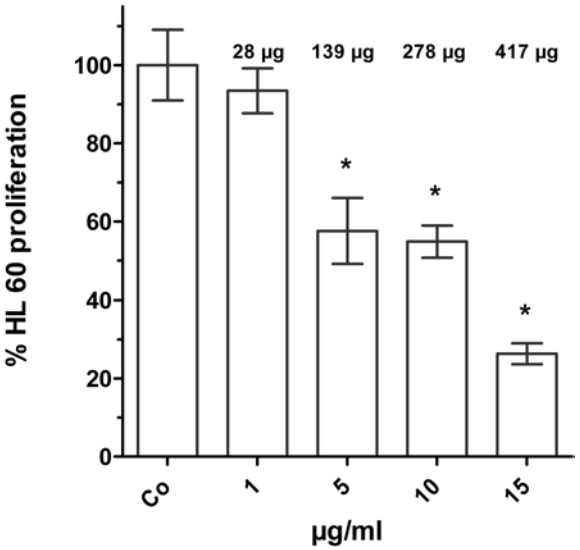

Figure 1. Anti-proliferative effects of *Pluchea odorata* CH_2Cl_2 crude extract. HL60 cells were seeded into T-25 flasks (1 x 10^5 cells/ml), grown for 24 hours, and treated with solvent (0.5 % EtOH) or the specified concentrations of CH_2Cl_2 extract. After 24 hours the proliferation was calculated as percentage of control. Values are mean ± SEM of experiments performed in triplicate. *$p<0.05$ as compared to untreated control.

activity of the fractions (10 µg/ml) was determined in HL-60 cells (Figure 2a). Fractions F2/11 – F2/16 showed effective growth inhibitory activity; fractions F2/11, F2/12, F2/13 and F2/15 inhibited cell growth up to nearly 100 %, F2/16 up to 95 % and F2/14 up to 80 %. Hence, CC-I facilitated the enrichment of the bioactive properties. The TLC profile of the active fractions F2/11 – F2/16 indicated the presence of chlorophyll (data not shown). In order to exclude the possibility that chlorophyll contributed to the anti-proliferative effect, fractions F2/11 – F2/16 were subjected to separation of chlorophyll and then re-evaluated for activity. The results indicated that the anti-proliferative activity was preserved in the chlorophyll-free fractions (Figure 2b). Moreover, the effect of fraction F2/14 was increased after the removal of chlorophyll.

4.3. Anti-proliferative activity of F3 (CC-II) fractions derived from F2/13

Since CC-I fractionation was successful in enriching the anti-proliferative activity, we then selected one of the most active chlorophyll-free fractions for further fractionation. Fraction F2/13 contained the least restrictive amount of material, which was 2.8 % of the F1/3 input (1.46 g). Hence, fraction F2/13 was subjected to a second step CC separation (CC-II). Based on similarities of the TLC profile, five main fractions (F3/1 – F3/5) were obtained (Table 3). In order to determine the anti-proliferative effect, HL-60 cells were treated with the indicated concentrations of fractions (Figure 3). The results suggested fraction F3/4 to be the most potent of the F3 fractions. Fraction F3/4 inhibited proliferation with a calculated IC_{50} of ~0.4 µg/ml; therefore, the increase of the activity compared to the crude extract was ~25-fold.

Additional separations of F3 fractions with reversed phase solid phase extraction resulted in decreased bio-activities (data not shown). Therefore, these fractions seemed to separate different active principles that were additive in F3/4. This evidences that controlled multi-compound preparations of plant extracts, such as F3/4 or i.e. Avemar (20), can be more effective than isolated single compounds. The attempt to identify these active principles would have exceeded the frame of this investigation.

4.4. Western blot analysis of cell cycle and checkpoint regulators

Fractions F2/11, F2/13 and F3/4 showed the highest anti-proliferative activity. Hence, their effect on the expression of cell cycle regulatory proteins was analyzed by Western blotting, because protagonists such as the proto-oncogenes Cyclin D1 and Cdc25A, which are both up-regulated in hyper-proliferative diseases, are goals for new anti-neoplastic therapies (21, 22). The lowest common concentration of fractions F2/11, F2/13 and F3/4, which completely inhibited HL-60 cell proliferation, was 3 µg/ml and therefore, the following analyses were performed with this concentration. Fraction F2/11 suppressed Cyclin D1 expression after 24 h, whereas F2/13 reduced the Cyclin D1 level after 8 h and its derivative fraction F3/4 already after 30 minutes (Figure 4). Temporally the D-family of cyclins appears in early G1 of the cell cycle (23-25) and Cyclin D1 is required for the activation of Cdk4 and Cdk6 (21, 26) and it is also known as the Prad1 proto-oncogene (27).

The intra-S-phase checkpoint prevents the duplication of damaged or broken DNA which would eventually lead to genomic instability. This checkpoint is i.e. regulated by ATM/ATR-Chk2-Chk1-Cdc25A (28). Depending on the type of DNA damage (genotoxic stress), ATM or ATR phosphorylates Chk2 or Chk1, which in turn phosphorylates Cdc25A (29, 30). Thereby, Cdc25A becomes inactivated and causes the inhibition of Cdk2 and Cdc2 (31). Here we demonstrate that Chk2 was phosphorylated at the activating Thr68 site upon treatment with all three tested fractions. F2/11 caused a rapid and transient phosphorylation of Chk2 within 2 h, which returned to constitutive levels after 24 h. In contrast, fraction F2/13 induced phosphorylation of Chk2 after 24 h and fraction F3/4 after 8 h which sustained for 24 h. Therefore, activation of Chk2 by F3/4 was not transient and was caused by a different trigger than by F2/11. Chk2 protein levels remained unchanged upon incubation with F2/13 and F3/4, but the level decreased upon incubation with F2/11 after 24 h (Figure 4). The analysis of Chk2 phosphorylation- and protein levels supported the notion that different active principles are contained in F2/11 compared to F2/13 and its derivative F3/4. The activation of Chk2 by F2/11 was the earliest effect observed in this protein expression study, whereas it was the latest event upon treatment with F2/13 and F3/4. The rapid Chk2 induction indicated that F2/11 caused DNA damage, which was supported by the fact that the phosphorylation of H2AX (gamma-H2AX) was induced even before Chk2-activation (Figure 6) and that the subsequent alterations of gene expression and cellular responses were most likely the consequences of this property. The induction of gamma-

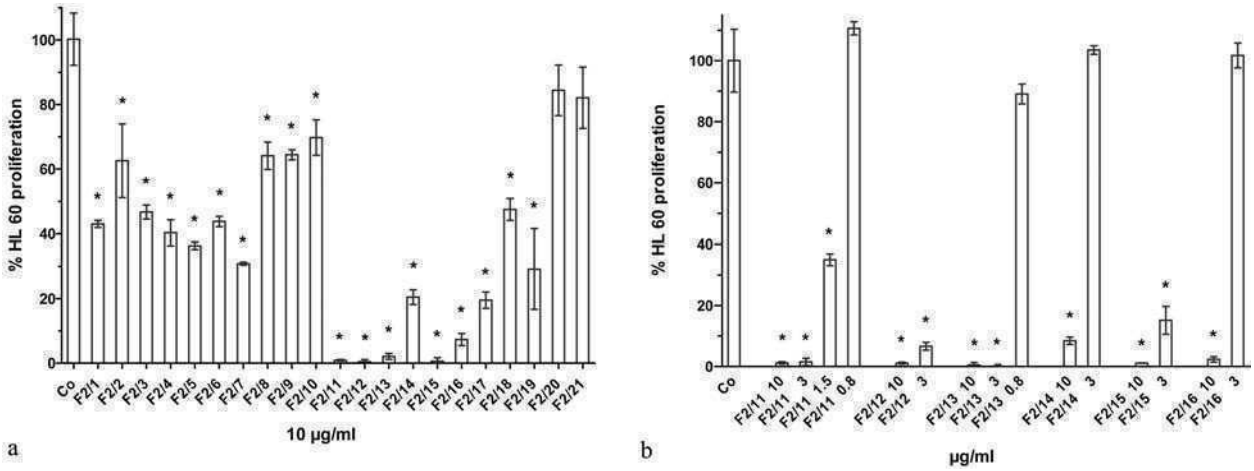

Figure 2. Anti-proliferative effects of *Pluchea odorata* fractions F2/1 – F2/21. HL60 cells were seeded into 24-well plates (1 x 10^5 cells/ml) and grown for 24 hours, and incubated with solvent (0.5 % DMSO) or (a) 10 µg/ml fraction F2/1 – F2/21 and (b) the specified concentrations of chlorophyll-free fraction F2/11 – F2/16. After 24 hours the proliferation was calculated as percentage of control. Values are mean ± SEM of experiments performed in triplicate. *p<0.05 as compared to untreated control.

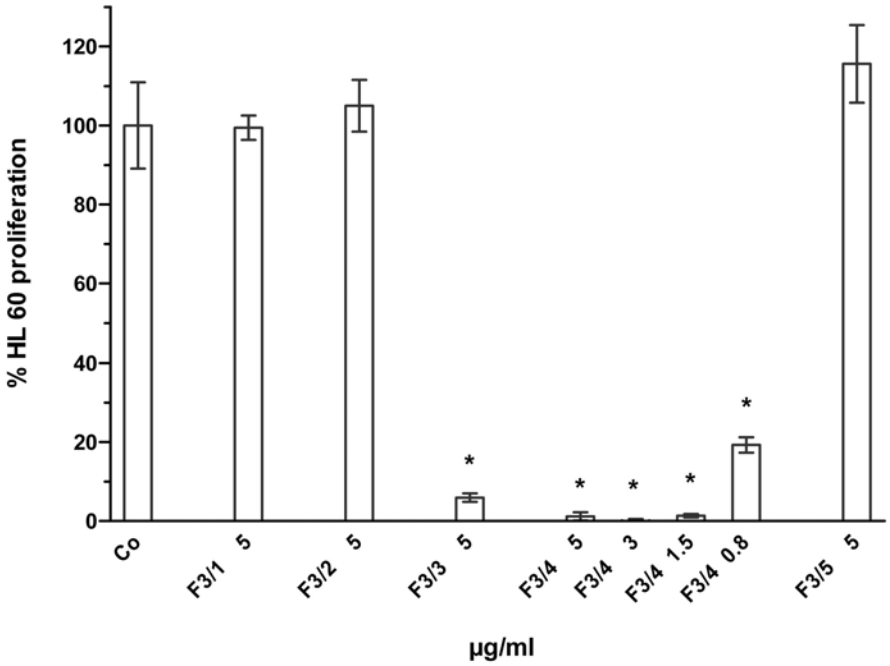

Figure 3. Anti-proliferative effects of *Pluchea odorata* fractions F3/1 – F3/5. Cells were seeded into 24-well plates (1 x 10^5 cells/ml), grown for 24 hours, and incubated with solvent (0.5 % DMSO) or with the specified concentrations of fractions F3/1 – F3/5 for 24 hours. Cell proliferation was calculated as percentage of control. Values are mean ± SEM of experiments performed in triplicate. *p<0.05 as compared to untreated control.

H2AX is among the earliest indicators of DNA strand breaks (32). In contrast, the activation of Chk2 by F3/4 and F2/13 (Figure 4) correlated with the comparatively late activation of caspase 3, respectively (Figure 6) that causes the degradation of DNA as one of several downstream effects. Cdc25A is a direct target of Chk2 and Chk1 and activation of Chk2 can cause the phosphorylation of Ser177 of Cdc25A, Chk1 the phosphorylation of Ser75 of Cdc25A, and both phosphorylations inactivate Cdc25A (33, 34). F2/11 caused an intense phosphorylation of (Ser177)Cdc25A within 4 h and shortly after the activation of Chk2 (Figure 4). Also (Ser75)Cdc25A became phosphorylated, but this was not due to Chk1 because this kinase did not become activated (data not shown). As a consequence, the phosphorylation level of (Tyr15)Cdc2 increased, because inactivated Cdc25A phosphatase did not resume to constitutively de-phosphorylate this Cdc2 site (35). Thus, the kinase activity

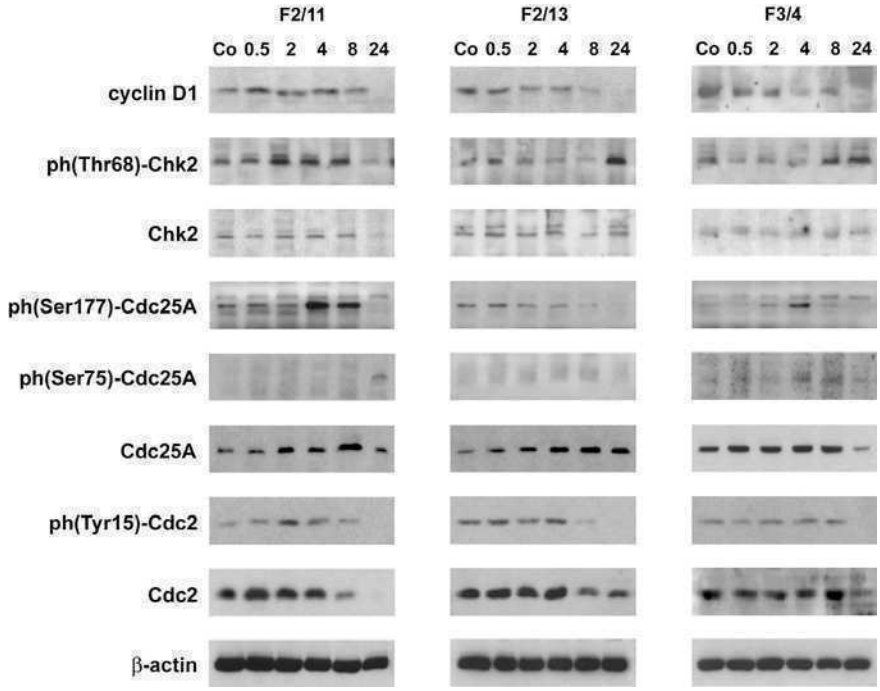

Figure 4. Influence of fraction F2/11, F2/13 and F3/4 on cell cycle and checkpoint regulators**.** Cells were cultivated in T-75 tissue culture flasks (1 x 10^5 cells/ml), grown for 24 hours, and incubated with 3µg/ml fraction F2/11, F2/13 and F3/4 for the specified periods of time. Then, isolated protein samples were subjected to 10 % SDS-PAGE separation and subsequent Western blot analysis using the indicated antibodies. Equal sample loading was controlled by Poinceau S staining and β-actin analysis.

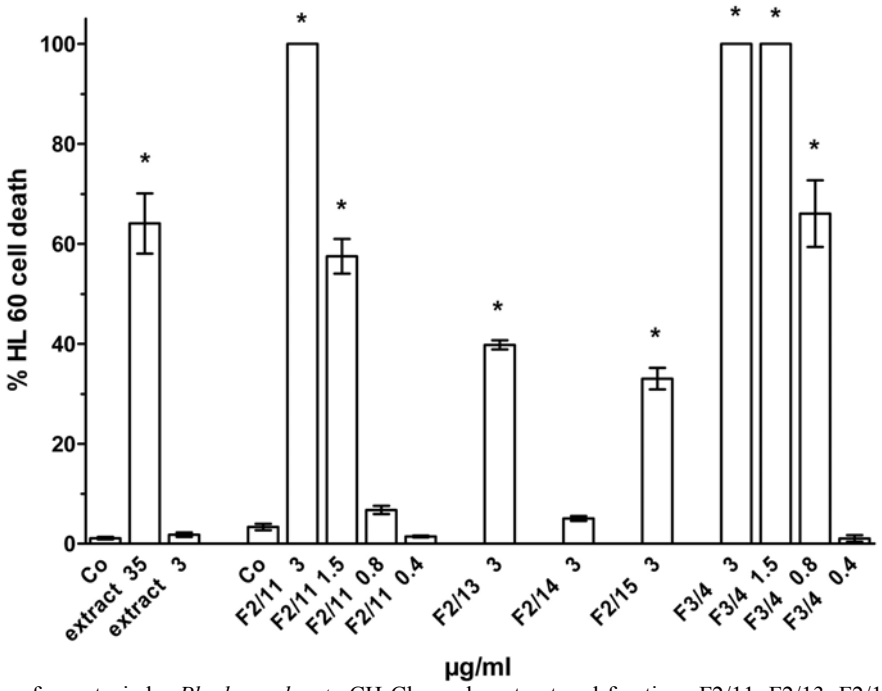

Figure 5. Induction of apoptosis by *Pluchea odorata* CH_2Cl_2 crude extract and fractions F2/11, F2/13, F2/14, F2/15 and F3/4. HL60 cells were seeded into 24-well plates (1 x 10^5 cells/ml) for 24 hours and treated with solvent (0.5% EtOH or DMSO) or the indicated concentrations of CH_2Cl_2 crude extract and fractions F2/11, F2/13, F2/14, F2/15 and F3/4. After 24 hours cells were double stained with Hoechst 33258 and propidium iodide and examined under the microscope with UV light connected to a DAPI filter. Cells with morphological changes indicative for apoptosis were counted and the percentage of cell death was calculated. Values are mean ± SEM of experiments performed in triplicate. *$p<0.05$ as compared to untreated control.

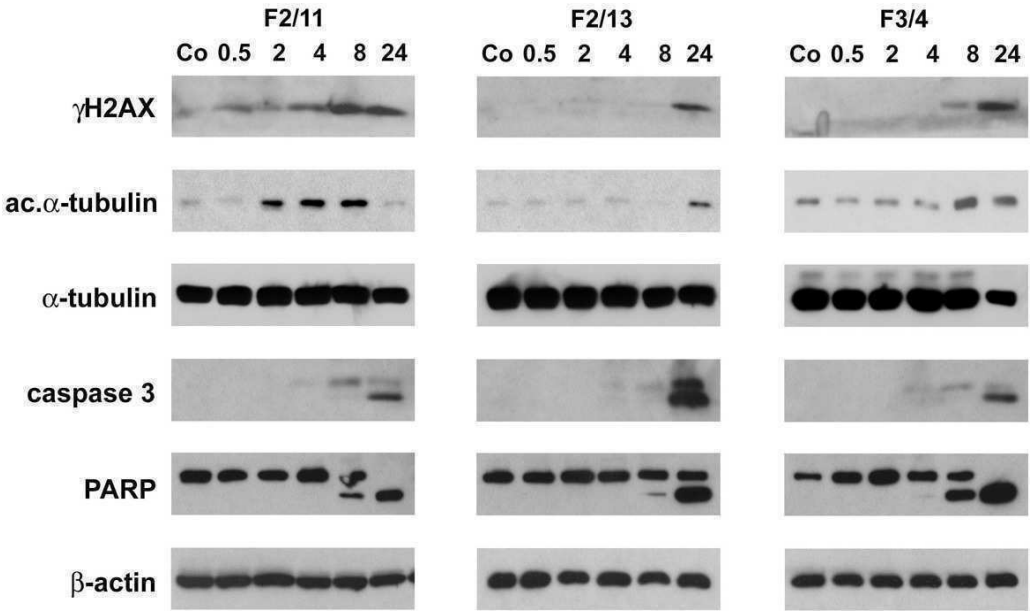

Figure 6. Effect of fraction F2/11, F2/13 and F3/4 on apoptosis-related proteins. Cells were cultivated in T-75 tissue culture flasks (1 x 10^5 cells/ml), grown for 24 hours, and incubated with 3µg/ml fraction F2/11, F2/13 and F3/4 for the specified periods of time. Then, isolated protein samples were subjected to 10 % SDS-PAGE separation and subsequent Western blot analysis using the indicated antibodies. Equal sample loading was controlled by Poinceau S staining and β-actin analysis.

of Wee1 prevailed, which gave rise to a transient accumulation of (Tyr15)Cdc2 phosphorylation upon treatment with F2/11 (36).

In contrast, F2/13 caused the de-phosphorylation of (Ser177)Cdc25A and hence, its activation (37). This was reflected by the de-phosphorylation of (Tyr15)Cdc2 after 8 h. Cdc2 is mandatory for orchestrated G2-M transit. Cdc25A and Cdc25C de-phosphorylate Cdc2, which causes the activation of its kinase domain (30). Cdc2 protein levels were much more stable in cells treated with F2/13 than in those treated with F2/11. In fact, Cdc2 was undetectable upon treatment with F2/11 after 24 h, such as Cyclin D1, and this was most likely causal for cessation of cell proliferation.

F3/4 caused a very transient phosphorylation of (Ser177)Cdc25A and a weak but more sustained phosphorylation of (Ser75)Cdc25A, which correlated with the degradation of this protein after 24 h, and with a slight increase of (Tyr15)Cdc2 phosphorylation levels (Figure 4). We investigated, whether the stress response protein p38/MAPK may have caused phosphorylation of (Ser75)Cdc25A (38). However, constitutive p38 phosphorylation levels were even reduced upon treatment with F3/4 (data not shown). After 24 h the lack of detectable (Tyr15)Cdc2 phosphorylation suggested that this cell cycle protagonist was fully activated. Therefore, suppression of Cyclin D1 together with the activation of Cdc2, as it was observed upon treatment with F3/4 and F 2/13, caused conflicting signals regarding an orchestrated cell cycle progression.

4.5. Fractions F2/11, F2/13 and F3/4 induce apoptosis

Since fractions F2/11, F2/13, and its derivative F3/4 were the most potent inhibitors of proliferation, they were also studied regarding their pro-apoptotic activities. We analyzed apoptosis with a highly sensitive method that identifies very early hallmark phenotypes long before the metabolism collapses and cells actually die (14-16).

HL-60 cells were incubated with the indicated concentrations of the respective fractions (F2/11, F2/13, F2/14, F2/15, F3/4), and with 35 µg/ml of *P. odorata* CH_2Cl_2 crude extract for 24 h, to investigate cell death induction. For the CH_2Cl_2 crude extract ,the calculated concentration which induced 50 % apoptosis (A_{IC50}) was ~25µM (Figure 5). Fraction F2/11 and F3/4 were the most potent fractions, inducing 100 % apoptosis. Interestingly, F2/13, which was the precursor of F3/4, induced only 40 % apoptosis, similar to F2/15, and F2/14 was ineffective at the tested concentration. To unravel which of the two fractions was more potent, further dilutions to 1.5 µg/ml, 0.8 µg/ml, and 0.4 µg/ml enabled to calculate the A_{IC50} after 24 h, which was ~1.4 µg/ml for fraction F2/11 and ~0.6 µg/ml for fraction F3/4. In addition, fraction F2/11 und F3/4 were analyzed after 8 h of treatment and the results indicated F3/4 to be twice as active as F2/11 (Table 4). Therefore, in fraction F3/4 the pro-apoptotic activity was 45-fold enriched compared to the crude CH_2Cl_2 extract (Figure 5).

Since in F3/4 the anti-proliferative and pro-apoptotic activities accumulated, we tested, whether an anti-migratory/metastatic property was contained as well and assessed F3/4 in a novel anti-metastasis assay based on the formation of gaps in lymphendothelial cell monolayers generated by MCF-7 breast cancer cell spheroids (39). However, F3/4 did not prevent the formation of gaps (data not shown).

Table 4. Induction of apoptosis by *Pluchea odorata* fractions F2/11, F2/13 and F3/4.

Fractions3 µg/ml	Apoptosis 8h treatment
F2/11	~20 %
F2/13	~5 %
F3/4	~40 %

Induction of apoptosis by *Pluchea odorata* fractions F2/11, F2/13 and F3/4. HL60 cells were seeded into 24-well plates (1 x 10^5 cells/ml) for 24 hours and treated with solvent (0.5% DMSO) or 3 µg/ml fractions F2/11, F2/13 and F3/4. After 8 hours cells were double stained with Hoechst 33258 and propidium iodide and examined under the microscope with UV light connected to a DAPI filter. Cells with morphological changes indicative for apoptosis were counted and the percentage of cell death was calculated. Values are mean ± SEM of experiments performed in triplicate. *$p<0.05$ as compared to untreated control.

4.6. Western blot analysis of apoptosis related proteins

When HL-60 cells were treated with 3 µg/ml of the indicated fractions, the cleavage of caspase 3 to a 19 kDa and a 12 kDa fragment was observed, which is a prerequisite for its activation that was confirmed by signature type cleavage of the downstream target PARP (40). F2/11 caused the induction of gamma-H2AX within 30 minutes (Figure 6) followed by the rapid activation of Chk2 (Figure 4), thereby indicating genotoxicity and the presence of a DNA targeting component in F2/11. In contrast, F2/13 induced gamma-H2AX after 24 h and F3/4 after 8 h, which correlated with caspase 3 activity (Figure 6). In this case, the induction of gamma-H2AX, and also the activation of Chk2 (Figure 4), were most likely the consequence of the activation of Caspase-Activated-DNAse (CAD) through caspase 3 (41).

Fractions F2/11, F2/13, and F3/4 induced the acetylation of alpha-tubulin and therefore, the stabilization of microtubule (42-44). This was reminiscent of the mechanism of taxol that causes mitotic arrest (3, 4). Tilting the fine-tuned equilibrium of polymerized/de-polymerized microtubule is incompatible with normal cell division and this causes cell cycle arrest and apoptosis (5), and therefore, tubulin-targeting drugs are validated anti-cancer therapeutics (45). The effect of fraction F2/11 differed from those of fractions F2/13 and F3/4 in that the acetylation of tubulin was rapid and severe upon treatment with F2/11, whereas fraction F2/13 induced tubulin acetylation only after 24 h and less pronounced. F3/4 induced tubulin acetylation already after 8 h which correlated with the enrichment of bio-activity compared to F2/13 (Figure 6). Therefore, we could separate two very distinct anti-neoplastic properties in fractions that were derived from the *P. odorata* CH_2Cl_2 crude extract. Firstly, a genotoxic property in fraction F2/11, which also triggered strong tubulin polymerization and which was certainly causal for both, cell cycle arrest and apoptosis. Secondly, an even stronger pro-apoptotic property in F3/4, which had more impact on the expression of the oncogenes Cyclin D1 and Cdc25A. The conflicting signals generated by cyclin D1 suppression and Cdc2 activation would specifically affect constantly cycling cancer cells. This was confirmed in experiments utilizing slowly cycling normal human lung fibroblasts, which were affected significantly less by fraction F3/4 than by fraction F2/11 (data not shown).

Previous studies on the genus *Pluchea* showed that the methanol extracts of *P. odorata* exhibited activity against *Giardia lamblia trophozoites* (46), and in the methanol extract of *P. indica* plucheol A and B, which are unique to species of *Pluchea*, were discovered (47). From the chloroform extract of *P. arabia*, godotol A and B were isolated, which exert weak anti-bacterial activity (48). In addition, in the chloroform extract of the aerial parts of *P. sagittalis*, the eudesmane-type sesquiterpenoids cuauthemone was found, which has anti-feedant activity (49), and cuauthemone, pluchin, plucheinol, among other eudesmane-type sesquiterpenoids, were isolated from *P. chingaio* (50). Cuauthemone was furthermore found in *P. odorata* (51), and thus, cuauthemone is a likely constituent of the dichloromethane extract, which was shown to exert anti-inflammatory activity (11, 52). Flavonoids are well known for their anti-oxidant, anti-inflammatory, and anti-neoplastic effects and quercetin and isorhamnetin have been found in the leaves of *P. lanceolata* (53). It is however unlikely, that polar flavonoids were contained in the here described dichloromethane extract of *P. odorata*. In a broad search for eudesmane-type sesquiterpenoids in the Asteraceae family only eudesmane ketones were found in *P. odorata* (54, 55). Whether cuauthemone or other eudesmane ketones may have contributed to the anti-neolpastic effects of the here studied fractions of the *P. odorata* dichloromethane extract remains to be established. The TLC profile after detection with anisaldehyde sulphuric acid reagent proposes the presence of sesquiterpenes in the active fractions.

This study evidenced that the traditional Maya healing plant *P. odorata* used for the treatment of severe and chronic inflammations, has also anti-neoplastic potential. The separation of a genotoxic property in F2/11 from a cell cycle-interfering property in F3/4 is a relevant step to rid off extract components that may cause unspecific and therefore, undesired therapeutic side effects.

5. ACKNOWLEDGEMENTS

We wish to thank Toni Jaeger for preparing the figures. The work was supported by the Funds for Innovative and Interdisciplinary Cancer Research to M.F.-S and G.K and the Hochschuljubilaeumsstiftung der Stadt Wien to G.K.

6. REFERENCES

1. Gordon Cragg, David Newman: Antineoplastic agents from natural sources: achievements and future directions, *Expet Opin Investig Drugs* 9, 2783-2797 (2000)

2. Gordon Cragg, David Newman, Stringner Yang: Natural product extracts of plant and marine origin having antileukemia potential. The NCI experience. *J NatProd* 69, 488 - 498 (2006)

3. Raphael Geney, Liang Sun, Paula Pera, Ralph Bernacki, Shujun Xia, Susan Horwitz, Carlos Simmerling, Iwao

Ojima: Use of the tubulin bound paclitaxel conformation for structure-based rational drug design. *Chem Biol* 12, 339 - 348 (2005)

4. Adam Marcus, Jun Zhou, Aurora O'Brate, Ernest Hamel, Jason Wong, Michael Nivens, Adel El-Naggar, Tso-Pang Yao, Fadlo Khuri, & Paraskevi Giannakakou: The synergistic combination of the farnesyl transferase inhibitor lonafarnib and paclitaxel enhances tubulin acetylation and requires a functional tubulin deacetylase. *Cancer Res* 65, 3883 - 3893 (2005)

5. Gianni Piperno, Margaret Fuller: Monoclonal antibodies specific for an acetylated form of alpha-tubulin recognize the antigen in cilia and flagella from a variety of organisms. *J Cell Biol* 101, 2085 - 2094 (1985)

6. Gordon Cragg, David Newman: Plants as source of anticancer agents. *J Ethnopharmacol* 100, 72 - 79 (2005)

7. Leland Cseke, Ara Kirakosyan, Peter Kaufman, Sara Warber, James Duke, & Harry Brielmann: Natural Products from Plants. *CRC Press*, FL (2006)

8. John Borchardt: Medicine of the Maya Ameridians. *Drug News Perspect* 17, 347 - 351 (2004)

9. Joydeb Kundu, Young-Joon Surh: Inflammation: gearing the journey to cancer. *Mutat Res* 659, 15 - 30 (2008)

10. Rosita Arvigo, Michael Balick: Rainforest Remedies. *Lotus Press*, Twin Lakes (1998)

11. Manuela Gridling, Nicole Stark, Sibylle Madlener, Andreas Lackner, Ruxandra Popescu, Birgit Benedek, Rene Diaz, Foster Tut, Thanh Vo, Daniela Huber, Michaela Gollinger, Phillip Saiko, Ali Oezmen, Wilhelm Mosgoeller, Rainer De Martin, Ruth Eytner, Karl-Heinz Wagner, Michael Grusch, Monika Fritzer-Szekeres, Thomas Szekeres, Brigitte Kopp, Richard Frisch, Georg Krupitza: *In vitro* anti-cancer activity of two ethno-pharmacological healing plants from Guatemala *Pluchea odorata* and *Phlebodium decumanum*. *Int J Oncol* 34, 1117 - 1128 (2009)

12. Sibyle Madlener, Jana Svacinova, Miloslav Kitner, Jiri Kopecky, Ruth Eytner, Andreas Lackner, Thanh Vo, Richard Frisch, Michael Grusch, Rainer De Martin, Karel Dolezal, Miroslav Strnad, Georg Krupitza: *In vitro* anti-inflammatory and anticancer activities of extracts of *Acalypha alopecuroidea* (Euphorbiaceae). *Int J Oncol* 35, 881 - 891 (2009)

13. Nicole Stark, Manulela Gridling, Sibylle Madlener, Sabine Bauer, Andreas Lackner, Ruxandra Popescu, Rene Diaz, Foster Tut, Thanh Vo, Caroline Vonach, Benedikt Giessrigl, Philipp Saiko, Michael Grusch, Monika Fritzer-Szekeres, Thomas Szekeres, Brigitte Kopp, Richard Frisch, Georg Krupitza: A polar extract of the Maya healing plant *Anthurium schlechtendalii* (Aracea) exhibits strong *in vitro* anticancer activity. *Int J Mol Med* 24, 513 - 521 (2009)

14. Georg Rosenberger, Gerhard Fuhrmann, Michael Grusch, Sandra Fassl, Howard Elford, Kees Smid, Godefridus Peters, Thomas Szekeres, Georg Krupitza: The ribonucleotide reductase inhibitor trimidox induces c-myc and apoptosis of human ovarian carcinoma cells. *Life Sci* 67, 3131 - 3142 (2000)

15. Monika Fritzer-Szekeres, Michael Grusch, Cornelia Luxbacher, Susanna Horvath, Georg Krupitza, Howard Elford, Thomas Szekeres: Trimidox, an inhibitor of ribonucleotide reductase, induces apoptosis and activates caspases in HL-60 promyelocytic leukemia cells. *Exp Hematol* 28, 924 - 930 (2000)

16. Michael Grusch, Monika Fritzer-Szekeres, Gerhard Fuhrmann, Georg Rosenberger, Cornelia Luxbacher, Howard Elford, Kees Smid, Godefridus Peters, Thomas Szekeres, Georg Krupitza: Activation of caspases and induction of apoptosis by novel ribonucleotide reductase inhibitors amidox and didox. *Exp Hematol* 29, 623 - 632 (2001)

17. Musa Khan, Benedikt Giessrigl, Caroline Vonach, Sibylle Madlener, Sonja Prinz, Irene Herbaceck, Christine Hoelzl, Sabine Bauer, Katharina Viola, Wolfgang Mikulits, Rizwana Quereshi, Siegfried Knasmueller, Michael Grusch, Brigitte Kopp, Georg Krupitza: Berberine and a *Berberis lycium* extract inactivate Cdc25A and induce alpha-tubulin acetylation that correlate with HL-60 cell cycle inhibition and apoptosis. *Mut Res* 683, 123 - 130 (2010)

18. Ali Oezmen, Sabine Bauer, Manuela Gridling, Judith Singhuber, Stanimira Krasteva, Sibylle Madlener, Than Vo, Nicole Stark, Philipp Saiko, Monika Fritzer-Szekeres, Thomas Szekeres, Tulay Askin-Celik, Liselotte Krenn, Georg Krupitza: *In vitro* anti-neoplastic activity of the ethno-pharmaceutical plant *Hypericum adenotrichum* Spach endemic to Western Turkey. *Oncol Rep* 22, 845 - 852 (2009)

19. Ali Oezmen, Sibylle Madlener, Sabine Bauer, Stanimira Krasteva, Caroline Vonach, Benedikt Giessrigl, Manuela Gridling, Katharina Viola, Nicole Stark, Philipp Saiko, Barbara Michel, Monika Fritzer-Szekeres, Thomas Szekeres, Tulay Askin-Celik, Liselotte Krenn, Georg Krupitza: *In vitro* anti-leukemic activity of the ethno-pharmacological plant *Scutellaria orientalis* ssp. carica endemic to western Turkey. *Phytomed* 17, 55 - 62(2010)

20. Philipp Saiko, Maria Ozsvar-Kozma, Sibylle Madlener, Astrid Bernhaus, Andreas Lackner, Michael Grusch, Zsuzsanna Horvath, Georg Krupitza, Walter Jaeger, Kirsten Ammer, Monika Fritzer-Szekeres, Thomas Szekeres: Avemar, a nontoxic fermented wheat germ extract, induces apoptosis and inhibits ribonucleotide reductase in human HL-60 promyelocytic leukemia cells. *Cancer Lett* 250, 323 - 328 (2007)

21. John Alao: The regulation of cyclin D1 degradation: roles in cancer development and the potential for therapeutic invention. *Mol Cancer* 6, 24 (2007)

22. Dipankar Ray, Hiroaki Kiyokawa: CDC25A phosphatase: a rate-limiting oncogene that determines genomic stability. *Cancer Res* 68, 1251 - 1253 (2008)

23. Yue Xiong, Joan Menninger, David Beach, David Ward: Molecular cloning and chromosomal mapping of CCND genes encoding human D-type cyclins. *Genomics* 13, 575 - 584 (1992)

24. Yue Xiong, Hui Zhang, David Beach: D type cyclins associate with multiple protein kinases and the DNA replication and repair factor PCNA. *Cell* 71, 504 - 514 (1992)

25. Toshiya Inaba, Hitoshi Matsushime, Markus Valentine, Martine Roussel, Charles Cherr, Thomas Look: Genomic organization, chromosomal localization, and independent expression of human cyclin D genes. *Genomics* 13, 565 - 574 (1992)

26. Kong Lingfei, Ying Pingzhang, Liu Zhengguo, Gen Jianhua, Zhao Yaowu: A study on p16, pRb, cdk4 and cyclinD1 expression in non-small cell lung cancers. *Cancer Lett* 130, 93 - 101 (1998)

27. Carol Rosenberg, Emily Wong, Elizabeth Petty, Allen Bale, Yoshihide Tsujimoto, Nancy Harris, Andrew Arnold: PRAD1, a candidate BCL1 oncogene: mapping and expression in centrocytic lymphoma. *Proc Natl Acad Sci U S A* 88, 9638 - 9642 (1991)

28. Syed Meeran, Santosh Katiyar: Cell cycle control as a basis for cancer chemoprevention through dietary agents. *Front Biosci* 13, 2191 - 2202 (2008)

29. Christina Karlsson-Rosenthal, Jonathan Millar: Cdc25: mechanisms of checkpoint inhibition and recovery. *Trends Cell Biol* 16, 285 - 292 (2006)

30. James Mailer: Mitotic control. *Curr Opin Cell Biol* 3, 269 - 275 (1991)

31. Jennifer Pietenpol, Zoe Stewart: Cell cycle checkpoint signaling: Cell cycle arrest versus apoptosis. *Toxicology* 181 - 182 475 - 481 (2002)

32. Matthew Wasco, Robert Pu, Limin Yu, Lyndon Su, Linglei Ma: Expression of gamma-H2AX in melanocytic lesions. *Hum Pathol* 39, 1614 - 1620 (2008)

33. Zhan Xiao, Zehan Chen, Angelo Gunasekera, Thomas Sowin, Saul Rosenberg, Steve Fesik, Haiying Zhang: Chk1 mediates S and G2 arrests through Cdc25A degradation in response to DNA-damaging agents. *J Biol Chem* 278, 21767 - 21773 (2003)

34. Jacob Falck, Niels Mailand, Randi Syljuasen, Jiri Bartek, Jiri Lukas: The ATM-Chk2-Cdc25A checkpoint pathway guards against radioresistant DNA synthesis. *Nature* 410, 842-847 (2001)

35. Arne Lindqvist, Veronica Rodriguez-Bravo, Rene Medema: The decision to enter mitosis: feedback and redundancy in the mitotic entry network. *J Cell Biol* 185, 193 - 202 (2009)

36. Douglas Kellogg: Wee1-dependent mechanisms required for coordination of cell growth and cell division. *J Cell Sci* 116, 4883 - 4890 (2003)

37. Sibylle Madlener, Margit Rosner, Sigurd Krieger, Benedikt Giessrigl, Manuela Gridling, Thanh Vo, Christina Leisser, Andreas Lackner, Ingrid Raab, Michael Grusch, Markus. Hengstschlaeger, Helmut Dolznig, Georg Krupitza: Short 42 degrees C heat shock induces phosphorylation and degradation of Cdc25A which depends on p38MAPK, Chk2 and 14.3.3. *Hum Mol Genet* 18, 1990 - 2000 (2009)

38. Annette Khaled, Dmitry Bulavin, Christina Kittipatarin, Wen Li, Michelle Alvarez, Kyungjae Kim, Howard Young, Albert Fornace, Scott Durum: Cytokine-driven cell cycling is mediated through Cdc25A. *J Cell Biol* 169, 755 - 763 (2005)

39. Sibylle Madlener, Philipp Saiko, Caroline Vonach, Katharina Viola, Nicole Huttary, Nicole Stark, Ruxandra Popescu, Manuela Gridling, Than Vo, Irene Herbacek, Agnes Davidovits, Benedikt Giessrigl, Somepalli Venkateswarlu, Silvana Geleff, Walter Jaeger, Michael Grusch, Dontscho Kerjaschki, Wolfgang Mikulits, Trimurtulu Golakoti, Monika Fritzer-Szekeres, Thomas Szekeres, Georg Krupitza: Multifactorial anticancer effects of digalloyl-resveratrol encompass apoptosis, cell-cycle arrest, and inhibition of lymphendothelial gap formation *in vitro*. *Brit J Cancer* 102, 1361 - 1370 (2010)

40. Teresa Fernandes-Alnemri, Gerald Litwack, Emad Alnemri: CPP32, a novel human apoptotic protein with homology to Caenorhabditis elegans cell death protein Ced-3 and mammalian interleukin-1 beta- converting enzyme. *J Biol Chem* 269, 30761-30764 (1994)

41. Brian Larsen, Shravanti Rampalli, Leanne Burns, Steve Brunette, Jeffrey Dilworth, Lynn Megeney: Caspase 3/caspase-activated DNase promote cell differentiation by inducing DNA strand breaks. *Proc Natl Acad Sci U S A* 107, 4230 - 4235 (2010)

42. Gianni Piperno, Michel LeDizet, Xiao Chang: Microtubules containing acetylated alpha-tubulin in mammalian cells in culture. *J Cell Biol* 2, 289 - 302 (1987)

43. Paula Wilson, Arthur Forer: Effects of nanomolar taxol on crane-fly spermatocyte spindles indicate that acetylation of kinetochore microtubules can be used as a marker of poleward tubulin flux. *Cell Motil Cytoskeleton* 37, 20 - 32 (1997)

44. Akihisa Matsuyama, Tadahiro Shimazu, Yuko Sumida, Akiko Saito, Yasuhiro Yoshimatsu, Daphne Seigneurin-Berny, Hiroyuki Osada, Yasuhiko Komatsu, Norikazu Nishino, Saadi Khochbin, Sueharu Horinouchi, Minoru Yoshida: *In vivo* destabilization of dynamic microtubules by HDAC6-mediated deacetylation. *EMBO J* 21, 6820 - 6831 (2002)

45. Mary Jordan, Leslie Wilson: Microtubules as a target for anticancer drugs (Review). *Nat Rev Cancer* 4, 253 - 265 (2004)

46. Sergio Peraza-Sanchez, Seydi Poot-Katun, Luis Torres-Tapia, Filogonio May-Pat, Paulino Sima-Polanco, Roberto Cedillo-Rivera: Screening of native plants of Yucatan for anti-*Giardia lamblia* activity. *Pharm Biol* 43 594 - 598 (2005)

47. Taketo Uchiyama, Toshio Miyase, Akira Ueno, Khan Usmanghani: Terpene and lignan glycosides from *Pluchea indica*. *Phytochemistry* 30, 655 - 657 (1991)

48. Majekodunmi Fatope, Rani Nair, Ruchi Marwah, Haifaa Al-Nadhiri: New sesquiterpenes from *Pluchea arabica*. *J Nat Prod* 67, 1925-1928 (2004)

49. Nancy Vera, Rosana Misico, Manuel Sierra, Yoshinori Asakawa, Alicia Bardon: Eudesmanes from *Pluchea sagittalis*. Their antifeedant activity on *Spodoptera frugiperda*. *Phytochemistry* 69, 1689 - 1694 (2008)

50. Volker Zlabel, William Watson: Plucheinol and (3alphaH)-Pluicheinol. *Acta Crystallographica* B38, 584 - 588(1982)

51. Koji Nakanishi, Rosalie Crouch, Iwao Miura, Xorge Dominguez, Acosta Zamudio, Roberto Villarreal: Structure of a sesquiterpene, cuauhtemone, and its derivative. Application of partially relaxed Fourier transform carbon-13 nuclear magnetic resonance. *J Am Chem Soc* 96, 609 – 611 (1974)

52. Francisco Perez-Garcia, Esther Marin, Salvador Canigueral, Tomas Adzet: Anti-inflammatory action of *Pluchea sagittalis*: involvement of an antioxidant mechanism. *Life Sci* 59, 2033 - 2040 (1996)

53. Amrik Chawla, Balbir Kaith, Sukhdev Handa, Dinesh Kulshreshtha & Rikhab Srimal: Chemical investigation and anti-inflammatory activity of *Pluchea lanceolata. Fitoterapia* 62, 441 - 444 (1991)

54. Quan-Xiang Wu, Yan-Ping Shi, Zhong-Jian Jia: Eudesmane sesquiterpenoids from the Asteraceae family. *Nat Prod Rep* 23, 699 - 734 (2006)

55. Javier Arriaga-Giner, Juan Borges-del-Castillo, Teresa Manresa-Ferrero, Purificacion Vazquez-Bueno, Francisco Rodriguez-Luis, S. Valdes-Iraheta: Eudesmane derivatives from *Pluchea odorata*. *Phytochemistry* 22, 1767-1769 (1983)

Abbreviations: ASE accelerated solvent extractor, ASR anisaldehyde sulphuric acid reagent, CC-I column chromatography I, CC-II column chromatography II, CHCl3 chloroform, CH2Cl2 dichloromethane, SDS-PAGE sodiumdodecylsulfonate polyacrylamide gel electrophoresis, PE petroleum ether, PIC Protease Inhibitor Cocktail, PMSF phenylmethylsulfonylfluorid, TLC thin layer chromatography, VLC vacuum liquid chromatography

Key Words: *Pluchea odorata*, anti-neoplastic, apoptosis, HL-60, genotoxic, H2AX, cyclin D1, Cdc25A, Cdc2, acetylated tubulin

Send correspondence to: Ruxandra Popescu, Department of Pharmacognosy, University of Vienna, Althanstrasse 14, A-1090, Vienna, Austria, Tel: 43-1-4277-55261, Fax: 43-1-4277-9552, E-mail: ruxandra.popescu@univie.ac.at

Bay11-7082 and xanthohumol inhibit breast cancer spheroid-triggered disintegration of the lymphendothelial barrier; the role of lymphendothelial NF-κB.

Viola K., Vonach C., Kretschy N., Teichmann M., Rarova L., Strnad M., **Giessrigl B.**, Huttary N., Raab I., Stary S., Krieger S., Keller T, Bauer S, Jarukamjorn K., Hantusch B., Szekeres T., de Martin R., Jäger W., Knasmüller S., Mikulits W., Dolznig H., Krupitza G. and Grusch M.

Br. J. Cancer, ***submitted.***

Bay11-7082 and xanthohumol inhibit breast cancer spheroid-triggered disintegration of the lymphendothelial barrier; the role of of lymphendothelial NF-κB

Running title: The role of NF-κB in lymph-intravasation of breast cancer cells

Katharina Viola[1,2], Caroline Vonach[1,2], Nicole Kretschy[1,2], Mathias Teichmann[1,3], Lucie Rarova[4], Miroslav Strnad[4], Benedikt Giessrigl[1], Nicole Huttary[1], Ingrid Raab[1], Susanne Stary[1], Sigurd Krieger[1], Thomas Keller[1], Sabine Bauer[1], Kanokwan Jarukamjorn[5,6], Brigitte Hantusch[1], Thomas Szekeres[7], Rainer de Martin[8], Walter Jäger[5], Siegfried Knasmüller[2], Wolfgang Mikulits[2], Helmut Dolznig[3], Georg Krupitza[1] and Michael Grusch[2]

[1] Institute of Clinical Pathology, Medical University of Vienna, Vienna, Austria.
[2] Department of Medicine I, Institute of Cancer Research, Comprehensive Cancer Center, Medical University of Vienna, Vienna, Austria
[3] Institute of Medical Genetics, Medical University of Vienna, Vienna, Austria
[4] Centre of the Region Haná for Biotechnological and Agricultural Research, Faculty of Science, Palacký University, Šlechtitelů 11, 783 71 Olomouc, Czech Republic
[5] Department of Clinical Pharmacy and Diagnostics, University of Vienna, Vienna, Austria
[6] Department of Pharmaceutical Chemistry, Faculty of Pharmaceutical Sciences, Khon Kaen University, Khon Kaen 40002, Thailand
[7] Department of Medical and Chemical Laboratory Diagnostics, Medical University of Vienna, General Hospital of Vienna, Vienna, Austria
[8] Department of Vascular Biology and Thrombosis Research, Medical University of Vienna, Austria

Correspondence: Michael Grusch
Department of Medicine I, Institute of Cancer Research, Medical University of Vienna, Waehringer Guertel 18-20, A-1090 Vienna, Austria.
Tel.: +431427765144
Fax: +431427765149
e-mail: michael.grusch@meduniwien.ac.at

Abstract

BACKGROUND: Many cancers spread through lymphatic routes and mechanistic insights of tumour intravasation into the lymphatic vasculature and targets for intervention are limited. The major emphasis of research focuses currently on the molecular biology of tumour cells, whereas still little is known regarding the contribution of lymphatics.

METHODS: Breast cancer cell spheroids attached to lymphendothelial cell (LEC) monolayers enable to study the process of intravasation by measuring the areas of "circular chemorepellent-induced defects" (CCID), which can be considered as gates for bulky tumour transmigration. Pro-metastatic mechanisms of tumour and lymphendothelial cells and anti-intravasative properties of compounds were studied by the CCID bio-assay and through simplification of the assay by replacing cancer spheroids with the CCID-triggering compound 12(S)- hydroxyeicosatetraenoic acid (HETE). Here we analysed xanthohumol, a prenylated hop-derived flavonoid contained in beer, to learn more about its activity spectrum regarding the modulation of CCIDs.

RESULTS: The formation of CCIDs was mediated by NF-κB dependent i) binding of LECs to MCF-7 spheroids, which correlated with ICAM-1 expression of LECs and ii) LEC migration, which correlated with the expression of the prometastatic factor S100A4. Also the expression of semaphorine 3F, a well documented cell repellent, depended on NF-κB in MCF-7 cells. Simultaneous inhibition of NF-κB with Bay11-7082 and of ALOX15 with baicalein, which was previously shown to attenuate CCIDs, prevented CCID formation synergistically. Furthermore, xanthohumol was a strong inhibitor of MCF-7-triggered CCID formation, whereas MDA-MB231-triggered CCIDs were much less affected. This correlated with the potential of xanthohumol to inhibit the activity of CYP1A1 in these cell lines.

CONCLUSIONS: The CCID bio-assay, which was recently validated in mouse xenograft assays and human patient samples, was used to elucidate NF-κB-dependent processes in ALOX15-induced tumour intravasation through the lymphatic barrier.

In this setting, well described compounds such as i.e. Bay11-7082 and baicalein, or less known molecules, i.e. xanthohumol, can be studied regarding their anti-intravasative properties. Compounds identified by this functional assay represent excellent candidates as anti-metastatic agents for cancer therapy.

Key words: lymphatic endothelium; migration; tumour spheroid intravasation; NFkappaB; xanthohumol; CCID

Introduction

Mostly, metastatic outgrowth demands an early step of intravasation of primary tumour cells into the blood- and lymphatic vasculature, whereby breast cancer cells seem to more commonly frequent the lymphatic route. Therefore, the number of axillar lymph nodes that are colonised by tumour cells is a reliable clinical predictor for patient outcome (**Carlson et al. 2009**). We found that post-sentinel lymph node colonisation and organ invasion correlate with intravasation of tumour cell clusters into lymphatics of sentinel lymph node metastases ("intrametastatic lymphatic carcinosis"; **Kerjaschki et al. 2011**). If intrametastatic lymphatic carcinosis of the sentinel lymph node does not take place, post-sentinel lymph nodes remain metastasis free. Therefore, this step is considered as critical for breast cancer cell spread. Lymph node intravasation involves partly the expression of the lipoxygenases ALOX12 and ALOX15 and their metabolite 12(S)- hydroxyeicosatetraenoic acid (HETE), which is secreted i.e. by MCF-7 cells (**Uchide et al. 2007**). *In vitro* 12(S)-HETE causes the retraction of lymphatic endothelial cells (LECs) thereby causing "circular chemorepellent-induced defects" (CCID) in LEC walls. CCIDs are entry gates through which breast cancer cells intravasate (transmigrate) into the lymphatic vasculature. Immunodeficient mice orthotopically xenografted with ALOX15-proficient or ALOX15-deficient breast cancer cells provided *in vivo* pathophysiological evidence of this mechanism. The relevant protagonists, ALOX12, ALOX15 and 12(S)-HETE, were also detected in paraffin sections of human metastatic lymph nodes and the expression of ALOX15 correlated inversely with metastasis free survival of the patients (**Kerjaschki et al. 2011**). The process of intravasation through lymphatics is only partly triggered by 12(S)-HETE and effectors that act in parallel and/or downstream are unkown. Therefore, the elucidation of the mechanistic details, which are causal for CCID formation, is important. The transcription factor NF-κB plays a role in murine lung alveolar carcinoma metastasis, pulmonary metastasis of murine osteosarcomas, and lung metastasis of invasive breast cancer MDA-MB-468 cells orthotopically xenografted in BALB/c nude mice (**Andela et al. 2000, Nishimura et al. 2010, Srivastava et al. 2010,**). In a recent study we demonstrated that VE-cadherin expression increased upon inhibition of NF-κB, which stabilised the integrity of LEC monolayers **(Vonach et al. 2011**). Therefore, besides ALOX12/15, also NF-κB activity was involved in the corruption of lymph vessel integrity and in CCID formation. In the present study we investigated the contribution of NF-κB to the attachment of MCF-7 spheroids to LECs and to LEC mobility. Furthermore, we tested the applicability of the CCID bio-assay and studied the effect of the phyto-flavonoid and *bona fide* NF-κB inhibitor xanthohumol (**Gao et al. 2009**) a major active component in hop cones

(**Magalhães et al. 2009**). Xanthohumol is a constitutent of beer (**Stevens and Page 2004**) and was reported to possess strong anti-neoplastic properties (**Monteghirfo et al. 2008**).

Materials and Methods

Chemicals: The I-κBα phosphorylation inhibitor (E)-3-[(4-methylphenylsulfonyl]-2-propenenitrile (Bay11-7082) and baicalein (EI-106) were purchased from Biomol (Hamburg, Germany), 12(S)-HETE from Cayman Chemical (Ann Arbor, MI, USA). Wogonin Cat was purchased from Calbiochem (Darmstadt, Germany), xanthohumol from Naturalchemics (Homburg, Germany). Mouse monoclonal anti-CD54 (ICAM-1) antibody was from Immunotech (Marseille, France) and polyclonal rabbit anti-paxillin (H-114) (SC-5574) from Santa Cruz Biotechnology (Heidelberg, Germany). Polyclonal rabbit anti-semaphorin 3F antibody was from Chemicon (Tenecula, CA, USA), and monoclonal mouse anti-phospho-p44/42 MAPK (Erk1/2) (Thr202/Tyr204) (E10), monoclonal rabbit anti-p44/42 MAPK (Erk1/2) (137F5), polyclonal rabbit anti-phospho-Myosin Light Chain 2 (Ser19), polyclonal rabbit anti-Myosin Light Chain 2, and polyclonal rabbit anti-MYPT1 were from Cell Signaling (Danvers, MA, USA). Monoclonal mouse anti-β-actin (clone AC-15) and polyclonal rabbit anti-S100A4 were from Sigma-Aldrich (Munich, Germany), polyclonal rabbit anti-phospho-MYPT1 (Thr696) from Upstate (Lake Placid, NY, USA). Monoclonal mouse anti-CD31 (JC70A), polyclonal rabbit anti-mouse and anti-rabbit IgGs were from Dako (Glostrup, Denmark).

Cell culture: Human MCF-7 and MDA-MB231 breast cancer cells were purchased from the American Type Culture Collection (ATCC, Rockville, MD, USA) and grown in MEM medium supplemented with 10% fetal calf serum (FCS), 1% penicillin/streptomycin (PS), 1% NEAA (Invitrogen, Karlsruhe, Germany). Telomerase immortalized human lymphendothelial cells (LECs) were grown in EGM2 MV (Clonetics CC-4147, Allendale, NJ, USA), all at 37°C in a humidified atmosphere containing 5% CO_2. For CCID formation assays, LECs were stained with cytotracker green purchased from Invitrogen (Karlsruhe, Germany). Human umbilical vein endothelial cells (HUVECs) were isolated and cultured in M199 medium supplemented with 20% FCS, antibiotics, endothelial cell growth supplement and heparin as previously described **(Zhang et al. 1998)**.

3-D co-cultivation of breast cancer spheroids with LEC monolayers: MCF-7 or MDA-MB231 cells were transferred to 30 ml MEM medium containing 6 ml of a 1.6% methylcellulose solution (0.3% final concentration; Cat. No.: M-512, 4000 centipoises; Sigma-Aldrich, Munich, Germany). 150 µl of this cell suspension were transferred to each well of a 96 well plate (Greiner Bio-one, Cellstar 650185, Kremsmünster, Austria) to allow spheroid formation within 48 h. Then, MCF-7 spheroids were washed in PBS and transferred to cytotracker-stained LEC monolayers that were seeded into 24-well plates (Costar 3524, Sigma-Aldrich, Munich, Germany) in 2 ml EGM2 MV medium.

CCID assay: MCF-7 cell spheroids (3000 cells/spheroid) were transferred to 24-well plates containing LEC monolayers. After four hours of incubation, the CCID areas in the LEC monolayers underneath the MCF-7 spheroids were photographed using an Axiovert (Zeiss, Jena, Germany) fluorescence microscope to visualise cytotracker(green)-stained LECs underneath the spheroids. CCID areas were calculated with the Axiovision Re. 4.5 software (Zeiss, Jena, Germany). MCF-7 spheroids were treated with solvent (DMSO) as negative control. Each experiment was performed in triplicate and for each condition, the CCID size of 12 or more spheroids (unless otherwise specified) was measured.

Western blotting: LECs were seeded in 6 cm dishes and treated with the indicated compounds (10 µM Bay11-7082 and or 1 µM 12(S)-HETE). Cells were washed twice with ice cold PBS and lysed in buffer containing 150 mM NaCl, 50 mM Tris pH 8.0, 0.1% Triton-X100, 1 mM phenylmethylsulfonylfluorid (PMSF) and protease inhibitor cocktail (PIC). Afterwards, the lysate was centrifuged at 12000 rpm for 20 min at 4°C and the supernatant stored at -20°C until further analysis. Equal amounts of protein were separated by SDS polyacrylamide gel electrophoresis and electro-transferred onto Hybond PVDF-membranes at 100V for 1 h at 4°C. To control equal sample loading, membranes were stained with Ponceau S (Sigma-Aldrich, Munich, Germany). After washing with PBS/T (PBS/Tween 20; pH: 7.2) or TBS/T (Tris Buffered Saline/Tween 20; pH: 7.6), membranes were immersed in blocking solution (5% non-fat dry milk in TBS containing 0.1% Tween or in PBS containing 0.5% Tween 20) at room temperature for 1 h. Membranes were washed and incubated with primary antibodies (in blocking solution; dilution 1:500 – 1:1000) by gently rocking at 4°C overnight or at room temperature for 1 h. Thereafter, the membranes were washed with PBS/T or TBS/T and incubated with secondary antibodies (peroxidase-conjugated goat anti-rabbit IgG or anti-mouse IgG; dilution 1:2000) at room temperature for 1 h. Chemiluminescence was

detected by ECL detection Kit (Thermo Scientific, Portsmouth, USA), and the membranes were exposed to Amersham Hyperfilms (GE-Healthcare, Buckinghamshire, UK).

SELE (CD62E, E-selectin, ELAM)-induction assay: Each well of a 96-well plate was coated with gelatine by applying 200 µl of 1.0% gelatine for 10 minutes at room temperature. Outer wells (A1-A12, H1-H12, 1-H1 and A12-H12) contained only 200 µl/well medium and served as an evaporation barrier. 1×10^4 HUVECs were seeded in each of the other wells in 200 µl medium and grown for 48 hours to optimal confluence. Increasing concentrations of xanthohumol were then added to the HUVEC-containing wells in triplicates, and the cells were incubated for 30 min, after which 10 ng/ml TNFα was added per well to stimulate NFκB, and thus SELE. After a further four hours incubation, the levels of SELE in each of the HUVEC-containing wells were determined by enzyme-linked activity assays (ELISAs) as described below.
Cell-surface ELISA SELE: Cells were washed once with PBS and fixed with 100 µl/well 25% glutaraldehyde (40µl in 10ml PBS, Sigma-Aldrich (Munich, Germany), stored at –20°C in aliquots) for 15 min at room temperature. Then, cells were washed 3 x with 200 µl per well PBS/0.05% Tween 20, blocked with 200 µl/well 5% BSA/PBS for 1 hour, and washed again 3 x with 200 µl per well PBS/0.05% Tween 20. Then, anti-SELE-antibody (clone BBA-1, R&D Systems, Minneapolis, MN, USA) diluted 1:5000 in 0.1% BSA/PBS (100µl per well) was added for 1 hour at room temperature and washed thereafter 5 x with 200 µ per well PBS/0.05% Tween 20. Subsequently, goat anti mouse-HRP antibody (Sigma-Aldrich, Munich, Germany) diluted 1:10000 in 0.1% BSA/PBS (100µl per well) was applied and the cells were incubated for a further hour in the dark at room temperature and, after decanting, washed five times with 200 µl per well PBS/0.05 % Tween 20. The HRP-activity of the cells in each of the wells was estimated using Fast-OPD (o-phenylenediamine dihydrochloride) (Sigma-Aldrich, Munich, Germany) assay as described (**Gridling et al. 2009**) and absorbance was measured at OD_{492nm} in a vertical spectrophotometer.

Cytotoxicity testing: For the SELE expression assay the toxicity of xanthhohumol was assessed in HUVECs by Calcein AM cytotoxicity assays in 96-well microtitre plates (**Madlener et al. 2009**). 20 µL portions of each of the xanthohumol concentrations were added in triplicate to the cells, which were then incubated at 37°C in an atmosphere containing 5 % CO_2 for 4 hours, after which Calcein AM solution (Molecular Probes, Invitrogen, Karlsruhe, Germany) was added for 1 hour according to the manufacturer's

instructions. The fluorescence of viable cells was quantified using a Fluoroskan Ascent instrument (Labsystems, Finland) reader and on the basis of triplicate experiments the cytotoxic concentrations were calculated.

Ethoxyresorufin-*O*-deethylase (EROD) assay selective for CYP1A1 activity: MDA-MB-231 and MCF-7 breast cancer cells were grown in phenol red-free RPMI 1640 tissue culture medium (PAN Biotech, Aldenbach, Germany), supplemented with 10% FCS and 1% PS (Invitrogen, Karlsruhe, Germany) under standard conditions at 37°C in a humidified atmosphere containing 5% CO_2 and 95% air. Twenty-four hours before treatment, the cells were transferred to RPMI 1640 medium (Invitrogen, Karlsruhe, Germany) supplemented with 2.5% charcoal-stripped FCS (PAN Biotech, Aldenbach, Germany) and 1% PS. Test compounds were dissolved in DMSO and diluted with medium (final DMSO concentration < 0.1%) to 5-25 µM. Experiments under each set of condition were carried out in triplicate. Blanks contained DMSO in the medium of the test compounds. After 18 h of incubation, ethoxyresorufin (final concentration 5.0 µM, Sigma-Aldrich, Munich, Germany) was added and 0.4 ml aliquots of the medium were sampled after 200 min. Subsequently, the formation of resorufin was analyzed by spectrofluorometry (PerkinElmer LS50B, Waltham, MA, USA) with an excitation wavelength of 530 nm and an emission wavelength of 585 nm.

Real-time PCR: LECs were seeded in 12 well plates, then they were pre-treated with 10 µM Bay11-7082 for 30 min and thereafter stimulated with 1.0 µM 12(S)-HETE or with TNFα (20ng/ml). Total RNA was isolated using the RNeasy Mini Kit 50 and QIAshredder 50 (QIAGEN, Hamburg, Germany). 1.0 µg of total RNA was reverse transcribed with Superscript First Strand Synthesis System (Invitrogen, Karlsruhe, Germany), the resulting cDNA was amplified using TaqMan Universal PCR Master mix (No AmpErase UNG; PartNo 4324018; Applied Biosystems, Vienna, Austria) with the E-selectin Primer (TaqMan Gene Expression Assays Part No 4331182; Applied Biosystems, Vienna, Austria). PCR products were analysed on the Abi Prism 7000 sequence detection system. Duplicate samples were analyzed in parallel. Glyceraldehyde-3-phosphate dehydrogenase (GAPDH) served as internal control. Relative transcript expression was calculated using the $\Delta\Delta C_T$ method.

Statistical analysis: Dose-response curves were analysed using Prism 4 software (La Jolla, CA, USA) and significance was determined by paired Student's t-test. Significant differences between experimental groups were * $p<0,05$.

Results

NF-κB inhibition interferes with MCF-7 spheroid-induced CCID formation in lymphendothelial monolayers

MCF-7 spheroids placed on LEC monolayers were treated with the NF-κB inhibitor Bay11-7082 and this dose-dependently suppressed LEC-CCID formation (**Fig 1a**). It is known that Bay11-7082 irreversibly stabilizes I-κBα and prevents NF-κB activation (**Pierce et al. 1997**), which facilitated to study how NF-κB in MCF-7 cancer cells and in LECs independently contributes to tumor cell intravasation into the lymphatic vasculature. The individual pretreatment of either MCF-7 spheroids or LEC monolayers with Bay11-7082 blocked CCID formation and this evidenced, that NF-κB of MCF-7 as well as that of LECs played a role for CCIDs (**Fig 1b**). ALOX12/15 and its metabolite 12(S)-HETE, which is shedded by MCF-7 spheroids (**Uchide et al. 2007**), was shown to be a trigger factor of CCID **(Kerjaschki et al. 2011,Vonach et al. 2011, Madlener et al. 2010**). Since the pretreatment of MCF-7 spheroids with Bay11-7082 had a stronger inhibitory effect on CCIDs than the pretreatment of LECs this suggests that a second major CCID-forming mechanism, which was different from ALOX12/15, controls MCF-7 cell intravasation into the lymphatic vasculature. SEMA3F was shown to repel endothelial and breast cancer cells (**Bielenberg et al. 2004, Nasarre et al. 2005**). MCF-7 cells expressed SEMA3F NF-κB dependently (**Fig.1 c**) and this can explain why the treatment of MCF-7 spheroids with Bay11-7082 inhibited CCIDs.

Inhibition of LEC migration by Bay11-7082

The treatment of LECs with 10 µM Bay11-7082 inhibited the MCF-7 spheroid-triggered CCID formation and this correlated with the inhibition of the mobility- and EMT- marker S100A, and the phosphorylation of Erk, but not with the activating phosphorylation of threonine-696 of MYPT (**Fig. 2a**). Therefore, MYPT activation was independent of NF-κB, evidencing that also other mechanisms contribute to LEC plasticity.

In earlier studies we could demonstrate that adherence among LECs was facilitated by VE-cadherin. The exposure of LECs to MCF-7 spheroids or to 12(S)-HETE downregulated VE-cadherin expression causing the disruption of the intercellular VE-cadherin bonds, which was demonstrated by Western blotting and confocal immunofluorescence of VE-cadherin (**Kerjaschki et al. 2011, Vonach et al. 2011**). Here we show that, in consequence to MCF-7 spheroid-mediated downregulation of VE-cadherin, the projected cell surface area of Bay11-7082 treated LECs appeared on average smaller compared to untreated controls, due to the

loss of contacts to the neighboring cells and concommittant rounding up (**Fig. 2b**). It further led to an increase of the peri-cellular areas, and alltogether to an affection of the intact LEC monolayer. However, the peri-cellular space between the cells did not increase because the migration of LECs was inhibited.

NFkB-dependent expression of adhesion molecules on LECs

15 µM Bay11-7082 caused the gradual loss of MCF-7 spheroid adhesion to the LEC monolayer (by ~30 %) and the treatment with 25 µM Bay11-7082 completely prevented the attachment of MCF-7 spheroids to LECs and CCID formation (**Fig.1a**). Therefore, NF-κB-dependent expression of adhesion molecules could account for the stable contact of MCF-7 spheroids to LECs. CD31, E-selectin (SELE), and intracellular adhesion molecule 1 (ICAM-1) are known to be expressed in endothelial cells. They contribute to adhesion to other cell types through counter-receptors i.e. $\alpha_v\beta_3$ integrin (vitronectin receptor), CD44, and $\alpha_L\beta_2$ integrin (LFA-1), respectively, which were all reported to be expressed in MCF-7 cells **(Deryungina et al. 2000, Budinsky et al. 1997).** 12(S)-HETE induced the expression of ICAM-1 and CD31 in LECs, but only ICAM-1 induction was inhibited by 15 µM Bay11-7082 (**Fig. 3a,b**). Therefore, ICAM-1 may have contributed to NF-κB dependent adhesion of MCF-7 spheroids to LEC monolayers. SELE was neither constitutively expressed in LECs nor induced by 12(S)-HETE (**Fig 3c**). In summary, we describe two NF-κB regulated mechanisms, which were required for the formation of CCIDs in LEC monolayers: 1) LEC motility, and 2) the adherence of LECs to MCF-7 spheroids.

Simultaneous blocking of NF-kB and lipoxygenase activities synergistically inhibits CCID

Consistent with the role of ALOX12/15 in the formation of CCIDs was the fact that ALOX12/15 inhibitor baicalein (100 µM), or the closely related compound wogonin (75 µM), attenuated LEC-CCID formation by 40-50 % (**Fig. 4a**). Simultaneous treatment with baicalein plus Bay11-7082 inhibited CCIDs synergistically (**Fig. 4b**). This inhibition was controlled in several ways: 1) By the CCID-inducing activity of ALOX15, which was restricted to MCF-7 cells because in 12(S)-HETE-stimulated LECs the expression of S100A4 and the phosphorylation patterns of MYPT1, MLC2, and Erk1/2, remained unchanged in presence of baicalein (**Fig. 4c**). 2) By the CCID-inducing activity of NF-κB, which controlled the mobility and the adhesion of LECs to MCF-7 spheroids (**Fig. 1-3**). The contribution of NF-κB

dependent SEMA3F expression of MCF-7 cells to the formation of CCIDs needs to be further analysed.

Xanthohumol attenuates LEC-CCID formation

Since we established the CCID bio-assay, which faithfully resembles intravasation of breast cancer emboli into intrametastatic lymphatics (**Kerjaschki et al. 2011**), the mechanisms of the underlying cellular processes as well as the anti-metastatic effects of pharmaceutic and natural compounds can be investigated. To challenge the assay we studied the prenylated flavonoid xanthohumol (2,4´,4-trihydroxy-6´-methoxy3´-prenylchalcone), because it was reported to possess health beneficial and anti-carcinogenic properties and to inhibit NF-κB activation in benign and malignant BHP-1 and PC3 prostate epithelial cells (**Colgate et al. 2007**). Xanthohumol, which is well tolerated by humans, is a component of the Chinese medicinal plant *Sophora flavescens Ait.* and of hop cones (*Humulus lupulus L.*), and is present in beer and hop cone tea (**Stevens and Page 2004, Stevens et al. 1999**), and more concentrated also in enriched beverage formulations.

CCIDs triggered by MCF-7 spheroids were dose-dependently inhibited with an IC-50 (the concentration of xanthohumol inhibiting 50% of the CCID-formation effect) of ~5 µM (**Fig. 5a, 5b**), whereas the IC-50 of xanthohumol for MDA-MB231 spheroid-triggered CCIDs was ~100 µM. Notably, the NF-κB inhibitor Bay11-7082 was active in a similar range (~10 µM) in both cell lines (**Fig.5c**). Therefore, we tested whether xanthohumol can inhibit NF-κB activity in endothelial cells. In HUVECs TNFα induced SELE expression (**Table 1**), which is indicative for NF-κB activity. However, xanthohumol reduced SELE expression only insignificantly suggesting that the flavonoid did not inhibit NF-κB activity in this *in vitro* model.

Xanthohumol has been shown to be metabolised by Cytochrome P450 (CYP; **Guo et al. 2006**) and CYP activity contributes to CCID (**in preparation**) and promotes metastasis (**Jiang et al. 2007**). Proadifen (2-Diethylaminoethyl 2,2-diphenylpentanoate; SKF 525-A), an inhibitor of the CYP family which is used as a local anaesthetic, significantly attenuates CCIDs (**in preparation**). In fact, xanthohumol as well as proadifen, significantly inhibited CYP1A1 activity in MCF-7 cells (5 µM) (**Fig. 6a**), as assessed by ethoxyresorufin-*O*-deethylase (EROD) catalytic assay. At higher concentration (25µM) xanthohumol inhibited CYP1A1 also in MDA-MB231 cells, yet less efficiently.

12(S)-HETE, which is secreted by MCF-7 (**Uchide et al. 2007),** but not by MDA-MB231 cells, contributes to ~50 % CCID formation triggered by MCF-7 spheroids (**Kerjaschki et al.**

2011). Therefore, LECs were directly treated with 12(S)-HETE to study the effect of xanthohumol on protein expression that is related to cell motility. Xanthohumol treatment dephosphorylated (inactivated) MLC2 and downregulated S100A4 and paxillin expression, and it reversed 12(S)-HETE-modulated suppression of Erk1/2 phosphorylation (**Fig. 6b**). Only a part of these effects was also observed upon Bay11-7082 treatment (**Fig. 2g**). Therefore, we describe a new property of xanthohumol, which inhibited the migration of LECs and suppressed marker proteins typical for an endothelial-mesenchymal transition type of cell plasticity. This correlated with the inhibition of CYP1A1 activity and with ALOX15 expression in breast cancer cells. Both, CYP and ALOX12/15 metabolise arachidonic acid and are contributing to CCID formation induced by MCF-7 spheroids.

Discussion

In this investigation we mimicked the interactive process of breast cancer cell intravasation into the lymphatic vasculature using a 3D co-culture system consisting of MCF-7 cancer cell spheroids (**Madlener et al. 2010)** and telomerase-immortalised human LEC monolayers (**Schoppmann et al. 2004**). Intravasation of tumor cells depends on cell attachment and on the motility of tumor cells and endothelial cells alike, whereby LEC movement has not been studied in this respect. We recently elucidated one prime intravasation mechanism of MCF-7 breast cancer spheroids and reported that 12(S)-HETE, which is secreted by MCF-7 cells (**Uchide et al. 2007**), causes LECs to respond with the formation of CCIDs (**Vonach et al. 2011, Kerjaschki et al. 2011)**. Under physiologic conditions, 12(S)-HETE is mainly produced by platelets, leukocytes, smooth muscle, epithelium, neuron, and fibroblast cells (**Spector et al. 1988**) and induces retraction of microvascular endothelial cells (**Uchide et al. 2007, Honn et al. 1994).** Under pathophysiologic conditions, 12(S)-HETE increases tumour cell adhesion to exposed ECM (**Honn et al. 1989**). Here, we investigated the 12(S)-HETE triggered effects in LECs and tried to elucidate how downstream signaling was mediated. Since the deregulation of NF-κB is associated with cancer development (**Folmer et al. 2009**) promoting oncogenesis through the transcriptional activation of genes associated with cell proliferation, angiogenesis and metastasis (**Orlowski and Baldwin 2002**), we focussed on the role of NF-κB on CCID formation. The interaction of MCF-7 spheroids with LECs was necessary for CCIDs and this was corrupted by Bay11-7082 concentrations >15 μM and correlated with the NF-κB-dependent downregulation of ICAM-1 in LECs. ICAM-1 is a member of the immunoglobulin gene superfamily and an inducible counter receptor for several leukocyte β_2 integrins (**Rosenstein et al. 1991**), i.e. $\alpha_L\beta_2$ integrin (synonym: LFA-1), which is expressed in MCF-7 cells (**Budinsky et al. 1997**).

Mobility is mediated in microvascular endothelial cells through enhanced phosphorylation (activation) of proteins comigrating with myosin light chain, actin and vimentin (**Tang et al. 1993**). It was showed that 12(S)-HETE treatment results in an increase in the filamentous polymeric F-actin content in the cytoskeleton, and enhanced phosphorylation of myosin light chain (**Rice et al. 1998**). MCF-7 spheroids and 12(S)-HETE induced also the migration of LECs and blood endothelial cells (**Kerjaschki et al. 2011, Uchide et al. 2007, Honn et al. 1994**) and here we describe the mobility components that become activated by 12(S)-HETE. S100A4, an angiogenic factor and a marker for a mesenchymal phenotype (**Zeisberg and Neilson 2009**), stimulates the mesenchymal motility and invasiveness of endothelial cells

(**Takenaga et al. 1994, Jenkinson et al. 2004, Ambartsumian et al. 2001, Schmidt-Hansen et al. 2004**). S100A4 was enhanced upon 12(S)-HETE treatment of LECs and thus, 12(S)-HETE-induced a mobile, mostly mesenchymal, phenotype in LECs. The expression of S100A4 correlated with the formation of CCIDs in the LEC monolayer underneath MCF-7 spheroids, which was found in earlier studies (**Vonach et al. 2011, Kerjaschki et al. 2011; Madlener et al. 2010**). This is furthermore consistent with a significant reduction of CCID sizes in the LEC monolayer underneath Bay11-7082 treated MCF-7 spheroids, which indicates reduced LEC motility. Besides S100A4, the mobility markers MYPT1, MLC2 and paxillin were also shown to be induced in LECs growing underneath MCF-7 spheroids or by synthetic 12(S)-HETE (**Vonach et al. 2011**), but Bay11-7082 could reverse only S100A4 induction, indicating additional mechanisms of cell mobility regulation.

In conclusion, this part of the study revealed that NF-κB controls not only the adhesion of MCF-7 spheroids to LECs, but also the movement of LECs and therefore the formation of CCIDs. In principle, it is also possible that NF-κB executed its effect only by one but not two mechanisms i.e. by facilitating the adherence of MCF-7 spheroids to LECs, infering that this contact through ICAM-1 was at the same time the trigger factor for LEC migration. However, it was shown that 12(S)-HETE stimulates NF-κB activation and NF-κB dependent ICAM-1 expression through RhoA and PKCα **(Bolick et al. 2005)**. This indicates that RhoA is an upstream regulator of ICAM-1 and Rho/Rac family GTPases are also prominent regulators of cell migration. Therefore ICAM-1 expression and LEC motility are most likely parallel but not serial events.

Co-treatment of the 3D cell system with Bay11-7082 together with the ALOX12/15 inhibitor baicalein synergised in the prevention of CCID formation. These results underscore the potential of combination therapies for the management of metastasising cancer and provide evidence that several distinct mechanisms contribute to tumour intravasation. The LOX inhibitor baicalein showed no effects in LECs and this is in agreement with the observation that inhibition of CCID by baicalein affected only the ALOX12/15 and 12(S)-HETE metabolism in MCF-7 cells, but not in MDA-MB321 cells, which do not express ALOX12/15 **(Kerjaschki et al. 2011**).

In search of new anti-neoplastic drugs natural products like xanthohumol are of particular interest, because of their availabilty, tolerability, and multi-target properties that may synergize to achieve the anticipated effects. The root of *Sophora flavescens Ait*., which contains Isoxanthohumol and other anti-neoplastic compounds, is used in traditional Chinese medicine to treat viral hepatitis and cancer. Xanthohumol possesses antiproliferative activities

in several cancer lines such as human breast cancer (MCF-7), colon cancer (HT-29) and ovarian cancer (A-2780) cells (**Miranda et al. 1999**), and significantly induces apoptosis in HCT 116 colon cancer cells by downregulation of Bcl-2 and activation of the caspase cascade (**Pan et al. 2005**). Xanthohumol was shown to repress both, NF-κB and Akt pathways in endothelial cells, and interfered with the angiogenic process, including inhibition of growth, and of endothelial cell migration (**Albini et al. 2006**). This is in agreement with our data because the 12(S)-HETE-induced expression of paxillin (focal adhesion phosphoprotein), was inhibited by xanthohumol. Paxillin is associated *in vivo* and *in vitro* with enhanced endothelial cell motility and necessary for cell-ECM contact **(Huang et al. 2003, Zaidel-Bar et a. 2003**). Furthermore, 12(S)-HETE activated MLC2 and MYPT1 and induced S100A4 expression, which are markers for cell mobility. Whereas Bay11-7082 blocked only S100A4 induction, xanthohumol prevented that of S100A4, MLC2 and paxillin. This suggests that xanthohumol exhibits a wider spectrum of effects that may synergise in the inhibition of CCIDs i.e by inhibition of paxillin and MLC2 (both are unaffected by Bay11-7082). This could be the reason, why xanthohumol is much less toxic than Bay11-7082, which powerfully and most and for all, inhibits a central mechanism necessary for cell survival.

Xanthohumol has been shown to possess antioxidant (**Hartkorn et al. 2009**) as well as radical-inducing properties (**Strathmann et al. 2010**). Radicals however, are not involved in CCID formation (**Madlener et al. 2010, Kerjaschki et al. 2011**).

CYP is an arachidonic acid metabolising enzyme. It was shown to be involved also in the metabolism of isoxanthohumol (**Guo et al. 2006**) and xanthohumol interfered with CYP1A1 activity. Other arachidonic acid metabolising enzymes are ALOXs and COX1/2, but the known role of xanthohumol in the inhibition of COX1/2 (**Gerhäuser et al. 2002**) did not contribute to the inhibition of CCID formation, because this is independent of COX1/2 (**Kerjaschki et al. 2011, Madlener et al. 2010**).

The inhibition of ALOX15 in MCF-7 spheroids by xanthohumol is conceivable, and the inefficiency of xanthohumol to inhibit CCIDs that were induced by MDA-MB231 spheroids could have been due to the fact that MDA-MB231 cells are ALOX12/15 deficient (**Kerjaschki et al. 2011**). Note in this context that also baicalein did not inhibit MDA-MB231-spheroid induced CCID formation (**Fig. 5c**). This shows that CCID formation was exclusively mediated by the ALOX15 activity of MCF-7 spheroids but not by the ALOX12/15 activity of LECs.

Furthermore, MCF-7 cells in contrast to MDA-MB231 breast cancer cells are estrogen-receptor (ER) positive (**Roomi et al. 2005**) and previous studies have shown that

xanthohumol blocks the effects of estrogens. The flavonoid binds to the ER and it was postulated that this property may prevent breast cancer (**Gerhäuser et al. 2002**). It is however, unlikely that binding to estrogen receptor was the reason why xanthohumol inhibited CCID formation induced by MCF-7 cell spheroids, because some colon cancer spheroids induce gaps by the same mechanisms as MCF-7 cells (**Kerjaschki et al. 2011**), yet colon cancer cells do not express ER receptors. With MCF-7 spheroids, both, Bay11-7082 and xanthohumol exhibit their CCID-inhibitory properties at rather low concentrations (IC_{50} ~5-10 μM), whereas with MDA-MB231 spheroids the efficiency of xanthohumol was dramatically reduced (IC_{50} ~ 100μM). The weak inhibitory effect of xanthohumol in MDA-MB231 spheroids regarding CCID formation indicates again that Bay11-7082 and xanthohumol target different mechanisms. Our data suggest novel targets for anti-carcinogenic effects of xanthohumol. Whether inhibition of ALOX12/15 in MCF-7 cells is part of the CCID-inhibitory effect of xanthohumol is going to be addressed in future studies. Summing up, we show that the CCID assay is a reliable tool to study new compounds that can inhibit the intravasation of tumour emboli into lymphatics and to elucidate the respective mechanisms. Furthermore, we provide evidence of a new anti-metastatic property of xanthohumol that could be exploited for the treatment of breast cancer.

Acknowledgments

Grant Nos. GACR (P505/11/1163) and ED0007/01/01 (both to M.S.) from the Centre of the Region Haná for Biotechnological and Agricultural Research, a grant of the Fellinger foundation (to G.K.), grants of the Herzfelder family foundation (to T.S., H.D. and M.G.), a scholarship from the Austrian exchange sevice OeAD (to K.J.), and grants by the Austrian Science Fund, FWF, grant numbers P19598-B13 and P20905-B13 (W.M.) and by the European Union, FP7 Health Research, project number HEALTH-F4-2008-202047 (W.M.) are gratefully acknowledged.

Literature

Albini A, Dell'Eva R, Vené R, Ferrari N, Buhler DR, Noonan DM, Fassina G (2006) Mechanisms of the antiangiogenic activity by the hop flavonoid xanthohumol: NF-kappaB and Akt as targets. FASEB J 20(3): 527-529

Ambartsumian N, Klingelhofer J, Grigorian M, Christensen C, Kriajevska M, Tulchinsky E, Georgiev G, Berezin V, Bock E, Rygaard J, Cao R, Cao Y, Lukanidin E (2001) The metastasis-associated Mts1 (S100A4) protein could act as an angiogenic factor. Oncogene 20: 4685-4695

Andela VB, Schwarz EM, Puzas JE, O'Keefe RJ, Rosier RN (2000) Tumor metastasis and the reciprocal regulation of prometastatic and antimetastatic factors by nuclear factor kappaB. Cancer Res 60(23): 6557-6562

Bielenberg DR, Hida Y, Shimizu A, Kaipainen A, Kreuter M, Kim CC, Klagsbrun M (2004) Semaphorin 3F, a chemorepulsant for endothelial cells, induces a poorly vascularized, encapsulated, nonmetastatic tumor phenotype. J Clin Invest 114(9): 1260-1271

Budinsky AC, Brodowicz T, Wiltschke C, Czerwenka K, Michl I, Krainer M, Zielinski CC (1997) Decreased expression of ICAM-1 and its induction by tumor necrosis factor on breast-cancer cells in vitro. Int J Cancer 71(6): 1086-1090

Bolick DT, Orr AW, Whetzel A, Srinivasan S, Hatley ME, Schwartz MA, Hedrick CC (2005) 12/15-Lipoxygenase regulates intercellular adhesion molecule-1 expression and monocyte adhesion to endothelium through activation of RhoA and nuclear factor-κB. Artersioscler Thromb Vasc Biol 25(2): 2301-2307

Carlson RW, Allred DC, Anderson BO, Burstein HJ, Carter WB, Edge SB, Erban JK, Farrar WB, Goldstein LJ, Gradishar WJ, Hayes DF, Hudis CA, Jahanzeb M, Kiel K, Ljung BM, Marcom PK, Mayer IA, McCormick B, Nabell LM, Pierce LJ, Reed EC, Smith ML, Somlo G, Theriault RL, Topham, NS, Ward JH, Winer EP, Wolff AC (2009) Breast Cancer: Clinical Practice Guidelines in Breast Cancer, NCCN Cancer Clinical Practice Panel, J Natl Compr Canc Netw 7: 122-192

Colgate EC, Miranda CL, Stevens JF, Bray TM, Ho E (2007) Xanthohumol, a prenylflavonoid derived from hops induces apoptosis and inhibits NF-kappaB activation in prostate epithelial cells. Cancer Lett 246(1-2): 201-209

Deryugina EI, Bourdon MA, Jungwirth K, Smith JW, Strongin AY (2000) Functional activation of integrin alpha V beta 3 in tumor cells expressing membrane-type 1 matrix metalloproteinase. Int J Cancer 86(1): 15-23

Ferk F, Huber WW, Filipic M, Bichler J, Haslinger E, Misík M, Nersesyan A, Grasl-Kraupp B, Zegura B, Knasmüller S (2010) Xanthohumol, a prenylated flavonoid contained in beer, prevents the induction of preneoplastic lesions and DNA damage in liver and colon induced by the heterocyclic aromatic amine amino-3-methyl-imidazo[4,5-f]quinoline (IQ). Mutat Res 691(1-2): 17-22

Folmer F, Jaspars M, Solano G, Cristofanon S, Henry E, Tabudravu J, Black K, Green DH, Küpper FC, Aalbersberg W, Feussner K, Dicato M, and Diederich M (2009) The inhibition of TNF-α induced NF-κB activation by marine natural products. Biochem Pharmacol 78: 592-606

Gao X, Deeb D, Liu Y, Gautam S, Dulchavsky SA, Gautam SC (2009) Immunomodulatory activity of xanthohumol: inhibition of T cell proliferation, cell-mediated cytotoxicity and Th1 cytokine production through suppression of NF-kappaB. Immunopharmacol Immunotoxicol 31(3): 477-484

Gerhäuser C, Alt A, Heiss E, Gamal-Eldeen A, Klimo K, Knauft J, Neumann I, Scherf HR, Frank N, Bartsch H, Becker H (2002) Cancer chemopreventive activity of Xanthohumol, a natural product derived from hop. Mol Cancer Ther 1(11): 959-969

Gridling M, Stark N, Madlener S, Lackner A, Popescu R, Benedek B, Diaz R, Tut FM, Nha Vo TP, Huber D, Gollinger M, Saiko P, Ozmen A, Mosgoeller W, De Martin R, Eytner R, Wagner KH, Grusch M, Fritzer-Szekeres M, Szekeres T, Kopp B, Frisch R, Krupitza G. (2009) In vitro anti-cancer activity of two ethno-pharmacological healing plants from Guatemala Pluchea odorata and Phlebodium decumanum. Int J Oncol 34(4): 1117-1128

Guo J, Nikolic D, Chadwick LR, Pauli GF, van Breemen RB (2006) Identification of human hepatic cytochrome P450 enzymes involved in the metabolism of 8-prenylnaringenin and isoxanthohumol from hops (Humulus lupulus L.). Drug Metab Dispos 34(7): 1152-1159

Hartkorn A, Hoffmann F, Ajamieh H, Vogel S, Heilmann J, Gerbes AL, Vollmar AM, Zahler S (2009) Antioxidant effects of xanthohumol and functional impact on hepatic ischemia-reperfusion injury. J Nat Prod 72(10): 1741-1747

Honn KV, Tang DG, Grossi I, Duniec ZM, Timar J, Renaud C, Leithauser M, Blair I, Johnson CR, Diglio CA, Kimler VA, Taylor JD, Marnett LJ (1994) Tumour cell-derived 12(S)-hydroxyeicosatetraenoic acid induces microvascular endothelial cell retraction. Cancer Res 54: 565-574

Honn KV, Grossi IM, Diglio CA, Wojtukiewicz M, Taylor JD (1989) Enhanced tumor cell adhesion to the subendothelial matrix resulting from 12(S)-HETE-induced endothelial cell retraction. FASEB J 3(11): 2285-2293

Huang, C, Rajfur, Z, Borchers, C, Schaller, MD, Jacobson, K (2003) JNK phosphorylates paxillin and regulates cell migration. Nature 424: 219-223

Jenkinson SR, Barraclough R, West CR, Rudland PS (2004) S100A4 regulates cell motility and invasion in an in vitro model for breast cancer metastasis. Br J Cancer 90: 253-262

Jiang JG, Ning YG, Chen C, Ma D, Liu ZJ, Yang S, Zhou J, Xiao X, Zhang XA, Edin ML, Card JW, Wang J, Zeldin DC, Wang DW (2007) Cytochrome p450 epoxygenase promotes human cancer metastasis. Cancer Res 67(14): 6665-6674

Kerjaschki D, Bago-Horvath Z, Rudas M, Sexl V, Schneckenleithner C, Wolbank S, Bartel G, Krieger S, Kalt R, Hantusch B, Keller T, Nagy-Bojarszky K, Huttary N, Raab I, Lackner K, Krautgasser K, Schachner H, Kaserer K, Rezar S, Madlener S, Vonach C, Davidovits A, Nosaka H, Hämmerle M, Viola K, Dolznig H, Schreiber M, Nader A, Mikulits W, Gnant M, Hirakawa S, Detmar M, Alitalo K, Nijman S, Offner F, Maier TJ, Steinhilber D, Krupitza G (2011) Lipoxygenase mediates invasion of intrametastatic lymphatic vessels and propagates

lymph node metastasis of human mammary carcinoma xenografts in mouse. J Clin Invest 121(5): 2000-2012

Madlener S, Svacinová J, Kitner M, Kopecky J, Eytner R, Lackner A, Vo TP, Frisch R, Grusch M, De Martin R, Dolezal K, Strnad M, Krupitza G (2009) In vitro anti-inflammatory and anticancer activities of extracts of Acalypha alopecuroidea (Euphorbiaceae). Int J Oncol 35(4): 881-891

Madlener S, Saiko P, Vonach C, Viola K, Huttary N, Stark N, Popescu R, Gridling M, Vo NT, Herbacek I, Davidovits A, Giessrigl B, Venkateswarlu S, Geleff S, Jäger W, Grusch M, Kerjaschki D, Mikulits W, Golakoti T, Fritzer-Szekeres M, Szekeres T, Krupitza G (2010) Multifactorial anticancer effects of digalloyl-resveratrol encompass apoptosis, cell-cycle arrest, and inhibition of lymphendothelial gap formation in vitro. Br J Cancer 102(9): 1361-1370

Magalhães PJ, Carvalho DO, Cruz JM, Guido LF, Barros AA (2009) Fundamentals and health benefits of xanthohumol, a natural product derived from hops and beer. Nat Prod Commun 4(5): 591-610

Miranda CL, Stevens JF, Helmrich A, Henderson MC, Rodriguez RJ, Yang YH, Deinzer ML, Barnes DW, Buhler DR (1999) Antiproliferative and cytotoxic effects of prenylated flavonoids from hops (Humulus lupulus) in human cancer cell lines. Food Chem Toxicol 37(4): 271-285

Monteghirfo S, Tosetti F, Ambrosini C, Stigliani S, Pozzi S, Frassoni F, Fassina G, Soverini S, Albini A, Ferrari N (2008) Antileukemia effects of xanthohumol in Bcr/Abl-transformed cells involve nuclear factor-kappaB and p53 modulation. Mol Cancer Ther 7(9): 2692-2702

Nasarre P, Kusy S, Constantin B, Castellani V, Drabkin HA, Bagnard D, Roche J (2005) Semaphorin SEMA3F has a repulsing activity on breast cancer cells and inhibits E-cadherin-mediated cell adhesion. Neoplasia 7(2): 180-189

Nishimura A, Akeda K, Matsubara T, Kusuzaki K, Matsumine A, Masuda K, Gemba T, Uchida A, Sudo A (2010) Transfection of NF-κB decoy oligodeoxynucleotide suppresses pulmonary metastasis by murine osteosarcoma. Cancer Gene Ther Dec 24 PMID: 21183950

Orlowski RZ, Baldwin Jr AS (2002) NF-κB as a therapeutic target in cancer. Trends Mol Med 8(8): 385-389

Pan L, Becker H, Gerhäuser C (2005) Xanthohumol induces apoptosis in cultured 40-16 human colon cancer cells by activation of the death receptor- and mitochondrial pathway. Mol Nutr Food Res 49(9): 837-843

Pierce JW, Schoenleber R, Jesmok G, Best J, Moore SA, Collins T, Gerritsenet ME (1997) Novel inhibitors of cytokine-induced IκBα phosphorylation and endothelial cell adhesion molecule expression show anti-inflammatory effects invivo. J Biol Chem 272(34): 21096-21103

Rice RL, Tang DG, Hddadi M, Honn KV, Taylor JD (1998) 12(S)-Hydroxyeicosatetraenoic acid increases microfilament content in B16a melanoma cells: a protein kinase-dependent process. Int J Cancer 77: 271–278

Rosenstein Y, Park JK, Hahn WC, Rosen FS, Bierer BE, Burakoff SJ (1991) CD43, a molecule defective in Wiskott-Aldrich syndrome, binds ICAM-1. Nature 354: 233-235

Roomi MW, Ivanov V, Kalinovsky T, Niedzwiecki A, Rath M (2005) In vitro and in vivo antitumorigenic activity of a mixture of lysine, proline, ascorbic acid, and green tea extract on human breast cancer lines MDA-MB-231 and MCF-7. Med Oncol 22(2): 129-138

Schmidt-Hansen B, Ornås D, Grigorian M, Klingelhöfer J, Tulchinsky E, Lukanidin E, Ambartsumian N (2004) Extracellular S100A4 (mts1) stimulates invasive growth of mouse endothelial cells and modulates MMP-13 matrix metalloproteinase activity. Oncogene 23: 5487-5495

Schoppmann SF, Soleiman A, Kalt R, Okubo Y, Benisch C, Nagavarapu U, Herron GS, Geleff S (2004) Telomerase-immortalized lymphatic and blood endothelial cells are functionally stable and retain their lineage specificity. Microcirculation 11: 261-269

Spector AA, Gordon JA, Moore SA (1988) Hydroxyeicosatetraenoic acids (HETEs). Prog Lipid Res 27: 271-323

Srivastava RK, Kurzrock R, Shankar S (2010) MS-275 sensitizes TRAIL-resistant breast cancer cells, inhibits angiogenesis and metastasis, and reverses epithelial-mesenchymal transition in vivo. Mol Cancer Ther 9(12): 3254-3266

Stevens JF, Taylor AW, Deinzer ML (1999) Quantitative analysis of xanthohumol and related prenylflavonoids in hops and beer by liquid chromatography-tandem mass spectrometry. J Chromatogr A. 832(1-2): 97-107

Stevens JF, Page JE (2004) Xanthohumol and related prenylflavonoids from hops and beer: to your good health! Phytochemistry 65(10): 1317-1330

Strathmann J, Klimo K, Sauer SW, Okun JG, Prehn JH, Gerhäuser C (2010) Xanthohumol-induced transient superoxide anion radical formation triggers cancer cells into apoptosis via a mitochondria-mediated mechanism. FASEB J 24(8): 2938-2950

Takenaga K, Nakamura Y, Endo H, Sakiyama S (1994) Involvement of S100-related calcium-binding protein pEL98 (or mts1) in cell motility and tumor cell invasion. Jpn J Cancer Res 85: 831-839

Tang DG, Timar J, Grossi IM, Renaud C, Kimler VA, Diglio CA, Taylor JD, Honn KV (1993) The lipoxygenase metabolite, 12(S)-HETE, induces a protein kinase C-dependent cytoskeletal rearrangement and retraction of microvascular endothelial cells. Exp Cell Res 207: 361-375

Uchide K, Sakon M, Ariyoshi H, Nakamori S, Tokunaga M, Monden M (2007) Cancer cells cause vascular endothelial cell retraction via 12(S)-HETE secretion; the possible role of cancer cell derived microparticle. Ann Surg Oncol 14: 862-868

Vonach C, Viola K, Giessrigl B, Huttary N, Raab I, Kalt R, Krieger S, Vo TPN, Madlener S, Bauer S, Marian B, Hämmerle M, Kretschy N, Teichmann M, Hantusch B, Stary S, Unger C, Seelinger M, Eger A, Mader R, Jäger W, Schmidt W, Grusch M, Dolznig H, Mikulits W, Krupitza G (2011) NF-κB mediates the 12(S)-HETE-induced endothelial to mesenchymal transition of lymphendothelial cells during the intravasation of breast carcinoma cells. Br J Cancer in print

Zaidel-Bar R, Ballestrem C, Kam Z, Geiger B (2003) Early molecular events in the assembly of matrix adhesions at the leading edge of migrating cells. J Cell Sci 116(22): 4605-4613

Zeisberg M, Neilson EG (2009) Biomarkers for epithelial-mesenchymal transitions. J Clin Invest 119(6): 1429-1437

Zhang JS, Nelson M, Wang L, Liu W, Qian CP, Shridhar V, Urrutia R, Smith DI (1998) Identification and chromosomal localization of CTNNAL1, a novel protein homologous to alpha-catenin. Genomics 54: 149-154

Table 1

Selectin E (SELE) expression in TNFα -induced HUVECs						
Analysis		Control	TNFα	TNFα & **1 µM X**	TNFα & **10 µM X**	TNFα & **30 µM X**
Inflammatory reaction	SELE (OD)	**0.053** SD 0.002	**0.130** SD 0.01	**0.115** SD 019	**0.121** SD 0.024	**0.112** SD 0.022
Cytotoxicity	CalceinAM (OD)	46.4 SD 2.7	44.5 SD 6.4	44.6 SD 3.9	43.8 SD 5.3	38.5 SD 8.0

1 x 10^4 HUVECs /well were seeded into 96-well plates and grown to confluence. Indicated concentrations of xanthohumol (X) were added 1 h prior to application of 10 ng/ml TNFα for another 4 h. Then cells were fixed and SELE levels analysed by ELISA. In parallel, extracts were analysed by CalceinAM assay to monitor non-specific extract toxicity.

Viola et al. Figure legends

Figure 1: Inhibition of CCIDs by Bay11-7082
a) MCF-7 spheroids were placed on LEC monolayers and co-cultivated for 4 h either with medium alone and solvent (DMSO; Co), or with increasing concentrations Bay11-7082 (1-25 µM) and then the areas of CCIDs were measured. **b)** MCF-7 spheroids and LEC monolayers (MCF-7&LEC), or MCF-7 spheroids alone, or LEC monolayers alone were pretreated for 30 min with 15 µM Bay11-7082, then the inhibitor was thoroughly removed and the pretreated cell types were co-cultivated with the respective untreated partner cell line (either untreated LECs or MCF-7, respectively) for 4h, and then CCID areas were measured.
The CCIDs underneath 12 spheroids were analysed for each condition. Experiments were done in triplicate, error bars indicate SEM and asterisks significance ($p<0.05$).
c) MCF-7 cells were grown as monolayer and treated with 15 µM Bay11-7082 for the indicated times (0, 0.2h, 0.5h, 1h, 2h). Then cells were lysed, proteins separated by SDS gel electrophoresis and subjected to Western blotting using anti-semaphorine 3F (SEMA3F) antibody. Staining with Ponceau S and immunoblotting with anti-β-actin antibody controlled equal sample loading.

Figure 2: Inhibition of LEC migration by Bay11-7082
a) LECs were grown to confluence and then pretreated with 10 µM Bay11-7082 or solvent (DMSO) for 0.5 h and then LECs were stimulated with 1 µM 12(S)-HETE for 1 h. Then cells were lysed, protein separated by SDS gel electrophoresis and subjected to Western blotting using the indicated antibodies. Staining with Ponceau S and immunoblotting with anti-β-actin antibody controlled equal sample loading. **b) Upper panel:** LEC monolayers were pretreated with 10 µM Bay11-7082 for 0.5 h and then untreated MCF-7 spheroids were placed onto the LEC monolayers and the size of LECs underneath the spheroid was measured after 4 h of co-incubation. Average LEC size (length): 36.25 µm (n=15). **Lower panel:** This is the reciprocal experiment in which MCF-7 spheroids were pretrated with 10 µM Bay11-7082 for 0.5 h and then placed onto untreated LEC monolayers and the size of LECs underneath the spheroid was measured after 4 h of co-incubation. Average LEC size (length): 53.25 µm (n=15). Pictures were taken using a Zeiss Axiovert microscope and Axiovision software to measure cell sizes. LECs were stained with cell tracker (green).

Figure 3: Analysis of adhesion protein expression upon 12(S)-HETE and Bay11-7082 treatment
LECs growing in 6-well plates were treated with 1 µM 12(S)-HETE for 0.2, 0.5, 2, 4 and 8 h (**a, b, left panels)**, or LECs were pre-treated with 15 µM Bay11-7082 or solvent (DMSO) for 0.5 h and then stimulated with 1 µM 12(S)-HETE for 0.5 h (**a, b, right panels**). Then, cells were harvested and protein lysates were analysed by Western blotting using antibodies against (**a**) CD31 and (**b**) ICAM-1. Equal sample loading was controlled by β-actin expression.
c) Analysis of E-selectin expression. LECs were grown in 12 well plates and pre-treated with Bay11-7082 for 0.5 h and thereafter stimulated with 20 ng/ml TNF-α or solvent (Co) for 0.5 h, or with 1 µM 12(S)-HETE for the indicated times. PCR products were analysed on the Abi Prism 7000 sequence detection system. Duplicate samples were analyzed. GAPDH served as internal control. Relative expression numbers were calculated using the $\Delta\Delta C_T$ method.

Figure 4: a) Inhibition of CCIDs by wogonin and baicalein
MCF-7 spheroids were placed on LEC monolayers and co-cultivated for 4 h either with solvent (DMSO; Co) or with increasing concentrations of wogonin (5-75 µM) or 100 µM baicalein and then the areas of CCIDs were measured.
b) Synergistic inhibition of CCIDs by baicalein and Bay11-7082
MCF-7 spheroids and LEC co-cultures were treated with 10 µM Bay11-7082 and/or 100 µM baicalein for 4 h.Then the CCID areas underneath at least 12 spheroids (per condition) were measured using a Zeiss Axiovert microscope and Axiovision software. Error bars indicate SEM, asterisks significe compared to control ($p<0.05$).
c) Analysis of LEC protein expression upon treatment with baicalein
LECs were grown to confluence and then pretreated with 100 µM baicalein or solvent (DMSO) for 0.5 h and then LECs were stimulated with 1 µM 12(S)-HETE for 1 h. Cells were lysed, proteins separated by SDS gel electrophoresis, and subjected to Western blotting using the indicated antibodies. Staining with Ponceau S and immunoblotting with anti-β-actin antibody controlled equal sample loading.

Figure 5: Inhibition of CCIDs by xanthohumol
a) MCF-7 spheroids were placed on LEC monolayers and co-cultivated either with solvent (DMSO; Co) or with 10 µM xanthohumol for 4 h and then the areas of CCIDs were photographed. Left panel: microscopic power field of a CCID underneath a MCF-7 spheroid of an untreated co-culture and right side: of a co-culture treated with 25 µM xanthohumol. Scale bars: 700 µm
b) MCF-7 spheroids and **c)** MDA-MB231 spheroids were placed on LEC monolayers and co-cultivated either with solvent (DMSO; Co) or with the indicated concentrations of xanthohumol, or 100 µM baicalein, or 10 µM Bay11-7082 for 4 h and then the areas of CCIDs were measured using a Zeiss Axiovert microscope and Axiovision software. Error bars indicate SEM, asterisks significance compared to control ($p<0.05$).

Figure 6:
a) Inhibition of CYP1A1 activity in breast cancer cells by xanthohumol and proadifen
MCF-7 and MDA-MB231 cells were kept under steroid-free conditions and treated with proadifen (5 µM; P), or xanthohumol (5 µM, 25 µM; X), or solvent (DMSO; Co). Then, 5 µM ethoxyresorufin was added and after 200 min the formation of resorufin was analysed, which is specific for CYP1A1 activity. Experiments were done in triplicate, error bars indicate SEM and asterisks significance ($p<0.05$).
b) Analysis of migratory markers in LECs upon treatment with xanthohumol
LECs were grown to confluence and then pretreated with 25 µM xanthohumol or solvent (DMSO) for 0.5 h and then LECs were stimulated with 1 µM 12(S)-HETE for 1 h. Cells were lysed, proteins separated by SDS gel electrophoresis, and subjected to Western blotting using the indicated antibodies. Staining with Ponceau S and immunoblotting with anti-β-actin antibody controlled equal sample loading.

F1a

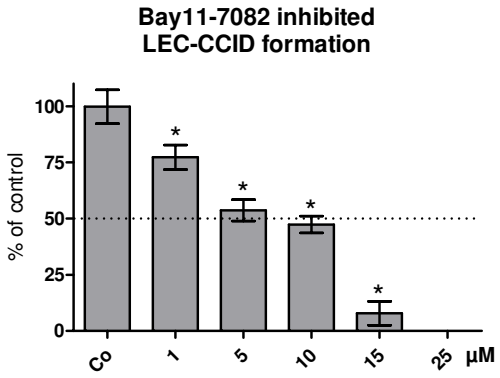

F1b

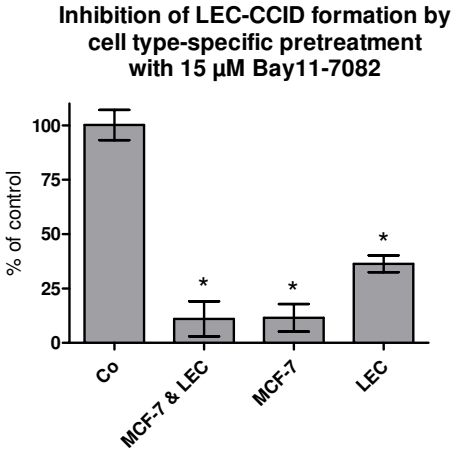

F1c

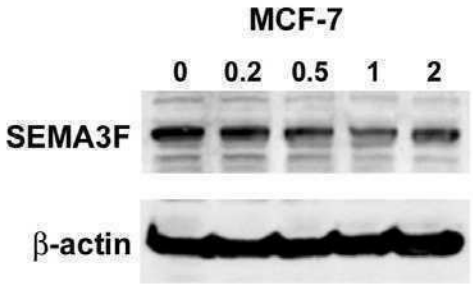

Viola et al Figure 1

F2a

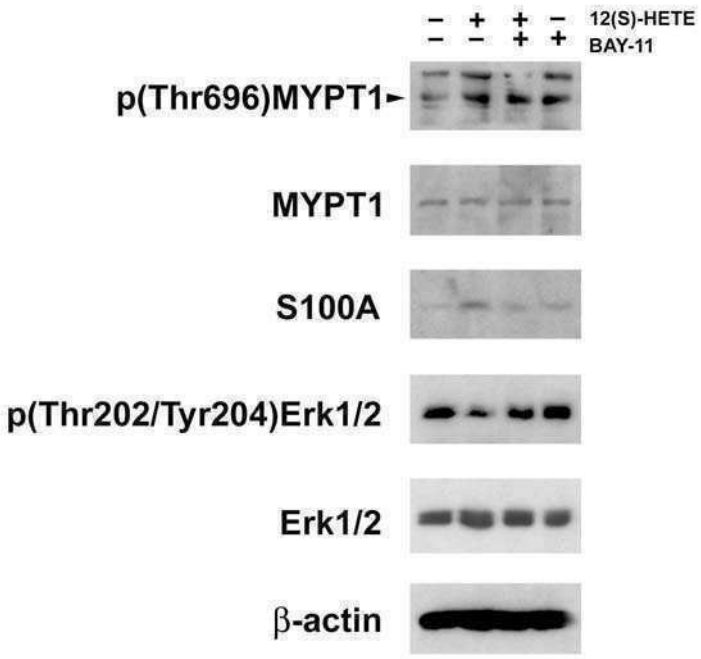

F2b

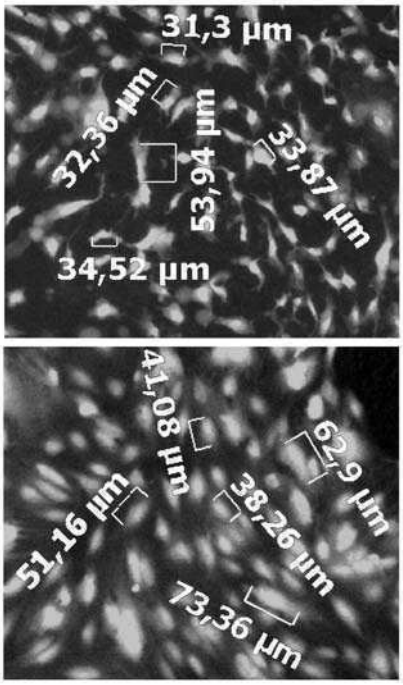

Viola et al Figure 2

F3a

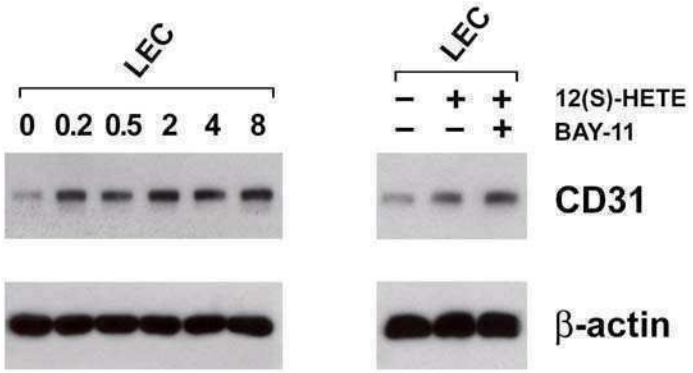

F3b

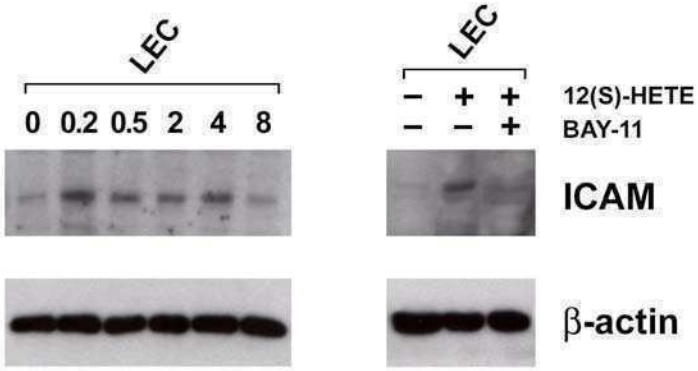

F3c

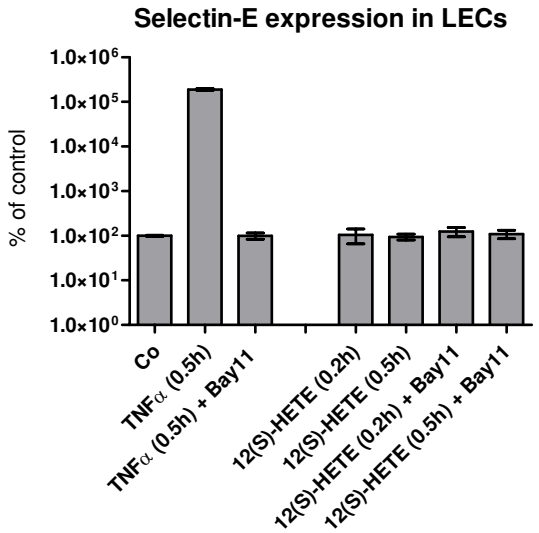

Viola et al Figure 3

F4a

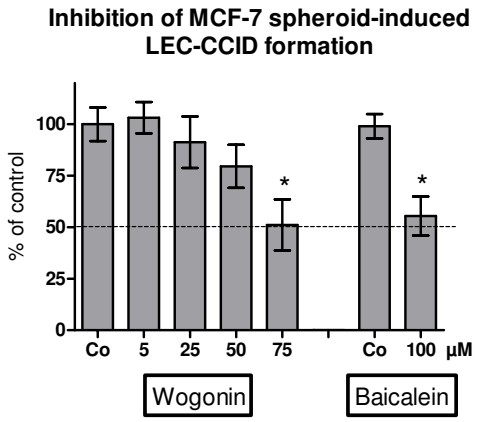

F4b

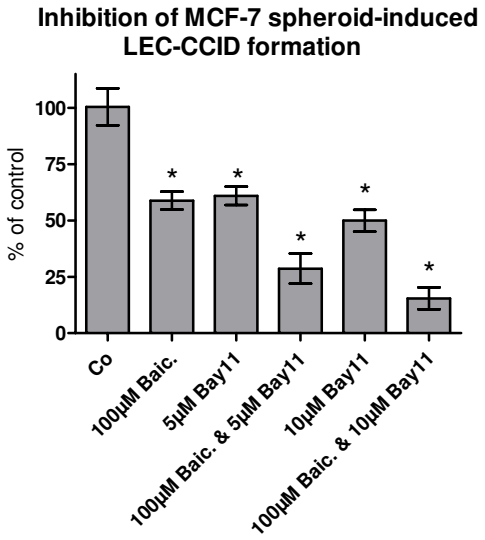

F4c

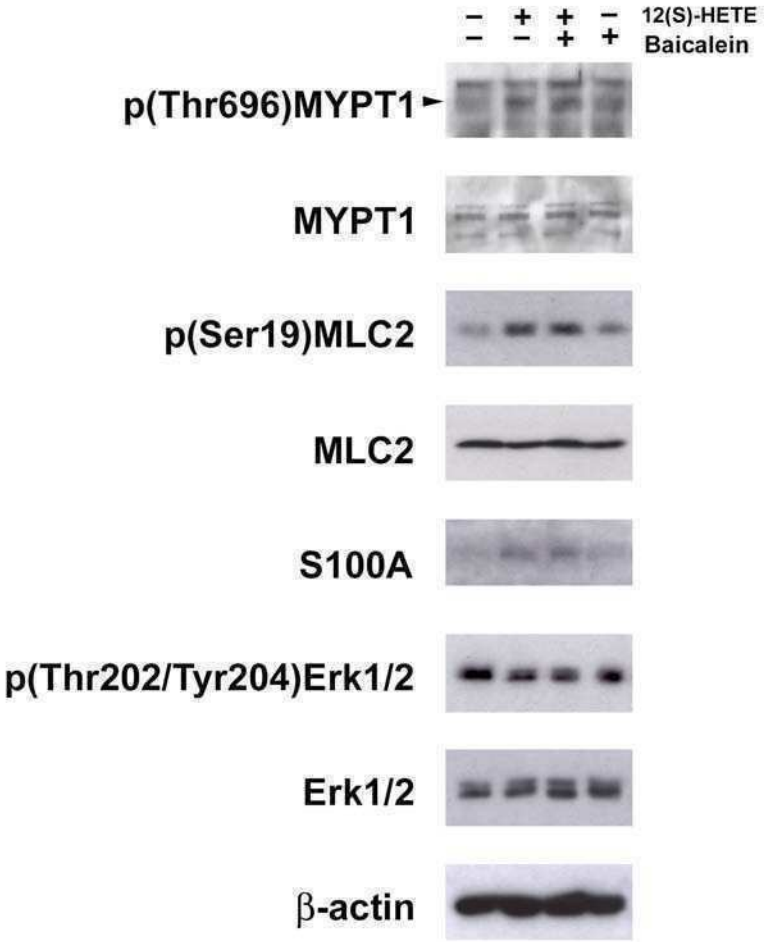

Viola et al Figure 4

F5a

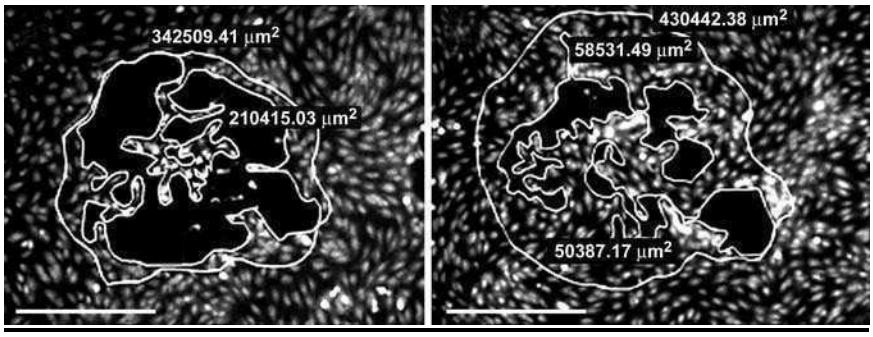

F5b

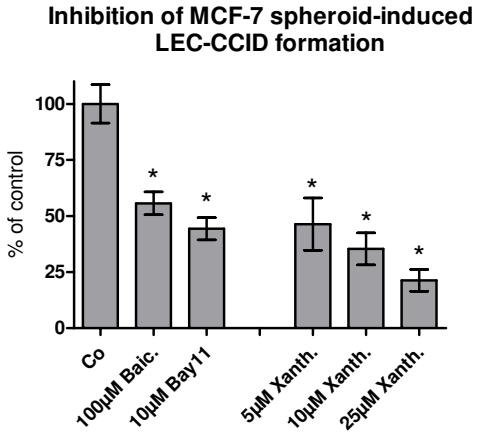

F5c

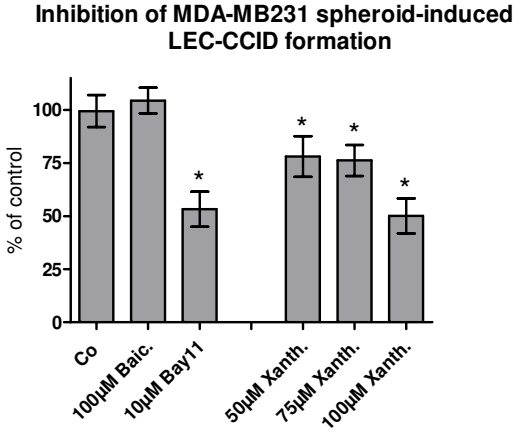

Viola et al Figure 5

F6a

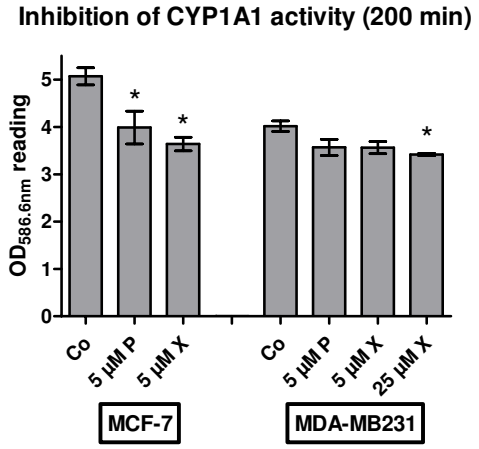

F6b

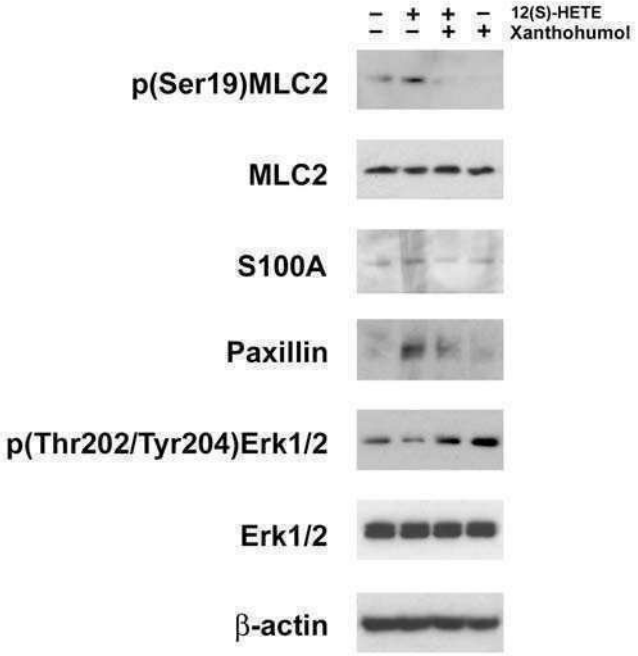

Viola et al Figure 6

Fractionation of an anti-neoplastic extract of *Pluchea odorata* eliminates a property typical for a migratory cancer phenotype.

Seelinger M., Popescu R., Seephonkai P., Singhuber J., **Giessrigl B.**, Unger C., Bauer S., Wagner K.H., Fritzer-Szekeres M., Szekeres T., Diaz R., Tut F.T., Frisch R., Feistel B., Kopp B. and Krupitza G.

Evidence-based Compl. and Alt. Medicine, ***submitted.***

Fractionation of an anti-neoplastic extract of *Pluchea odorata* eliminates a property typical for a migratory cancer phenotype

Mareike Seelinger[1], Ruxandra Popescu[2], Prapairat Seephonkai[2], Judith Singhuber[2], Benedikt Giessrig[1], Christine Unger[1], Sabine Bauer[1], Karl-Heinz Wagner[3], Monika Fritzer-Szekeres[4], Thomas Szekeres[4], Rene Diaz[5], Foster M. Tut[5], Richard Frisch[5], Björn Feistel[6], Brigitte Kopp[2], Georg Krupitza[1].

[1] Institute of Clinical Pathology, Medical University of Vienna, Waehringer Guertel 18-20, A-1090 Vienna, Austria
[2] Department of Pharmacognosy, Faculty of Life Sciences, University of Vienna, Althanstrasse 14, A-1090 Vienna, Austria
[3] Department of Nutritional Sciences, University of Vienna, Althanstrasse 14, Austria
[4] Clinical Institute of Medical and Chemical Laboratory Diagnostics, Medical University of Vienna, Waehringer Guertel 18-20, Austira;
[5] Institute for Ethnobiology, Playa Diana, San José/Petén, Guatemala;
[6] Finzelberg GmbH & Co.KG, Koblenzer Strasse 48-54, D-56626 Andernach, Germany

Short title: Distinct pharmacological activities in fractions of the Maya healing plant *Pluchea odorata*

Key words: *Pluchea odorata*, oncogenes, mobility proteins, metastasis,

Correspondence:
Georg Krupitza, Institute of Clinical Pathology, Medical University of Vienna, Waehringer Guertel 18-20, A-1090, Vienna, Austria
e-mail: georg.krupitza@meduniwien.ac.at,

Abstract

Introduction: Several studies demonstrated that anti-inflammatory remedies exhibit excellent anti-neoplastic properties. An extract of the *Asteracea Pluchea odorata,* which is used for wound healing and against inflammatory conditions, was fractionated and properties correlating to anti-neoplastic- and wound healing effects were separated.
Methods: Up to six fractionation steps using silica gel, sephadex columns and distinct solvent systems were used and eluted fractions were analysed by thin layer chromatography, apoptosis- and proliferation assays. The expression of oncogenes and proteins regulating cell migration was investigated by immuno-blotting after treating HL60 cells with the most active fractions.
Results: Sequential fractionations enriched anti-neoplastic activities which suppressed oncogene expression of i.e. JunB, c-Jun, c-Myc, and Stat3. Furthermore, a fraction (F4.6.3) inducing-, or keeping-up expression of the mobility markers MYPT, ROCK1 and paxillin could be separated from another fraction (F5.3.3.7), which inhibited these markers.
Conclusions: Wound healing builds up scar- or specific tissue and hence, compounds enhancing cell migration support this process. In contrast, successful anti-neoplastic therapy combats tumour progression and thus, suppression of cell migration is mandatory.

Introduction

Drug discovery is a constant need for bio-medical research and clinical progress. Particularly mega-bio-diversity areas such as the tropical rainforests of Central America are very promising for the discovery of new pharmaceutical lead compounds. Therefore, we chose an ethno-medical approach to drug discovery and focussed on traditional remedies of the Maya to pre-select plants with proven health effects.

Traditional medicine plants are often used for hundreds of years (**Fabricant and Farnsworth 2001**), which is the reason why no or only little toxic effects in humans can be expected. Especially in Africa and Central and South America traditional medicine is advised by a shamans, curanderos or herbalists who often keep the use of the healing plants as a secret (**Rastogi and Dhawan 1982**). Although these plants are used since ages little is known about the "Pinciples of Activity" and/or the targeted cellular mechanisms and hence, these remedies have a great potential for drug development. We aimed for the separation and isolation of distinct properties of the Maya healing plant *Pluchea odorata* which are relevant for anticancer treatment. *P. odorata* grows in the USA, Mexico, Belize, Guatemala, Panama, Cayman Islands, Guadeloupe, Jamaica, Puerto Rico, St. Lucia, Venezuela and Ecuador (Germplasm Resources Information Network, United States Department of Agriculture, 9 November 2004, http://www.ars-grin.gov/cgi-bin/npgs/html/taxon p.104497) and is still used by the Maya to treat common cold, fever, flu, head colds, headache, hypertension, neuralgia, ophthalmia, palsy, pneumonia, snake bite, swellings, inflammation, and bruises of the skin (**Arvigo and Balick 1998**). The medical solution is prepared by boiling two handfuls of leaves in one gallon of water and then it is frequently applied on the affected area until the inflammation subsides (**Balick and Lee 2005**). Further the plant is described as being antidote, astringent, diaphoretic, and haemostatic (**Johnson 1999**), as well as traditionally used by mothers after giving birth to decrease the risk for infections and conveyance of tissue recovery (**Arvigo and Balick 1998**). **Gridling et al. (2009**) and **Bauer et al. (2011**) describe a strong anti-neoplastic effect of the dichloromethane extract in HL60 and MCF-7 cells and an anti-inflammatory response in HUVECs.

Pharmaceutical drugs are prepared under standardised conditions and usually contain just one Active Principle. In contrast, ethno-pharmacologic remedies are mixtures of a vast number of compounds, which are in many cases unknown, and vary in their composition and activity depending on the growth area and the time of collection. This makes them difficult for application and trading. Moreover, plant extracts can also contain compounds that are

systemically toxic or counteract the desired effect of the Active Principle(s). On the other hand, some of the different compounds in a plant extract can synergise. The present work will give examples of this phenomenon. A common reason to terminate *a priori* successful therapies of all kinds of cancer and other diseases is the acquisition of drug resistance. However, it has not been reported so far that complex plant mixtures induce treatment resistances in patients, most likely because several distinct Active Principles target various intra- and inter-cellular signalling pathways simultaneously thereby preventing that the organism develops an "escape mechanism". Thus, the development of complex extracts should be considered as a strategy to treat cancer. Standardisation procedures for such mixtures must be individually developed to provide therapeutics which are effective and safe and do not exhibit from batch to batch variations. The fractionation and accompanying testing in bio-assays and by appropriate analyses are a feasible concept for standardisation and remedies emerging along such procedures can be approved by national agencies (i.e. Avemar, **WO 2004014406 (A1):** "Use of a fermented wheat germ extract as anti-inflammatory agent" by Hidvegi and Resetar).

Here we describe a fractionation approach of the dichloromethane extract of *P. odorata*, which was constantly controlled regarding its activity by bio-assays and analyses that can be standardised. This resulted in fractions causing distinct cellular responses indicative for wound healing or anti-neoplastic properties.

Material and Methods

Plant material

The aerial parts (leaves, caulis, florescence) of *Pluchea odorata* (L.) Cass. was collected in Guatemala, Departamento Petén, near the north-western shore of Lago Petén Itzá, San José, within an area of four year old secondary vegetation ~1 km north of the road from San José to La Nueva San José (16°59'30" N, 89°54'00" W). Voucher specimens (leg. G. Krupitza & R. O. Frisch, Nr. 1-2009, 08. 04. 2009, Herbarium W) were archived at the Museum of Natural History, Vienna, Austria. 6 kg of air dried plant material have been extracted with dichloromethane by Björn Feistel (Finzelberg GmbH & Co.KG, Andernach, Germany), and the extract stored in an exiccator in the dark at 4°C until use.

Plant extraction and fractionation

Plant extracion with dichloromethane was essentially as described earlier (**Gridling et al. 2009, Bauer et al. 2011**).

Vacuum Liquid Chromatography (VLC) was used for the separation of large amounts of extract. 36 g crude dichloromethane extract was re-dissolved in dichloromethane, mixed with 70 g silica gel and evaporated to dryness and ground in a mortar to obtain a homogenous powder. A 12 x 40 cm column was packed with 900 g silica gel, on top the silica gel-containing extract, and covered with sea sand to ballast the sample. The mobile phase was passed through by application of vacuum. **Table 1** shows the mobile phases used. After checking the collected fractions by TLC, those with similar bands were recombined.

Table 1 Mobile phases used for VLC of the dichloromethane extract

Mobile phase	**Relation**	**Volume (l)**
Petroleum ether		4
Petroleum ether: chloroform	9 : 1	5
Chloroform		12
Chloroform: methanol	9 : 1	9
Chloroform: methanol	7 : 3	9
Chloroform: methanol	5 : 5	9
Chloroform: methanol	3 : 7	9
Chloroform: methanol	1 : 9	9
Methanol		9

VLC-fractionation of F1: 10 g of F1 were dissolved in dichloromethane, mixed with 20 g silica gel, evaporated to dryness, refined in a mortar and applied on top a 5 x 60 cm silica gel column. Compounds were eluted with the mobile phases shown in **table 2** by applying vacuum. Collected fractions were checked by TLC and similar fractions were recombined.

Table 2 Mobile phases used for VLC of F1

Mobile phase	**Relation**	**Volume (l)**
Dichloromethane: hexan	8 : 2	2
Dichloromethane		2
Dichloromethane: ethyl acetate	8 : 2	1
Dichloromethane: ethyl acetate	6 : 4	1
Dichloromethane: ethyl acetate	4 : 6	1
Dichloromethane: ethyl acetate	2 : 8	1
Ethyl acetate		1
Ethyl acetate: methanol	8 : 2	1
Ethyl acetate: methanol	6 : 4	1

Column chromatography (CC)-fractionation of F2.6: Fractions with less than 2 g CC were eluted without vacuum. 1.6 g F2.6 were dissolved in dichloromethane, mixed with 3 g silica gel, evaporated to dryness, placed on top a 5 x 50 cm silcia gel column and eluted with mobile phases shown in **table 3**. The collected fractions were checked by TLC and those with similar band patterns were recombined.

Table 3 Mobile phases used for CC of F2.6

Mobile phase	**Relation**	**Volume (l)**
Dichloromethane	100 %	1
Dichloromethane: ethyl acetate	80 : 20	2
Dichloromethane: ethyl acetate	60 : 40	1
Dichloromethane: ethyl acetate	40 : 60	1
Dichloromethane: ethyl acetate	20 : 80	1
Ethyl acetate	100 %	1

CC-fractionation of F3.3 and F3.6: 1.14 g of F3.3 or 0.32 g of F3.6 were dissolved in dichloromethane and methanol (90:3.5) and applied on top a 3.5 x 40 cm sephadex column which was conditioned with methanol (2.5 x 40 cm for 3.6). Then, the loaded column was covered with some more sephadex to protect the sample. Methanol was used as mobile phase. Fractions were collected, checked by TLC and those with similar band patterns were recombined.

CC-fractionation of F4.3.3: 1.08 g F3.3 was dissolved in dichloromethane, placed on top of a 2 x 30 cm silica gel column and covered with silica gel. Mobile phases were used as illustrated in **table 4**. Fractions were checked by TLC and those with similar band patterns were recombined.

Table 4 Mobile phases used for CC of F4.3.3

Mobile phase	**Relation**	**Volume (ml)**
Dichloromethane	100 %	500
Dichloromethane: ethyl acetate	90 : 10	500
Dichloromethane: ethyl acetate	80 : 20	500
Dichloromethane: ethyl acetate	60 : 40	500
Dichloromethane: ethyl acetate	40 : 60	500
Dichloromethane: ethyl acetate	20 : 80	500
Ethyl acetate	100 %	500

CC-fractionation of F5.3.3.7: 145.64 mg F5.3.3.7 was dissolved dichloromethane and applied on a dichloromethane-conditioned 80 x 1.5 cm silica gel column and fractionated with one litre solvent (chloroform: methanol: water, 95:1.5:0.1). Fractions were collected in tubes, ten drops per minute, and every 30 minutes the tubes were changed. Afterwards the column was washed with 300 ml methanol. Fractions were checked by TLC and those with similar band patterns were recombined.

CC-fractionation of F4.6.3: 20 mg F4.6.3 (very oily) was dissolved in dichloromethane, mixed with silica gel and applied on top a 2.5 x 15 cm dichloromethane conditioned silica gel column. Successful elution was achieved with dichloromethane:ethylacetate (50:50). Fractions were checked by TLC and those with similar band patterns were recombined.

Thin layer chromatography (TLC)

TLC was used for detecting the best solvent combination for VLC or CC or as a finger print of new fractions. Stationary phase and mobile phases are described in **table 5**. The mobile phase varied between six solvent systems. Plates were detected under UV_{254}, UV_{366} and visible light, before and after spraying with anisaldehyd sulphuric acid reagent (ASR). ASR consisted of 0.5 ml anisaldehyd, 10 ml glacial acetic acid, 85 ml methanol and 5 ml H_2SO_4 (sulfuric acid). The sprayed plate was heated at 100 °C for five minutes and then compounds were detected at UV and visible light. Unless otherwise stated 8 µl extract or fraction were applied to the plate.

Table 1 Stationary phase, mobile phases and detection methods used for TLC

Stationary phase	silica gel plates 60 F254 (Merck, Darmstadt, Germany)	
Mobile phase	TLC system 1: chloroform: methanol: water	90:22:3.5
	TLC system 2: chloroform: methanol: water	90:3.5:0.2
	TLC system 3: chloroform: methanol: water	70:30:10
	TLC system 4: dichloromethane: ethyl acetate	80:20
	TLC system 5: dichloromethane: ethyl acetate	85:15
	TLC system 6: chloroform: methanol: water	70:22:3.5
Detection	UV_{254}, UV_{366}, visible light Anisaldehyd sulphuric acid reagent (ASR)	

Cell culture

HL-60 (human promyelocytic leukaemia cell) cells were purchased from American Type Culture Collection (ATCC). The cells were grown in RPMI 1640 medium which was supplemented with 10 % heat-inactivated fetal calf serum (FCS), 1 % Glutamax and 1 % Penicillin-Streptomycin. Both, medium and supplements were obtained from Life Technologies (Carlsbad, CA, USA). The cells were kept in humidified atmosphere at 37 °C containing 5 % CO_2.

Proliferation assay

Proliferation assays were performed to analyse the inhibition of proliferation of HL-60 cells treated with extract or fractions of *P. odorata*. Extract and fractions were dissolved in ethanol (final concentration was 0.2 %). HL-60 cells were seeded in 24-well plates at a concentration of 1 x 10^5 cells per ml RPMI medium allowing logarithmic growth within the time of treatment with plant extract or fractions. The control was treated with solvent. After 24 and 48 hours the number of cells was determined using the Sysmex Cell Counter (Sysmex Corp., Kobe, Japan). Experiments were done in triplicate. Percentage of cell division progression compared to the untreated control was calculated by applying the following formula:

$$\frac{C_{48\,or\,72h} + drug - C_{24h} + drug}{C_{48\,or\,72h} - drug - C_{24h} + drug} \times 100 = \%\ cell\ division$$

Apoptosis assay

Determination of cell death by Hoechst 33258 (HO) and propidium iodide (PI) double staining (both Sigma, St. Louis, MO) allows identifying the amount and the type of cell death

(early or late apoptosis or necrosis). Therefore HL-60 cells were seeded in a 24-well plate at a concentration of 1 x 10^5 cells per ml RPMI medium. Cells were treated with fractions or extract of *P. odorata.* The cells were incubated for 8, 24, 48 and/or 72 hours, depending on the experiment. At each time point 100 µl cell suspension of each well were transferred into separate wells of a 96-well plate and Hoechst 33285 and propidium iodide were added at final concentrations of 5 µg/ml and 2 µg/ml, respectively. After one hour of incubation at 37 °C, stained cells were examined and photographed with an Axiovert fluorescence microscope (Zeiss, Jena, Germany) equipped with a DAPI filter. Type and number of cell deaths were evaluated by visual examination of the photographs according to the morphological characteristics revealed by HOPI staining. Experiments were done in triplicate.

Western Blotting

Preparation of lysates: HL60 cells were seeded in a tissue culture flask at a concentration of 1 x 10^6 cells per ml RPMI medium. *P. odorata* fractions F1, F4.6.3 and F5.3.6.7 were analysed by western blots. HL60 cells were either incubated with 40 µg/ml F1 or with 10 µg/ml of one of the other two *P. odorata* fractions for the indicated times. At each time point, 4 x 10^6 cells were harvested, placed on ice and centrifuged (1000 rpm, 4 °C, 4 min). Then, the supernatant (medium) was discarded and the pellet was washed twice with cold phosphate buffered saline (PBS, pH 7.2), and centrifuged (1000 rpm, 4 °C, 4 min). The cell pellet was lysed in a buffer containing 150 mM NaCl, 50 mM Tris (pH 8.0), 1 % Triton-X-100, 1 mM phenylmethylsulfonyl fluoride (PMSF) and 1 mM protease inhibitor cocktail (PIC) (Sigma, Schnelldorf, Germany). Afterwards the lysate was centrifuged at 12000 rpm for 20 min at 4 °C. Supernatant was transferred into a 1.5 ml tube and stored at -20 °C for further analyses.
Gel electrophoresis (SDS-PAGE) and blotting: Equal amounts of protein samples (lysate) were mixed with sodium dodecyl sulfate (SDS) sample buffer (1:1) and loaded onto a 10 % polyacrylamide gel. Proteins were separated by polyacrylamide gel electrophoresis (PAGE) at 120 Volt for approximately one hour. To make proteins accessible to antibody detection, they were electrotransferred from the gel onto a polyvinylidene difluoride (PVDF) Hybond membrane (Amersham, Buckinghamshire, UK) at 95 Volt for 80 minutes. Membranes were allowed to dry for 30 minutes to provide fixing of the proteins on the membrane. Methanol was used moist the membranes. Equal sample loading was checked by staining the membrane with Ponceau S (Sigma, Schnelldorf, Germany).
Protein detection: After washing with PBS or TBS (Tris buffered saline, pH 7.6), membranes were blocked in PBS- or TBS-milk (5 % non-fat dry milk in PBS containing 0.5 % Tween 20

or TBS containing 0.1 % Tween 20) for one hour at room temperature. Then membranes were washed with PBS/T (PBS containing 0.5 % Tween 20) or TBS/T (TBS containing 0.1 % Tween 20), changing the washing solution four to five times every five minutes. Then every membrane was incubated with a primary antibody (1:500) in blocking solution (according to the data sheet TBS-, PBS- milk or TBS-, PBS- BSA), at 4 °C over night gently shaking. Subsequently the membrane was again washed with PBS/T or TBS/T, and incubated with the second antibody (peroxidase-conjugated goat anti-rabbit IgG or anti-mouse IgG) diluted 1:2000 for one hour at room temperature. After washing the membranes chemiluminescence was developed with enhanced chemiluminescence (ECL) plus detection kit (Amersham, UK) (two seconds to ten minutes) and membranes were exposed to the Lumi-Imager TM F1 (Roche) for increasing times.

Antibodies

Monoclonal mouse ascites fluid anti-acetylated α-tubulin (6-11B-1), and β actin (AC-15) antibodies were from Sigma (St. Louis, MO, USA). Monoclonal mouse α-tubulin (DM1A), β-tubulin (H-235), Cdc25A (F-6), and polyclonal rabbit paxillin (H-114), ROCK-1 (C8F7), c-Jun (H-79), Jun b (210) were from Santa Cruz Biotechnology, Inc.(Santa Cruz, CA, USA). Monoclonal rabbit cleaved caspase 8 (Asp391) (18C8) and phospho-Stat3 (Tyr705)(D3A7) antibodies and polyclonal rabbit cleaved caspase 3 (Asp175), human specific cleaved caspase 9 (Asp330), phospho-Chk2 (Thr68), Chk2, phospho-myosin light chain 2 (MLC2-Ser19), myosin light chain 2, Stat3, and MYPT1 were from Cell Signaling (Danvers, MA, USA). Polyclonal rabbit phospho-Cdc25A (Ser177) antibody was from Abgent (San Diego, CA, USA), polyclonal rabbit Phospho-MYPT1 (Thr696) from Upstate (NY, USA), mouse monoclonal γH2AX (pSer139) (DR 1017) from Calbiochem (San Diego, CA, USA), and mouse monoclonal c-Myc Ab-2 (9E10.3) from Thermo Fisher Scientific, Inc. (**xxxxxxxxxxxxxxxxxxxxxxx**). The secondary antibodies peroxidase-conjugated anti-rabbit IgG and anti-mouse IgG were purchased from Dako (Glostrup, Denmark).

Statistical Analysis

For statistical analyses Excel 2003 software and Prism 5 software package (GraphPad, San Diego, CA, USA) were used. The values were expressed as mean ± standard deviation and the Student's T-test was applied to compare differences between control samples and treatment groups. Statistical significance level was set to $p < 0.05$.

Results and Discussion

The dichloromethane extract of *P. odorata* exhibits strong anti-neoplastic activity (**Fig. 1a**). Therefore, we fractionated this extract and constantly monitored the activities by bio-assays measuring apoptosis- and/or proliferation rates to get closer to the Active Principles. In the first round the crude extract was split in three distinct fractions of which fraction F1 exhibited the strongest anti-proliferative and pro-apoptotic activity (**Fig 1b, c**). 40 µg F1/ml induced caspase 3 and decreased β-actin- and α-tubulin levels and therefore, also reduced acetylation levels of α-tubulin were detected within 4 h of treatment (**Fig.1d**). This suggested that the overall protein decrease was due to the early activation of caspase 3 and subsequent cell death.

Fig 1a

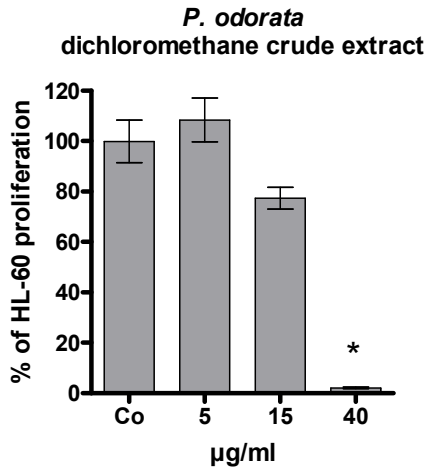

Fig 1b

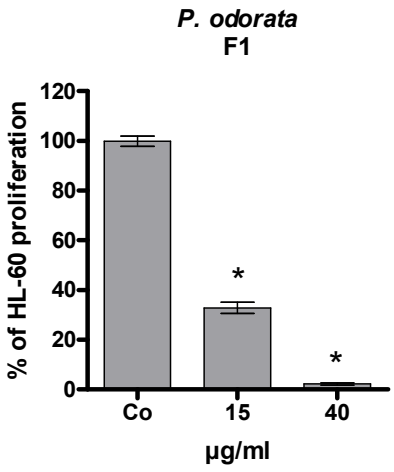

Fig 1c

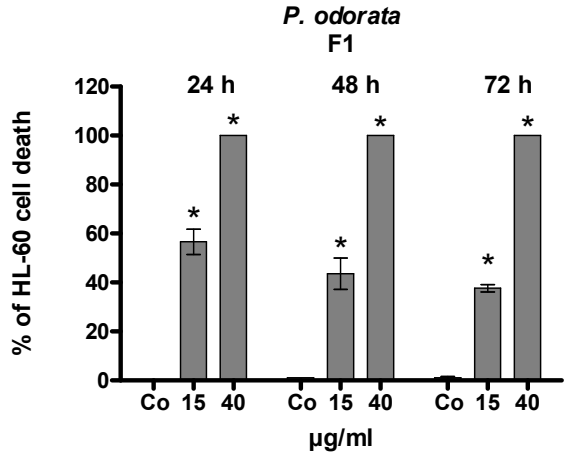

Fig 1d

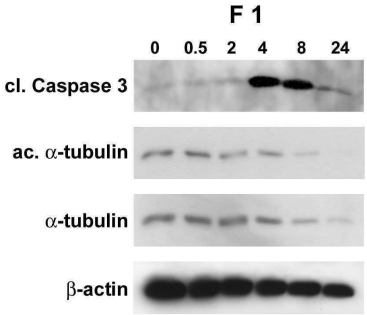

Legend figure 1: Anti-proliferative effect of a) dichloromethane crude extract, b) fraction F1 in HL60 cells; 1 x 10^5 cells/ml were seeded into 24-well plate, incubated with 5, 15 and 40 µg/ml extract or fraction F1 and the percentage of proliferation was calculated relative to solvent treated control within a 24 h period; c) Induction of apoptosis by F1, F2 and F3; Cells were grown as described and incubated with 15 and 40 µg/ml of each fraction for 72 h. Then, cells were double stained with Hoechst 33258 and propidium iodide and examined under the microscope with UV light connected to a DAPI filter. Nuclei with morphological changes which indicated cell death were counted and the percentages of dead cells were calculated. Experiments were performed in triplicate. Asterisks indicate significance compared to untreated control ($p<0.05$) and error bars indicate ±SD. d) 1 x 10^6 cells/ml were incubated with 40 µg/ml F1 and harvested after 0.5, 2, 4, 8 and 24 h of treatment, lysed and total protein applied to SDS-PAGE. Western blot analysis was conducted with the indicated antibodies. Equal sample loading was confirmed by Ponceau S staining and β-actin analysis.

F1 was further processed yielding fractions F2.1-F2.9. F2.6 was nearly as active F2.7 (**Fig 2a**), but contained ~10 times more fraction material (1.9g versus 0.2g, respectively). Therefore F2.6 was further processed yielding fractions F3.1-F3.10 (**Fig 2b, 2c**).

Fig 2a

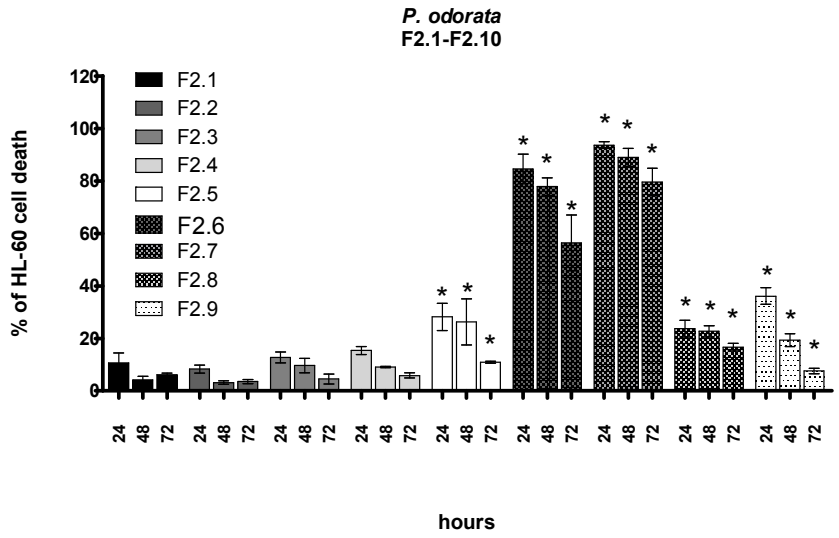

Fig 2b

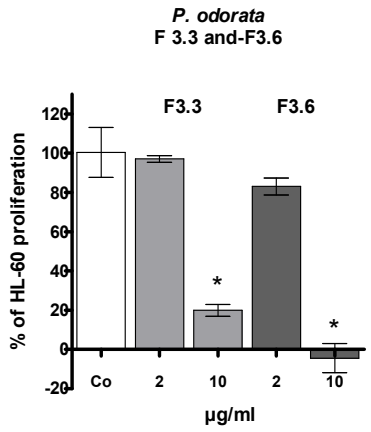

Fig 2c

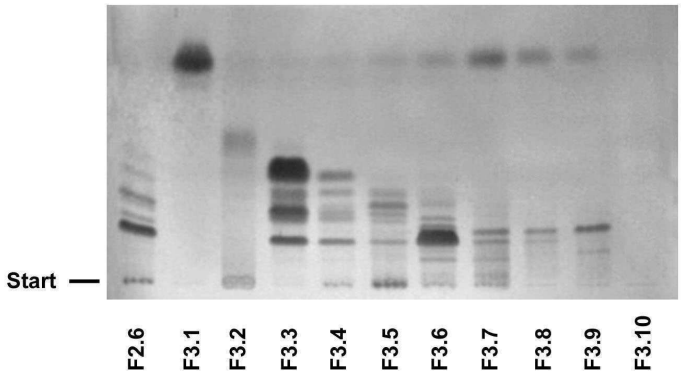

Legend figure 2: a) Induction of apoptosis of HL60 cells by F2.1-F2.9
1 x 105 cells/ml were seeded in 24-well plates and incubated with 10 µg/ml of each fraction for 72 h. Then, cells were double stained with Hoechst 33258 and propidium iodide and examined under the microscope with UV light connected to a DAPI filter. Nuclei with morphological changes which indicated cell death were counted and the percentages of dead cells were calculated. Significance was calculated in comparison to F2.2. b) Anti-proliferative effect of F3.3 and F3.6; 1 x 105 cells/ml were seeded into 24-well plate, incubated with 2 and 10 µg/ml of each fraction and the percentage of proliferation was calculated relative to solvent treated control within a 24 h period. Experiments were performed in triplicate. Asterisks indicate significance compared to untreated control ($p<0.05$) and error bars indicate ±SD. c) thin layer chromatography (TLC) of F2.6 (0) and F3.1-F3-10 (1-10); Mobile phase: TLC system 2; Detection: visible light with ASR.

10 µg/ml of F3.4-F3.6 exhibited potent anti-proliferative properties in HL60 cells suppressing cell growth by 100 %. The TLC analysis showed that both, F3.3 and F3.6, contained a distinct main compound, and therefore, F3.3 and F3.6 were further fractionated. Also F3.2 was processed however this yielded only several low-activity fractions (**data not shown**).

i) The sub-fractionation of F3.3 by sephadex produced three main fractions with similar TLC patterns and these were also similar to the one shown in **figure 2c.** Therefore, they were recombined (and termed **F.4.3.3**) and re-fractionated on a silica gel column yielding the potent anti-proliferative and pro-apoptotic fraction F5.3.3.7 (**Fig. 3a, 3b**). Further fractionation of F5.3.3.7 caused the decomposition of the strong cytotoxic activity into many low active fractions (F6.3.3.7.1-F6.3.3.7.12; **Fig 3c**), which in sum approximated the activity of the precursor.

Fig 3a

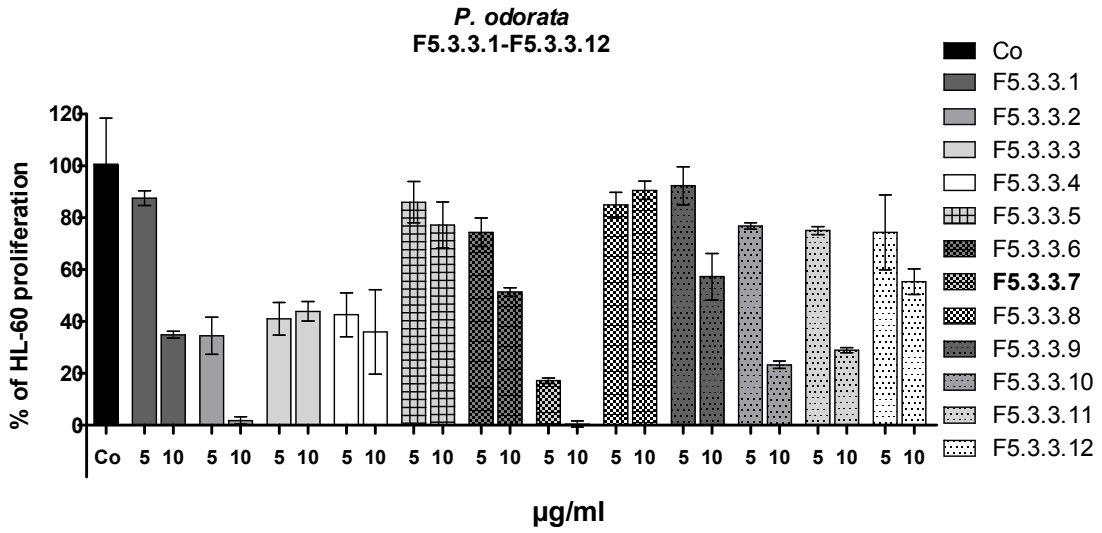

Fig. 3b

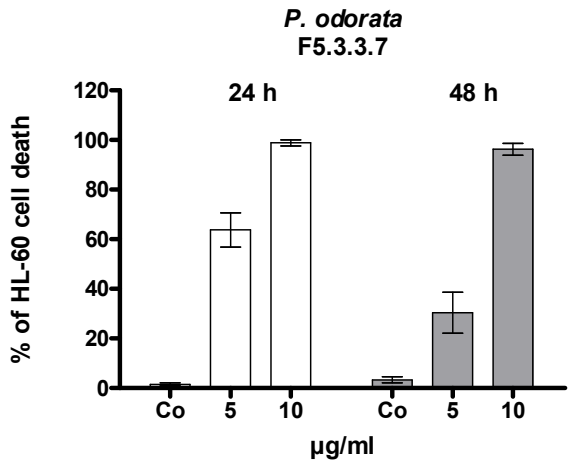

Fig 3c

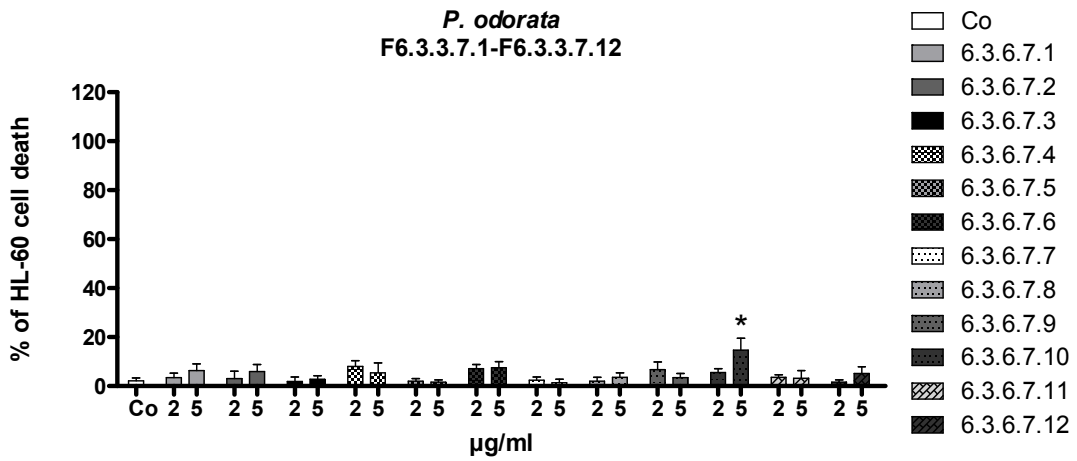

Legend figure 3: a) Anti-proliferative effect of F5.3.3.1-F5.3.3.12 in HL60 cells; 1 x 10^5 cells/ml were seeded into 24-well plates, incubated with 5 and 10 µg/ml of each fraction and the percentage of proliferation was calculated relative to solvent treated control within a 24 h period. b) Induction of apoptosis by F5.3.3.7 and c) by F6.3.3.7.1-F6.3.3.7.12 in HL60 cells; 1 x 10^5 cells/ml were seeded in 24-well plates and incubated with b) 5 and 10 µg/ml of F5.5.3.7 for 24 and 48 h and c) with 2 and 5 µg/ml of each fraction for 24 h. Then, cells were double stained with Hoechst 33258 and propidium iodide and examined under the microscope with UV light connected to a DAPI filter. Nuclei with morphological changes which indicated cell death were counted and the percentages of dead cells were calculated. Experiments were performed in triplicate. Asterisks indicate significance compared to untreated control ($p<0.05$) and error bars indicate ±SD.

ii) The sub-processing of F3.6 yielded fraction F4.6.3 as the most pro-apoptotic one which was very oily (**Fig 4a**). Upon further fractionation the activity of F4.6.3 also decomposed into several low-activity fractions (F5.6.3.1-F5.6.3.6; **Fig 4b**).

Fig 4a

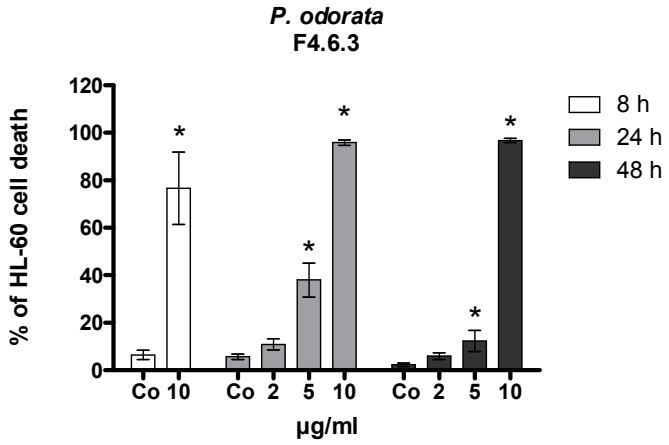

Fig 4b

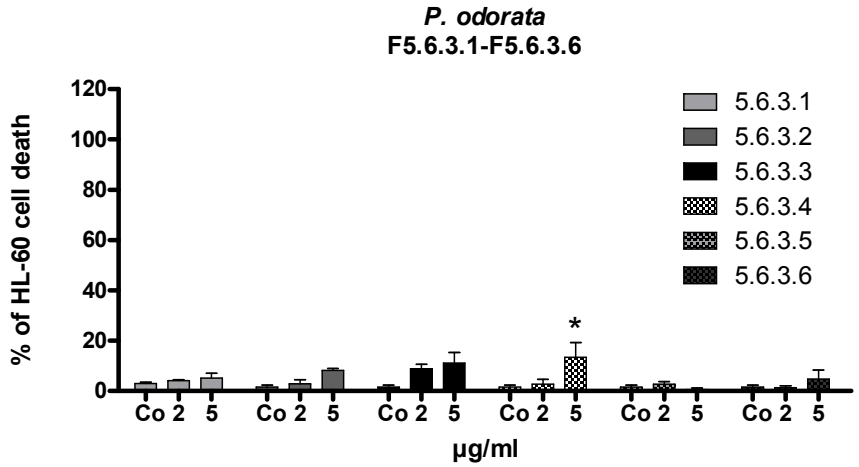

Legend figure 4: a) Induction of apoptosis; 1 x 10^5 HL60 cells/ml were seeded in 24-well plates and incubated with 2 and/or 10 µg/ml of F4.6.3 for 8, 24 and 48 h or b) 2 and 5 µg/ml of F5.6.3.1-F5.6.3.6 for 24 h. Then, cells were double stained with Hoechst 33258 and propidium iodide and examined under the microscope with UV light connected to a DAPI filter. Nuclei with morphological changes which indicated cell death were counted and the percentages of dead cells were calculated. Experiments were performed in triplicate. Asterisks indicate significance compared to untreated control ($p<0.05$) and error bars indicate ±SD.

Therefore, we went back to F5.3.3.7 and F4.6.3 and continued analyses with these two distinct high activity fractions. The TLC patterns of F5.3.3.7 and F4.6.3 were clearly different of each other evidencing that they contain different compounds (**Fig 5a**). To characterise the two distinct fraction types post-translational modifications and expression levels of proteins, which are relevant for apoptosis and cell cycle arrest, were investigated. F5.3.3.7 slightly

induced Chk2 phosphorylation and hence, its activation, whereas F4.6.3 did not (**Fig 5b**). Chk2 was shown to phosphorylate Cdc25A at Ser177 and tags it for proteasomal degradation (**Madlener et al 2009, Karlsson-Rosenthal and Millar 2006)**. However, treatment of HL60 cells with F5.3.3.7 caused the de-phosphorylation of Ser177 and protein stabilisation. Also F4.6.3 stabilised Cdc25A despite Ser177 phosphorylation. This implicated that Cdc25A was not regulated by Chk2 activity in this scenario. Moreover Cdc25A stabilisation suggested an increase in cell cycle activity (**Blomberg and Hoffmann 1999**). Nevertheless, cell proliferation was inhibited.

Fig 5a

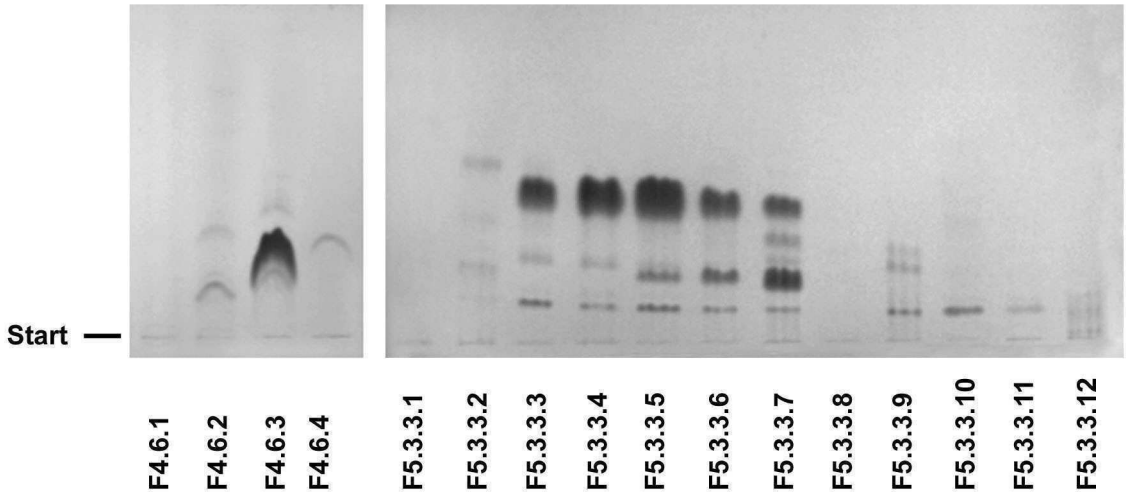

Fig 5b

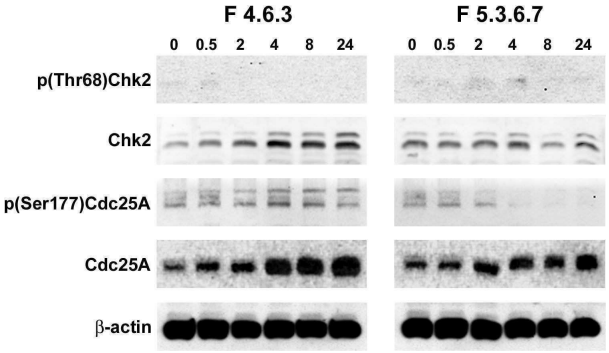

Fig 5c

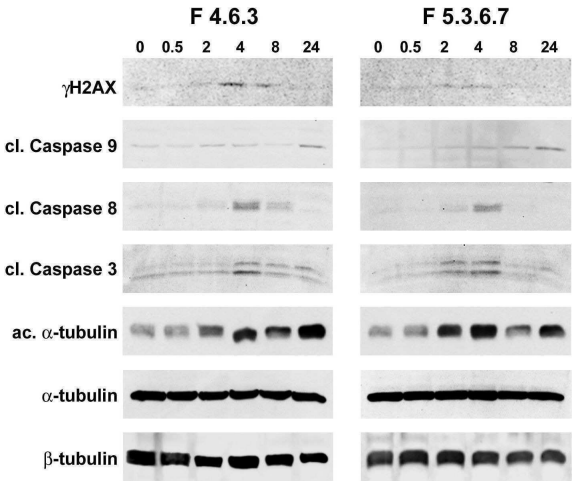

Fig 5d

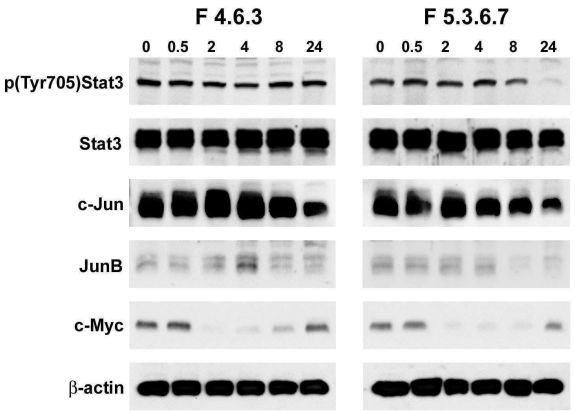

Fig 5e

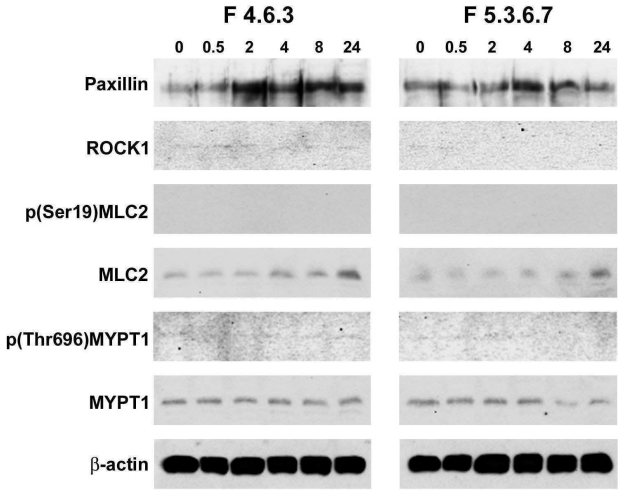

Legend figure 5: a) Thin layer chromatography (TLC) of F 4.6.3 (left panel) and F5.3.3.7 (right panel); Mobile phase: TLC system 2; Detection: UV254.
Analysis of b) Cell cycle and checkpoint regulators, c) apoptosis related proteins, d) oncogenes, e) proteins required for mobility; 1 x 106 HL60 cells/ml were incubated with 10 µg/ml F4.6.3 and F5.3.3.7, respectively and harvested after 0.5, 2, 4, 8 and 24 h of treatment. Cells were lysed and obtained proteins samples applied to SDS-PAGE. Western blot analysis was performed with the indicated antibodies. Equal sample loading was confirmed by Ponceau S staining and β-actin analysis.

In search of molecular causes for reduced proliferation, we found that the fractionation steps enriched a spindle toxin or an indirect microfilament-targeting activity). This was reflected by induced α-tubulin acetylation, which is an indicator of the polymerisation status of tubulin microfilaments (**Piperno et al. 1987, Hubbert et al. 2002**), within 2 h of treatment with F5.3.3.7 and F4.6.3 (**Fig. 5c**). Thereafter, caspase 3 became activated. Also the phosphorylation of H2AX occurred after treatment with both fractions indicating DNA damage presumably due to caspase 3-induced DNAse activity of DNA fragmentation factor (DFF; **Liu et al. 1997**), because caspase 3 activation and H2AX phosphorylation appeared simultaneously (**Paull et al., 2000**). Evidently, the molecular onset of apoptosis occurred faster than the orchestrated expression of the investigated cell cycle regulators. Interestingly, the activation of caspase 3 concurred with the activation of caspase 8, but not with activation of caspase 9, indicating that the extrinsic apoptosis pathway became activated and not the intrinsic one. The signature-type processing of caspase 3 into the active fragment was more prominent by F1 than by F5.3.3.7 and F4.6.3. This was most likely due to the four times

higher F1 concentration used (40 µg/ml), which caused also the degradation of α-tubulin and β-actin as consequence of swift onset of cell death.
The low or absent activation of Chk2 (respectively) suggested that a genotoxic activity, which was formerly present in the crude extract (**Gridling et al. 2009**) and in other subfractions (**Bauer et al. 2011**), was eliminated throughout the described fractionations. Avoiding genotoxicity can be beneficial, because it reduces DNA damage and subsequent mutations that may cause secondary malignancies. Cdc25A, a classified oncogene (**Kiyokawa and Ray 2008, Ray and Kiyokawa 2008**) was up-regulated by both fraction types and therefore, we investigated also the expression of other oncogenes, which are related to tumour growth and progression. F4.6.3 had a substantial effect on the repression of c-Myc and only a minor effect on c-Jun. Even more effective, F5.3.3.7 suppressed also the phosphorylation of Tyr705 of Stat3 and thus inhibited its function, which is known to play a role in tumour progression (**Devarajan and Huang 2009**). This fraction further repressed JunB and c-Jun and c-Myc more effectively than F4.6.3.

Since *P. odorata* is used also as a wound healing remedy, this property also involves tissue regeneration and the regulation of a process called "epthelial to mesenchymal transition" (EMT, **van Zijl et al. 2011, Thiery et al. 2009**). The most prominent feature of EMT is the acquisition of a mobile phenotype (**Kalluri and Weinberg 2009, Vonach et al. 2011)**. If transient and tightly regulated EMT is beneficial for the organism because it contributes to acute inflammation and tissue repair (**Lu et al. 2006, Grivennikov et al. 2010, Lopez-Novoa and Nieto 2009**). In contrast, the chronic status occurrence of EMT causes pathologies such as progression of cancer (**Wu and Zhou 2009**). The mobility of cancer cells is a prerequisite for the intra- and extra-vasation of the vasculature, tissue invasion and metastatic spread (**Krupitza et al. 1996, van Zijl et al. 2011**) and it is mediated by proteins that allow cell plasticity and movement. Therefore, the alteration of motility-related gene products in cancerous cells, such as paxillin (**Schaller 2001, Deakin and Turner 2008**), ROCK1 (**Sahai and Marshall 2003**), MLC2 for the formation of stress fibres (**Totsukawa et al. 2000**) and MYPT (**Vetterkind et al. 2010**), are indicators for increased mobility and hence, cancer progression. Also leukaemia cells such as differentiated HL60 attach to the ECM and vascular cells and transmigrate through vessel walls, invade tissues (**Liu et al 2009, Wang et al. 2010, Raman et al. 2010**) and add to the progression of the disease. Hence, HL60 cells possess a repertoire of proteins facilitating cell movement although they normally grow in suspension. Treatment with F5.3.3.7 caused ROCK1 repression below constitutive and detectable levels, which was not the case with F4.6.3 (**Fig. 5d**). Also MYPT expression decreased upon

treatment with F5.3.3.7. Paxillin became up-regulated by F4.6.3 treatment and marginally by F5.3.3.7 and this was also the case for the phosphorylation of MLC2. Since *P. odorata* is successfully used for tissue recovery and healing of skin bruises the increased mobility of cells (fibroblasts, epithelial cells, macrophages etc) is required to close the tissue disruption. This very property however, is detrimental throughout cancer treatment and elimination of this activity might be beneficial for this purpose. Therefore, future research has to address the question whether F5.3.3.7 is advantageous for cancer cell treatment, whereas F4.6.3 exhibits advanced wound healing properties.

Conclusions

A spindle-damaging activity became enriched by fractionations, which was reflected by increased α-tubulin acetylation followed by the activation of caspases 8 and 3 and the typical nuclear morphology of apoptosis. The impact on apoptosis and the orchestration of apoptosis regulator activation were similar for both fractions. In comparison to earlier work genotoxic components activating Chk2 were eliminated.
Importantly, F4.6.3 induced mobility markers, whereas F5.3.3.7 inhibited the expression of mobility markers or did not interfere with their constitutive expression. This property implicates an inhibitory effect of F5.3.3.7 on tumour progression which was also reflected by the down-regulation of the Jun family of oncogenes and the suppression of Stat3 activity. These findings can provide a basis for the development of remedies 1) supporting wound healing in case of F.6.3 or 2) interfering with tumour progression in case of F5.3.37.

Acknowledgements

We wish to thank Toni Jäger for preparing the figures. The work was supported by the Funds for Innovative and Interdisciplinary Cancer Research to G.K.

Literature

R. Arvigo and M. Balick, "One Hundred Healing Herbs of Belize," in *Rainforest Remedies,* pp. 72-73, Lotus Press, Twin Lakes WI, 2nd edition, 1998.

M. Balick and R. Lee, "Inflammation and ethnomedicine: looking to our past," *Explore (NY)*, vol. 1, no. 5, pp. 389-392, 2005.

S. Bauer, J. Singhuber, M. Seelinger, C. Unger, K. Viola, C. Vonach, B. Giessrigl, S. Madlener, N. Stark, B. Wallnofer, K.H. Wagner, M. Fritzer-Szekeres, T. Szekeres, R. Diaz, F. Tut, R. Frisch, B. Feistel, B. Kopp, G. Krupitza and R. Popescu, "Separation of anti-neoplastic activities by fractionation of a Pluchea odorata extract," *Frontiers Bioscience* (Elite Ed), vol. 3, pp.1326-1336, 2011.

I. Blomberg and I. Hoffmann, "Ectopic expression of Cdc25A accelerates the G(1)/S transition and leads to premature activation of cyclin E- and cyclin A-dependent kinases," *Molecular Cell Biology*, vol. 19, no. 9, pp. 6183-6194, 1999.

N.O. Deakin and C.E. Turner, "Paxillin comes of age," *Journal of Cell Science*, vol. 121, pt. 15, pp. 2435-2444, 2008.

E. Devarajan and S. Huang, "STAT3 as a central regulator of tumor metastases", *Current Molecular Medicine*, vol. 9, no.5, pp. 626-633, 2009.

D.S. Fabricant and N.R. Farnsworth, "The Value of Plants Used in Traditional Medicine for Drug Discovery," *Environmental Health Perspectives*, vol. 109, no.1, pp. 69-75, Review, 2001.

M. Gridling, N. Stark, S. Madlener, A. Lackner, R. Popescu, B. Benedek, R. Diaz, F.M. Tut, T.P. Nha Vo, D. Huber, M. Gollinger, P. Saiko, A. Ozmen, W. Mosgoeller, R. De Martin, R. Eytner, K.H. Wagner, M. Grusch, M. Fritzer-Szekeres, T. Szekeres, B. Kopp, R. Frisch and G. Krupitza, "In vitro anti-cancer activity of two ethno-pharmacological healing plants from Guatemala Pluchea odorata and Phlebodium decumanum," *International Journal of Oncology*, vol. 34, no.4, pp. 1117-1128, 2009.

S.I. Grivennikov, F.R. Greten and M. Karin, “Immunity, inflammation, and cancer”, *Cell,* vol. 140, no. 6, pp.883-399, Review, 2010.

C. Hubbert, A. Guardiola, R. Shao, Y. Kawaguchi, A. Ito, A. Nixon, M. Yoshida, X.F. Wang and T.P. Yao, “HDAC6 is a microtubule-associated deacetylase,” *Nature*, vol. 417, no. 6887, pp. 455-458, 2002.

T. Johnson, *CRC Ethnobotany Desk Reference*, p. 641, CRC Press LLC, Boca Raton, 1999.

R. Kalluri and R.A. Weinberg, „The basics of epithelial-mesenchymal transition”, *Journal of Clinical Investigations*, vol. 119, no. 6, pp. 1420-1428, 2009.

C. Karlsson-Rosenthal and J.B.A. Millar, “Cdc25: mechanisms of checkpoint inhibition and recovery”, *Trends in Cell Biology*, vol. 16, no. 6, pp. 285-292, 2006.

H. Kiyokawa and D. Ray, “In vivo roles of CDC25 phosphatases: biological insight into the anti-cancer therapeutic targets,” *Anticancer Agents in Medicinal Chemistry*, vol. 8, no. 8, pp. 832-836, 2008.

G. Krupitza, S .Grill, H. Harant, W. Hulla, T. Szekeres, H. Huber and C. Dittrich, “Genes related to growth and invasiveness are repressed by sodium butyrate in ovarian carcinoma cells”, *British Journal of Cancer*, vol. 73, no. 4, pp. 433-438, 1996.

P. Liu, J. Li, H. Lu and B. Xu, “Thalidomide inhibits leukemia cell invasion and migration by upregulation of early growth response gene 1,” *Leukemia and Lymphoma*, vol. 50, no. 1, pp. 109-113, 2009.

X. Liu, H. Zou, C. Slaughter and X. Wang, “DFF, a heterodimeric protein that functions downstream of caspase-3 to trigger DNA fragmentation during apoptosis”, *Cell*, vol. 89, no. 2, pp. 175-184, 1997.

J.M. López-Novoa and M.A. Nieto, “Inflammation and EMT: an alliance towards organ fibrosis and cancer progression”, *EMBO Molecular Medicine*, vol. 1, no. 6-7, pp. 303-314, Review, 2009.

H. Lu, W. Ouyang and C. Huang, “Inflammation, a key event in cancer development”, *Molecular Cancer Resarch*, vol. 4, no. 4, pp. 221-233, 2006.

S. Madlener, M. Rosner, S. Krieger, B. Giessrigl, M. Gridling, T.P. Vo, C. Leisser, A. Lackner, I. Raab, M. Grusch, M. Hengstschläger, H. Dolznig and G. Krupitza, “Short 42 degrees C heat shock induces phosphorylation and degradation of Cdc25A which depends on p38MAPK, Chk2 and 14.3.3,” *Human Molecular Genetics*, vol. 18, no. 11, pp. 1990-2000, 2009.

T.T. Paull, E.P. Rogakou, V. Yamazaki, C.U. Kirchgessner, M. Gellert and W.M. Bonner, “A critical role for histone H2AX in recruitment of repair factors to nuclear foci after DNA damage,” *Current Biology*, vol. 10, no. 15, pp. 886-895, 2000.

G. Piperno, M. LeDizet and X.J. Chang, “Microtubules containing acetylated alpha-tubulin in mammalian cells in culture,” *Journal of Cell Biology*, vol. 104, no. 2, pp. 289-302, 1987.

D. Raman, J. Sai, N.F. Neel, C.S. Chew and A. Richmond, “LIM and SH3 protein-1 modulates CXCR2-mediated cell migration,” *PLoS One*, vol. 5, no. 4, pp. e10050, 2010.

R.P. Rastogi and B.N. Dhawan, “Research on medicinal plants at the Central Drug Research Institute, Lucknow (India),” *Indian Journal of Medical Research*, vol. 76, pp. 27-45, 1982.

D. Ray and H. Kiyokawa, “CDC25A phosphatase: a rate-limiting oncogene that determines genomic stability”, *Cancer Research*, vol. 68, no. 5, pp. 1251-1253, Review, 2008.

E. Sahai and CJ Marshall, “Differing modes of tumour cell invasion have distinct requirements for Rho/ROCK signalling and extracellular proteolysis,” *Nature Cell Biology*, vol. 5, no. 8, pp. 711-719, 2003.

M.D. Schaller, “Paxillin: a focal adhesion-associated adaptor protein,” *Oncogene*, vol. 20, no. 44, pp. 6459-6472, 2001.

J.P. Thiery, H. Acloque, R.Y. Huang and M.A. Nieto,”Epithelial-mesenchymal transitions in development and disease,” *Cell*, vol. 139, no. 5, pp. 871-890, 2009.

G. Totsukawa, Y. Yamakita, S. Yamashiro, D.J. Hartshorne, Y. Sasaki and F. Matsumura, “Distinct roles of ROCK (Rho-kinase) and MLCK in spatial regulation of MLC phosphorylation for assembly of stress fibers and focal adhesions in 3T3 fibroblasts,” *Journal of Cell Biology*, vol. 150, no. 4, pp. 797-806, 2000.

F. van Zijl, G. Krupitza and W. Mikulits, “Initial steps of metastasis: Cell invasion and endothelial transmigration,” *Mutation Research*, 2011.

S. Vetterkind, E. Lee, E. Sundberg, R.H. Poythress, T.C. Tao, U. Preuss and K.G. Morgan, “Par-4: a new activator of myosin phosphatise,” *Molecular Biology of the Cell*, vol. 21, no. 7, pp. 1214-1224, 2010.

C. Vonach, K. Viola, B. Giessrigl, N. Huttary, I. Raab, R. Kalt, S. Krieger, T.P. Vo, S. Madlener, S. Bauer, B. Marian, M. Hämmerle, N. Kretschy, M. Teichmann, B. Hantusch, S. Stary, C. Unger, M. Seelinger, A. Eger, R. Mader, W. Jäger, W. Schmidt, M. Grusch, H. Dolznig, W. Mikulits and G. Krupitza, “NF-κB mediates the 12(S)-HETE-induced endothelial to mesenchymal transition of lymphendothelial cells during the intravasation of breast carcinoma cells,” *British Journal of Cancer*, vol. 105, no. 2, pp. 263-271, 2011.

L. Wang, J. Learoyd, Y. Duan, A.R. Leff and X. Zhu, “Hematopoietic Pyk2 regulates migration of differentiated HL-60 cells,” *Journal of Inflammation (London, England)*, vol. 7, pp. 26, 2010.

Y. Wu Y and B.P. Zhou, “Inflammation: a driving force speeds cancer metastasis”, *Cell* Cycle, vol. 8, no. 20, pp. 3267-3273, Review, 2009.

Effects of *Scrophularia* Extracts on Tumor Cell Proliferation, Death and Intravasation through Lymphendothelial Cell Barriers.

Giessrigl B., Yazici G., Teichmann M., Kopf S., Ghassemi S., Atanasov A.G., Dirsch V.M., Grusch M., Jäger W., Özmen A. and Krupitza G.

Evidence-based Compl. and Alt. Medicine, ***submitted.***

Effects of *Scrophularia* Extracts on Tumor Cell Proliferation, Death and Intravasation through Lymphendothelial Cell Barriers

Giessrigl Benedikt[1,3,*], Yazici Gökhan[2,*], Teichmann Mathias[1], Kopf Sabine[1], Ghassemi Sara[5], Atanasov Atanas G.[4], Dirsch Verena M.[4], Grusch Michael[5], Jäger Walter[3], Özmen Ali[2], Krupitza Georg[1]

[1] Institute of Clinical Pathology, Medical University of Vienna, Waehringer Guertel 18-20, A-1090 Vienna, Austria
[2] Institute of Biology, Fen-Edebiyat Fakültesi, Adnan Menderes Üniversitesi, Aydin, Turkey
[3] Department for Clinical Pharmacy and Diagnostics, Faculty of Life Sciences, University of Vienna, Althanstrasse 14, A-1090 Vienna, Austria
[4] Department of Pharmacognosy, University of Vienna, Althanstrasse 14, A-1090 Vienna, Austria
[5] Institute of Cancer Research, Department of Medicine I, Medical University of Vienna, Borschkegasse 8a, A-1090 Vienna, Austria

[*] contributed equally

Key words: *Scrophularia lucida*, cell-proliferation, cell-death, oncogenes, intravasation

Correspondence:
Georg Krupitza, Institute of Clinical Pathology, Medical University of Vienna, Waehringer Guertel 18-20, A-1090, Vienna, Austria
e-mail: georg.krupitza@meduniwien.ac.at,
Ali Özmen, Biyoloji Bölümü, Fen-Edebiyat Fakültesi, Adnan Menderes Üniversitesi, 09010 - Aydin, Turkey
e-mail: aozmen@adu.edu.tr

Abstract

Introduction: Different studies describe the anti-inflammatory effects of *Scrophularia* species, a medicinal plant widely used in folk medicine since ancient times. As knowledge regarding the anti-neoplastic properties of this species is rather limited, we investigated the influence of methanolic extracts of different *Scrophularia* species on cell proliferation, cell death, and tumour cell intravasation through the lymphendothelial barrier.
Methods: HL-60 leukaemia cells were treated with methanolic extracts of different *Scrophularia* species leading to strong growth inhibition and high cell death rates. The expression of cell cycle regulators, oncogenes and cell death inducers was checked by Western blot analysis. Furthermore the effect of *S. lucida* was studied in a NF-κB reporter assay, and in a novel assay measuring "circular chemorepellent-induced defects" (CCID) in lymphendothelial monolayers that were induced by MCF-7 breast cancer spheroids.
Results: Methanol extracts of *Scrophularia* species exhibited strong anti-proliferative properties. *S. floribunda* extract inhibited G2/M- and later on S-phase and *S.lucida* inhibited S-phase and in both cases this was associated with the down-regulation of c-Myc expression. Extracts of *S. floribunda* and *S. lucida* led to necrosis and apoptosis, respectively. Furthermore, *S. lucida,* but not *S. floribunda,* effectively attenuated tumor cell intravasation through lymphendothelial cell monolayers, which correlated with the inhibition of NF-κB.
Conclusions: *S. lucida* exhibited promising anti-neoplastic effects and this was most likely due to the down-regulation of various cell cycle regulators, proto-oncogenes and NF-κB and the activation of caspase 3.

Introduction

While only ~1% of the estimated 300 000 different species of higher plants have a history in food use, up to 10-15% have extensive documentation for application in traditional medicine (**1**). Natural products have played a significant role in human healthcare for thousands of years, especially in the treatment of infectious diseases (**2**). Even today, more than 60% of all drugs used are either natural products or directly derived thereof and are used to treat even diseases such as cancer. Among these are very important agents like vinblastine, vincristine, the camptothecin derivatives, topotecan and irinotecan, etoposide, derived from epidopodophyllotoxin, and paclitaxel (**3, 4, 5**).

Ethno-medicine does not only explore written sources i.e. Traditional Chinese Medicine or Ayurveda, but in particular also gives strong attention to the many kinds of folk medicine that was practiced in all parts of the world for centuries.

A very rich plant diversity is found in Turkey, because the Taurus peninsula has seas on three sides and various climatic zones and topographies. The flora of Turkey is rich in medicinal and aromatic plants that have been used to treat different diseases in Turkish and antique folk medicine (**6, 7**). Since ancient times, different *Scrophularia* species have been used as remedies for some medical treatments, including scabies, eczema, psoriasis, inflammatory diseases and tumors (**8**). There are more than 220 genera of the Scrophulariaceae family in which the genus *Scrophularia* is known for the rich presence of sugar esters and iridoid glycosides (**9, 10**), and a few publications describe the anti-inflammatory properties of different *Scrophularia* species (**11, 12**). Oleanonic and ursolonic acids extracted from the root of *S. ningpoensis* Hemsl were found to be cytotoxic against a series of human cancer cell lines (MCF7, K562 and A549) (**10**).

We have investigated the anti-proliferative and pro-apoptotic potency of the methanol extracts of five different *Scrophularia* species (two endemic to Turkey: *S. libanotica* and *S. pinardii*) and elucidated the corresponding pathways of those two species that showed the strongest antineoplastic effect. Furthermore, we discovered a property in *S. lucida*, which correlates with the inhibition of lymph node metastasis of breast cancer cells.

Methods

Plant material: *Scrophularia floribunda*, *S. lucida*, *S. peregrina*, *S. pinardii* and *S. libanotica subsp. libanotica var. mesogitana* were collected in the south-west of Turkey at a height around 250 m in Aydin and Marmaris, respectively. Flowering times of these plants were identified from books for specifying the collection time. Plants were recognized in the field survey by various plant parts (flower, leaf, stamen, colouring of petals and etc.) and by comparing with previously prepared herbarium samples. Taxonomic determinations were made by Dr. Özkan Eren using the serial "Flora of Turkey and the East Aegean Islands" (Davis, 1965-1988). Voucher specimens (voucher numbers: *S. floribunda* AYDN 432; *S. lucida* AYDN 433), in duplicates were deposited in the herbarium of the Department of Biology, Adnan Menderes University.

Sample preparation: Plants were freeze dried, subsequently milled and extracted with methanol at the ratio of 1:10. Extraction was carried out on a shaker at room temperature overnight. After filtration, methanol was evaporated with a rotary evaporator and extract weight was determined (**table 1**). For the experiments, the extracts were dissolved in ethanol. For the proliferation- and apoptosis assays the following concentrations as calculated for dried plant material were used: 500 µg/ml, 1 mg/ml, 4 mg/ml and 10 mg/ml. To exclude an effect of ethanol on cell proliferation and apoptosis, controls were treated with same concentrations of ethanol as used for sample treatment (in general 0.2 % EtOH) (**13,14**).

Species	**Wet weight** (g)	**Dry weight** (g)	**Extract weight** (g)
S. floribunda	349	87	17
S. lucida	295	87	14
S. peregrine	243	55	11.6
S. pinardii	383	88	17
S. libanotica	280	88	12.5

Table 1 Extract yields after sample preparation

Detannification: For removal of tannins 5 g of the total methanol extract of *S. floribunda* and *S. lucida*, respectively, were dissolved in 60 ml of a methanol/water mixture (10:1). After triple solvent extraction with 60 ml petroleum ether for withdrawal of chlorophyll, waxes and fats, the methanol fraction was diluted with 60 ml of water and subsequently this aqueous solution was extracted three times with 120 ml chloroform. To gain the detannified extract,

the collected chloroform fraction was washed three times with 360 ml sodium chloride solution (1%) and after drying with sodium sulphate, the chloroform was evaporated with a rotary evaporator. *S. floribunda* and *S. lucida* total methanol extract yielded 0.24 g and 0.11 g per g, respectively.

Cell culture: HL-60 promyeloic leukaemia cells were purchased from ATCC. Cells were grown in RPMI 1640 medium supplemented with 10 % heat inactivated fetal calf serum (FCS), 1 % L-glutamine and 1 % penicilline/streptomycin. Human MCF-7 breast cancer cells were cultivated in MEM medium supplemented with 10% FCS, 1 % penicillin/streptomycin, 1 % NEAA. Telomerase immortalized human lymphendothelial cells (LECs) were grown in EGM2 MV (Clonetics CC-4147, Allendale, NJ, USA). For CCID formation assays, LECs were stained with cytotracker green. HEK293-NFκB-Luc cells were cultivated in high glucose DMEM containing phenol red, supplemented with 10% FCS, 1% penicillin/streptomycin and 1% L-glutamine. GFP transfection of HEK293-NFκB-Luc cells using lipofectamin2000 was carried out in medium without penicillin/streptomycin.
All cells were grown at 37°C in a humidified atmosphere containing 5% CO_2. If not mentioned otherwise, all media and supplements were obtained from Invitrogen Life Technologies (Karlsruhe, Germany).

3-D co-cultivation of MCF-7 cancer cells with LECs: MCF-7 mock cells were transferred to 30 ml MEM medium containing 6 ml of a 1.6 % methylcellulose solution (0.3 % final concentration; Cat. No.: M-512, 4000 centipoises; Sigma, Munich, Germany). 150 µl of this cell suspension were transferred to each well of a 96 well plate (Greiner Bio-one, Cellstar 650185, Kremsmünster, Austria) to allow spheroid formation within the following two days. Then, MCF-7 spheroids were washed in PBS and transferred to cytotracker-stained LEC monolayers that were seeded into 24 well plates (Costar 3524, Sigma, Munich, Germany) in 2 ml EGM2 MV medium (**15, 16**).

Circular chemorepellent induced defect (CCID) assay: MCF-7 cell spheroids (3000 cells/spheroid) were transferred to the 24 well plate containing LEC monolayers. After four hours of incubating the MCF-7 spheroids-LEC monolayer co-cultures, the CCID sizes in the LEC monolayer underneath the MCF-7 spheroids were photographed using an Axiovert (Zeiss, Jena, Germany) fluorescence microscope to visualise cytotracker (green)-stained LECs underneath the spheroids (**17**). Gap areas were calculated with the Axiovision Re. 4.5

software (Carl Zeiss, Jena, Germany). MCF-7 spheroids were treated with solvent (ethanol) as negative control. The gap sizes of at least 12 spheroids per experiment were measured.

Reagents and antibodies: Hoechst 33258 and propidium iodide were purchased from Sigma (Munich, Germany). Amersham ECLPlus Western Blotting Detection System was from GE Healthcare (Buckinghamshire, UK).

Antibodies: Mouse monoclonal (ascites fluid) anti-acetylated tubulin clone 6-11B1 Cat# AT6793 and mouse monoclonal (ascites fluid) anti-β-actin clone AC-15 Cat# A5441 were from Sigma (Munich, Germany). Anti α-tubulin (TU-02) Cat# sc-8035, PARP-1 (F-2) Cat# sc 8007, anti cyclin D1 (M-20) Cat# sc-718, p21 (C-19) Cat# sc-397, cdc25a (F-6) Cat# sc-7389, cdc25b (C-20) Cat# sc-326, cdc25c (C-20) Cat# sc-327, c-jun (C-20) Cat# sc-1694 and jun-B (210) Cat+# sc-73 were from Santa Cruz Biotechnologies Inc. (Santa Cruz, CA, USA) Phospho-p44/42 MAPK (Erk1/2) (Thr^{202}/Tyr^{204}) (E10) Cat# 9106, p44/42 MAPK (Erk1/2) (137F5) Cat# 4695, phospho-p38 MAPK (Thr^{180}/Tyr^{182}) (12F8) Yat# 4631, p38 MAPK Cat# 9212, cleaved caspase 3 (Asp^{175}) Cat# 9661, phospho-Wee1 (Ser^{642}) (D47G5) Cat# 4910, Wee1 Cat# 4936, phospho-chk2 (Thr^{68}) Cat# 2661, chk2 Cat# 2662, Myosin Light Chain 1 Cat# 3672 and phospho-Myosin Light Chain 2 (Ser^{19}) Cat# 3671 were purchased from Cell Signalling (Danvers, MA, USA). Anti c-myc antibody Ab-2 (9E10.3) was from Neomarkers (Fremont, CA, USA) and rabbit polyclonal phospho detect anti-H2AX ($pSer^{139}$) Cat# dr-1017 from Calbiochem (Merck, Darmstadt, Germany). Anti mouse and anti rabbit IgG were from Dako (Glostrup, Denmark).

Proliferation inhibition analysis: HL-60 cells were seeded in T-25 Nunc tissue culture flasks at a concentration of $1x10^5$/ml and incubated with increasing concentrations of plant extracts (corresponding to 500 µg/ml, 1 mg/ml, 4 mg/ml and 10 mg/ml of the dried plant). Cell counts and IC_{50} values were determined at 24, 48 and 72 hours using a Casy TTC cell counter (Roche, Basel, Switzerland), respectively.

The percent of cell divisions compared to the untreated control were calculated as follows: $((C_{72h + drug} - C_{24h + drug})/(C_{72h - drug} - C_{24h - drug})) \times 100 = \%$ cell division, where $C_{72h + drug}$ is the cell number after 72 h of extract treatment, $C_{24h + drug}$ is the cell number after 24 h of extract treatment, $C_{72h - drug}$ and $C_{24h - drug}$ are the cell numbers after 72 and 24 h without extract treatment (**18,19**).

Cell death analysis: The Hoechst propidium iodide double staining was performed according to the method described by **Grusch et al. (20, 21)**. HL-60 cells ($1x10^5$) were seeded in T-25 Nunc tissue culture flasks and exposed to 20 µg/ml detannified extract (corresponding to 0.42 mg/ml of dried *S. floribunda* and 1.10 mg/ml of dried *S. lucida*) for 24 and 48 h. Hoechst 33258 and propidium iodide (Sigma, Munich, Germany) were added directly to the cells at final concentrations of 5 and 2 µg/ml, respectively. After 60 min of incubation at 37°C cells were examined on a Zeiss Axiovert fluorescence microscope (Zeiss, Jena, Germany) equipped with a DAPI filter. Cells were photographed and analysed by visual examination to distinguish between apoptosis and necrosis (**22**). Cells were judged according to their morphology and the integrity of their cell membranes by propidium iodide staining.

FACS analysis: HL-60 cells ($1x10^6$ per ml) were seeded in T-25 Nunc tissue culture flasks and incubated with 20 µg/ml detannified extract (corresponding to 0.42 mg/ml of dried *S. floribunda* and 1.10 mg/ml of dried *S. lucida*) for 8 and 24 h, respectively. Then, cells were washed with 5 ml cold PBS, centrifuged (800 rpm for 5 min), and resuspended and fixed in 3 ml cold ethanol (70%) for 30 min at 4˚C. After two further washing steps with cold PBS, RNAse A and propidium iodide were added to a final concentration of 50 µg/ml each and incubated at 4˚C for 60 min before measurement (**23, 24**). Cells were analysed on a FACSCalibur flow cytometer (BD Biosciences, San Jose, CA, USA) and cell cycle distribution was calculated with ModFit LT software (Verity Software House, Topsham, ME, USA).

NF-κB Luciferase Assay: $10x10^6$ HEK293-NFκB-Luc cells (Panomics, Fremont, USA) were seeded in 20 ml full growth DMEM medium in a 15 cm dish. Next day, cells were transfected with the cDNA of green fluorescence protein (GFP). A total of 30 µl Lipofectamin 2000 (Invitrogen, Karlsruhe, Germany) and 7.5 µg DNA were mixed in 2 ml transfection medium and incubated for 20 min at room temperature followed by adding this mixture to the cells. After incubation for 6 hours in humidified atmosphere containing 5% CO_2, $4x10^4$ cells per well were seeded in serum- and phenol red-free DMEM in a 96 transparent well plate. On the next day cells were treated with detannified *S. lucida* extract (corresponding to 0.5 mg/ml, 2 mg/ml and 4 mg/ml of the dried plant) and 15 µM Bay 11-7082 (Sigma Aldrich Cat# B5556) as a specific inhibitor of NFκB (control). One hour after treatment cells were stimulated with 2 ng/ml human recombinant TNF-α for additional 4 hours. Luminescence of the firefly luciferase and fluorescence of the GFP were quantified on a GeniusPro plate reader (Tecan,

Grödig, Austria). The luciferase signal derived from the NF-κB reporter was normalized by the GFP-derived fluorescence to account for differences in the cell number or transfection efficiency.

Western Blotting: HL-60 cells (0.5 x 10^6) were seeded into T-75 Nunc tissue culture flasks and incubated with 20 µg/ml detannified extract (corresponding to 0.4 mg/ml of dried *S. floribunda* and 1.1 mg/ml of dried *S. lucida*) for 0.5, 2, 4, 8 and 24 h, respectively. At each time point 2 x 10^6 cells were harvested, washed twice with cold PBS, centrifuged (175 x g) for 5 min and lysed in a buffer containing 150 nM NaCl, 50 mM Tris, 1 % Triton-X-100, 1 mM phenylmethylsulfonylfluride (PMSF) and 2.5 % PIC (Cat#P8849 Sigma, Munich, Germany). After centrifugation (12 000 x g) for 20 min at 4°C the supernatant was stored at -20°C until further analysis. Equal amounts of protein samples were separated by polyacrylamide gel electrophoresis and electrotransferred onto PVDV-membranes (Hybond-P, Amersham) at 4°C overnight. Staining membranes with Ponceau S controlled equal sample loading. After washing with Tris buffered saline (TBS) ph 7.6, membranes were blocked for 1 h in 5 % non-fat dry milk in TBS containing 0.1% Tween-20. Membranes were incubated with the first antibody (in blocking solution, dilution 1:500-1:1000) by gently rocking overnight at 4°C, washed with TBS containing 0.1% Tween-20 and further incubated with the second antibody (peroxidase-conjugated swine anti-rabbit IgG or rabbit anti-mouse IgG, dilution 1:2000-1:5000 in blocking solution) for 1 h. Chemoluminescence was developed by the ECL plus detection kit (GE Healthcare, Buckinghamshire, UK) and detected using a Lumi-Imageer F1 Workstation (Roche, Basel, Switzerland).

Statistics: All experiments were performed in triplicate and analysed by t-test (GraphPad Prism 5.0 program, GraphPad (San Diego, CA, USA).

Results

Anti-proliferative activity

The methanol extracts of the tested Scrophularia species inhibited cell growth of HL-60 promyeloic leukaemia cells, whereof *S. floribunda* and *S. lucida* showed the strongest inhibition with IC_{50} values of 0.54 mg/ml and 0.41 mg/ml, respectively (calculated for dried plant material; **table 2, figure 1**). Methanol extracts contain tannins, which may have caused this effect non-specifically. Therefore, the extracts of those plants exhibiting the strongest activities were purified to remove chlorophyll and fatty ingredients in a first step and then tannins and other polar substances in a second step. The obtained detannified extracts (dt) were tested again regarding their anti-proliferative activity and they still showed approximately the same strong growth inhibition (IC_{50} values of 0.3 mg/ml and 0.4 mg/ml for *S. floribunda dt* and *S. lucida dt*, respectively, **figure 2**). To compare the two *Scrophularia* species regarding their potency, 20 µg/ml of the detannified extracts (corresponding to 1.1 mg/ml *S. lucida* and 0.4 mg/ml *S. floribunda*, respectively) were used for all further experiments.

Methanol extract	**IC_{50} (mg/ml)**
S. floribunda	0.5
S. lucida	0.4
S. peregrina	3.7
S. pinardii	0.9
S. libanotica	0.9

Table 2 IC_{50} values in HL-60 cells after **72h** of treatment with the total methanol extracts of indicated *Scrophularia* species

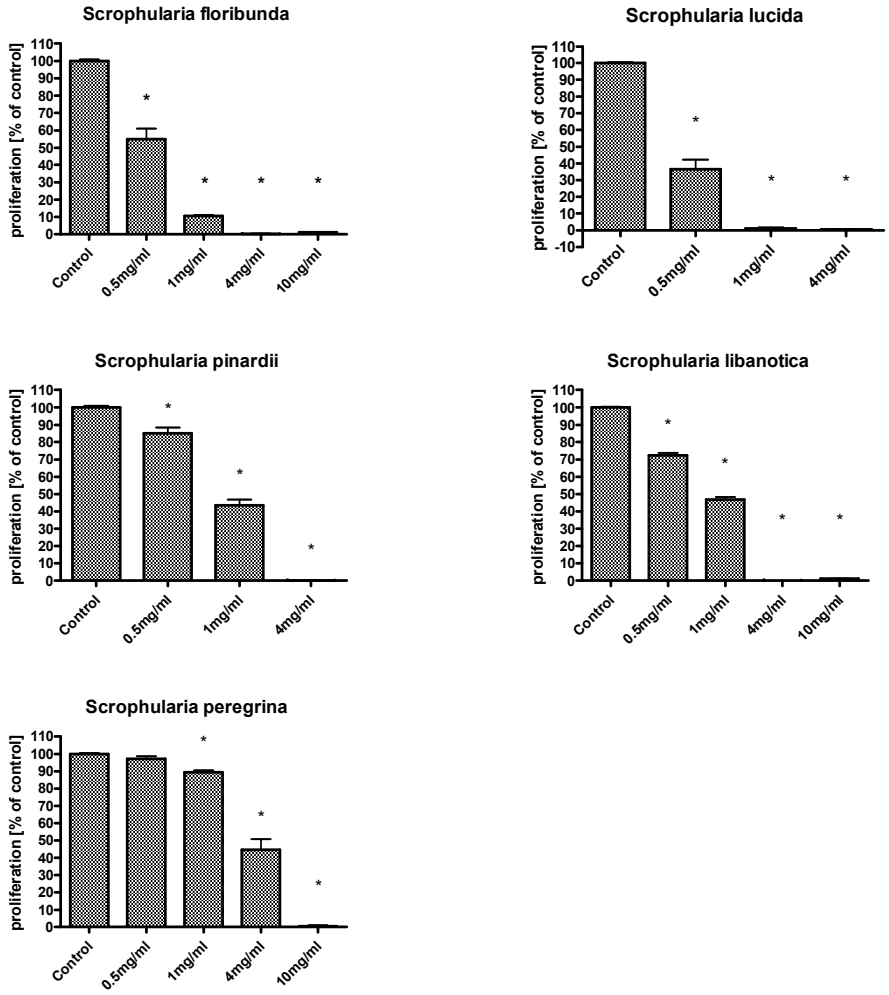

Figure 1 Proliferation inhibition upon treatment with total methanol extracts for 72 h. HL-60 cells ($1x10^5$ cells/ml) were seeded in T-25 tissue culture flasks and were incubated with total methanolic extracts corresponding to 0.5 mg/ml, 1 mg/ml, 4 mg/ml and 10 mg/ml of the dried plant. Experiments were performed in triplicate. To avoid unspecific effects caused by the solvent, ethanol concentration was the same in all samples (0.2%). Asterisks indicate significance compared to untreated control ($p<0.05$) and error bars indicate ±SD.

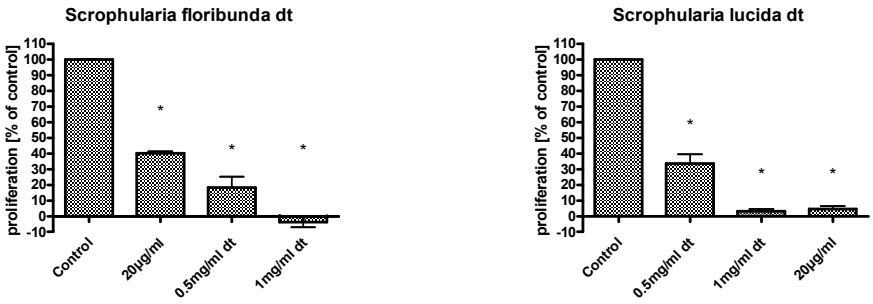

Figure 2 Proliferation inhibition upon treatment with the detannified extracts (corresponding to 0.4, 0.5, 1.0 and 1.1 mg dried plant / ml medium) for 72 h. For *S. floribunda* or *S. lucida* 20 µg dtMeOH extract corresponded to 0.4 or 1.1 mg dried plant weight, respectively. Experiments were performed in triplicate. To avoid unspecific effects caused by the solvent, ethanol concentration was the same in all samples (0.2%). Asterisks indicate significance compared to untreated control ($p<0.05$) and error bars indicate ±SD.

Cell cycle distribution

To investigate the cell cycle distribution, logarithmically growing HL-60 cells were exposed to 20 µg/ml detannified methanol extract of *S. lucida* and *S. floribunda* for 8 an 24 h, respectively. Both extracts caused a rapid reduction of G1 cells (**figure 3**). *S. floribunda* treatment induced a strong G2/M arrest after 8 h and a significant accumulation of cells in the S-phase after 24 h. In contrast *S. lucida* did not elicit a G2/M arrest, but a strong accumulation in the S-phase after 8 h and a distinct sub-G1 peak indicating loss of DNA typical for apoptosis.

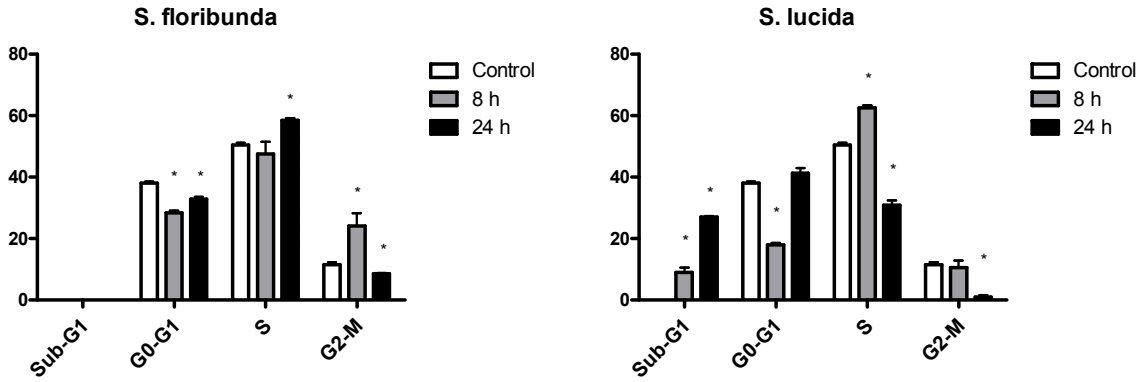

Figure 3 Effects of Scrophularia extracts on cell cycle distribution; HL-60 cells ($1x10^6$ per ml) were seeded in T-25 tissue culture flasks and incubated with 20 µg/ml detannified extract (corresponding to 0.4 mg/ml of dried *S. floribunda* and 1.1 mg/ml of dried *S. lucida*) for 8 and 24 h. Experiments were performed in triplicate. To avoid unspecific effects caused by the solvent, ethanol concentration was the same in all samples (0.2%). Asterisks indicate significance compared to untreated control ($p<0.05$) and error bars indicate ±SD.

Potential mechanisms arresting cell proliferation

To investigate the underlying mechanisms responsible for the strong proliferation inhibition we analysed the expression profiles of different positive and negative cell cycle regulators (**figure 4, figure 5**). *S. floribunda* clearly increased the p21 level after 4 h, while *S. lucida* extract inhibited p21 expression within 4 h. Although p21 is a prominent transcriptional target of p53 another pathway must have triggered the p21 increase since HL-60 cells are p53 deficient (**25**). As also the activation of the MEK-Erk pathway was shown to up-regulate p21 (**26, 27**), we checked the phosphorylation status of Erk1/2. *S. floribunda* showed a slight increase of the phosphorylation status of Erk1/2 at the 4 h time point going along with the p21 up regulation. In contrast *S. lucida* strongly phosphorylated Erk1/2 already after 2 h, followed by a decrease after 8 h and a drop below control level after 24 h. Therefore, p21 must have

been regulated independent of Erk1/2. However, both extracts lead to Erk phosphorylation for an unusually long time, which is known in other contexts to be activated only for some 10-20 min (**28**).

Another prominent inducer of cell cycle arrest and apoptosis is cellular stress. p38 MAPK presents an important member in a signalling cascade controlling its responses to cellular stress. Phosphorylation of p38 at Thr180 and Tyr182 leads to its activation and binding to Jnk or Max modulates transcription (**29, 30**). Both extracts were capable to activate p38 within 2 h indicating that cellular stress was another important factor that may have caused growth arrest.

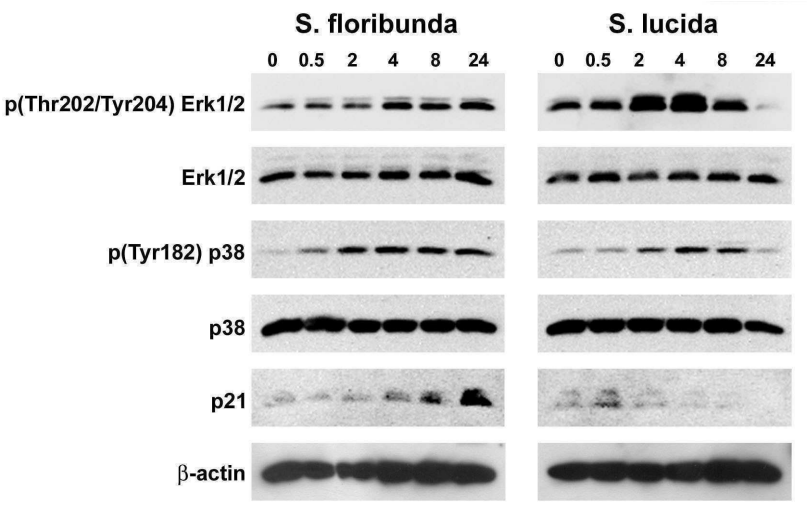

Figure 4 Western blot analysis of different proteins of the MAPK pathway. 1 x 10^6 HL-60 cells/ml were incubated with 20 µg/ml detannified extract and harvested after 0.5, 2, 4, 8 and 24 h of treatment. Cells were lysed and obtained protein samples applied to SDS-PAGE. Western blot analysis was performed with the indicated antibodies. Equal sample loading was confirmed by Ponceau S staining and β-actin analysis.

The activation of Chk2 by *S. floribunda* (**figure 5**) was in time with the phosphorylation of Erk1/2 and the induction of p21. The inhibition of the cell cycle was due to the inactivation of Cdc2, which was reflected by the increased phosphorylation of Tyr15. Interestingly, Tyr15-Cdc2 phosphorylation correlated with over-expression of Wee1, which specifically phosphorylates this site, but not with Cdc25A and Cdc25C, because these phosphatases responsible for the de-phosphorylation of Tyr15-Cdc2 became up-regulated. This was in sharp contrast to the effects on cell cycle regulators elicited by *S. lucida* extract, because Chk2 was induced much earlier and this correlated with the degradation of the Cdc25 family, which

is in accordance with the reported mechanisms of cell cycle inhibition upon DNA check point activation (**31, 32**). It was expected that this would result in hyper-phosphorylation and inactivation of the effector-kinase Cdc2, but the contrary was the case due to inhibition and down-regulation of Wee1. Therefore, the phosphorylation status of Cdc2 primarily correlates with Wee1 but not with Cdc25A and Cdc25C. Also Cdc25B became down-regulated by *S. lucida* but was expressed unchanged upon treatment with *S. floribunda*. This evidenced that *S. floribunda* and *S. lucida* contained distinct "Active Principles". Although potential mechanisms as to how the extract of *S. floribunda* inhibits cell division could be outlined, it was still unclear how the extract of *S. lucida* arrested cell proliferation.

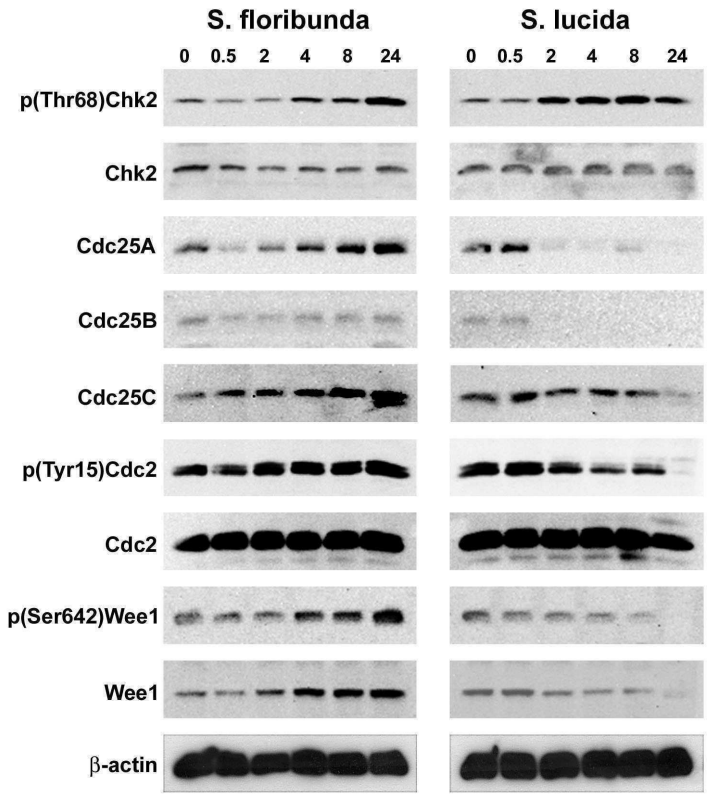

Figure 5 Western blot analysis of cell cycle and checkpoint regulators. 1 x 10^6 HL-60 cells/ml were incubated with 20 µg/ml detannified extract and harvested after 0.5, 2, 4, 8 and 24 h of treatment. Cells were lysed and obtained protein samples applied to SDS-PAGE. Western blot analysis was performed with the indicated antibodies. Equal sample loading was confirmed by Ponceau S staining and β-actin analysis.

Downregulation of oncogenes

Hence, we investigated the expression of proto-oncogenes, which are involved in tumour cell proliferation. C-Myc, a member of the Myc family of oncogenes, is essential for promoting cell growth by regulating the transcription of target genes required for proliferation and c-Myc was shown to be over-expressed in a wide spectrum of tumors (**33**). As an over-expression leads to constitutive signals that promote proliferation and angiogenesis of the tumor (**34**), we checked the expression levels of the c-Myc protein to investigate whether the two *Scrophularia* extracts were capable to down regulate that oncogene. In fact, treatment of HL-60 cells with the two extracts resulted in c-Myc protein decrease, in particular with *S. lucida* that showed a dramatic down regulation within 2 hours (**figure 6**). Together with Fos family members, Jun family members form the group of AP-1 proteins which, after dimerisation, bind to responsive elements in the promoter regions of different target genes (**35**). AP-1 heterodimers are important regulators of genes playing a major role in proliferation, differentiation, invasion and metastasis (**36**). Therefore, we also checked the expression status of c-Jun, JunB and Fos after incubation with the two *Scrophularia* extracts. While Fos was slightly up regulated by both extracts, and *S. floribunda* did not affect Jun and JunB, *S. lucida* showed a strong down regulation of these two oncogenes after 24 hours.

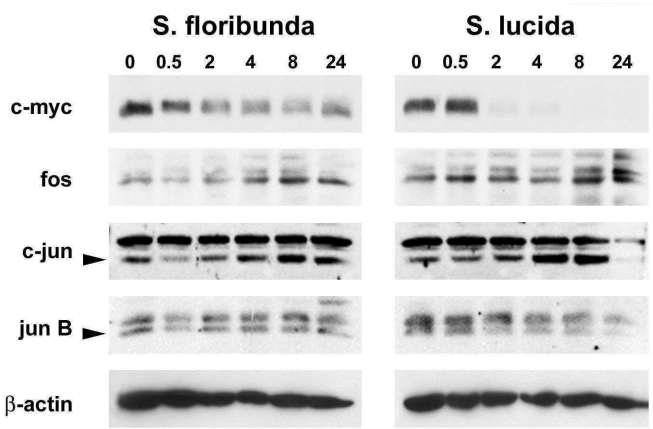

Figure 6 Western blot analysis of different oncogenes. 1 x 10^6 HL-60 cells/ml were incubated with 20 µg/ml detannified extract and harvested after 0.5, 2, 4, 8 and 24 h of treatment. Cells were lysed and obtained proteins samples applied to SDS-PAGE. Western blot analysis was performed with the indicated antibodies. Equal sample loading was confirmed by Ponceau S staining and β-actin analysis.

Cell death induction

Treatment of HL-60 cells with the detannified *S. lucida* and *S. floribunda* extract resulted in high cell death rates (**figure 7**). While incubation with detannified extract of *S. lucida* corresponding to 1 mg/ml of the dried plant induced up to 70 % of apoptosis after 48 h, HL-60 cells treated with *S. floribunda* extract showed a para-typical apoptosis phenotype with almost instantaneous incorporation of propidium iodide indicating necrosis, which was substantiated in respective western blots (see below).

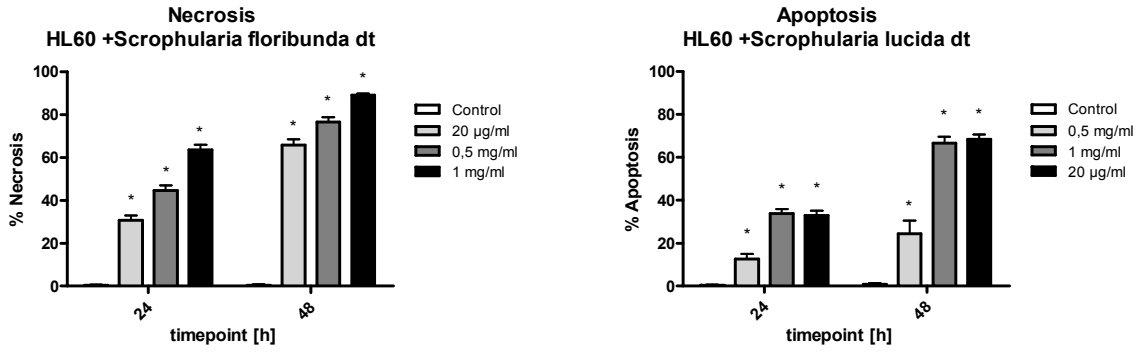

Figure 7 Induction of cell death of HL-60 cells treated with detannified *Scrophularia* extracts. $1x10^5$ HL-60 cells/ml were seeded in 24-well plates and incubated with 0.5 mg/ml and 1 mg/ml extract corresponding to dried plant and 20 µg/ml to pure extract (corresponding to 1.1 mg/ml *S. lucida* and 0.4 mg/ml *S. floribunda*, respectively). Then, cells were double stained with Hoechst 33258 and propidium iodide and examined under the microscope with UV light connected to a DAPI filter. Nuclei with morphological changes which indicated cell death were counted and the percentages of dead cells were calculated. Experiments were performed in triplicate. Asterisks indicate significance compared to untreated control ($p<0.05$) and error bars indicate ±SD.

Cell death mechanisms

FACS analyses (**figure 3**) and HOPI staining (**figure 7**) indicated that *S. lucida* induced apoptosis but not necrosis, while the extract of *S. floribunda* did not show a sub G1 peak. As both compounds led to cell death, we further investigated the two extracts regarding the mechanisms involved. Caspase 3 plays a critical role in the execution of the apoptotic program and is one of the key enzymes for the cleavage of the 113 kDa nuclear enzyme poly-(ADP-ribose) polymerase (PARP) that is cleaved in fragments of 89 and 24 kDa during apoptosis (**37, 38**).

S. lucida caused the specific cleavage of Caspase 3 to the active 17 kDa and the proteolytic cleavage of the death substrate PARP into the large 89 kDa fragment demonstrating that caspase 3 was functional and responsible for the pro-apoptotic property of *S. lucida* methanol extract (**figure 8**). In contrast, *S. floribunda* did not show caspase 3 activation and signature

type PARP cleavage. Instead of the 89 kDa cleavage product we found a smaller 55 kDa fragment. It was demonstrated that also necrotic cell death of HL-60 cells goes along with degradation of PARP, but different from that observed during apoptosis (**39, 40**). **Gobeil et al.** (**41**) revealed that necrotic treatment of Jurkat T cells did not cause caspase activation and provoked the appearance of multiple PARP cleavage products mediated by lysosomal proteases. The main fragment was at 55 kDa, which was also found here after treatment of Hl-60 cells with *S. floribunda* extract and which correlated with the necrotic phenotype observed by HO/PI double staining (**20, 21, 42**).

To investigate whether genotoxicity of the two extracts was responsible for cell death, we analysed the phosphorylation status of the histone H2AX (γ-H2AX), because this core histone variant becomes rapidly phosphorylated in response to DNA double strand breaks. Interestingly both extracts, *S. lucida* and as well *S. floribunda*, caused severe phosphorylation of H2AX after 2 and 4 h incubation, respectively.

Tubulin is the major constituent of microtubuli, which facilitates chromosome disjunction during mitosis, and therefore, affecting the tubulin structures is incompatible with functional cell division (**43**). Alterations of the fine tuned balance of microtubuli polymerisation/de-polymerisation, such as by taxol are reflected by the acetylation status of α-tubulin (**44**). Both methanol extracts increased the acetylation of α-tubulin demonstrating that cytotoxicity can be attributed to tubulin polymerization.

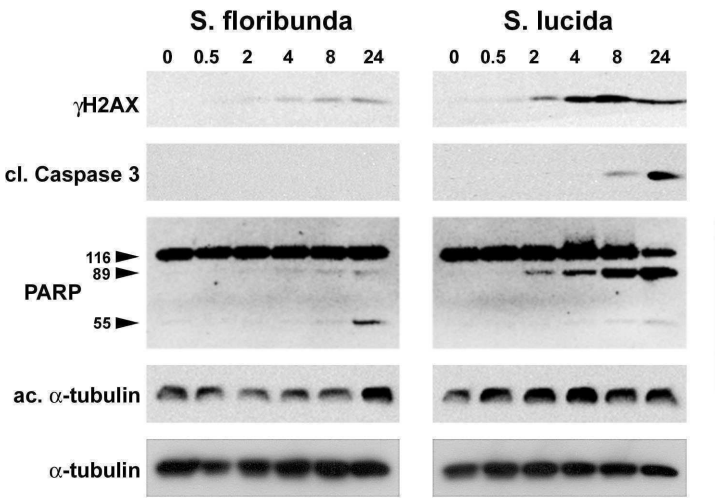

Figure 8 Western blot analysis of apoptosis related proteins. 1 x 10^6 HL-60 cells/ml were incubated with 20 µg/ml detannified extract and harvested after 0.5, 2, 4, 8 and 24 h of treatment. Cells were lysed and obtained protein samples applied to SDS-PAGE. Western blot analysis was performed with the indicated antibodies. Equal sample loading was confirmed by Ponceau S staining and α-tubulin analysis.

Inhibition of lymphendothelial gap formation induced by co-cultivated tumour cell spheroids

Tissue invasion and metastasis is one of the hallmarks of cancer described by **Hanahan and Weinberg** (**45, 46**) and for most tumor types patients are not threatened by the primary tumour but by metastases that destroy the function of infested organs. We tested the extracts of both plants in a recently developed three-dimensional cell culture assay measuring the area of **c**ircular **c**hemorepellent-**i**nduced **d**efects CCIDs in the lymphendothelial cell (LEC) barrier (**figure 9**) which are induced by exudates (i.e. 12(S)-hydoxyeicosatetraenoic acid) of MCF-7 cancer cell spheroids. CCIDs can be considered as entry gates for tumor cells and are directly responsible for lymph node- and distant metastases (**15, 16, 17**). The extract of *S. floribunda* did not prevent CCID formation but affected the viability of LECs and because of the toxic effect of 1 mg/ml MeOH extract to LECs, the precise effect on CCID formation could not be evaluated. Both extracts of *S. lucida* (MeOH and detannified dtMeOH) significantly inhibited CCID formation in LECs up to 40%. The total MeOH extract showed extremely high fluorescence that disappeared after detannification.

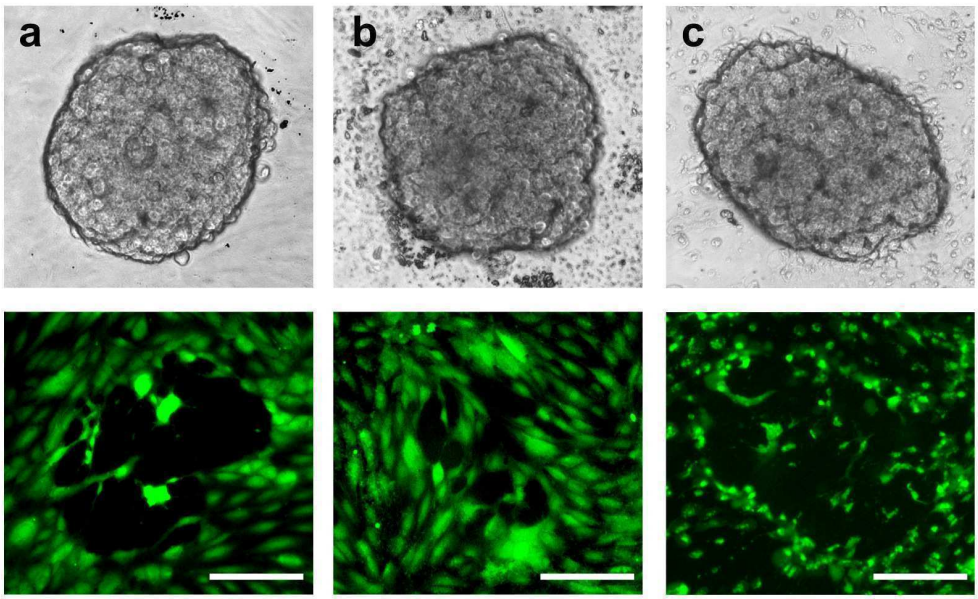

d

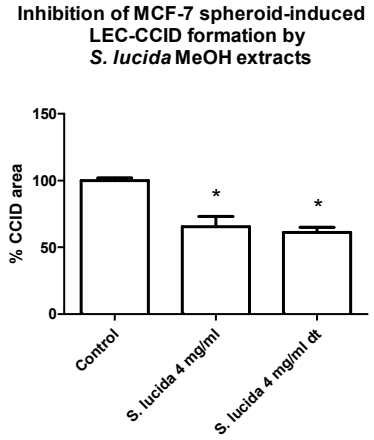

Figure 9 Effect of different *Scrophularia* extracts on MCF-7 spheroid induced gap formation in lymphendothelial cell monolayers. Upper panel: MCF-7 tumor cell spheroids; lower panel: same microscopical frame showing LECs underneath MCF-7 spheroids. The 3D co-cultures were treated either with a) solvent (ethanol) or with dtMeOH extracts of b) *S. lucida* or c) *S. floribunda* corresponding to 4 mg dried plant weight /ml medium. When the 3D co-cultures were treated with *S. lucida* extract the generated CCIDs in LECs underneath the MCF-7 spheroids were d) on average ~40 % smaller than those in controls. dt: detannified MeOH extract; scale bars: 150 µm

NF-κB inhibition by *S. lucida* extract

Besides exudates like 12-S-HETE mentioned above, also NF-κB activation was reported to be associated with tumor cell proliferation, survival, angiogenesis and invasion (**47, 48**). We could show that the inhibition of NF-κB translocation with Bay11-7082, an irreversible inhibitor of I-κBα phosphorylation, blocked MCF-7 spheroid-induced gap formation of LECs in a dose-dependent fashion (**16**). To check whether the significant inhibition of CCID formation in LECs caused by *S. lucida* extracts may be induced through inhibition of NF-κB activity, we tested the detannified extract in a NF-κB luciferase reporter gene assay. Cells were stimulated with 2 ng/ml TNF-α, and luciferase activity was measured after incubation with the selective NF-κB inhibitor Bay11-7082 and different concentrations of *S. lucida* (corresponding 0.5 g/ml, 2 g/ml and 4 g/ml of the dried plant) and compared with a TNF-α/ethanol treated control. As expected, 15 µM of Bay11-7082 (as positive control) inhibited NF-κB activity by nearly 70%. *S. lucida* also decreased the expression of the reporter gene dose-dependently (**figure 10**).

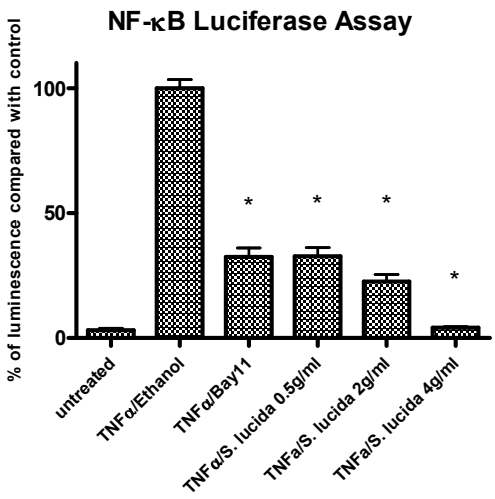

Figure 10 Effect of *S. lucida* extract on the NF-κB transactivation activity. $10x10^6$ HEK293-NFκB-Luc cells were transfected with the cDNA of green fluorescence protein (GFP). After incubation for 6 hours, $4x10^4$ cells per well were seeded in serum- and phenol red-free DMEM in a 96 transparent well plate. On the next day cells were treated with detannified *S. lucida* extract (corresponding to 0.5, 2 and 4 mg dried plant /ml medium), 15 µM Bay 11-7082 as a specific inhibitor of NF-κB, or solvent (ethanol). One hour after treatment cells were stimulated with 2 ng/ml human recombinant TNF-α for additional 4 hours. Luminescence of the firefly luciferase and fluorescence of the GFP were quantified on a GeniusPro plate reader. The luciferase signal derived from the NF-κB reporter was normalized by the GFP-derived fluorescence to account for differences in cell number or transfection efficiency. Experiments were performed in triplicate. Asterisks indicate significance compared to untreated control ($p<0.05$) and error bars indicate ±SD.

Discussion

Different species of the *Scrophularia* family are used since ancient times as remedies for some medical conditions including inflammatory diseases and tumors (**8, 10**). While most publications focus on the anti-inflammatory properties (**11, 12**), this work demonstrates for the first time the anti-proliferative and pro-apoptotic properties of different *Scrophularia species*, and beyond that we show that *S. lucida* inhibits LEC-CCID formation by co-cultivated MCF-7 cancer cell spheroids (**14, 17**) and inhibited NF-κB activity. Recently we could demonstrate that NF-κB activity contributed to LEC-CCID formation through inhibition of VE-cadherin expression and loss of intra-specific LEC adhesion (**16, 49**).

As of the different tested methanolic *Scrophularia* extracts *S. lucida* and *S. floribunda* showed the strongest anti-proliferative properties, these two extracts were chosen to check the underlying mechanisms. Treating HL-60 cells with the detannified *S. floribunda* extract resulted in a strong G2/M arrest after 8 hours. This increase of the cell number in G2/M correlated with the phosphorylation status of Cdc2, which is indicative for its inhibition. In contrast, 8 hour treatment with *S. lucida* showed a strong accumulation in the S-phase and after 24 hours there was a severe G2/M decrease (correlating with Cdc2 activation). The subsequent increase of the subG1 peak suggests that the cells are directly running into death from G2/M. Interestingly, the Cdc2 phosphorylation status did not correlate with the expression levels of Cdc25 phosphatases neither after treatment with the extract of *S. floribunda* nor with that of *S. lucida*, but it correlated with the expression of Wee1. Therefore, *Scrophularia* extracts most likely regulated Cdc2 activity through Wee1 and not Cdc25, demonstrating that Wee1 activity dominates over Cdc25 activity. However, tilting fine tuned Cdc25 activities and expression may trigger cell cycle arrest and finally apoptosis although Cdc2 is active.

The accumulation of HL-60 cells in S-phase after 8 hour treatment with *S. lucida* might be caused through degradation of c-myc oncogene. c-Myc is associated with a wide range of cancers and is an essential regulator of G1/S transition (**50, 51**). While in normal cells inhibition of c-myc usually results in a G0/G1 cell cycle arrest (**52, 53**), tumor cells exhibit significant heterogeneity with regard to the positioning of cell cycle arrest in response to c-Myc depletion (**54**). **Cannell et al.** (**55**) showed that in response to DNA damage c-myc is translationally repressed by the induction of miR-34c microRNA and that this induction is induced by p38 MAPK/MK2 signalling resulting in S-phase arrest. As c-myc is over-

expressed primarily in cancer cells, its down-regulation may inhibit proliferating cancer cells specifically (**56, 57**).

Another important property of a good anti cancer remedy is its ability to kill cancer cells and beside their anti-proliferative properties both extracts led to cell death in HL-60 cells. Strong phosphorylation of the histone H2AX demonstrates that both extracts are genotoxic. Treatment of HL-60 cells with *S. lucida* resulted in high apoptosis rate after 48 hours, driven through caspase 3 activation and subsequent cleavage of PARP into the active 89 kDa fragment. In contrast, *S. floribunda* showed severe necrosis and neither caspase 3 activation nor signature type cleavage of PARP. The main fragment was at 55 kDa and is described as necrotic PARP cleavage product (**41**). This extremely toxic effect was also observed in the CCID assay, where *S. floribunda* killed the LECs already after 4 hours. Due to this generally toxic effect also against normal cells *S. floribunda* has to be dismissed as an anti-cancer remedy.

As mentioned above, most publications highlight anti-inflammatory properties of *Scrophularia* species. **Giner et al.** (**11**) investigated the activity of four glycoterpenoids (two saponins, verbascosaponin A and verbascosaponin, and two iridoids, scropolioside A and scrovalentinoside) isolated from *S. auriculata* ssp. *pseudoauriculata* in different models of acute and chronic inflammation and demonstrated the anti-inflammatory activity in mice against different endema inducers. In another publication (**12**) five phenylpropanoid glycosides isolated from the roots of *S. scordonia* L. have been evaluated as potential inhibitors of some macrophage functions involved in the inflammatory process. They were shown to perform inhibitory effects on enzymes of the arachidonate cascade (COX-1, COX-2) and significant reduction of LPS-induced TNF-α production without relevant effects on the ALOX5 pathway. Treating LEC monolayers with 1 μM synthetic 12(S)-HETE, a metabolite of arachidonic acid generated by ALOX12/15, caused the phosphorylation of MLC2 (**16**) indicating that 12(S)-HETE induced the motility of LECs thereby provoking an early step of metastasis (**15, 17**). This observation is also consistent with an inflammatory process, which is accompanied by the acquisition of a mobile phenotype of the affected cells reflecting "epithelial to mesenchymal transition" (EMT; **58).** Interestingly, the extract of *S. lucida* activated the mobility marker MLC2 (data not shown). It was expected that MLC2 would become inhibited, because of the markedly attenuated formation of CCIDs. Therefore, other activities suppressing LEC migration must have prevailed over MLC2 activation and the NF-κB inhibitory property of *S. lucida* is a likely candidate for this effect. As *Scrophularia* species have been used as remedies for different skin diseases, including scabies, eczema and

psoriasis (**8**) the partly pro-migratory property inducing MLC2 phosphorylation could be an explanation for this wound healing effect, which depends on the plasticity of cells.
Furthermore, an ethanol extract prepared from the aerial parts of *S. striata* Boiss significantly and dose-dependently inhibited matrix metalloproteinases (MMPs) activity (**59**). According to the critical role of MMPs in tumor invasion, metastasis and neovascularisation, the inhibition of the degradation of components of the extracellular matrix is a promising approach for the prevention of cancer progression. In order to develop distal metastasis a tumor cell has to encompass different steps: local infiltration into the adjacent tissue, intravasation, survival within the circulatory system, extravasation and subsequent proliferation leading to colonization (**58, 60**). Inhibiting the first steps of this multi step process must be a major goal of cancer therapy. We could demonstrate that *S. lucida* exhibited significant inhibition of CCID formation and MMP2 and MMP9 play a significant role in this particular assay (**15**).

Conclusion

Here we could show that the species *S. lucida*, which is a genus widely used as folk remedy, exhibits severe anti-proliferative and killing effects on cancer cells and strong anti-invasive properties. The fractionation of the methanol extract will be a mandatory future approach to identify the compounds responsible for the anti-proliferative and anti-metastatic properties.

Acknowledgements

We wish to thank Toni Jäger for preparing the figures.

References

1. M.W. Wang, X. Hao and K. Chen, "Biological screening of natural products and drug innovation in China" *Philos Trans R Soc Lond B Biolo Sci*, vol. 362, no. 1482, pp. 1093-1105, 2007.

2. G.F. Gonzales, and L.G. Valerio jr., "Medicinal plants from Peru: a review of plants as potential agents against cancer", *Anticancer Agents Med Chem*, vol. 6, no. 5, pp. 429-444, 2006.

3. G.M. Cragg and D.J. Newman "Plants as a source of anti –cancer agents", *J Ethophrmacol*, vol. 100, no. 1-2, pp. 72-79, 2005.

4. G.M. Cragg and D.J. Newman, "Antineoplastic agents fom natural sources: achievements and future directions", *Expert Opin Investig Drugs*, vol. 9, pp. 2783-2797, 2000.

5. D.J. Newman and G.M. Cragg, "Natural products as sources of new drugs over the last 25 years", *J Nat Prod*, vol. 70, no. 3, pp. 461-477, 2007.

6. T. Baytop, "Türkiyede Bitkiler ile Tedavi", *Istanbul University Press*, Faculty of Pharmacy No: 3255, 1999.

7. Vienna Dioscurides, 6th century, National Library, Vienna, Austria

8. J. Galindez, A.M. Diaz Lanza and L. Fernandez Metallano, "Biologically Active Substances from the Genus Scrophularia", *Pharmaceutical Biology*, vol. 40, no. 1, pp. 45-59, 2002.

9. I. Çalis, G.A. Gross and O. Sticher O., "Phenylpropanoid glycosides isolated from Scrophularia scopolii" *Phytochemistry*, vol: 26, pp. 2057–2061, 1987.

10. A.T. Nguyen, J. Fontaine, H. Malonne, M. Claeys, M. Luhmer and P. Duez, "A sugar ester and an iridoid glycoside from Scrophularia ningpoensis", *Phytochemistry*, vol. 66, pp. 1186-1191, 2005.

11. R.M. Giner, M.L. Villalba, M.C. Recio, S. Manez, M. Cerda-Nicolas and J.L. Rios, "Anti-inflammatory glycoterpenoids from *Scrophularia auriculata*", *Eur J Pharmacol*, vol. 389, pp. 243-252, 2000.

12. A.M. Díaz, M.J. Abad, L. Fernández, A.M. Silván, J. de Santos and P. Bermejo, "Phenylpropanoid glycosides from Scrophularia scorodonia: In vitro anti-inflammatory activity", *Life Sci*, vol. 74, pp. 2515-2526, 2004.

13. A. Özmen, S. Madlener, S. Bauer, S. Krasteva, C. Vonach, B. Giessrigl, M. Gridling, K. Viola, N. Stark, P. Saiko, B. Michel, M. Fritzer-Szekeres, T. Szekeres, T. Askin-Celik, L. Krenn and G. Krupitza, "In vitro anti-leukemic activity of the ethno-pharmacological plant Scutellaria orientalis ssp. carica endemic to western Turkey", *Phytomedicine*, vol. 17, no. 1, pp. 55-62, 2010.

14. A. Özmen, S. Bauer, M. Gridling, J. Singhuber, S. Krasteva, S. Madlener, N. T. P. Vo, N. Stark, P. Saiko M. Fritzer-Szekeres, T. Szekeres, T. Askin-Celik, L. Krenn and G. Krupitza, "In vitro anti-neoplastic activity of the ethno-pharmaceutical plant Hypericum adenotrichum Spach endemic to Western Turkey", *Oncology Reports*, vol. 22, no. 4, pp. 845-852, 2009.

15. D. Kerjaschki, Z. Bago-Horvath, M. Rudas, V. Sexl, C. Schneckenleithner, S. Wolbank, G. Bartel, S. Krieger, R. Kalt, B. Hantusch, T. Keller, K. Nagy-Bojarszky, N. Huttary, I. Raab, K. Lackner, K. Krautgasser, H. Schachner, K. Kaserer, S. Rezar, S. Madlener, C. Vonach, A. Davidovits, H. Nosaka, M. Hämmerle, K. Viola, H. Dolznig, M. Schreiber, A. Nader, W. Mikulits, M. Gnant, S. Hirakawa, M. Detmar, K. Alitalo, S. Nijman, F. Offner, T.J. Maier, D. Steinhilber and G. Krupitza, "Lipoxygenase mediates invasion of intrametastatic lymphatic vessels and propagates lymph node metastasis of human mammary carcinoma xenografts in mouse" *J Clin Inves.*, vol. 121, no. 5, pp. 2000–2012, 2011.

16. C. Vonach, K. Viola, B. Giessrigl, N. Huttary, I. Raab, R. Kalt, S. Krieger, N.T. Vo, S. Madlener, S. Bauer, B. Marian, M. Hämmerle, N. Kretschy, M. Teichmann, B. Hantusch, S. Stary, C. Unger, M. Seelinger, A. Eger, R. Mader, W. Jäger, W. Schmidt, M. Grusch, H. Dolznig, W Mikulits and G. Krupitza, "NF-κB mediates the12(S)-HETE-induced endothelial to mesenchymal transition of lymphendothelial cells during the intravasation of breast carcinoma cells", *Br J Cancer*, vol. 105, no. 2, pp. 263-271, 2011.

17. S. Madlener, P. Saiko, C. Vonach, K. Viola, N. Huttary, N. Stark, R. Popescu, M. Gridling, N.T. Vo, I. Herbacek, A. Davidovits, B. Giessrigl, S. Venkateswarlu, S. Geleff, W. Jäger, M. Grusch, D. Kerjaschki, W. Mikulits, T. Golakoti, M. Fritzer-Szekeres, T. Szekeres and G. Krupitza, "Multifactorial anticancer effects of digalloyl-resveratrol encompass apoptosis, cell-cycle arrest, and inhibition of lymphendothelial gap formation in vitro", *Br J Cancer*, vol. 102, no. 9, pp. 1361-1370, 2010.

18. S. Maier, S. Strasser, P. Saiko, C. Leisser, S. Sasgary, M. Grusch, S. Madlener, Y. Bader, J. Hartmann, H. Schott, R. M. Mader, T. Szekeres, M. Fritzer-Szekeres and G. Krupitza, „Analysis of mechanisms contributing to AraC-mediated chemoresistance and re-establishment of drug sensitivity by the novel heterodinucleoside phosphate 5-FdUrd-araC", *Apoptosis*, vol. 11, no. 3, pp. 427-440, 2006.

19. S. Strasser, S. Maier, C. Leisser, P. Saiko, S. Madlener, Y. Bader, A. Bernhaus M. Gueorguieva, S. Richter, R. M. Mader, J. Wesierska-Gadek, H. Schott, T. Szekeres, M. Fritzer-Szekeres and G. Krupitza, "5-FdUrd-araC heterodinucleoside re-establishes sensitivity in 5-FdUrd- and AraC- resistant MCF-7 breast cancer cells overexpressing ErbB2", *Differentiation*, vol. 74, pp. 488-498, 2006.

20. M. Grusch, M. Fritzer-Szekeres, G. Fuhrmann, G. Rosenberger, C. Luxbacher, H.L. Elford, K. Smid, G.J. Peters, T. Szekeres and G. Krupitza, "Activation of caspases and induction of apoptosis by amidox and didox", *Exp Haematol*, vol. 29, pp. 623-632, 2001.

21. M. Grusch, D. Polgar, S. Gfatter, K. Leuhuber, S. Huettenbrenner, C. Leisser, G. Fuhrmann, F. Kassie, H. Steinkellner, K. Smid, G.J. Peters, H. Jayaram, T. Klepal, T. Szekeres, S. Knasmüller and G. Krupitza, "Maintainance of ATP favours apoptosis over necrosis triggered by benzamide riboside", *Cell Death Differ*, vol. 9, pp. 169-178, 2002.

22. S. Hüttenbrenner, S. Maier, C. Leisser, D. Polgar, S. Strasser, M. Grusch and G.Krupitza, „The evolution of cell death programs as prerequisites of multicellularity", *Reviews in Mutation Research*, vol. 543, pp. 235-249, 2003.

23. S. Madlener, J. Svacinová, M. Kitner, J. Kopecky, R. Eytner, A. Lackner, N. T. P. Vo, R. Frisch, M. Grusch, R. de Martin, K. Dolezal, M. Strnad and G. Krupitza", In vitro anti-

inflammatory and anticancer activities of extracts of Acalypha alopecuroidea (Euphorbiaceae)", *International Journal of Oncology,* vol. 35, no. 4, pp. 881-891, 2009.

24. M. Gridling, N. Stark, S. Madlener, A. Lackner, R. Popescu, B. Benedek, R. Diaz, F. M. Tut , N. T. P. Vo, D. Huber, M. Gollinger, P. Saiko, A. Özmen, W. Mosgoeller, R. de Martin, R. Eytner, K. H. Wagner, M. Grusch, M. Fritzer-Szekeres, T. Szekeres, B. Kopp, R. Frisch and G. Krupitza, "In vitro anti-cancer activity of two ethno-pharmacological healing plants from Guatemala Pluchea odorata and Phlebodium decumanum", *International Journal of Oncology*, vol. 34, no. 4, pp. 1117-1128, 2009.

25. A. Biroccio, D. del Bufalo, A. Ricca, C. D'Angelo, G. d'Orazi, A. Sacchi, S. Soddu and G. Zupi, "Increase of BCNU sensitivity by wt-p53 gene therapy in glioblastoma lines depends on the administration schedule", *Gene Ther*, vol. 6, pp. 1064-1072, 1999.

26. K.S. Park, S.H. Jeon J.W. Oh and K.Y. Choi, "p21Cip/WAF1 activation is an important factor for the ERK pathway dependent anti-proliferation of colorectal cancer cells", *Exp Mol Med*, vol. 36, pp. 557-562, 2004.

27. M.M. Facchinetti, A. de Siervi, D. Toskos and A.M. Senderowicz, "UCN-01-induced cell cycle arrest requires the transcriptional induction of p21(waf1/cip1) by activation of mitogen-activated protein/extracellular signal-regulated kinase kinase/extracellular signal regulated kinase pathway", *Cancer Res*, vol. 64, pp. 3629-3637, 2004.

28. H.L. Ebner, M. Blatzer, M. Nawaz and G. Krumschnabel, "Activation and nuclear translocation of Erk in response to ligand-dependent and –independent stimuli in liver and gill cells from rainbow trout", *J Exp Biol*, vol. 210, pp. 1036-1045, 2007.

29. C.M. Lee, D. Onésime, C.D. Reddy, N. Dhanasekaran, E.P.J.L.P. Reddy, "A scaffolding protein that tethers JNK/p38MAPK signaling modules and transcription factors", *Proc Natl Acad Sci USA*, vol. 99, no. 22, pp. 14189-1494, 2002.

30. A.S. Zervos, L. Faccio, J.P. Gatto, J.M. Kyriakis and R. Brent, "Mxi2, a mitogen-activated protein kinase that recognizes and phosphorylates Max protein", *Proc Natl Acad Sci USA*, vol. 92, no. 23, pp.10531-1054, 1995.

31. M. Donzelli and G.F. Draetta GF, “Regulating mammalian checkpoints through Cdc25 inactivation” *EMBO Rep*, vol. 4, pp. 671-677, 2003.

32. J. Falck, N. Mailand, R.G. Syljuasen, J. Bartek and J. Lukas, “The ATM-Chk2-Cdc25A checkpoint pathway guards against radioresistant DNA synthesis”, *Nature*, vol. 410, pp. 842-847, 2001.

33. T.A. Baudino and J.L. Cleveland JL, “The Max network gone mad”, *Mol Cell Biol*, vol. 21, no. 3, pp. 691-702, 2001.

34. C.V. Dang, “c-Myc target genes involved in cell growth, apoptosis and metabolism”, *Mol Cel Biol,* vol. 19, no. 1, pp. 1-11, 1999.

35. K. Milde-Langosch, “The Fos family of transcription factors and their role in tumourigenesis”, *Eur J Cancer*, vol. 41, pp. 2449-2461, 2005

36. E. Tulchinsky, “Fos family members: regulation, structure and role in oncogenic transformation”, *Histol Histopathol*, vol. 15, pp. 921–928, 2000.

37. T. Fernandes-Alnemri, G. Litwack and E.S. Alnemri, “CPP32, a novel human apoptotic protein with homology to Caenorhabditis elegans cell death protein Ced-3 and mammalian interleukin-1 beta-concerting enzyme”, *J Biol Chem*, vol. 269, pp. 30761-30764, 1994.

38. M. Germain, E.B. Affar, D. d’Amours, V.M. Dixit, G.S. Salvesen and G.G. Poirier GG, “Cleavage of poly(ADP-ribose)polymerase during apoptosis” *J Biol Chem*, vol. 274, pp. 28379-28384, 1999.

39. G.M. Shah, R.G. Shah, and G.G.Poirier, “Different cleavage pattern for poly(ADP-Ribose) polymerase during necrosis and apoptosis in HL-60 cells”, *Biochem Biophys Res Commun*, vol. 229, pp. 838-844, 1996.

40. C.A. Casiano, R.L. Ochs and E.M. Tan, “Distinct cleavage products of nuclear proteins in apoptosis and necrosis revealed by autoantibody probes”, *Cell Death Differ,* vol. 5, pp. 183-190, 1998.

41. S. Gobell, C.C. Boucher, D. Nadeau and G.G. Poirier, “Characterization of the necrotic cleavage of poly(ADP-ribose) polymerase (PARP-1): implication of lysosomal proteases”, *Cell Death Differ,* vol. 8, pp. 588-594, 2001.

42. M. Fritzer-Szekeres, M. Grusch, C. Luxbacher, Z. Horvath, G. Krupitza, H.L. Elford and T. Szekeres, “Trimidox, an inhibitor of ribonucleotide reductase, induces apoptosis and activates caspases in HL-60 promyelocytic leukemia cells”, *Exp Haematol*, vol. 28, pp. 924-930, 2000.

43. G. Piperno and M. Fuller, “Monoclonal antibodies specific for an acetylated form of alpha-tubulin recognize the antigen in cilia and flagella from a variety of organisms”, *J Cell Biol*, vol. 101, pp. 2085-2094, 1985.

44. H. Xiao, P. Verdier-Pinard, N. Fernandez-Fuentes, B. Burd, R. Angeletti, A. Fiser, S.B. Horwitz and G.A. Orr, “Insights into the mechanism of microtubule stabilization by taxol”, *Proc Natl Acad Sci USA*, vol. 103, pp. 10166-10173, 2006.

45. D. Hanahan and R.A. Weinberg, “The Hallmarks of Cancer”, *Cell*, vol. 100, pp. 57-70, 2000.

46. D. Hanahan and R. A. Weinberg, “Hallmarks of cancer: the next generation“, *Cell*, vol. 144, no. 5, pp. 646-674, 2011.

47. M. Brown, J. Cohen, D. Arun, Z. Chen and C. Van Waes, “NF-kappa B in carcinoma therapy and prevention.”, *Expert Opin Targets*, vol. 12, no. 9, pp. 1109-1122, 2008.

48. M.J. Flister, A. Wilber, K.L. Hall, C. Iwata, K. Miyazona, R.E. Nisato, M.S. Pepper, D.C. Zawieja and S. Ran, “Inflammation induces lymphangiogenesis through up-regulation of VEGFR-3 mediated by NF-kappaB and Pro1”, *Blood*, vol. 115, no. 2, pp. 418-429, 2010.

49. K. Viola, C. Vonach, N. Kretschy, M. Teichmann, L. Rarova, M. Strnad, B. Giessrigl, N. Huttary, I. Raab, S. Stary, S. Krieger, T. Keller, S. Bauer, K. Jarukamjorn, B. Hantusch, T. Szekeres, R. de Martin. W. Jäger, S. Knasmüller, W. Mikulits, H. Dolznig, G. Krupitza and M. Grusch, “Bay11-7082 and xanthohumol inhibit breast cancer spheroid-triggered

disintegration of the lymphendothelial barrier; the role of lymphendothelial NF-κB", *Br J Cancer,* 2011, submitted, **2011.**

50. S. Adhikary and M. Eilers, "Transcriptional regulation and transformation by Myc proteins", *Nat Rev Mol Cell Biol*, vol. 6, no. 8, pp. 635-645, 2005.

51. C.E. Gauwerky and C.M. Croce, "Chromosomal translocations in leukaemia", *Semin Cancer Biol*, vol. 4, no.6, pp. 333-340, 1993.

52. I.M. de Alboran, R.C. O'Hagan, F. Gartner, B. Malynn, L. Davidson and R. Rickert, "Analysis of c.myc function in normal cells via conditional gene-target mutation", *Immunity*, vol. 14, pp. 45-55, 2001.

53. T. Prathapam, S. Tegen, T. Oskarsson, A. Trumpp and G.S. Martin, "Activated Src abrogates the myc requirement for the G0/G1 transition but not for the G1/S transition", *Proc Natl Acad Sci USA*, vol. 103, pp. 2695-2700, 2006.

54. H. Wang, S. Mannava, V. Grachtchouk, D. Zhuang, M.S. Soengas, A.V. Gudkov, E.V. Prochownik and M.A. Nikiforov, "c-Myc depletion inhibits proliferation of human tumor cells at various stages of cell cycle", *Oncogene*, vol. 27, no. 13, pp. 1905-1915, 2008.

55. I.G. Cannell, Y.W. Kong, S.J. Johnston, M.L. Chen, H.M. Collins, H.C. Dobbyn, A. Elia, T.R. Kress, M. Dickens, M.J. Clemens, D.M. Heery, M. Gaestel, M. Eilers, A.E. Willis and M. Bushell, "p38 MAPK/MK2-mediated induction of miR-34c following DNA damage prevents Myc-dependent DNA replication", *Proc Natl Acad Sci USA*, vol. 107, no. 12, pp. 5375-5380, 2010.

56. G. Krupitza, H. Harant, E. Dittrich, T. Szekeres, H. Huber and C. Dittrich, "Sodium butyrate inhibits c-myc splicing and interferes with signal transduction in ovarian carcinoma cells" *Carcinogenesis*, vol. 16, pp. 1199-1205, 1995.

57. G. Krupitza, S. Grill, H. Harant, W. Hulla, T. Szekeres, H. Huber and C. Dittrich, "Genes related to growth and invasiveness are repressed by sodium butyrate in ovarian carcinoma cells", *Br J Cancer*, vol. 73, pp. 433-438, 1996.

58. F. van Zijl, G. Krupitza and W. Mikulits, “Initial steps of metastasis: Cell invasion and endothelial transmigration”, *Mutat Res*, vol. 728, no. 1-2, pp. 23-34, 2011.

59. R. Hajiaghaee, H.R. Monsef-Esfahani, M.R. Khorramizadeh, F. Saadat, A.R. Shahverdi and F. Attar, “Inhibitory Effect of Aerial Parts of Scrophularia striata on Matrix Metalloproteinases Expression”, *Phytother Res*, vol. 21, pp. 1127-1129, 2007.

60. A. Eger and W. Mikulits, “Models of epithelial-mesenchymal transition”, *Drug Disc Today; Disease models*, vol. 2, pp. 57-63, 2005.

Digalloylresveratrol, a novel resveratrol analog attenuates the growth of human pancreatic cancer cells by inhibition of ribonucleotide reductase *in situ* activity.

Saiko P., Graser G., **Giessrigl B.**, Lackner A., Grusch M., Krupitza G., Jaeger W., Golakoti T., Fritzer-Szekeres M. and Szekeres.

J. of Gastroenterology, ***submitted.***

Digalloylresveratrol, a novel resveratrol analog attenuates the growth of human pancreatic cancer cells by inhibition of ribonucleotide reductase *in situ* activity

Short title: Antitumor effect of digalloylresveratrol

Philipp Saiko[1], Geraldine Graser[1], Benedikt Giessrigl[2], Andreas Lackner[3], Michael Grusch[3], Georg Krupitza[2], Walter Jaeger[4], Trimurtulu Golakoti[5], Monika Fritzer-Szekeres[1], and Thomas Szekeres[1,*]

[1]Department of Medical and Chemical Laboratory Diagnostics, Medical University of Vienna, General Hospital of Vienna, Waehringer Guertel 18-20, A-1090 Vienna, Austria

[2]Institute of Clinical Pathology, Medical University of Vienna, General Hospital of Vienna, Waehringer Guertel 18-20, A-1090 Vienna, Austria

[3]Department of Medicine I, Division of Cancer Research, Medical University of Vienna, Borschkegasse 8a, A-1090 Vienna, Austria

[4]Department of Clinical Pharmacy and Diagnostics, University of Vienna, Althanstrasse 14, A-1090 Vienna, Austria

[5]Laila Impex R&D Center, Jawahar Autonagar, Vijayawada, 520 007 India

*Corresponding author:

Phone: +43 1 40400 5365

FAX: +43 1 320 33 17

Email: thomas.szekeres@meduniwien.ac.at

Abstract

Introduction: Digalloylresveratrol (DIG) is a newly synthesized compound aimed to combine the biological effects of the plant polyphenolics gallic acid and resveratrol, which are both radical scavengers exhibiting anticancer activity. In this study, we investigated the effects of DIG in the human AsPC-1 and BxPC-3 pancreatic adenocarcinoma cell lines.

Methods: The colony formation of cells was determined by clonogenic assay, the induction of apoptosis was evaluated by a specific Hoechst dye 33258 and propidium iodide double staining, cell cycle distribution was analyzed by FACS, and RR *in situ* activity was quantified by incorporation of ^{14}C-cytidine into nascent DNA. Alterations of deoxyribonucleoside triphosphate (dNTP) pools were measured by HPLC, and protein expression was investigated by western blotting.

Results: DIG dose-dependently inhibited the formation of tumor cell colonies and caused an accumulation of cells in the S phase. The incorporation of ^{14}C-cytidine into nascent DNA was significantly inhibited at all DIG concentrations employed, being equivalent to an *in situ* inhibition of RR and this was consistent with the observed S phase arrest. Furthermore, Erk1/2 became inactivated and moderated p38 phosphorylation indicating a mild replication stress. DIG led to a significant depletion of the dATP pool in AsPC-1 cells, activated ATM and Chk2, and induced the phosphorylation and degradation of the proto-oncogene Cdc25A, whereas DIG-induced phosphorylation of Akt compromised apoptosis.

Conclusion: DIG strongly inhibits colony formation, cell cycle progression, and RR *in situ* activity in AsPC-1 and BxPC-3 cells. Due to these promising results, further preclinical and *in vivo* investigations are warranted.

Key words: Digalloylresveratrol, ribonucleotide reductase, pancreatic cancer, AsPC-1 cells, BxPC-3 cells.

Introduction

Pancreatic cancer is an aggressive malignancy with poor prognosis, suffering from the lack of early diagnosis and appropriate treatment options. The 5-year survival rate remains beyond 5%, with the median survival period being less than 6 months [1]. Pancreatic cancer accounts for 6% of all cancer deaths, and is the fourth leading cause of cancer death in the United States [2-3]. The introduction of potentially curative resection has led to improved survival, but patients eventually relapse from local recurrence and metastasis, which renders pancreatic cancer an incurable disease given the currently available treatment modalities. Accordingly, more effective therapeutic strategies are needed for an ameliorated control of unresectable and/or metastatic disease.

Naturally occurring compounds with putative cancer chemopreventive properties, such as the phytoalexin resveratrol (3,4',5-trihydroxy-*trans*-stilbene; RV) or the virostatic and antimycotic agent gallic acid (3,4,5-trihydroxybenzoic acid; GA), guide the design of novel agents with improved pharmacologic potential. RV has initially been identified as the main ingredient of (red) wine being responsible for the so-called *French paradox* [4]. The latter is the fact that the heart infarction rate in France is at least 40% lower than in all other European countries and the United States, despite a diet rich in saturated fat [5]. As part of the tannin molecule, GA is also present in (red) wine and has been proposed to contribute to the *French paradox* [6].

During the past years, numerous studies revealed the distinct free radical-scavenging activity of RV and GA and their anticancer effects [7-9]. RV and GA were shown to induce differentiation and programmed cell death in a wide variety of tumor cell lines [10] and to effectively inhibit the enzyme ribonucleotide reductase (RR; EC 1.17.4.1) [8, 11]. RR catalyzes

the rate-limiting step of *de novo* DNA synthesis, which is the reduction of ribonucleotide diphosphates into the corresponding deoxyribonucleotide diphosphates. RR is significantly upregulated in tumor cells and in order to meet the increased need for deoxyribonucleoside triphosphates (dNTPs) for DNA synthesis [12] and is therefore considered an excellent target for cancer chemotherapy. Difluorodeoxycytidine (Gemcitabine; dFdC) is a commonly used RR inhibitor that has been the mainstay of systemic treatment of pancreatic cancer for more than a decade but with only limited therapeutic efficacy [1, 13-14].

The enzyme is an $\alpha 2\beta 2$ complex consisting of two subunits [15]. The effector binding R1 subunit possesses an $\alpha 2$ homodimeric structure with substrate and allosteric effective sites that control enzyme activity and substrate specificity. The nonheme iron R2 subunit, a $\beta 2$ homodimer, forms two dinuclear iron centers each stabilizing a tyrosyl radical. The inhibition of the nonheme iron subunit can be caused, for instance, by iron chelation or radical scavenging of the tyrosyl radical [16]. Additionally, a p53-inducible R2-homologue (p53R2) has been described recently [16]. Expression of the R2 and p53R2 subunits is induced by DNA damage and it has been reported that p53R2 supplies dNTPs for DNA repair in G_0/G_1 cells in a p53-dependent manner [17].

Based on the promising cytotoxic effects of the single compounds, we recently synthesized an ester of one molecule RV and two molecules GA, digalloylresveratrol (DIG). To date, we have already shown that an equimolar combination of RV and GA (ratio 1:2) inhibited the growth of human HT-29 colon cancer cells to a lesser extent than DIG. The latter also diminished RR activity in this cell line [18]. In human HL-60 promyelocytic leukemia cells, treatment with DIG led to induction of apoptosis, cell cycle arrest, attenuation of RR activity, and inhibition of lymphendothelial gap formation *in vitro* [19].

We therefore hypothesized that DIG may be also effective in solid malignancies showing an even worse prognosis, such as pancreatic cancer. Following this strategy, we investigated the biochemical effects of DIG in the AsPC-1 and BxPC-3 human pancreatic adenocarcinoma cell lines in order to identify possible beneficial effects that might lead to further preclinical and *in vivo* studies.

DIG was examined for its cytotoxicity employing clonogenic assays. The induction of apoptosis was quantified using a Hoechst/propidium iodide double staining method and cell cycle distribution effects were evaluated by FACS. Expression levels of cell cycle regulating proteins were determined by western blotting: We investigated the phosphorylation of ATM, Chk2, p38, and Akt kinases as well as the phosphorylation of Cdc25A phosphatase. The question of whether DIG inhibits the *in situ* activity of RR and/or affects the steady state of deoxynucleosidetriphosphate pools (dNTPs), which are the products of RR metabolism, was addressed by incorporation of radio-labeled ^{14}C-cytidine into nascent DNA of tumor cells and by employing a specific HPLC method, respectively. In addition, the radical scavenging potential of DIG was measured by DPPH assay because the tyrosyl radical harbored in the R2 subunit of RR serves as an additional target for inhibiting the enzyme.

Methods

Chemicals and supplies

Digalloylresveratrol (DIG) was synthesized and provided by Laila Impex R&D Center, Jawahar Autonagar, Vijayawada, 520 007 India. Resveratrol (3,4,5-trihydroxy-*trans*-stilbene; RV), gallic acid (3,4,5-trihydroxybenzoic acid; GA), and solvent DMSO were obtained from Sigma-Aldrich GmbH, Vienna, Austria. Structural formulas of DIG, GA, and RV including nomenclature, molecular weight, and molecular formula are given in figure 1. All other chemicals and reagents were commercially available and of highest purity.

Cell culture

Human AsPC-1 and BxPC-3 pancreatic adenocarcinoma cells were purchased from ATCC (American Type Culture Collection, Manassas, VA, USA) and were grown in RPMI 1640 Medium with GLUTAMAX supplemented with 10% heat inactivated fetal calf serum (FCS), 1% Sodium Pyruvate, and 1% Penicillin-streptomycin. Both cell lines were maintained at 37°C in a humidified atmosphere containing 5% CO_2 using a Heraeus cytoperm 2 incubator (Heraeus, Vienna, Austria). Cells were grown in a monolayer culture using 25cm^2 tissue culture flasks and were periodically detached from the flask surface by 0.25% trypsin-ethylenediaminetetraacetic acid (trypsin-EDTA) solution. All media and supplements were obtained from Life Technologies (Paisley, Scotland, UK). Cell counts were determined using a microcellcounter CC-110 (SYSMEX, Kobe, Japan). Cells being in the logarithmic phase of growth were used for all experiments described below.

Clonogenic assay

Cells ($1x10^3$ per well) were plated in 24-well plates and allowed to attach overnight at 37°C in a humidified atmosphere containing 5% CO_2. Then cells were incubated with increasing concentrations of DIG for 6 days. Subsequently, the medium was carefully removed from the wells and the plates were stained with 0.5% crystal violet solution for 5 minutes. Colonies of more than 50 cells were counted using an inverted microscope at 40-fold magnification.

Hoechst dye 33258 and propidium iodide double staining

The Hoechst staining was performed according to the method described by our group [20]. Cells ($0.2x10^6$ per ml) were seeded in $25cm^2$ Nunc tissue culture flasks and exposed to increasing concentrations of DIG for 72 hours. Hoechst 33258 (HO, Sigma, St. Louis, MO, USA) and propidium iodide (PI, Sigma, St. Louis, MO, USA) were added directly to the cells to final concentrations of 5 µg/ml and 2 µg/ml, respectively, followed by 60 minutes of incubation at 37°C. Cells were examined on a Nikon Eclipse TE-300 Inverted Epi-Fluorescence Microscope (Nikon, Tokyo, Japan) equipped with a Nikon DS-5M-L1 Digital Sight Camera System including appropriate filters for Hoechst 33258 and PI. This method allows distinguishing between early apoptosis, late apoptosis, and necrosis and is therefore superior to TUNEL assay that fails to discriminate among apoptosis and necrosis [21-22] and does not provide any morphological information. In addition, the HO/PI staining is more sensitive than a customary FACS based Annexin V binding assay [22-24]. The Hoechst dye stains the nuclei of all cells and thus allows monitoring cellular changes associated with apoptosis, such as chromatin condensation and nuclear fragmentation. In contrast, PI is excluded from viable and early apoptotic cells; consequently, PI uptake indicates loss of membrane integrity being characteristic of late apoptotic and necrotic cells. In combination

with fluorescence microscopy to evaluate the morphologies of nuclei, the selective uptake of the two dyes enables studying the apoptosis induction of intact cultures and distinguishing it from non-apoptotic cell death by means of necrosis. The latter is characterized by nuclear PI uptake without chromatin condensation or nuclear fragmentation [25]. Cells were judged according to their morphology and the integrity of their cell membranes, counted under the microscope and the number of apoptotic cells was given as percentage value.

DPPH radical scavenging activity assay

The radical scavenging activity of DIG was determined using the free radical 2,2-diphenyl-1-picrylhydrazyl (DPPH). In its radical form, DPPH absorbs at 515nm but upon reduction by an antioxidant or radical species, its absorption decreases. The reaction was started by the addition of DIG, RV, GA, or an equimolar combination of RV and GA (10µl; 1–100µM final concentration) to 3.0ml of 0.1mM DPPH in methanol. The bleaching of DPPH was followed using an HP 8453 diode array spectrometer equipped with a magnetically stirred quartz cell. Absorbance was recorded for up to 15 min, although steady states of reaction were reached within 5 min in most cases. The reference cuvette contained up to 0.1mM DPPH in 3.0ml of methanol. The DPPH radical scavenging activity obtained for each compound was compared with that of ascorbic acid and α-Tocopherol.

Cell cycle distribution analysis

Cells ($0.4x10^6$ per ml) were seeded in $25cm^2$ Nunc tissue culture flasks and incubated with increasing concentrations of DIG at 37°C under cell culture conditions. After 48 hours, cells were harvested and suspended in 5 ml cold PBS, centrifuged, resuspended and fixed in 3 ml cold ethanol (70%) for 30 minutes at 4°C. After two washing steps in cold PBS RNAse A and

propidium iodide were added to a final concentration of 50 µg/ml each and incubated at 4°C for 60 minutes before measurement. Cells were analyzed on a FACSCalibur flow cytometer (BD Biosciences, San Jose, CA, USA) and cell cycle distribution was calculated with ModFit LT software (Verity Software House, Topsham, ME, USA).

Incorporation of ^{14}C-labeled cytidine into DNA

To analyze the effect of DIG treatment on the *in situ* activity of RR, an assay was performed as described previously [26]. Radiolabeled ^{14}C-cytidine has to be reduced by RR in order to be incorporated into the DNA of cells following incubation with DIG. Cells (0.4×10^6 cells per ml) were incubated with various concentrations of DIG for 24 hours. Subsequently, cells were counted and pulsed with ^{14}C-cytidine (0.3125 µCi, 5 nM) for 30 minutes at 37°C. Afterwards, cells were collected by centrifugation and washed with PBS. Total DNA from 5×10^6 cells was purified by phenol-chloroform-isoamyl alcohol extraction and specific radioactivity of the samples was determined using a Wallac 1414 liquid scintillation counter (PerkinElmer, Boston, MA) whose read out was normalized by a Hitachi U-2000 Double Beam Spectrophotometer to ensure equal amounts and purity of DNA.

Determination of deoxyribonucleoside triphosphates (dNTPs)

AsPC-1 cells were seeded in 175 cm^2 tissue culture flasks (5×10^7 per flask) and then incubated with increasing concentrations of DIG for 24 hours. The cells were then centrifuged at 1800 g for 5 min, resuspended in 100 µl of PBS, and extracted with 10 µl of trichloracetic acid (90%). The lysate was allowed to rest on ice for 30 min and neutralized by the addition of 1.5 volumes of freon containing 0.5 mol/l tri-n-octylamine. Concentrations of dNTPs were then determined using the method described by Garrett and Santi [27]. Aliquots

(100 µl) of the samples were analyzed using a Merck ''La Chrom'' high-performance liquid chromatography (HPLC) system (Merck, Darmstadt, Germany) equipped with D-7000 interface, L-7100 pump, L-7200 autosampler, and L-7400 UV detector. Detection time was set at 80 min, with the detector operating on 280 nm for 40 min and then switched to 260 nm for another 40 min. Samples were eluted with a 3.2 M ammonium phosphate buffer (pH 3.6, adjusted by the addition of 3.2 mM H_3PO_4) containing 20 M acetonitrile using a 4.6x250 mm PARTISIL 10 SAX column (Whatman Ltd., Kent, UK). Separation was performed at constant ambient temperature and a flow rate of 2 ml per minute. The concentration of each dNTP was calculated as percentage of the total area under the curve for each sample.

Western blotting

After incubation with 40µM DIG, AsPC-1 cells ($2x10^6$ per ml) were harvested, washed twice with ice-cold PBS (pH 7.2) and lysed in a buffer containing 150 mM NaCl, 50 mM Tris-buffered saline (Tris pH 8.0), 1% Triton X-100, 2.5% 100mM phenylmethylsulfonylfluoride (PMSF) and 2.5% protease inhibitor cocktail (PIC; from a 100x stock). The lysate was centrifuged at 12000 rpm for 20 minutes at 4°C, and the supernatant was stored at -20°C until further analysis. Equal amounts of protein samples were separated by polyacrylamide gel electrophoresis (PAGE) and electroblotted onto PVDF membranes (Hybond, Amersham) overnight at 4°C. Equal sample loading was controlled by staining membranes with Ponceau S. After washing with PBS/Tween-20 (PBS/T) pH 7.2 or Tris/Tween-20 (TBS/T) pH 7.6, membranes were blocked for 60 minutes in blocking solution (5% non-fat dry milk in PBS containing 0.5% Tween-20 or in TBS containing 0.1% Tween-20). Then membranes were incubated with the first antibody (in blocking solution, dilution 1:500 to 1:1000) by gently rocking at 4°C, overnight. Subsequently, the membranes were washed with PBS or TBS and

further incubated with the second antibody (peroxidase-conjugated goat anti-rabbit IgG, anti-mouse IgG, or donkey anti-goat IgG – dilution 1:2000 to 1:5000 in PBS/T or TBS/T) at room temperature for 60 minutes. Chemoluminescence was developed by the ECL detection kit (Amersham, Buckinghamshire, UK) and then membranes were exposed to Amersham Hyperfilms. Equal numbers of cells were lysed for each sample and PVDF membranes were checked by Ponceau S staining. Equal sample loading was controlled by β-actin expression, which appeared to be stable when inspected in short term exposures to x-ray films. Each western blot experiment was performed at least twice, and specific experimental points were done more often as they served as internal controls.

Antibodies directed against p(Ser1981)-ATM, p(Thr68)-Chk2, Chk2, cleaved Caspase-3 (Asp175), p(Thr202/Tyr204)-Erk1/2, Erk1/2, p(Thr180/Tyr182)-p38MAPK, p38MAPK, p(Ser473)-Akt, Akt, and goat anti-rabbit IgG were from Cell Signaling (Danvers, MA, USA), against p(Ser177)-Cdc25A from Abgent (San Diego, CA, USA), against R2 (I-15), Cdc25A (F-6), and donkey anti-goat IgG from Santa Cruz (Santa Cruz, CA, USA), against β-actin from Sigma (St. Louis, MO, USA), and goat anti-mouse IgG was from Dako (Glostrup, Denmark).

Statistical calculations

Dose-response curves were calculated using the Prism 5.01 software package (GraphPad, San Diego, CA, USA) and significant differences between controls and each drug concentration applied were determined by unpaired *t*-test. All p-values beyond 0.05 were considered significant and marked with an asterisk (*).

Results

Effect of DIG on the colony formation of AsPC-1 and BxPC-3 cells

Logarithmically growing cells were incubated with various concentrations of drugs for 6 days. After that time, cell colonies were counted as described in the methods section. In AsPC-1 cells, incubation with DIG, GA, and RV led to IC_{50} values (50% inhibition of colonies) of 21.5, 21, and 18µM, respectively. DIG, GA, and RV inhibited the growth of BxPC-3 cell colonies with IC_{50} values of 8.5, 41, and 13 µM, respectively (table 1).

Induction of apoptosis in AsPC-1 and BxPC-3 cells by DIG

Pancreatic cancer cells were exposed to increasing concentrations of DIG for 72 hours and double stained with Hoechst 33258 and propidium iodide to analyze whether apoptotic cell death was induced. However, the number of apoptotic cells did not significantly differ from untreated controls, which is in line with the results of similar studies performed by our group [18] and others [28].

Upon treatment with 30µM DIG, 8.5% of AsPC-1 cells underwent apoptosis (figure 2a). Accordingly, western blot analysis after incubation of AsPC-1 cells with 40µM DIG showed that caspase 3 protein levels remained unchanged (data not shown). Interestingly, Akt kinase became highly phosphorylated at Ser473 within 2 hours, which was shown to provide a survival advantage by inhibiting apoptosis (figure 2b). For technical reasons (rapid agglomeration) apoptosis induction could not be evaluated in BxPC-3 cells.

Cell cycle distribution in AsPC-1 and BXPC-3 cells after treatment with DIG

Cells were incubated with different concentrations of DIG for 48 hours. Treatment of both AsPC-1 and BxPC-3 cells led to an arrest in the S Phase. In AsPC-1 cells, 80µM DIG increased this cell population from 36.7% to 53.3%, whereas G2-M phase cells decreased from 11.4% to 0%. In BxPC-3 cells, exposure to 40µM DIG elevated this cell population from 11.6% to 29.1% while depleting cells in the G0-G1 phase from 85.6% to 68.5% (figures 3a-b). In both cell lines, no subG1 peaks could be observed by FACS at the time points measured.

Inhibition of incorporation of ^{14}C-cytidine into DNA of AsPC-1 and BxPC-3 cells after treatment with DIG

The incorporation of ^{14}C-cytidine into nascent DNA (to determine RR *in situ* activity) was measured in AsPC-1 and BxPC-3 cells after incubation with increasing concentrations of DIG for 24 hours. After exposure of AsPC-1 cells to 20, 25, 30, and 35µM DIG for 24 hours, the incorporation of ^{14}C-cytidine was significantly reduced to 7%, 5%, 5%, and 4% of untreated controls, respectively. BxPC-3 cells were treated with 5, 10, 15 and 20µM DIG, which significantly decreased the incorporation of ^{14}C-cytidine to values beyond 5% at every concentration applied (figures 4a-b).

dNTP alterations after treatment with DIG

Constitutive RR activity maintains balanced dNTP pools, whereas RR inhibition tilts this balance. In line with this, DIG treatment caused an imbalance of dNTPs in AsPC-1 cells after 24 hours, which was determined by HPLC analysis as described in the methods section. Incubation of cells with 20 µM DIG resulted in a significant depletion of intracellular dATP pools to 31% when compared to controls. In contrast, treatment with 30 µM DIG increased

dTTP pools to 130% of control values. Regarding the dCTP pools, treatment with DIG led to only marginal changes. All dGTP pools remained beyond the detectability of the method (figure 5).

Antioxidant activity of DIG, RV, and GA

The *in vitro* free radical-scavenging activity of DIG, RV, GA, and equimolar combinations of RV and GA was determined employing a DPPH-assay. After incubation for 10 min DIG, RV, and GA inhibited 50% of DPPH activity with IC_{50} values of 1.83, 98.3, and 3.12µM, respectively. Although the radical-scavenging activity of RV was notably rather weak when compared with GA, this finding is in agreement with the literature [29-31]. The combination of RV and GA inhibited 50% of DPPH activity at 4.82µM, thus indicating that the antioxidant potential of DIG is superior to an equimolar application of the single agents by about 2.5-fold. Tocopherol and ascorbic acid were used as reference compounds resulting in IC_{50} values of 6.98µM and 9.63µM, respectively (table 2).

Expression of RR subunit R2 after treatment with DIG

To monitor the effect of RR inhibitors on the expression of RR subunit R2, AsPC-1 cells were incubated with 40µM DIG for 0.5, 2, 4, 8, and 24 hours and subjected to western blot analysis. The protein level of the inducible R2 subunit remained unchanged during the time course being consistent with the fact that the activity of the enzyme can be attenuated without influencing the protein levels of its subunits [32] (data not shown).

Expression of checkpoint and cell cycle regulating proteins after treatment of AsPC-1 cells with DIG

To investigate whether stalling of the replication fork caused activation of cell cycle checkpoint kinases, AsPC-1 cells were treated with 40µM DIG for 0.5, 2, 4, 8, and 24 hours and subjected to western blot analysis. Treatment with DIG resulted in phosphorylation at Ser1981 of ATM kinase within 2 hours. ATM is activated upon DNA damage and in turn caused phosphorylation of Chk2 at the activating Thr68 site. Furthermore, DIG phosphorylated Ser177 of Cdc25A, which is a target of Chk2, finally resulting in reduction/degradation of Cdc25A after 24 hours (figure 6).

Expression of mitogen-activated protein (MAP) kinases after treatment of AsPC-1 cells with DIG

AsPC-1 cells were incubated with 40µM DIG for 0.5, 2, 4, 8, and 24 hours and subjected to western blotting to determine the effect on MAP kinases. Phosphorylation of Erk1/2 was reduced within 2 hours. However, DIG showed an induction of p38 kinase phosphorylation indicating a stress response (figure 7).

Discussion

Gallic acid (GA) and resveratrol (RV) are naturally occurring polyphenolics previously reported to scavenge free radicals, to inhibit ribonucleotide reductase (RR), and to induce cell cycle arrest and apoptosis [8, 11, 33-35]. Pancreatic cancer is a very aggressive, malignant neoplasm with poor prognosis correlating to short overall survival. In this study, we tested a novel synthetic ester of GA and RV, digalloylresveratrol (DIG) in the AsPC-1 and BxPC-3 pancreatic cancer cell lines, assuming that this compound may exhibit stronger activity than GA or RV itself.

It has already been demonstrated that growth inhibition of human HT-29 colon cancer cells after treatment with DIG surpasses incubation with an equimolar combination of RV and GA [18]. In human HL-60 promyelocytic leukemia cells, the inhibition of cell proliferation of DIG exceeded that of GA by 10-fold [11]. These results support the conclusion that the RV backbone, to which the galloyl-residues are connected, is responsible for the improved effects seen with DIG [19].

Employing clonogenic assays, we show that DIG inhibited the colony formation of BxPC-3 cells with an IC_{50} of 8.5 µM being superior to treatment with GA or RV resulting in IC_{50} values of 41 µM and 13 µM, respectively. Unexpectedly, in AsPC-1 cells, DIG yielded an IC_{50} of 21.5 µM thus not exceeding the inhibition of colony formation caused by GA (21 µM) and RV (18 µM). Different cellular morphology and pharmacology might be the reason for these findings. Cui et al recently reported that the sensitivity of various pancreatic cancer cell lines to RV is different [36], which could also be an explanation for our observations since RV serves as backbone in the DIG molecule. Furthermore, the same group also demonstrated

that RV exerts less pronounced growth inhibition activity in AsPC-1 cells than in BxPC-3 cells [36] suggesting that in pancreatic cancer cell lines, RV might be the active principle of DIG.

The analysis of the *in situ* RR activity evidenced that DIG is a powerful RR inhibitor even at low concentrations. In addition, DIG caused alterations of deoxyribonucleoside triphosphate (dNTP) pool balance: dATP pools were significantly depleted while dTTP pools were elevated. A similar depletion of dATP pool sizes could previously be observed with Gemcitabine [37-38], a mechanism mainly contributing to the antitumor properties of this clinically established anticancer drug. By misbalancing the concentration of precursors for *de novo* DNA synthesis, the latter is blocked in proliferating cells. Growth arrest and cell cycle perturbations are the consequences, as it was monitored in the course of DIG treatment.

The prime effect of DIG was an S-phase arrest, which is consistent with the role of RR as the rate limiting enzyme for S-phase transit and the fact that inhibition of RR leads to accumulation of cells in S-phase [39]. DNA damage or disrupted dNTP balance and incomplete DNA synthesis activate cell cycle checkpoints to prevent DNA synthesis and cell cycle progression [40-42] and to provide time for repair before the damage gets passed on to daughter cells or to allow for the reconstitution of the dNTP pools. These regulatory pathways govern the order and timing of cell cycle transitions to ensure completion of one cellular event prior to commencement of another. Before mitosis, cells have to pass G1-S, intra-S, and G2-M cell cycle checkpoints, which are controlled by their key regulators, ATR and ATM protein kinases, through activation of their downstream effector kinases Chk1 and Chk2, respectively [42-43]. Exposure of AsPC-1 cells to DIG resulted in phosphorylation of ATM at Ser1981 and in turn caused phosphorylation of Chk2. These observations are in line with the fact that ATM activation is not limited to an ionizing radiation-induced response [44], but seemingly plays an important role in response to DNA damage caused by

chemotherapeutic agents as well. Activated Chk2 phosphorylates the Cdc25A phosphatase at Ser177 targeting it for proteasomal degradation as it was observed in AsPC-1 cells upon DIG treatment. Cdc25A is a proto-oncogene [45] required for cell cycle transit [46], and its overexpression often correlates with more aggressive diseases and poor prognosis [45]. A similar effect was observed on short 42°C heat shock treatment, which also induced the ATM-Chk2 pathway, resulting in subsequent degradation of Cdc25A in human HEK293 embryonic kidney cells [47].

Apart from the ATM-Chk2 pathway, various groups have reported an involvement of mitogen activated protein kinases (MAPK) activation in attenuating cells in the S phase of the cell cycle [44, 48-49]. MAP kinases are important mediators between cell surface receptors and transcription factors transducing signals triggered by i.e. physical and chemical stress (e.g. after exposure to chemotherapeutic agents) and regulate numerous cellular processes such as proliferation and programmed cell death [50]. Western blot analysis revealed that DIG eventually blocked Erk1/2 phosphorylation thereby inhibiting cell division driven by extracellular mitogens. This was paralleled by phosphorylation of p38 reflecting increased cellular stress.

Another prominent anticancer attribute of chemotherapeutics is the induction of apoptosis. DIG exhibited strong pro-apoptotic properties in HL-60 cells and triggered apoptosis by the caspase 3 pathway [19]. Caspases are a family of cysteases being involved in regulating the activation of apoptotic signal transmission that cleave protein substrates after their Asp residues [36]. In contrast, apoptosis upon DIG treatment occurred in only 8.5% of AsPC-1 cells, indicating that cell cycle inhibition rather than induction of programmed cell death seems to be the primary antineoplastic effect of DIG. Consistently, the expression level of caspase 3 protein in AsPC-1 cells remained unchanged throughout the time course (data not

shown), whereas Akt became phosphorylated. Akt plays a critical role in inhibiting caspase activation and apoptosis thus promoting cell survival [51]. This protein kinase is activated by phospholipid binding and activation loop phosphorylation at Thr308 by PDK1 [52] and by phosphorylation within the carboxy terminus at Ser473 by PDK2. Phosphorylation at Ser473 is accomplished by mammalian target of rapamycin (mTOR) in a rapamycin-insensitive complex with rictor and Sin1 [53-54] or by DNA-PK [55]. DNA-PK becomes activated upon DNA damage and cellular stress [56-57] and this, most likely, caused the phosphorylation at Ser473 rendering AsPC-1 cells resistant to apoptosis. Reportedly, increased Akt signaling is accompanied by a poor clinical outcome in many tumor types including pancreatic cancer [58].

GA was shown to inhibit RR by scavenging the tyrosyl radical being essential for the activity of the enzyme [11], and RV diminished RR activity through a similar mechanism [59]. The *in vitro* radical-scavenging activity of DIG exceeded that of an equimolar combination of RV and GA by about 2.5-fold, suggesting that the RV backbone synergizes with the GA molecules resulting in a more pronounced inhibition of the DPPH radical. Since the measurement of ^{14}C-cytidine incorporation revealed a significant inhibition of RR *in situ* activity in both AsPC-1 and BxPC-3 cells, we strongly believe that DIG also attenuates RR activity by tyrosyl radical scavenging.

Taken together, DIG shows remarkable *in vitro* radical-scavenging properties, significantly inhibits RR *in situ* activity, and induces cell cycle arrest. We demonstrate that the novel RR inhibitor DIG exerts pronounced antitumor activity in human pancreatic cancer cell lines and therefore deserves further preclinical and *in vivo* testing.

Acknowledgements

This investigation was supported by the Medical-Scientific Fund of the Mayor of Vienna, grant #09059 to M.F.-S., the "Hochschuljubilaeumsstiftung der Stadt Wien", grant #H-756/2005 to T.S., and by the Fellinger Cancer Research Association (Fellinger Krebsforschung Gemeinnuetziger Verein) to G.K. as a mission-oriented grant (Auftragsforschung). The authors wish to thank Toni Jaeger for preparing the western blotting figures.

Conflict of interest

The authors declare that they have no conflict of interest.

References

[1] Almhanna K, Philip PA. Defining new paradigms for the treatment of pancreatic cancer. Curr Treat Options Oncol 2011;12:111-25.

[2] Jemal A, Siegel R, Ward E, Hao Y, Xu J, Thun MJ. Cancer statistics, 2009. CA Cancer J Clin 2009;59:225-49.

[3] Xu Q, Zhang TP, Zhao YP. Advances in early diagnosis and therapy of pancreatic cancer. Hepatobiliary Pancreat Dis Int 2011;10:128-35.

[4] Renaud S, de Lorgeril M. Wine, alcohol, platelets, and the French paradox for coronary heart disease. Lancet 1992;339:1523-6.

[5] Richard JL. [Coronary risk factors. The French paradox]. Arch Mal Coeur Vaiss 1987;80 Spec No:17-21.

[6] Appeldoorn CC, Bonnefoy A, Lutters BC, Daenens K, van Berkel TJ, Hoylaerts MF, et al. Gallic acid antagonizes P-selectin-mediated platelet-leukocyte interactions: implications for the French paradox. Circulation 2005;111:106-12.

[7] Salucci M, Stivala LA, Maiani G, Bugianesi R, Vannini V. Flavonoids uptake and their effect on cell cycle of human colon adenocarcinoma cells (Caco2). British journal of cancer 2002;86:1645-51.

[8] Horvath Z, Saiko P, Illmer C, Madlener S, Hoechtl T, Bauer W, et al. Synergistic action of resveratrol, an ingredient of wine, with Ara-C and tiazofurin in HL-60 human promyelocytic leukemia cells. Experimental hematology 2005;33:329-35.

[9] Saiko P, Szakmary A, Jaeger W, Szekeres T. Resveratrol and its analogs: defense against cancer, coronary disease and neurodegenerative maladies or just a fad? Mutation research 2008;658:68-94.

[10] Kawada M, Ohno Y, Ri Y, Ikoma T, Yuugetu H, Asai T, et al. Anti-tumor effect of gallic acid on LL-2 lung cancer cells transplanted in mice. Anti-cancer drugs 2001;12:847-52.

[11] Madlener S, Illmer C, Horvath Z, Saiko P, Losert A, Herbacek I, et al. Gallic acid inhibits ribonucleotide reductase and cyclooxygenases in human HL-60 promyelocytic leukemia cells. Cancer letters 2007;245:156-62.

[12] Takeda E, Weber G. Role of ribonucleotide reductase in expression in the neoplastic program. Life sciences 1981;28:1007-14.

[13] Noble S, Goa KL. Gemcitabine. A review of its pharmacology and clinical potential in non-small cell lung cancer and pancreatic cancer. Drugs 1997;54:447-72.

[14] Toschi L, Finocchiaro G, Bartolini S, Gioia V, Cappuzzo F. Role of gemcitabine in cancer therapy. Future Oncol 2005;1:7-17.

[15] Kolberg M, Strand KR, Graff P, Andersson KK. Structure, function, and mechanism of ribonucleotide reductases. Biochim Biophys Acta 2004;1699:1-34.

[16] Shao J, Zhou B, Chu B, Yen Y. Ribonucleotide reductase inhibitors and future drug design. Curr Cancer Drug Targets 2006;6:409-31.

[17] Bourdon A, Minai L, Serre V, Jais JP, Sarzi E, Aubert S, et al. Mutation of RRM2B, encoding p53-controlled ribonucleotide reductase (p53R2), causes severe mitochondrial DNA depletion. Nat Genet 2007;39:776-80.

[18] Bernhaus A, Fritzer-Szekeres M, Grusch M, Saiko P, Krupitza G, Venkateswarlu S, et al. Digalloylresveratrol, a new phenolic acid derivative induces apoptosis and cell cycle arrest in human HT-29 colon cancer cells. Cancer letters 2009;274:299-304.

[19] Madlener S, Saiko P, Vonach C, Viola K, Huttary N, Stark N, et al. Multifactorial anticancer effects of digalloyl-resveratrol encompass apoptosis, cell-cycle arrest, and inhibition of lymphendothelial gap formation in vitro. British journal of cancer 2010;102:1361-70.

[20] Grusch M, Polgar D, Gfatter S, Leuhuber K, Huettenbrenner S, Leisser C, et al. Maintenance of ATP favours apoptosis over necrosis triggered by benzamide riboside. Cell death and differentiation 2002;9:169-78.
[21] Grasl-Kraupp B, Ruttkay-Nedecky B, Koudelka H, Bukowska K, Bursch W, Schulte-Hermann R. In situ detection of fragmented DNA (TUNEL assay) fails to discriminate among apoptosis, necrosis, and autolytic cell death: a cautionary note. Hepatology 1995;21:1465-8.
[22] Rosenberger G, Fuhrmann G, Grusch M, Fassl S, Elford HL, Smid K, et al. The ribonucleotide reductase inhibitor trimidox induces c-myc and apoptosis of human ovarian carcinoma cells. Life sciences 2000;67:3131-42.
[23] Grusch M, Fritzer-Szekeres M, Fuhrmann G, Rosenberger G, Luxbacher C, Elford HL, et al. Activation of caspases and induction of apoptosis by novel ribonucleotide reductase inhibitors amidox and didox. Experimental hematology 2001;29:623-32.
[24] Fritzer-Szekeres M, Grusch M, Luxbacher C, Horvath S, Krupitza G, Elford HL, et al. Trimidox, an inhibitor of ribonucleotide reductase, induces apoptosis and activates caspases in HL-60 promyelocytic leukemia cells. Experimental hematology 2000;28:924-30.
[25] Huettenbrenner S, Maier S, Leisser C, Polgar D, Strasser S, Grusch M, et al. The evolution of cell death programs as prerequisites of multicellularity. Mutation research 2003;543:235-49.
[26] Szekeres T, Gharehbaghi K, Fritzer M, Woody M, Srivastava A, van't Riet B, et al. Biochemical and antitumor activity of trimidox, a new inhibitor of ribonucleotide reductase. Cancer chemotherapy and pharmacology 1994;34:63-6.
[27] Garrett C, Santi DV. A rapid and sensitive high pressure liquid chromatography assay for deoxyribonucleoside triphosphates in cell extracts. Anal Biochem 1979;99:268-73.
[28] Guo Y, Xu X, Qi W, Xie C, Wang G, Zhang A, Ge Y. Synergistic anti-tumor interactions between gemcitabine and clofarabine in human pancreatic cancer cell lines. Mol Med Report 2011. In press.
[29] Hoshino J, Park EJ, Kondratyuk TP, Marler L, Pezzuto JM, van Breemen RB, et al. Selective synthesis and biological evaluation of sulfate-conjugated resveratrol metabolites. Journal of medicinal chemistry 2010;53:5033-43.
[30] Shang YJ, Qian YP, Liu XD, Dai F, Shang XL, Jia WQ, et al. Radical-scavenging activity and mechanism of resveratrol-oriented analogues: influence of the solvent, radical, and substitution. J Org Chem 2009;74:5025-31.
[31] Gamez EJ, Luyengi L, Lee SK, Zhu LF, Zhou BN, Fong HH, et al. Antioxidant flavonoid glycosides from Daphniphyllum calycinum. J Nat Prod 1998;61:706-8.
[32] Saiko P, Graser G, Giessrigl B, Lackner A, Grusch M, Krupitza G, et al. A novel N-hydroxy-N'-aminoguanidine derivative inhibits ribonucleotide reductase activity: Effects in human HL-60 promyelocytic leukemia cells and synergism with arabinofuranosylcytosine (Ara-C). Biochemical pharmacology 2011;81:50-9.
[33] Faried A, Kurnia D, Faried LS, Usman N, Miyazaki T, Kato H, et al. Anticancer effects of gallic acid isolated from Indonesian herbal medicine, Phaleria macrocarpa (Scheff.) Boerl, on human cancer cell lines. International journal of oncology 2007;30:605-13.
[34] Hsu CL, Lo WH, Yen GC. Gallic acid induces apoptosis in 3T3-L1 pre-adipocytes via a Fas- and mitochondrial-mediated pathway. Journal of agricultural and food chemistry 2007;55:7359-65.
[35] Horvath Z, Murias M, Saiko P, Erker T, Handler N, Madlener S, et al. Cytotoxic and biochemical effects of 3,3',4,4',5,5'-hexahydroxystilbene, a novel resveratrol analog in HL-60 human promyelocytic leukemia cells. Experimental hematology 2006;34:1377-84.
[36] Cui J, Sun R, Yu Y, Gou S, Zhao G, Wang C. Antiproliferative effect of resveratrol in pancreatic cancer cells. Phytother Res 2010;24:1637-44.
[37] Gandhi V, Estey E, Plunkett W. Modulation of arabinosylcytosine metabolism during leukemia therapy. Advances in experimental medicine and biology 1994;370:119-24.
[38] Robinson BW, Im MM, Ljungman M, Praz F, Shewach DS. Enhanced radiosensitization with gemcitabine in mismatch repair-deficient HCT116 cells. Cancer research 2003;63:6935-41.

[39] Chimploy K, Diaz GD, Li Q, Carter O, Dashwood WM, Mathews CK, et al. E2F4 and ribonucleotide reductase mediate S-phase arrest in colon cancer cells treated with chlorophyllin. International journal of cancer 2009;125:2086-94.
[40] Kastan MB, Bartek J. Cell-cycle checkpoints and cancer. Nature 2004;432:316-23.
[41] Shiloh Y. ATM and related protein kinases: safeguarding genome integrity. Nat Rev Cancer 2003;3:155-68.
[42] Bartek J, Lukas J. Chk1 and Chk2 kinases in checkpoint control and cancer. Cancer Cell 2003;3:421-9.
[43] Abraham RT. Cell cycle checkpoint signaling through the ATM and ATR kinases. Genes Dev 2001;15:2177-96.
[44] Zhu KQ, Zhang SJ. Involvement of ATM/ATR-p38 MAPK cascade in MNNG induced G1-S arrest. World J Gastroenterol 2003;9:2073-7.
[45] Ray D, Kiyokawa H. CDC25A phosphatase: a rate-limiting oncogene that determines genomic stability. Cancer research 2008;68:1251-3.
[46] Gao G, Peng M, Zhu L, Wei Y, Wu X. Human papillomavirus 16 variant E7 gene induces transformation of NIH 3T3 cells via up-regulation of cdc25A and cyclin A. Int J Gynecol Cancer 2009;19:494-9.
[47] Madlener S, Rosner M, Krieger S, Giessrigl B, Gridling M, Vo TP, et al. Short 42 degrees C heat shock induces phosphorylation and degradation of Cdc25A which depends on p38MAPK, Chk2 and 14.3.3. Hum Mol Genet 2009;18:1990-2000.
[48] Iguchi T, Miyakawa Y, Yamamoto K, Kizaki M, Ikeda Y. Nitrogen-containing bisphosphonates induce S-phase cell cycle arrest and apoptosis of myeloma cells by activating MAPK pathway and inhibiting mevalonate pathway. Cell Signal 2003;15:719-27.
[49] Lin KL, Su JC, Chien CM, Tseng CH, Chen YL, Chang LS, et al. Naphtho[1,2-b]furan-4,5-dione induces apoptosis and S-phase arrest of MDA-MB-231 cells through JNK and ERK signaling activation. Toxicol In Vitro 2010;24:61-70.
[50] Johnson GL, Lapadat R. Mitogen-activated protein kinase pathways mediated by ERK, JNK, and p38 protein kinases. Science 2002;298:1911-2.
[51] Franke TF, Kaplan DR, Cantley LC. PI3K: downstream AKTion blocks apoptosis. Cell 1997;88:435-7.
[52] Alessi DR, Andjelkovic M, Caudwell B, Cron P, Morrice N, Cohen P, et al. Mechanism of activation of protein kinase B by insulin and IGF-1. EMBO J 1996;15:6541-51.
[53] Sarbassov DD, Guertin DA, Ali SM, Sabatini DM. Phosphorylation and regulation of Akt/PKB by the rictor-mTOR complex. Science 2005;307:1098-101.
[54] Jacinto E, Facchinetti V, Liu D, Soto N, Wei S, Jung SY, et al. SIN1/MIP1 maintains rictor-mTOR complex integrity and regulates Akt phosphorylation and substrate specificity. Cell 2006;127:125-37.
[55] Bozulic L, Hemmings BA. PIKKing on PKB: regulation of PKB activity by phosphorylation. Curr Opin Cell Biol 2009;21:256-61.
[56] Surucu B, Bozulic L, Hynx D, Parcellier A, Hemmings BA. In vivo analysis of protein kinase B (PKB)/Akt regulation in DNA-PKcs-null mice reveals a role for PKB/Akt in DNA damage response and tumorigenesis. J Biol Chem 2008;283:30025-33.
[57] Bozulic L, Surucu B, Hynx D, Hemmings BA. PKBalpha/Akt1 acts downstream of DNA-PK in the DNA double-strand break response and promotes survival. Mol Cell 2008;30:203-13.
[58] Schlieman MG, Fahy BN, Ramsamooj R, Beckett L, Bold RJ. Incidence, mechanism and prognostic value of activated AKT in pancreas cancer. British journal of cancer 2003;89:2110-5.
[59] Fontecave M, Lepoivre M, Elleingand E, Gerez C, Guittet O. Resveratrol, a remarkable inhibitor of ribonucleotide reductase. FEBS letters 1998;421:277-9.

Table 1

Effect of DIG, GA, and RV on the colony formation of human AsPC-1 and BxPC-3 pancreatic cancer cells (IC_{50} values)

Compound	AsPC-1	BxPC-3
DIG	21.5µM	8.5µM
GA	21.0µM	41.0µM
RV	18.0µM	13.3µM

Table 2

DPPH activity after incubation with DIG, GA, RV, 1 Mol RV + 2 Mol GA, Ascorbic acid, and Tocopherol for 15 minutes

Compound	IC_{50} (µM)
DIG	1.8
GA	3.1
RV	95.0
RV + GA (1+2)	4.7
Ascorbic acid	9.5
Tocopherol	7.0

Figure legends

Figure 1. Structural formulas of DIG, GA, and RV including nomenclature and molecular weight (MW).

Figure 2a. Induction of apoptosis in AsPC-1 cells after incubation with DIG. Cells ($0.2x10^6$ per ml) were exposed to increasing concentrations of DIG for 72 hours. Hoechst 33258 (HO, Sigma, St. Louis, MO, USA) and propidium iodide (PI, Sigma, St. Louis, MO, USA) were added directly to the cells to final concentrations of 5 µg/ml and 2 µg/ml, respectively. After 60 minutes of incubation at 37°C, cells were counted under a fluorescence microscope and the number of apoptotic cells was given as percentage value. Data are means ± standard errors of three determinations.

Figure 2b. Expression levels of p(Ser473)Akt and Akt after incubation with DIG. After incubation with 40µM DIG for 0.5, 2, 4, 8, and 24 hours, AsPC-1 cells ($2x10^6$ per ml) were harvested, washed twice with ice-cold PBS (pH 7.2) and lysed in a buffer containing 150 mM NaCl, 50 mM Tris-buffered saline (Tris pH 8.0), 1% Triton X-100, 1 mM phenylmethylsulfonylfluoride (PMSF) and protease inhibitor cocktail (PIC; from a 100x stock). The lysate was centrifuged at 12000 rpm for 20 minutes at 4°C, and the supernatant was subjected to western blot analysis.

Figure 3. Cell cycle distribution in AsPC-1 (a) and BxPC-3 (b) cells after incubation with DIG. Cells ($0.4x10^6$ per ml) were seeded in $25cm^2$ Nunc tissue culture flasks and incubated with increasing concentrations of DIG for 48 hours under cell culture conditions. Cells were

analyzed on a FACSCalibur flow cytometer (BD Biosciences, San Jose, CA, USA) and cell cycle distribution was calculated with ModFit LT software (Verity Software House, Topsham, ME, USA). Data are means ± standard errors of three determinations.

Figure 4. Inhibition of incorporation of ^{14}C-cytidine into DNA of AsPC-1 (a) and BxPC-3 (b) cells after treatment with DIG. Cells ($0.4x10^6$ cells per ml) were incubated with increasing concentrations of DIG for 24 hours. After the incubation period, cells were counted and pulsed with ^{14}C-cytidine (0.3125 µCi, 5 nM) for 30 minutes at 37°C. Then cells were collected by centrifugation and washed with PBS. Total DNA was extracted from $5x10^6$ cells and specific radioactivity of the samples was determined using a Wallac 1414 liquid scintillation counter (PerkinElmer, Boston, MA). Data are means ± standard errors of three determinations. Values significantly ($p<0.05$) different from control are marked with an asterisk (*).

Figure 5. Concentration of dNTP pools in AsPC-1 cells upon treatment with DIG. Cells ($0.4x10^6$ cells per ml) were incubated with 20, 30, and 40 µM DIG for 24 hours. Afterwards, $5x10^7$ cells were separated for the extraction of dNTPs. The concentration of dNTPs was calculated as percent of total area under the curve for each sample. Data are means ± standard errors of three determinations. Values significantly ($p<0.05$) different from control are marked with an asterisk (*).

Figure 6. Expression levels of p(Ser1981)ATM, p(Thr68)Chk2, Chk2, p(Ser75)Cdc25A, p(Ser177)Cdc25A, and Cdc25A after incubation with DIG. After incubation with 40µM DIG for 0.5, 2, 4, 8, and 24 hours, AsPC-1 cells ($2x10^6$ per ml) were harvested, washed twice with

ice-cold PBS (pH 7.2) and lysed in a buffer containing 150 mM NaCl, 50 mM Tris-buffered saline (Tris pH 8.0), 1% Triton X-100, 1 mM phenylmethylsulfonylfluoride (PMSF) and protease inhibitor cocktail (PIC; from a 100x stock). The lysate was centrifuged at 12000 rpm for 20 minutes at 4°C, and the supernatant was subjected to western blot analysis.

Figure 7. Expression levels of p(Thr202/Tyr204)Erk1/2, Erk1/2, p(Thr180/Tyr182)p38MAPK, and p38MAPK after incubation with DIG. After incubation with 40µM DIG for 0.5, 2, 4, 8, and 24 hours, AsPC-1 cells ($2x10^6$ per ml) were harvested, washed twice with ice-cold PBS (pH 7.2) and lysed in a buffer containing 150 mM NaCl, 50 mM Tris-buffered saline (Tris pH 8.0), 1% Triton X-100, 1 mM phenylmethylsulfonylfluoride (PMSF) and protease inhibitor cocktail (PIC; from a 100x stock). The lysate was centrifuged at 12000 rpm for 20 minutes at 4°C, and the supernatant was subjected to western blot analysis.

Figure 1.

Structural formulas of DIG, GA, and RV including nomenclature and molecular weight (MW)

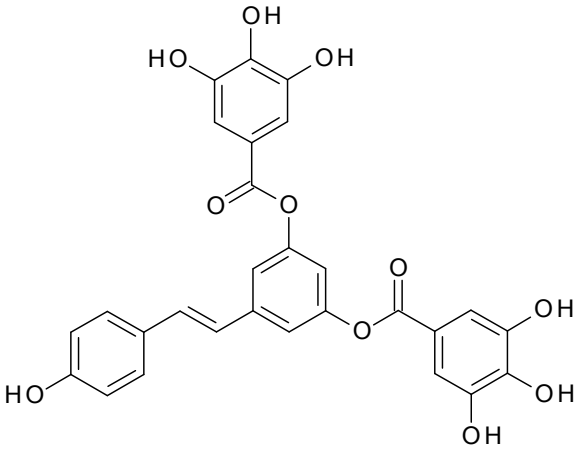

DIG (3,5-O-digalloyl-resveratrol)

MW = 532.47

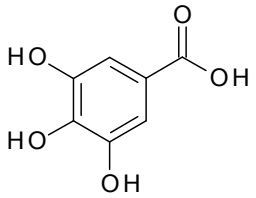

Gallic acid (3,4,5-trihydroxybenzoic acid)

MW = 170.12

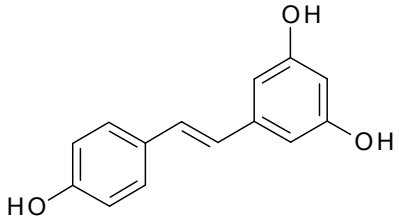

Resveratrol (3,4',5-trihydroxy-*trans*-stilbene)

MW = 228.25

Figure 2.

(a) Induction of apoptosis in AsPC-1 cells after incubation with DIG for 72 hours.

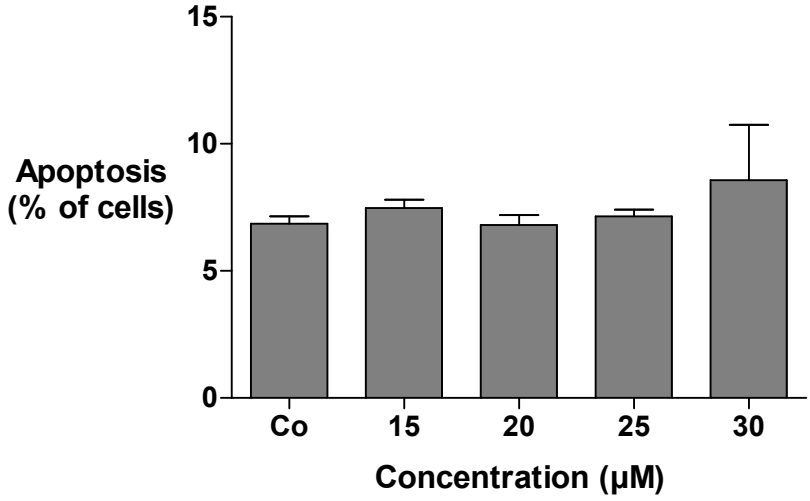

(b) Expression levels of p(Ser473)Akt and Akt after incubation of AsPC-1 cells with DIG.

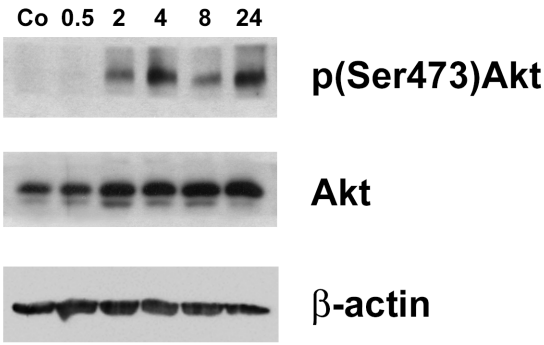

Figure 3.

Effect of DIG on the cell cycle distribution of AsPC-1 (a) and BxPC-3 (b) cells

(a)

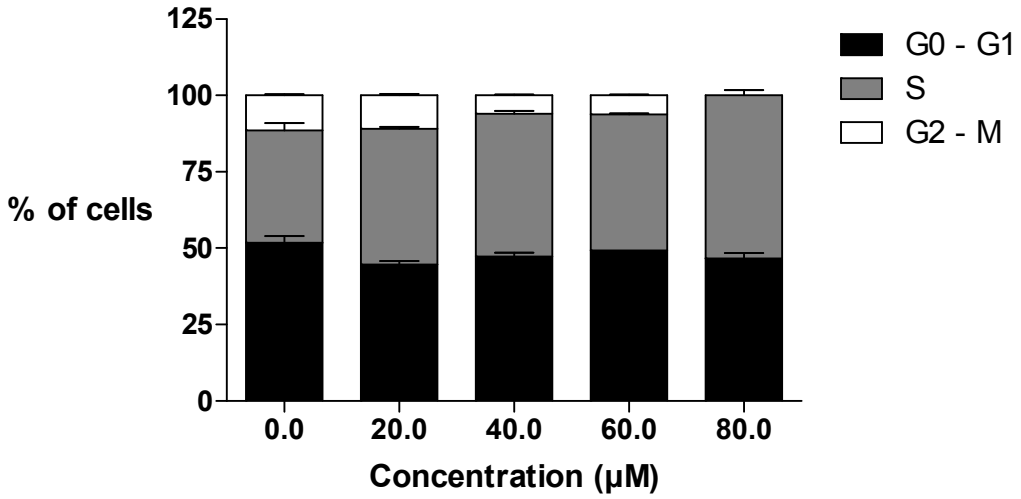

(b)

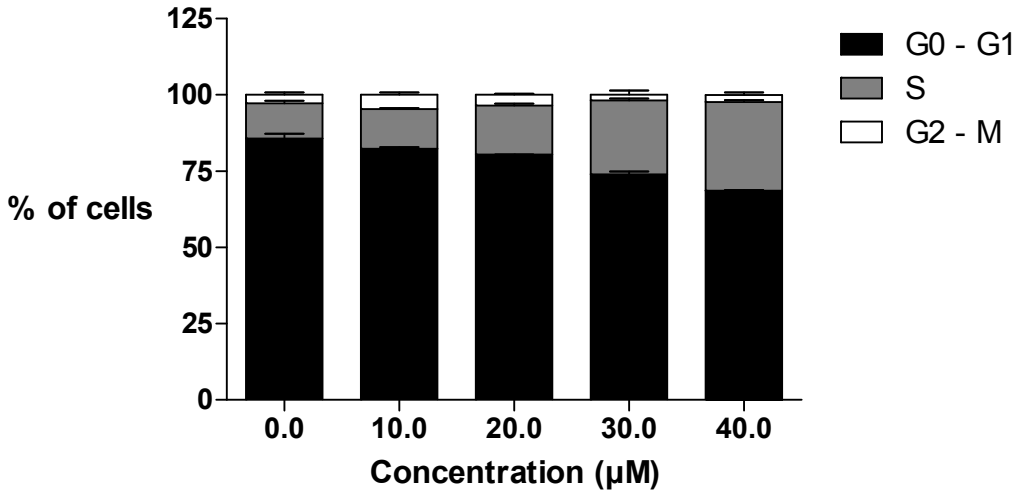

Figure 4.

In situ **measurement of ribonucleotide reductase activity in AsPC-1 (a) and BxPC-3 (b) cells after treatment with DIG for 24 hours**

(a)

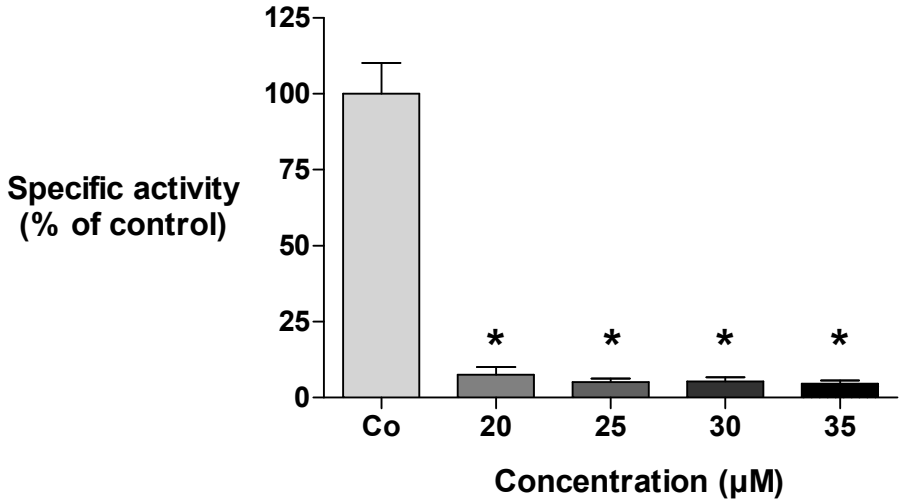

(b)

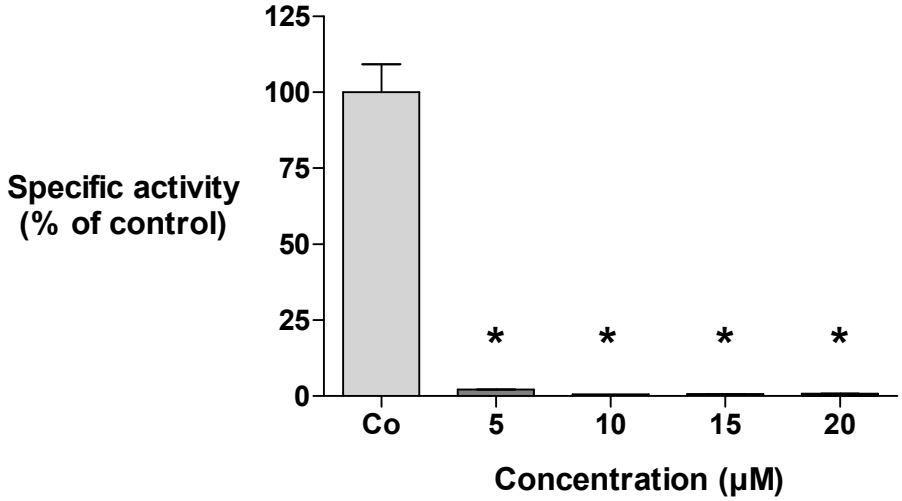

Figure 5.

Concentration of dNTP pools in AsPC-1 cells after treatment with DIG for 24 hours

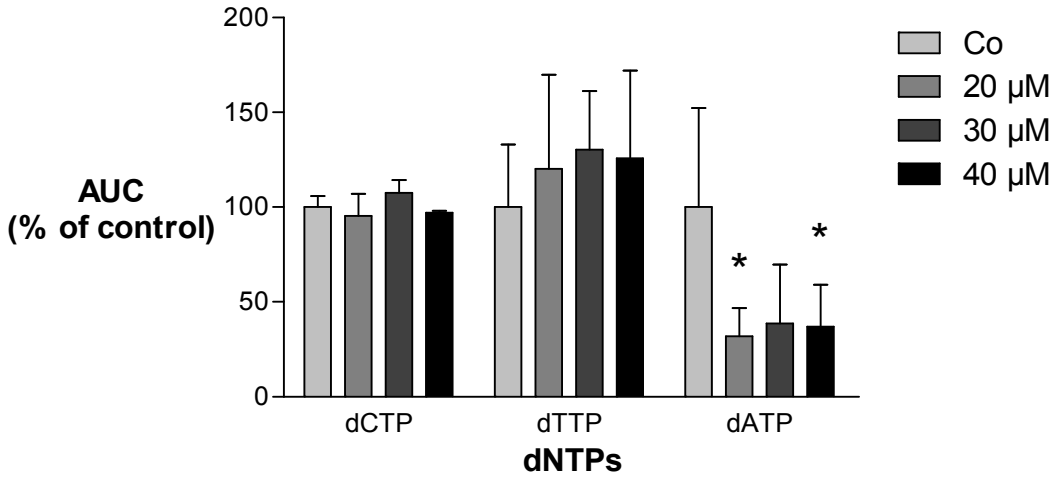

Figure 6.

Expression of checkpoint and cell cycle regulating proteins after treatment of AsPC-1 cells with DIG

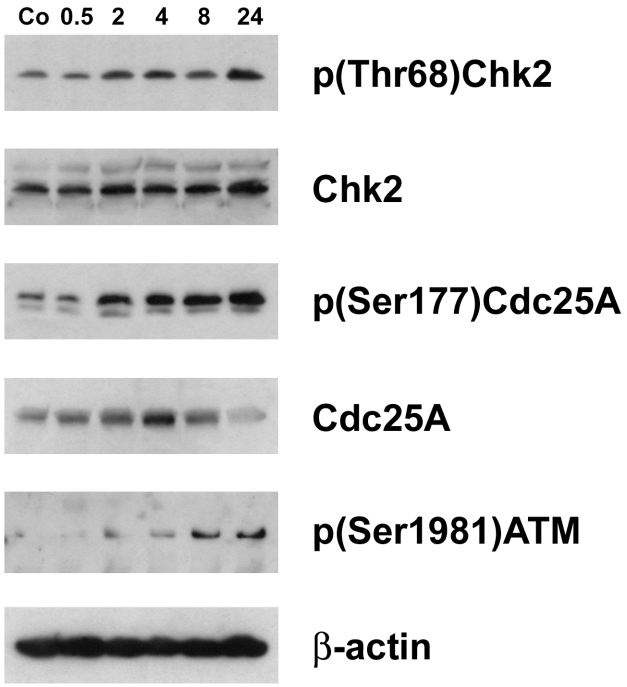

Figure 7.

Expression of mitogen-activated protein (MAP) kinases after treatment of AsPC-1 cells with DIG

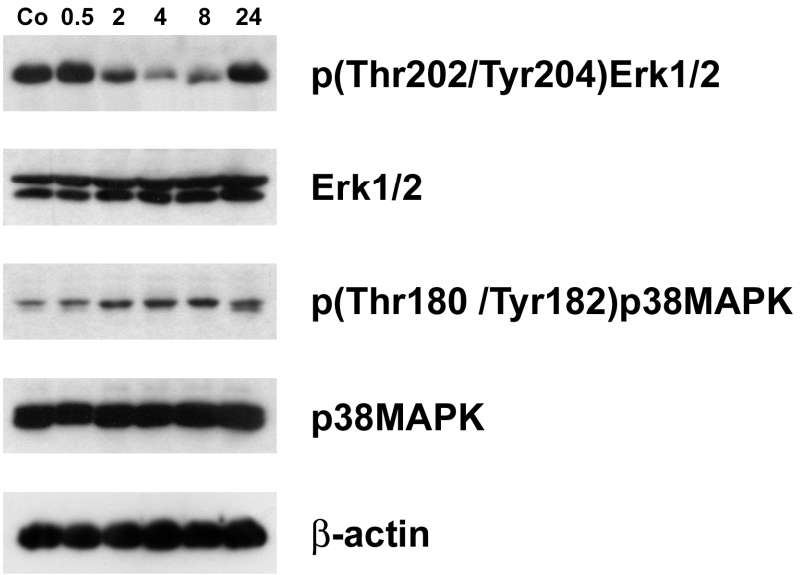

Hsp90 stabilises Cdc25A and counteracts heat shock mediated Cdc25A degradation and cell cycle attenuation in pancreas carcinoma cells.

Giessrigl B., Krieger S., Huttary N., Saiko P., Alami M., Maciuk A., Gollinger M., Mazal P., Szekeres T., Jäger W. and Krupitza G.

Hum Mol Genet., ***submitted.***

Hsp90 stabilises Cdc25A and counteracts heat shock mediated Cdc25A degradation and cell cycle attenuation in pancreas carcinoma cells

Benedikt Giessrigl[1,2], Sigurd Krieger[1], Nicole Huttary[1], Philipp Saiko[3], Mouad Alami[4], Alexandre Maciuk[5], Michaela Gollinger[1], Peter Mazal[1], Thomas Szekeres[3], Walter Jäger[2], Georg Krupitza[1]

[1] Institute of Clinical Pathology, Medical University of Vienna, Waehringer Guertel 18-20, A-1090 Vienna, Austria

[2]Department of Clinical Pharmacy and Diagnostics, Faculty of Life Sciences, University of Vienna, Althanstrasse 14, A-1090 Vienna, Austria

[3]Department of Medical and Chemical Laboratory Diagnostics, Medical University of Vienna, General Hospital of Vienna, Waehringer Guertel 18-20, A-1090 Vienna, Austria

[4] Laboratory of Therapeutic Chemistry, UMR CNRS 8076 BioCIS, Faculty of Pharmacy, University Paris-South 11

[5]Laboratoire de Pharmacognosie - UMR CNRS 8076 BioCIS, Faculty of Pharmacy, University Paris-South 11

Short title: Heat shock and inhibition of Hsp90 destabilises Ccd25A and arrests the cell cycle

Key words: Hsp90, Cdc25A stability, cell cycle, heat shock

Correspondence:
Georg Krupitza, Institute of Clinical Pathology, Medical University of Vienna, Waehringer Guertel 18-20, A-1090, Vienna, Austria
e-mail: georg.krupitza@meduniwien.ac.at,

Abstract

Pancreas cancer cells escape most treatment options. Heat shock protein (Hsp)90 is frequently over-expressed in pancreas carcinomas and protects a number cell cycle regulators such as the proto-oncogene Cdc25A. We show that inhibition of Hsp90 with geldanamycine (GD) destabilises Cdc25A independent of Chk1/2 whereas the standard drug for pancreas carcinoma treatment, gemcitabine (GEM), causes Cdc25A degradation through activation of Chk2. Both agents applied together additively inhibit the expression of Cdc25A and proliferation of pancreas carcinoma cells thereby demonstrating that both Cdc25A-destabilising/degrading pathways are separated. The role of Hsp90 as stabiliser of Cdc25A in pancreas carcinoma cells is further supported by two novel synthetic inhibitors 4-TCNA and 7-TCNA and specific Hsp90AB1 (Hsp90β) shRNA. The here presented data open a treatment option for cancers, which are hardly responding to drugs, such as pancreas carcinomas or cancers with acquired resistances. We conclude that targeting i.e. Hsp90 is a hypothesis driven and tailored approach for drug intervention.

Introduction

Pancreatic cancer is the tenth most common type of cancer in western countries and ranks fourth in cancer mortality statistics and in spite of intensive research and significant improvement in the survival of pancreatic cancer patients (**Mihaljevic et al., 2010**, **Fahrig et al. 2006, Heinrich et al. 2011**) this cancer entity is still amongst the most malignant ones. Because of the lack of early detection, the absence of symptoms and effective screening tests, high rate of relapse and limited effective therapies, prognosis is very poor with a 5 year survival rate of less than 5% and a 1 year survival rate of less than 20% (**Evans et al., 2001**). Due to metastasis more than 80% of these carcinomas are not resectable (**Niederhuber et al., 1995**) and therefore systemic chemotherapy plays an important role in the treatment of this extremely aggressive cancer with the goal to provide symptomatic relief and prolong survival. Besides 5-fluorouracil, gemcitabine (GEM) was identified as the two main treatment options (**Huguet et al., 2009**) but in particular metastatic pancreatic cancer is highly chemoresistant and response rates of single agent therapies are less than 20% (**Evans et al., 2001**). Because of this lack of effective therapy, research for new capable treatment options represents an important challenge. Heat shock proteins (Hsps) represent a highly conserved set of proteins that have a pivotal role in cell cycle progression and cell death (apoptosis) as well as in maintaining cellular homeostasis under stress (**Khalil et al., 2011**). Various insults like hypoxia, ischemia, exposure to UV light or chemicals, nutritional deficiencies or other stress rapidly induce their expression (**Cotto and Morimoto, 1999; Lindquist and Craig, 1998**) and Hsp90A (further on termed Hsp90) over-expression was shown among others e.g. for pancreatic, breast and lung cancer and for leukemia (**Khalil et al., 2011**).
In a recent study we could show that heat shock (HS) induces Cdc25A degradation and that Hsp90 stabilises Cdc25A in HeLa and HEK293 cells (**Madlener et al., 2009**). The cell cycle promoting phosphatase Cdc25A is an oncogene and indispensable for embryonic development (**Nilsson and Hoffmann, 2000**) and can substitute for Cdc25B and Cdc25C. Therefore, Cdc25A is mandatory for cell cycle progression and the fact that HS, in presence of the Hsp90 inhibitor geldanamycine (GD, which is currently investigated in clinical trials), destabilises Cdc25A in HEK293 and HeLa cells tempted us to test whether this is also the case in pancreas carcinoma cells. As there is still no cure for this cancer entity and gemcitabine (GEM) therapy has more of a palliative than life-extending effect, we investigated whether Hsp90 inhibition combination with high-fever-range HS might affect pancreas carcinoma cells and contributes to cell cycle arrest.

Results

HS and GD cause destabilisation of Cdc25A and other cell cycle regulators

BxPC-3 cells were treated with HS (41.5 C, 90 min) or with 250 nM GD, or both, and the protein expression of Cdc25A, B, and C was investigated. Whereas HS had no effect and GD only little effect on the expression of Cdc25 proteins, the combination of HS plus GD dramatically suppressed the expression of Cdc25A, B, and C in BxPC-3 cells (**Fig 1a**). The expression of Cdc25A reversed to control level when cells were cultivated for further 6h in absence of GD (post-treatment) before cells were lysed for western blot analyses. In contrast, Cdc25C levels of BxPC-3 cells were still reduced post-treatment with HS plus GD. The protein level of cyclin D1, another cell cycle regulating oncogene, was also down-regulated upon combinatorial treatment and also within the post-treatment period.
To test whether this was a cell line effect the expression of Cdc25s and cyclin D1 was analysed also in two other pancreas carcinoma cell lines, PANC-1 and ASPC-1 (**Fig 1b, c**). In PANC-1 HS alone had an already strong suppressing effect on Cdc25A and GD further reduced its expression below levels of detection. The removal of GD for a 6h post-treatment period reversed the levels of Cdc25A and Cdc25B back to that of control. Post-treatment of PANC-1 and ASPC-1 with HS plus GD still suppressed Cdc25C. This indicated that Cdc25A and Cdc25C were regulated by a mechanism that was common to all three pancreas carcinoma cell lines. Immediately after treatment, also Cdc25B expression responded similarly in the three cell lines. In the post-treatment period, Cdc25B levels even increased in BxPC-3 cells that experienced combinatorial treatment. Cyclin D1 decreased upon HS in PANC-1 and ASPC-1 cells and recovered in ASPC-1 to control levels upon post-treatment incubation, whereas in PANC-1 cells cyclin D1 even increased during HS post-treatment.

Such as Cdc25C (**García-Morales et al. 2007**), Wee1 is a client of Hsp90 in HCT116 colon cancer cells (**Tse et al., 2009**). Therefore, we tested whether HS & GD treatment would affect Wee1 stability also in pancreas carcinoma cell lines. Indeed, Wee1 levels decreased in BxPC-3 cells upon treatment with GD, and HS & GD and this caused also the reduction of phosphorylated (active) Wee1 kinase and consequently the reduction of the phosphorylation level of its target Cdc2 (**Fig 2a, b**). Furthermore, in PANC-1 cells Wee1 became down-regulated after treatment with HS, and GD & HS which resulted in decreased phosphorylation levels of Cdc2. This implicated that Cdc2 became activated and induced the cell cycle and proliferation. In contrast, the down-regulation of cyclinD1, which reflects the status of cycling

and therefore proliferating cells, indicated an attenuation of cell proliferation. The dis-regulated expression of cell cycle protagonists may induce cell cycle inhibitors to arrest cell cycle progression in order to re-orchestrate the cell cycle. Hence, we investigated the expression/activation of p53 and p21 in Bx-PC-3 cells after treatment with HS and GD, but neither p53 became activated nor p21 induced (**Fig. 3a**). P53 is a client of Hsp90 (**Park et al., 2011**) and therefore, p53 became degraded upon treatment with GD and its expression was completely suppressed by the combinatorial treatment with HS. HS causes Chk2 activation and induces Cdc25A degradation in HEK 293 and HeLa cells (**Madlener et al. 2009**) and also exposure to UV causes Chk activation and Cdc25A degradation (**Chen et al. 2003)**. In BxPC-3 cells the check point kinases Chk1 and Chk2 remained inactive upon HS, GD, or HS & GD (**Fig. 3b**). Ser75 and Ser177 of Cdc25A are specifically phosphorylated by Chk1 and Chk2, respectively, tagging it for proteasome-mediated degradation. Since neither of the checkpoint kinases became activated, also the constitutive phosphorylation of Cdc25A did not increase at the specific amino acid residues.
To test whether the effects of HS and GD on cell cycle proteins were specific for pancreas carcinoma cells the experiments were expanded to breast cancer cell lines. In the highly metastatic $ER^{negative}$ breast cancer cell line MDA-MB231 Cdc25 family proteins and Wee1 were degraded and consequently Cdc2 was de-phosphorylated (**Fig. 4a**). Also in the $ER^{positive}$ MCF-7 breast cancer cell line the levels of Cdc25A, Wee1, and Cdc2 phosphorylation were reduced. Derivatives of MCF-7 that were made resistant to tamoxifen (TR) and fulvestrant (FR) maintained their sensitivity to HS and GD and the expression of Cdc25A and Wee1 and the phosphorylation of Cdc2 were down-regulated (**Fig. 4b**). Hence, HS induced degradation of Cdc25s, which was enforced by GD, was a general phenomenon and not limited to pancreas carcinoma cells, and Hsp90 protected the proto-oncogene Cdc25A from constitutive and high-fever-range induced degradation. This implicates that HS and GD treatment caused Cdc25A destabilisation and attenuated cell cycle progression independent of DNA checkpoint activators.

Novel Hsp90 inhibitors and specific knock-down destabilise Cdc25A

To obtain additional proof that Cdc25A is a client of Hsp90 in pancreas carcinoma cells BxPC-3 cells were treated with two novel synthetic Hsp90 inhibitors, 4- and 7-tosylcyclonovobiocic acid (4-TCNA and 7-TCNA). While GD binds the N-terminal ATP-binding pocket of Hsp90 and impairs its chaperone function, the coumarin antibiotic

novobiocin was demonstrated to bind an ATP-binding domain in the C-terminal region of Hsp90 and the removal of the noviose moiety together with introduction of a tosyl substituent at C-4 or C-7 coumerins provided A-TCNA and /-TCNA as lead compounds (**Radanyi et al., 2008; Marcu et al., 2000; Le Bras et al., 2007**). These two analogues were shown to down-regulate a subset of Hsp90 client proteins in breast, colon, ovarian and endometrial cancer cell lines (**Radanyi C et al.**). 7-TCNA destabilised Cdc25C, which is a *bona fide* client of Hsp90 (**García-Morales et al., 2007**). In combination with HS both, 4-TCNA and 7-TCNA, caused the down-regulation of Cdc25C thereby demonstrating the specificity of these inhibitors (**Fig 5**). Even more pronounced was the effect of 4-TCNA and 7-TCNA on the expression of Cdc25A further indicating that Cdc25A is a client of Hsp90 in BxPC-3 cells.

To provide firm evidence that Cdc25A is a client of Hsp90 the mRNA expression of the constitutively expressed gene (Hsp90AB1/Hsp90β) was knocked-down by specific shRNA (**Fig. 6a**) and also Hsp90 protein expression was reduced to different extent in the ten analysed clones (**Fig. 6b**). As anticipated, in the knockdown clone (no. 2 from **figs 6a, 6b**) the expression of the client proteins Cdc25A, Cdc25C, Wee1 and p53 was down-regulated (**Fig. 6c**). However, HS did not further reduce the expression levels of Wee1, Cdc25C, and Cdc25A in the knock-down clone. Most likely, another chaperone overtook the function of Hsp90 and protected the client proteins upon HS. It was reported that Hsp70 can replace Hsp90 (**Bottoni et al., 2009**). In future studies we are going to address this issue. Nevertheless, it was demonstrated that Hsp90 prevented Cdc25A degradation. BrdU incorporation studies together with FACS analyses confirmed that directly after HS BxPC-3 cells were arrested in G1 phase, whereas Hsp90 knock-down cells were arrested in G2 and the incorporation of BrdU in these cells was inhibited during S phase (**Fig. 6d**). Therefore, Hsp90 significantly contributes to BxPC-3 cell cycle progression and could be therapeutically targeted in pancreas carcinoma cells.

<u>GD and gemcitabine additively inhibit Cdc25A and cell proliferation</u>

The only current chemotherapy against pancreas carcinoma is with gemcitabine (GEM). Although pancreas carcinoma cells were reported to be devoid of functional DNA checkpoints (**Myasaka et al. 2007**) GEM induced the phosphorylation of Chk2, but not Chk1 (**Fig. 7a**). This was accompanied by an inhibition of Cdc25A expression. Therefore, we studied whether GD and HS in combination with GEM could support the anti-neoplastic effect in pancreas carcinoma cells. The short incubation times of the previous experiments (1h

preincubation with GD followed by 1.5h HS) just served to study the basic cellular mechanisms of HS and in this part of the work, we also investigated the effects of GEM and GD after longer incubation times. For this BxPC-3 cells were incubated with GEM and GD for 8 h, whereas HS still lasted only for 90 min because in clinical applications this is the usually applied and tolerated time which does not threat the patients (**Skitzki et al., 2009; Dewhirst et al., 2005; Kraybill et al., 2002**). As shown before, HS or GD alone had no effect on Cdc25A expression after this incubation period but the combination of HS & GEM, or GD & GEM, or HS & GD & GEM reduced the expression of Cdc25A below the levels of GEM treatment alone (**Fig. 7b**). On Cdc25C, GEM had only an effect in combination with HS. In long term experiments (72 h) cell numbers were measured but for this, the concentrations of GEM and GD were reduced to inhibit BxPC-3 cell proliferation not more than 50 %. In detail, 5 nM GEM reduced the cell number by approximately 40 % and 10 nM GD by nearly 20 % (**Fig. 7c**). The effect of the combination of 5 nM GEM and 10 nM GD was roughly additive reducing the cell number by more than 55 %. A single HS (90 min) at the beginning of the experiment had no additional effect in long term experiments. In knockdown cells GEM alone reduced the cell number by 53 % which was similar to the cell number reduction achieved by GEM & GD in wild type cells. Interestingly, in knockdown cells, HS & GEM further reduced the cell number by 70 %. Thus, the exposure to HS and the targeting of Hsp90 strongly supported GEM standard treatment of pancreas carcinoma cells.

Discussion

Pancreas cancer cells are highly resistant to various in vitro treatments and also clinical therapy regimens are largely ineffective (**Jemal et al. 2003**). GEM is the main standard agent and the major beneficial effect seems to be a palliative one (**Bayraktar et al., 2010**). Pancreas cancer cells tend to acquire resistance to GEM and this was reported to be caused by the activation of the NF-kB pathway (**Uwagawa et al. 2009, Fujiwara et al. 2011**). Undoubtly, the resistance to drug treatment involves mutations of $p16^{INK}$ or alternatively, mutations of p53 (**Okamoto et al. 1994, Chen et al., 2011**). Furthermore, disease progression correlates with an inactivation of the Chk2 DNA damage check point (**Miyasaka et al. 2007**). Nevertheless, we demonstrate that isolated BxPC-3 pancreas carcinoma cells respond to GEM treatment with the phosphorylation of Chk2, Cdc25A degradation, and concomitant cell cycle attenuation. Recently it was shown that HS induced Chk2 in HEK293 cells (**Madlener et al. 2009**) and hence, the observation that HS did not induce Chk2 phosphorylation in BxPC-3 pancreas carcinoma cells was unexpected. Thus, the activation of Chk2 by GEM or by HS was through distinct pathways, whereby the HS induced pathway remained silent in BxPC-3 cells. Despite this fact, HS caused cell cycle arrest in a background of inhibited Hsp90 (by GD) or reduced Hsp90 expression (by shRNA). However, the attenuation of cell cycle progression was transient and only occurred immediately after HS-treatment and this was most likely due to disabled DNA checkpoint activation and lack of p21 induction. The Hsp90 client p53 was also degraded, which however does not play a role in this scenario, because p53 is anyway mutated in BxPC-3 cells (**Park et al. 2006**). Despite the transient nature of cell cycle inhibition, we show that the cell cycle was arrested independent of functional DNA check point kinases Chk1 and Chk2. Otherwise, we would have detected the specific and destabilising Cdc25A phosphorylations at Ser75 and Ser177. Instead, targeting Hsp90 was sufficient to attenuate cell cycle progression and cell proliferation which correlated with the destabilisation of the Cdc25 family of phosphatases and other cell cycle regulators like Wee1, cyclin D1 and to some extent also Cdc2. We already provided evidence that HS caused the degradation of Cdc25A, B, and C in HEK293 and HeLa cells through the activity of Chk2 and inhibition of Hsp90 just accelerated the destabilisation of Cdc25A in these cell lines (**Madlener et al. 2009**). Degradation of Cdc25A was due to phosphorylations at Ser75 and Ser177 (through p38 and Chk2) and subsequent sequestration of Cdc25A by 14.3.3 proteins to the cytoplasm where Cdc25A became ubquitinylated and subjected to proteasomal destruction (**Madlener et al. 2009, Goloudina et al. 2003, Busino et al. 2004, Busino et al.**

2003). Here, we show for the first time that the degradation of Cdc25A depended on the inhibition (reduction) of Hsp90 without the necessity to activate Chk2.

The combination of HS together with the Hsp90 inhibitor GD resulted in an impressive suppression of Cdc25A, B, and C particularly in BxPC-3 and PANC-1 cells. This effect was not restricted to pancreas carcinoma cells but was also observed in MDA-MB231 and MCF-7 breast cancer cells and tamoxifen and fulvestrant-resistant derivatives. Also the novel synthetic Hsp90 inhibitors 4-TCNA and 7-TCNA strongly down-regulated Cdc25A expression, which substantiated the hypothesis that inhibition of Hsp90 can be a strategy to combat pancreas cancer cell expansion. We observed that HS did not produce an additional effect on Cdc25A-, Cdc25C, or Wee1- degradation in BxPC-3 cells, in which Hsp90 expression was knocked down by specific shRNA. Thus, another chaperone might have slipped in place of Hsp90. To accomplish its chaperon function, Hsp90 forms a dynamic complex known as the Hsp90 chaperone machinery with Hsp70 and different co-chaperones (**Pratt and Toft, 2003**). Furthermore, the over-expression of Hsp27 has been shown to correlate with the induction of chemoresistance for GEM in pancreatic cancer cells and therefore this protein could be a possible marker for predicting the response of pancreatic cancer patients to treatment with GEM (**Bottoni et al., 2009**). This strongly suggests that limited Hsp90 levels allow other chaperones, such as Hsp70 or Hsp27, to fill the former position of Hsp90 (**Bottoni et al., 2009; Yun et al., 2010**) on i.e. Cdc25A and (partly) fulfil its function. The role of other heat shock proteins after inhibiting Hsp90 will be investigated in further studies.

GEM induced Chk2 and added up to the cell cycle inhibitory effect induced by GD &/- HS. This evidenced that a GEM-based therapy can be improved by a combination treatment targeting Hsp90 and cell cycle regulators. Hsp90-dependent cell cycle inhibition was only short but very strong. This effect was vastly prolonged when GD (+/-GEM) was applied for the entire experimental period (which better reflects a clinical setting) despite a single and short (90 min) HS exposure.

Materials and methods

Cell culture: BxPC-3, AsPC-1 and PANC-1 pancreatic cancer cell lines and MCF-7 and MDA-MB-231 breast cancer cell lines were purchased from ATCC. BxPC-3 and AsPC-1 cells were cultured in RPMI 1640 medium supplemented with 10 % heat inactivated fetal calf serum (FCS), 1 % L-glutamine, 1 % sodiumpyruvate and 1 % penicilline/streptomycin. PANC-1 cells were grown in high glucose DMEM medium supplemented with 10 % heat inactivated FCS, 1 % L-glutamine and 1 % penicilline/streptomycin. MCF-7 and MDA-MB-231 breast cancer cells were cultivated in DMEM/F-12 1:1 medium supplemented with 10 % heat inactivated FCS, 1 % L-glutamine and 1 % penicilline/streptomycin. Tamoxifen and fulvestrant resistance were obtained by treating MCF-7 cells with increasing concentrations (up to 500nM) of tamoxifen and fulvestrant, respectively, and the resistant cell lines (tamoxifen resistant (TR500-MCF-7); fulvestrant resistant (FR500-MCF-7)) were grown in DMEM/F-12 1:1 medium supplemented with 10 % heat inactivated FCS, 1 % L-glutamine, 1 % penicilline/streptomycin and 500nM of the corresponding anti-estrogen.
All cells were grown at 37°C in a humidified atmosphere containing 5% CO_2. If not mentioned otherwise, all media and supplements were obtained from Invitrogen Life Technologies (Karlsruhe, Germany).

Heat shock and inhibitor treatment: Cells were grown up to 80 % confluence and after pre-incubation with 250 nM GD for 1 h, cells were exposed to 41.5°C for 1.5 h in a humidified atmosphere containing 5% CO_2. After HS treatment cells were prepared for analysis as described thereafter.

Western Blotting: After incubation with corresponding compounds and exposure to 41.5°C HS cells were harvested, washed twice with cold PBS and lysed in a buffer containing 150 nM NaCl, 50 mM Tris, 1 % Triton-X-100, 1 mM phenylmethylsulfonylfluride (PMSF) and 2.5 % PIC (Cat#P8849 Sigma, Munich, Germany). After centrifugation (12 000 x g) for 20 min at 4°C the supernatant was stored at -20°C until further analysis. Equal amounts of protein samples were separated by polyacrylamide gel electrophoresis and electrotransferred onto PVDV-membranes (Hybond-P, Amersham), 4°C overnight. Staining membranes with Ponceau S controlled equal sample loading. After washing with Tris buffered saline (TBS) pH 7.6, membranes were blocked in 5 % non-fat dry milk in TBS containing 0.1% Tween-20 for 1 h. Membranes were incubated with the first antibody (in blocking solution, dilution 1:500-

1:1000) by gently rocking at 4°C overnight, washed with TBS containing 0.1% Tween-20 and further incubated with the second antibody (peroxidase-conjugated swine anti-rabbit IgG or rabbit anti-mouse IgG, dilution 1:2000-1:5000 in blocking solution) for 1 h. Chemoluminescence was developed by the ECL plus detection kit (GE Healthcare, Buckinghamshire, UK) and analysed using a Lumi-Imager F1 Workstation (Roche, Basel, Switzerland).

Reagents and antibodies: Tamoxifen (Cat# T5648), fulvestrant (Cat# I4409), geldanamycin (Cat# G3381), hexadimethrine bromide (Cat# H9268) and puromycin (Cat# P9620) were purchased from Sigma (Munich, Germany). Amersham ECLPlus Western Blotting Detection System was from GE Healthcare (Buckinghamshire, UK). The synthetic HSP90 inhibitors 4-TCNA and 7-TCNA were provided by Dr. Mouâd Alami, Université Paris Sud.
Antibodies: Mouse monoclonal (ascites fluid) anti-β-actin clone AC-15 Cat# A5441 was from Sigma (Munich, Germany). Anti cyclin D1 (M-20) Cat# sc-718, p21 (C-19) Cat# sc-397, Cdc25A (F-6) Cat# sc-7389, Cdc25B (C-20) Cat# sc-326, Cdc25C (C-20) Cat# sc-327 were from Santa Cruz Biotechnologies Inc. (Santa Cruz, CA, USA). Phospho-Wee1 (Ser^{642}) (D47G5) Cat# 4910, Wee1 Cat# 4936, phospho-Chk2 (Thr^{68}) Cat# 2661, Chk2 Cat# 2662, phospho-Chk1 (Ser^{345}) Cat# 2341, Chk1 Cat# 2345, phospho-p53 (Ser^{20}), acetylated-p53 (Lys^{382}) Cat# 2525 and Hsp90 Cat# 4877 were from Cell Signalling (Danvers, MA, USA). p53 antibody Cat# 1767 was purchased from Immunotech (Marseille, France), phospho-Cdc25A (Ser^{75}) Cat# ab47279 from Abcam (Cambridge, UK) and phospho-Cdc25A (Ser^{177}) Cat# AP3046 was from Abgent (San Diego, CA, USA). Anti mouse and anti rabbit IgG were from Dako (Glostrup, Denmark).

Quantitative RT-PCR: BxPC-3 cells (0.25×10^5) were seeded in 6 wells and after 24 h cultivation they were harvested and homogenised using Qia-shredder (Cat# 79654, Qiagen, Hilden, Germany). The cells were further processed according to the instructions of RNeasy Mini Kit (Cat# 74104, Qiagen). Final RNA concentration was measured using a NanoDrop Fluorospectrometer (Thermo Fisher Scientific, Inc., Waltham, MA, USA). cDNA synthesis from 1 µg RNA was performed using Superscript-first-strand synthesis systems for RT-PCR (Cat# 11904-018, Invitrogen, Carlsbad, CA, USA). Hsp90AB1 transcript levels were investigated by real-time PCR using Taqman detection system (Applied Biosystems, Carlsbad, CA, USA). The housekeeping-gene glyceralaldehyde 3-phosphate dehydrogenase (GAPDH) served as reference gene. Assay ID numbers of the Taqman gene expression kits

were: GAPDH: HS99999905_m1; HSP90AB1 (this is the constitutively expressed form of Hsp90A, which for reasons of simplicity is shortened throughout the manuscript to Hsp90): HS01546474_g1. Cycle program (95°C for 10 min to activate polymerase followed by 40 cycles of 95°C for 15 s and 60°C for 1 min) was started on an Abi Prism 7000 Sequence Detection System (Applied Biosystems). Real time-PCR was performed in duplicates for each cDNA template and gene investigated. Negative controls, containing water instead of cDNA, confirmed the absence of RNA/DNA in all reagents applied in the assay.

Lentiviral shRNA transduction: BxPC-3 cells (1 x 10^4) were seeded in 24 well plates and were cultivated overnight. The next day hexadimethrine bromide (8ng/ml) and 1 x 10^5 transducing units of the lentiviral shRNA vectors were added. Transduction particles (HSP90AB1: TRCN0000008748; clone ID NM_007355.2-232s1c1; negative control: Cat# SHC002H) were obtained from Sigma (Munich, Germany). After 24 hours of incubation, fresh media and further 24 h later puromycin (10µg/ml) were added to identify resistant BxPC-3 Hsp90 knockdown colonies (BxPC-3 knockdown).

Proliferation inhibition analysis: BxPC-3 cells and BxPC3 knockdown (1 x 10^5) were seeded in 6 well plates, cultivated overnight and treated with 5 nM GEM and 10 nM GD, respectively. A single HS was performed 1 h after the beginning of the treatment. To avoid unspecific effects caused by the solvent, DMSO concentration was the same in all samples (0.05%). Cell counts were determined after 72 h using a Casy TTC cell counter (Roche, Basel, Switzerland).

BrdU incorporation: BxPC-3 and BxPC-3 knockdown cells were seeded in 6-wells, pre-treated with GD for 1 h and incubated with 10 µM of BrdU exposed to 41.5°C for 1.5 h. Cells were prepared following the instructions of the manufacturer (BrdU Flow Kit Cat# 552598, BD Pharmingen), except for the incubation with fluorescent anti-BrdU antibody, which was incubated overnight at 4°C (dilution 1:50). Afterwards, the BrdU incorporation was measured and analysed by a FACSCalibur flow cytometer.

Statistics: All experiments were performed in triplicate and analysed by t-test (GraphPad Prism 5.0 program, GraphPad (San Diego, CA, USA).

Acknowledgements

We wish to thank Toni Jäger for preparing the figures. This work was supported by the Fellinger Cancer Research Association (Fellinger Krebsforschung Gemeinnütziger Verein) with a grant to G.K as a mission-oriented grant (Auftragsforschung), and by the Herzfelder´sche Family foundation with a grant to T.S.

References

Bayraktar S., Bayraktar U.D. and Rocha-Lima C.M. Recent developments in palliative chemotherapy for locally advanced and metastatic pancreas cancer. *World J Gastroenterol.* 16: 673-682, **2010.**

Bottoni P., Girdina B. and Scatena R. Proteomic profiling of heat shock proteins: an emerging molecular approach with direct pathophysiological and clinical implications. *Proteomics Cli Appl*. 3: 636-653, **2009.**

Busino L., Donzelli M., Chiesa M., Guardavaccaro D., Ganoth D., Dorrello N.V. Hershko A., Pagano M. and Draetta G.F. Degradation of Cdc25A by beta-TrCP during S phase and in response to DNA damage. *Nature* 426: 87-91, **2003.**

Busino L., Chiesa M., Draetta G.F. and Donzelli M. Cdc25A phosphatase: combinatorial phosphorylation, ubiquitylation and proteolysis. *Oncogene* 23: 2050-2056, **2004.**

Chen M.S., Ryan C.E. and Piwnica-Worms H. Chk1 kinase negatively regulates mitotic function of Cdc25A phosphatase through 14-3-3 binding. *Mol. Cell. Biol.* 23 7488-7497, **2003.**

Chen Y.W., Liu J.Y., Lin S.T., Li J.M., Huang S.H., Chen J.Y., Wu J.Y., Kuo C.C., Wu C.L., Lu Y.C., Chen Y.H., Fan C.Y., Huang P.C., Law C.H., Lyu P.C., Chou H.C. and Chan HL. Proteomic analysis of gemcitabine-induced drug resistance in pancreatic cancer cells. *Mol Biosyst.* 7: 3065-74, **2011.**

Cotto J.J. and Morimoto R.I. Stress induced activation of the heat shock response: cell and molecular biology of heat shock factors. *Biochem. Soc. Symp.* 64: 105-118, **1999.**

Dewhirst M.W., Vujaskovic Z., Jones E. and Thrall D. Re-setting the biologic rationale for thermal therapy. *Int J Hyperthermia.* 21:779-790, **2005.**

Evans D.B., Abbruzzese J.L. and Willett C.G. Cancer of the pancreas. In: DeVita V.T., Hellman S., and Rosenberg S.A., editors. Cancer: principles & practice of oncology. Philadelphia: Lipincott: 1126-1161, **2001.**

Fahrig R., Quietzsch D., Heinrich J.C., Heinemann V., Boeck S., Schmid R.M., Praha C., Liebert A., Sonntag D., Krupitza G. and Hänel M. RP101 improves the efficacy of chemotherapy in pancreas carcinoma cell lines and pancreatic cancer patients. *Anticancer Drugs* 17:1045-56, **2006.**

Fujiwara Y., Furukawa K., Haruki K., Shimada Y., Iida T., Shiba H., Uwagawa T., Ohashi T. and Yanaga K. Nafamostat mesilate can prevent adhesion, invasion and peritoneal dissemination of pancreatic cancer thorough nuclear factor kappa-B inhibition. *J Hepatobiliary Pancreat Sci.*18: 731-739, **2011.**

García-Morales P., Carrasco-García E., Ruiz-Rico P., Martínez-Mira R., Menéndez-Gutiérrez M.P., Ferragut J.A., Saceda M. and Martínez-Lacaci I. Inhibition of Hsp90 function by ansamycins causes downregulation of cdc2 and cdc25c and G(2)/M arrest in glioblastoma cell lines. *Oncogene* 26: 7185-7193, **2007.**

Goloudina A., Yamaguchi H., Chervyakova D.B., Appella E., Fornace Jr. A.J. and Bulavin D.V. Regulation of human Cdc25A stability by serine 75 phosphorylation is not suficient to activate a S-phase checkpoint. *Cell Cycle* 2: 473-478, **2003.**

Heinrich J.C., Tuukkanen A., Schroeder M., Fahrig T. and Fahrig R. RP101 (brivudine) binds to heat shock protein HSP27 (HSPB1) and enhances survival in animals and pancreatic cancer patients. *J Cancer Res Clin Oncol* 1371349-61, **2011.**

Huguet F. Girard N., Guerche C.S., Hennequin C., Mornex F. and Azria D. Chemoradiotherapy in the management of locally advanced pyncreatic carcinoma: a qualitative systematic review. *J Clin Oncol.* 27: 2269-2277, **2009.**

Jemal A., Murray T., Samuels A., Ghafoor A., Ward E., and Thun M.J. *Cancer statistics, 2003.CA Cancer J Clin.* 53: 5-26, **2003.**

Khalil A.A., Kabapy N.F., Deraz S.F. and Smith C. Heat shock proteins in oncology: Diagnostic biomarkers or therapeutic targets? *Biochimica and Biophysica*, in press, **2011.**

Kraybill W.G., Olenki T., Evans S.S., Ostberg J.R., O'Leary K.A., Gibbs J.F. and Repasky E.A. A phase I study of fever-range whole body hyperthermia (FR-WBH) in patients with advanced solid tumours: correlation with mouse models. *Int J Hyperthermia*. 18: 253-266, **2002.**

Le Bras G., Radanyi C., Peyrat J.F., Brion J.D., Alami M., Marsaud V., Stella B. and Renoir J.M. New novobiocin analogues as antiproliferative agents in breast cancer cells and potential inhibitors of heat shock protein 90. *J. Med Chem.* 50: 6189-6200, **2007.**

Lindquest S. and Craig E.A. The heat-shock proteins. *Annu Rev Genet.* 22: 631-677, **1998.**

Madlener S., Rosner M., Krieger S., Giessrigl B., Gridling M., Vo T.P., Leisser C., Lackner A., Raab I., Grusch M., Hengstschläger M., Dolznig H. and Krupitza G. Short 42°C heat shock induces phosphorylation and degradation of Cdc25A which depends on p38MAPK, Chk2 and 14.3.3. *Human Molecular Genetics* 18: 1990-2000, **2009.**

Marcu M.G., Chadli A., Bouhouche I., Catelli M. and Neckers L.M. The heat shock protein 90 antangonist novobiocin interacts with a previously unrecognized ATP-binding domain in the carboxyl terminus of the chaperone. *J. Biol. Chem.* 275: 37181-37186, **2000.**

Mihaljevic A.L., Michalski C.W., Firess H. and Kleeff J. Molecular mechanisms of pancreatic cancer – understanding proliferation, invasion and metastasis. *Langenbecks Arch Surg* 395: 295-308, **2010.**

Miyasaka Y., Nagai E., Yamaguchi H., Fujii K., Inoue T., Ohuchida K., Yamada T., Mizumoto K., Tanaka M. and Tsuneyoshi M.. The role of the DNA damage checkpoint pathway in intraductal papillary mucinous neoplasms of the pancreas. *Clin Cancer Res.* 13: 4371-4377, **2007.**

Niederhuber J.E., Brennan M.F. and Menck H.R. The national cancer data base report on pancreatic cancer. Cancer 76: 1671-1677, **1995.**

Nilsson I. and Hoffmann I. Cell cycle regulation by the Cdc25 phosphatase family. *Prog. Cell Cycle Res.* 4: 107-114, **2000.**

Okamoto A., Demetrick D.J., Spillare E.A., Hagiwara K., Hussain S.P., Bennett W.P., Forrester K., Gerwin B., Serrano M., Beach D.H., and Harris C.C. Mutations and altered expression of p16INK4 in human cancer. *Proc Natl Acad Sci U S A.* 91:11045-11049, **1994.**

Park S.J., Kostic M. and Dyson H.J. Dynamic Interaction of Hsp90 with Its Client Protein p53. *J Mol Biol* 411: 158-173, **2011.**

Park Y.J., Wen J., Bang S., Park S.W. and Song S.Y. (6)-Gingerol induces cell cycle arrest and cell death of mutant p53-expressing pancreatic cancer cells. *Yonsei Med J.* 47:688-697, **2006.**

Pratt W.B. and Toft D.O. Regulation of signalling protein function and trafficking by the hsp90/hsp70 based chaperone machinery. *Exp. Biol. Med. (Maywood)* 228: 111-133, **2003.**

Radanyi C., Le Bras G., Marsaud V., Peyrat J.F., Messaoudi S., Catelli M.G., Brion J.D., Alami M. and Renoir J.. Antiproliferative and apoptotic activities of tosylcyclonovobiocic acids as potent heat shock protein 90 inhibitors in human cancer cells. *Cancer Letters* 274: 88-94, **2009.**

Skitzki J.J., Repasky E.A. and Evans S.S. Hyperthermia as an immunotherapy strategy for cancer. *Curr Opin Investig Drugs.* 10:550-558, **2009.**

Tse A.N., Sheikh T.N., Alan H., Chou T.C. and Schwartz GK. 90-kDa heat shock protein inhibition abrogates the topoisomerase I poison-induced G2/M checkpoint in p53-null tumour cells by depleting Chk1 and Wee1. *Mol Pharmacol* 75: 124-133, **2009.**

Uwagawa T., Chiao P.J., Gocho T., Hirohara S., Misawa T. and Yanaga K. Combination chemotherapy of nafamostat mesilate with gemcitabine for pancreatic cancer targeting NF-kappaB activation. *Anticancer Res. 29*: 3173-3178, **2009.**

Yun C.H., Yoon S.Y., Nguyen T.T., Cho H.Y., Kim T.H., Kim S.T., Kim B.C., Hong Y.S., Kim S.J., Lee H.J. Geldanamycin inhibits TGF-beta signaling through induction of Hsp70. *Arch Biochem Biophys.* 495: 8-13, **2010.**

Figure legends

Figure 1

Western blot analysis of the Cdc25 phosphatases and cyclin D1 in (a) BxPC-3, (b) PANC-1 and (c) AsPC-1 pancreatic cancer cells. After pre-incubation with 250 nM GD for 1 h, cells were exposed to 41.5°C for 1.5 h. Cells were lysed directly after HS (left panel "treatment") or after 6 h post-incubation in the absence of GD (right panel "post-treatment"). The obtained protein samples were applied to SDS-PAGE. Western blot analysis was performed with the indicated antibodies. Equal sample loading was confirmed by Ponceau S staining and β-actin analysis.

Figure 2

Western blot analysis of the cell cycle regulators Cdc2 and Wee1 in (a) BxPC-3 and (b) PANC-1 pancreatic cancer cells. After pre-incubation with 250 nM GD for 1 h, cells were exposed to 41.5°C for 1.5 h. Cells were lysed directly after HS (left panel "treatment") or after 6 h post-incubation in the absence of GD (right panel "post-treatment"). The obtained protein samples were applied to SDS-PAGE. Western blot analysis was performed with the indicated antibodies. Equal sample loading was confirmed by Ponceau S staining and β-actin analysis.

Figure 3

Western blot analysis of (a) p53 and p21 and (b) the checkpoint kinases Chk1 and Chk2 and the site-specific phosphorylation of Cdc25A (as indicated) in BxPC-3 pancreatic cancer cells. After pre-incubation with 250 nM GD for 1 h, cells were exposed to 41.5°C for 1.5 h. Cells were lysed directly after HS and the obtained protein samples were applied to SDS-PAGE. Western blot analysis was performed with the indicated antibodies. Equal sample loading was confirmed by Ponceau S staining and β-actin analysis.

Figure 4

Western blot analysis of different cell cycle regulators in (a) MDA-MB-231 and (b) MCF-7, tamoxifen resistent (TR500-MCF-7) and fulvestrant resistent (FR-MCF-7) breast cancer cells. After pre-incubation with 250 nM GD for 1 h, cells were exposed to 41.5°C for 1.5 h. Cells were lysed directly after HS (a, left panel "treatment"; b) or after 6 h post incubation in the absence of GD (a, right panel "post-treatment"). The obtained protein samples were applied to

SDS-PAGE. Western blot analysis was performed with the indicated antibodies. Equal sample loading was confirmed by Ponceau S staining and β-actin analysis.

Figure 5

Western blot analysis of Cdc25A and Cdc25C in BxPC-3 pancreatic cancer cells. After pre-incubation with 50 µM 4-TCNA and 7-TCNA, respectively, for 1 h, cells were exposed to 41.5°C for 1.5 h. Cells were lysed directly after HS and the obtained protein samples were applied to SDS-PAGE. Western blot analysis was performed with the indicated antibodies. Equal sample loading was confirmed by Ponceau S staining and β-actin analysis.

Figure 6

Knockdown of Hsp90AB1 with specific shRNA. (a) mRNA levels of Hsp90AB1 of BxPC-3 scrambled control (1) cells and different knockdown clones (2-11). RNA of lentiviral transduced clones was isolated, transcribed into cDNA and subjected to quantitative real time-PCR using specific primers for Hsp90AB1 and GAPDH (as internal control). Experiments were performed in duplicate. (b) Western blot analysis of Hsp90 of BxPC-3 scrambled control cells (1) and different knockdown clones (2-11). Equal sample loading was confirmed by Ponceau S staining and β-actin analysis. (c) Western blot analysis of different cell cycle regulators in BxPC-3 control cells (Co) and BxPC-3 knockdown cells (k.d.) Cells were exposed to 41.5°C for 1.5 h and lysed directly after HS and the obtained protein samples were applied to SDS-PAGE. Western blot analysis was performed with the indicated antibodies. Equal sample loading was confirmed by Ponceau S staining and β-actin analysis. (d) Effects of HS on cell cycle distribution of BxPC-3 wildtype and knockdown cells. Cells were incubated with 10 µM of BrdU, exposed to 41.5°C for 1.5 h and prepared following the instructions of the manufacturer (BrdU Flow Kit, BD Pharmingen). The BrdU incorporation was measured and analysed by a FACSCalibur flow cytometer. Experiments were performed in sextuple. Asterisks indicate significance compared to the corresponding control ($p<0.05$) and error bars indicate ±SD.

Figure 7

Effects of GEM on BxPC-3 pancreatic cancer cells in combination with GD/HS. (a) BxPC-3 cells were treated with 0.5 µM GEM for 2, 4 and 8 h. (b) After pre-incubation with 250 nM GD and 0.5 µM GEM for 1 h, BxPC-3 cells were exposed to 41.5°C for 1.5 h. After 8 h post-incubation in the presence of GEM/GD, cells were lysed and the obtained protein samples

were applied to SDS-PAGE. Western blot analysis was performed with the indicated antibodies. Equal sample loading was confirmed by Ponceau S staining and β-actin analysis. (c) Proliferation inhibition of BxPC-3 wildtype and BxPC-3 knockdown cells upon treatment with 5 nM GEM and 10 nM GD for 72 h. A single HS (41.5°C for 1.5 h) was carried out 1 h after treatment start. Experiments were performed in triplicate. Asterisks and triangles indicate significance compared to the corresponding controls ($p<0.05$) and error bars indicate ±SD.

Fig Compilation

1a

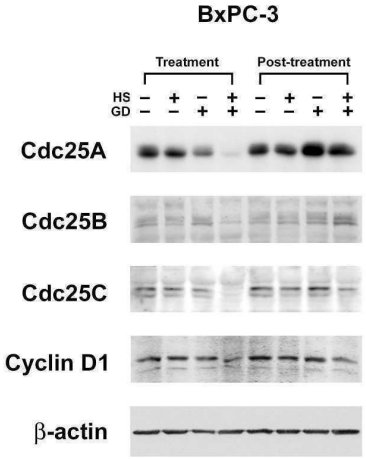

1b

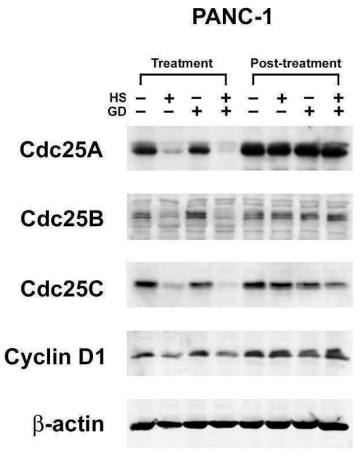

1c

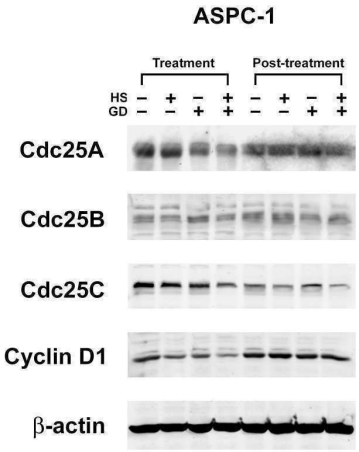

2a

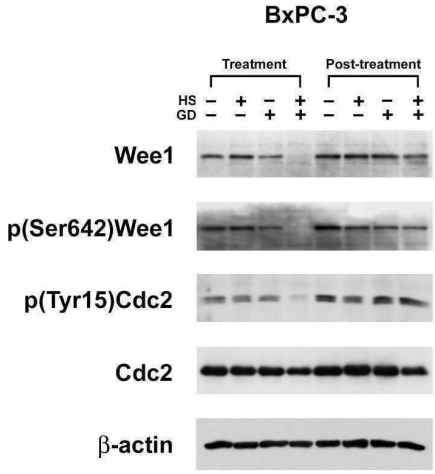

2b

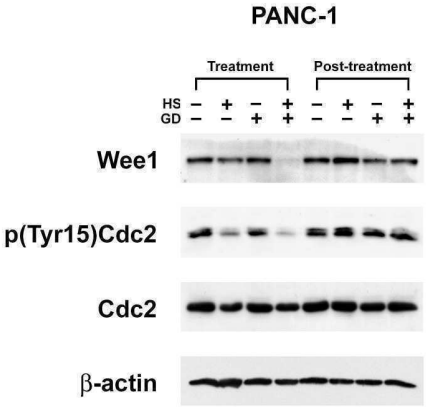

3a

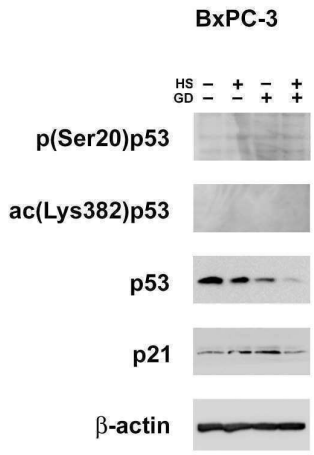

3b

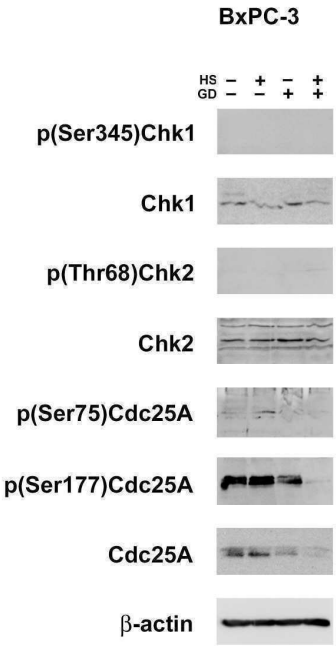

4a

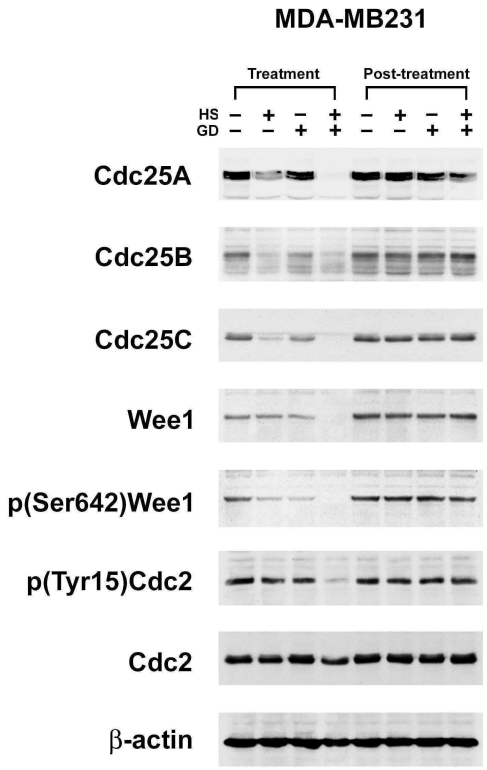
MDA-MB231
Treatment
Post-treatment
HS
GD
Cdc25A
Cdc25B
Cdc25C
Wee1
p(Ser642)Wee1
p(Tyr15)Cdc2
Cdc2
β-actin

4b

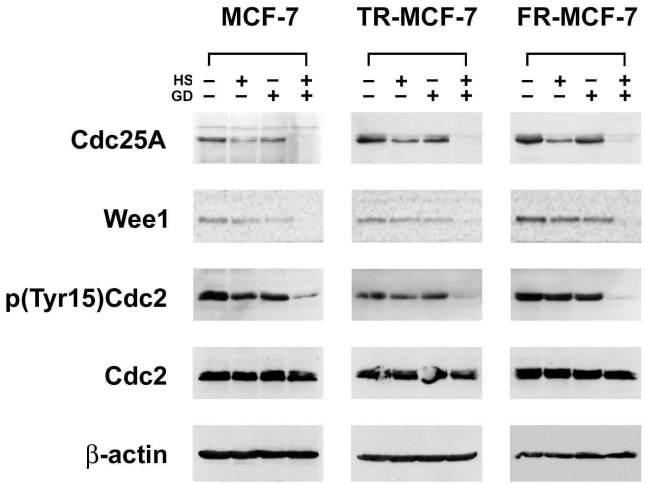
MCF-7
TR-MCF-7
FR-MCF-7
HS
GD
Cdc25A
Wee1
p(Tyr15)Cdc2
Cdc2
β-actin

5

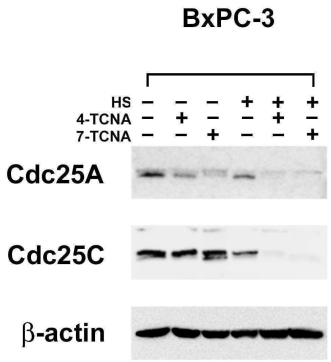
BxPC-3
HS
4-TCNA
7-TCNA
Cdc25A
Cdc25C
β-actin

6a

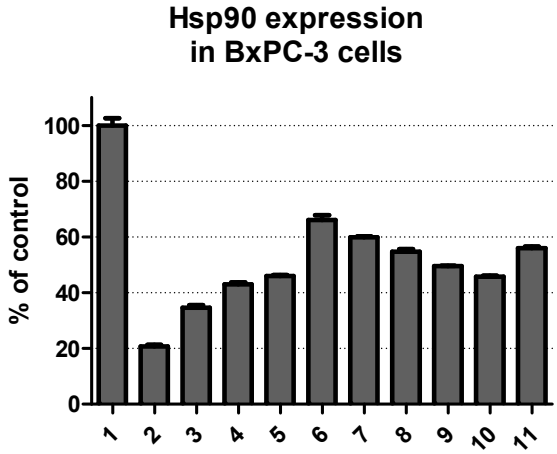

6b

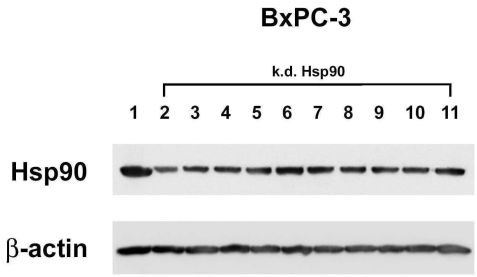

6c

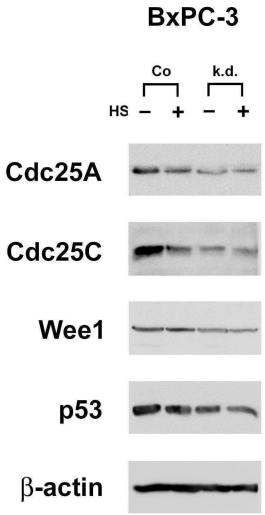

6d

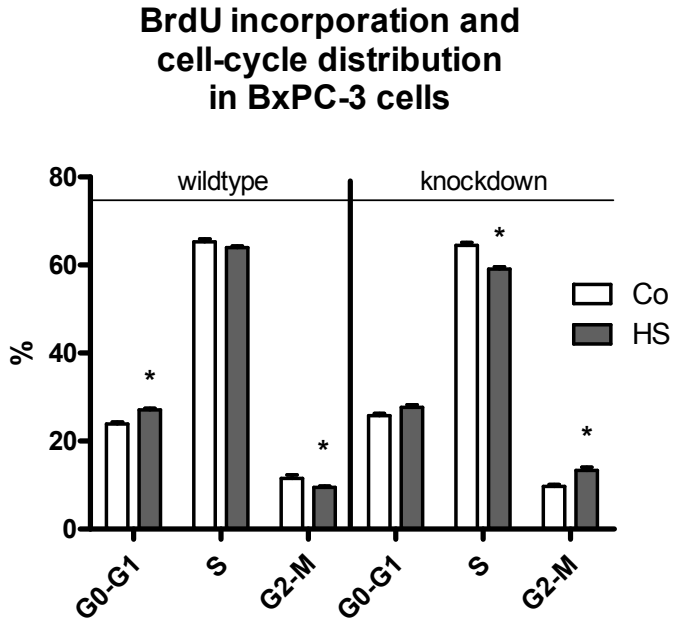

7a

7b

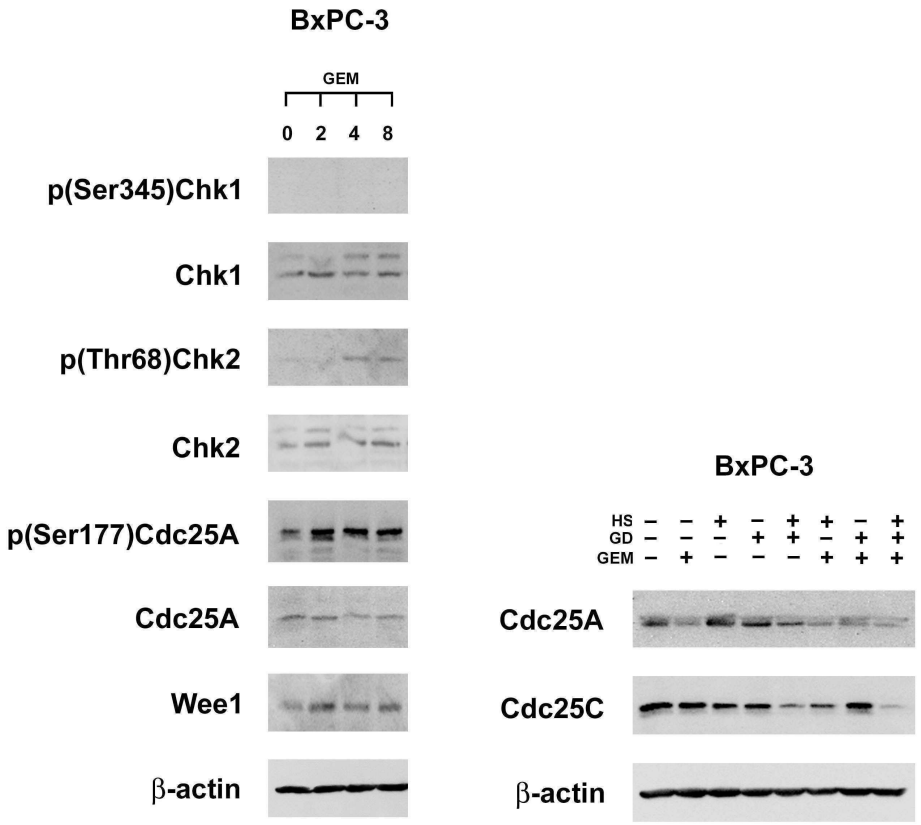
BxPC-3
GEM
0 2 4 8
p(Ser345)Chk1
Chk1
p(Thr68)Chk2
Chk2
p(Ser177)Cdc25A
Cdc25A
Wee1
β-actin
BxPC-3
HS – – + – + + – +
GD – – – + + – + +
GEM – + – – – + + +
Cdc25A
Cdc25C
β-actin

7c

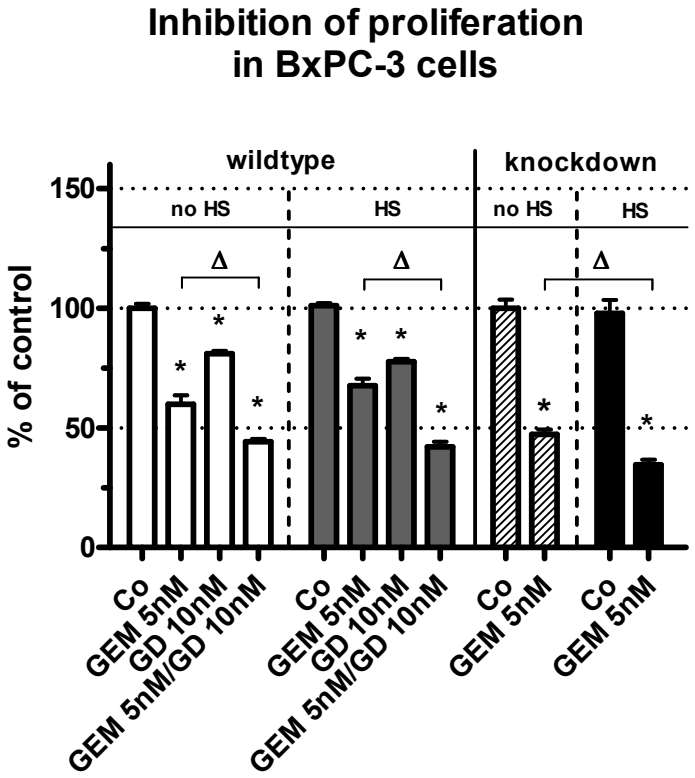
Inhibition of proliferation
in BxPC-3 cells
wildtype
knockdown
no HS
HS
no HS
HS
Δ
Δ
Δ
% of control
150
100
50
0
Co
GEM 5nM
GD 10nM
GEM 5nM/GD 10nM
Co
GEM 5nM
GD 10nM
GEM 5nM/GD 10nM
Co
GEM 5nM
Co
GEM 5nM

7 CURRICULUM VITAE

Name:	Benedikt Giessrigl
Date of birth:	23.06.1982
Place of birth:	Vienna, Austria
Nationality:	Austria

Education

1988-1992	Primary School, Vienna
1992-2000	Grammar School, Vienna
16.06.2000	Final exam
2001-2005	Studies of Pharmacy, University of Vienna
06/2005-12/2005	Diploma thesis at the Institute of Pharmaceutical Chemistry, University of Vienna. Title: *"Zwitterionische Antisense Oligonukleotide"*
21.12.2005	Graduation; Academic degree: Mag. pharm.
since 10/2008	PhD studies at the Department of Clinical Pharmacy and Diagnostics, University of Vienna

Professional experience

2006 - 2007	Practical training in a pharmacy – „Aspirantenjahr"[1]
02/2007	Final examination – "Fachprüfung für den Apothekerberuf"[1]
04/2007 - 10/2007	Pharmacist in a public pharmacy
11/2007 - 06/2008	Ludwig Boltzmann Institute for Applied Cancer Research (LBI-ACR Vienna)

[1]graduates have to complete one year of practical training in a pharmacy followed by a final examination in order to be qualified as pharmacists.

11/2007 - 12/2008	Pharmacist in the hospital pharmacy of the "Kaiser Franz Josef Spital", Vienna, division of cytostatic production
since 07/2008	practical work for the PhD studies at the Department of Clinical Pathology, Medical University of Vienna
since 01/2009	Part-time pharmacist in a public pharmacy

Teaching experience

2008 - 2009	Lecturer for undergraduate students of pharmacy („Qualitative pharmazeutische Analytik") at the Department of Clinical Pharmacy and Diagnostics
since 2009	Lecturer for undergraduate students of „FH-Studienlehrgang Biotechnologie" („Analytische Chemie I LAB") at the Department of Clinical Pharmacy and Diagnostics

8 LIST OF SCIENTIFIC PUBLICATIONS

1. Madlener S., Rosner M., Krieger S., **Giessrigl B.**, Gridling M., Vo T.P., Leisser C., Lackner A., Raab I., Grusch M., Hengstschläger M., Dolznig H. and Krupitza G. Short 42 degrees C heat shock induces phosphorylation and degradation of Cdc25A which depends on p38MAPK, Chk2 and 14.3.3. *Hum Mol Genet.* 18: 1990-2000, **2009.**

2. Stark N., Gridling M., Madlener S., Bauer S., Lackner A., Popescu R., Diaz R., Tut F.M., Vo T.P., Vonach C., **Giessrigl B.**, Saiko P., Grusch M., Fritzer-Szekeres M., Szekeres T., Kopp B., Frisch R. and Krupitza G. A polar extract of the Maya healing plant Anthurium schlechtendalii (Aracea) exhibits strong in vitro anticancer activity. *Int J Mol Med.* 24: 513-521, **2009.**

3. Ozmen A., Madlener S., Bauer S., Krasteva S., Vonach C., **Giessrigl B.**, Gridling M., Viola K., Stark N., Saiko P., Michel B., Fritzer-Szekeres M., Szekeres T., Askin-Celik T., Krenn L. and Krupitza G. In vitro anti-leukemic activity of the ethno-pharmacological plant Scutellaria orientalis ssp. carica endemic to western Turkey. *Phytomedicine* 17: 55-62, **2010.**

4. Winkler J., Giessrigl B., Novak C., Urban E. and Noe C.R. 2′-*O*-Lysylaminohexyladenosine modified oligonucleotides. *Chemical Monthly* 141: 809-815, **2010.**

5. Khan M., **Giessrigl B.**, Vonach C., Madlener S., Prinz S., Herbaceck I., Hölzl C., Bauer S., Viola K., Mikulits W., Quereshi R.A., Knasmüller S., Grusch M., Kopp B. and Krupitza G. Berberine and a Berberis lycium extract inactivate Cdc25A and induce alpha-tubulin acetylation that correlate with HL-60 cell cycle inhibition and apoptosis. *Mutat Res.* 683: 123-130, **2010.**

6. Vo T.P., Madlener S., Bago-Horvath Z., Herbacek I., Stark N., Gridling M., Probst P., **Giessrigl B.**, Bauer S., Vonach C., Saiko P., Grusch M., Szekeres T., Fritzer-Szekeres M., Jäger W., Krupitza G. and Soleiman A. Pro- and anti-

carcinogenic mechanisms of piceatannol are activated dose-dependently in MCF-7 breast cancer cells. *Carcinogenesis* 31: 2074-2081, **2010.**

7. Madlener S., Saiko P., Vonach C., Viola K., Huttary N., Stark N., Popescu R., Gridling M., Vo N.T., Herbacek I., Davidovits A., **Giessrigl B.**, Venkateswarlu S., Geleff S., Jäger W., Grusch M., Kerjaschki D., Mikulits W., Golakoti T., Fritzer-Szekeres M., Szekeres T. and Krupitza G. Multifactorial anticancer effects of digalloyl-resveratrol encompass apoptosis, cell-cycle arrest, and inhibition of lymphendothelial gap formation in vitro. *Br. J. Cancer* 102: 1361-137, **2010.**

8. Saiko P., Graser G., **Giessrigl B.**, Lackner A., Grusch M., Krupitza G., Basu A., Sinha B.N., Jayaprakash V., Jaeger W., Fritzer-Szekeres M. and Szekeres T. A novel N-hydroxy-N'-aminoguanidine derivative inhibits ribonucleotide reductase activity: Effects in human HL-60 promyelocytic leukemia cells and synergism with arabinofuranosylcytosine (Ara-C). *Biochem Pharmacol.* 81: 50-59, **2011.**

9. Minorics R., Szekeres T., Krupitza G., Saiko P., **Giessrigl B.**, Wölfling J., Frank E. and Zupkó I. Antiproliferative effects of some novel synthetic solanidine analogs on HL-60 human leukemia cells in vitro. *Steroids* 76: 156-162, **2010.**

10. Bauer S., Singhuber J., Seelinger M., Unger C., Viola K., Vonach C., **Giessrigl B.**, Madlener S., Stark N., Wallnofer B., Wagner K.H., Fritzer-Szekeres M., Szekeres T., Diaz R., Tut F., Frisch R., Feistel B., Kopp B., Krupitza G. and Popescu R. Separation of anti-neoplastic activities by fractionation of a Pluchea odorata extract. *Front Biosci. (Elite Ed)* 1: 1326-36, **2011.**

11. Jäger W., Gruber A., **Giessrigl B.**, Krupitza G., Szekeres T. and Sonntag D. Metabolomic analysis of resveratrol-induced effects in the human breast cancer cell lines MCF-7 and MDA-MB-231. *OMICS* 15: 9-14, **2011.**

12. Vonach C., Viola K., **Giessrigl B.**, Huttary N., Raab I., Kalt R., Krieger S., Vo T.P., Madlener S., Bauer S., Marian B., Hämmerle M., Kretschy N., Teichmann M., Hantusch B., Stary S., Unger C., Seelinger M., Eger A., Mader R., Jäger W.,

Schmidt W., Grusch M., Dolznig H., Mikulits W. and Krupitza G. NF-κB mediates the 12(S)-HETE-induced endothelial to mesenchymal transition of lymphendothelial cells during the intravasation of breast carcinoma cells. *Br. J. Cancer* 105: 263-271, **2011.**

13. Viola K., Vonach C., Kretschy N., Teichmann M., Rarova L., Strnad M., **Giessrigl B.**, Huttary N., Raab I., Stary S., Krieger S., Keller T, Bauer S, Jarukamjorn K., Hantusch B., Szekeres T., de Martin R., Jäger W., Knasmüller S., Mikulits W., Dolznig H., Krupitza G. and Grusch M. Bay11-7082 and xanthohumol inhibit breast cancer spheroid-triggered disintegration of the lymphendothelial barrier; the role of lymphendothelial NF-κB. *Br. J. Cancer,* 2011, submitted, **2011.**

14. Seelinger M., Popescu R., Seephonkai P., Singhuber J., **Giessrigl B.**, Unger C., Bauer S., Wagner K.H., Fritzer-Szekeres M., Szekeres T., Diaz R., Tut F.T., Frisch R., Feistel B., Kopp B. and Krupitza G. Fractionation of an anti-neoplastic extract of *Pluchea odorata* eliminates a property typical for a migratory cancer phenotype. *Evidence-based Compl. and Alt. Medicine,* submitted, **2011.**

15. **Giessrigl B.,** Yazici G., Teichmann M., Kopf S., Ghassemi S., Atanasov A.G., Dirsch V.M., Grusch M., Jäger W., Özmen A. and Krupitza G. Effects of *Scrophularia* Extracts on Tumor Cell Proliferation, Death and Intravasation through Lymphendothelial Cell Barriers. *Evidence-based Compl. and Alt. Medicine,* submitted, **2011.**

16. Saiko P., Graser G., **Giessrigl B.**, Lackner A., Grusch M., Krupitza G., Jaeger W., Golakoti T., Fritzer-Szekeres M. and Szekeres. Digalloylresveratrol, a novel resveratrol analog attenuates the growth of human pancreatic cancer cells by inhibition of ribonucleotide reductase *in situ* activity, *J. of Gastroenterology*, ***submitted.***

17. **Giessrigl B.,** Krieger S., Huttary N., Saiko P., Alami M., Maciuk A., Gollinger M., Mazal P., Szekeres T., Jäger W. and Krupitza G. Hsp90 stabilises Cdc25A

and prevents heat shock mediated cell cycle arrest in pancreas carcinoma cells. *Hum. Mol. Genet.* ***submitted.***

18. Unger C., Popescu R., **Giessrigl B.**, Laimer D., Heider S., Seelinger M., Diaz R., Tut F.M., Wallnöfer B., Egger G., Hassler M., Knöfler M., Saleh L., Sahin E., Wagner K.H., Grusch M., Frisch R., Fritzer-Szekeres M., Szekeres T., Kenner L., Kopp B. and Krupitza G. The dichloromethane extract of the ethno-medicinal plant *Neurolaena lobata* inhibits NPM/ALK expression which contributes to anaplastic large cell lymphomas. ***in preparation*.**